WELL COMPLETION REPORT
INTERPRETIVE

THYLACINE-1

T/30P

OFFSHORE OTWAY BASIN

SEPTEMBER 2003

Origin Energy Resources
339 Coronation Drive
MILTON, 4064
Brisbane, Queensland
Australia

TABLE OF CONTENTS

TABLES

1. Thylacine-1 Reservoir Summary
2. Predicted versus Actual Formation tops
3. Previous drilling history

FIGURES

1. Thylacine-1 Location Map
2. Depth Structure Map over Thylacine Prospect
3. Offshore Otway Stratigraphic Section
4. Predicted versus Actual Stratigraphy
5. Investigator 3D and 2D Seismic Survey Location Map
6. 3D xline 1200 through Thylacine-1
7. 3D xline 1260 through Thylacine Prospect
8. Variance Cube Time Slice (1512 ms TWT) through Thylacine Prospect
9. 3D Inline 1100 showing Top Porosity seismic amplitude anomaly over Thylacine Prospect
10. Thylacine-1 Time-Depth curve
11. Tectonic Elements – Otway Basin

APPENDICES

1. Petrophysics Report
2. MDT Report
3. Geochemistry Report
4. Palynological Report
5. Micropalaeontological Report
6. Petrology Report
7. Core Description and Interpretation (SEDSTRAT Pty Ltd)
8. Core Description and Interpretation (Core Laboratories Australia)
9. Special Core Analysis

ENCLOSURES

1. Composite Log

1. WELL INDEX SHEET

Permit Interests:	Origin Energy Resources Ltd (30%) - OPERATOR Woodside Energy Ltd (50%) Benaris International NV (20%)
Rig on Location:	04/05/2001
Spud:	05/05/2001
Reached TD:	18/05/2001
Rig Released:	28/05/2001
Total Rig Days:	25
Rig Name:	Ocean Bounty
Drilling Contractor:	Diamond Offshore General Co.
Total Depth:	2710 mMDRT (D & L)
Well Status:	Gas Discovery; Plugged and Suspended

Well Name:	Thylacine-1
Basin:	Offshore Otway
Permit:	T/30P
Type:	Vertical Exploration Well
Water Depth:	101.4m (LAT to seabed)
Elevation:	25m (RT-sea level)
Latitude:	39° 14' 27.592"S
Longitude:	142° 54' 44.169"E
Easting:	665 030.3 metres
Northing:	5 654 721.5 metres
(AGD 84; AMG Zone 54, Central Meridian 141° East). Deviation from intended location = 6.8m toward 110.8°	
Seismic Reference:	Inline 700/CDP 1200: Investigator 3D survey
Actual Well Cost:	A$14,099,513

Formation Tops:

FORMATION / *MARKER*	TOPS (m)				REMARKS/SHOWS
	MDRT	SUBSEA	THICK	TWT(ms)	
Port Campbell Limestone	126.4	101.4	272.6	127	No Returns 126.4 - 752 mMDRT
Gellibrand Marl			717.0		
Upper Gellibrand Marl	401.0	376.0	(430)	387	Calcareous claystone interbedded with minor sandstone and argillaceous calcilutite
Middle Miocene Seismic Marker	-	-	-	565	
Lower Gellibrand Marl *Base Miocene Seismic Marker*	831.0	806.0	(285.0)	735	Calcareous claystone interbedded with minor argillaceous calcilutite
Narrawaturk Marl	1116.0	1091.0	55.0	942	Calcilutite interbedded with calcareous claystone
Mepunga Formation	1171.0	1146.0	65.0	981	Sandstone with rare claystone interbeds
Dilwyn Formation	1236.0	1211.0	164.6	1025	Claystone with interbedded sandstone
Paaratte Formation	1400.6	1375.6	303.4	1134	Claystone and silty claystone with minor sandstone and argillaceous calcilutite interbeds
Belfast Formation	1704.0	1679.0	454.0	1324	Claystone with trace siltstone and sandstone stringers towards the base
Thylacine Member	2048.5	2023.5	(109.5)	1524	Interbedded sandstone, siltstone and claystone. **Gas shows.**
Flaxman Formation	2158.0	2133.0	115.1	1585	Interbedded sandstone, siltstone and claystone. **Gas shows.**
Waarre Formation			436.9+		
Upper Waarre Formation	2273.1	2248.1	(150.8)	1647	Interbedded fluvial sandstone, siltstone, claystone & minor coal. **Gas shows.**
Lower Waarre Formation	2423.9	2398.9	(189.1)	1727	Interbedded sandstone and claystone
Top coals	2652.0	2627.0		1843	
TOTAL DEPTH	2710.0	2685.0			

Formation Evaluation While Drilling:

Suite #	Run #	Interval (mMDRT)	Logs Acquired
1	1	1845.4 – 2709.5	DGR-ARC 5

Wireline Logs:

Suite #	Run #	Interval (mMDRT)	Logs Acquired
1	1	1835.7 – 116.8	Pex(HLRA)-DSI-HNGS
2	1	2715.5 – 1657.8	Pex(HLRA)-DSI-HNGS
2	2	2628.0 – 2049.0	MDT-GR
2	3	2230.0 – 2050.0	MSCT-GR
2	4	2503.0 – 2019.9	FMI-GR ***Refer to *Bal A.A (2002)* for full processing report**
2	5	2707.0 – 130.5	CSI (VSP/checkshot survey; Rig source zero offset)
2	6	2700.0 – 1865.0	CST-GR (60 SWC)

Cores:

Conventional:

Core #	Interval (mMDRT)	Cut (m)	Rec (m)	Formation
1	2165-2201	36	35.73 (99.73%)	Flaxman Formation

Sidewall:

Suite#	Run#	Type	Interval (mMDRT)	Bullets	Misfired	Empty	Lost	Recovered
2	3	Rotary (MSCT)	2050-2230	14	0	0	2	12
2	6	Percussion	1865-2700	60	1	2	5	52

Pressure Testing and Fluid Sampling:

Suite#	Run#	Type	Interval (mMDRT)	Total Tests	Valid Tests	Supercharged	Tight	Samples Collected
2	2	MDT	2049.0 – 2279.1	79	47	2	15	5

Hole & Casing Details:

Hole Size	Interval (mMDRT)	Casing Size	Shoe Setting Depth (mMDRT)
36"	126.4 – 182.2	30"/20"	181.0
17 ½ "	182.2 – 752.0	13 $^{3}/_{8}$ "	745.3
12 ¼ "	752.0 – 1855.0	9 $^{5}/_{8}$ "	1849.9
8 ½ "	1855.0 – 2710.0 (TD)	7"	2708.2

Suspension Plugs:

Suspension Plug #	Interval (mMDRT)
1	1610.0 – 1680.0
2	1245.0 – 1300.0

2. WELL SUMMARY

Thylacine 1 was drilled as a vertical exploration well designed to test a large horst structure within the Shipwreck Trough. The well is located in the offshore Otway Basin within petroleum exploration permit T/30P, approximately 240 km southwest of Melbourne, 70 km south of Port Campbell and 155 km southeast of Portland (Figure 1). Thylacine-1 was spudded on the 5th May 2001 in 101.4 m of water by the Semi-submersible 'Ocean Bounty'. It was drilled to a total depth of 2710 mMDRT.

The Thylacine structure is a composite horst developed at the southern end of a major N-NE trending ridge. It is fault-bounded to the south and northeast, forming a large, triangular-shaped horst that pitches to the west (Figure 2). The primary reservoir target was the Turonian Waarre Formation. However, the overlying Flaxman Formation also proved to be hydrocarbon bearing, with the gas column extending upwards into a new, previously unknown, younger Santonian reservoir unit herein named the Thylacine Member of the Belfast Formation. The well is interpreted to have encountered a 277.1 m gross gas column with a net gas-bearing sand pay of 139.5 m (N:G = 50.3%) with an average effective porosity of 16.4% and average effective water saturation of 49.4%. The top of the reservoir section coincides with a strong amplitude anomaly over the crest and in the western areas of the structure. A well-developed flat spot is also interpreted in the main horst.

Based on wireline log data and preliminary formation evaluation, Thylacine-1 was not tested. Instead, a 7" liner was run, and the well was plugged and suspended as a future gas producer. The rig was released on 28th May 2001.

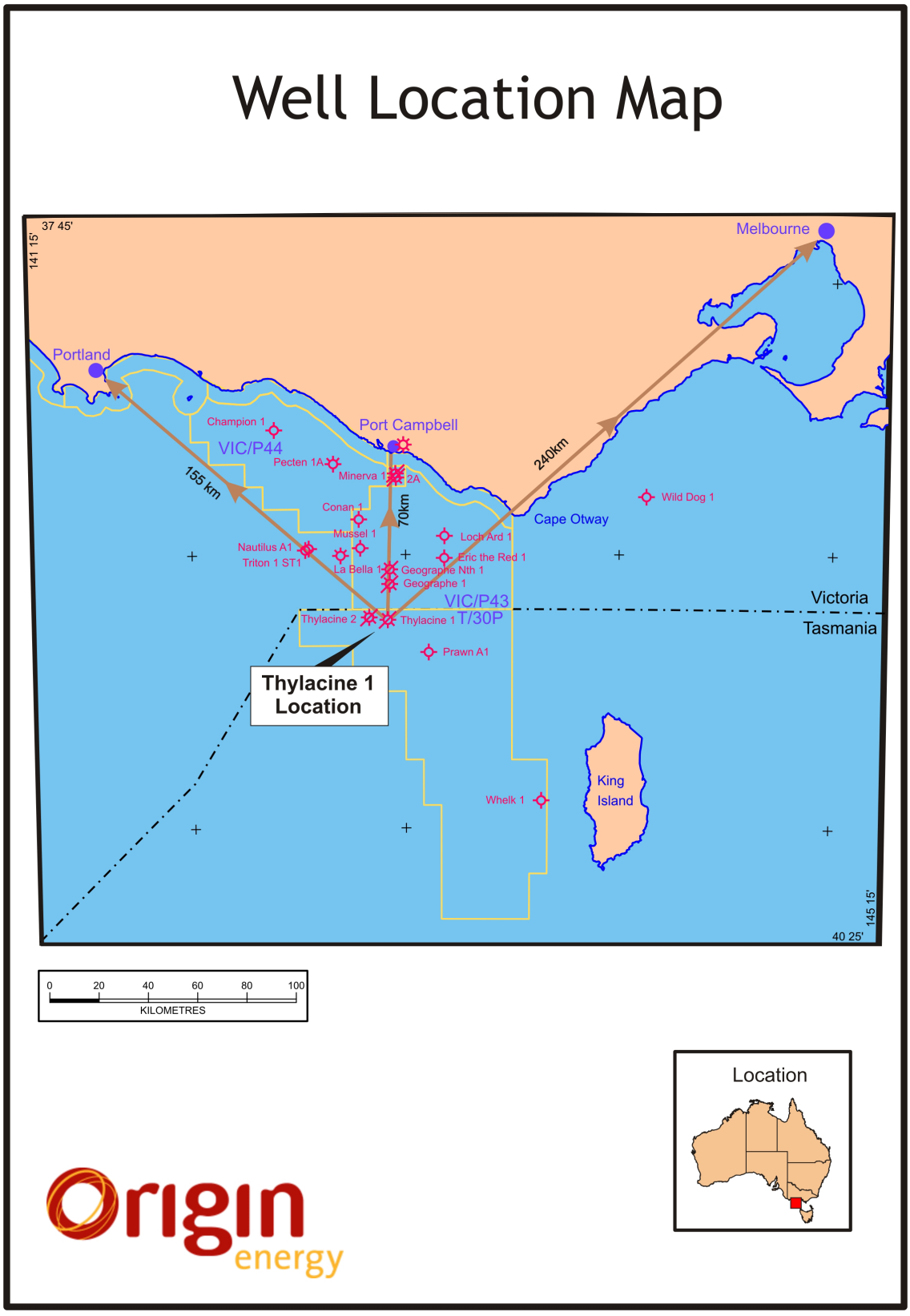

Figure 1. Thylacine-1 Location Map

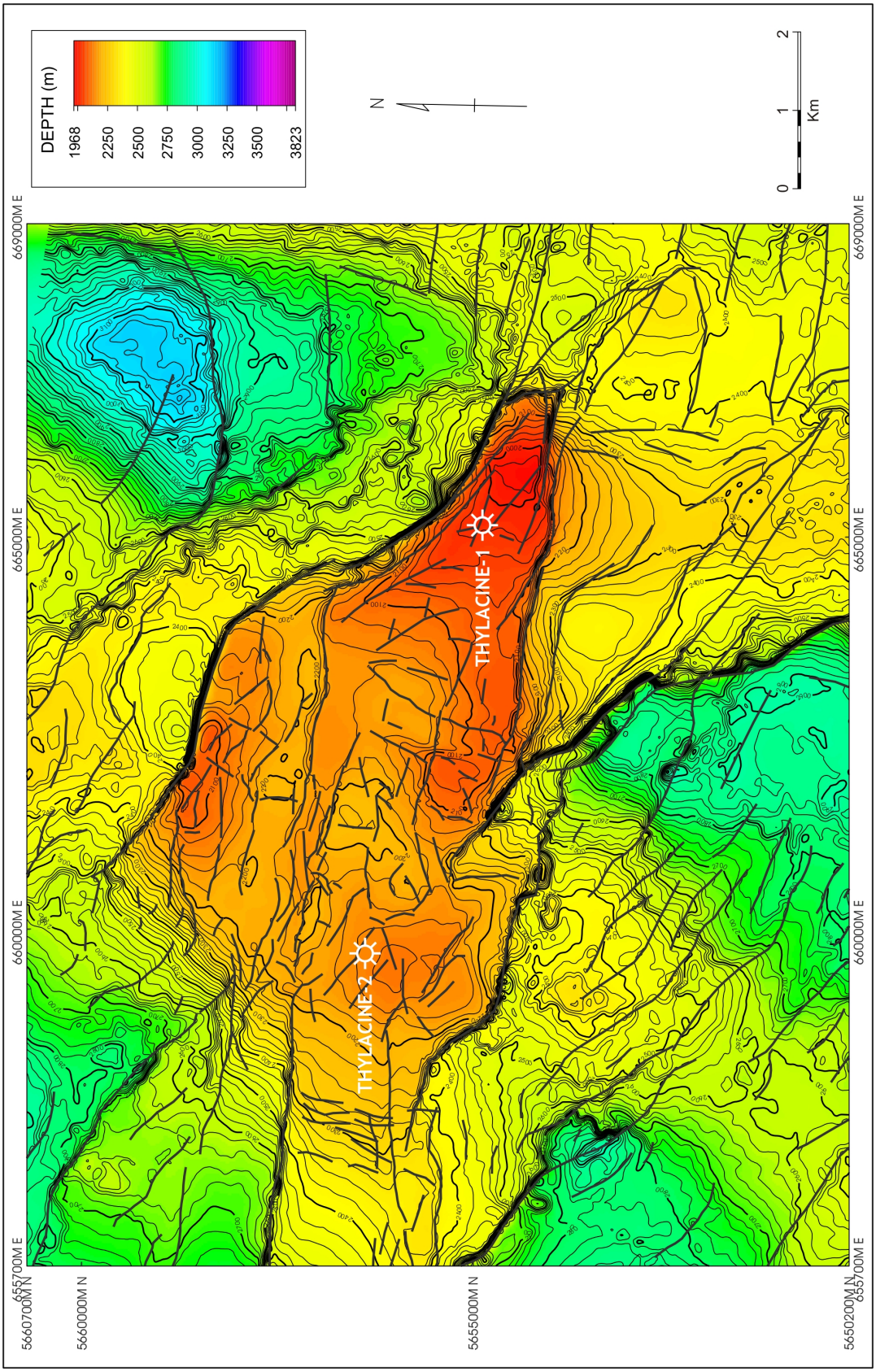

Figure 2. Top Porosity depth structure map over Thylacine Prospect

3. HYDROCARBONS

No fluorescence was observed in the Tertiary section in Thylacine 1. Background gas readings between 777 - 1483 mMDRT ranged from 0.01 - 0.05%, peaking at 0.96% near the top of the Mepunga Formation between 1180 –1250 mMDRT. The gas readings then started to gradually climb upon entering the Late Cretaceous Paaratte and Belfast formations, reaching 0.3% at the base of the Belfast. On penetrating the Thylacine Member (2048.5 – 2158.0 mMDRT), the gas readings increased dramatically to a maximum of 13.6% at 2050 mMDRT, and then fluctuated between 0.4 and 10.1% through the middle of the unit, before peaking again at 18.1% between 2129 – 2158 mMDRT near the base. The average reading for the entire unit was 5.5%. The average gas reading then dropped back to 2.5% (range: 0.7 – 9.6%) in the underlying Flaxman Formation (2158.0 – 2273.3 mMDRT), with peaks at 2163.0 m (9.6%), 2180 m (6.1%) and 2257.0 m (7.3%). In the Upper Waarre Formation, the average gas reading down to the GWC was 1.0% (range: 0.08 – 6.2%), with a peak (6.2%) near the top of the unit at 2304 mMDRT.

Direct fluorescence was observed at several levels in core from the upper sands of the Flaxman Formation (Core #1: 2165.0 – 2201.0 mMDRT). Between 2165.0 – 2184.0 m, trace dull yellow to off white fluorescence with nil to thin yellow white residual ring was noted, but this fluorescence was attributed to mud invasion as the glycol based mud filtrate shows similar fluorescence (DGR, 16/05/01). At 2185.0 m trace dull yellow pinpoint to patchy natural fluorescence with slow dull off white to pale yellow and thin dull off white to pale yellow residue was observed. The only other natural fluorescence noted was at a depth of 2188.0 m where trace to 5% pinpoint moderately bright yellow direct fluorescence with a slow dull off white to pale yellow cut fluorescence was observed.

Log analysis (Appendix 1) indicates a 275 m gas column was intersected in Thylacine-1 spanning (in descending stratigraphic order) the Thylacine Member (basal Belfast Formation), Flaxman Formation and Upper Waarre Formation. MDT data (Appendix 2) indicates the presence of a single gas column with a FWL between 2324 mMDRT and 2328 mMDRT, which straddles the log-derived GWC of 2325.6 mMDRT. Five gas samples were collected during the MDT run, one from the Thylacine Member (2053.8 mMDRT), two from the Flaxman Formation (2165.8 mMDRT and 2236.8 mMDRT), and two from the Upper Waarre Formation (2279.1 mMDRT and 2302.4 mMDRT). Analysis of two gas samples recovered from the Thylacine Member and Flaxman Formation revealed the two gases have almost identical compositions consisting of 82% methane, 9% CO_2, 8% wet gas and 1%

nitrogen (Appendix 3). The gas contains approximately 15 bbl/mmscf of LPG and 11 bbl/mmscf of condensate (C_{5+} basis). Isotope data indicate the CO_2 is diagenetic in origin and not volcanic-related.

4. STRATIGRAPHY

A generalised stratigraphy of the eastern offshore Otway Basin is illustrated in Figure 3 and the stratigraphic section intersected by Thylacine-1 is illustrated in Figure 4. As can be seen in Figure 4, the 'actual' stratigraphy differs from the 'prognosed' stratigraphy in a number of areas. These include: 1) the penetration of a previously unencountered Late Oligocene carbonaceous claystone at the top of the Mepunga Formation, 2) a new sandstone unit at the base of the Belfast Formation here termed the Thylacine Member, and 3) a thicker, sandier (and more complex) Flaxman Formation.

Reports by Dr Roger Morgan (Morgan Palaeo Associates), and Dr John Rexilius and Mr Scott Powell (International Stratigraphic Consultants Pty Ltd), on the age of the sediments penetrated in Thylacine 1 are included in Appendices 4 and 5 respectively. The detailed palynological sampling programme conducted during the drilling of Thylacine 1 (48 core, side wall core and cuttings samples) has, in co-ordination with the Geographe 1 and Thylacine 2 sampling programmes, allowed Dr Morgan to significantly refine the existing Late Cretaceous spore-pollen and dinoflagellate zonation schemes for the Otway Basin, thereby dramatically increasing its resolution. Consequently, it is now possible to correlate units between wells in the Shipwreck Trough far more accurately than before.

Lithological descriptions from ditch cuttings, sidewall core and conventional core, together with the MWD / wireline log interpretation, provide the basis for the stratigraphic breakdown in Enclosure 1.

HEYTESBURY GROUP

Port Campbell Limestone (126.4 – 401.0 mMDRT)

The Port Campbell Limestone in Thylacine 1 is approximately 272 m thick. Its presence is inferred from seismic ties to nearby wells such as La Bella 1, Mussel-1 and Conan 1 as first returns were not established until 752 mMDRT. Onshore, to the north in the Port Campbell area, the Port Campbell Limestone is a light grey to white, medium-hard, poorly sorted, shallow marine calcarenite with abundant fossils (corals, bryozoans, foraminifera) and up to 3% glauconite. Micropalaeontological data indicates it is Miocene in age onshore (Tickell et al., 1992).

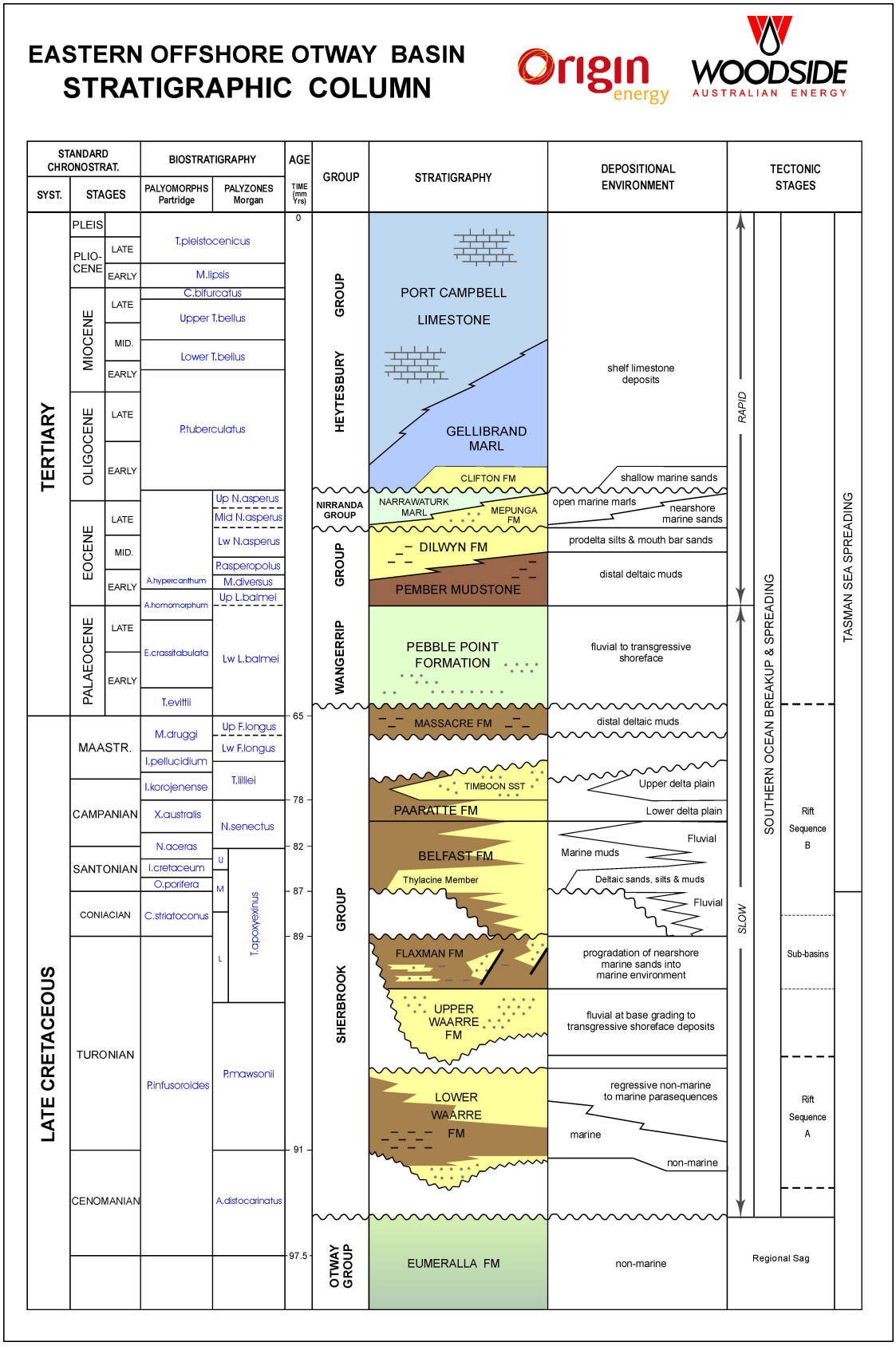

Figure 3. Offshore Otway Stratigraphic Section

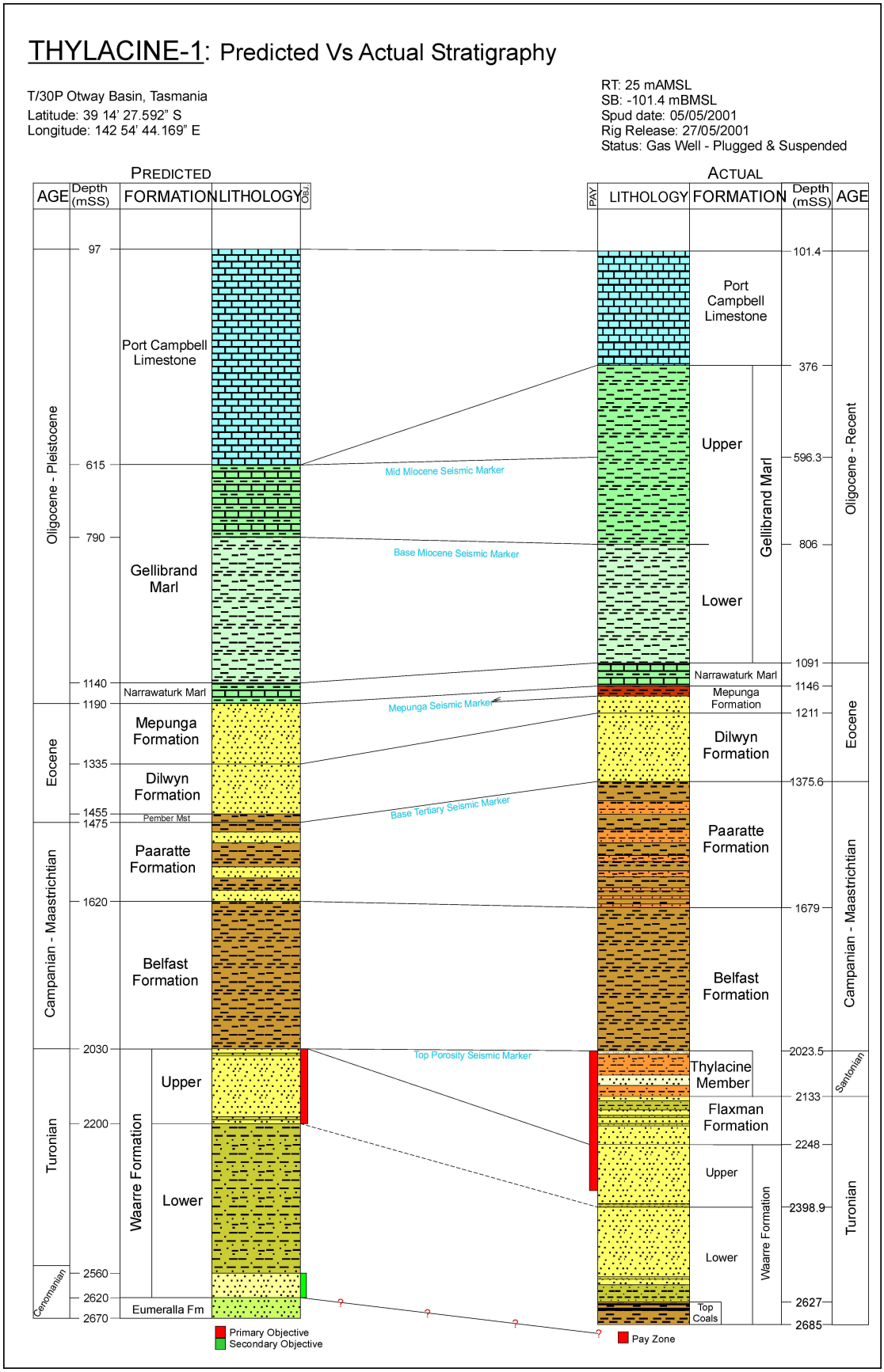

Figure4. Predicted versus Actual Stratigraphy

Gellibrand Marl (401.0 – 1116.0 mMDRT)

The Gellibrand Marl is a shallow marine calcareous mudstone that gradationally underlies the Port Campbell Limestone onshore in the Port Campbell area (Tickell et al., 1992). In the Shipwreck Trough, the Gellibrand Marl can be seismically divided into two units separated by a prominent seismic marker called the 'Base Miocene Seismic Marker'. The two units are here called the Upper Gellibrand Marl and Lower Gellibrand Marl. Both units are present in Thylacine 1 where they have a combined thickness of 717.0 m.

Upper Gellibrand Marl (401.0 – 831.0 mMDRT)

The Upper Gellibrand Marl in Thylacine 1 is 430 m thick. Prior to drilling, the top of the Gellibrand Marl in the Shipwreck Trough was correlated with a prominent seismic marker called the 'Mid Miocene Seismic Marker'. This event is an unconformity surface with local canyon development that is mappable across the entire Shipwreck Trough area. In this report, the top of the Gellibrand Marl was picked based on a significant drop in ROP at 401 mMDRT, as it is difficult to pick a contact on the casing-corrected GR log (the only log that extends above the casing shoe) and first returns were not established until 752 mMDRT. The 'Mid Miocene Seismic Marker' occurs approximately 220 m stratigraphically below the top Upper Gellibrand Marl pick.

Returns from the base of the Upper Gellibrand Marl indicate calcareous mudstone is the dominant lithology with minor interbedded limestone, sandstone, claystone and calcilutite. The mudstone is light grey in colour, soft, fossiliferous, pyritic and carbonaceous. Micropalaeontological data (Appendix 5) indicate the base of the Upper Gellibrand Marl in Thylacine 1 is early Early Miocene in age.

Lower Gellibrand Marl / Base Miocene Seismic Marker (831.0 – 1116.0 mMDRT)

The 'Base Miocene' seismic event defines the top of the Lower Gellibrand Marl. This event is another unconformity surface with local canyon development that is mappable across the entire Shipwreck Trough area.

The Lower Gellibrand Marl in Thylacine 1 is 285 m thick and composed almost entirely of calcareous claystone. The claystone is light grey to olive grey in colour, soft, amorphous, sub-blocky – blocky, silty in parts, and contains trace crystalline calcite, carbonaceous matter, glauconite, pyrite nodules and fossil fragments.

Micropalaeontological data (Appendix 5) indicate it is mid – late Early Oligocene to mid – late Late Oligocene in age.

NIRRANDA GROUP

Narrawaturk Marl (1116.0 – 1171.0 mMDRT)

The Narrawaturk Marl in Thylacine 1 is represented by 55 m of interbedded calcilutite, limestone and minor sandstone. The calcilutite is light grey in colour, soft to firm, with trace pyrite, glauconite and fossil fragments. The age of the Narrawaturk Marl in Thylacine 1 is not known as the unit was not sampled, but it is probably Middle Eocene to mid – late Early Oligocene based on the age of the underlying Mepunga Formation and overlying Lower Gellibrand Marl.

Mepunga Formation (1171.0 – 1236.0 mMDRT)

The Mepunga Formation in Thylacine 1 is a 164.6 m thick sequence of sandstone and minor claystone. The sandstone is clear to pale yellow in colour, medium- to very coarse-grained, poorly sorted, and predominately loose with minor aggregates cemented by pyrite and dolomite. Visual porosity is described as poor to fair. The claystone interbeds are predominately dark brown to olive brown-green in colour, soft to firm, dispersive, with trace glauconite and pyrite. The top of the formation is characterised by the presence of an 11 m thick claystone not previously encountered in the offshore Otway Basin. The claystone is greyish brown to dusky brown – dusky yellowish brown in colour, soft, sub-blocky to blocky, slightly calcareous, with trace glauconite, pyrite and crystalline calcite.

Palynological data (Appendix 4) indicates the Mepunga Formation in Thylacine 1 is early to middle Eocene age based on the presence of *P.asperopolus* Zone spore-pollen at the base of the unit and *D.heterophylcta* Zone dinoflagellate in the claystone at the top. The sediments are interpreted to have had be deposited in a nearshore to inner shelf environment based on the percentage of dinoflagellate present in the formation and their diversity.

WANGERRIP GROUP

Dilwyn Formation (1236.0 – 1400.5 mMDRT)

The Dilwyn Formation in Thylacine-1 is a 164.6 m thick sequence of sandstone that underlies the Mepunga Formation. The sandstone is greyish brown to light grey in colour, medium- to coarse-grained, quartzose, sub-rounded, and is moderately to well sorted. It has trace to common iron staining and has good to very good visual porosity. Palynological dating (Appendix 4) indicates the formation is Early Eocene in age in Thylacine 1 based on the presence of *K.thompsoniae – W.ornatum* Zone dinoflagellate near the base of the unit and *P.asperopolus* Zone spore-pollen towards the top. The low percentage of dinoflagellate in the unit suggests the sediments probably accumulated in a nearshore to very nearshore marine environment

SHERBROOK GROUP

Paaratte Formation (1400.6 – 1704.0 mMDRT)

The Paaratte Formation in Thylacine 1 is represented by a 303.4 m thick sequence of claystone with occasional bands of calcilutite at the top of the formation and rare sandstone beds dispersed throughout. The claystone is typically dark to greenish grey and brownish grey in colour, soft, dispersive, and contains glauconite and pyrite. The interbedded sandstones are typically quartzose, light grey in colour, and very fine- to medium-grained with scattered coarse grains.

Palynological data (Appendix 4) indicate the Paaratte Formation in Thylacine 1 spans the *X.australis* (lower d) to *M.druggi* (upper) dinoflagellate zones, and *N.senectus* (upper) - *F.longus* spore-pollen zones, and is early Campanian to Maastrichtian in age. The sediments are interpreted as having had been deposited in a predominantly nearshore marine environment based on the low percentage of dinoflagellate present and their low diversity.

Belfast Formation (1704.0 – 2048.5 mMDRT)

The Belfast Formation in Thylacine 1 is represented by a monotonous, 344.5 m thick sequence of light to dark grey, non-calcareous claystone and minor siltstone. Palynological data (Appendix 4) indicates the Belfast Formation in Thylacine 1 spans the *upper O.porifera – lower X.australis* dinoflagellate zones and *T.apoxyexinus – N.senectus* spore-

pollen zones, and is Santonian to early Campanian in age. The formation is undifferentiated except for a sequence of interbedded sandstone – claystone at the base of the formation called here the Thylacine Member (see below). A shelfal marine environment of deposition is inferred for the shales at the base of the formation based on the co-dominant moderately diverse dinoflagellate and highly diverse spore – pollen assemblages recovered. Further up-section, dinoflagellate are less common and less diverse, suggesting the shales in the upper part of the formation were probably deposited in a shallower nearshore environment.

Thylacine Member (2048.5 – 2158.0 mMDRT)

The Thylacine Member is a 109.5 m thick sequence of interbedded sandstone, siltstone and minor claystone consisting of several coarsening-up cycles. The sandstones are light grey to white in colour, fine to medium-grained, predominantly well sorted, sublitharenites and litharenites (Appendix 6). The claystones at the base of the cycles are medium to dark grey, soft to firm with trace glauconite, pyrite and carbonaceous material. Palynological data (Appendix 4) indicates the Thylacine Member in Thylacine 1 spans the *upper O.porifera –I.cretaceum lower 'a'* dinoflagellate zones and *T.apoxyexinus* spore-pollen zone, and is Santonian in age. A nearshore marine environment of deposition is inferred for the sediments based on the predominance of spore - pollen over dinoflagellate and their high diversity.

Flaxman Formation (2158.0 – 2273.1 mMDRT)

The Flaxman Formation in Thylacine 1 is an 115 m thick sequence of interbedded sandstone, siltstone and claystone, with individual sandstone beds up to 10 m thick. The sandstones are light grey to white, poorly to well sorted, fine to coarse-grained litharenites and quartzarenites. Palynological dating (Appendix 4) indicates the Flaxman Formation in Thylacine 1 spans the *P.infusorioides upper 'a'* – *P.infusorioides upper 'c'* dinoflagellate zones and *P.mawsonii* spore-pollen zone, and is Turonian in age. Environments of deposition range from marine near the base of the unit, to very nearshore / marginal marine toward the top.

A detailed lithological and palaeoenvironmental interpretation of the core recovered from the Flaxman Formation can be found in Appendices 7 (SEDSTRAT Pty Ltd) and 8 (Core Laboratories Australia) respectively.

Waarre Formation (2273.1 – 2710.0 mMDRT [TD])

The Waarre Formation in the Shipwreck Trough can informally divided into two units based largely on environment of deposition. The two units are called (in ascending stratigraphic order) the Lower Waarre and Upper Waarre, and are separated by a major sequence boundary located within the mid *P.infusoroides* dinoflagellate Zone. The Lower Waarre is interpreted as a largely regressive unit ranging from marine at the base to non-marine near the top, whereas the Upper Waarre is interpreted as a transgressive unit grading from fluvial at the base to shoreface toward the top. The two units have similar high net : gross values, but the Upper Waarre sand bodies are generally thicker and have a distinctive blocky profile on the GR log. Both units were intersected in Thylacine 1 where they have a combined thickness of 436.9 m.

Upper Waarre Formation (2273.1 – 2423.9 mMDRT)

The Upper Waarre Formation in Thylacine 1 is represented by a 150.9 m thick interval of interbedded sandstone, siltstone and minor claystone with a N:G of 66.9%. The sandstones, which are up to 15 m thick, are moderate to moderately-well sorted, fine to coarse grained, quartz–rich (Appendix 6).

Palynological dating (Appendix 4) indicates the Upper Waarre in Thylacine 1 spans the *P.infusorioides middle 'c'* to *upper 'a'* dinoflagellate zones and *P.mawsonii* spore-pollen zone, and is Turonian in age. Environments of deposition range from nonmarine at the base to marginal marine or very nearshore in the middle and upper parts of the unit.

Lower Waarre Formation (2423.9 – 2710.0 mMDRT [TD])

The Lower Waarre Formation in Thylacine 1 is represented by more than 286 metres (base not intersected) of interbedded sandstone, siltstone, claystone and minor coal. It differs from the Upper Waarre in that it contains more siltstone and less sandstone and claystone. Consequently, its N:G (33.1%) is significantly lower than the Upper Waarre and its GR log response has a distinctive spikey character. The Lower Waarre sandstones are also moderate to moderately-well sorted, fine to coarse grained, and quartz–rich like the Upper Waarre sandstones (Appendix 6).

Palynological dating (Appendix 4) indicates the Lower Waarre Formation in Thylacine 1 spans the *P.infusorioides lower 'd'* to *middle 'b'* dinoflagellate zones and *P.mawsonii* spore-pollen zone, and is Cenomanian to early Turonian in age. The

sediments at the top of the Lower Waarre between 2449.0 mMDRT and 2501.5 mMDRT are interpreted to have had been deposited in a marginal marine environment based on the extremely rare low diversity dinoflagellate assemblage and abundant and diverse spore – pollen assemblage. At 2425.7 m, a non-marine environment is indicated by the total absence of saline markers, and minor freshwater algae suggest fluvial rather than lacustrine sediments. Between 2571.0 mMDRT and 2636.2 mMDRT, the Lower Waarre appears to have been deposited in a non-marine to marginal marine environment shifting to very nearshore marine near the base at 2667.5 mMDRT.

'Top Coals' (2652 - 2710.0 mMDRT [TD])

The 'Top Coals' horizon is a prominent seismic marker that is interpreted to coincide with the top of a 20 m thick interval of four to five thin (< 1 m thick) coal seams near the base of the Lower Waarre Formation in Thylacine 1. The coals are black to very dark brown in colour, dull, moderately hard, subblocky to angular, with 10% argillaceous material.

5. PETROPHYSICAL AND CORE SUMMARY

5.1 Petrophysical Summary

A petrophysical review was conducted to assess the reservoir quality and hydrocarbon saturation of the Late Cretaceous sediments intersected whilst drilling Thylacine-1. The study entailed an analysis of all available lithological data, and a complete petrophysical analysis. Results are summarised in Table 1.

The Thylacine Member (2048.5 - 2158.0 mMDRT) encountered at Thylacine-1 is interpreted to have moderate reservoir quality. The sandstones that are present contain high clay volumes, averaging 26.4%. Calculated effective porosities average only 15.5% for these reservoirs. As a result, the log-derived gas permeability is considerably reduced in comparison to other cleaner reservoirs, averaging only 8.6mD, which will negatively affect this unit's producibility and recovery factor. The average effective water saturation is 52.5%, and the net reservoir to gross is 43%.

The Flaxman Formation (2158.0 - 2273.3 mMDRT) appears to have better reservoir development. The sandstones present, on average, are cleaner than those above and have an average clay volume of 16.9%. The average effective porosity is higher (16.7%), and the gas permeability is significantly higher, averaging 20.8mD. This unit has a net reservoir to gross of 43%, and an average effective water saturation of 47%.

The interval between the top of the Upper Waarre Formation and the interpreted GWC (2273.3 - 2325.6 mMDRT) has the best average reservoir parameters. The average clay volume in this unit was only 14.6%, whilst the average effective porosity was similar to that for the Flaxman Formation (17.0%). This unit is interpreted to have an 80% net reservoir to gross ratio, average effective water saturation of 16%, and very good gas permeabilities, averaging 27mD.

Between the four wells now present on the Thylacine and Geographe fields, sufficient core analysis data are present to calibrate the log responses, and no more core analysis is considered necessary.

The spectral gamma ray data are in agreement with the petrological analysis, in that the dominant clay mineral is kaolinite. These spectral gamma ray data also imply that the clay type present in the sandstones is of the same chemistry to those present in the shales. Therefore, little value is being added by this log, and it is recommended that acquisition of the spectral gamma ray tool is not necessary in future wells.

The LWD data acquired by Anadrill were not utilised in the interpretation of fluid saturations, as they are responding with lower values than those measured using the wireline devices, presumably due to the highly porous and permeable nature of these reservoirs encouraging the deep invasion of mud filtrate. It is not recommended that LWD be acquired in future wells for the purposes of petrophysical evaluation.

See Appendix 1 for detailed petrophysical information.

5.2 Core Analysis Summary

See Appendix 9 for Special Core Analysis Report.

Table 1. Thylacine 1 reservoir summary

FORMATION	INTERVAL				AVERAGE							NET /GROSS %
	FROM (mMDRT)	TO (mMDRT)	GROSS (m)	NET PAY (m)	VCL %	PHIT (%)	PHIE (%)	AIR PERM (mD)	GAS PERM (mD)	WATER PERM (mD)	SW (%)	
Thylacine Member	2048.50	2158.00	109.50	47.50	26.42	20.51	15.46	10.89	8.61	3.17	52.50	43.38
Flaxman Formation	2158.00	2273.30	115.30	50.07	16.91	19.92	16.70	25.90	20.82	7.74	46.73	43.43
Upper Waarre Fm-GWC	2273.30	2325.60	52.30	41.94	14.58	19.58	16.95	33.62	27.16	10.13	49.06	80.19
		TOTAL	**277.10**	**139.51**	**19.45**	**20.02**	**16.35**	**20.86**	**16.69**	**6.19**	**49.39**	**50.35**
Upper Waarre Formation	2273.30	2424.20	150.90	101.40	17.79	19.15	16.01	8.90	7.01	2.58	77.16	67.20
Lower Waarre Formation	2424.20	2684.00	259.80	88.73	24.73	17.81	13.65	2.22	1.70	0.62	95.54	34.15

Cut-offs Applied		
Net Pay	K_gas >	0.1mD
	VCl <	40.0%

6. GEOPHYSICAL DISCUSSION

6.1 Seismic Data

The Investigator 3D seismic survey, acquired in 2000, covers an area of 986.4 km^2 across permits VIC/P43 and T/30P in the central Shipwreck Trough (Figure 5). It included coverage of the Thylacine Structure, providing excellent structural definition as well as significant stratigraphic detail of the feature (Figure 6).

Seismic data quality over the Thylacine Structure is generally very good. Excellent control on the spatial distribution of high density faulting was achieved, and the top of the intra-Santonian reservoir objective was readily discernible over the prospect. The event is a trough (hard kick, negative amplitude, red on colour displays) on the seismic data, except within closure at Thylacine where a phase reversal occurs, consistent with a gas accumulation. High quality Variance Cube™ time slices and amplitude images extracted from the 3D seismic data were also an essential part of the prospectivity assessment.

Miocene canyoning slightly degrades the seismic quality over the eastern part of the structure, and may be responsible for a minor amount of velocity "pull-up", but this will need to be confirmed through detailed velocity analysis. Data quality deteriorates to the northeast of the Thylacine Structure, due to high density faulting. Overall the 3D data is of a high standard, which helped to lower the pre-drill exploration risks.

6.2 Structure

The Thylacine Structure is a composite horst located close to the axis of the Shipwreck Trough. It is fault-bounded to the south and north-east, forming a large, triangular shaped horst that pitches to the west (Figure 7). The core of the structure is interpreted to be underlain by a relatively rigid basement block that has undergone less subsidence than surrounding areas. The fault mapping was assisted by excellent imaging of the Variance Cube™ time slices (Figure 8).

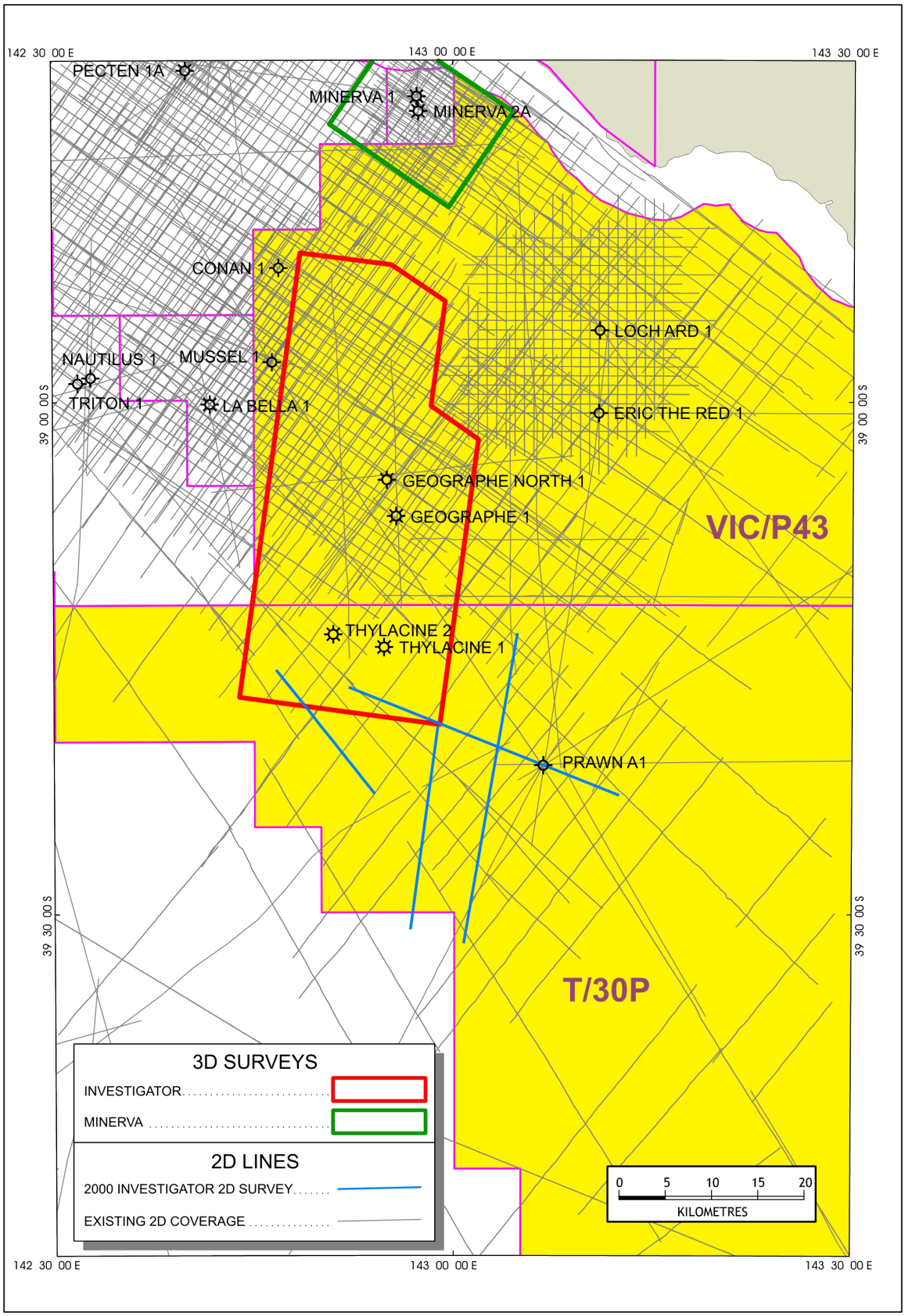

Figure 5. Investigator 3D and 2D Seismic Survey location map

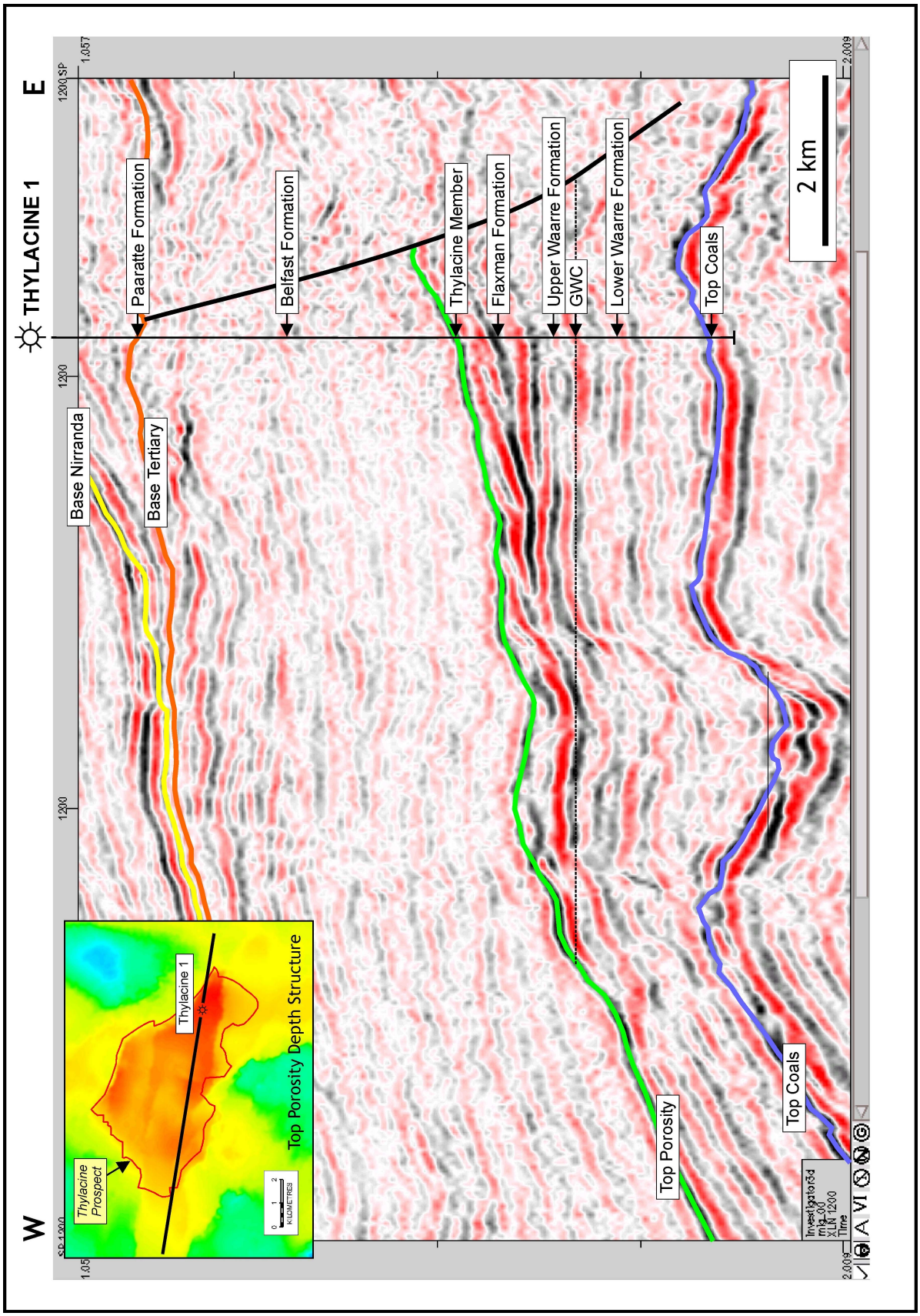

Figure 6. 3D xline 1200 through Thylacine-1

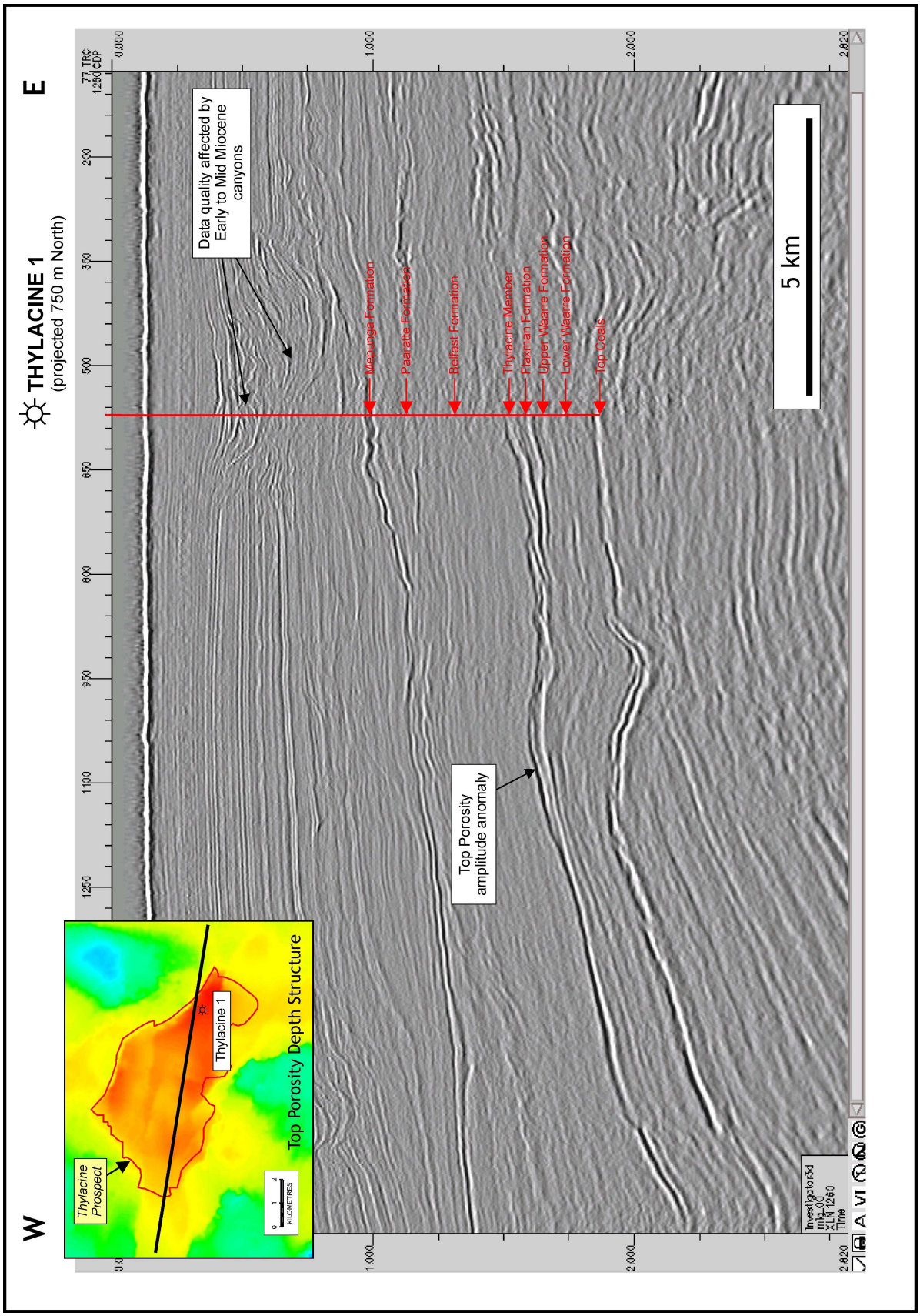

Figure 7. 3D xline 1260 through Thylacine Prospect

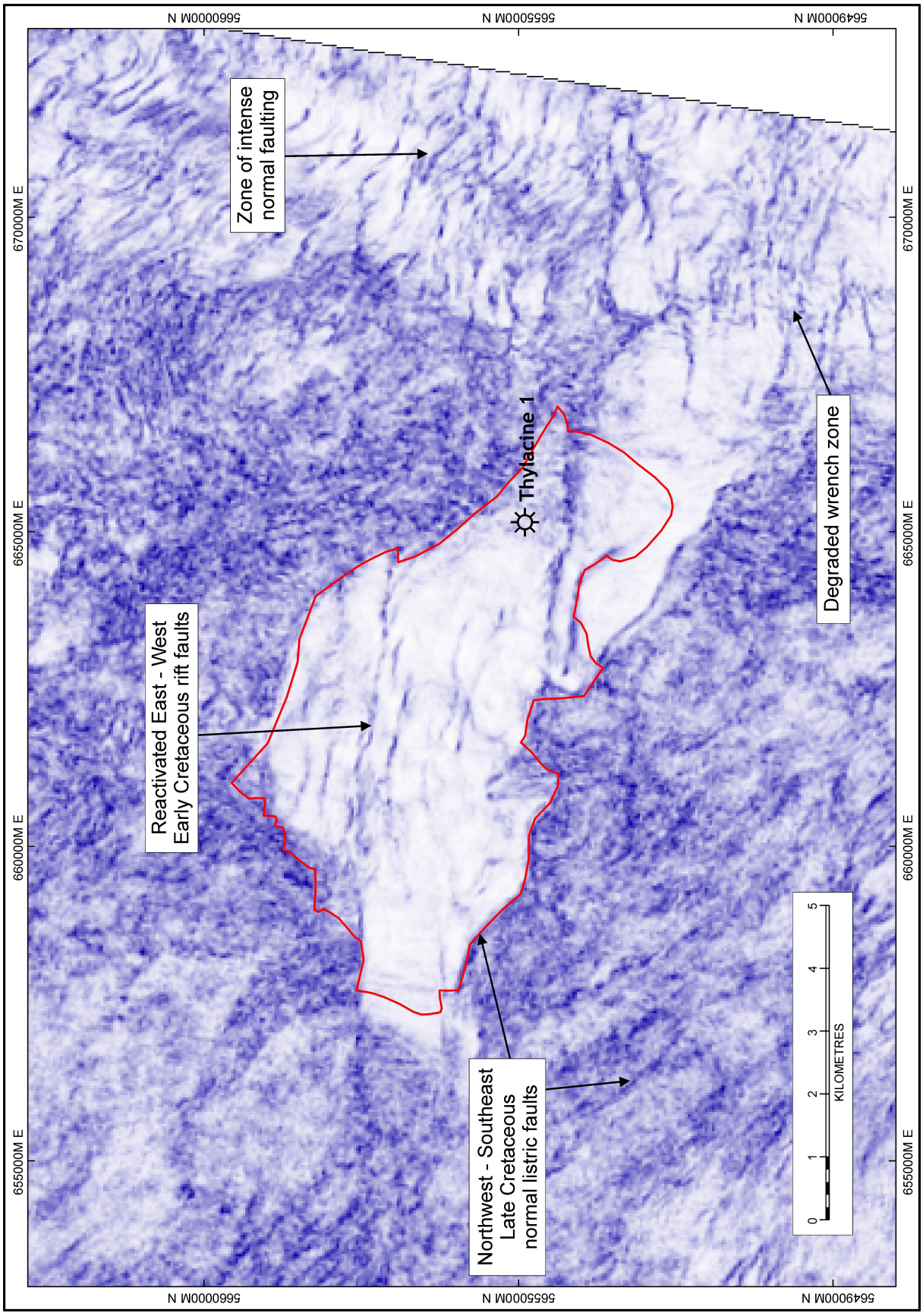

Figure 8. Variance Cube Time Slice (1512 ms TWT) through Thylacine Prospect

The Thylacine Structure is interpreted to have developed in response to repeated episodes of rifting during the break-up of Australia and Antarctica in the Late Jurassic to Late Cretaceous. The primary extension direction varied from N-S to NE-SW, resulting in normal faults orientated E-W to NW-SE. Evidence from elsewhere in the basin suggests that the E-W faults are likely to be the oldest and are associated with the earliest phases of rifting in the Late Jurassic/Early Cretaceous. They tend to be steep and probably extend well into basement. The Late Cretaceous faulting episode is dominated by ENE to NE trending normal faults, that are less steep. Many of the Early Cretaceous faults were also reactivated during this Late Cretaceous faulting episode. The most recent faulting in the Tertiary section is mainly orientated NNE-SSW.

The eastern end of the Thylacine structure is controlled by the N-S striking Sorrell transfer zone which marks the eastern limit of west to east rifting that separated Australia and Antarctica. Fault orientations change abruptly along this zone due to the long history of repeated strike-slip movement. The Sorell Transfer Zone is also the primary control on the Shipwreck Trough, which developed in response to the trans-tensional movement.

Thylacine is bounded to the south by a large E-W normal fault and to the north by a large NW-SE fault. The primary faults defining the horst penetrate up to the base of the Tertiary, indicating significant growth of the structure during deposition of the Belfast Formation.

The structure contains three main sub-culminations. Thylacine-1 tested the overall crest, at the eastern end of the structure, where the main faults intersect at an acute angle. Based on the seismic mapping, ultimate structural closure of the top porosity horizon is defined by a spill-point across the northeast bounding fault. This point is approximately coincident with the gas-water contact (GWC) in Thylacine 1 at a depth of 2298 mSS (2323 mMDRT). Seismic amplitudes indicate that the field may also extend into a folded, downthrown block, juxtaposed against the southern side of the main horst. This block is partly encompassed by the overall closure.

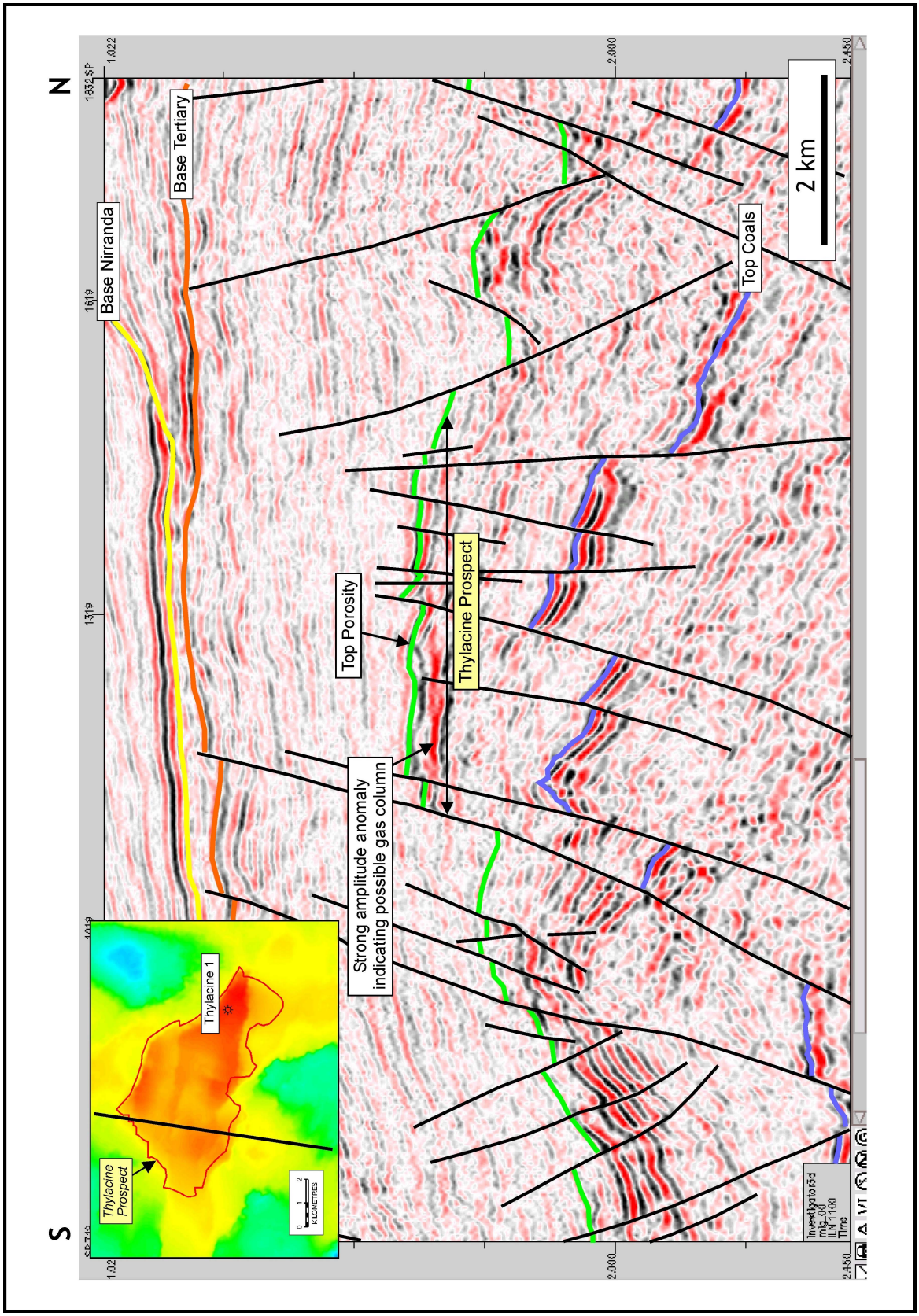

Figure 9. 3D Inline 1100 showing Top Porosity seismic amplitude anomaly over Thylacine Prospect

6.3 Seismic Amplitudes

Seismic amplitudes in both the full and far stack volumes were an essential part of the prospectivity assessment. At the top porosity horizon there is a distinct amplitude anomaly over the Thylacine structure (Figure 9). The anomaly closely correlates to the time closure, thereby supporting the conclusion that the structure is gas charged. This helped to reduce the pre-drill risk.

Also supporting gas charge into the structure were several discontinuous flat reflections at approximately the level of the structural spill-point. They were not all at precisely at the same level in two-way-time (TWT), and hence it was difficult to be certain whether they represented a single GWC, multiple contacts, or no contact at all. Lateral velocity changes and interference by reflections from stratigraphic boundaries can result in GWCs that are not flat in time sections. Despite the ambiguity in their interpretation, the flat spots were considered most likely to be indicative of a GWC, and hence a contact was predicted in Thylacine 1. However, the actual GWC came in 60.6 m deeper than expected (see below).

6.4 Actual versus Predicted depths

The depth conversion of the time structure maps, on which the predicted depths for the well were based, was done by calibrating seismic stacking velocities to nearby well control. The main method of depth conversion used was an interval velocity approach that was applied to each of the following horizons: a) Water bottom, b) Mid Miocene Event, c) Top Mepunga Horizon, d) Base Tertiary and e) Top Porosity. As a crosscheck, an average velocity approach was used to depth convert the Top Porosity horizon. Both methods gave similar results. The final predicted depths, for intermediate horizons were based on two-way-time picks and interval velocities derived from checkshot data in La Bella 1. All final predicted depths together with the actual depths are shown in Table 2.

The uncertainty in the depth prognosis was estimated at +/- 50 m based on the range of T-D curves from nearby wells. All tops down to the Top Porosity were within error except the Upper Gellibrand Marl, Dilwyn Formation and Paaratte Formation which were 239 m, 124 m and 99.4 m high to prognosis respectively. The higher than expected picks for these units is largely due to the lack of well control in this part of the basin and difficulty in picking some events on seismic, in particular the Base Tertiary. The Top Porosity pick, in

comparison, was only 7 m high to prognosis. However, the Waarre Formation, which was thought to represent top porosity, came in 105 m low, due to the unexpectedly thick overlying section of Flaxman Formation and lower Belfast sands (Thylacine Member) that formed the upper part of the gas reservoir. The GWC prediction came in 60.6 m low. This large depth error is thought to be due to the lack of precision with which the flat-spot event can be picked off the seismic, and not a significant error in the velocity estimation itself.

A time depth curve based on the check-shot survey for Thylacine 1 shows that the velocity trend is similar to nearby wells (Figure 10). Details of the velocity survey and VSP can be found in the Thylacine-1 Basic Data Report.

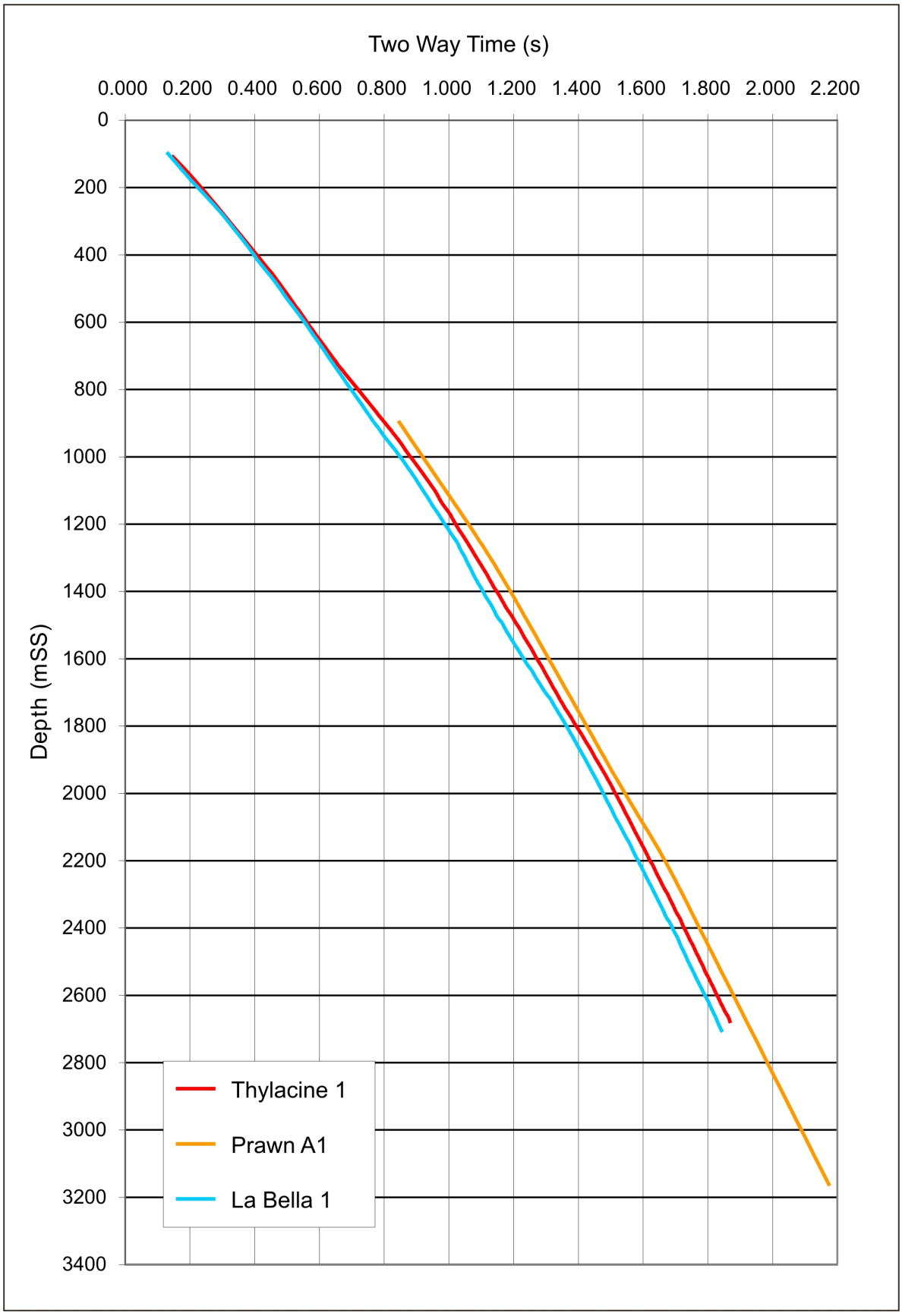

Figure 10. Thylacine-1 Time-Depth curve

Table 2. Predicted vs Actual Formation Tops

Thylacine 1 (Inline 700 CDP 1200)
RT = 25 m ASL
Water Depth = 101.4 m

	Formation / *Seismic Marker*	Two-way time (ms)	Predicted Depth (mKB)	Actual Depth (mKB)	Actual Depth (mSS)	Thickness (m)	High/Low (-ve = high)
TERTIARY	*Seabed* / Port Campbell Lst	127	122.0	126.4	101.4	274.6	4.4
	Upper Gellibrand Marl	565	640.0	401.0	376.0	430.0	-239.0
	*Mid Miocene Seismic Marker**	565	640.0	621.3	596.3	-	-18.7
	Lower Gellibrand Marl / *Base Miocene Seismic Marker*	700	815.0	831.0	806.0	285.0	16.0
	Narrawaturk Marl	964	1165.0	1116.0	1091.0	55.0	-49.0
	Mepunga Formation	994	1215.0	1171.0	1146.0	65.0	-44.0
	Dilwyn Formation	1078	1360.0	1236.0	1211.0	164.6	-124.0
	Pember Mudstone	Not Picked	1480.0	Not Intersected	Not Intersected	Not Intersected	Not Intersected
CRETACEOUS	Paaratte Formation / *Base Tertiary*	1161	1500.0	1400.6	1375.6	303.4	-99.4
	Belfast Formation	1256	1645.0	1704.0	1679.0	454.0	59.0
	Thylacine Member	Not Prognosed		2048.5	2023.5	(109.5)	-
	Flaxman Formation	Not Prognosed		2158.0	2133.0	115.1	-
	Upper Waarre Formation	1521	2055.0	2273.1	2248.1	150.8	218.1
	Lower Waarre Formation	1615	2225.0	2423.9	2398.9	189.1+	198.9
	GWC	1650	2265.0	2325.6	2300.6	-	60.6
	Top Coals	Not Prognosed		2652.0	2627.0	-	-
	Top Eumeralla Formation	1829	2645.0	Not Intersected	Not Intersected	Not Intersected	Not Intersected
	TD		**2695.0**	**2710.0**	**2685.0**	-	15.0

7. GEOLOGICAL DISCUSSION

7.1 Previous Exploration

The drilling history in the eastern offshore Otway Basin is summarized in Table 3. Only two wells had been drilled in the area encompassed by T/30P prior to Thylacine 1: Prawn A1 (1967) and Whelk-1 (1970). Both wells were drilled by Esso, but no hydrocarbon shows were recorded.

Well	Year	Operator	TD (m)	Status	Result
Pecten 1A	1967	Shell	2850	P&A	Gas show, 145 mcf from 17 m of tight Waarre
Prawn A1	1967	Esso	3193	P&A	No valid closure, good reservoir, poor seal
Nautilus 1A	1968	Esso	2011	P&A	Tertiary wedge play, no reservoir found
Mussel 1	1969	Esso	2450	P&A	Not drilled in crestal location
Whelk 1	1970	Esso	1466	P&A	No seal
Triton 1	1982	Esso	3545	P&A	Poor reservoir, no closure mapped to date
La Bella 1	1993	BHP	2710	GAS	Estimated 210 bcf OGIP
Minerva 1	1993	BHP	2425	GAS	Estimated 575 bcf OGIP
Eric the Red 1	1993	BHP	1875	P&A	No cross fault seal
Minerva 2A	1993	BHP	2170	GAS	Thick Waarre sand development
Loch Ard 1	1993	BHP	1397	P&A	No Top Seal for Waarre reservoir
Conan 1	1995	BHP	2175	P&A	Ineffective fault seal
Champion 1	1995	BHP	1882	P&A	Upper Waarre absent, no cross fault seal

Table 3: Drilling history in the eastern offshore Otway Basin.

In early 2000, the Joint Venture partners for T/30P acquired a 250 sq. km 3D seismic survey over the Thylacine prospect. Thylacine-1 was the first well to be drilled based on the interpretation of these seismic data.

7.2 Regional Geology

The Otway Basin formed in response to rifting between Australia and Antarctica during the Late Jurassic - Late Cretaceous. The basin has a two-stage rift history, with the first stage spanning the Late Jurassic and Early Cretaceous, followed by the second in the Late Cretaceous. The second event was responsible for the formation of the Shipwreck Trough,

which is where are the known gas discoveries to date in the offshore eastern Otway Basin are located (see Figure 11).

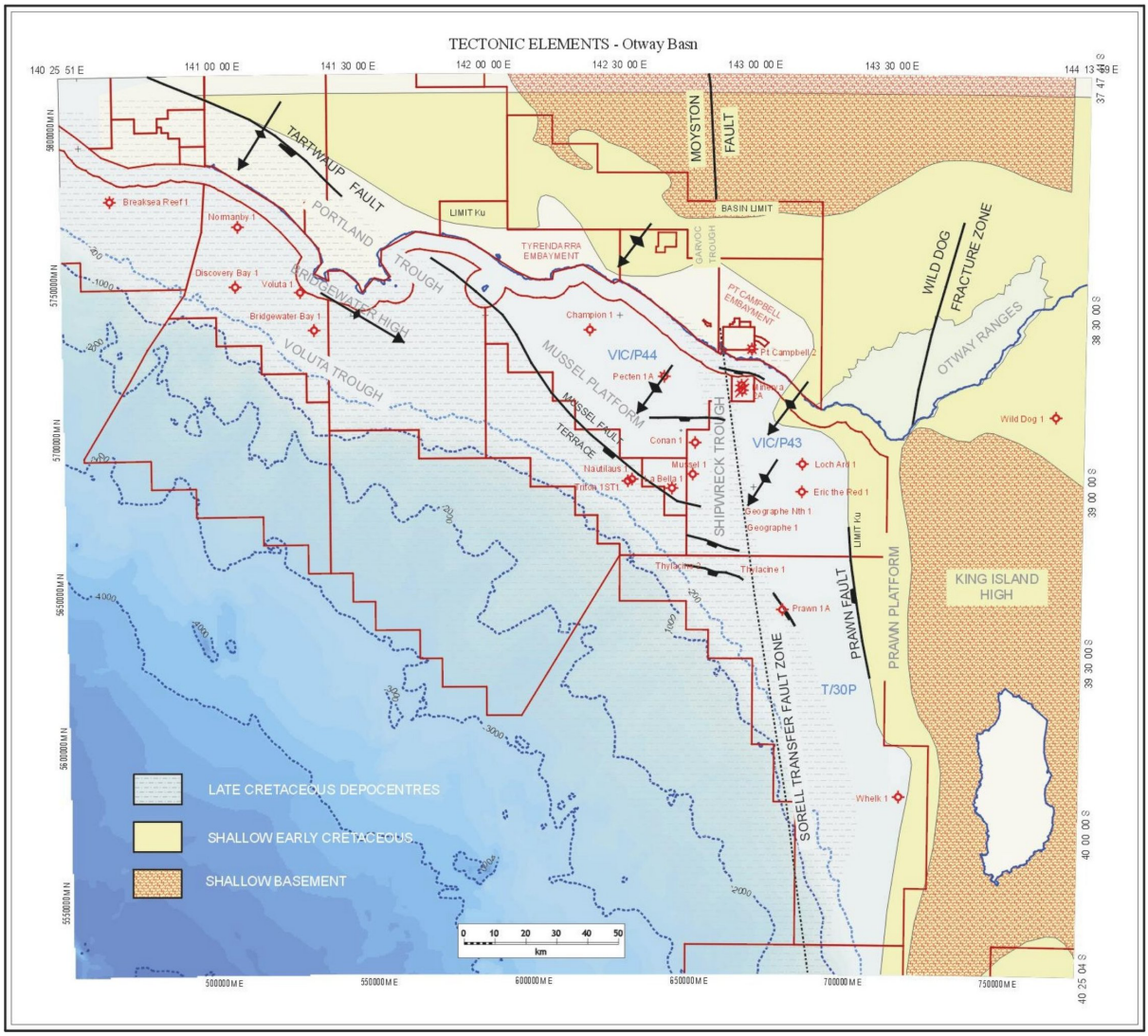

Figure 11. Tectonic elements, Otway Basin

The Shipwreck Trough formed in response to sinistral transtension along the Sorell Transfer Fault during the Late Cretaceous, with significant thickening of Late Cretaceous sediments centred along the axis of the trough. Initial sedimentation commenced in the Cenomanian with the deposition of axially-dispersed marginal marine to fluvial-dominated sediments of the Waarre Formation. This section thickens significantly into the trough and deposition and preservation is dependant on the palaeotopography of the basin, which in turn was dependent upon accommodation created by transpression adjacent to the Sorell Fault.

During the mid Turonian, an increase in rifting resulted in significant growth basinward of the Mussel Fault Zone and Tartwaup Hingeline. This was followed by a major transgression

culminating in the deposition of the Flaxman Formation in the late Turonian. A significant increase in structural activity during the Coniacian and Santonian resulted in marked relative uplift east of the Sorell Fault Zone and significant fault movement within the trough itself. This change in structural style resulted in a complete reorganization of sedimentation patterns within the Shipwreck Trough. On the high parts of fault blocks, this period is marked by a depositional hiatus recorded by the absence of the *C .striatoconus* dinoflagellate zone and by bathyl sedimentation in low areas. Subsequent progradation from the east into the trough resulted in deltaic sequences within middle and late Santonian such as those intersected in the Thylacine and Geographe Fields (i.e. the Thylacine Member). A final widespread regional transgression in the Late Santonian (lower *I. cretaceum* dinoflagellate zone) resulted in the deposition of a thick sequence of deep-marine shale (Belfast Formation) throughout most areas of the basin east of the Sorell Fault Zone. This shale forms the regional seal for the reservoir section in the Thylacine and Geographe fields, and is also the top seal at other gas fields within the Shipwreck Trough (eg. La Bella, Minerva).

Directly adjacent to, and to the east the Sorell Fault Zone, the Cenomanian through to the base Tertiary was dominated by continental and nearshore sedimentation reflecting higher palaeotopography and proximity to sediment source areas. These areas provided vast volumes of sediment into the low area adjacent to the Sorell Fault Zone. This is evident within the Late Cretaceous (Santonian to Campanian) sedimentary sections intersected in Prawn A1 and Whelk 1, which are sandstone-dominated fluvial sequences. Within T/30P, interpreted sand-dominated depositional sequences are evident on seismic data within the Late Cretaceous and extend east of the Sorell Fault Zone into the structurally lower area to the west.

Regional fold trends that plunge to the southwest are essential to defining prospectivity within the Shipwreck Trough. Three such anticlines have been identified along the north – south orientated Shipwreck Trough play fairway within the Investigator 3D area. One of them, the 'Geographe Anticline', underlies the Geographe and Thylacine prospects, and is interpreted to control the migration of hydrocarbons from the source kitchens. The folding and stress field orientations are a composite of at least three different phases of deformation. The first phase began in the Albian / Cenomanian with the initial uplift of the Otway Ranges (crustal kink) in response to rift propagation from the west. The second phase occurred during the Santonian in response to the opening of the Tasman Sea. The third (and final) phase occurred towards the end of the Tertiary in the Mid to Late Miocene

in response sea floor spreading inertia following the collision of Australian northern plate margin with the Banda Arc.

Major east-west trending rift faults occur along the Shipwreck Trough together with the transfer fault deformations. The Albian to Turonian east-west trending rift faults are inferred to be perpendicular to the direction of extension. The rift and post rift deformations mean that there are three main fault sets that dominate the Shipwreck Trough. Extensional tectonics are accentuated towards the shelf margin by gravitational effects. Features such as Thylacine occur over remnant resistant basement highs surrounded by intense deformation.

The northwest-southeast trending listric normal faulting commenced in the middle of the Late Cretaceous and terminated at the end of the Cretaceous with very little penetration above the Palaeocene Pebble Point Formation. These faults commonly sole out on the earlier fault sets. Secondary synthetic and antithetic faulting and rollover anticline development is also present. Inversion due to north-northwest transpression is inferred to have affected most structures in the eastern Otway, especially at Minerva.

A degraded north-south oriented wrench zone is present in the east of the Investigator 3D and is best shown on the variance cube data (see Figure 8). This wrenching, which is the result of crustal transtension, is manifest as a vertical north-trending fault that splays vertically with keystone development. En echelon relay geometries are evident within the 3D, north of Geographe. The complex structural geometry south of Thylacine in the vicinity of Prawn A1 is interpreted to be the product of wrench tectonics.

7.3 Contributions to Geological Concepts and Conclusions

Thylacine-1 was drilled as a vertical exploration well in T/30P designed to test the hydrocarbon prospectivity of a large horst at the Late Cretaceous Waarre Formation level at the southern end of the Shipwreck Trough. Prior to drilling, it was anticipated that Thylacine-1 would intersect reservoir in both the Upper and Lower Waarre Formations. Instead, Thylacine-1 encountered reservoir quality sandstone in the Flaxman and Upper Waarre Formation and also intersected gas-saturated sandstone in a previously unknown unit above the Flaxman Formation here termed the Thylacine Member.

Thylacine-1 proved the hydrocarbon potential of the Late Cretaceous interval in the southern part of the Shipwreck Trough. The well showed significant thickening of the

Flaxman and Waarre Formations compared with the equivalent section intersected in wells such as Minerva 1 and La Bella 1. MDT data indicate a single gas column of 274.5 m was intersected with a FWL of 2297.6mSS. The well contains a combined total of 138.3 m of net pay in the Thylacine Member, Flaxman and Upper Waarre Formations. The Thylacine Member is interpreted to have 47.5 m of net pay (N:G = 43.4%) with an average effective porosity (PHIE) of 15.5%, average gas permeability of 8.6 mD, and average effective water saturation (Swe) of 52.5%. The Flaxman Formation is interpreted to have 50.1 m of net pay (N:G = 43.4%) with an average effective porosity of 16.7%, average gas permeability of 20.8 mD, and average water saturation of 43.4%. The Upper Waarre Formation is interpreted to have 40.9 m of net pay (N:G = 80.2%) with an average effective porosity of 17.0%, average gas permeability of 27.2 mD, and average effective water saturation of 49.1%. Core data has confirmed fair to excellent reservoir quality within the fluvio-deltaic Flaxman Formation.

The newly encountered Thylacine Member comprises a series of coarsening-upwards progradational sequences that form a part of a large fluvio-deltaic sequence sourced from the Prawn Platform to the east. Palynological data confirms that this unit is younger than the Flaxman Formation and belongs to the Santonian *O. porifera* dinoflagellate zone.

A detailed palynological sampling programme using core, sidewall core and cuttings data has, in co-ordination with the Geographe 1 and Thylacine 2 sampling programme, added significant resolution to the dinoflagellate zonation scheme adopted herein. This has allowed increased accuracy in the correlation between units within the Late Cretaceous in this region.

Geochemical analyses from gas sampled at Thylacine 1 indicate a Type III source for the hydrocarbon. The gas composition of the two MDT samples (2054 mMDRT and 2166 mMDRT) from the Thylacine Member and Flaxman Formation are very similar with 82% methane, 9% CO_2, 8% wet gases and 1% nitrogen. The composition is similar to that analysed at La Bella 1. Carbon isotope data indicates that the CO_2 is derived from a diagenetic source rather than igneous.

Vitrinite reflectance data and RockEval analyses indicate the gas in Thylacine 1 has not been generated in-situ, but is derived instead from source rocks elsewhere at depths in excess of 3500m and maturities > 1.0 – 1.3% Ro. The source rocks are interpreted to be carbonaceous siltstones and coals of the underlying Eumeralla Formation and/or more

deeply buried Waarre and Flaxman Formation carbonaceous siltstones and coals to the south. RockEval analysis of argillaceous sandstones and siltstones from the lower Belfast Formation, Thylacine Member, Upper Waarre Formation and Lower Waarre Formation in Thylacine 1 indicate these units contain Type III gas-prone kerogen with S2 yields of between 0.6 to 4.6 kg/tonne (typically < 2 kg/tonne). This suggests hydrocarbon expulsion from these units would only be possible at thermal maturity levels considerably higher than the present-day maturity of the Lower Waarre Formation (0.70% Ro) in the well.

Bright seismic amplitudes on good quality seismic data have provided a low risk indicator for the presence of gas in Cretaceous reservoirs in the offshore Otway Basin. However, Thylacine has shown that there is no precise correlation between seismic amplitudes or flat spots and the presence of gas pore fill.

8. REFERENCES

Jason R. (Origin Energy)	Thylacine-1 Basic Data Report, T/30P, December 2001.
Bal A.A. (Baker Atlas Geoscience)	Thylacine-1 and Thylacine-2 Structural and Sedimentological Interpretation of FMI Images. Volumes 1 & 2, April 2002
Tickell, S.J., Edwards, J. and Abele, C., 1992.	Port Campbell Embayment 1:100 000 map geological report. Geological Survey of Victoria Report 95.

APPENDIX 1
PETROPHYSICS REPORT

T/30P, OTWAY BASIN, TASMANIA

THYLACINE - 1

PETROPHYSICAL REPORT

THYLACINE MEMBER, FLAXMANS FORMATION, AND WAARRE FORMATION

2048-2684 mMDRT

Origin Energy Resources Limited
Second Floor, South Court, John Oxley Centre
339 Coronation Drive
MILTON QLD 4064

Chris Shield, March 2003
N:\chris\otway\thylacine\thylacine-1\petro\2003-03\Thylacine-1 Petro Report.doc

EXECUTIVE SUMMARY

This report details a review of the reservoir quality and hydrocarbon saturation of three Late Cretaceous formations intersected whilst drilling the exploration well, Thylacine-1 in T/30P in the Otway Basin, Tasmania. The study entails an analysis of all available lithological data, and a complete petrophysical analysis (Table 1).

The Thylacine Member (2048.5-2158.0 mMDRT) encountered at Thylacine-1 is interpreted to have moderate reservoir quality. The sandstones that are present contain high clay volumes, averaging 26.4%. Calculated effective porosities average only 15.5% for these reservoirs. As a result, the log-derived gas permeability is considerably reduced in comparison to other cleaner reservoirs, averaging only 8.6mD, which will negatively affect this unit's producibility and recovery factor. The average effective water saturation is 52.5%, and the net reservoir to gross is 43%.

The Flaxmans Formation (2158.0-2273.3 mMDRT) appears to have better reservoir development. The sandstones present, on average, are cleaner than those above and have an average clay volume of 16.9%. The average effective porosity is higher (16.7%), and the gas permeability is significantly higher, averaging 20.8mD. This unit has a net reservoir to gross of 43%, and an average effective water saturation of 47%.

The interval between the top of the upper Waarre Formation and the interpreted GWC (2273.3-2325.6mMDRT) has the best average reservoir parameters. The average clay volume in this unit was only 14.6%, whilst the average effective porosity was similar to that for the Flaxmans Formation (17.0%). This unit is interpreted to have an 80% net reservoir to gross ratio, average effective water saturation of 16%, and very good gas permeabilities, averaging 27mD.

Between the four wells now present on the Thylacine and Geographe fields, sufficient core analysis data is present to calibrate the log responses, and no more core analysis is considered necessary.

The spectral gamma ray data are in agreement with the petrological analysis, in that the dominant clay mineral is kaolinite. These spectral gamma ray data also infer that the clay type present in the sandstones, is of the same chemistry to those present in the shales. Therefore, little benefit is being added by this log, and it is recommended that acquisition of the spectral gamma ray tool is not necessary in future wells.

The LWD data acquired by Anadrill were not utilised in the interpretation of fluid saturations, as they are responding with lower values than those measured using the wireline devices, presumably due to the highly porous and permeable nature of these reservoirs encouraging the deep invasion of mud filtrate. It is not recommended that LWD be acquired in future wells for the purposes of petrophysical evaluation.

FORMATION	TOP	BASE	GROSS	NET PAY	AVE.	AVE.	AVE.	AVE.	AVE.	AVE.	AVE.	NET RES /
NAME	FROM	TO	INTERVAL	INTERVL	VCL	PHIT	PHIE	AIR PERM	GAS PERM	WATER PERM	SWE	GROSS
	mMDRT	mMDRT	mMDRT	mMDRT	%	%	%	mD	mD	mD	%	%
Thylacine Member	2048.50	2158.00	109.50	47.50	26.42	20.51	15.46	10.89	8.61	3.17	52.50	43.38
Flaxmans Formation	2158.00	2273.30	115.30	50.07	16.91	19.92	16.70	25.90	20.82	7.74	46.73	43.43
Upp. Waarre Fm-GWC	2273.30	2325.60	52.30	41.94	14.58	19.58	16.95	33.62	27.16	10.13	49.06	80.19
		TOTAL	**277.10**	**139.51**	**19.45**	**20.02**	**16.35**	**20.86**	**16.69**	**6.19**	**49.39**	**50.35**
Upper Waarre Fm	2273.30	2424.20	150.90	101.40	17.79	19.15	16.01	8.90	7.01	2.58	77.16	67.20
Lower Waarre Fm	2424.20	2684.00	259.80	88.73	24.73	17.81	13.65	2.22	1.70	0.62	95.54	34.15

Table-1. Petrophysical Summary

TABLE OF CONTENTS

Figures

Tables

Appendices

A. Log depth-matching Summary

B. Petrophysical Model and Constant Listing

C. Core Analysis cross-plots

Enclosures

1.	Composite and petrophysical summary plot, 2048-2684 mMDRT	1:500
2.	Composite and petrophysical summary plot, 2048-2380 mMDRT	1:200

INTRODUCTION

Thylacine-1 is an exploration well drilled in 2001, and is located within the current T/30P permit (Figure-1).

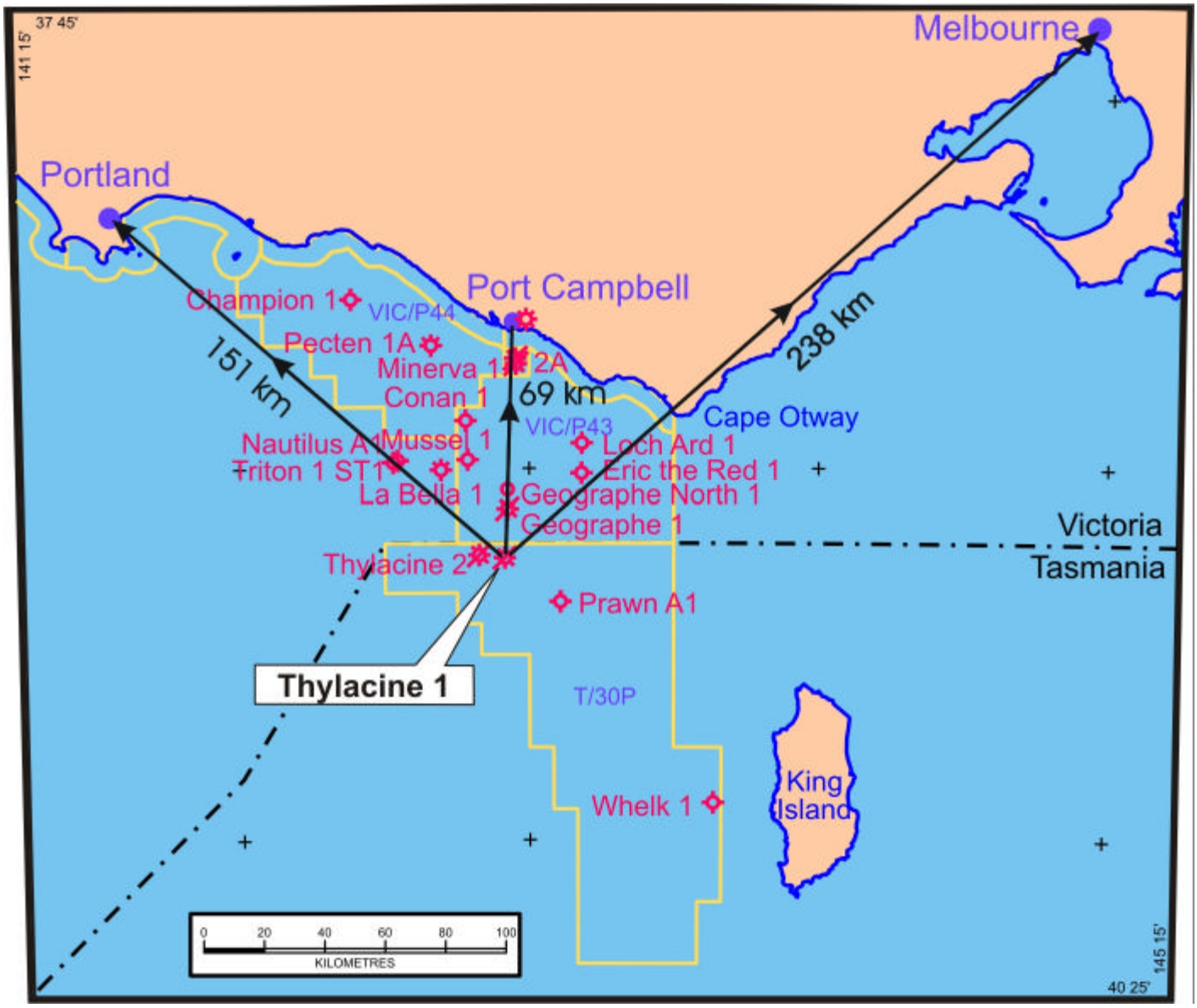

Figure 1. Location Map

The well intersected interbedded claystones, and moderate to excellent quality sandstones displaying weak fluorescence and very good gas shows within the basal Belfast (Thylacine Member), Flaxmans and Waarre Formations (Table-2). This report addresses the reservoir and hydrocarbon-producing potential of all strata intersected between 2000 metres and the base of complete log coverage at 2711.0 mMDRT.

FORMATION / *MARKER*	**TOPS (m)**				**REMARKS/SHOWS**
	MDRT	SUBSEA	THICK	TWT(ms)	
Port Campbell Limestone	126.4	101.4	272.6	127	No Returns 126.4 - 752 mDRT
Gellibrand Marl			717.0		
Upper Gellibrand Marl	401.0	376.0	(430)	387	Calcareous claystone interbedded with minor sandstone and argillaceous calcilutite
Middle Miocene Seismic Marker	-	-	-	565	
Lower Gellibrand Marl *Base Miocene Seismic Marker*	831.0	806.0	(285.0)	735	Calcareous claystone interbedded with minor argillaceous calcilutite
Narrawaturk Marl	1116.0	1091.0	55.0	942	Calcilutite interbedded with calcareous claystone
Mepunga Formation	1171.0	1146.0	65.0	981	Sandstone with rare claystone interbeds
Dilwyn Formation	1236.0	1211.0	164.6	1025	Claystone with interbedded sandstone
Paaratte Formation	1400.6	1375.6	303.4	1134	Claystone and silty claystone with minor sandstone and argillaceous calcilutite interbeds
Belfast Formation	1704.0	1679.0	454.0	1324	Claystone with trace siltstone and sandstone stringers towards the base
Thylacine Member	2048.5	2023.5	(109.5)	1524	Interbedded sandstone, siltstone and claystone. **Gas shows.**
Flaxman Formation	2158.0	2133.0	115.1	1585	Interbedded sandstone, siltstone and claystone. **Gas shows.**
Waarre Formation			436.9+		
Upper Waarre Formation	2273.1	2248.1	(150.8)	1647	Interbedded fluvial sandstone, siltstone, claystone & minor coal. **Gas shows.**
Lower Waarre Formation	2423.9	2398.9	(189.1)	1727	Interbedded sandstone and claystone
Top coals	2652.0	2627.0		1843	
TOTAL DEPTH	2710.0	2685.0			

Table 2. Stratigraphic Table

DATA AVAILABILITY AND QUALITY

Lithological Data

One conventional core cut between 2165.0 and 2201.0 mMDRT, had a 99.3% recovery. In order to allow comparison of routine and special core analysis data with the results of the log analysis, it was necessary to depth match the core to wireline depths. As a result of depth-matching the core gamma ray to the wireline gamma ray, a bulk depth shift of 3.1 metres was necessary. To allow for the fine scale variations in wireline depth due to cable stretch, core plug total porosity and log derived total porosity were used to provide a fine tuning of the depth shift required, resulting in a

further depth match that varied between -0.35 and 0.07 metres. A listing on the depth shifts applied is included in Appendix-A.

Lithological information is provided by core, and mechanical and percussion sidewall core descriptions, and cuttings descriptions summaries.

Mudlog Data

Baker Hughes were contracted to provide mudlogging services. A variable depth match was applied to this mudlog data to conform to wireline log depths. The ROP and total gas curves were used as the seed to depth match the mudlog data, to the wireline gamma ray and density curve data. The depth match applied varied between –1.6 and 2.7 metres. A listing of the depth shifts applied is included in Appendix-A. The raw and depth-shifted data are available in LAS ASCII format on a CD-ROM adjoining this report.

Electric Log Data

MWD and LWD services were provided by Anadrill. Although the LWD logs were not used in this interpretation, these data were variably depth matched to wireline depths in order to produce a fully depth matched composite log suite, as the LWD gamma ray was logged to a deeper depth than any wireline tool. The LWD gamma ray was match to the wireline gamma ray, and the depth match varied between 1.7 and 4.3 metres. A summary of the tools and intervals acquired is in Table-3, and a listing of the depth shifts applied is included in Appendix-A. The raw and depth-shifted data are available in LAS ASCII format on a CD-ROM adjoining this report.

Schlumberger, who provided wireline services, logged the well in two suites. Suite-1 was logged in a 12.25-inch hole, whilst Suite-2 was logged in an 8.5-inch hole. Table-2 contains a summary of the logging tools run on the relevant log intervals. Comments upon log quality, herein discussed, are limited to the first run in the hole as this is the super-combo run. The raw, edited, and merged data are available in LAS ASCII format on a CD-ROM adjoining this report.

Overall the data is of a high quality, although there are two logs for which the data must be questioned from both logging suites. This hole was drilled with a mud containing barite. Barite, however settles out as a solid, and therefore tends to concentrate in the mudcake. In a hole displaying limited wash out, such as this one, the thickness of the mudcake build-up opposite

porous sandstones can be estimated by the difference between the bit size and the caliper. Despite several attempts at correcting the photo-electric factor (PEF) for this mudcake thickness, a log resulted that displayed values as low as 1.0 opposite porous and permeable quartzose sandstones, where the range of value should be between 1.8 and 2.2. As a result the PEF curve was utilised in this analysis in a qualitative sense only.

Suite/Run	Tool String	Interval (mMDRT)	BHT (degC)
1/1	DGR-ARC5 (LWD)	1845.4-2709.5	
1/1	PEx(HRLA)-DSI-HNGS-SP	744.0-1833.3	78
1/2	PEx(HRLA)-DSI-HNGS-SP	1675.5-2713.0	104
2/2	MDT-GR	2049.0-2628.2	113
2/3	MSCT-GR	2050.0-2240.0	98
2/4	FMI-GR	2022.0-2503.0	106
2/5	CSI-GR	130.5-2707.0	114
5/6	CST-GR	1874.6-2704.2	

Table-3. Log Data Acquired

The spontaneous potential (SP) log displays limited definition in differentiating the highly porous and permeable sandstones from the intervening shales. Since both the mud, and the sea water where the reference electrode was located, have a salinity of twice that of the formation water, greater definition of sands and shales would have been expected on the SP log. As such, the SP log was not utilised as a clay indicator or as an indicator of formation water chemistry.

Formation Test Data

One successful Modular Dynamics Tester (MDT) run resulted in the acquisition of 43 valid pressure tests and three samples, plus a number of tight and super-charged pressure points. These data are discussed in Appendix-3 of the Well Completion Report, and thus will not be considered here further.

Routine and Special Core Analysis Data

A comprehensive routine (RCA) and special (SCAL) core analysis programme was undertaken from horizontal and vertical plugs taken from Core-1. The range of analyses were measured including ambient and overburden helium porosities; ambient, overburden, and Klinkenburg-corrected horizontal and vertical permeabilities; probe permeabilities; grain densities; cation exchange capacities; capillary pressures; relative permeabilities; cementation exponents; and

saturation exponents. The results of many of these analyses are utilised in the petrophysical model discussed herein, and for calibration and quality control of the results of the petrophysical model. A selection of the cross-plots relevant to this petrophysical evaluation is included in Appendix-C

Details of the acquisition, measurement and quality control of these data is discussed in Appendix-2 of the Well Completion Report, and thus will not be considered here further.

As discussed earlier, these core analysis results have been depth matched to wireline depths using the core gamma ray. The raw and depth shifted core analysis data are available in LAS ASCII on a CD-ROM adjoining this report.

BOREHOLE DATA

Hole Conditions

The borehole is in good condition within the 12.25-inch hole, displaying up to a 0.5 inch thick mudcake build-up over good quality sands. Washouts do not exceed 0.5 inches, except for between 1170 and 1230 metres, where the hole-size exceeds the bitsize by up to 2 inches. Hole rugosity is commonly excessive within this interval, described as a marl, causing a loss in signal from the pad contact wireline log tools.

Apart from directly beneath the 9.625-inch casing shoe, the hole condition within 8.5-inch hole section is excellent. The caliper does not exceed the bitsize by any more than 0.5 inch, and the mudcake build-up is limited to less than 0.2 inch. Hole rugosity is also minimal, except for one peak at 2537 metres.

Mud Properties

The section encompassing the Thylacine Member, Flaxmans and Waarre Formations reservoirs was drilled with a KCl-PHPA-Glycol-barite mud (Table-4).

Bottom Hole Temperature

A Horner temperature plot generated for Suite-2 (Figure-2) yielded an extrapolated bottom hole temperature of 116.5 degree Celsius at 2711.0 mMDRT. The maximum-recorded temperatures from the individual logging runs were used to environmentally correct the wireline log data.

Depth	Mud Type	Mud Weight (g/cc)	R_{mf} @ Temp (Ωm @ °C)	Viscosity (sec/litre)	Chlorides (ppm)
2713	KCl-PHPA	1.33	0.074 @ 20	65	59,000
Solids (%)	**Potassium (ppm)**	**R_m @ Temp (Ωm @ °C)**	**R_{mc} @ Temp (Ωm @ °C)**	**Fluid Loss (cc)**	**Barite (%)**
11.0	44,000	0.094 @ 20	0.455 @ 20	2.3	6.1

Table-4. Mud Properties

RESERVOIR QUALITY

The upper part of the interpreted interval down to 2048.5 metres is described as light to dark grey, non-calcareous shale, and forms part of the Belfast Formation.

The Thylacine Member (2048.5–2158.0m) is described as light grey to white, fine to medium grained, well-sorted sublitharenite to litharenite, interbedded with siltstones and minor claystone.

Between 2158.0 and 2273.3 m, the Flaxmans Formation is described as fine to coarse-grained, poorly sorted sandstone, interbedded with siltstone and claystone.

The upper Waarre Formation between 2273.3 and 2423.9m is described as fine to coarse-grained moderately well-sorted quartzose sandstones interbedded with siltstone and minor claystone.

The basal reservoir, the lower Waarre Formation (2423.9 – 2710.0m) contains a similar lithology to the upper Waarre Formation, except that several thin coal seams are present, particularly in the lower part of this unit.

HORNER TEMPERATURE PLOT

Thylacine-1 Suite-2

WELL:	Thylacine-1	**LOG SUITE:**	Suite-2	
PERMIT:	T/30P	**LOG DATE:**	19-May-01	
NOTES:	Sensor measure points estimated.	**T.D.:**	2713.0	(Logger)
		Geologist:	Chris Shield	

LOG TYPE	BOTTOM DEPTH OF LOGGED INTERVAL mRT {Sensor Measure Point}	Tx (hrs)	T (hrs)	T/(Tx+T)	Max. TEMP Deg C	Eq. Max TEMP Deg C
PEx(HRLA)-DSI-HNGS	2711.0	0.75	11.67	0.940	104	104.00
MDT-GR	2626.2	0.75	46.57	0.984	113	116.65
MSCT-GR	2238.0	1.25	11.92	0.905	98	118.71
FMI-GR	2501.0	1.25	19.92	0.941	106	114.90
CSAT	2705.0	1.25	27.92	0.957	114	114.25

Where: Tx = CIRCULATION TIME
T = TIME SINCE CIRCULATION STOPPED

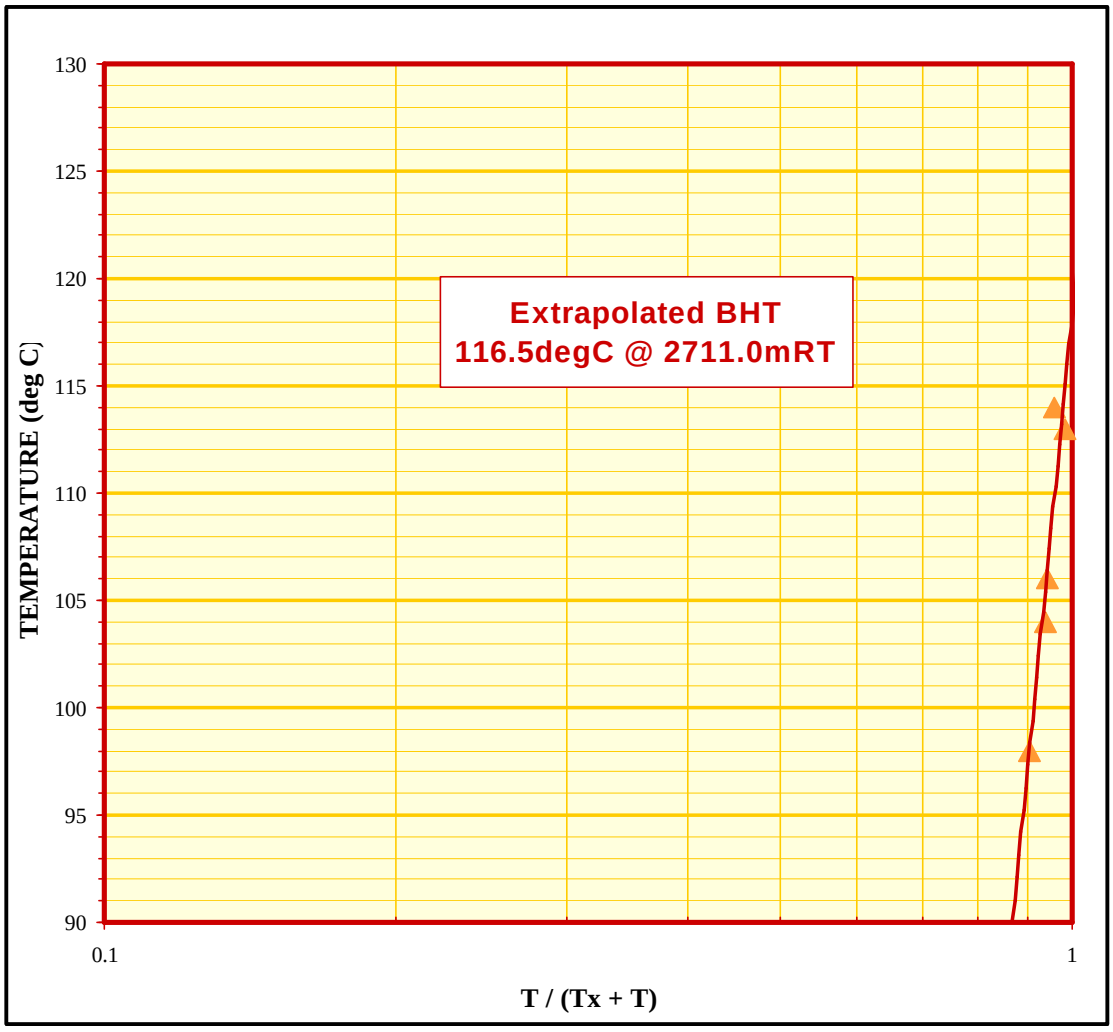

Figure-2. Suite-2 Extrapolated Borehole Temperature Plot

LOG ANALYSIS METHODOLOGY

A complete listing of all reservoir zonations, petrophysical models, constants, and parameters applied in the interpretation are included as Appendix-B.

Preparation

The final Schlumberger wireline data were loaded from Origin Energy's master digital well log database into the Crocker Data Processing (CDP) Petrolog v9.1.7 software. As there was data of various resolutions, wireline data at 5 and 15cm, mudlog data at 50cm, and core plug data at 1cm spacings, all available data were re-sampled to the finest 1cm resolution. This ensured that the core plug data could be accurately depth-matched, and maximise the degree of correlation between core and log-derived results.

Environmental Corrections

With the Platform Express tool, many environmental corrections are applied at the wellsite. The field prints contain a parameter listing, that details which environmental corrections that have been applied by the wireline engineer. This section summarises which corrections were applied, and whether they were applied at the wellsite, or in the Petrolog software in the office.

The gamma ray (GR) curve was corrected for borehole size using the density caliper at the wellsite. A KCl concentration correction was applied in the Petrolog software. For the purposes of creating a composite log suite, the GR was corrected for casing thickness, where necessary, in the Petrolog software.

The borehole size and bed thickness corrections were applied to the laterolog data via inverse resistivity modelling at the wellsite. Invasion corrections were applied at the wellsite, resulting in a true formation resistivity (Rt) and invaded zone resistivity (Rxo) curve provided by Schlumberger. Mudcake thickness corrections were applied to the microlaterolog data at the wellsite.

The density (RHOB) log data were corrected for borehole size and mud density at the wellsite. The compensated neutron (NPHI) log was corrected for borehole size and salinity, formation temperature and pressure, mudcake thickness, and mud density at the wellsite. Formation salinity and barite corrections were applied in the Petrolog software.

.

Zonation

The well was zoned according to the formation tops in Table-1. These formational zones were further subdivided into petrophysical facies, thus enabling the recognition of sand, silt, and clay-rich rock types. Figure-3 displays an example of how these data were subdivided on a density neutron cross plot.

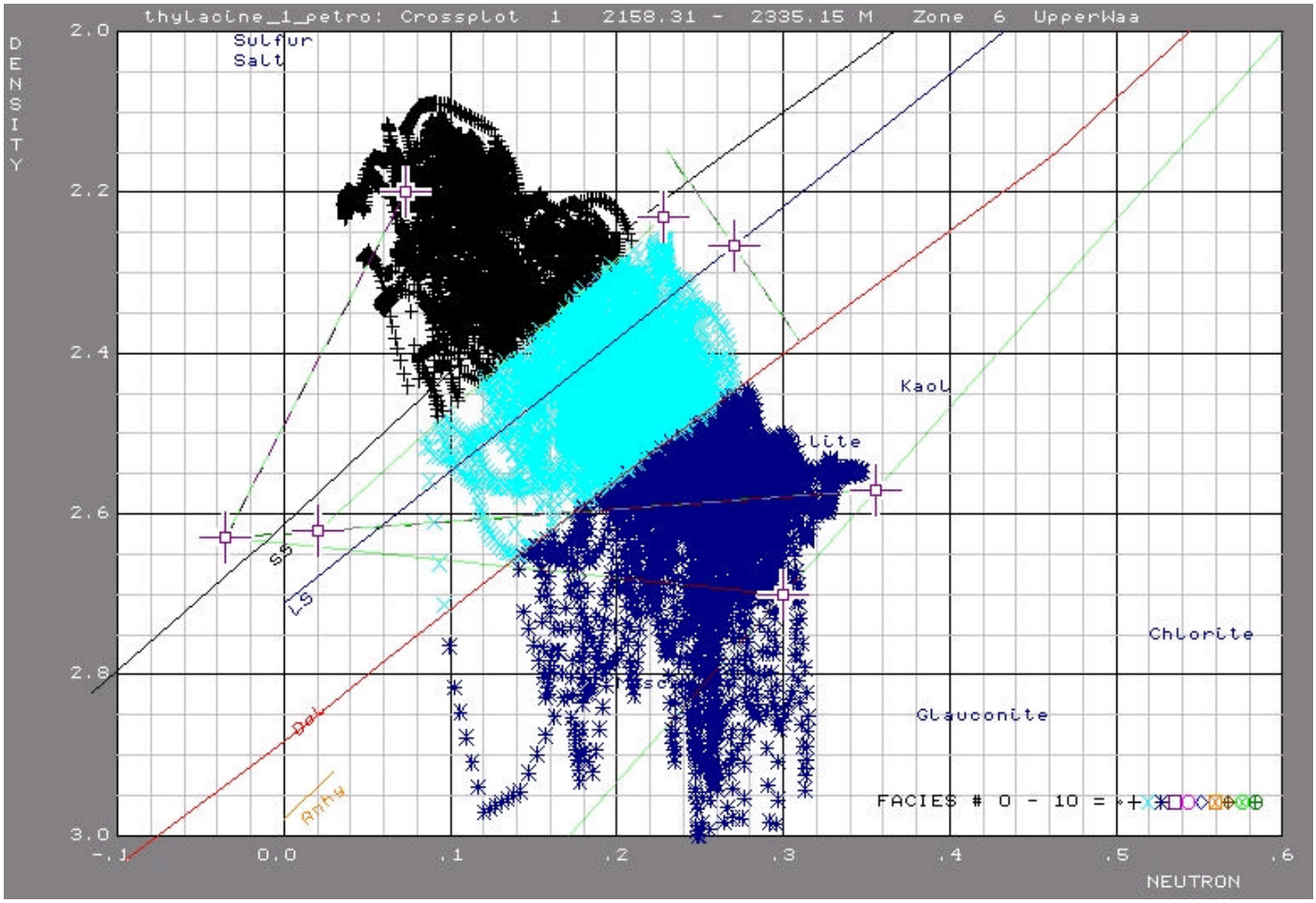

Figure-3. Petrophysical facies sub-division of lithostratigraphic zones.

This subdivision enabled different inputs and constants to be applied to the different petrological facies within each lithological unit. The identification of clay volume parameters and of clay resistivity values was made more accurate is cross plot to be generated that displayed only those points dominated by clay. By the same token the identification of formation water resistivity and hydrocarbon density could now be evaluated using only sand-rich data points.

Clay Volume and Porosity

Clay volume (VCl) was defined by application of a linear GR, RHOB-NPHI cross-plot, RHOB-DT cross-plot, and sonic (DT) models (Figure-4). The minimum VCl calculated from all techniques was applied as the VCl in the interpretation. VCl parameters were set to ensure that the average values calculated from logs matched the core, sidewall cores and cuttings descriptions.

A linear density-neutron model was applied to derive porosity (PHIT), with a Wyllie sonic porosity model being applied in badhole areas. Badhole was defined using cut-offs for differential caliper, DRHO, and hole rugosity. The density and neutron data were corrected for hydrocarbon density prior to determining the log derived total porosity. The total porosity was then matched to the overburden helium core porosity, prior to the correction for Clay volume and the subsequent derivation of effective porosity (Figure-5).

$$PHIT = \frac{((r_{ma} - r_b)/(r_{ma} - r_f)) + j_N}{2}$$

The log derived hydrocarbon density was calculated at 0.6 g/cc, by cross plotting effective porosity versus the apparent grain density. As we know the hydrocarbon in these reservoirs is gas, and therefore significantly less dense than 0.6 g/cc, it can be inferred that the area of investigation of the density tool was affected by the presence of mud filtrate.

Lithology

Petrological studies, detailed in Appendix-7 of the Well Completion Report, and conducted on core and sidewall cores samples from Thylacine-1, indicate that some of the sandstone reservoirs contained significant amounts of carbonate cements and argillaceous matter. To allow for this variable mineralogy, particularly the carbonate cementation, a complex lithology petrophysical model was applied in preference to a silty sand petrophysical model. The application of this complex lithology model aims to optimise the calculation of total porosity for subtle changes in the matrix density as a result of changing concentration in carbonate cement.

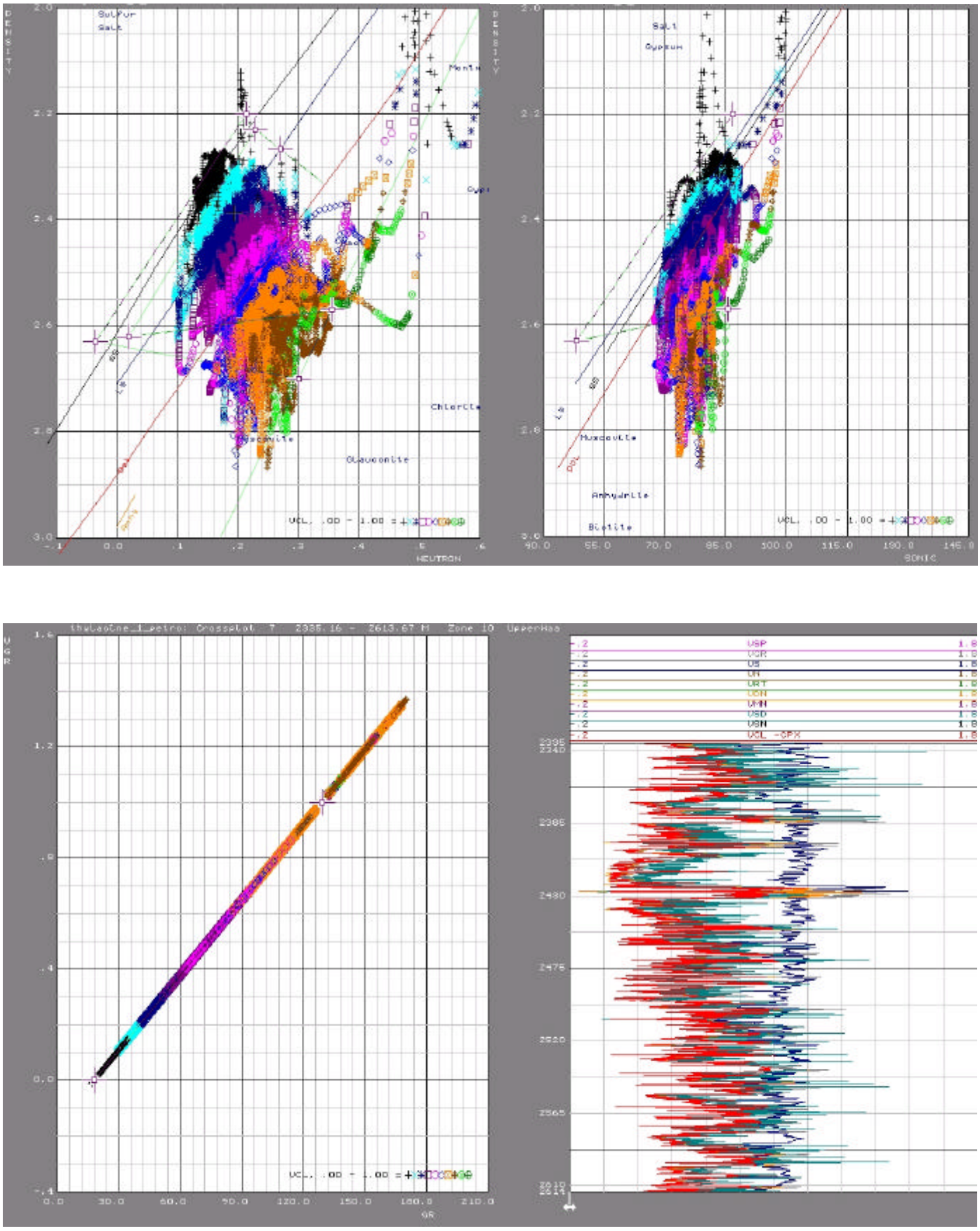

Figure 4. Clay volume determination. Comparison of results from the RHOB-NPHI, RHOB-DT, and GR techniques for the upper Waarre Formation, 2335.2-2613.0 mMDRT.

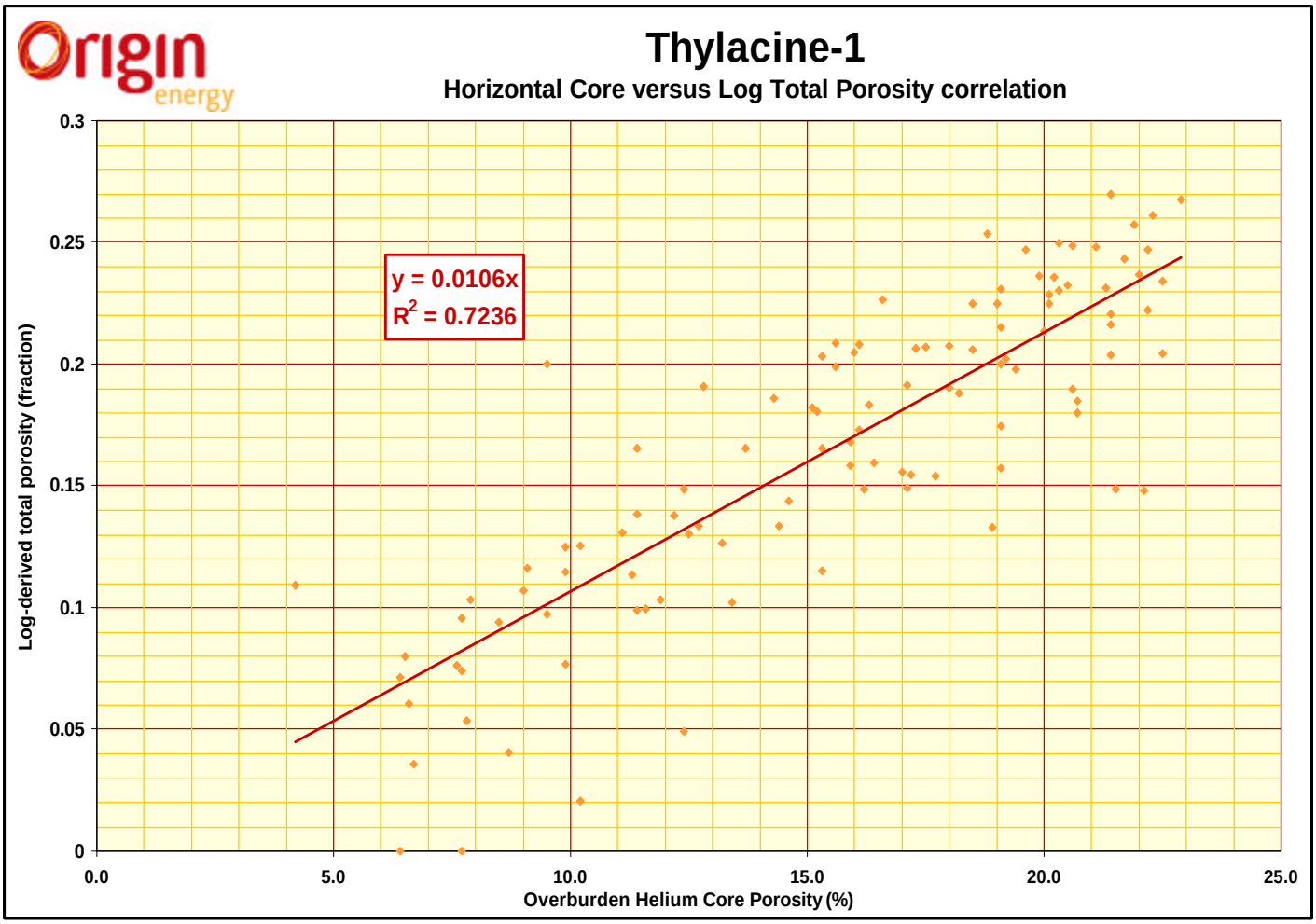

Figure 5. Comparison of overburden Helium core porosity and log-derived total porosity.

This model however, does have its drawbacks. As previously discussed, the PEF log, which is an essential component of the complex lithology model, is considered to be of dubious quality for quantitative assessment, but valid qualitatively. It was therefore necessary to add a bulk correction factor of 0.45 to the PEF data in order to optimise the distinction between quartz and carbonate cements. The application of a complex lithology model also limits be type of water saturation equation that can be applied to only those equations that utilise effective porosity, and not total porosity.

Formation Water Resistivity

Although a water sample was recovered using the MDT tool, subsequent analysis proved it to be and undefinable mixture of mud filtrate and formation water. As discussed previously, the SP log is considered to be of dubious quality, and therefore was not utilised to derive a formation water resistivity. Ultimately, the formation water resistivity was defined using the Rwa technique by the

application of Hingle (Figure-7) and Pickett (Figure-8) crossplots of sandstone-dominated zones beneath the gas water contact.

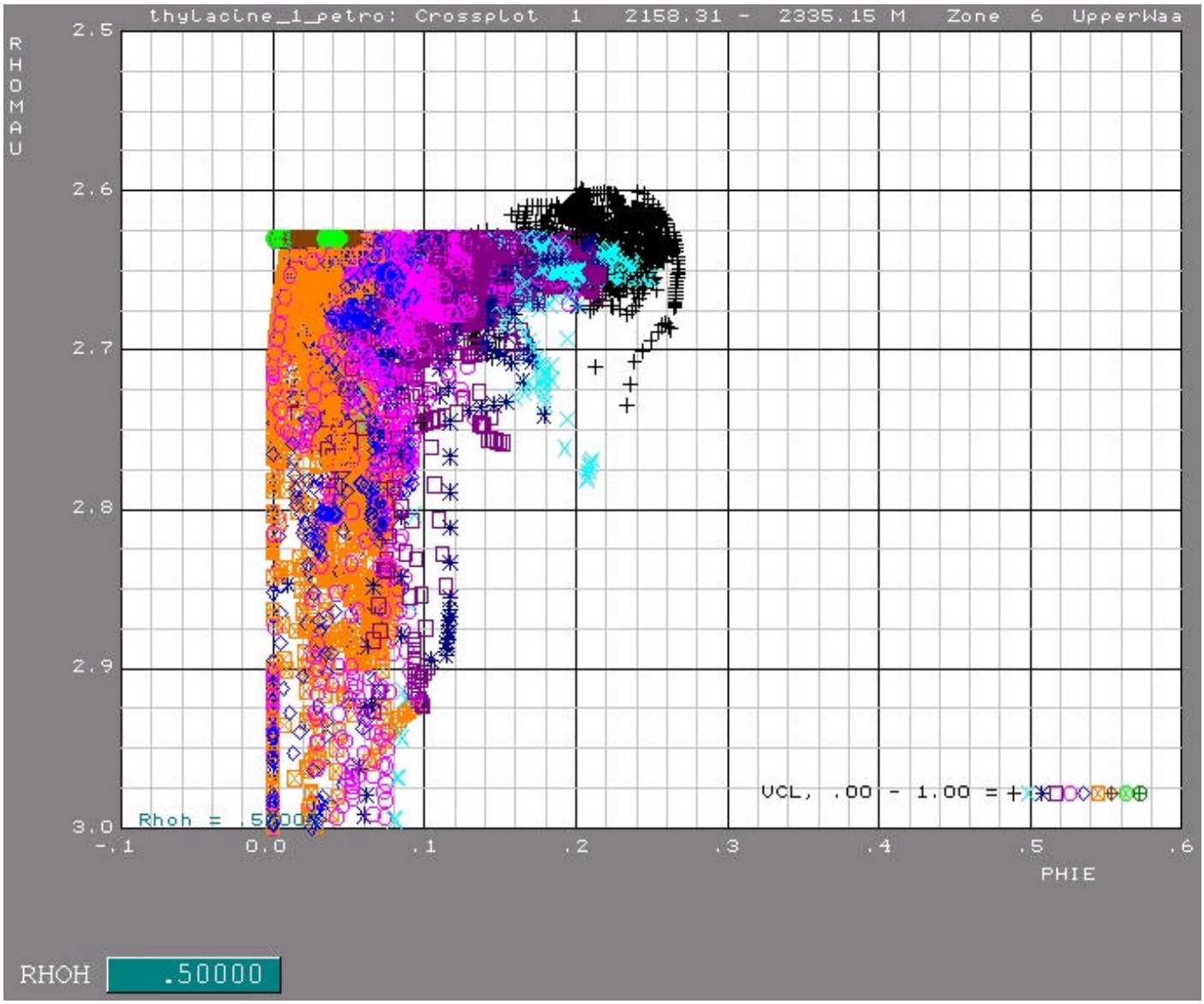

Figure 6. Hydrocarbon density derivation from cross-plot of effective porosity versus apparent grain density.

A review of offset well data with reliable formation water chemistries was conducted prior to the drilling of Thylacine-1. The results of this study, and of the formation water resistivity derived from logs and utilised in this study, are summarised in Table-5.

Well	Depth (m)	Rw@ Temp (Ωm @ °C)	Salinity (ppm NaCl	Source
Thylacine-1	2335-2613	0.46 @ 25	13,000	Rwa derived from logs
Minerva-1	1816-1838	0.48 @ 25	13,800	DST-1 fluid recovery
Pecten-1A	1771-1784	0.32 @ 25	20,700	Production test fluid recovery
Conan-1	1830-1950	0.50 @ 25	11,700	Rwa derived from logs

Table-5. Waarre Formation water chemistry data

Water Saturation

Two water saturation equations were used to determine the optimal method of determining hydrocarbon saturation from the wireline logs, an Indonesian equation and a Waxman-Smits equation.

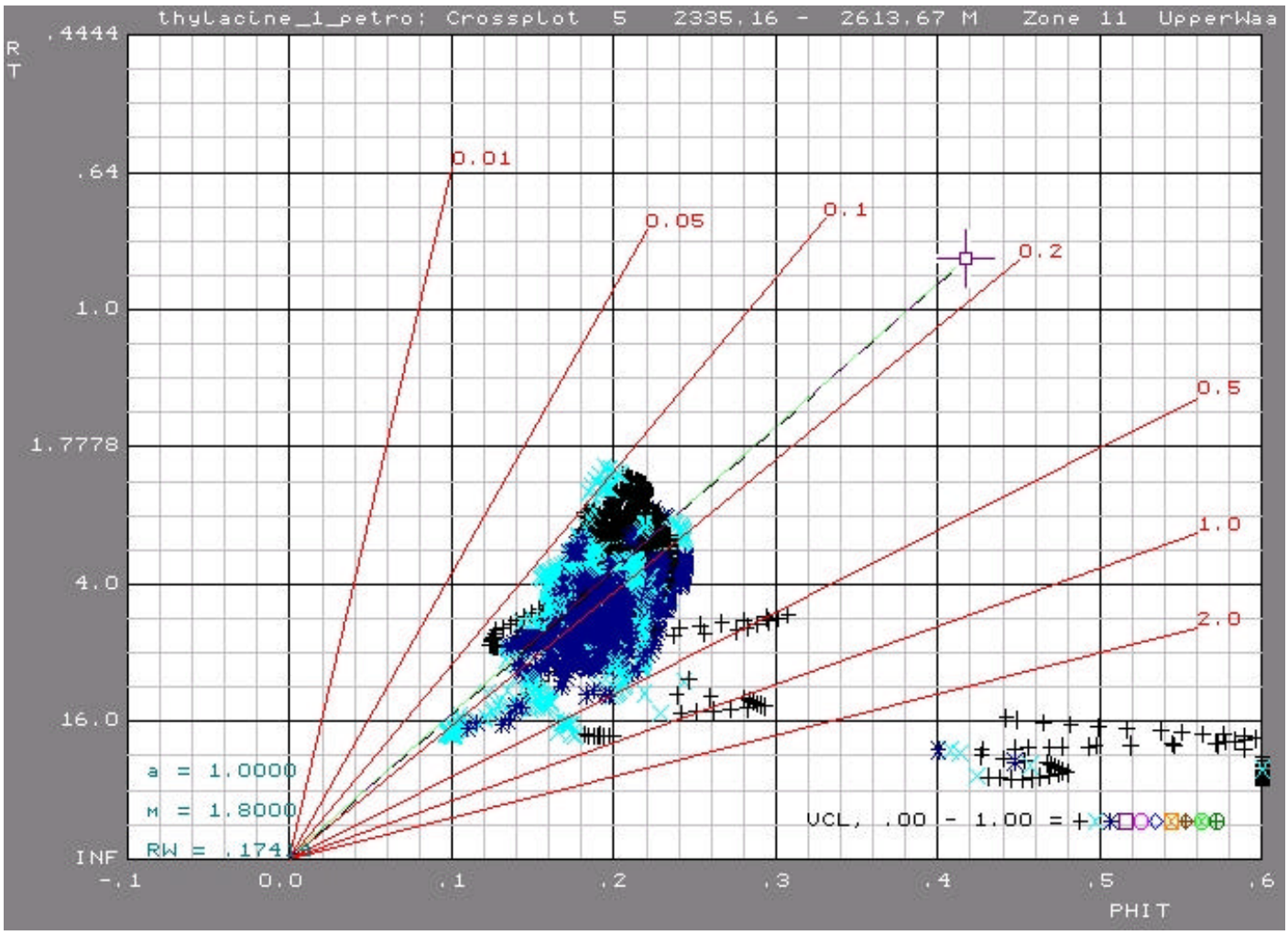

Figure 7. Hingle cross-plot defining formation water resistivity from upper Waarre Formation below the GWC. Sand petrofacies displayed.

The tortuosity factor (a) was kept constant at one. Values for the cementation exponent (m) and the saturation factor (n) were determined from the results of the special core analysis study. These values remained constant for each petrophysical facies, and across the various lithostratigraphic units (Table-6,7).

Petro-facies	Tortuosity Factor (a)	Cementation Exponent (m)	Saturation Exponent (n)	Clay Resistivity (RCl)
Sandstone	1.00	1.80	1.75	49.0 ohmm
Siltstone	1.00	2.00	1.95	49.0 ohmm
Claystone	1.00	2.35	2.15	49.0 ohmm

Table-6. Summary of electrical properties applied in the Indonesian Equation

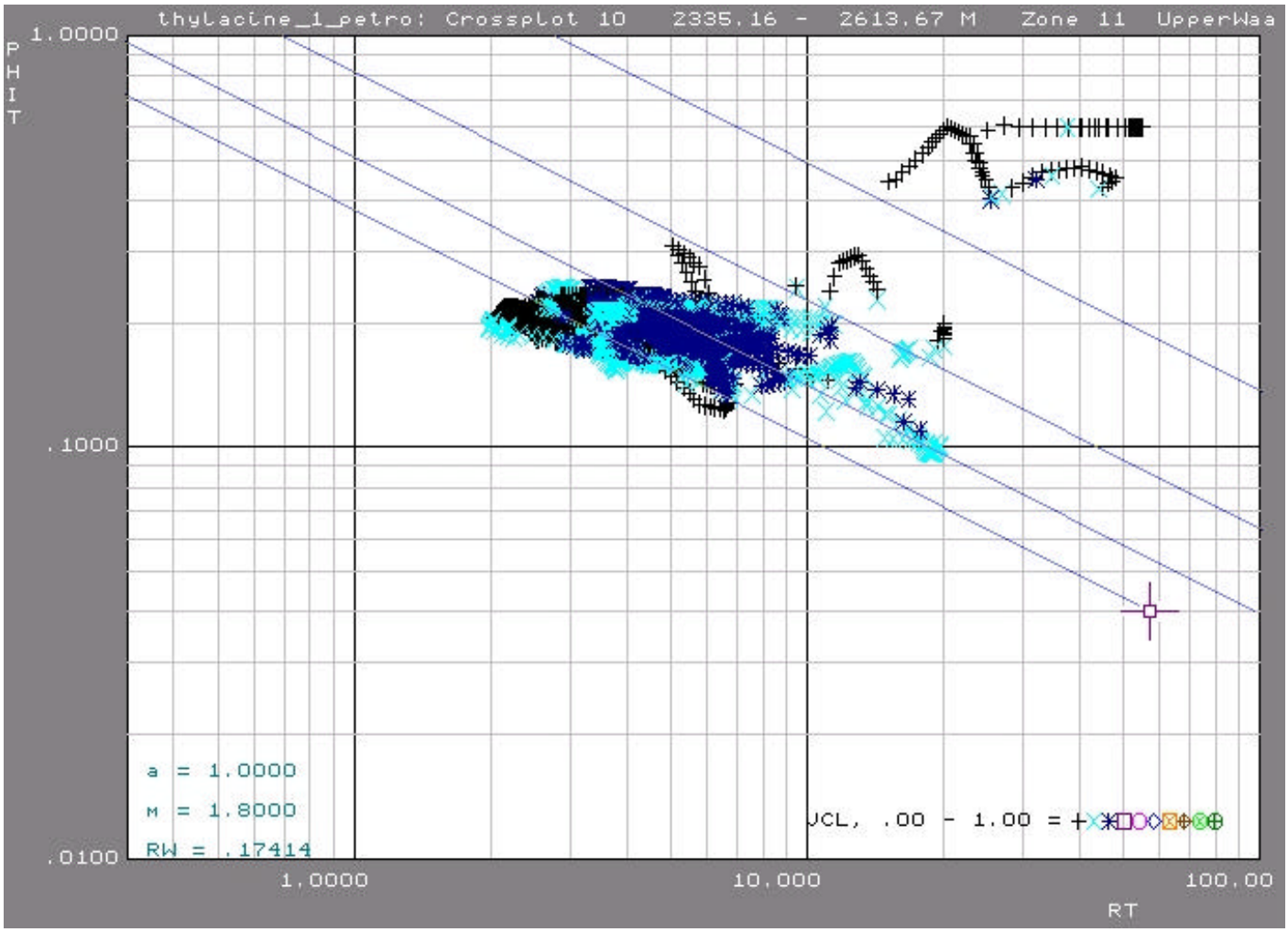

Figure 8. Pickett cross-plot defining formation water resistivity from upper Waarre Formation below the GWC. Sand petrofacies displayed.

Petro-facies	Tortuosity Factor (a)	Waxman-Smits Cementation Exponent (m*)	Waxman-Smits Saturation Exponent (n*)
Sandstone	1.00	1.95	2.05
Siltstone	1.00	2.15	2.25
Claystone	1.00	2.50	2.45

Table-7. Summary of electrical properties applied in the Waxman-Smits Equation

The Indonesian equation, which is an effective porosity system that calculates an effective water saturation, derives its shale conductivity factor from the wireline resistivity log-derived Rt. A log derived clay resistivity (RCl) is defined by cross plotting the apparent formation water resistivity (Rwa) versus GR for the clay-rich petrophysical facies (Figure-9). This RCl value remains a constant across all zones that are deemed to contain similar clay properties.

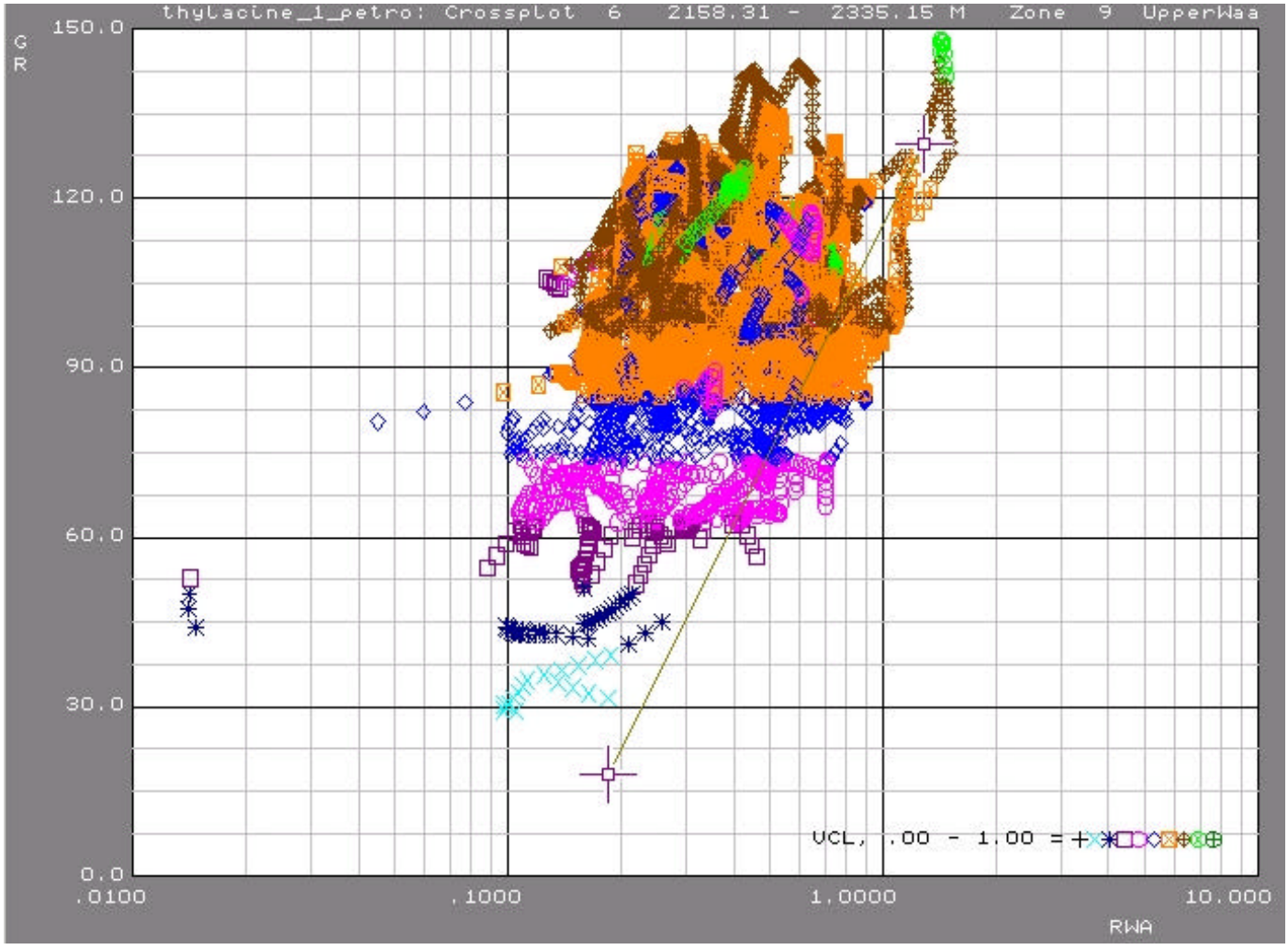

Figure 9. Clay resistivity derivation as applied in the Indonesian water saturation equation. Clay petrofacies displayed.

The Waxman-Smits equation contains total porosity as an input parameter, and therefore derives a total water saturation. The shale conductivity factor for this equation is stated in terms of BQv, where BQv is a function of formation water resistivity, formation temperature, and the concentration of exchangeable cations (Qv). A relationship exists between Qv and the cation exchange capacity (CEC), which is a parameter measured on all special core analysis plugs obtained from this well.

$$B = \frac{0.225T - 1.28 - 0.0004059T^2}{1 + Rw^{1.23}(0.045T - 0.27)}$$

$$Qv = \frac{CEC(1 - PHIT) \times graindensity}{100 \times PHIT}$$

A good relationship between core-derived CEC and log-derived VCl (Figure-10,11) enabled the application of a variable Qv to be applied in the Waxman-Smits equation.

Applying a total porosity water saturation equation to a shaley sand petrophysical model is optimal, as the matrix density is kept constant (i.e.2.65 g/cc) and changes in porosity only occur with changes in clay content, given a constant fluid content. However, if applying a total porosity water saturation equation to a complex lithology model, there are too many unknowns to provide a unique answer as neither the matrix density nor the clay volume are fixed. An effective porosity water saturation equation is better suited to application to a complex lithology model as the clay volume is already taken into consideration in the conversion from total to effective porosity.

Both saturation equations were processed, but the Waxman-Smits equation encountered problems when the clay volume was high. To enable comparison of the results of the two equations, it was necessary to filter out all data values from the water saturation curve where the clay volume was greater than 50%. Figure-12 displays a comparison of the results from these two equations over a section of the gas-bearing reservoir.

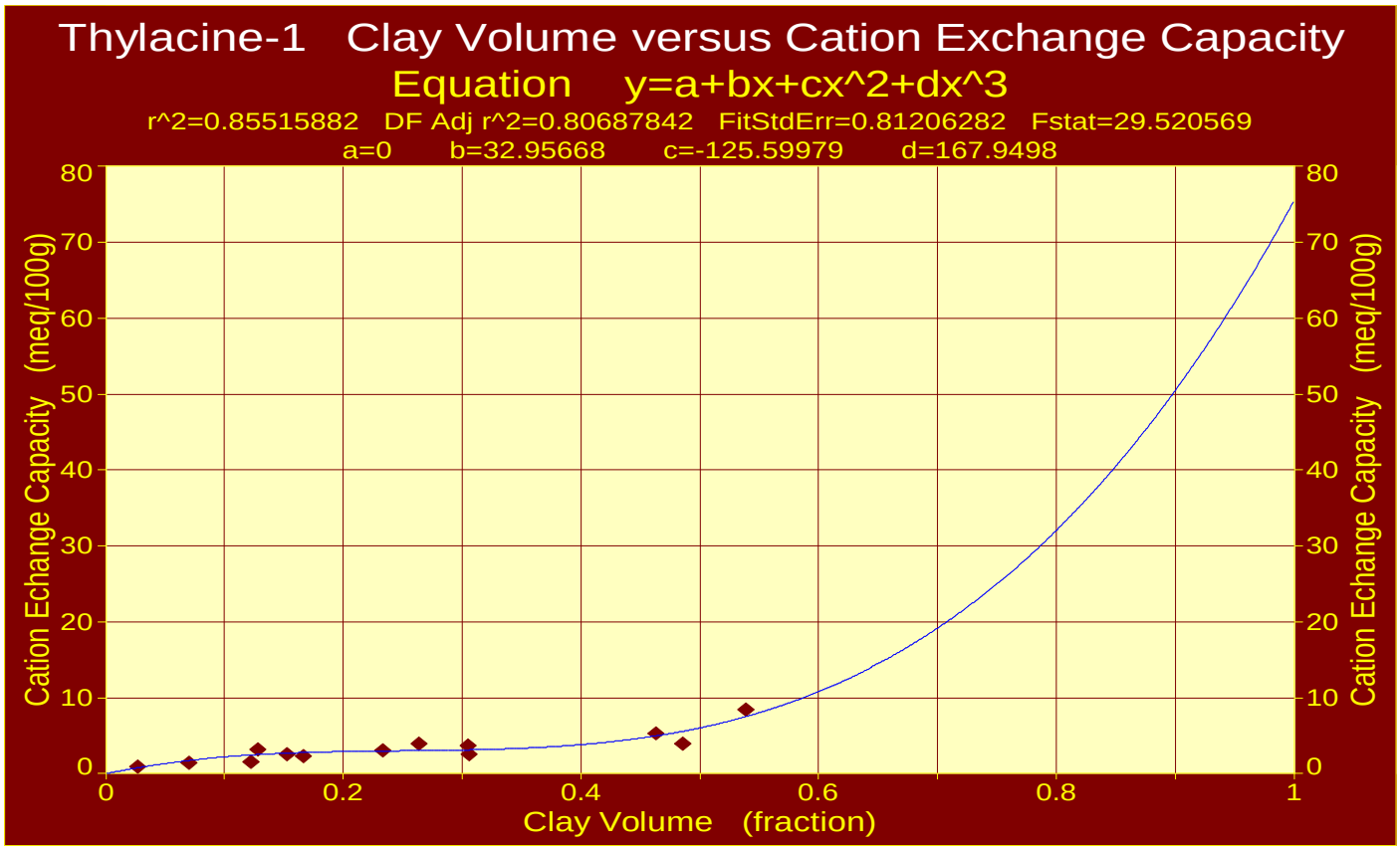

Figure-10. Derivation of a variable Qv, via the relationship between core-derived CEC and log-derived VCl.

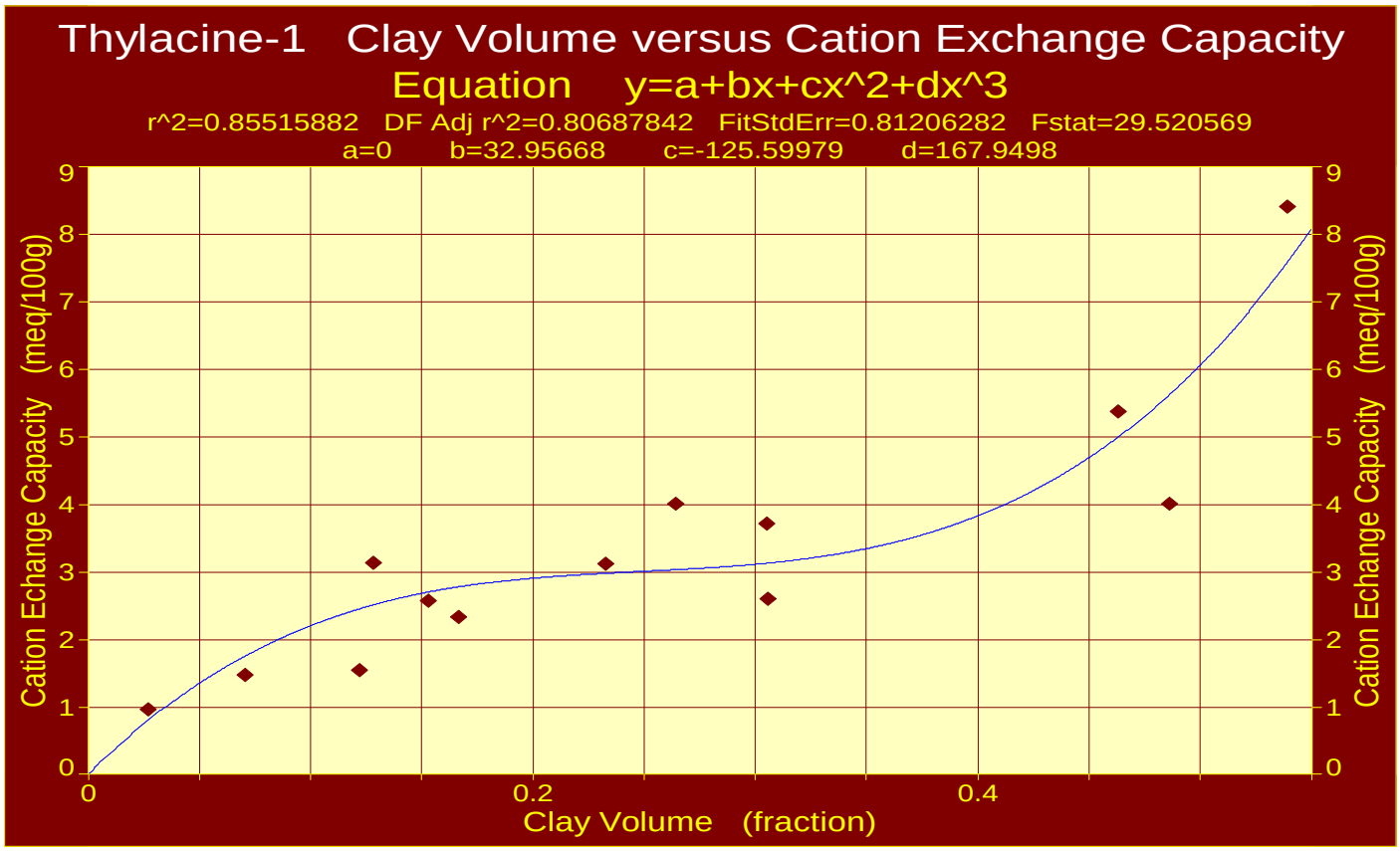

Figure-11. Zoomed view of the derived relationship between core-derived CEC and log-derived VCl.

It is evident that the derived water saturation from the Waxman-Smits saturation equation obtains a closer match to the core-derived irreducible water saturation (Cswi) capillary pressure measurements than does the Indonesian equation. Whilst this would suggest that the water saturations derived from the Waxman-Smits equation are more correct, significant portions of the reservoirs exhibiting the lowest clay volumes exhibit 99% hydrocarbon saturation, which is not considered to be possible.

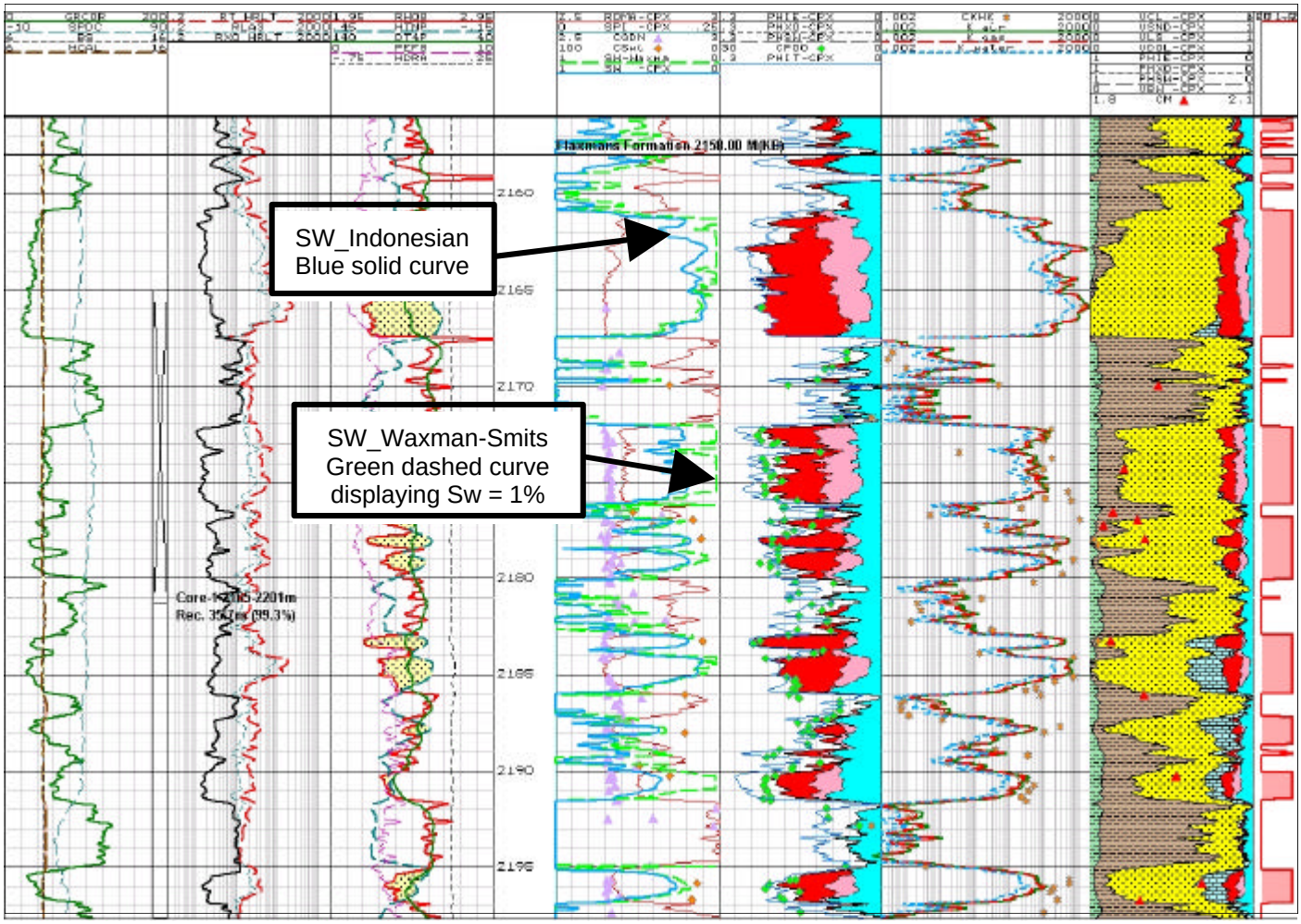

Figure-12. Comparison of results between the Indonesian and Waxman-Smits water saturation equations.

The y-intercept of the CEC versus VCl plots (Figures-10, 11) must be zero, so that in a perfectly clean sandstone (i.e. VCl = 0), the Waxman-Smits equation reverts to an Archie Equation. However, if the slope of the curve-fit of CEC versus VCl were higher between 0 and 10% VCl, this would reduce the calculated Sw from the Waxman-Smits Equation for these clean sandstones. This section of the curve is constrained by only two data points. With the addition of more data from Thylacine-2 and Geographe-1, it is envisaged that this correlation will be improved. However,

based on the current data, the results from the Indonesian Equation are considered more realistic and are quoted in the following text, and reservoir summaries.

Permeability

As a component of the special core analysis study, gas-slippage and Klinkenburg-corrected overburden permeabilities were measured from both horizontal and vertical core plugs. These data act as a reference for any log-derived permeability equation. Permeability is often correlated to porosity alone, but this correlation is fraught with inaccuracy, as there are other rock parameters that can affect permeability. The intrinsic permeability of a rock is affected by its clay content, as increasing clay content in the pore space will decrease the flow rate at which a fluid can pass, and also increase the pressure gradient required to make the fluid flow. A useful qualitative indicator of the distance which a fluid has been able to flow into a formation is given by the difference between the true formation resistivity and the invaded zone resistivity (Rt-Rxo). With decreasing flow rates of mud filtrate into a formation, the difference between these values diminishes.

As the core analysis data have been accurately depth-matched to wireline depths, it is possible to conduct a multiple linear regression of VCl, PHIT, and Rt-Rxo to derive an effective air permeability curve. This log-derived permeability is displayed on Enclosure-1, and is derived as

$$K_{Air} = 5.831 \times PHIT - 4.320 \times VCl - 0.849 \times \log(Rt - Rxo) - 0.100$$

This technique produces a 76% correlation co-efficient between the measured overburden Klinkenburg-corrected permeabilities and the log-derived gas permeabilities. This equation is valid only for this well, as data from Thylacine-2 and Geographe-1 have not been considered here. It is planned to produce a single permeability equation that is valid for the gas-bearing reservoirs in both fields as a component of a future study. This equation is only valid for reservoirs above the gas water contact (GWC), as the values for Rt and Rxo are affected by the nature of the fluid in the pore space. Although average permeabilities have been quoted for rocks below the GWC in subsequent sections of this report, it should be remembered that any reported average log-derived permeabilities in water-bearing strata would be expected to under-estimate true values.

The SCAL data were used to derive a correlation between the overburden air, and both gas and water permeabilities (Figures-13,14). These relationships were used to generate gas and water permeability curves, which are also only quantitative above the GWC.

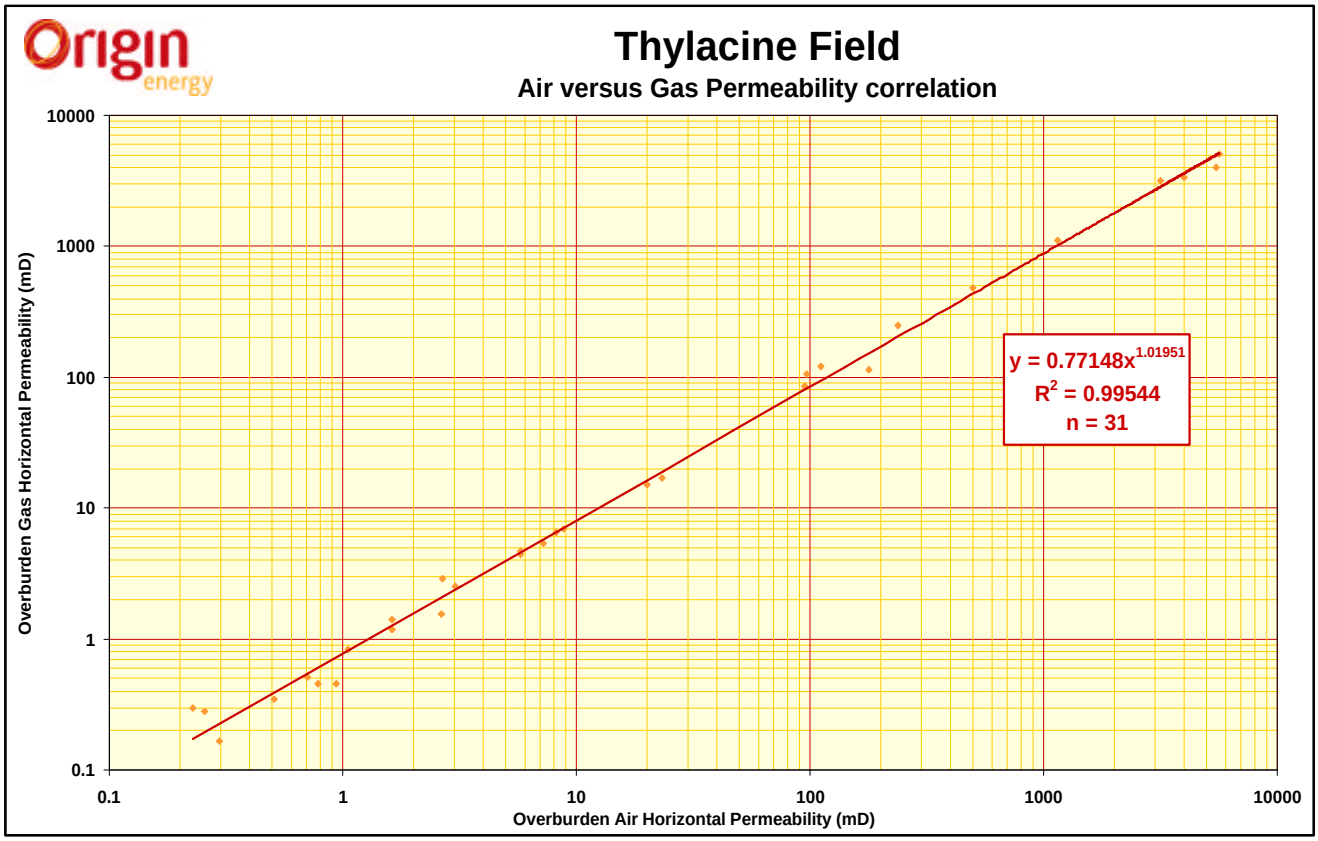

Figure-13. Relationship between core-derived overburden air permeability and gas permeability.

Reservoir Summary Parameters

The cut-off limits for petrophysical parameters are detailed in Table-8. A maximum clay volume of 40% is the basis of the net rock calculation. Net reservoir is defined as those net rocks having a log-derived overburden Klinkenburg-corrected horizontal air permeability of 0.1mD. Average effective water saturations are reported for zones above the gas-water contact. The petrophysical results are summarised in Table-9.

Reservoir	VCl < (%)	K > (mD)
Thylacine Member, Flaxmans Formation, Waarre Formation	40	0.1

Table-8. Cut Off Parameters

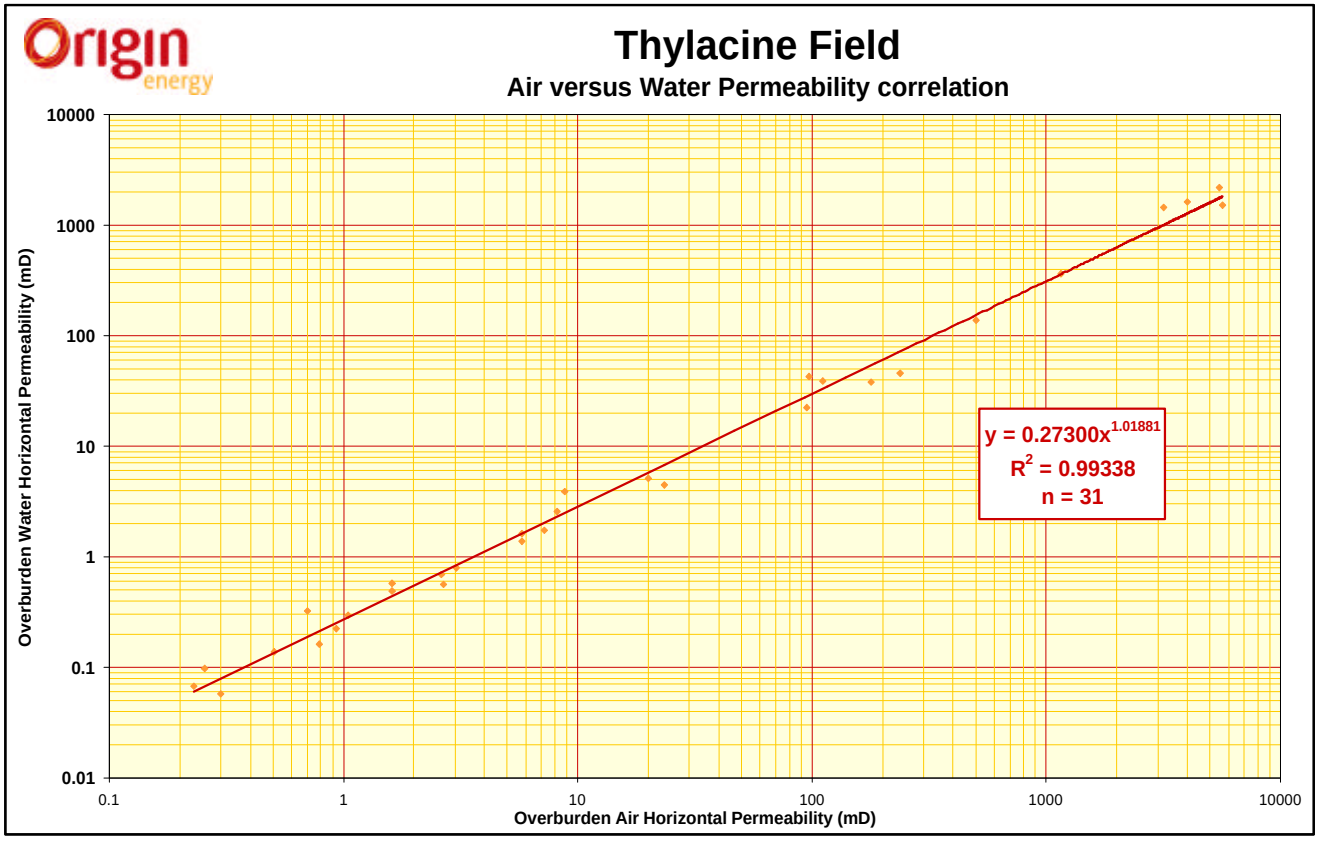

Figure-14. Relationship between core-derived overburden air permeability and water permeability.

FORMATION	TOP	BASE	GROSS	NET PAY	AVE.	AVE.	AVE.	AVE.	AVE.	AVE.	AVE.	NET RES /
NAME	FROM	TO	INTERVAL	INTERVL	VCL	PHIT	PHIE	AIR PERM	GAS PERM	WATER PERM	SWE	GROSS
	mMDRT	mMDRT	mMDRT	mMDRT	%	%	%	mD	mD	mD	%	%
Thylacine Member	2048.50	2158.00	109.50	47.50	26.42	20.51	15.46	10.89	8.61	3.17	52.50	43.38
Flaxmans Formation	2158.00	2273.30	115.30	50.07	16.91	19.92	16.70	25.90	20.82	7.74	46.73	43.43
Upp. Waarre Fm-GWC	2273.30	2325.60	52.30	41.94	14.58	19.58	16.95	33.62	27.16	10.13	49.06	80.19
		TOTAL	**277.10**	**139.51**	**19.45**	**20.02**	**16.35**	**20.86**	**16.69**	**6.19**	**49.39**	**50.35**
Upper Waarre Fm	2273.30	2424.20	150.90	101.40	17.79	19.15	16.01	8.90	7.01	2.58	77.16	67.20
Lower Waarre Fm	2424.20	2684.00	259.80	88.73	24.73	17.81	13.65	2.22	1.70	0.62	95.54	34.15

Table-9. Reservoir Summary

Fluid Contacts

A gas-oil contact cannot be identified from the logs, and it is assumed that the reservoir at the Thylacine-1 location does not contain an oil-leg. The lowermost gas-bearing sandstone is present at 2324.8-2325.5 mMDRT. A three-metre shale separates this sandstone from another this sandstone at 2328.5-2329.4 mMDRT, which is interpreted to contain only residual hydrocarbons. Therefore a gas-water contact is identified between 2325.5 and 2328.5 mMDRT, based upon these logs (Figure-12).

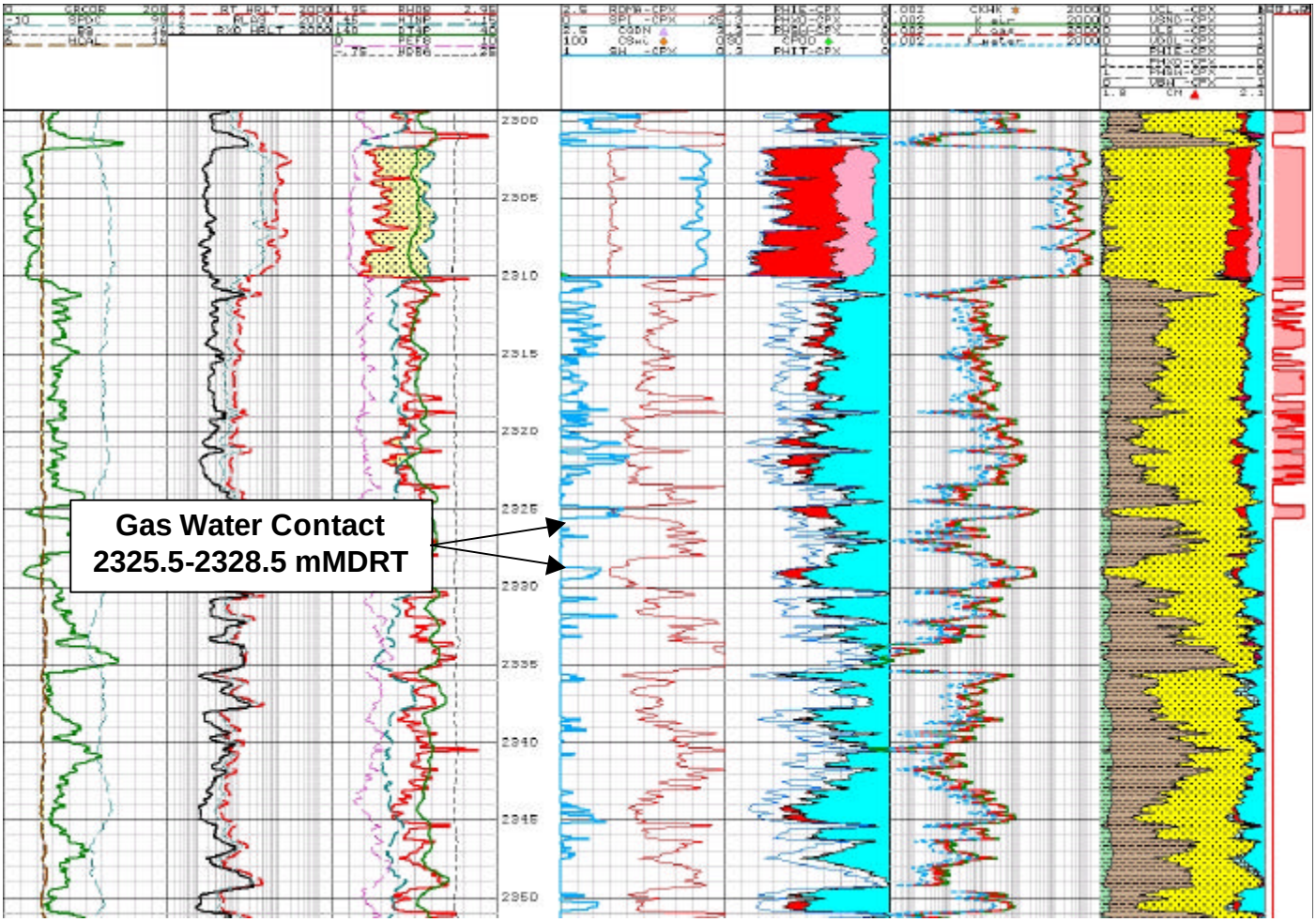

Figure-12. Gas-water contact, located between 2325.5 and 2328.5 mMDRT, as defined by the log analysis

DISCUSSION

The Thylacine Member (2048.5-2158.0 mMDRT) encountered at Thylacine-1 is interpreted to have moderate reservoir quality. The sandstones that are present contain high clay volumes, averaging 26.4%. Calculated effective porosities average only 15.5% for these reservoirs. As a result, the log-derived gas permeability is considerably reduced in comparison to other cleaner reservoirs,

averaging only 8.6mD, which will negatively affect this unit's producibility and recovery factor. The average effective water saturation is 52.5%, and the net reservoir to gross is 43%.

The Flaxmans Formation (2158.0-2273.3 mMDRT) appears to have better reservoir development. The sandstones present, on average, are cleaner than those above and have an average clay volume of 16.9%. The average effective porosity is higher (16.7%), and the gas permeability is significantly higher, averaging 20.8mD. This unit has a net reservoir to gross of 43%, and an average effective water saturation of 47%.

The interval between the top of the upper Waarre Formation and the interpreted GWC (2273.3-2325.6mMDRT) has the best average reservoir parameters. The average clay volume in this unit is only 14.6%, whilst the average effective porosity is similar to that for the Flaxmans Formation (17.0%). This unit is interpreted to have an 80% net reservoir to gross ratio, average effective water saturation of 16%, and very good gas permeabilities, averaging 27mD.

Between the four wells now present on the Thylacine and Geographe fields, sufficient core analysis data is present to calibrate the log responses, and no more core analysis is considered necessary.

Given the thinly-bedded nature of the Thylacine Member and Flaxmans Formation, it is recommended that all wireline logs are acquired in high resolution mode. To enable consistency in logging responses, and avoid subtle variations in the measurement of different company's logging tools, it is recommended that the same principle logging suite (PEx(HRLA)-DSI-SP) be run in subsequent wells. This is particularly relevant, as core to log correlations have been made using these data, and subsequent wells on these fields are unlikely to contain further cores.

The nature of the PEF data acquired by Schlumberger is of particular concern, as the quality of this curve directly affects the ability to distinguish the presence and volume of any carbonate cements present. The PEF data is severely affected by even small volumes of barite in the mud, as barite tends to come out of solution and concentrate in the mudcake. The estimation of the thickness and concentration of the barite in the mudcake is further hampered when the hole washes out. It is recommended that the addition of barite in the mud be limited, and if possible, not included.

The spectral gamma ray data are in agreement with the petrological analysis, in that the dominant clay mineral is kaolinite. These spectral gamma ray data also infer that the clay type present in the sandstones, is of the same chemistry to those present in the shales. Therefore, little benefit is being added by this log, and it is recommended that acquisition of the spectral gamma ray tool is not necessary in future wells.

The LWD data acquired by Anadrill were not utilised in the interpretation of fluid saturations, as they are responding with lower values than those measured using the wireline devices, presumably due to the highly porous and permeable nature of these reservoirs encouraging the deep invasion of mud filtrate. It is not recommended that LWD be acquired in future wells for the purposes of petrophysical evaluation.

CONCLUSIONS / RECOMMENDATIONS

- The Thylacine Member (2048.5-2158.0 mMDRT) contains sandstones that, due to their argillaceous nature, would be likely to be capable of only moderate producibility.
- The Flaxmans and upper Waarre Formations (2158.0-2325.6 mMDRT) contains cleaner and more porous and permeable sandstones that would be expected to achieve high gas production rates.
- The reservoirs are sufficiently simple mineralogically to warrant removing the spectral gamma ray from future logging suites.
- Core-to-log correlations of porosity and permeability are adequate to suggest that the acquisition of further core and core analysis data would not significantly increase the confidence level applied to the petrophysical analysis.
- The addition of barite to the mud should be limited or eradicated if possible, in order to improve the quality and reliability of PEF data in future wells.
- There is no petrophysical requirement to acquire LWD data in future wells, as the wireline resistivity data is considered a more reliable indicator of the nature and volume of the fluids in the pore space.

APPENDIX - A
Log Depth-matching Summary

MUDLOG TO WIRELINE

```
DEPTH MATCH LOGS - MNEMONIC
ROP TGAS WOB RPM SPP FLOW SPM TQAV TQMA LAG TPIN TPOT MWIN MWOT Dxc BITD BITT TBR TVD
C1 C2 C3 C4 iC4 nC4 C5 iC5 nC5 CO2 CALC DOLO
PRIMARY CURVE NO.  =   1

REFERENCE LOGS - MNEMONIC
ECGR RHOZ

DEPTH UNITS = M
   148.692   148.692
   622.402   623.316
   711.454   711.911
   784.504   785.927
   793.496   795.172
   830.885   831.545
   853.592   854.253
   940.562   941.527
   985.368   986.028
  1004.468  1005.332
  1046.480  1047.090
  1055.167  1055.370
  1078.687  1079.652
  1114.654  1114.654
  1128.522  1128.167
  1144.372  1143.864
  1152.398  1153.211
  1161.491  1161.339
  1170.584  1171.702
  1180.389  1182.167
  1215.644  1217.828
  1247.546  1249.223
  1267.460  1268.781
  1307.338  1307.744
  1345.692  1345.032
  1380.388  1379.982
  1400.708  1401.318
  1479.499  1479.296
  1517.396  1515.770
  1551.635  1551.432
  1576.527  1576.730
  1584.655  1585.265
  1608.531  1609.903
  1628.546  1629.563
  1665.529  1666.596
  1703.476  1704.289
  1724.609  1725.473
  1770.888  1770.990
  1788.516  1788.973
```

```
  1926.488  1926.285
  1968.551  1968.449
  2006.549  2005.330
  2048.662  2049.120
  2059.483  2060.651
  2089.556  2091.843
  2114.499  2115.515
  2137.461  2139.086
  2170.532  2172.208
  2177.695  2179.523
  2188.667  2190.496
  2220.468  2220.417
  2228.850  2229.460
  2238.197  2238.248
  2258.314  2257.806
  2270.455  2269.896
  2301.342  2300.123
  2311.552  2310.029
  2336.597  2335.937
  2345.538  2344.979
  2361.083  2361.997
  2379.574  2380.945
  2390.445  2392.528
  2411.578  2412.238
  2429.256  2429.561
  2448.357  2448.814
  2458.669  2459.685
  2481.936  2483.206
  2515.362  2516.327
  2544.470  2545.944
  2575.560  2577.541
  2604.211  2606.091
  2624.582  2627.274
  2636.622  2637.943
  2661.666  2662.479
```

MWD TO WIRELINE

```
DEPTH MATCH LOGS - MNEMONIC
GR_ARC_F A16H_UNC A22H_UNC A28H_UNC A34H_UNC A40H_UNC P16H_UNC P22H_UNC P28H_UNC
P34H_UNC P40H_UNC ROP5_RM
PRIMARY CURVE NO.  =   1

REFERENCE LOGS - MNEMONIC
ECGR

DEPTH UNITS = M
  1859.077  1861.160
  1865.935  1868.068
  1879.295  1881.683
  1897.583  1900.276
  1908.099  1910.740
  1914.246  1916.938
  1930.552  1932.940
```

1944.776	1947.113
1954.428	1956.664
1969.262	1971.446
2006.041	2008.022
2020.011	2021.942
2039.722	2041.754
2050.745	2052.574
2064.106	2066.392
2073.707	2075.993
2090.268	2092.604
2099.412	2101.799
2113.178	2115.719
2129.079	2131.873
2147.672	2150.466
2157.171	2159.915
2167.077	2170.430
2177.288	2180.844
2206.803	2208.530
2223.110	2224.989
2237.893	2239.620
2255.469	2257.349
2271.878	2274.113
2282.647	2284.984
2299.361	2301.901
2308.555	2311.197
2324.049	2326.691
2337.562	2340.509
2355.291	2358.441
2373.529	2376.830
2386.533	2390.242
2396.185	2399.843
2412.238	2415.794
2428.596	2431.796
2445.512	2448.865
2462.733	2466.340
2477.770	2481.428
2494.788	2498.344
2508.809	2512.568
2520.493	2524.151
2531.720	2535.377
2544.217	2548.179
2559.710	2563.724
2572.715	2576.779
2586.177	2590.241
2599.589	2603.805
2610.104	2614.168
2623.820	2628.087
2634.488	2638.552
2650.795	2654.707
2667.407	2671.064

CORE TO WIRELINE

DEPTH MATCH LOGS - MNEMONIC
CPOO COGR CKHP CPOR CKHK CKVK CGDN SNUM CM CM* CCEC CQv CN CN* CSw CSwi CKg CKw
PRIMARY CURVE NO. = 1

REFERENCE LOGS - MNEMONIC
PHIT-CPX

DEPTH UNITS = M

2168.800	2168.550
2172.440	2172.230
2173.340	2173.320
2176.530	2176.610
2178.010	2177.960
2182.010	2181.790
2183.460	2183.330
2187.300	2187.140
2189.800	2189.660
2196.230	2196.070
2202.850	2202.610

APPENDIX - B
Petrophysical Parameter Listing

```
LOG ANALYSIS REPORT BY PETROLOG REVISION  9.10
File name: thylacine_1_petro.pro    13/03/2003  13:36:51

          Company           : ORIGIN ENERGY RESOURCES LTD
          Well Name         : THYLACINE-1
          Field             : Thylacine
          Country           : Australia
          State             : Tasmania
          Field Location    : Otway Basin
          Latitude          : 039 14' 27.592" S    DMS
          Longitude         : 142 54' 44.169" E    DMS
          Permanent Datum   : LAT
          Elevation of PD   :        .00 M

          Hole depth M     Temperature C     Gradient Deg C / 100 M
              2713.0          104.40          3.0010
              1833.3           78.00          2.8001
                  .0           26.67

          Log data
          Column     Logs       Logs
          Position   Available  Used
              1      DEPT       DEPT
              2      ECGR
              3      SPDC       SP
              4      BS
              5      DT4S
              6      HCAL       CALI
              7      HDRA       DRHO
              8      PEFZ
              9      RHOZ
             10      RLA1
             11      RLA2
             12      RLA3       LLS
             13      RLA4
             14      RLA5
             15      RT_H       ERT
             16      RXO_       MSFL
             17      TNPH
             18      HCGR
             19      HFK        POTA
             20      HSGR
             21      HTHO       THOR
             22      HTPR       THK
             23      HTUR
             24      HUPR
             25      HURA       URAN
             26      RXOZ
             27      DT4P       DT
             28      RHO8       RHOB
             29      EHGR
             30      HTNP       NPHI
             31      PEF8       PEF
             32      RXO8
             33      SP
             34      LITH
             35      MUD_
             36      ROP
             37      WOB
             38      RPM
             39      SPP
             40      FLOW
             41      SPM
             42      TQAV
             43      TGAS
             44      C1
             45      C2
             46      C3
             47      C4
             48      iC4
             49      nC4
             50      C5
             51      iC5
```

52	nC5	
53	CO2	
54	CALC	
55	DOLO	
56	RCA_	
57	COGR	
58	CKHP	
59	CPOR	
60	CPOO	
61	CKHK	
62	CKVK	
63	CGDN	
64	SNUM	
65	CM	
66	CM*	
67	CCEC	
68	CQv	
69	CN	
70	CN*	
71	CSw	
72	CSwi	
73	CKg	
74	CKw	
75	GR_K	
76	GRCO	GR
77	FLAG	FLAG
78	Rt-R	
79	log(	
80	log(	
81	K_ai	
82	K_ga	
83	K_wa	
84	NET	
85	NET	

```
                        Caliper recorded in : Inches
                        Mud weight units    : g/cc
                        Density log units   : g/cc
                        DRHO    log units   : g/cc
                        Sonic   log units   : Us/ft
                        Neutron log units   : LS POR
                        Density tool type   : LDT
                        RHO (H,MA,f)  units : g/cc
                        Dens. X-plots units : g/cc
                        GRV units           : Mbbl
```

Log scaling data

Log Mnemonic	Scaling Option	Coeff. A	Coeff. B
PEF	1	.40000	1.00000

Mineral table

Zone no.	1	2	3	4	5	6	7	8	9	10
Formation Name	BelfastM	Flaxmans	Flaxmans	Flaxmans	Flaxmans	UpperWaa	UpperWaa	UpperWaa	UpperWaa	UpperWaa
Top depth	2000.000	2048.750	2048.750	2048.750	2048.750	2158.310	2158.310	2158.310	2158.310	2335.157
Bottom depth	2048.750	2158.310	2158.310	2158.310	2158.310	2335.148	2335.148	2335.148	2335.148	2613.670
USER Log type	RHO8	RHO8	RHO8	RHO8	RHO8	RHO8	RHO8	RHO8	RHO8	RHO8
Coal USER min	.000	.000	.000	.000	.000	.000	.000	.000	.000	.000
Coal USER max	2.000	2.000	2.000	2.000	2.000	2.000	2.000	2.000	2.000	2.000

Zone no.	11	12	13	14
Formation Name	UpperWaa	UpperWaa	UpperWaa	LowerWaa
Top depth	2335.157	2335.157	2335.157	2613.670
Bottom depth	2613.670	2613.670	2613.670	2713.000
USER Log type	RHO8	RHO8	RHO8	RHO8
Coal USER min	.000	.000	.000	.000
Coal USER max	2.000	2.000	2.000	2.000

Lithology models

1.	Sand-Dolomite	2.64 to	2.89
2.	Sand-Limestone	2.64 to	2.75
3.	Sand	2.64 to	2.69
4.	Limestone	2.67 to	2.75
5.	Dolomite	2.75 to	2.89
6.	Limestone-Dolomite	2.68 to	2.89

CPX flag values

1. VCL greater than 0.95
2. VN greater than 0.75
3. VS greater than 0.75

```
   4.  Bad hole condition
   5.  Matrix density greater than Lithological model
   6.  Matrix density less than Lithological model
   7.  Porosity derived from Sonic Log
   8.  Porosity derived from or limited by PHIMAX
   9.  Porosity derived from Density Log
   $.  Pay zone

Water saturation equations
   1.  Indonesia
   2.  Simandoux
   3.  Fertl & Hammock
   4.  Laminar
   5.  Bussian
   6.  User defined
   7.  Single Sonic

VGRTYPE :Vclay from GR Equations used
   0.  Not Used
                        IGR=(GR-GRmin)/(GRmax-GRmin)
   1.  Linear           VGR=IGR
   2.  Asymmetric (S shaped)
          Defined by 2 sets of intermediate points
          through which the S bend passes through.
          GR1, VGR1 and GR2, VGR2.
       Steiber equation:  VGR= IGR/(A + (A-1.0)*IGR)
   3.  Steiber 1  A = 2.0
   4.  Steiber 2  A = 3.0
   5.  Steiber 3  A = 4.0
   6.  Steiber 50%
        A is computed to give VGR= 0.5 when GR = GR50%)
   7.  Larinov Old Rocks: VGR= (2**(2*IGR)-1.0)/3.0
   8.  Larinov Tertiary : VGR= 0.083*(2.0*(3.7058*IGR)-1.0)
   9.  Clavier          : VGR= 1.7-SQRT(3.38-(IGR+0.7)**2.0)

Cementation factor m
   1.  Linear        m = m
   2.  Shell formula m = 1.87 + 0.019/PHI
   3.  Borai formula m = 2.2 -0.035/(PHI+0.042)

             THYLACINE-1                        Complex Lithology Results
             ORIGIN ENERGY RESOURCES LTD        13-03-2003
                           Neutron               RT Determination
Logging Company   Mud type    log type           Flags by priority
0. Schlumberger   0. NaCl     0. CNL CORR        23. ERT (external RT)
1. HLS            1. KCl %    1. TNPH             1. Dual Laterolog - RXO
2. Dresser        2. Oil-base 2. SNP             20. PHASOR-SFL
3. BPB/Reeves     3. Barite   3. N               21. PHASOR-RXO
4. Sperry MWD                 4. HLS DSN2         2. Dual Induction - LL8
5. Baker MWD                  5. CNL PRE 86       3. ILD-SFL-RXO
6. Anadril MWD                6. APLU            10. DIL-SFL
7. Computalog                 7. FPLU            11. DIL-LL3
8. Probe                      8. CDN 6.5"         8. ILD & 16 inch Normal
9. Tucker                     9. CDN 8.0"        17. LLD-LLS
Formation                    10. ADN 6.75        18. ID PHASOR
Water                        11. ATLAS 2435 CN    4. ILD
0=NaCl                       12. ATLAS 2420 CN    5. LLD
1=NaHCO3                     13. ATLAS SNP        6. LL3 or LL7
                             14. BPB/Reeves       7. Dual Laterolog
                             15. HLS G           13. LLS
                             16. Tucker_SNP      19. IM PHASOR
                             17. Tucker_CNL      14. ILM
                                                 15. LL8
                                                  9. 64 inch Normal Log
                                                 12. SFL
                                                 22. N16
                                                 16. RXO
                                                  0. No RT logs
```

Zone no.	1	2	3	4	5	6	7	8	9	10
Formation Name	BelfastM	Flaxmans	Flaxmans	Flaxmans	Flaxmans	UpperWaa	UpperWaa	UpperWaa	UpperWaa	UpperWaa
Top depth	2000.000	2048.750	2048.750	2048.750	2048.750	2158.310	2158.310	2158.310	2158.310	2335.157
Bottom depth	2048.750	2158.310	2158.310	2158.310	2158.310	2335.148	2335.148	2335.148	2335.148	2613.670
Logging Company	0	0	0	0	0	0	0	0	0	0
Mud type	4	4	4	4	4	4	4	4	4	4
Formation Water Type	0	0	0	0	0	0	0	0	0	0
Neutron Log Type	1	1	1	1	1	1	1	1	1	1

Zone no.	11	12	13	14
Formation Name	UpperWaa	UpperWaa	UpperWaa	LowerWaa
Top depth	2335.157	2335.157	2335.157	2613.670

Bottom depth	2613.670	2613.670	2613.670	2713.000
Logging Company	0	0	0	0
Mud type	4	4	4	4
Formation Water Type	0	0	0	0
Neutron Log Type	1	1	1	1

	Zone no.	1	2	3	4	5	6	7	8	9	10
	Formation	BelfastM	Flaxmans	Flaxmans	Flaxmans	Flaxmans	UpperWaa	UpperWaa	UpperWaa	UpperWaa	UpperWaa
1.	Top depth	2000.000	2048.750	2048.750	2048.750	2048.750	2158.310	2158.310	2158.310	2158.310	2335.157
2.	Bottom depth	2048.750	2158.310	2158.310	2158.310	2158.310	2335.148	2335.148	2335.148	2335.148	2613.670
3.	No logs										
4.	No logs	.000	.000	.000	.000	.000	.000	.000	.000	.000	.000
5.	RM	.0940000	.0940000	.0940000	.0940000	.0940000	.0940000	.0940000	.0940000	.0940000	.0940000
6.	Temp. RM	20.000	20.000	20.000	20.000	20.000	20.000	20.000	20.000	20.000	20.000
7.	RMF	.0742000	.0742000	.0742000	.0742000	.0742000	.0742000	.0742000	.0742000	.0742000	.0742000
8.	Temp. RMF	20.000	20.000	20.000	20.000	20.000	20.000	20.000	20.000	20.000	20.000
9.	RMC	.455	.455	.455	.455	.455	.455	.455	.455	.455	.455
10.	Temp. RMC	20.000	20.000	20.000	20.000	20.000	20.000	20.000	20.000	20.000	20.000
11.	Bit size	8.500	8.500	8.500	8.500	8.500	8.500	8.500	8.500	8.500	8.500
12.	Mud wt	1.330	1.330	1.330	1.330	1.330	1.330	1.330	1.330	1.330	1.330
13.	SSP	.000	.000	.000	.000	.000	.000	.000	.000	.000	.000
14.	RW (SP)	.0292780	.0286319	.0286319	.0286319	.0286319	.0275328	.0275328	.0275328	.0275328	.0259489
15.	Temperature	83.734	86.110	86.110	86.110	86.110	90.407	90.407	90.407	90.407	97.240
16.	RW @ FT	.196	.192	.192	.192	.192	.185	.185	.185	.185	.174
17.	RW@75F(23.9C	.455	.455	.455	.455	.455	.455	.455	.455	.455	.455
18.	RW salinity	13000.000	13000.000	13000.000	13000.000	13000.000	13000.000	13000.000	13000.000	13000.000	13000.000
19.	RMF @ FT	.0292780	.0286319	.0286319	.0286319	.0286319	.0275328	.0275328	.0275328	.0275328	.0259489
20.	RMF salinity	.115	.115	.115	.115	.115	.115	.115	.115	.115	.115
21.	RM @ FT	.0370907	.0362722	.0362722	.0362722	.0362722	.0348798	.0348798	.0348798	.0348798	.0328733
22.	RHO H	.500	.500	.500	.500	.500	.500	.500	.500	.500	.500
23.	Gas Flag	1.000	1.000	1.000	1.000	1.000	1.000	1.000	1.000	1.000	1.000
24.	RHO F	1.071	1.070	1.070	1.070	1.070	1.070	1.070	1.070	1.070	1.068
25.	t F	188.969	188.969	188.969	188.969	188.969	188.969	188.969	188.969	188.969	188.969
26.	RHOMA	2.680	2.650	2.650	2.650	2.650	2.630	2.630	2.630	2.630	2.630
27.	PHIN min	-.0350000	-.0350000	-.0350000	-.0350000	-.0350000	-.0350000	-.0350000	-.0350000	-.0350000	-.0350000
28.	t MA	55.500	55.500	55.500	55.500	55.500	55.500	55.500	55.500	55.500	55.500
29.	t MA min	48.000	48.000	48.000	48.000	48.000	48.000	48.000	48.000	48.000	48.000
30.	Sonic option	.000	.000	.000	.000	.000	.000	.000	.000	.000	.000
31.	Compact/Ovrt	1.000	1.000	1.000	1.000	1.000	1.000	1.000	1.000	1.000	1.000
32.	CAL cut off	16.000	16.000	16.000	16.000	16.000	16.000	16.000	16.000	16.000	16.000
33.	RUGO.cut off	1.000	1.000	1.000	1.000	1.000	1.000	1.000	1.000	1.000	1.000
34.	DRHO cut off	.150	.150	.150	.150	.150	.150	.150	.150	.150	.150
35.	Bad Hole	.000	.000	.000	.000	.000	.000	.000	.000	.000	.000
36.	No clay	SP	SP	SP	SP	SP	SP	SP	SP	SP	SP
		RT	RT	RT	RT	RT	RT	RT	RT	RT	RT
		N	N	N	N	N	N	N	N	N	N
		MN	MN	MN	MN	MN	MN	MN	MN	MN	MN
		SN	SN	SN	SN	SN	SN	SN	SN	SN	SN
37.	Vclay Flag	.000	.000	.000	.000	.000	.000	.000	.000	.000	.000
38.	Vclay type	.000	.000	.000	.000	.000	.000	.000	.000	.000	.000
39.	Vclay inp1	.200	.200	.200	.200	.200	.200	.200	.200	.200	.200
40.	Vclay out1	.150	.150	.150	.150	.150	.150	.150	.150	.150	.150
41.	Vclay inp2	.800	.800	.800	.800	.800	.800	.800	.800	.800	.800
42.	Vclay out2	.800	.800	.800	.800	.800	.800	.800	.800	.800	.800
43.	Vclay 50%	.500	.500	.500	.500	.500	.500	.500	.500	.500	.500
44.	VclayGR type	1.000	1.000	1.000	1.000	1.000	1.000	1.000	1.000	1.000	1.000
45.	GR clean	17.969	17.969	17.969	17.969	17.969	17.969	17.969	17.969	17.969	17.969
46.	GR clay	123.059	123.059	123.059	123.059	123.059	123.059	123.059	123.059	123.059	123.059
47.	GR1	36.000	36.000	36.000	36.000	36.000	36.000	36.000	36.000	36.000	36.000
48.	VGR1	.100	.100	.100	.100	.100	.100	.100	.100	.100	.100
49.	GR2	84.000	84.000	84.000	84.000	84.000	84.000	84.000	84.000	84.000	84.000
50.	VGR2	.800	.800	.800	.800	.800	.800	.800	.800	.800	.800
51.	GR50%	70.000	70.000	70.000	70.000	70.000	70.000	70.000	70.000	70.000	70.000
52.	R clay	49.000	49.000	49.000	49.000	49.000	49.000	49.000	49.000	49.000	49.000
53.	R limit	1000.000	1000.000	1000.000	1000.000	1000.000	1000.000	1000.000	1000.000	1000.000	1000.000
54.	Rclay1 flag	.000	.000	.000	.000	.000	.000	.000	.000	.000	.000
55.	Rclay1	1.000	1.000	1.000	1.000	1.000	1.000	1.000	1.000	1.000	1.000
56.	Vcl @ Rclay1	.150	.150	.150	.150	.150	.150	.150	.150	.150	.150
57.	RHOB sand	2.150	2.150	2.150	2.150	2.150	2.231	2.231	2.231	2.231	2.231
58.	RHOB silt	2.620	2.620	2.620	2.620	2.620	2.620	2.620	2.620	2.620	2.620
59.	RHOB clay	2.570	2.570	2.570	2.570	2.570	2.570	2.570	2.570	2.570	2.570
60.	RHO Dry Clay	2.700	2.700	2.700	2.700	2.700	2.700	2.700	2.700	2.700	2.700
61.	Rhob Calcite	2.850	2.850	2.850	2.850	2.850	2.850	2.850	2.850	2.850	2.850
62.	PHIN Sand	.250	.250	.250	.250	.250	.229	.229	.229	.229	.229
63.	PHIN silt	.0200000	.0200000	.0200000	.0200000	.0200000	.0200000	.0200000	.0200000	.0200000	.0200000
64.	PHIN clay	.356	.356	.356	.356	.356	.356	.356	.356	.356	.356
65.	Phin Calcite	.100	.100	.100	.100	.100	.100	.100	.100	.100	.100
66.	PHISILT	.0200000	.0200000	.0200000	.0200000	.0200000	.0200000	.0200000	.0200000	.0200000	.0200000
67.	Calcite Flag	.000	.000	.000	.000	.000	.000	.000	.000	.000	.000
68.	t clay	85.603	85.603	85.603	85.603	85.603	85.603	85.603	85.603	85.603	85.603
69.	M clay	.689	.689	.689	.689	.689	.689	.689	.689	.689	.688

70.	N clay	.430	.429	.429	.429	.429	.429	.429	.429	.429	.429
71.	PHIN 2.2	.235	.211	.211	.211	.211	.0733353	.0733353	.0733353	.0733353	.214
72.	t 2.2	90.000	90.000	90.000	90.000	90.000	86.692	86.692	86.692	86.692	86.692
73.	a	1.000	1.000	1.000	1.000	1.000	1.000	1.000	1.000	1.000	1.000
74.	A1	1.000	1.000	1.000	1.000	1.000	1.000	1.000	1.000	1.000	1.000
75.	m	2.350	2.000	1.800	2.000	2.350	2.000	1.800	2.000	2.350	2.000
76.	m1	2.500	2.150	1.950	2.150	2.500	2.150	1.950	2.150	2.500	2.150
77.	m Function	1.000	1.000	1.000	1.000	1.000	1.000	1.000	1.000	1.000	1.000
78.	n	2.150	2.000	1.750	1.950	2.150	2.000	1.750	1.950	2.150	2.000
79.	n1	2.450	2.250	2.050	2.250	2.450	2.250	2.050	2.250	2.450	2.250
80.	B from BQV	14.714	14.026	14.026	14.026	14.026	11.125	11.125	11.125	11.125	11.569
81.	A(QV)	.0003050	.0003050	.0003050	.0003050	.0003050	.0003050	.0003050	.0003050	.0003050	.0003050
82.	B(QV)	-3.450	-3.450	-3.450	-3.450	-3.450	-3.450	-3.450	-3.450	-3.450	-3.450
83.	Lithomod	1.000	1.000	1.000	1.000	1.000	1.000	1.000	1.000	1.000	1.000
84.	SXO limit	.200	.200	.200	.200	.200	.200	.200	.200	.200	.200
85.	PHI max	.309	.268	.268	.268	.268	.270	.270	.270	.270	.270
86.	PHI min c.o.	.0010000	.0010000	.0010000	.0010000	.0010000	.0010000	.0010000	.0010000	.0010000	.0010000
87.	EXPX	1.500	1.500	1.500	1.500	1.500	1.500	1.500	1.500	1.500	1.500
88.	Clay cut off	.400	.400	.400	.400	.400	.400	.400	.400	.400	.400
89.	PHIe cut off	.0500000	.0500000	.0500000	.0500000	.0500000	.0500000	.0500000	.0500000	.0500000	.0500000
90.	PHIt cut off	.100	.100	.100	.100	.100	.100	.100	.100	.100	.100
91.	SWe cut off	.500	.500	.500	.500	.500	.500	.500	.500	.500	.500
92.	SWt cut off	.600	.600	.600	.600	.600	.600	.600	.600	.600	.600
93.	GrossRockVol	.000	.000	.000	.000	.000	.000	.000	.000	.000	.000
94.	Oil Exp.Fact	1.200	1.200	1.200	1.200	1.200	1.200	1.200	1.200	1.200	1.200
95.	FormGeom.Fac	1.000	1.000	1.000	1.000	1.000	1.000	1.000	1.000	1.000	1.000
96.	RecoveryFact	.200	.200	.200	.200	.200	.200	.200	.200	.200	.200
97.	SWB max	1.000	1.000	1.000	1.000	1.000	1.000	1.000	1.000	1.000	1.000
98.	RWB	1.157	1.975	1.975	1.975	1.159	1.838	1.838	1.838	1.288	1.838
99.	SWB cut off	.300	.300	.300	.300	.300	.300	.300	.300	.300	.300
100.	RWF	.196	.192	.192	.192	.192	.185	.185	.185	.185	.174
101.	RMFF	.0292780	.0286319	.0286319	.0286319	.0286319	.0275328	.0275328	.0275328	.0275328	.0259489
102.	Sw Eq. CPX	1.000	1.000	1.000	1.000	1.000	1.000	1.000	1.000	1.000	1.000
103.	Sw Eq. SSS	1.000	1.000	1.000	1.000	1.000	1.000	1.000	1.000	1.000	1.000
104.	Glauconite	.000	.000	.000	.000	.000	.000	.000	.000	.000	.000
105.	SWirr.cutoff	.300	.300	.300	.300	.300	.300	.300	.300	.300	.300
106.	Perm Expon.	6.000	6.000	6.000	6.000	6.000	6.000	6.000	6.000	6.000	6.000
107.	PERM K coef	62500.000	62500.000	62500.000	62500.000	62500.000	62500.000	62500.000	62500.000	62500.000	62500.000
108.	RHOMA 1	2.680	2.650	2.650	2.650	2.650	2.630	2.630	2.630	2.630	2.630
109.	RHOMA 2	2.810	2.810	2.810	2.810	2.810	2.810	2.810	2.810	2.810	2.810
110.	RHOMA 3	3.488	3.488	3.488	3.488	3.488	3.488	3.488	3.488	3.488	3.488
111.	UMA 1	4.800	4.800	4.800	4.800	4.800	4.800	4.800	4.800	4.800	4.800
112.	UMA 2	27.896	27.896	27.896	27.896	27.896	27.896	27.896	27.896	27.896	27.896
113.	UMA 3	18.632	18.632	18.632	18.632	18.632	18.632	18.632	18.632	18.632	18.632
114.	UF	.400	.400	.400	.400	.400	.400	.400	.400	.400	.400
115.	UMACL	13.237	13.237	13.237	13.237	13.237	13.237	13.237	13.237	13.237	13.237
116.	GR Dispersed	96.470	96.470	96.470	96.470	96.470	96.470	96.470	96.470	96.470	96.470
117.	PHIT Dispers	.0003432	.0003432	.0003432	.0003432	.0003432	.0003432	.0003432	.0003432	.0003432	.0003432
118.	PHIT Laminat	.143	.143	.143	.143	.143	.143	.143	.143	.143	.143
119.	PHIT Sand	.225	.225	.225	.225	.225	.225	.225	.225	.225	.225
93.	PHINmat1	.200	.200	.200	.200	.200	.200	.200	.200	.200	.200
94.	PHIDmat1	.240	.240	.240	.240	.240	.240	.240	.240	.240	.240
95.	PHINmat2	.350	.350	.350	.350	.350	.350	.350	.350	.350	.350
96.	PHIDmat2	.200	.200	.200	.200	.200	.200	.200	.200	.200	.200
97.	PHINmat3	.050	.050	.050	.050	.050	.050	.050	.050	.050	.050
98.	PHIDmat3	.000	.000	.000	.000	.000	.000	.000	.000	.000	.000
99.	PHINmat4	.200	.200	.200	.200	.200	.200	.200	.200	.200	.200
100.	PHIDmat4	-.100	-.100	-.100	-.100	-.100	-.100	-.100	-.100	-.100	-.100

	Zone no.	11	12	13	14
	Formation	UpperWaa	UpperWaa	UpperWaa	LowerWaa
1.	Top depth	2335.157	2335.157	2335.157	2613.670
2.	Bottom depth	2613.670	2613.670	2613.670	2713.000
3.	No logs				
4.	No logs	.000	.000	.000	.000
5.	RM	.0940000	.0940000	.0940000	.0940000
6.	Temp. RM	20.000	20.000	20.000	20.000
7.	RMF	.0742000	.0742000	.0742000	.0742000
8.	Temp. RMF	20.000	20.000	20.000	20.000
9.	RMC	.455	.455	.455	.455
10.	Temp. RMC	20.000	20.000	20.000	20.000
11.	Bit size	8.500	8.500	8.500	8.500
12.	Mud wt	1.330	1.330	1.330	1.330
13.	SSP	.000	.000	.000	.000
14.	RW (SP)	.0259489	.0259489	.0259489	.0247668
15.	Temperature	97.240	97.240	97.240	102.909
16.	RW @ FT	.174	.174	.174	.166
17.	RW@75F(23.9C	.455	.455	.455	.455
18.	RW salinity	13000.000	13000.000	13000.000	13000.000
19.	RMF @ FT	.0259489	.0259489	.0259489	.0247668
20.	RMF salinity	.115	.115	.115	.115

21. RM @ FT	.0328733	.0328733	.0328733	.0313757
22. RHO H	.500	.500	.500	.500
23. Gas Flag	1.000	1.000	1.000	1.000
24. RHO F	1.068	1.068	1.068	1.067
25. t F	188.969	188.969	188.969	188.969
26. RHOMA	2.630	2.630	2.630	2.630
27. PHIN min	-.0350000	-.0350000	-.0350000	-.0350000
28. t MA	55.500	55.500	55.500	55.500
29. t MA min	48.000	48.000	48.000	48.000
30. Sonic option	.000	.000	.000	.000
31. Compact/Ovrt	1.000	1.000	1.000	1.000
32. CAL cut off	16.000	16.000	16.000	16.000
33. RUGO.cut off	1.000	1.000	1.000	1.000
34. DRHO cut off	.150	.150	.150	.150
35. Bad Hole	.000	.000	.000	.000
36. No clay	SP	SP	SP	SP
	RT	RT	RT	RT
	N	N	N	N
	MN	MN	MN	MN
	SN	SN	SN	SN
37. Vclay Flag	.000	.000	.000	.000
38. Vclay type	.000	.000	.000	.000
39. Vclay inp1	.200	.200	.200	.200
40. Vclay out1	.150	.150	.150	.150
41. Vclay inp2	.800	.800	.800	.800
42. Vclay out2	.800	.800	.800	.800
43. Vclay 50%	.500	.500	.500	.500
44. VclayGR type	1.000	1.000	1.000	1.000
45. GR clean	17.969	17.969	17.969	17.969
46. GR clay	123.059	123.059	123.059	123.059
47. GR1	36.000	36.000	36.000	36.000
48. VGR1	.100	.100	.100	.100
49. GR2	84.000	84.000	84.000	84.000
50. VGR2	.800	.800	.800	.800
51. GR50%	70.000	70.000	70.000	70.000
52. R clay	49.000	49.000	49.000	49.000
53. R limit	1000.000	1000.000	1000.000	1000.000
54. Rclay1 flag	.000	.000	.000	.000
55. Rclay1	1.000	1.000	1.000	1.000
56. Vcl @ Rclay1	.150	.150	.150	.150
57. RHOB sand	2.231	2.231	2.231	2.150
58. RHOB silt	2.620	2.620	2.620	2.620
59. RHOB clay	2.570	2.570	2.570	2.570
60. RHO Dry Clay	2.700	2.700	2.700	2.700
61. Rhob Calcite	2.850	2.850	2.850	2.850
62. PHIN Sand	.229	.229	.229	.250
63. PHIN silt	.0200000	.0200000	.0200000	.0200000
64. PHIN clay	.356	.356	.356	.356
65. Phin Calcite	.100	.100	.100	.100
66. PHISILT	.0200000	.0200000	.0200000	.0200000
67. Calcite Flag	.000	.000	.000	.000
68. t clay	85.603	85.603	85.603	85.603
69. M clay	.688	.688	.688	.688
70. N clay	.429	.429	.429	.429
71. PHIN 2.2	.214	.214	.214	.235
72. t 2.2	86.692	86.692	86.692	90.000
73. a	1.000	1.000	1.000	1.000
74. A1	1.000	1.000	1.000	1.000
75. m	1.800	2.000	2.350	2.000
76. m1	1.950	2.150	2.500	2.150
77. m Function	1.000	1.000	1.000	1.000
78. n	1.750	1.950	2.150	2.000
79. n1	2.050	2.250	2.450	2.250
80. B from BQV	11.569	11.569	11.569	16.260
81. A(QV)	.0003050	.0003050	.0003050	.0003050
82. B(QV)	-3.450	-3.450	-3.450	-3.450
83. Lithomod	1.000	1.000	1.000	1.000
84. SXO limit	.200	.200	.200	.200
85. PHI max	.270	.270	.270	.294
86. PHI min c.o.	.0010000	.0010000	.0010000	.0010000
87. EXPX	1.500	1.500	1.500	1.500
88. Clay cut off	.400	.400	.400	.400
89. PHIe cut off	.0500000	.0500000	.0500000	.0500000
90. PHIt cut off	.100	.100	.100	.100
91. SWe cut off	.500	.500	.500	.500
92. SWt cut off	.600	.600	.600	.600
93. GrossRockVol	.000	.000	.000	.000
94. Oil Exp.Fact	1.200	1.200	1.200	1.200
95. FormGeom.Fac	1.000	1.000	1.000	1.000
96. RecoveryFact	.200	.200	.200	.200
97. SWB max	1.000	1.000	1.000	1.000

98.	RWB	1.838	1.838	1.372	1.974
99.	SWB cut off	.300	.300	.300	.300
100.	RWF	.174	.174	.174	.166
101.	RMFF	.0259489	.0259489	.0259489	.0247668
102.	Sw Eq. CPX	1.000	1.000	1.000	1.000
103.	Sw Eq. SSS	1.000	1.000	1.000	1.000
104.	Glauconite	.000	.000	.000	.000
105.	SWirr.cutoff	.300	.300	.300	.300
106.	Perm Expon.	6.000	6.000	6.000	6.000
107.	PERM K coef	62500.000	62500.000	62500.000	62500.000
108.	RHOMA 1	2.630	2.630	2.630	2.630
109.	RHOMA 2	2.810	2.810	2.810	2.810
110.	RHOMA 3	3.488	3.488	3.488	3.488
111.	UMA 1	4.800	4.800	4.800	4.800
112.	UMA 2	27.896	27.896	27.896	27.896
113.	UMA 3	18.632	18.632	18.632	18.632
114.	UF	.400	.400	.400	.400
115.	UMACL	13.237	13.237	13.237	13.237
116.	GR Dispersed	96.470	96.470	96.470	96.470
117.	PHIT Dispers	.0003432	.0003432	.0003432	.0003432
118.	PHIT Laminat	.143	.143	.143	.143
119.	PHIT Sand	.225	.225	.225	.225
93.	PHINmat1	.200	.200	.200	.200
94.	PHIDmat1	.240	.240	.240	.240
95.	PHINmat2	.350	.350	.350	.350
96.	PHIDmat2	.200	.200	.200	.200
97.	PHINmat3	.050	.050	.050	.050
98.	PHIDmat3	.000	.000	.000	.000
99.	PHINmat4	.200	.200	.200	.200
100.	PHIDmat4	-.100	-.100	-.100	-.100

APPENDIX - C
Core Analysis Cross-plots

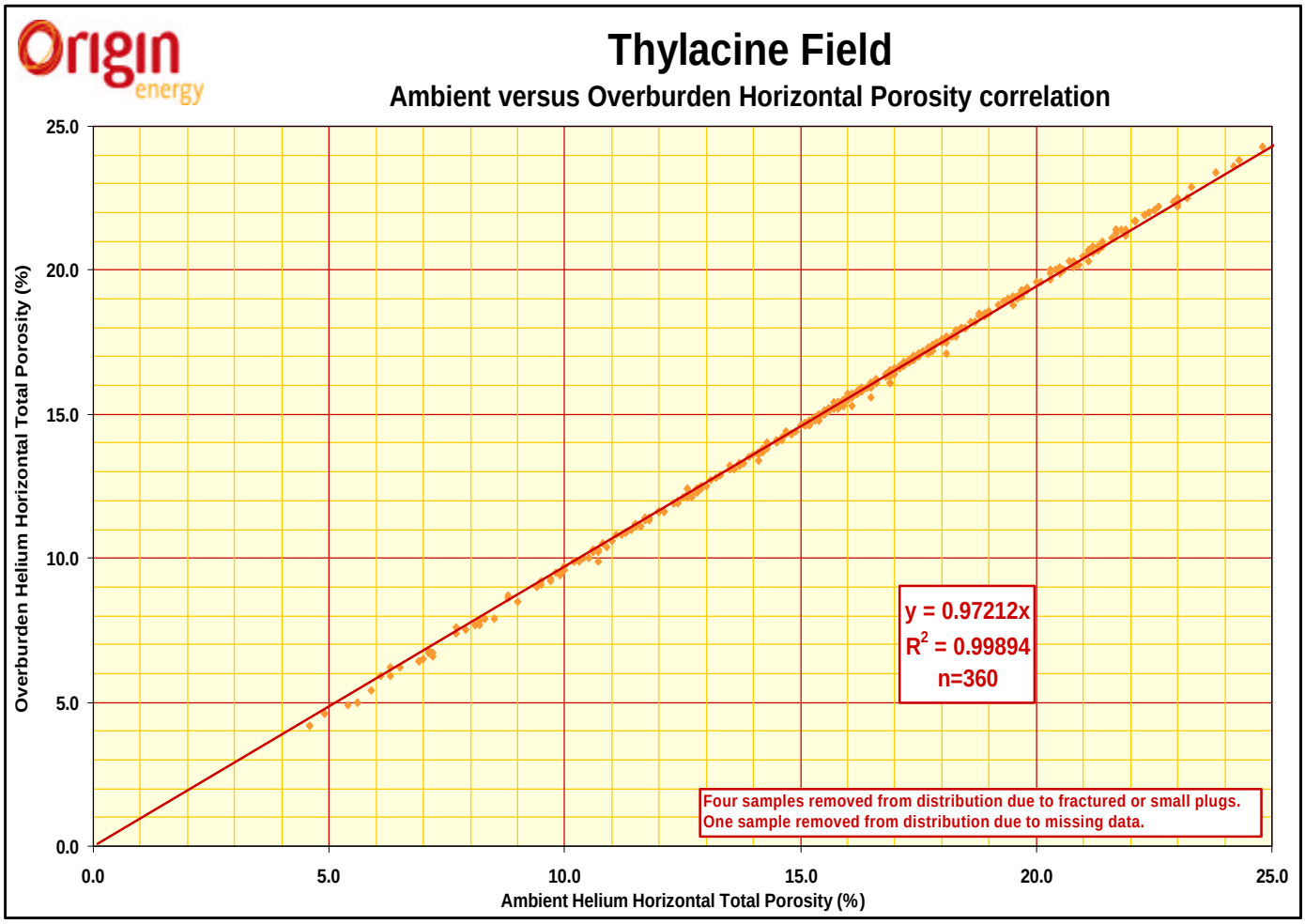

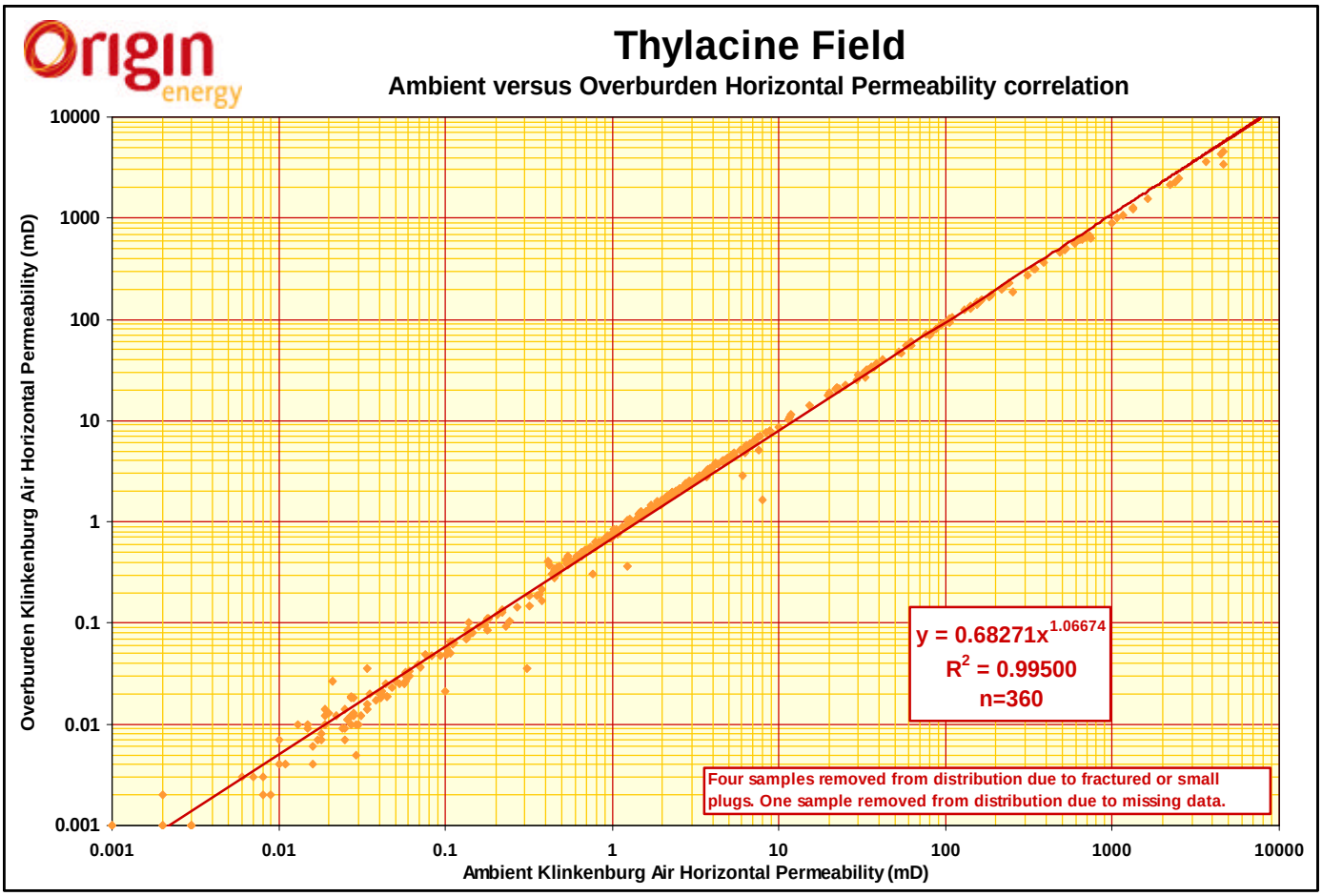
Thylacine Field
Ambient versus Overburden Horizontal Permeability correlation
Overburden Klinkenburg Air Horizontal Permeability (mD)
Ambient Klinkenburg Air Horizontal Permeability (mD)
y = 0.68271x^1.06674
R^2 = 0.99500
n=360
Four samples removed from distribution due to fractured or small plugs. One sample removed from distribution due to missing data.

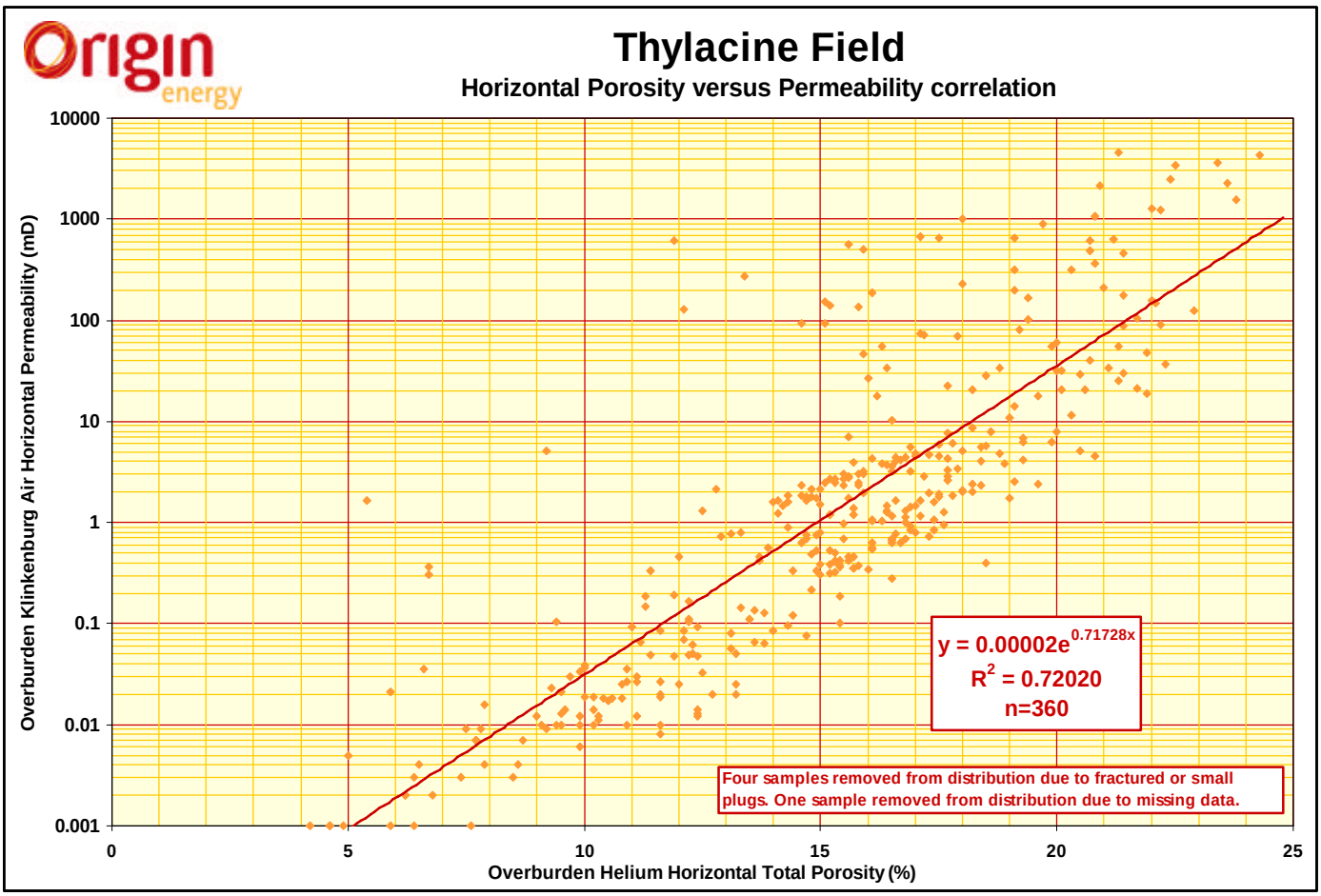
Thylacine Field
Horizontal Porosity versus Permeability correlation
Overburden Klinkenburg Air Horizontal Permeability (mD)
Overburden Helium Horizontal Total Porosity (%)
y = 0.00002e^0.71728x
R^2 = 0.72020
n=360
Four samples removed from distribution due to fractured or small plugs. One sample removed from distribution due to missing data.

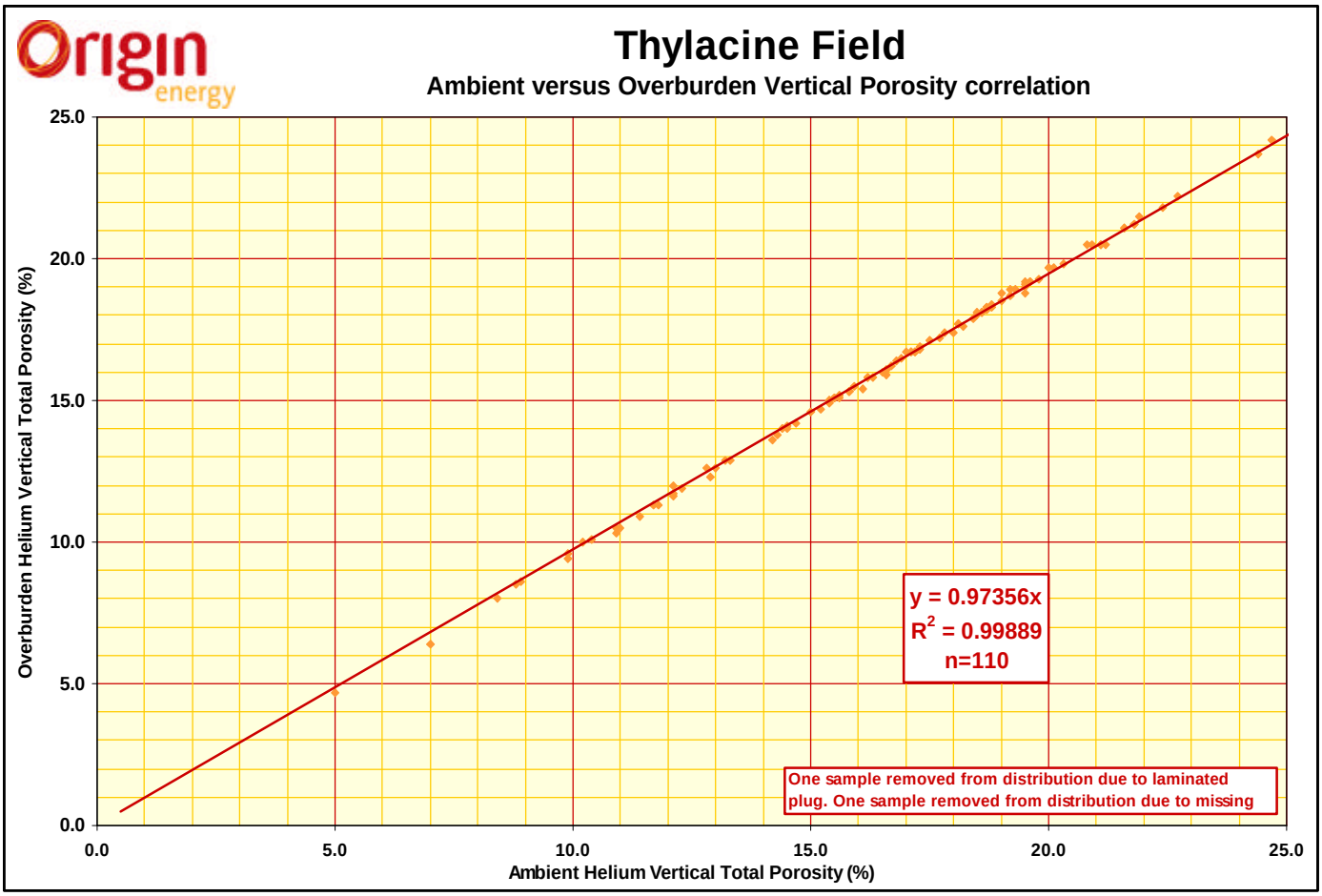
Thylacine Field
Ambient versus Overburden Vertical Porosity correlation
Overburden Helium Vertical Total Porosity (%)
Ambient Helium Vertical Total Porosity (%)
y = 0.97356x
R2 = 0.99889
n=110
One sample removed from distribution due to laminated plug. One sample removed from distribution due to missing
0.0
5.0
10.0
15.0
20.0
25.0

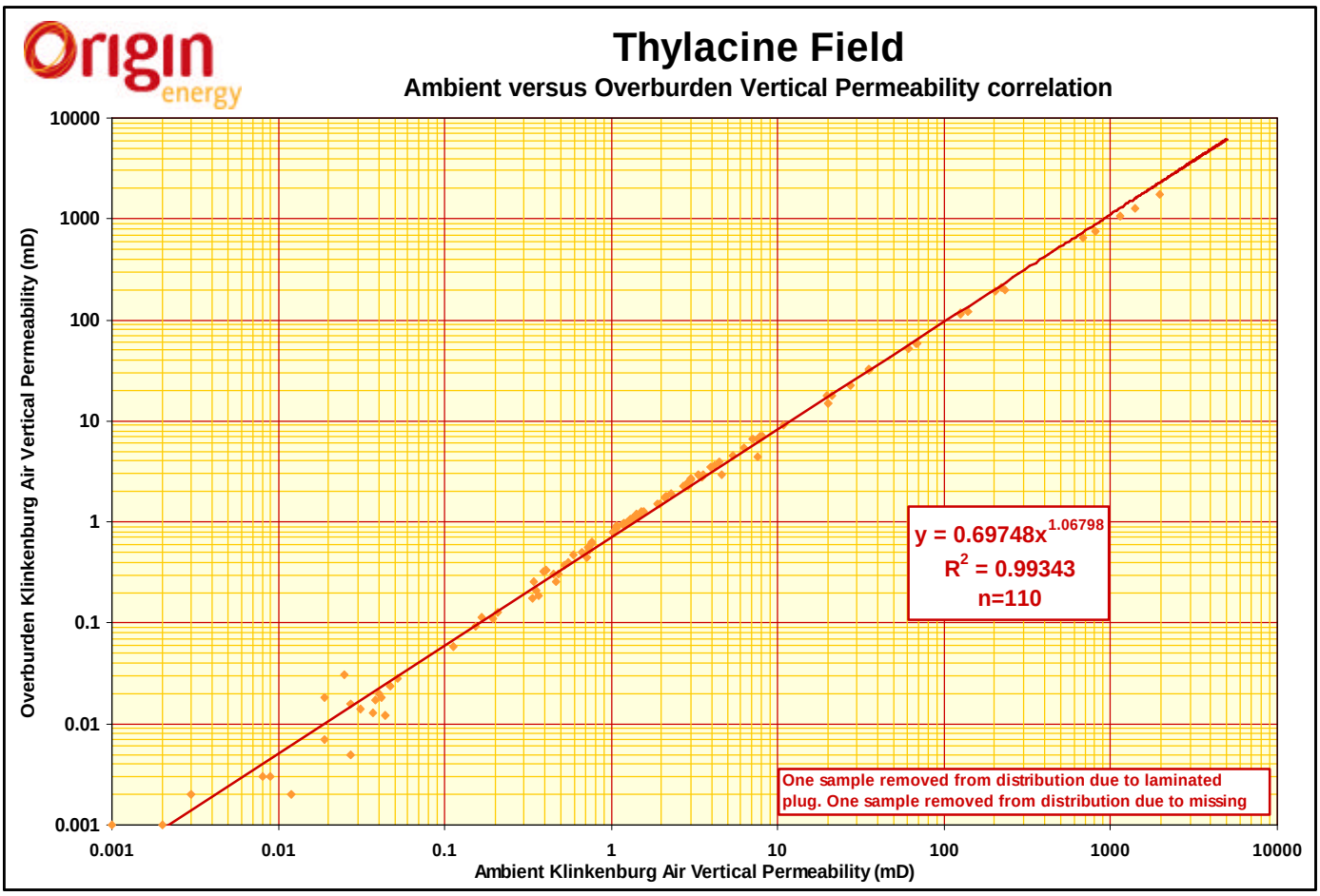
Thylacine Field
Ambient versus Overburden Vertical Permeability correlation
Overburden Klinkenburg Air Vertical Permeability (mD)
Ambient Klinkenburg Air Vertical Permeability (mD)
y = 0.69748x1.06798
R2 = 0.99343
n=110
One sample removed from distribution due to laminated plug. One sample removed from distribution due to missing
0.001
0.01
0.1
1
10
100
1000
10000

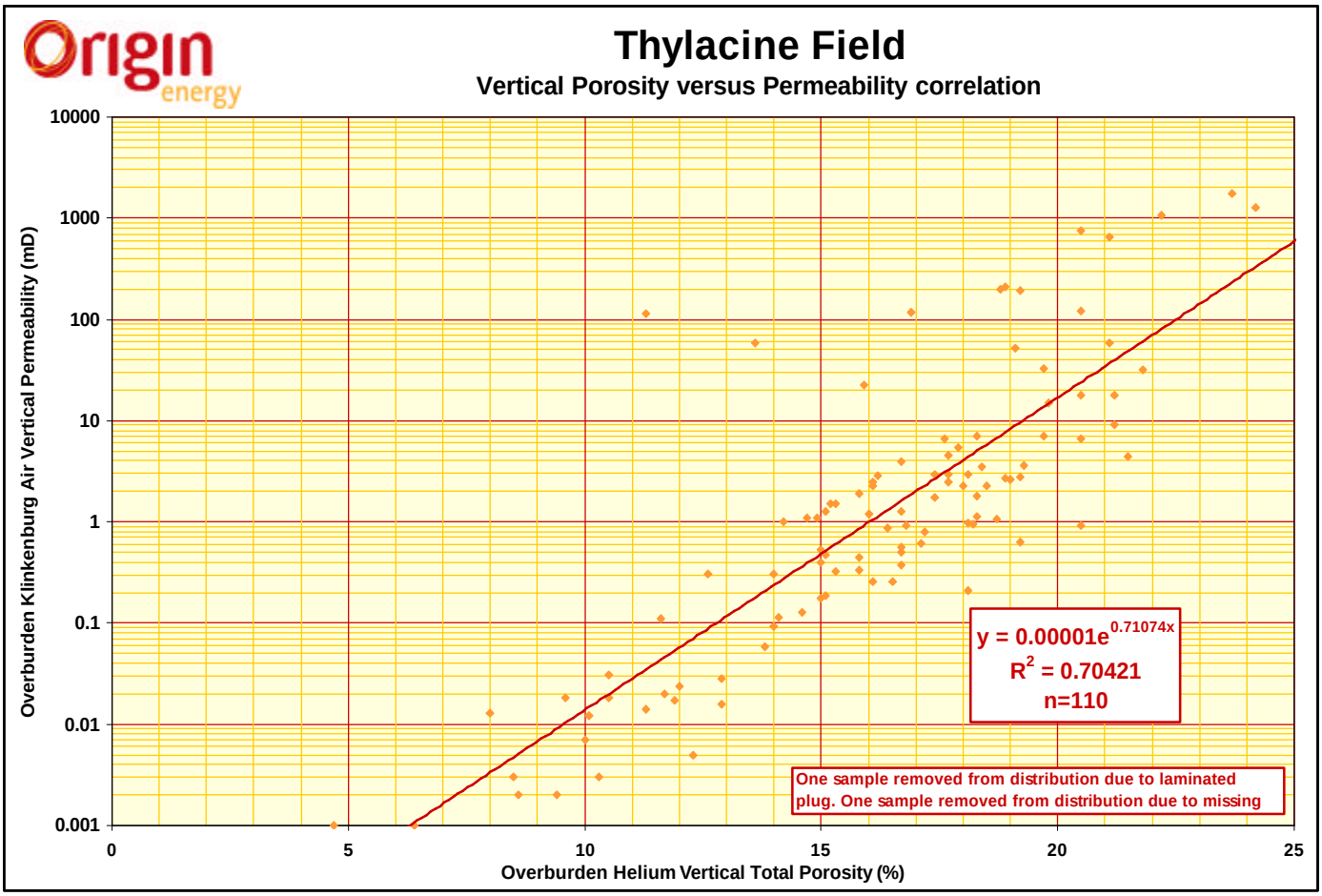
Thylacine Field
Vertical Porosity versus Permeability correlation
Overburden Klinkenburg Air Vertical Permeability (mD)
10000
1000
100
10
1
0.1
0.01
0.001
0
5
10
15
20
25
Overburden Helium Vertical Total Porosity (%)
y = 0.00001e^0.71074x
R^2 = 0.70421
n=110
One sample removed from distribution due to laminated plug. One sample removed from distribution due to missing

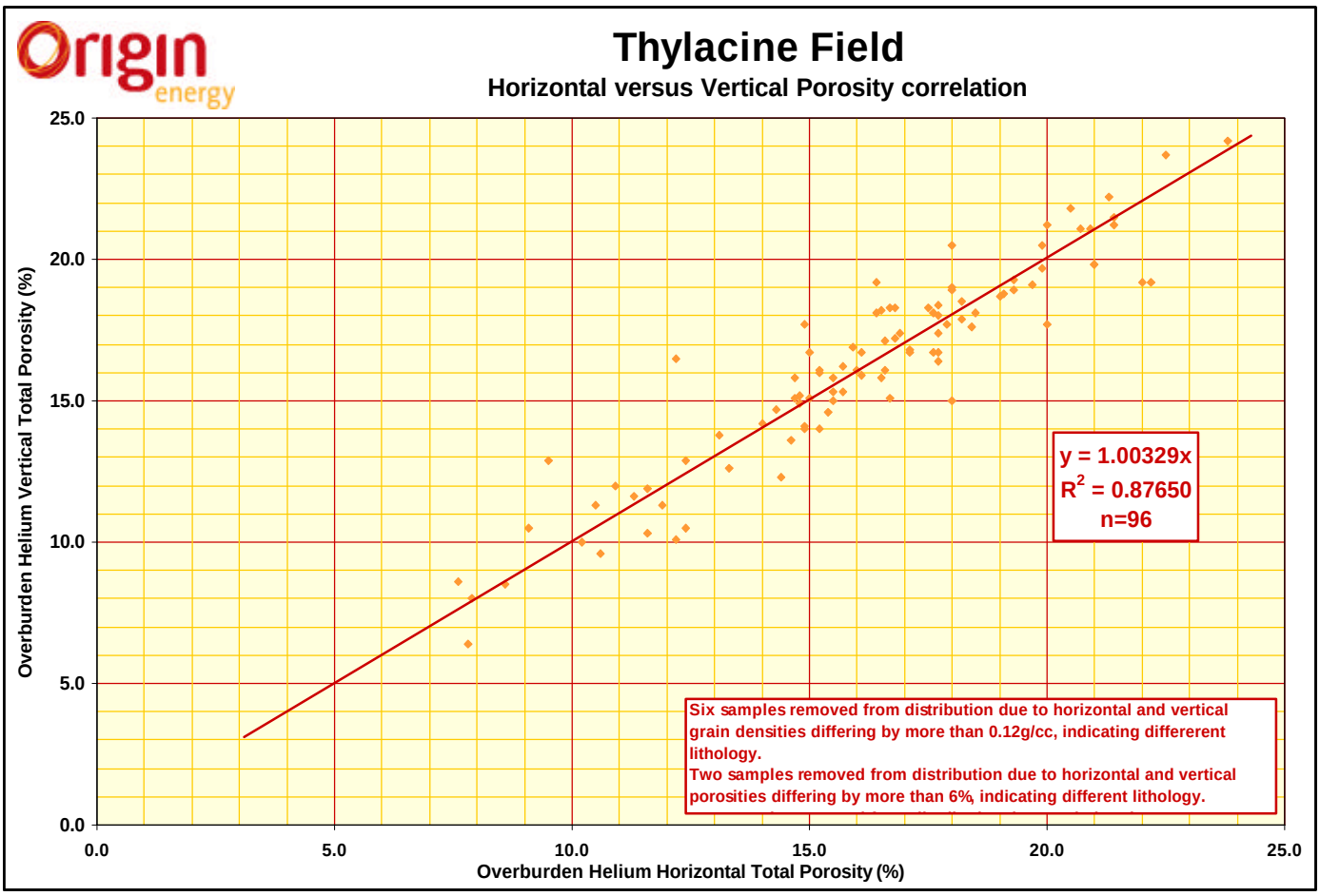
Thylacine Field
Horizontal versus Vertical Porosity correlation
Overburden Helium Vertical Total Porosity (%)
25.0
20.0
15.0
10.0
5.0
0.0
0.0
5.0
10.0
15.0
20.0
25.0
Overburden Helium Horizontal Total Porosity (%)
y = 1.00329x
R^2 = 0.87650
n=96
Six samples removed from distribution due to horizontal and vertical grain densities differing by more than 0.12g/cc, indicating differerent lithology.
Two samples removed from distribution due to horizontal and vertical porosities differing by more than 6%, indicating different lithology.

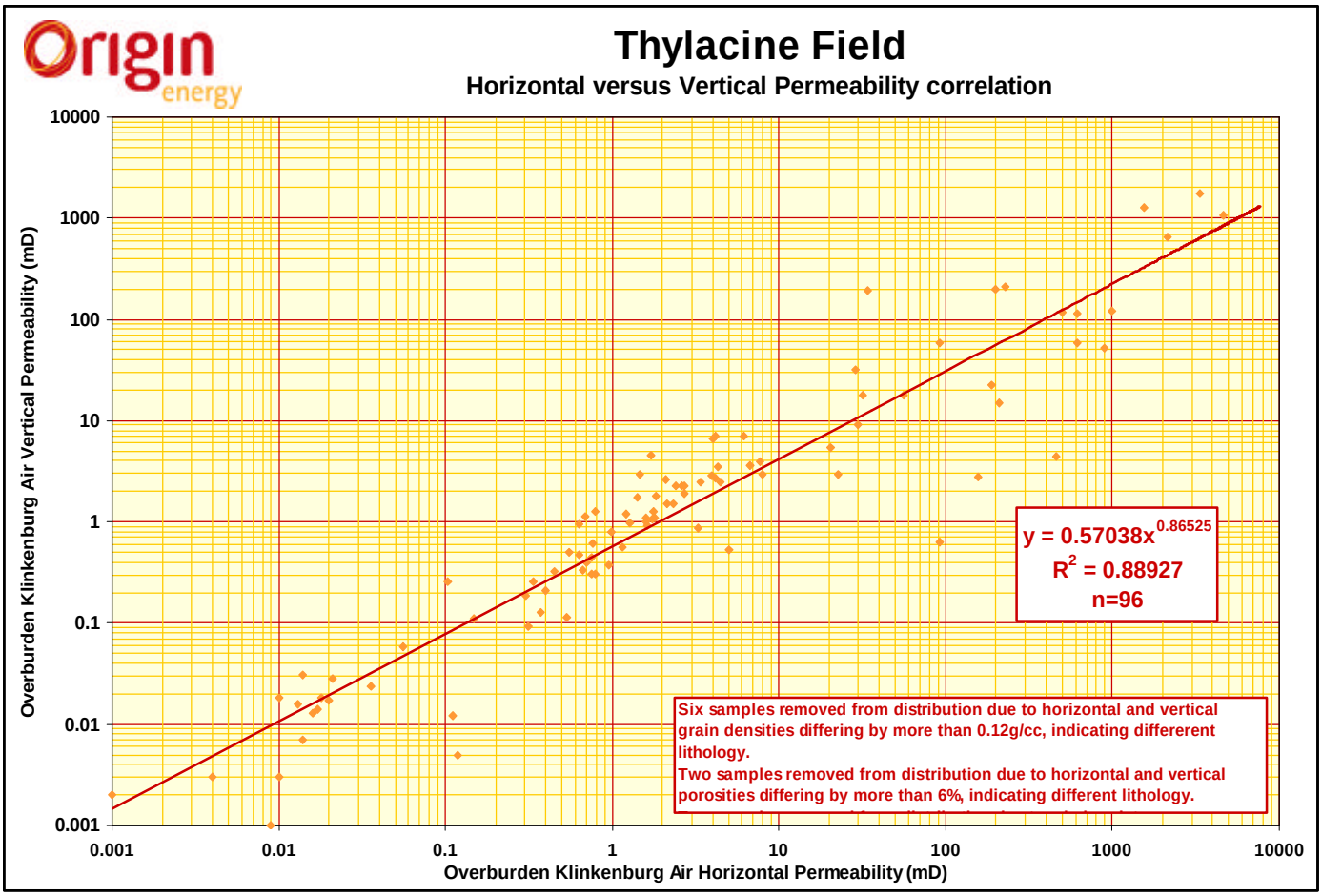
Thylacine Field
Horizontal versus Vertical Permeability correlation
Overburden Klinkenburg Air Vertical Permeability (mD)
Overburden Klinkenburg Air Horizontal Permeability (mD)
y = 0.57038x^0.86525
R2 = 0.88927
n=96
Six samples removed from distribution due to horizontal and vertical grain densities differing by more than 0.12g/cc, indicating differerent lithology.
Two samples removed from distribution due to horizontal and vertical porosities differing by more than 6%, indicating different lithology.

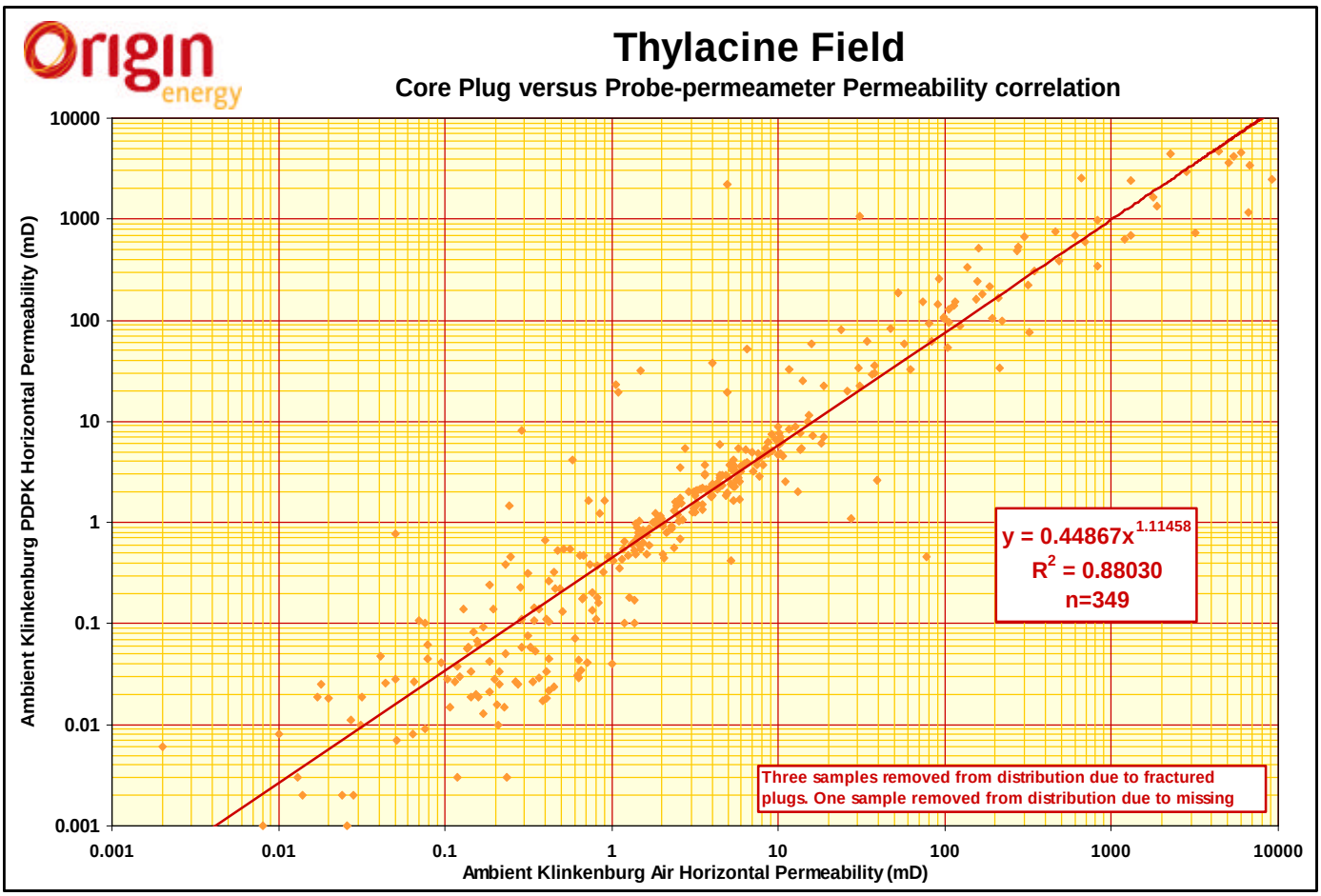
Thylacine Field
Core Plug versus Probe-permeameter Permeability correlation
Ambient Klinkenburg PDPK Horizontal Permeability (mD)
Ambient Klinkenburg Air Horizontal Permeability (mD)
y = 0.44867x^1.11458
R2 = 0.88030
n=349
Three samples removed from distribution due to fractured plugs. One sample removed from distribution due to missing

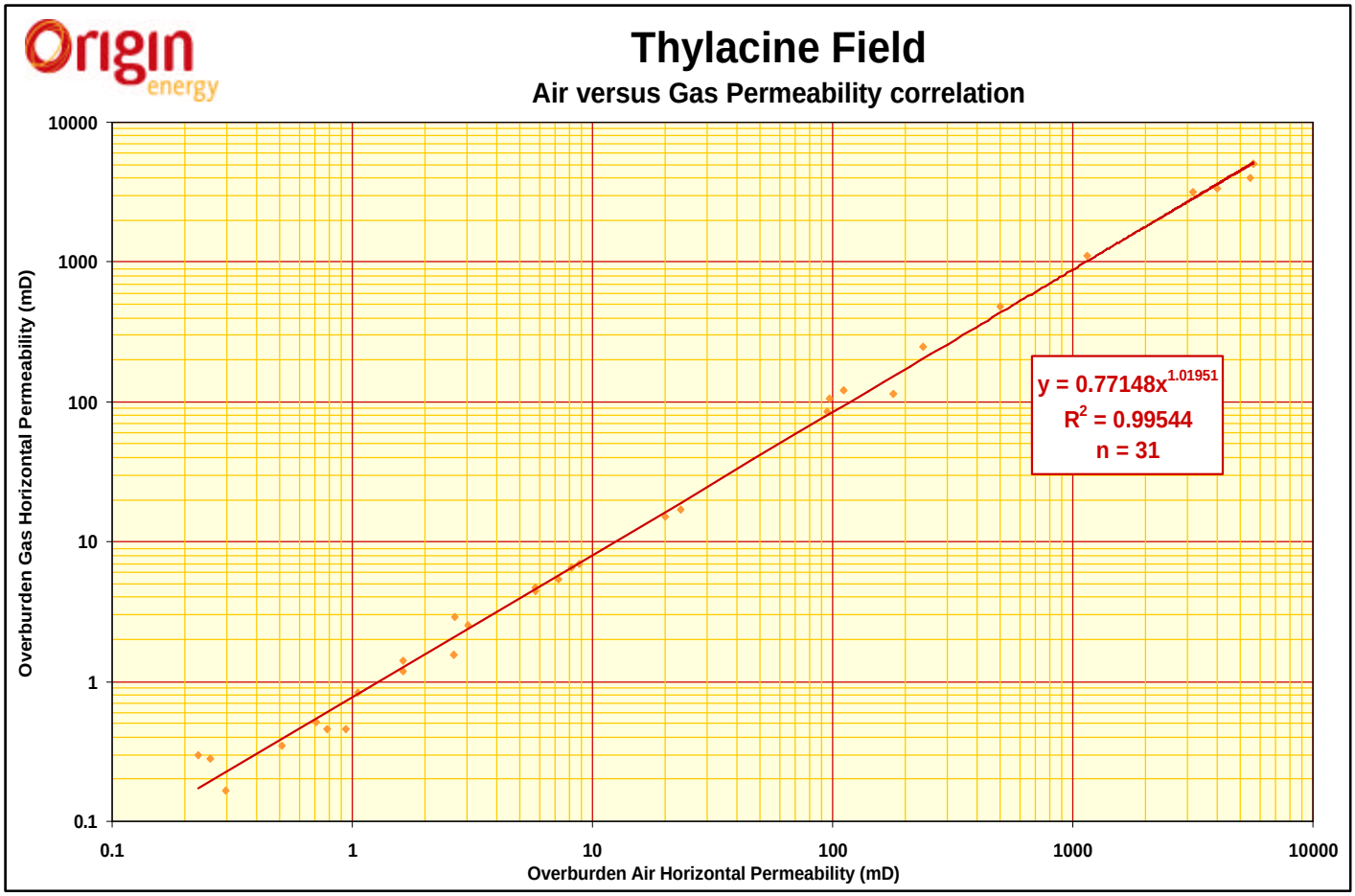
Thylacine Field
Air versus Gas Permeability correlation
Overburden Gas Horizontal Permeability (mD)
Overburden Air Horizontal Permeability (mD)
y = 0.77148x^1.01951
R^2 = 0.99544
n = 31
10000
1000
100
10
1
0.1
0.1
1
10
100
1000
10000

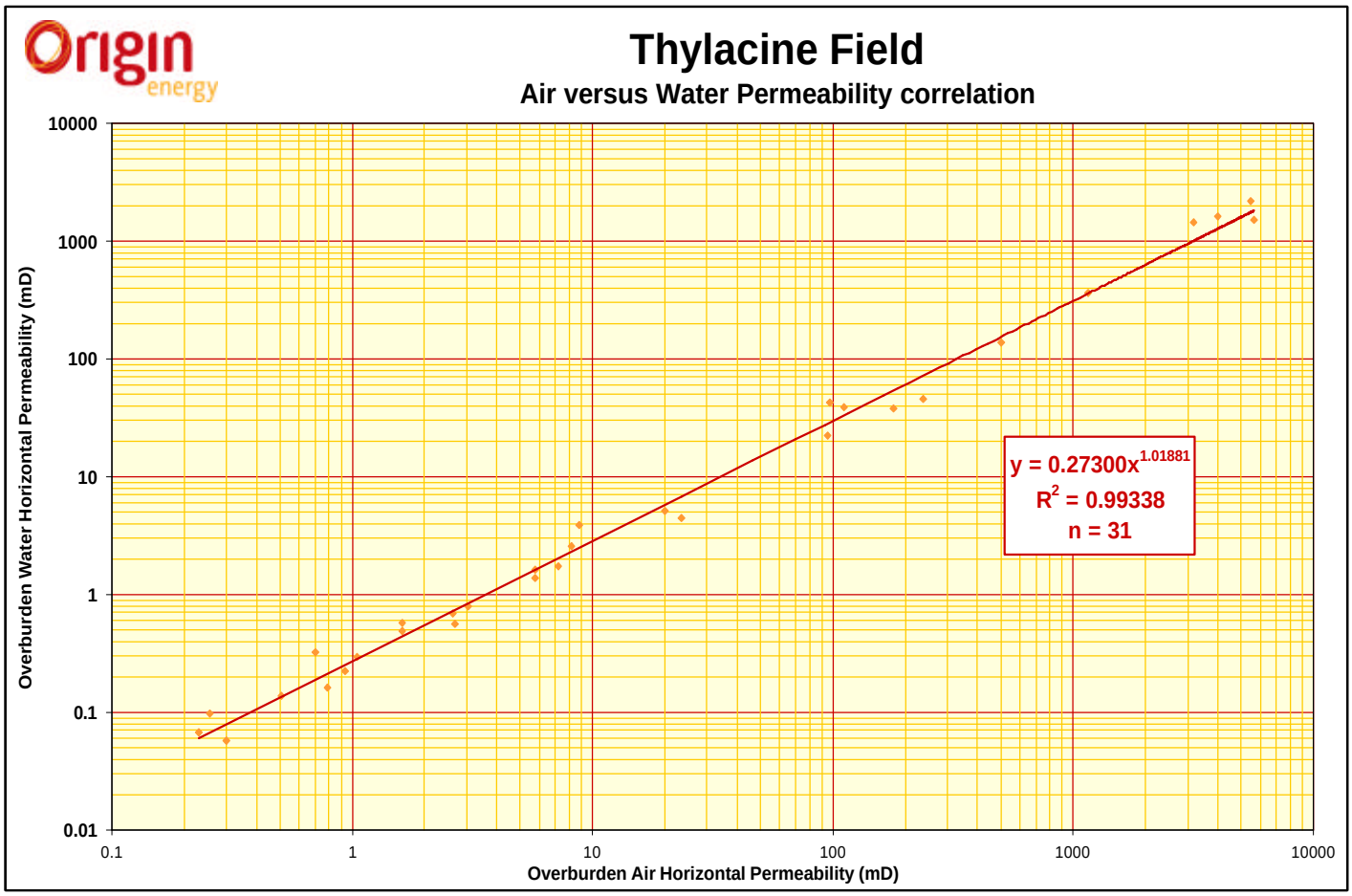
Thylacine Field
Air versus Water Permeability correlation
Overburden Water Horizontal Permeability (mD)
Overburden Air Horizontal Permeability (mD)
y = 0.27300x^1.01881
R^2 = 0.99338
n = 31
10000
1000
100
10
1
0.1
0.01
0.1
1
10
100
1000
10000

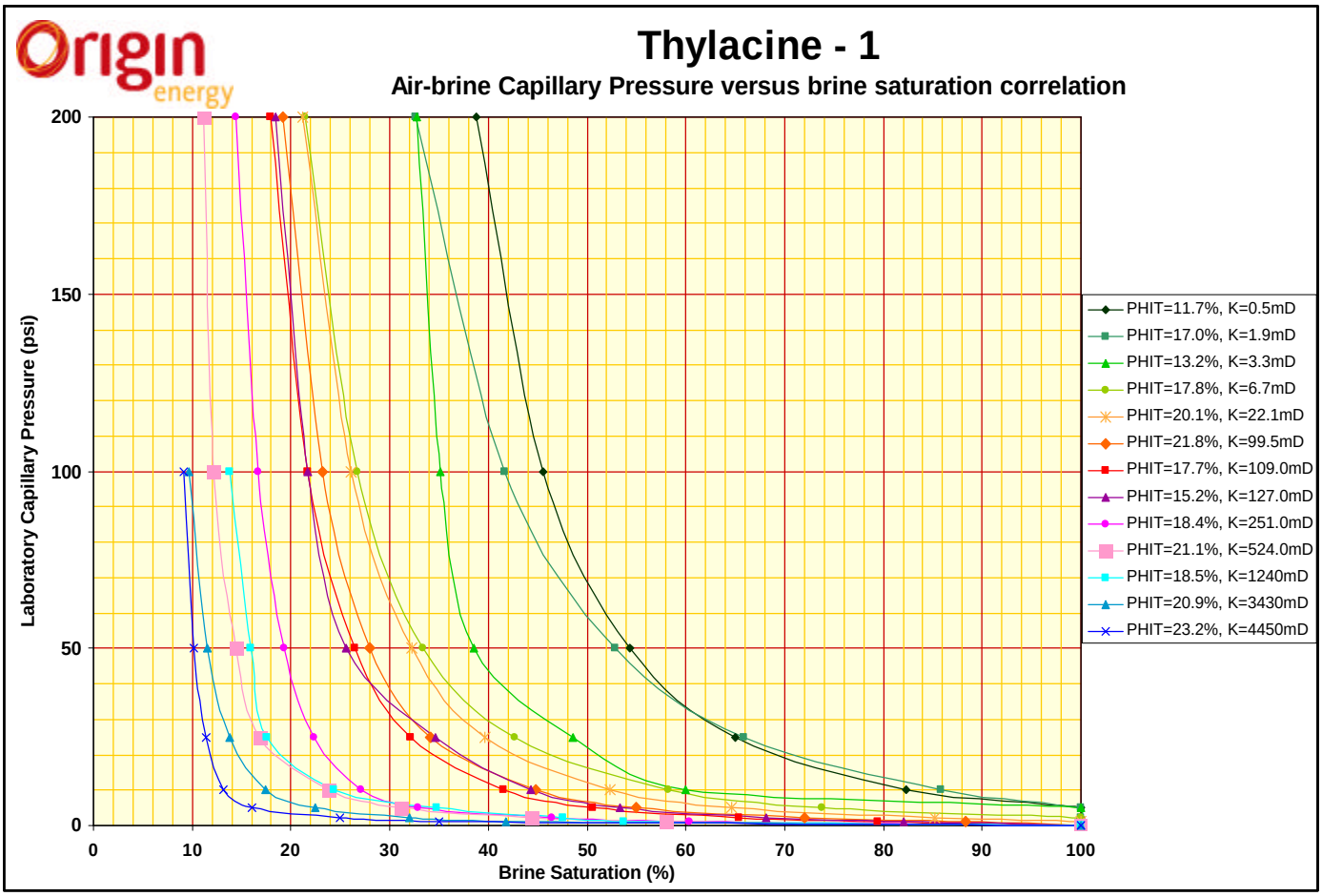
Thylacine - 1
Air-brine Capillary Pressure versus brine saturation correlation
Laboratory Capillary Pressure (psi)
Brine Saturation (%)
0
50
100
150
200
0
10
20
30
40
50
60
70
80
90
100
PHIT=11.7%, K=0.5mD
PHIT=17.0%, K=1.9mD
PHIT=13.2%, K=3.3mD
PHIT=17.8%, K=6.7mD
PHIT=20.1%, K=22.1mD
PHIT=21.8%, K=99.5mD
PHIT=17.7%, K=109.0mD
PHIT=15.2%, K=127.0mD
PHIT=18.4%, K=251.0mD
PHIT=21.1%, K=524.0mD
PHIT=18.5%, K=1240mD
PHIT=20.9%, K=3430mD
PHIT=23.2%, K=4450mD

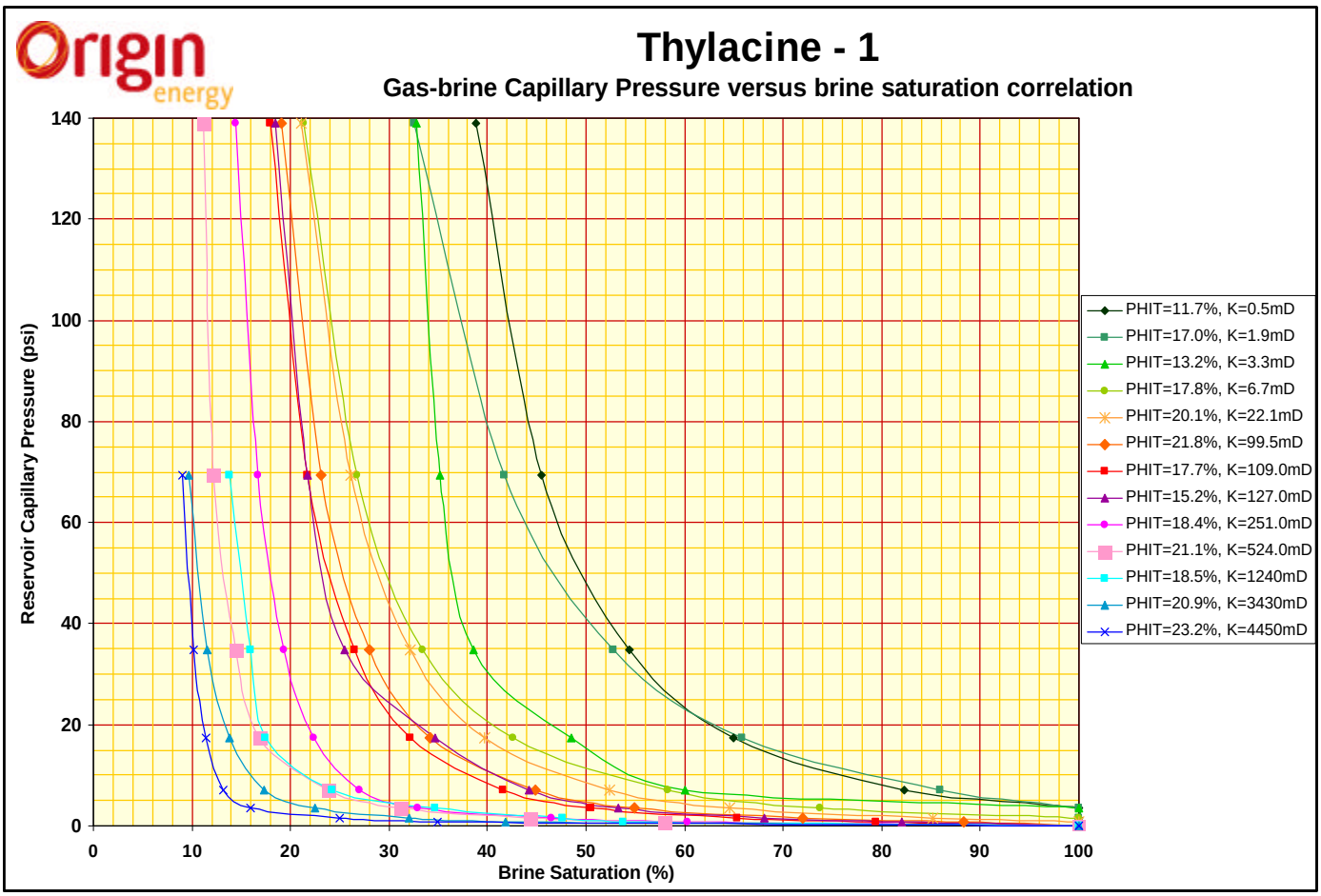
Thylacine - 1
Gas-brine Capillary Pressure versus brine saturation correlation
Reservoir Capillary Pressure (psi)
Brine Saturation (%)
0
20
40
60
80
100
120
140
0
10
20
30
40
50
60
70
80
90
100
PHIT=11.7%, K=0.5mD
PHIT=17.0%, K=1.9mD
PHIT=13.2%, K=3.3mD
PHIT=17.8%, K=6.7mD
PHIT=20.1%, K=22.1mD
PHIT=21.8%, K=99.5mD
PHIT=17.7%, K=109.0mD
PHIT=15.2%, K=127.0mD
PHIT=18.4%, K=251.0mD
PHIT=21.1%, K=524.0mD
PHIT=18.5%, K=1240mD
PHIT=20.9%, K=3430mD
PHIT=23.2%, K=4450mD

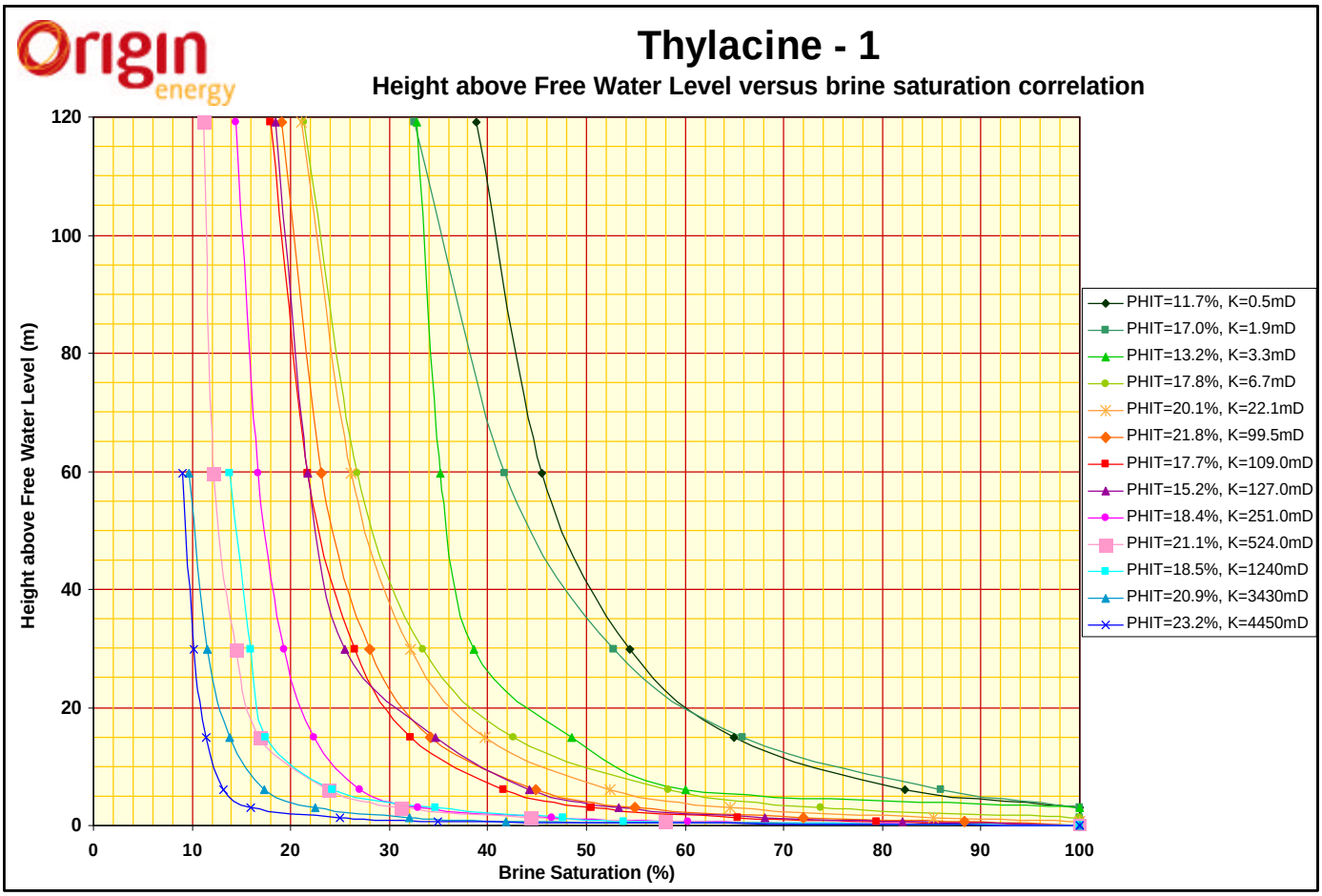
Thylacine - 1
Height above Free Water Level versus brine saturation correlation
Height above Free Water Level (m)
Brine Saturation (%)
0
20
40
60
80
100
120
0
10
20
30
40
50
60
70
80
90
100
PHIT=11.7%, K=0.5mD
PHIT=17.0%, K=1.9mD
PHIT=13.2%, K=3.3mD
PHIT=17.8%, K=6.7mD
PHIT=20.1%, K=22.1mD
PHIT=21.8%, K=99.5mD
PHIT=17.7%, K=109.0mD
PHIT=15.2%, K=127.0mD
PHIT=18.4%, K=251.0mD
PHIT=21.1%, K=524.0mD
PHIT=18.5%, K=1240mD
PHIT=20.9%, K=3430mD
PHIT=23.2%, K=4450mD

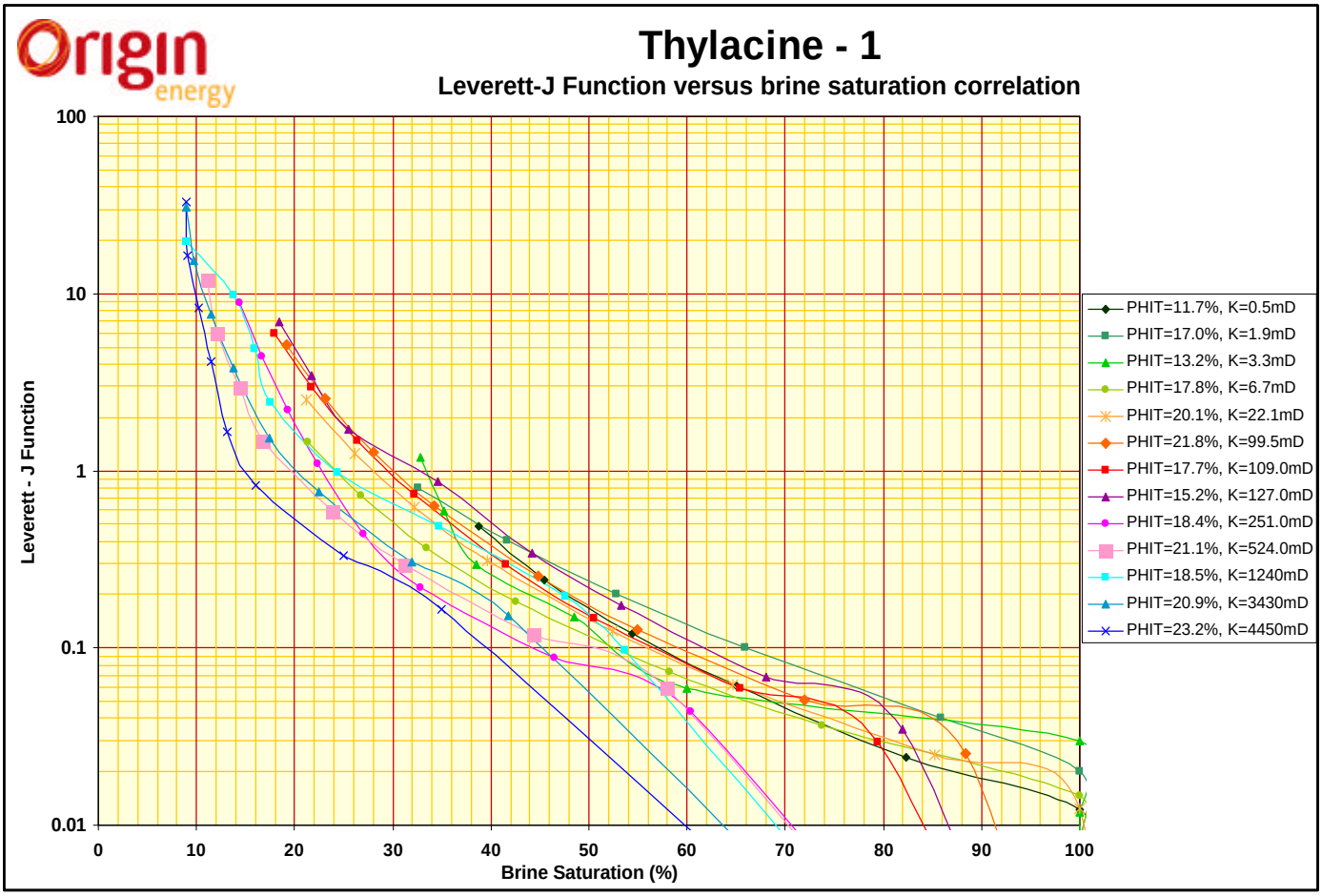
Thylacine - 1
Leverett-J Function versus brine saturation correlation
Leverett - J Function
Brine Saturation (%)
0.01
0.1
1
10
100
0
10
20
30
40
50
60
70
80
90
100
PHIT=11.7%, K=0.5mD
PHIT=17.0%, K=1.9mD
PHIT=13.2%, K=3.3mD
PHIT=17.8%, K=6.7mD
PHIT=20.1%, K=22.1mD
PHIT=21.8%, K=99.5mD
PHIT=17.7%, K=109.0mD
PHIT=15.2%, K=127.0mD
PHIT=18.4%, K=251.0mD
PHIT=21.1%, K=524.0mD
PHIT=18.5%, K=1240mD
PHIT=20.9%, K=3430mD
PHIT=23.2%, K=4450mD

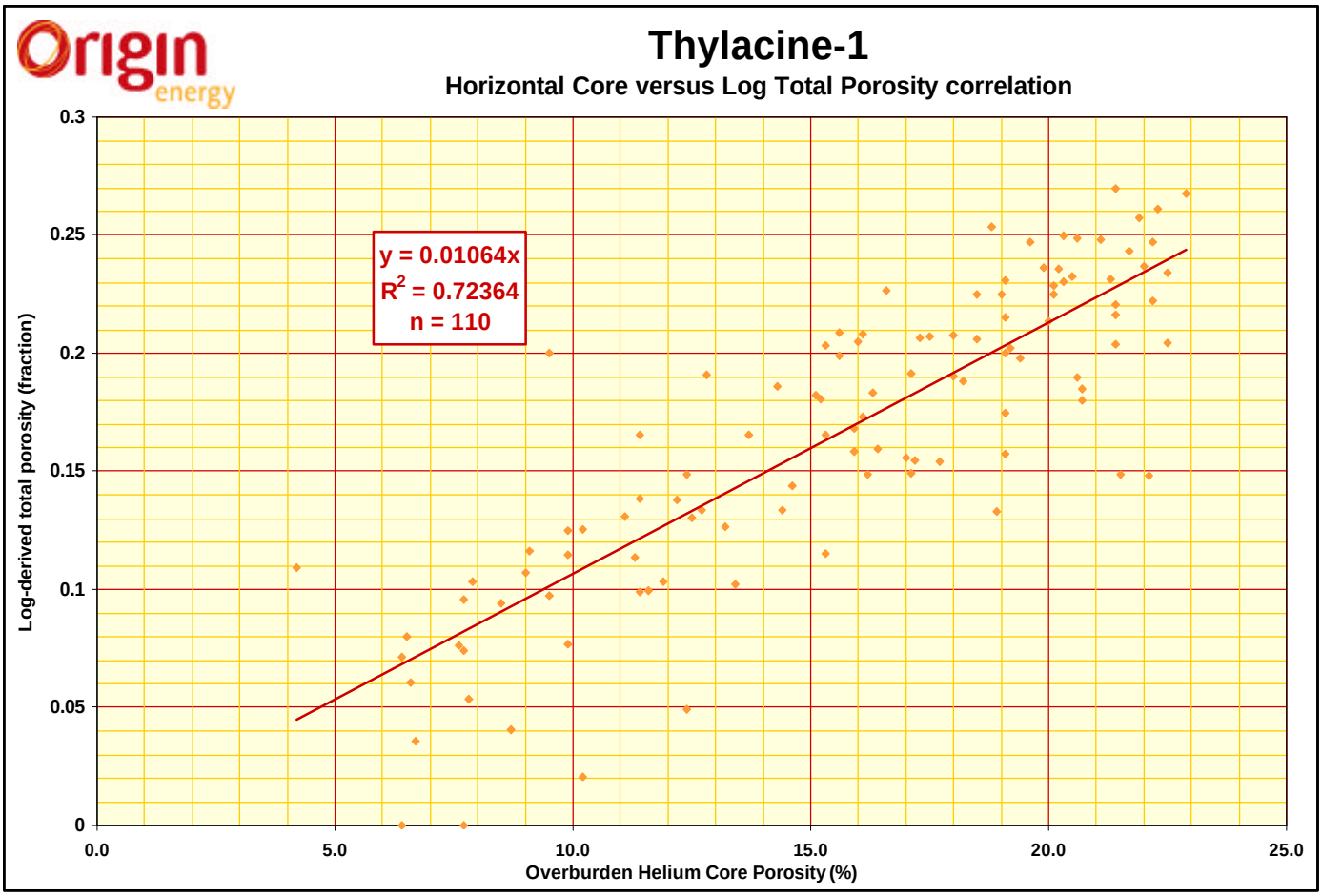
Thylacine-1
Horizontal Core versus Log Total Porosity correlation
y = 0.01064x
R2 = 0.72364
n = 110
Log-derived total porosity (fraction)
Overburden Helium Core Porosity (%)
0.3
0.25
0.2
0.15
0.1
0.05
0
0.0
5.0
10.0
15.0
20.0
25.0

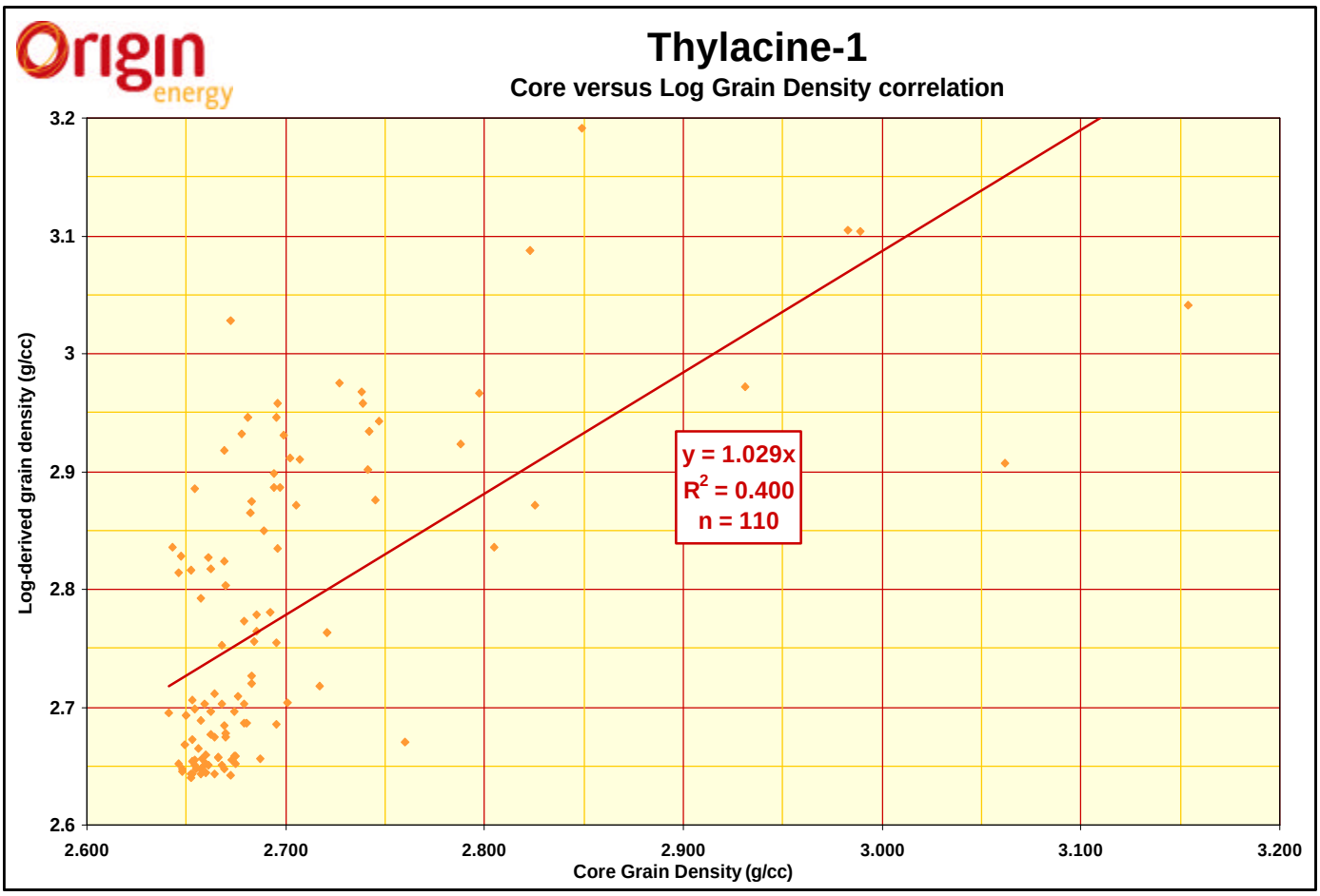
Thylacine-1
Core versus Log Grain Density correlation
y = 1.029x
R2 = 0.400
n = 110
Log-derived grain density (g/cc)
Core Grain Density (g/cc)
3.2
3.1
3
2.9
2.8
2.7
2.6
2.600
2.700
2.800
2.900
3.000
3.100
3.200

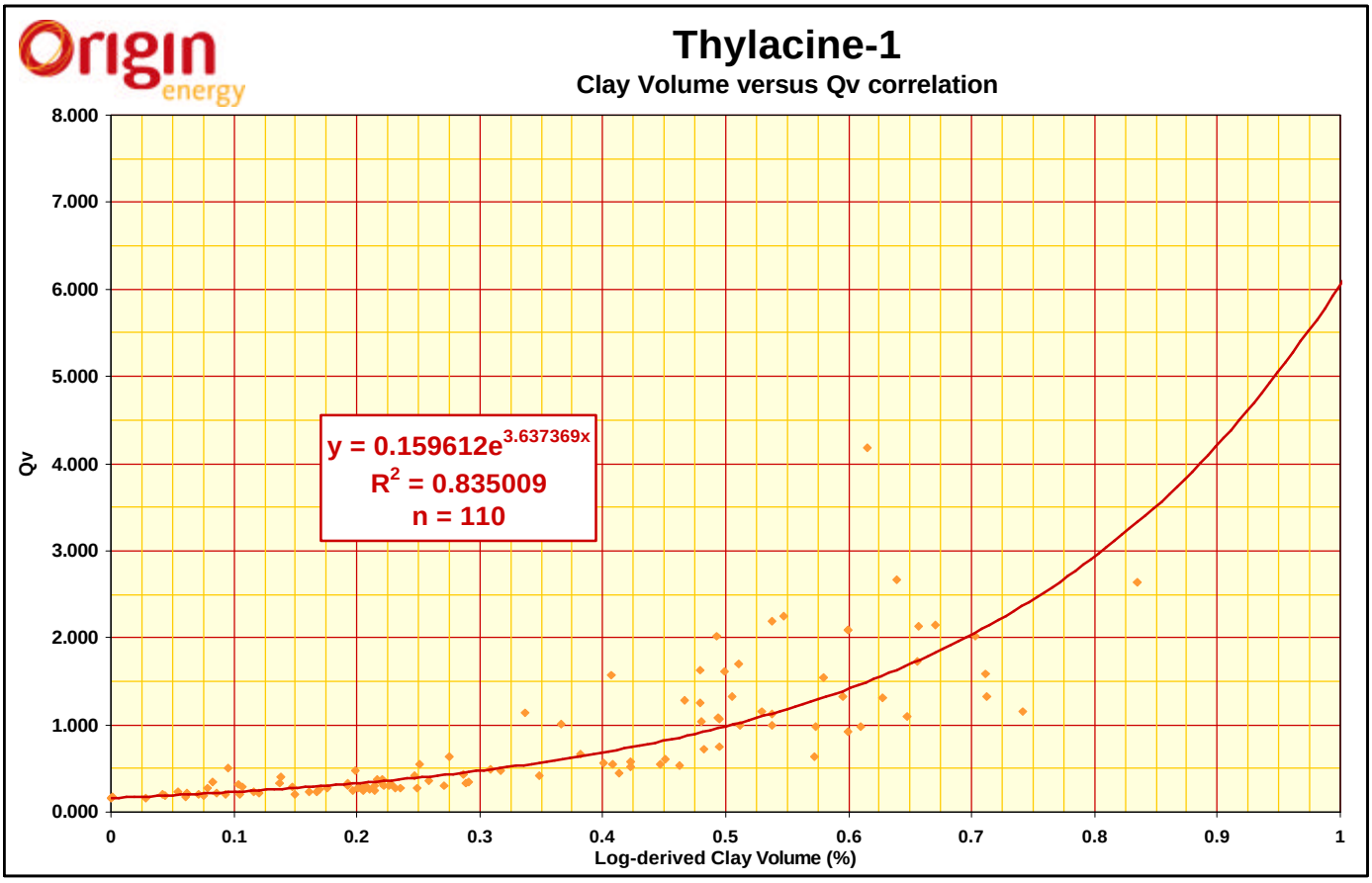
Origin energy
Thylacine-1
Clay Volume versus Qv correlation
y = 0.159612e^3.637369x
R^2 = 0.835009
n = 110
Qv
Log-derived Clay Volume (%)
8.000
7.000
6.000
5.000
4.000
3.000
2.000
1.000
0.000
0
0.1
0.2
0.3
0.4
0.5
0.6
0.7
0.8
0.9
1

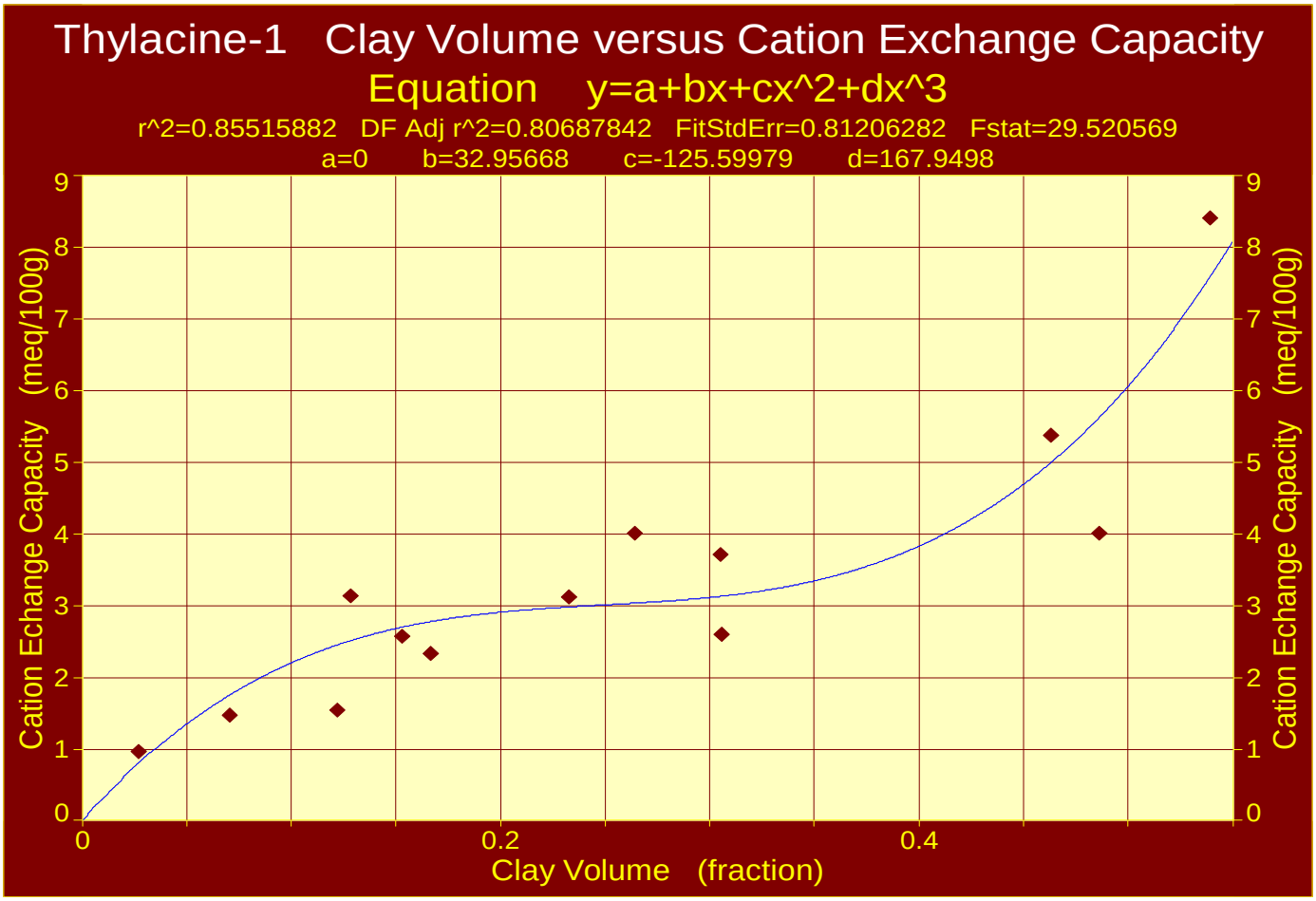
Thylacine-1 Clay Volume versus Cation Exchange Capacity
Equation y=a+bx+cx^2+dx^3
r^2=0.85515882 DF Adj r^2=0.80687842 FitStdErr=0.81206282 Fstat=29.520569
a=0 b=32.95668 c=-125.59979 d=167.9498
Cation Echange Capacity (meq/100g)
Clay Volume (fraction)
9
8
7
6
5
4
3
2
1
0
0
0.2
0.4

ENCLOSURE-1
Petrophysical and Composite Plot
2048-2684mMDRT (1:500)

THYLACINE-1

COMPOSITE AND PETROPHYSICAL SUMMARY

Company	ORIGIN ENERGY RESOURCES LTD
Well Name	THYLACINE-1
Field	Thylacine
Country	Australia
Nation	Australia
State	Tasmania
Province	Otway Basin
County or Rig name	Ocean Bounty
Field Location	Otway Basin
Field Locn. Line 1	Easting: 665030.3 m
Field Locn. Line 2	Northing: 5654721.5 m
Latitude	039 14' 27.592" S DMS
Longitude	142 54' 44.169" E DMS
Permanent Datum	LAT
Elevation of PD	.00 M
Elevation of RT	25.00 M
Elevation Ground lv	101.40 M
Elevation Log Zero	25.00 M
Above Perm. Datum	25.00 M
Log measured from	RT
Drill measured from	RT
Services	PEx(HRLA)-DSI-HNGS-SP
Other Services Ln 1	MDT-GR
Other Services Ln 2	MSCT-GR
Other Services Ln 3	FMI-GR
Other Services Ln 4	VSP-GR
Other Services Ln 5	CST-GR
Service company	Schlumberger
Number of runs	2
Well class	Exploration
Basin	Otway
Tenement/Concession	T30/P
On-Shore Flag	Off-shore
Log date	11-MAY-2001 19-May-2001
Date computed	26-03-03
Date plotted	27-03-2003
Time plotted	09:29:23

PETROLOG SOFTWARE Revision 9.10

CROCKER
DATA PROCESSING

RUN INFORMATION

Run number	1	2A
Log date	11-MAY-2001	19-May-2001
Depth-Driller	1855.50 M	2710.00 M
Depth-Logger	1833.50 M	2713.00 M
Bottom log interval	1833.30 M	2713.00 M
Top log interval	744.00 M	1657.50 M
Casing-Driller	745.30 M	1849.90 M
Casing-Logger	744.00 M	1850.00 M
Casing Diameter	13.3750 inch	9.6250 inch
Casing Weight		47.0000 lb/ft
Casing Depth		1850.00 M
Bit Size	12.2500 inch	8.5000 inch
Hole Fluid type	KCl PHPA Glycol	KCl PHPA Glycol
Fluid Density	1.1900 gm/cc	1.3300 gm/cc
Fluid Viscosity	64.0000 s	65.0000 s
Fluid PH	8.5	8.600000
Fluid Loss	3.3000 C3	2.3000 C3
Mud Sample Source	Active Pit	Active Pit
RM @ Surface	.0910 Ohmm	.0940 Ohmm
Mud temp Surface	18.00 degC	20.00 degC
RMF @ Surface	.0780 Ohmm	.0742 Ohmm
MF temp Surface	18.00 degC	20.00 degC
RMC @ Surface	.1820 Ohmm	.4547 Ohmm
MC Temp Surface	18.00 degC	20.00 degC
Source of RMF/RMC	Press	Press
Mud Sample Temp	78.00 degC	104.00 degC
Mud Filt.SampleTemp	78.00 degC	104.40 degC
MudCakeSample Sourc	Press	Press
Time circ. stopped	20:45	06:30
Date circ. stopped	10-MAY-2001	19-May-2001
Time logger at btm	08:25	18:10
Date logger at btm	11-MAY-2001	19-May-2001
Surface hole temp	26.67 degC	26.67 degC
Bottom hole temp	78.00 degC	104.40 degC
Surface temperature	18.00 degC	20.00 degC
Max recorded temp	78.00 degC	104.40 degC
Max recorded temp 1		106.00 degC
Max recorded temp 2		113.00 degC
Max recorded temp 3		114.00 degC
Logging unit No	25	25
Logging unit Loc	VEA-APG	VEA-APG
Logging Company ID	440	440
Recorded by	F.Marcano, R.Hill	F. Marcano, R. Hil
Witness	M.Bilek, P.Gibson	M. Bilek, P. Gibso
Program Version	9C2-303	9C2-303
Bore Hole Status	Open	Open
Fluid Level		.00 M
Avg Angular Deviat		.0000000
General.Temp Select		TEMP
Maximum Hole Deviat		2.9700 deg
Total depth		2710.00 M
Temp Conn.WaterSamp		37.78 degC
Filtrate Cl	59,000 ppm	59,000 ppm
% Solids	9.0	11.0

FIELD REMARKS

Suite-1 Run-1 PEx(HRLA)-DSI-HNGS-SP
1. This is the depth correlation log. Full depth control procedures followed.
2. Borehole corrections applied to the logs.
3. Limestone matrix-model and used in computation of Neutron Porosity.
4. Bottom hole temperature 7.8 degC at 08:25 on 11-May-2001.
5. Data acquired in HIRES mode for entire interval.
6. Sonic check in casing reading as expected (57 us/ft)
7. Caliper check inside casing reading 12.39 inches.
8. Tide level read from drill floor was 2.63 above LAT at 06:10 on 11-May-2001.
9. Wireline tools could not pass beyond 1833.5m. Driller's TD at 1855.0m.
10. Circulation on bottom for 55 minutes. Circulation stopped at 20:45 on 10-May-2001.
11. Tools run as per tool sketch.
12. Maximum well deviation of 1.88 degrees at 1855m.
13. DSI Modes: Lower dipole, P&S, FMD.
14. Neutron corrected for borehole size, borehole salinity, temperature, pressure, mud weight.
15. PEF corrected for barite content.

Suite-2 Run-1 PEx(HRLA)-DSI-HNGS-SP
1. Subsequent run in hole. Log correlated to PEx(HRLA)-DSI-HNGS-SP dated 11-May-2001.
2. Borehole corrections applied to the logs.
3. Limestone matrix-model and used in computation of Neutron Porosity.
4. Bottom hole temperature 104.4degC at 18:10 on 19-May-2001.
5. Data aquired in HIRES mode for entire interval.
6. Sonic check in casing reading as expected (57 us/ft).
7. Caliper check in casing reading 8.76 in. ID expected 8.75 in.
8. Circulation stoped at 06:30 on 19-may-2001.
9. Tool run as per tool sketch.
10. Well sketch as per driller's depths.
11. DSI modes: Lower dipole, P&S, FMD.
12. Neutron corrected for borehole size, borehole salinity, temperature, pressure, mud weight.
13. PEF corrected for barite content.

Suite-2 Run-2 MDT-GR
1. Log correlated to PEx(HRLA)-DSI-HNGS-SP dated 19-May-2001.
2. Tools ran as per tool sketch.
3. Low shock technique used to perform fluid sampling.
4. Both strain and quartz gauges were used during pressure measurements.
5. Pump out volume was used to clean invasion from formation prior to fluid sampling.
6. Fluid sample welssite analysis performed by Petrotech.

Suite-2 Run-3 MSCT-GR
1. Log correlated to PEx(HRLA)-DSI-HNGS-SP dated 19-May-2001.
2. Tools run as per tool sketch.
3. Mud circulated from 22:20 on 22-May-2001 and stopped at 22:55 on 22-May-2001.
4. No cores were recovered on Suite-2 Run-2 because weight on bit was too large.
5. 14 cores attempted, 12 recovered, 1 lost, and 1 aborted.

Suite-2 Run-4 FMI-GR
1. Log correlated to PEx(HRLA)-DSI-HNGS-SP dated 19-May-2001.
2. Tools run as per tool sketch.
3. 30% pad pressure applied for FMI.
4. FMI image processed to adjust image contrast.
5. BHT: 105.6 degC at 2550m.

Suite-2 Run-5 VSP-GR
1. Log correlated to PEx(HRLA)-DSI-HNGS-SP dated 19-May-2001.
2. Tools ran as per tool sketch.
3. TVD data obtained from anadrill survey.
4. Gun offset: 45m, gun azimuth: 140deg, gun depth: 30m.
5. Hydrophone offset: 45m, hydrophone azimuth: 140deg, hydrophone depth: 35m.
6. 3 compressed air guns operating at 1600psi were used for seismic acquisition. Individual gun volume was 150cc.

Suite-2 Run-6 CST-GR
1. Log correlated to PEx(HRLA)-DSI-HNGS-SP dated 19-May-2001.
2. Tools ran as per tool sketch.
3. 60 shots attempted, 52 recovered, 5 lost, 2 empty, 1 misfire.

COMPUTATION PARAMETERS

DEPTH INTERVAL	RW PPM	RW OHMM	TEMP C	GR MIN	GR MAX	R CLAY	RHOB CLAY	PHIN CLAY	t CLAY	RHOH	a	m
2000.0 - 2048.8	13000	.196	83.7	18	123	49	2.57	.356	86	.50	1.00	2.35
2048.8 - 2158.3	13000	.192	86.1	18	123	49	2.57	.356	86	.50	1.00	2.00
2048.8 - 2158.3	13000	.192	86.1	18	123	49	2.57	.356	86	.50	1.00	1.80
2048.8 - 2158.3	13000	.192	86.1	18	123	49	2.57	.356	86	.50	1.00	2.00
2048.8 - 2158.3	13000	.192	86.1	18	123	49	2.57	.356	86	.50	1.00	2.35
2158.3 - 2335.1	13000	.185	90.4	18	123	49	2.57	.356	86	.50	1.00	2.00
2158.3 - 2335.1	13000	.185	90.4	18	123	49	2.57	.356	86	.50	1.00	1.80
2158.3 - 2335.1	13000	.185	90.4	18	123	49	2.57	.356	86	.50	1.00	2.00
2158.3 - 2335.1	13000	.185	90.4	18	123	49	2.57	.356	86	.50	1.00	2.35
2335.2 - 2613.7	13000	.174	97.2	18	123	49	2.57	.356	86	.50	1.00	2.00
2335.2 - 2613.7	13000	.174	97.2	18	123	49	2.57	.356	86	.50	1.00	1.80
2335.2 - 2613.7	13000	.174	97.2	18	123	49	2.57	.356	86	.50	1.00	2.00
2335.2 - 2613.7	13000	.174	97.2	18	123	49	2.57	.356	86	.50	1.00	2.35
2613.7 - 2713.0	13000	.166	102.9	18	123	49	2.57	.356	86	.50	1.00	2.00

LOG DESCRIPTION

ROMA-CPX	Apparent Matrix Density (Complex Litho Model)
SPI -CPX	Secondary Porosity Indicator = PHIT-PHIS >=0 (Complex Litho Model)
PHIE-CPX	Effective Porosity (Complex Litho Model)
PHXO-CPX	Product (PHIE * SXO) (Complex Litho Model)
PHSW-CPX	Product (PHIE * SW) (Complex Litho Model)
MINERAL	Special Mineral Table output flag (Salt,Trona,Anhydrite,Gypsum,Coal)
VCL -CPX	Volume of clay (Complex Litho Model)
VSND-CPX	Volume of Sand (Complex Litho Model)
VLS -CPX	Volume of Limestone (Complex Litho Model)
VDOL-CPX	Volume of Dolomite (Complex Litho Model)
PHIE-CPX	Effective Porosity (Complex Litho Model)
PHXO-CPX	Product (PHIE * SXO) (Complex Litho Model)
PHSW-CPX	Product (PHIE * SW) (Complex Litho Model)
VBW -CPX	Volume of bound water (Complex Litho Model)
GRCOR	
SPDC	Spontaneous Potential - Drift-corrected
BS	Bit Size
HCAL	HRCC Caliper Calibrated
RHO8	HRDD High Resolution Formation Density
HTNP	High Resolution Thermal Neutron Porosity (Ratio Method) in Selected Lithology
DT4P	Delta-T Compressional - Monopole P&S
PEF8	HRDD High Resolution Formation Photoelectric Factor
HDRA	HRDD Spine and Ribs Density Correction
CPOO	
CKHK	
PHIT-CPX	Total porosity from CPX model after hydrocarbon correction (Complex Litho Model)
RT_HRLT	HRLT True Formation Resistivity
RLA3	Apparent Resistivity from Computed Focusing Mode 3
RXO_HRLT	HRLT Invaded Zone Resistivity
CGDN	
NET -PAY	
K_air	
K_gas	
K_water	
CSwi	
SW -CPX	Formation Water Saturation <=1.0 (Complex Litho Model)

LITHOLOGIES

▨ Bound Water	▨ Cristobilite	▨ Limestone	▨ Bound Water	🟩 OIL
🟥 GAS	🟩 MOVED OIL	🟥 MOVED GAS	🟦 Water	▨ Sandstone

SPECIAL MINERALS

■ Coal

DST/SWC/FET/Core/Shows Legend

☒ Partial recovery → Full sample → No sample ⇾ Partial sample ▶ Valid ◉ Sample

▷ Invalid ◢ Casing shoe

ENCLOSURE-2
Petrophysical and Composite Plot
2048-2380mMDRT (1:200)

THYLACINE-1

COMPOSITE AND PETROPHYSICAL SUMMARY

Company	ORIGIN ENERGY RESOURCES LTD
Well Name	THYLACINE-1
Field	Thylacine
Country	Australia
Nation	Australia
State	Tasmania
Province	Otway Basin
County or Rig name	Ocean Bounty
Field Location	Otway Basin
Field Locn. Line 1	Easting: 665030.3 m
Field Locn. Line 2	Northing: 5654721.5 m
Latitude	039 14' 27.592" S DMS
Longitude	142 54' 44.169" E DMS
Permanent Datum	LAT
Elevation of PD	.00 M
Elevation of RT	25.00 M
Elevation Ground lv	101.40 M
Elevation Log Zero	25.00 M
Above Perm. Datum	25.00 M
Log measured from	RT
Drill measured from	RT
Services	PEx(HRLA)-DSI-HNGS-SP
Other Services Ln 1	MDT-GR
Other Services Ln 2	MSCT-GR
Other Services Ln 3	FMI-GR
Other Services Ln 4	VSP-GR
Other Services Ln 5	CST-GR
Service company	Schlumberger
Number of runs	2
Well class	Exploration
Basin	Otway
Tenement/Concession	T30/P
On-Shore Flag	Off-shore
Log date	11-MAY-2001 19-May-2001
Date computed	26-03-03
Date plotted	27-03-2003
Time plotted	09:42:10

PETROLOG SOFTWARE Revision 9.10

CROCKER
DATA PROCESSING

RUN INFORMATION

Run number	1	2A
Log date	11-MAY-2001	19-May-2001
Depth-Driller	1855.50 M	2710.00 M
Depth-Logger	1833.50 M	2713.00 M
Bottom log interval	1833.30 M	2713.00 M
Top log interval	744.00 M	1657.50 M
Casing-Driller	745.30 M	1849.90 M
Casing-Logger	744.00 M	1850.00 M
Casing Diameter	13.3750 inch	9.6250 inch
Casing Weight		47.0000 lb/ft
Casing Depth		1850.00 M
Bit Size	12.2500 inch	8.5000 inch
Hole Fluid type	KCl PHPA Glycol	KCl PHPA Glycol
Fluid Density	1.1900 gm/cc	1.3300 gm/cc
Fluid Viscosity	64.0000 s	65.0000 s
Fluid PH	8.5	8.600000
Fluid Loss	3.3000 C3	2.3000 C3
Mud Sample Source	Active Pit	Active Pit
RM @ Surface	.0910 Ohmm	.0940 Ohmm
Mud temp Surface	18.00 degC	20.00 degC
RMF @ Surface	.0780 Ohmm	.0742 Ohmm
MF temp Surface	18.00 degC	20.00 degC
RMC @ Surface	.1820 Ohmm	.4547 Ohmm
MC Temp Surface	18.00 degC	20.00 degC
Source of RMF/RMC	Press	Press
Mud Sample Temp	78.00 degC	104.00 degC
Mud Filt.SampleTemp	78.00 degC	104.40 degC
MudCakeSample Sourc	Press	Press
Time circ. stopped	20:45	06:30
Date circ. stopped	10-MAY-2001	19-May-2001
Time logger at btm	08:25	18:10
Date logger at btm	11-MAY-2001	19-May-2001
Surface hole temp	26.67 degC	26.67 degC
Bottom hole temp	78.00 degC	104.40 degC
Surface temperature	18.00 degC	20.00 degC
Max recorded temp	78.00 degC	104.40 degC
Max recorded temp 1		106.00 degC
Max recorded temp 2		113.00 degC
Max recorded temp 3		114.00 degC
Logging unit No	25	25
Logging unit Loc	VEA-APG	VEA-APG
Logging Company ID	440	440
Recorded by	F.Marcano, R.Hill	F. Marcano, R. Hil
Witness	M.Bilek, P.Gibson	M. Bilek, P. Gibso
Program Version	9C2-303	9C2-303
Bore Hole Status	Open	Open
Fluid Level		.00 M
Avg Angular Deviat		.0000000
General.Temp Select		TEMP
Maximum Hole Deviat		2.9700 deg
Total depth		2710.00 M
Temp Conn.WaterSamp		37.78 degC
Filtrate Cl	59,000 ppm	59,000 ppm
% Solids	9.0	11.0

FIELD REMARKS

Suite-1 Run-1 PEx(HRLA)-DSI-HNGS-SP
1. This is the depth correlation log. Full depth control procedures followed.
2. Borehole corrections applied to the logs.
3. Limestone matrix-model and used in computation of Neutron Porosity.
4. Bottom hole temperature 7.8 degC at 08:25 on 11-May-2001.
5. Data acquired in HIRES mode for entire interval.
6. Sonic check in casing reading as expected (57 us/ft)
7. Caliper check inside casing reading 12.39 inches.
8. Tide level read from drill floor was 2.63 above LAT at 06:10 on 11-May-2001.
9. Wireline tools could not pass beyond 1833.5m. Driller's TD at 1855.0m.
10. Circulation on bottom for 55 minutes. Circulation stopped at 20:45 on 10-May-2001.
11. Tools run as per tool sketch.
12. Maximum well deviation of 1.88 degrees at 1855m.
13. DSI Modes: Lower dipole, P&S, FMD.
14. Neutron corrected for borehole size, borehole salinity, temperature, pressure, mud weight.
15. PEF corrected for barite content.

Suite-2 Run-1 PEx(HRLA)-DSI-HNGS-SP
1. Subsequent run in hole. Log correlated to PEx(HRLA)-DSI-HNGS-SP dated 11-May-2001.
2. Borehole corrections applied to the logs.
3. Limestone matrix-model and used in computation of Neutron Porosity.
4. Bottom hole temperature 104.4degC at 18:10 on 19-May-2001.
5. Data aquired in HIRES mode for entire interval.
6. Sonic check in casing reading as expected (57 us/ft).
7. Caliper check in casing reading 8.76 in. ID expected 8.75 in.
8. Circulation stoped at 06:30 on 19-may-2001.
9. Tool run as per tool sketch.
10. Well sketch as per driller's depths.
11. DSI modes: Lower dipole, P&S, FMD.
12. Neutron corrected for borehole size, borehole salinity, temperature, pressure, mud weight.
13. PEF corrected for barite content.

Suite-2 Run-2 MDT-GR
1. Log correlated to PEx(HRLA)-DSI-HNGS-SP dated 19-May-2001.
2. Tools ran as per tool sketch.
3. Low shock technique used to perform fluid sampling.
4. Both strain and quartz gauges were used during pressure measurements.
5. Pump out volume was used to clean invasion from formation prior to fluid sampling.
6. Fluid sample welssite analysis performed by Petrotech.

Suite-2 Run-3 MSCT-GR
1. Log correlated to PEx(HRLA)-DSI-HNGS-SP dated 19-May-2001.
2. Tools run as per tool sketch.
3. Mud circulated from 22:20 on 22-May-2001 and stopped at 22:55 on 22-May-2001.
4. No cores were recovered on Suite-2 Run-2 because weight on bit was too large.
5. 14 cores attempted, 12 recovered, 1 lost, and 1 aborted.

Suite-2 Run-4 FMI-GR
1. Log correlated to PEx(HRLA)-DSI-HNGS-SP dated 19-May-2001.
2. Tools run as per tool sketch.
3. 30% pad pressure applied for FMI.
4. FMI image processed to adjust image contrast.
5. BHT: 105.6 degC at 2550m.

Suite-2 Run-5 VSP-GR
1. Log correlated to PEx(HRLA)-DSI-HNGS-SP dated 19-May-2001.
2. Tools ran as per tool sketch.
3. TVD data obtained from anadrill survey.
4. Gun offset: 45m, gun azimuth: 140deg, gun depth: 30m.
5. Hydrophone offset: 45m, hydrophone azimuth: 140deg, hydrophone depth: 35m.
6. 3 compressed air guns operating at 1600psi were used for seismic acquisition. Individual gun volume was 150cc.

Suite-2 Run-6 CST-GR
1. Log correlated to PEx(HRLA)-DSI-HNGS-SP dated 19-May-2001.
2. Tools ran as per tool sketch.
3. 60 shots attempted, 52 recovered, 5 lost, 2 empty, 1 misfire.

COMPUTATION PARAMETERS

DEPTH INTERVAL	RW PPM	RW OHMM	TEMP C	GR MIN	GR MAX	R CLAY	RHOB CLAY	PHIN CLAY	t CLAY	RHOH	a	m
2000.0 - 2048.8	13000	.196	83.7	18	123	49	2.57	.356	86	.50	1.00	2.35
2048.8 - 2158.3	13000	.192	86.1	18	123	49	2.57	.356	86	.50	1.00	2.00
2048.8 - 2158.3	13000	.192	86.1	18	123	49	2.57	.356	86	.50	1.00	1.80
2048.8 - 2158.3	13000	.192	86.1	18	123	49	2.57	.356	86	.50	1.00	2.00
2048.8 - 2158.3	13000	.192	86.1	18	123	49	2.57	.356	86	.50	1.00	2.35
2158.3 - 2335.1	13000	.185	90.4	18	123	49	2.57	.356	86	.50	1.00	2.00
2158.3 - 2335.1	13000	.185	90.4	18	123	49	2.57	.356	86	.50	1.00	1.80
2158.3 - 2335.1	13000	.185	90.4	18	123	49	2.57	.356	86	.50	1.00	2.00
2158.3 - 2335.1	13000	.185	90.4	18	123	49	2.57	.356	86	.50	1.00	2.35
2335.2 - 2613.7	13000	.174	97.2	18	123	49	2.57	.356	86	.50	1.00	2.00
2335.2 - 2613.7	13000	.174	97.2	18	123	49	2.57	.356	86	.50	1.00	1.80
2335.2 - 2613.7	13000	.174	97.2	18	123	49	2.57	.356	86	.50	1.00	2.00
2335.2 - 2613.7	13000	.174	97.2	18	123	49	2.57	.356	86	.50	1.00	2.35
2613.7 - 2713.0	13000	.166	102.9	18	123	49	2.57	.356	86	.50	1.00	2.00

LOG DESCRIPTION

ROMA-CPX	Apparent Matrix Density (Complex Litho Model)
SPI -CPX	Secondary Porosity Indicator = PHIT-PHIS >=0 (Complex Litho Model)
PHIE-CPX	Effective Porosity (Complex Litho Model)
PHXO-CPX	Product (PHIE * SXO) (Complex Litho Model)
PHSW-CPX	Product (PHIE * SW) (Complex Litho Model)
MINERAL	Special Mineral Table output flag (Salt,Trona,Anhydrite,Gypsum,Coal)
VCL -CPX	Volume of clay (Complex Litho Model)
VSND-CPX	Volume of Sand (Complex Litho Model)
VLS -CPX	Volume of Limestone (Complex Litho Model)
VDOL-CPX	Volume of Dolomite (Complex Litho Model)
PHIE-CPX	Effective Porosity (Complex Litho Model)
PHXO-CPX	Product (PHIE * SXO) (Complex Litho Model)
PHSW-CPX	Product (PHIE * SW) (Complex Litho Model)
VBW -CPX	Volume of bound water (Complex Litho Model)
GRCOR	
SPDC	Spontaneous Potential - Drift-corrected
BS	Bit Size
HCAL	HRCC Caliper Calibrated
RHO8	HRDD High Resolution Formation Density
HTNP	High Resolution Thermal Neutron Porosity (Ratio Method) in Selected Lithology
DT4P	Delta-T Compressional - Monopole P&S
PEF8	HRDD High Resolution Formation Photoelectric Factor
HDRA	HRDD Spine and Ribs Density Correction
CPOO	
CKHK	
PHIT-CPX	Total porosity from CPX model after hydrocarbon correction (Complex Litho Model)
RT_HRLT	HRLT True Formation Resistivity
RLA3	Apparent Resistivity from Computed Focusing Mode 3
RXO_HRLT	HRLT Invaded Zone Resistivity
CGDN	
NET -PAY	
K_air	
K_gas	
K_water	
CSwi	
SW -CPX	Formation Water Saturation <=1.0 (Complex Litho Model)

LITHOLOGIES

▨ Bound Water	▨ Cristobilite	▦ Limestone	▨ Bound Water	🟩 OIL
🟥 GAS	🟩 MOVED OIL	■ MOVED GAS	■ Water	▨ Sandstone

DST/SWC/FET/Core/Shows Legend

☒ Partial recovery	→ Full sample	→ No sample	▷ Partial sample	◀ Valid	◉ Sample
▷ Invalid	◢ Casing shoe				

APPENDIX 2
MDT REPORT

Thylacine 1 MDT Report

Origin Energy Resources Ltd

December 2002

Thylacine 1 MDT Report

Contents

List of Figures

List of Tables

1 Summary

The Thylacine 1 MDT survey confirmed the presence of a 275 m gas column in the Thylacine Member, Flaxman Formation and Upper Waarre Formation. Sample derived gas gradients, corrected to reservoir conditions provide evidence of minor pressure discontinuities over the column.

The Free Water Level is estimated to be in the range 2299m to 2303 mSS depending on whether the pre-test pressures or sample derived gradient is used to describe the gas gradient.

Thylacine gas contains 9 - 10 % CO_2 and approximately 1.5% Nitrogen. The gas contains some natural gas liquids with approximately 15 bbl/MMscf of LPG's and 11 bbl/MMscf of condensate (C_5+ basis).

2 Background

The Thylacine 1 well was drilled in permit T/30P in the Otway Basin, offshore Victoria. The well intersected a gross gas column in excess of 250 m in the Santonian Thylacine Member and Turonian Flaxmans and Upper Waarre formations. An extensive MDT survey was conducted to evaluate the gas discovery.

The objectives of the survey included:

1. The establishment of reservoir fluid gradients and fluid contacts
2. Recovery of representative formation fluid samples for compositional and PVT analysis

The survey was conducted on May 20 – 21, 2001 and included 79 pre-test attempts and numerous sampling attempts.

3 Pre-Test Interpretation

3.1 Pressure Data

Formation pressures were measured with a quartz gauge and strain gauge. The quartz gauge functioned correctly throughout the survey, and showed excellent stability and repeatability in the measurement of hydrostatic pressures before and after each pre-test (Figure 1). Consequently, pressures from the quartz gauge were used for all interpretation due to their inherently greater accuracy and resolution.

The complete pressure dataset can be found in the Basic Data volume. A filtered and sorted dataset used for the analysis presented in this document can be found in Figure 2

3.2 Temperature

Figure 3 shows the temperatures measured in the Thylacine 1 well versus depth.

3.3 Pre Test Derived Fluid Gradients and Contacts

Figure 4 shows the pre-test derived formation pressures measured in the Thylacine 1 well versus depth. Initial inspection of this plot suggests a common gas gradient of 0.247 psi/m throughout the Thylacine Member, Flaxman Formation and Waarre Formation, with a Free Water Level around 2303 mSS.

There is some scatter above and below this apparent common gas gradient in the lower permeability Thylacine Member. Scatter above the gas gradient can be explained by a slight supercharging effect. However, if a common pressure regime is assumed, explanation of pressures measured below the gas gradient is more problematic. Figure 5 shows an expanded plot of pressures measured in the gas column. On the basis of this plot there is some evidence that the upper Thylacine Member sand intersected from 2049 – 2055 mMDRT (2024 – 2031 mSS) is not in hydraulic communication with deeper sands as the pressures measured are offset by approximately 5 psi from the common gas gradient. Pressures measured in this sand are described as 'valid' on the field report and permeability is sufficient to have obtained 2 gas samples at 2053.8 mMDRT (2028.8 mSS). Further discussion of possible pressure discontinuities can be found in Section 4.2 where sample derived in-situ fluid densities are used to determine expected fluid gradients.

3.4 Pre Test Derived Mobility

Figure 6 shows the pre-test derived formation mobility as measured in the Thylacine 1 well versus depth. The contrast between the high quality Flaxman and Upper Waarre reservoirs and the overlying Thylacine Member is evident.

3.5 Regional Pressure Comparison

Figure 7 shows the Thylacine 1 formation pressure plotted against the pressures reported in the nearby wells Minerva-1, Minerva-2, Eric The Red-1 and La Bella-1. Significant pressure discontinuities in the aquifer are evident with Thylacine 1 aquifer pressures approximately 50 psi greater than the pressure observed at Minerva and 100 psi under pressured relative to La Bella.

4 Sampling

4.1 Summary

11 reservoir gas samples and 3 water samples were collected with the MDT.

A summary of the depths from which these samples were obtained can be found in Table 1. Three samples were analysed onsite while the remainder were retained for later compositional and PVT analysis.

Full results of analysis of these samples can be found in the relevant report and a summary of the compositional analysis can be found in Table 2.

The Thylacine gas has a CO_2 content of approximately 9 - 10% and Nitrogen content of approximately 1.5% to give a total inerts content around 11.5%. The gas contains moderate levels of gas liquids with an LPG content (C_3/C_4) around 2% with approximately 1% C_5+. The corresponding LPG content is approximately 15 bbl/MMscf with a condensate content ($C5_+$ basis) of 11 bbl/MMscf.

4.2 Sample Derived Fluid Gradients and Fluid Contacts

Using the results of the compositional analysis, an estimate of reservoir fluid density and reservoir conditions has been made for selected samples over the Thylacine 1 gas column. The results of this analysis show a predicted gradient in the range 0.230 – 0.234 psi/m, somewhat lower than the 0.247 psi/m determined from the pre-test pressures.

Figure 8 shows the sample derived fluid gradients plotted for each sample depth with pre-test pressures over the gas column. This analysis suggests the presence of subtle pressure discontinuities of less than 1 psi over the lower Thylacine / Flaxman / Upper Waarre sand sequence and a more significant discontinuity of approximately 5 psi between the upper Thylacine Member sands and the remainder of the gas column.

The Free Water Level calculated using sample derived gas gradient is 2299 mSS for the lower Thylacine / Flaxman / Upper Waarre sequence and 2294 mSS for the upper Thylacine sand, assuming a common aquifer.

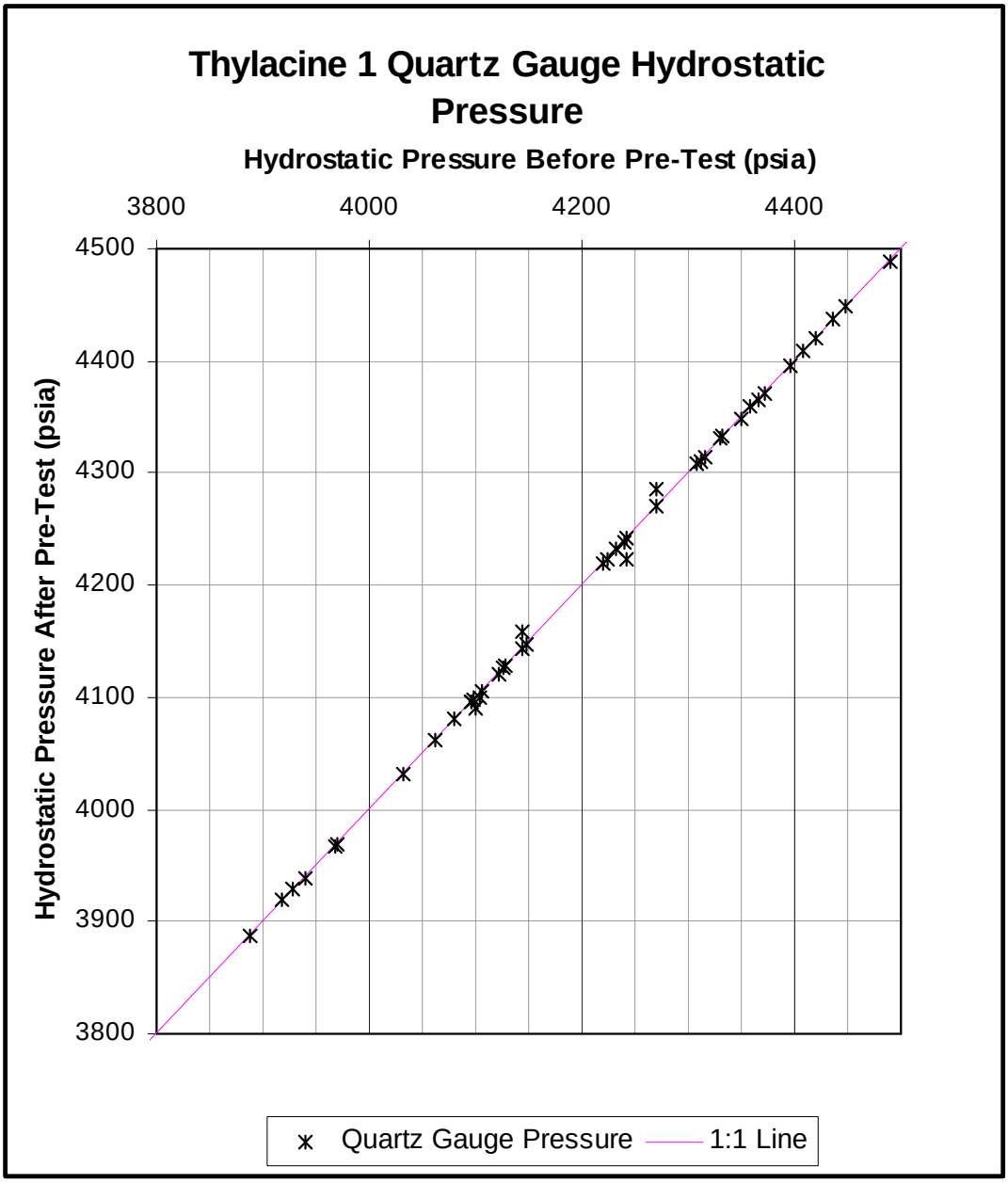
Thylacine 1 Quartz Gauge Hydrostatic Pressure
Hydrostatic Pressure Before Pre-Test (psia)
3800
4000
4200
4400
Hydrostatic Pressure After Pre-Test (psia)
4500
4400
4300
4200
4100
4000
3900
3800
Quartz Gauge Pressure
1:1 Line

Figure 1

Thylacine-1

KB Elevation **25.0** m ASL

Depth mKB	Depth mSS	Pressure psia	Mobility mD/cP	Comment
2049.0	2024.0	3280.20	4.20	* valid
2052.0	2027.0	3280.50		* valid
2052.0	2027.0	3282.30	12.70	* valid
2053.8	2028.8	3280.50		* valid
2053.8	2028.8	3280.00		* valid
2066.3	2041.3	3284.07	4.80	* valid
2071.7	2046.7	3287.90	0.30	* tight test
2077.5	2052.5	3285.46	0.20	* tight test
2092.4	2067.4	3294.42	95.10	* valid
2094.0	2069.0	3294.93	13.80	* valid
2143.7	2118.7	3307.63	19.70	* valid
2149.5	2124.5	3310.40	5.90	* valid
2153.0	2128.0	3311.96	2.60	* valid
2161.3	2136.3	3311.00	56.50	* valid
2161.5	2136.5	3310.79	0.30	* valid
2162.9	2137.9	3311.63	103.00	* seal failure
2163.4	2138.4	3311.98	122.00	* seal failure
2165.8	2140.8	3312.55	476.20	* seal failure
2165.8	2140.8	3312.66		* valid
2165.8	2140.8	3313.23	877.00	* valid
2167.0	2142.0	3313.16	3198.00	* valid
2175.5	2150.5	3314.66	41.50	* valid
2178.0	2153.0	3316.25	5.60	* valid
2179.1	2154.1	3316.00	17.20	* valid
2187.8	2162.8	3317.92	17.90	* valid
2196.0	2171.0	3320.00	132.60	* valid
2230.0	2205.0	3328.20	62.20	* valid
2236.2	2211.2	3330.58	5000.00	* valid
2236.8	2211.8	3329.90		* n/a
2238.6	2213.6	3330.28	369.70	* valid
2239.7	2214.7	3330.45	137.10	* valid
2240.7	2215.7	3330.71	240.90	* valid
2255.4	2230.4	3334.38	25.60	* valid
2263.4	2238.4	3336.77	87.10	* valid
2275.1	2250.1	3339.65	809.80	* n/a
2277.0	2252.0	3340.13	1029.00	* valid
2279.1	2254.1	3341.30	437.60	* valid
2279.1	2254.1	3340.45		* valid
2287.0	2262.0	3342.82	903.00	* valid
2288.0	2263.0	3342.68	5000.00	* valid
2297.5	2272.5	3345.26	849.80	* valid
2302.4	2277.4	3346.06	5000.00	* valid
2306.0	2281.0	3346.95	1114.80	* valid
2309.0	2284.0	3347.56	3608.90	* valid
2321.9	2296.9	3351.42	17.10	* valid
2329.1	2304.1	3353.30	13.10	* valid
2335.7	2310.7	3369.11	12.90	* valid
2344.5	2319.5	3376.60	6.10	* valid
2350.6	2325.6	3390.54	2.10	* valid
2372.6	2347.6	3413.20	490.40	* valid
2420.6	2395.6	3479.43	52.30	* valid
2448.0	2423.0	3517.30	55.70	* valid
2580.0	2555.0	3701.93	14.70	* valid
2607.0	2582.0	3747.70	5.00	* valid

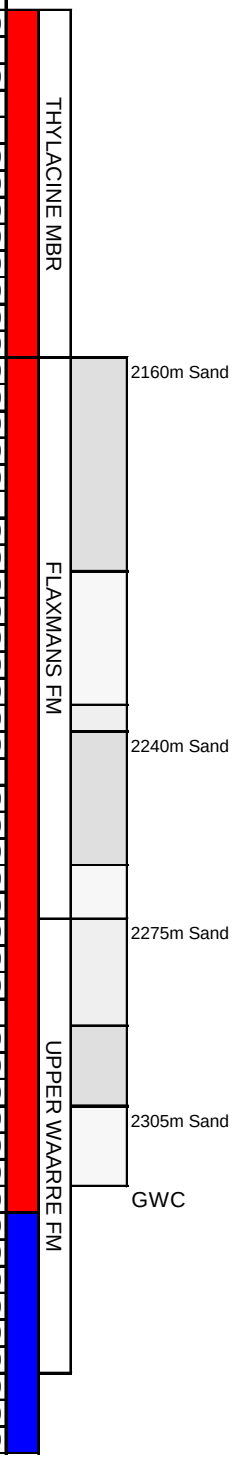

Figure 2

Thylacine 1 MDT Temperature Data

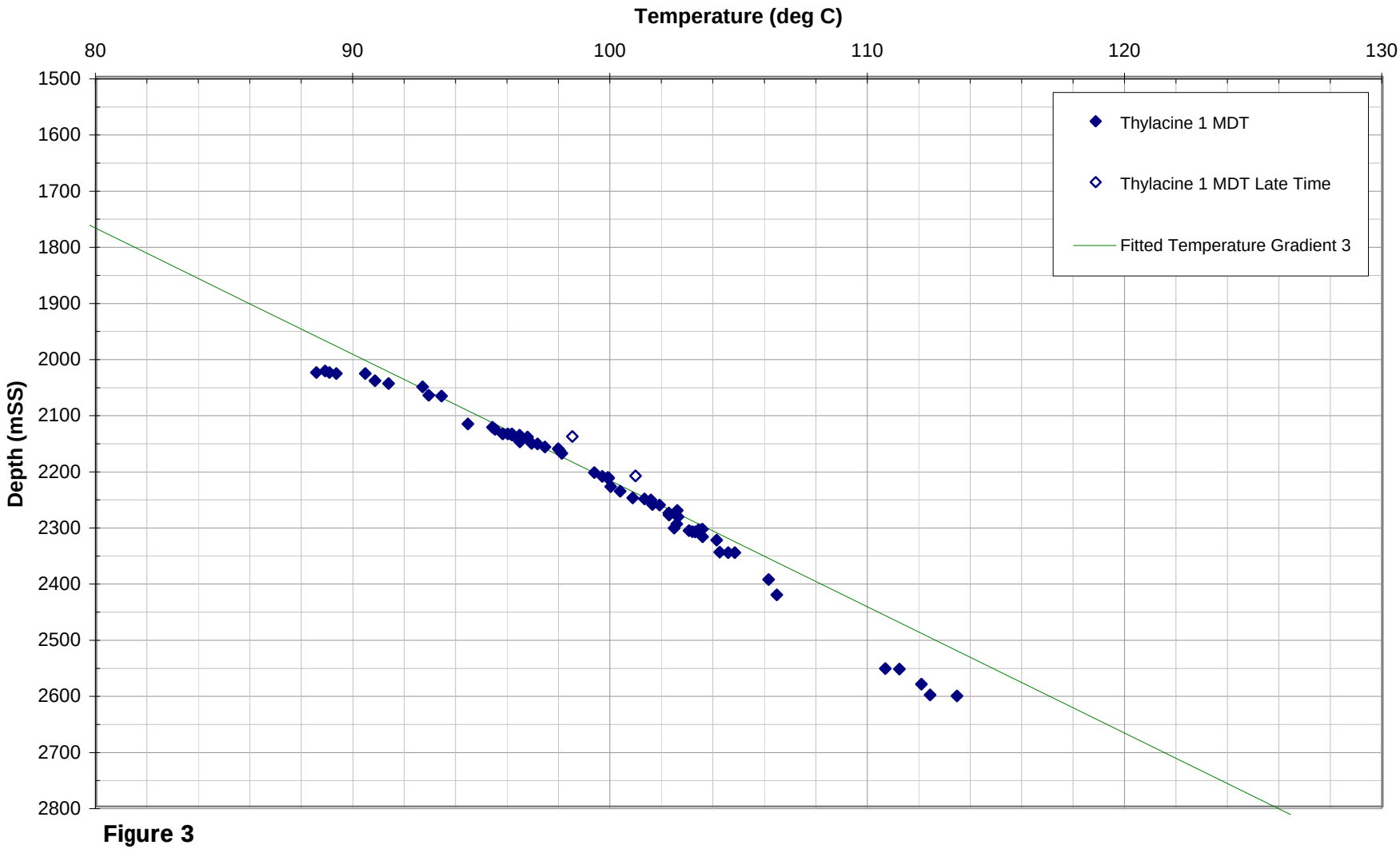

Figure 3

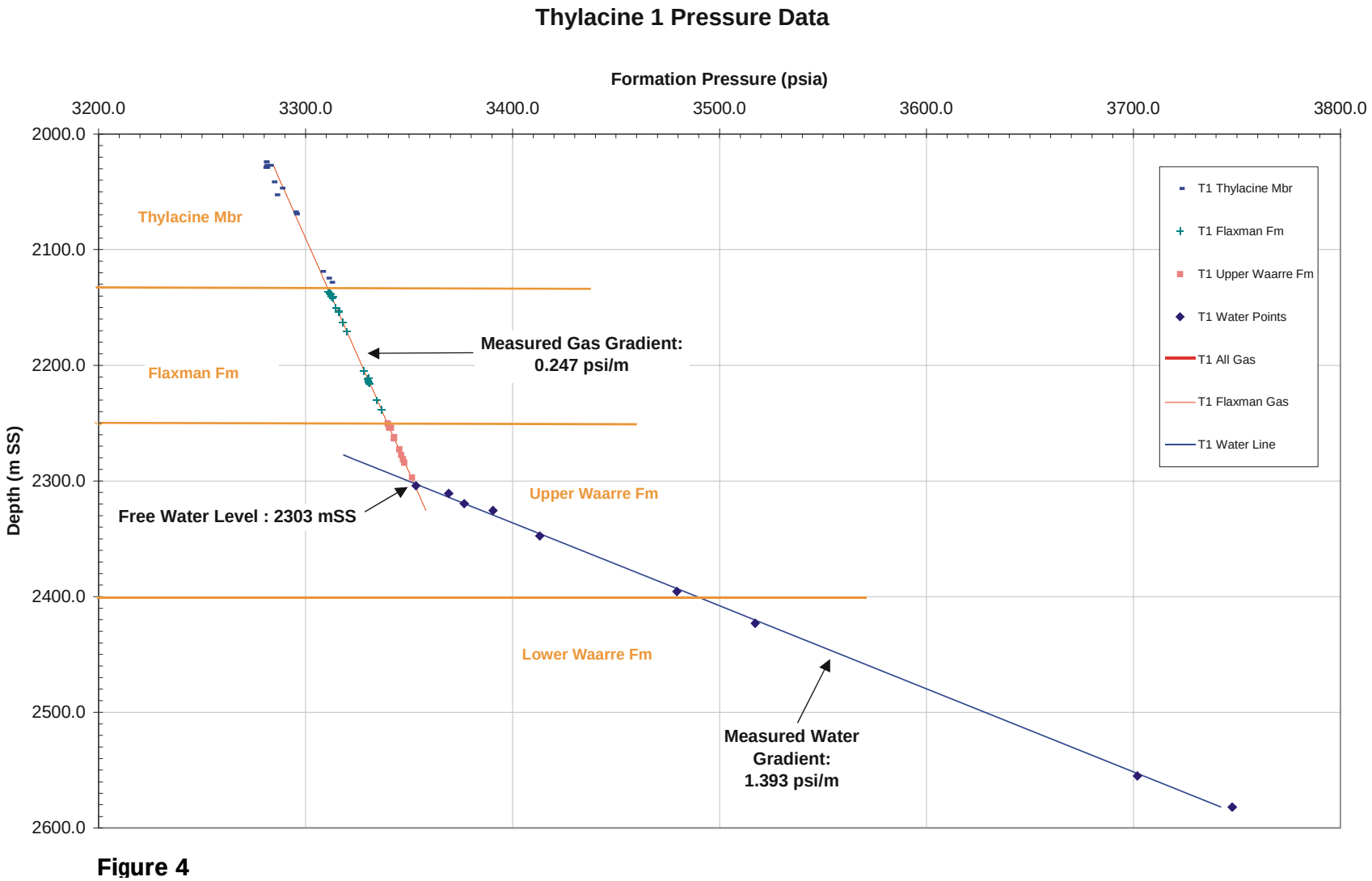
Thylacine 1 Pressure Data
Formation Pressure (psia)
3200.0
3300.0
3400.0
3500.0
3600.0
3700.0
3800.0
2000.0
2100.0
2200.0
2300.0
2400.0
2500.0
2600.0
Depth (m SS)
Thylacine Mbr
Flaxman Fm
Upper Waarre Fm
Lower Waarre Fm
Measured Gas Gradient:
0.247 psi/m
Free Water Level : 2303 mSS
Measured Water
Gradient:
1.393 psi/m
T1 Thylacine Mbr
T1 Flaxman Fm
T1 Upper Waarre Fm
T1 Water Points
T1 All Gas
T1 Flaxman Gas
T1 Water Line

Figure 4

Thylacine 1 Pressure Data

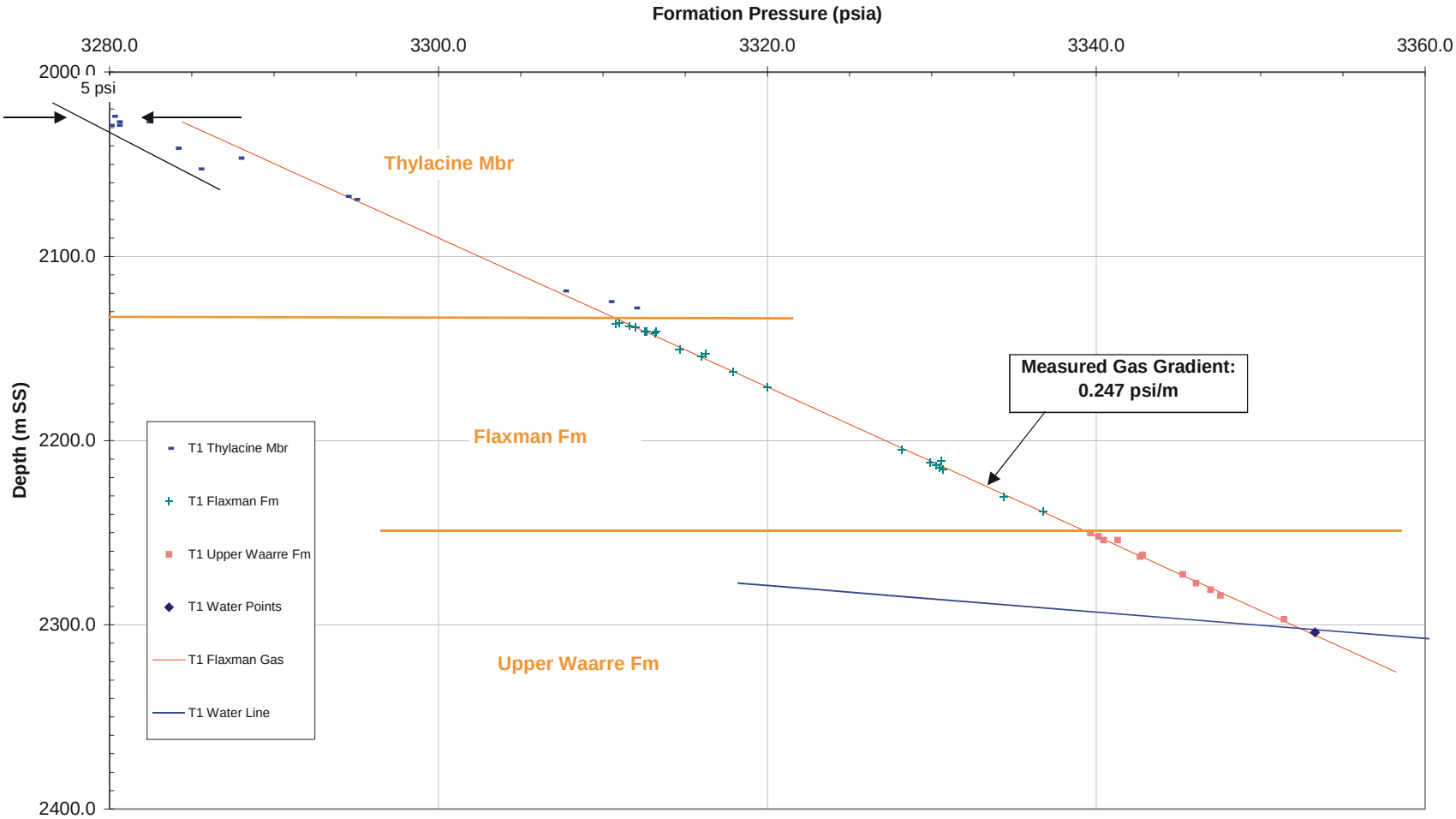

Figure 5

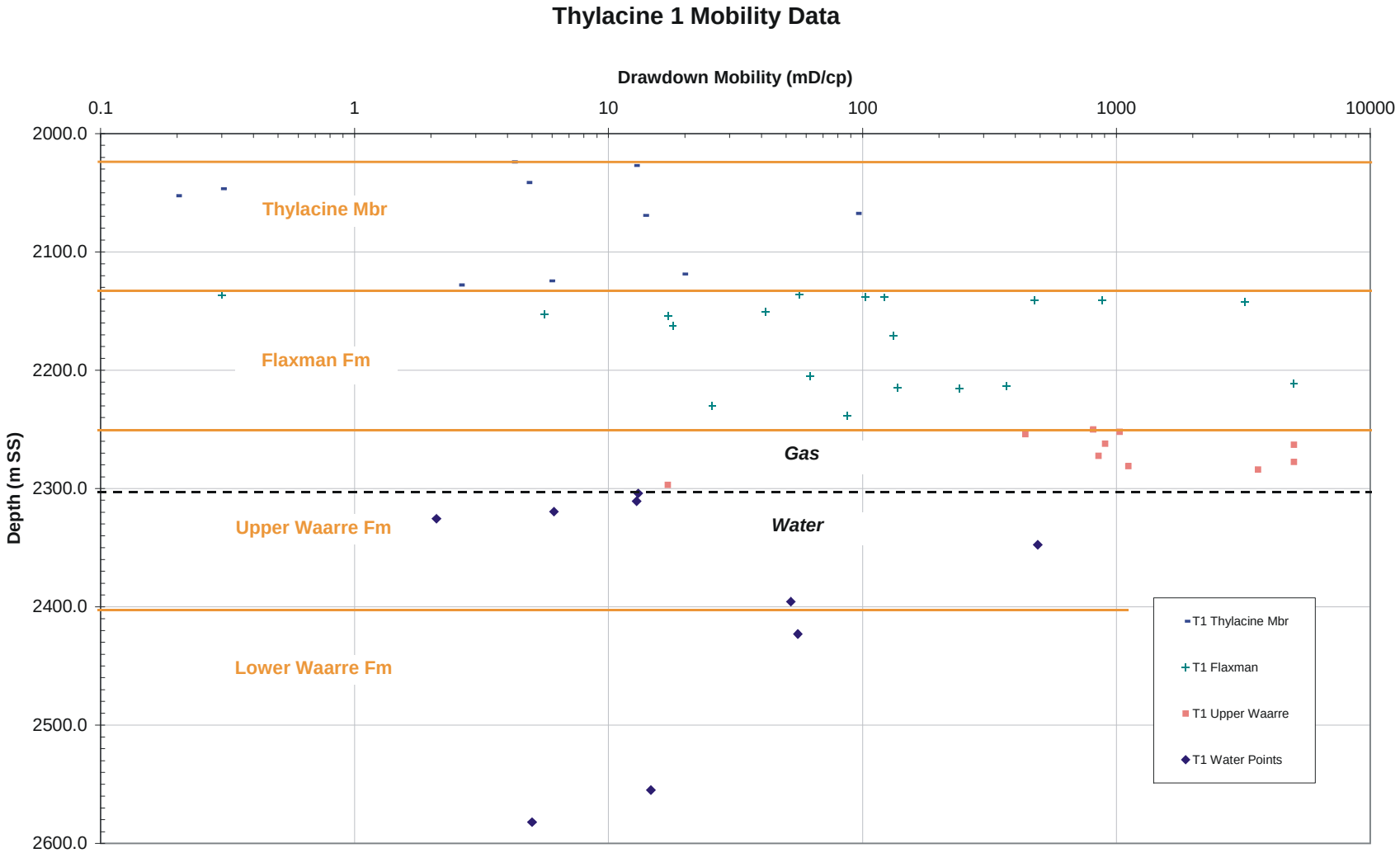
Thylacine 1 Mobility Data
Drawdown Mobility (mD/cp)
0.1
1
10
100
1000
10000
2000.0
2100.0
2200.0
2300.0
2400.0
2500.0
2600.0
Depth (m SS)
Thylacine Mbr
Flaxman Fm
Gas
Water
Upper Waarre Fm
Lower Waarre Fm
T1 Thylacine Mbr
T1 Flaxman
T1 Upper Waarre
T1 Water Points

Figure 6

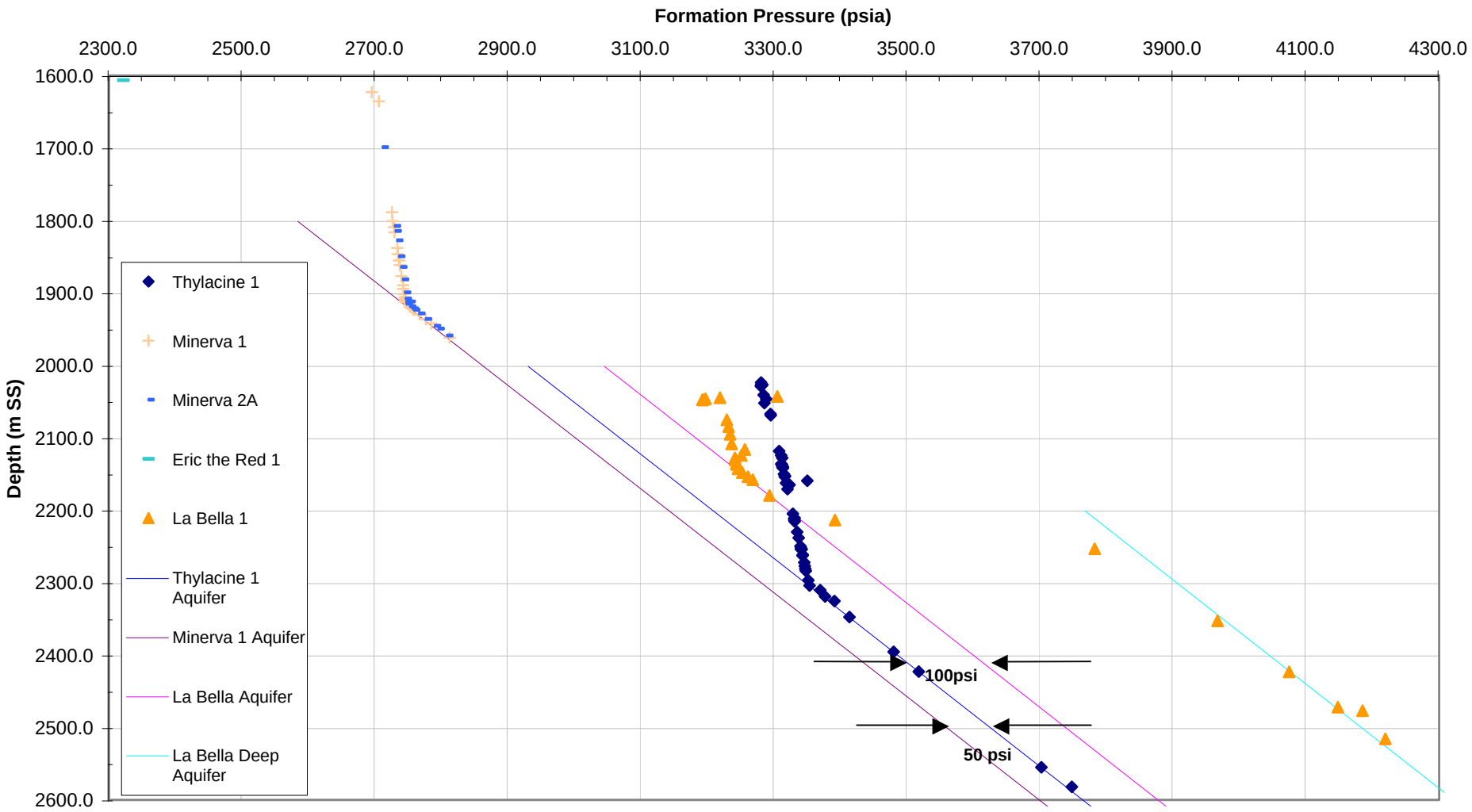
Otway Basin Regional Pressure Data - Offshore Wells
Formation Pressure (psia)
2300.0
2500.0
2700.0
2900.0
3100.0
3300.0
3500.0
3700.0
3900.0
4100.0
4300.0
Depth (m SS)
1600.0
1700.0
1800.0
1900.0
2000.0
2100.0
2200.0
2300.0
2400.0
2500.0
2600.0
Thylacine 1
Minerva 1
Minerva 2A
Eric the Red 1
La Bella 1
Thylacine 1 Aquifer
Minerva 1 Aquifer
La Bella Aquifer
La Bella Deep Aquifer
100psi
50 psi

Figure 7

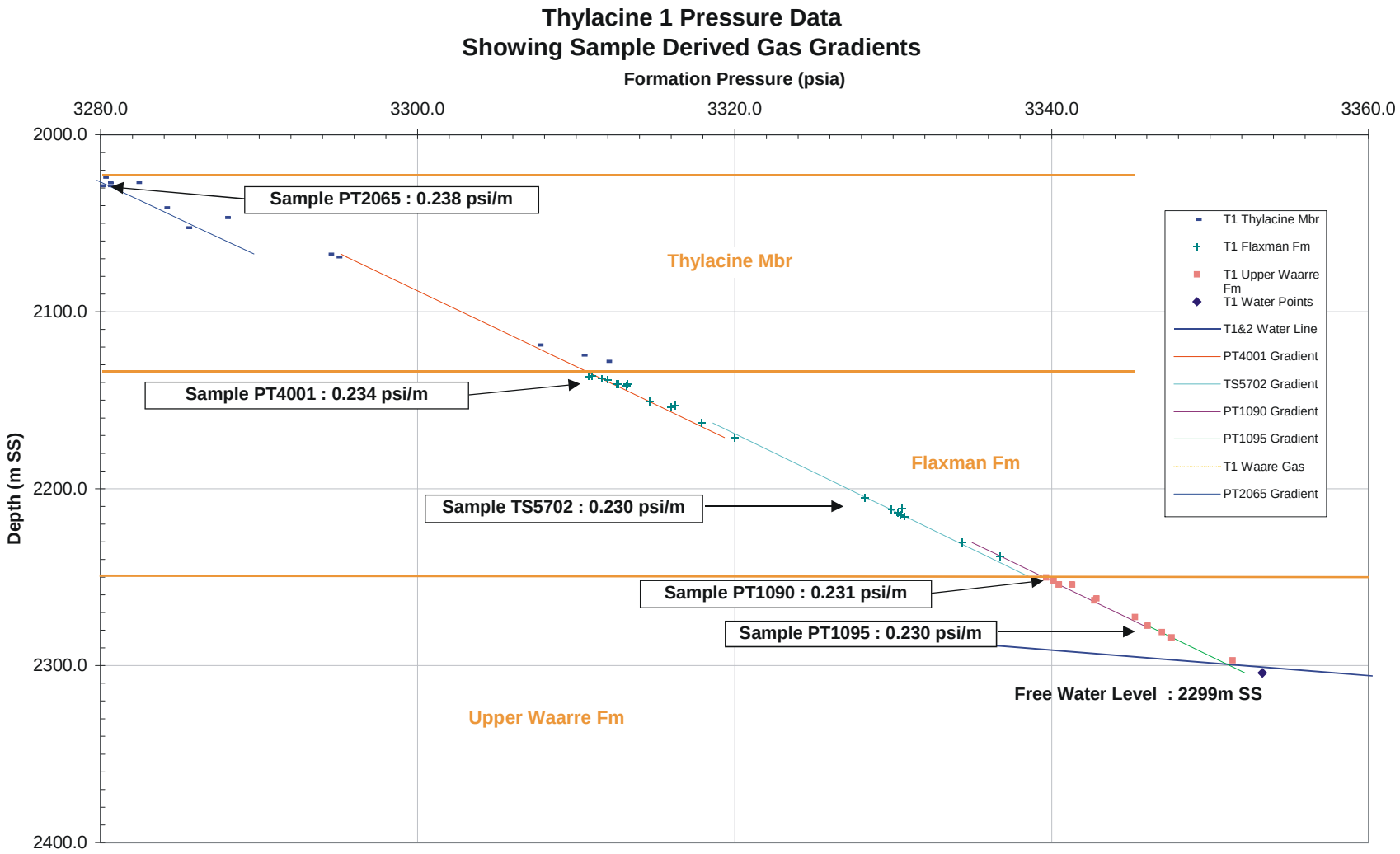
Thylacine 1 Pressure Data
Showing Sample Derived Gas Gradients
Formation Pressure (psia)
3280.0
3300.0
3320.0
3340.0
3360.0
2000.0
2100.0
2200.0
2300.0
2400.0
Depth (m SS)
Sample PT2065 : 0.238 psi/m
Sample PT4001 : 0.234 psi/m
Sample TS5702 : 0.230 psi/m
Sample PT1090 : 0.231 psi/m
Sample PT1095 : 0.230 psi/m
Thylacine Mbr
Flaxman Fm
Upper Waarre Fm
Free Water Level : 2299m SS
T1 Thylacine Mbr
T1 Flaxman Fm
T1 Upper Waarre Fm
T1 Water Points
T1&2 Water Line
PT4001 Gradient
TS5702 Gradient
PT1090 Gradient
PT1095 Gradient
T1 Waare Gas
PT2065 Gradient

Figure 8

MDT SAMPLE DATA

Client	**Woodside Energy Ltd**
Well	**Thylacine-1**
Proj. No.	**101053**

Depth (mah RT)	Chamber No.	Date Collected	Time Collected	Opening Pressure (psig)	Opening Temp. (°C)	Ambient Temp. (°C)	Sample Type	Comments
Sample 1								
2053.8	**MPSR 0157**	**20.05.01**	**08:11 - 08:25**	**4279**	**14**	**14.0**	**GAS**	**3rd sample for onsite analysis**
Sample 2								
2053.8	MPSR 0122	20.05.01	08:32 - 08:43	4264	13.6	13.6	GAS	**to be shipped in MPSR bottle**
Sample 3								
2165.8	**MPSR 0485**	**21.05.01**	**06:31 - 06:38**	**4221**	**13.7**	**13.7**	**GAS**	**1st sample for onsite analysis**
Sample 4								
2165.8	MPSR 0156	21.05.01	06:39 - 06:45	4134	13.6	13.6	GAS	**to be shipped in MPSR bottle**
Sample 5								
2165.8	MRSC BB90	21.05.01	06:47 - 06:59	3843	13.5	13.5	GAS	transfer to Petrotech cylinders
Sample 6								
2236.8	MPSR 0487	21.05.01	08:50 - 08:54	3873	13.5	13.5	GAS	not over pressurised as much as other samples ?
Sample 7								
2236.8	MPSR 0186	21.05.01	08:54 - 08:58	4119			GAS	transfer to Petrotech cylinders
Sample 8								
2279.1	MPSR 0497	21.05.01	09:50 - 09:54	4105	13.5	13.5	GAS	transfer to Petrotech cylinders
Sample 9								
2279.1	MPSR 0187	21.05.01	09:54 - 09:57	3989			GAS	transfer to Petrotech cylinders
Sample 10								
2302.4	**MPSR 0500**	**21.05.01**	**10:52 - 10:58**	**4076**	**13.5**	**13.5**	**GAS**	**2nd sample for onsite analysis**
Sample 11								
2302.4	MPSR 0192	21.05.01	10:59 - 11:04	3959			GAS	**to be shipped in MPSR bottle**
Sample 12								
2344.5	MPSR 0503	21.05.01	12:02 - 12:15	N/A	13.5	13.5	WATER	transfer to Petrotech cylinders
Sample 13								
2344.5	MPSR 0193	21.05.01	12:17 - 12:23	**no sample**			WATER	closing mechanism on valve failed
Sample 14								
2344.5	MRSC BB36	21.05.01	12:28 - 13:20	N/A	13.6	14	WATER	transfer to Petrotech cylinders

Table 1

Table 2: Compositional Data

Well	Formation	Depth	Sample ID	N2	CO2	C1	C2	C3	iC4	nC4	iC5	nC5	nC6	C7	C8	C9	C10	C11	C12+	Inerts	LPG's	C5+	C8+
		mMDKB		mol%	mol%	mol%	mol%	mol%	mol%	mol%	mol%	mol%	mol%	mol%	mol%	mol%	mol%	mol%	mol%	mol%	mol%	mol%	mol%
Thylacine-1	Thylacine Mbr	2053.8	PT2065	1.85	8.85	80.52	5.28	1.50	0.32	0.54	0.22	0.16	0.18	0.21	0.23	0.05	0.02	0.01	0.06	10.70	2.36	1.14	0.37
Thylacine-1	Flaxman Fm	2165.8	PT4001	1.38	9.29	81.13	4.88	1.61	0.29	0.39	0.15	0.11	0.14	0.23	0.21	0.06	0.03	0.02	0.08	10.67	2.29	1.03	0.40
Thylacine-1	Flaxman Fm	2165.8	PT1063	1.46	9.20	81.57	4.71	1.43	0.29	0.39	0.16	0.11	0.13	0.23	0.20	0.05	0.01	0.01	0.05	10.66	2.11	0.95	0.32
Thylacine-1	Flaxman Fm	2236.8	TS5702	1.23	9.40	81.82	4.56	1.41	0.26	0.36	0.14	0.10	0.13	0.22	0.20	0.06	0.02	0.01	0.08	10.63	2.03	0.96	0.37
Thylacine-1	Flaxman Fm	2236.8	TS5601	1.38	9.55	81.55	4.53	1.34	0.25	0.38	0.15	0.11	0.13	0.23	0.21	0.06	0.03	0.02	0.08	10.93	1.97	1.02	0.40
Thylacine-1	Upper Waarre Fm	2279.1	PT2037	1.49	9.84	80.62	4.82	1.52	0.28	0.42	0.17	0.12	0.14	0.22	0.19	0.05	0.02	0.02	0.08	11.33	2.22	1.01	0.36
Thylacine-1	Upper Waarre Fm	2279.1	PT1090	1.52	9.91	80.14	4.94	1.64	0.31	0.45	0.18	0.13	0.15	0.23	0.21	0.06	0.03	0.02	0.08	11.43	2.40	1.09	0.40
Thylacine-1	Upper Waarre Fm	2302.4	PT1095	1.50	9.83	80.71	4.81	1.43	0.27	0.44	0.18	0.12	0.14	0.22	0.19	0.06	0.02	0.01	0.07	11.33	2.14	1.01	0.35
			Mean	**1.42**	**9.57**	**81.08**	**4.75**	**1.48**	**0.28**	**0.40**	**0.16**	**0.11**	**0.14**	**0.23**	**0.20**	**0.06**	**0.02**	**0.02**	**0.07**	**11.00**	**2.17**	**1.01**	**0.37**

APPENDIX 3
GEOCHEMISTRY REPORT

GEOCHEMISTRY REPORT

1 Introduction

Following the completion of the Thylacine-1 well, a program was undertaken to evaluate the source rock character and thermal maturity of the drilled sequence and the fluids recovered from it.

This report provides a compilation of the petroleum geochemistry data from Thylacine-1 well, together with an interpretation of these data.

The evaluation consisted of the following analyses:

DESCRIPTION	TYPE	QUANTITY
Standard compositional gas analysis (C1 to C5, N2, O2, CO2)	GAS	2
Stable carbon isotope determination (CSIA) of gases	GAS	2
SCAN GC-MS whole oil	COND	2
Liquid chromatography	COND	2
SCAN GC-MS (saturate fraction)	COND	2
SIM GC-MS branched/cyclic alkane fraction	COND	2
SIM GC-MS aromatic fraction (including HPI)	COND	2
Stable carbon isotope determination (4 fractions)	COND	2
Compound specific isotope analysis (CSIA)	COND	2
Wax determination by high temperature gas chromatography (HTGC)	COND	1
Lithological description	SED	7
Rock-Eval pyrolysis	SED	5
Total organic carbon (TOC) determination (before cleanup)	SED	5
Rock-Eval pyrolysis (before cleanup)	SED	3
Small scale solvent extraction (for removal of HC based contaminants)	SED	24
Water extraction (for removal of glycol contamination)	SED	24
Total organic carbon (TOC) determination (after cleanup)	SED	24
Rock-Eval pyrolysis (after cleanup)	SED	23
Vitrinite reflectance	SED	14
Pyrolysis-gas chromatography (PGC) of extracted sediment	SED	2
Solvent extraction	SHOW	3
SCAN GC-MS (whole extract)	SHOW	1
Liquid chromatography	SHOW	3
SCAN GC-MS (saturate fraction)	SHOW	3
SIM GC-MS branched/cyclic alkane fraction incl. sep. - qualitative	SHOW	1

Table 1: Analytical program

Geotechnical Services Pty in Perth carried out the source rock and fluid analyses. In addition, Shell Global Solutions (SGS) in Houston carried out HTGC wax analysis of the condensate.

2 Source Rock Characterisation

2.1 Total Organic Carbon & Rock Eval Pyrolysis

As indicated in Table 1 and Table 2, a number of samples were selected for Rock-Eval pyrolysis from the Belfast Formation (incl. Thylacine Member), Flaxman Formation and Waarre Formation. These consisted largely of argillaceous sandstones and siltstones, only one true claystone being analysed from 1972 m. Although carbonaceous material was frequently observed within cuttings towards the base of the well, it proved impossible to pick sufficient for analysis, and Rock-Eval data represent bulk cuttings only. One high graded cuttings sample within the Lower Waarre Formation (2610-2630 m) yielded slightly higher TOC than bulked cuttings from the same interval, but there was insufficient material to obtain a Rock-Eval result.

ANALYSIS OF ORGANIC MATTER BY ROCK-EVAL PYROLYSIS

THYLACINE-1

GEOTECH

Depth (m)		Tmax	S1	S2	S3	S1+S2	S2/S3	PI	TOC	HI	OI
1972.0	ext	431	0.15	1.32	0.60	1.47	2.20	0.10	1.48	89	41
2040.0	ext	432	0.18	0.78	0.63	0.96	1.24	0.19	1.28	61	49
2090.0	ext	432	0.30	1.27	0.87	1.57	1.46	0.19	1.09	117	80
2131.5		462	1.99	3.12	1.39	5.11	2.24	0.39	1.41	221	99
2131.5	ext	435	0.21	1.16	0.64	1.37	1.81	0.15	1.35	86	47
2258.5	ext	433	0.10	0.59	0.53	0.69	1.11	0.14	0.61	97	87
2282.5	ext	435	0.18	1.35	0.77	1.53	1.75	0.12	1.33	102	58
2334.8	ext	436	0.20	1.09	0.90	1.29	1.21	0.16	1.22	89	74
2356.0		348	9.00	6.30	2.65	15.30	2.38	0.59	2.46	256	108
2397.7	ext	433	0.43	4.39	1.37	4.82	3.20	0.09	3.62	121	38
2417.0		nd	nd	nd	nd	nd	nd	nd	0.20	nd	nd
2425.7	ext	435	0.17	1.58	0.42	1.75	3.76	0.10	1.67	95	25
2438.0		nd	nd	nd	nd	nd	nd	nd	0.23	nd	nd
2449.0	ext	437	0.22	2.58	1.09	2.80	2.37	0.08	2.53	102	43
2515-2530	ext	434	0.15	1.21	1.19	1.36	1.02	0.11	1.13	107	105
2535-2550	ext	432	0.11	1.00	1.20	1.11	0.83	0.10	0.97	103	124
2552.2	ext	435	0.13	0.97	0.54	1.10	1.80	0.12	0.97	100	56
2571.0	ext	434	0.14	1.41	1.02	1.55	1.38	0.09	1.56	90	65
2597.0	ext	435	0.15	1.73	1.33	1.88	1.30	0.08	1.82	95	73
2610-2630	bulk ctgs	442	0.24	1.55	1.49	1.79	1.04	0.13	1.17	132	127
2610-2630	h/p ctgs	nd	nd	nd	nd	nd	nd	nd	1.97	nd	nd
2630-2650	ext	433	0.45	3.94	1.58	4.39	2.49	0.10	2.46	160	64
2636.2	ext	434	0.15	0.75	0.89	0.90	0.84	0.17	0.88	85	101
2650-2670	ext	435	0.33	2.13	1.48	2.46	1.44	0.13	1.70	125	87
2667.5		430	5.73	11.09	1.78	16.82	6.23	0.34	3.99	278	45
2667.5	ext	436	0.55	4.58	1.05	5.13	4.36	0.11	2.03	226	52
2670-2690	ext	356	0.56	1.92	2.03	2.48	0.95	0.23	1.31	147	155
2690-2710	ext	434	0.19	1.44	1.18	1.63	1.22	0.12	1.11	130	106
2695.5	ext	nd	0.03	0.19	0.53	0.22	0.36	0.14	0.16	119	331

Table 2: TOC and Rock-Eval pyrolysis data

Initial results indicated significant contamination with alkenes (Penetrex) and glycols from the mud system, and all samples were subsequently extracted prior to analysis (prefixed "ext" in Table 2). TOC of cleaned/extracted samples varies from 0.6% to 3.6%, and averages 1.5%. The geochemical well log (Figure 1) compares the results of unextracted (black points) with extracted samples (coloured points).

HI ranges from 61 to 278 but some of the higher values are due to contamination, and extracted samples had a maximum HI of 226, and average HI of 106, indicating a fair to rich, Type III gas-prone source rock (Figure 2). S2 yields from the extracted samples vary from 0.6 to 4.6 kg/tonne, but are typically below 2 kg/tonne (Figure 3) suggesting that expulsion would only be possible at relatively high levels of thermal maturity. At high maturity, considerable secondary cracking of liquids to gas would occur, producing the type of dry gas encountered in the offshore Otway gas fields found to date.

Group : Geological Services and Regional Review
Basin : Otway
Author : WOPRD9

WOODSIDE
AUSTRALIAN ENERGY

Petroleum Source Rock Summary: Thylacine-1

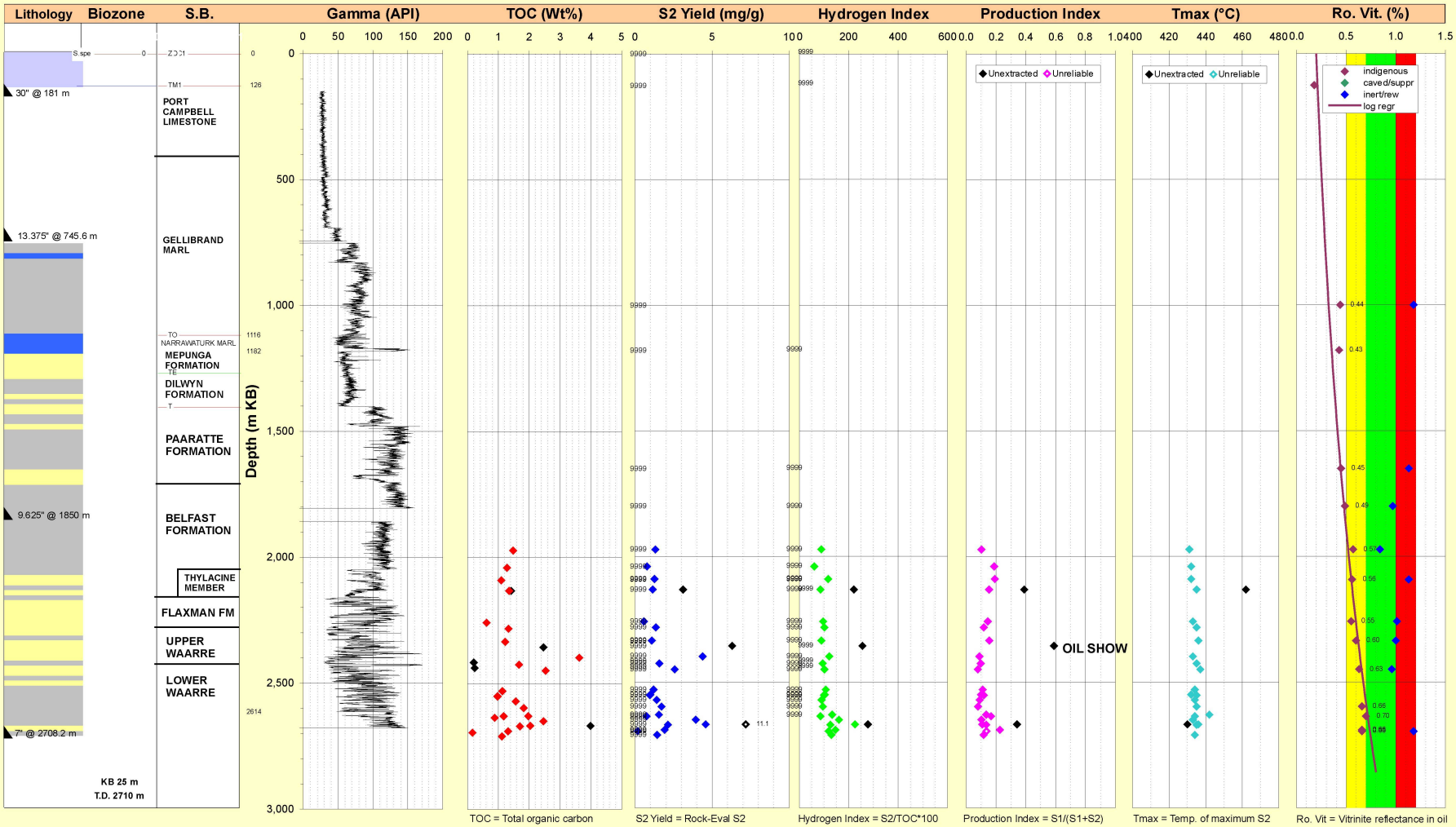

Last revision : 19/11/02

Figure 1: Geochemical well log, Thylacine-1

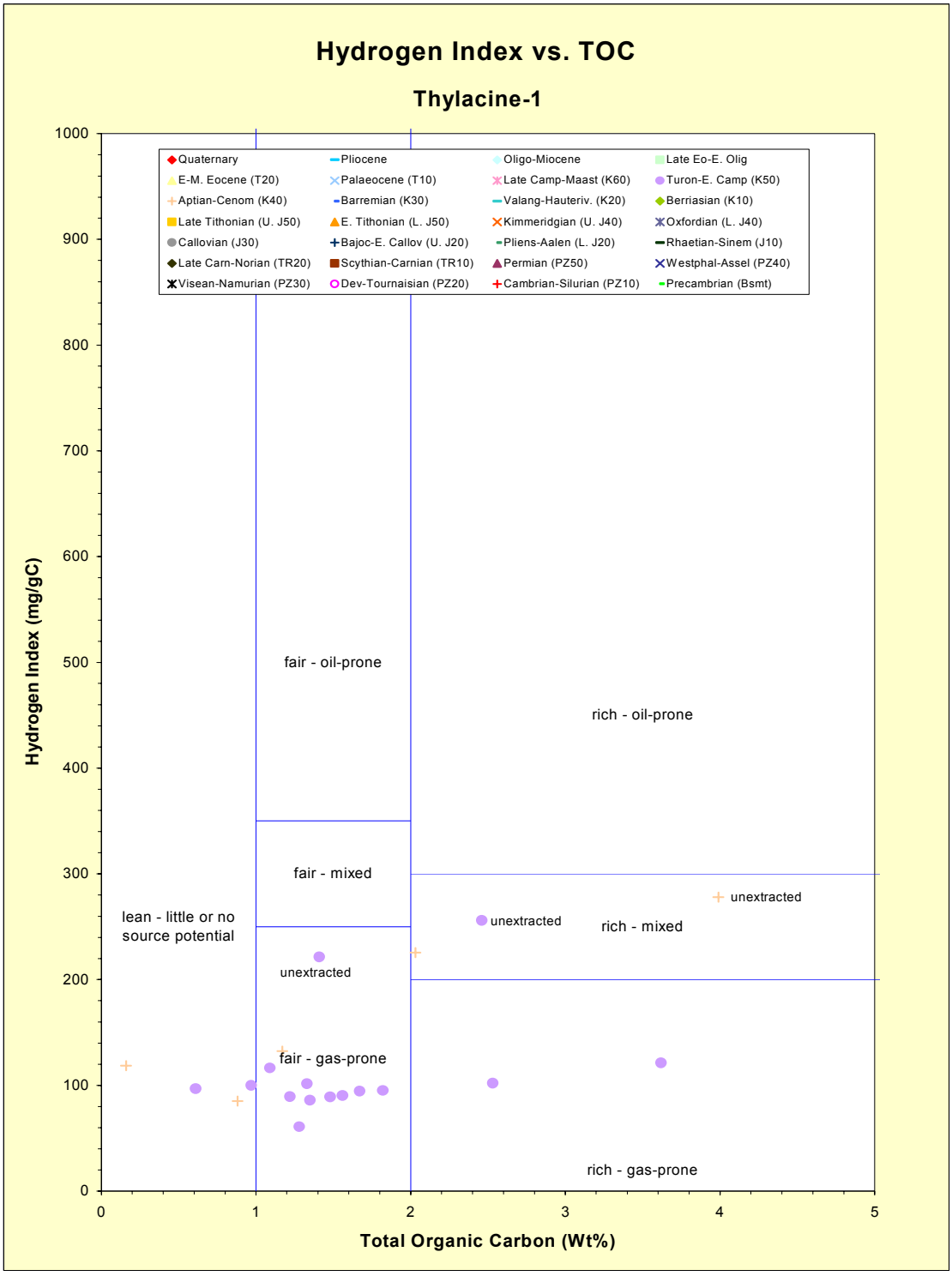

Figure 2: TOC vs. Hydrogen Index

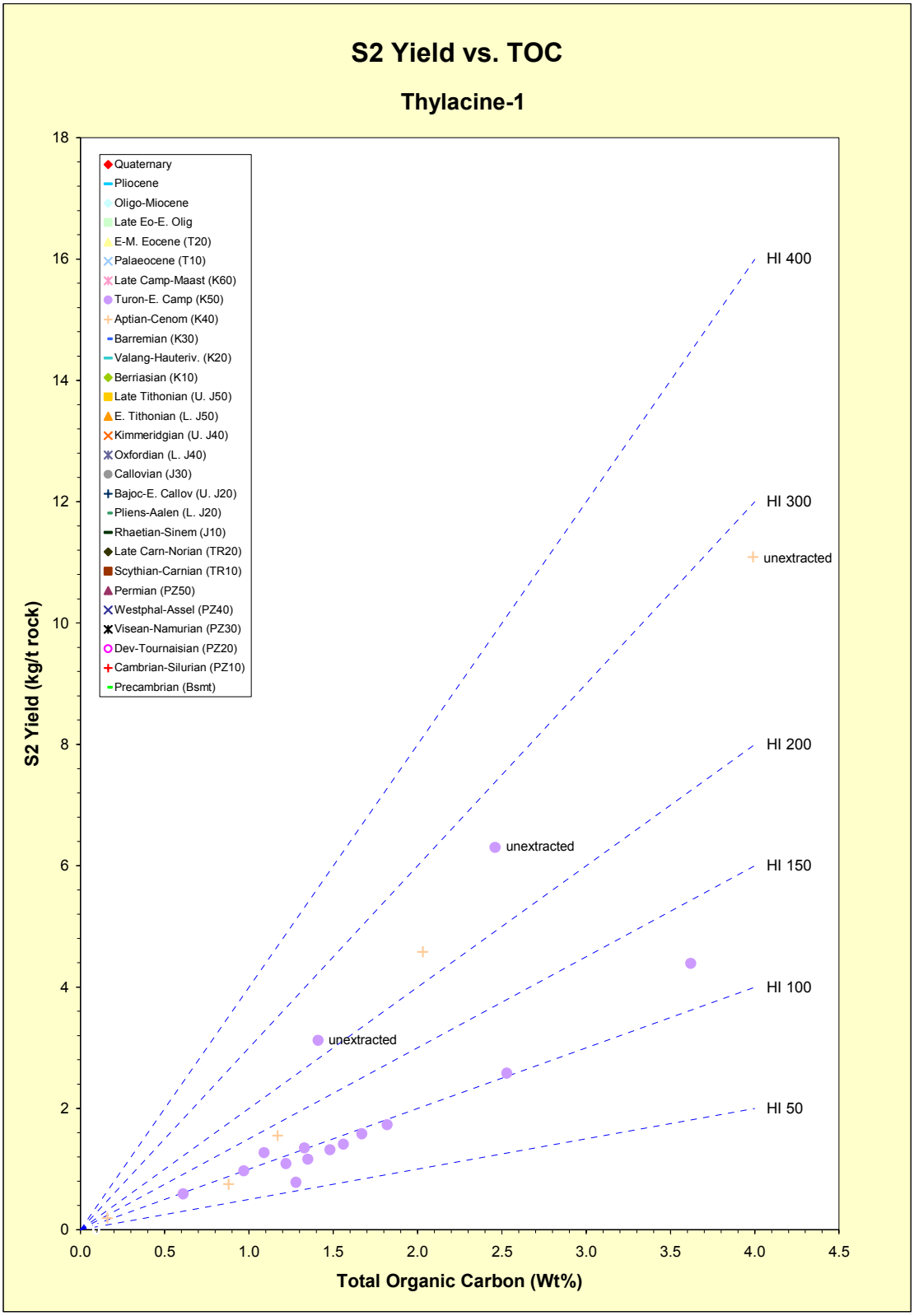

Figure 3: S2 yield vs. TOC

2.2 Pyrolysis-Gas Chromatography

Pyrolysis-gas chromatography was performed on two of the richer argillaceous siltstones from the Upper Waarre (2397.7 mKB) and Lower Waarre (2397.7 mKB). These yielded relatively high gas/oil generation indices (GOGI = C1-C5/C6+ HC's) of 1.63-1.79, consistent with primarily gas-prone source potential. Paraffins were generated out to at least C31, however, suggesting that any liquids expelled by these sediments could be relatively waxy (Figure 4).

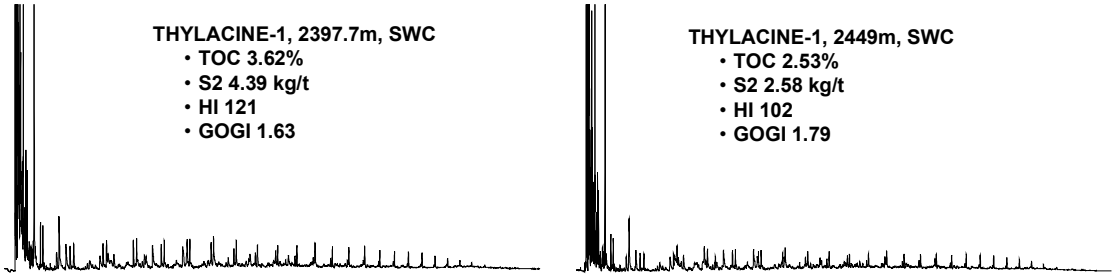

Figure 4: Pyrolysis-GC profiles, Upper and Lower Waarre Formations

On the basis of these data it is clear that the Late Cretaceous section in Thylacine-1 contains a gas-prone source facies which could be the source of the Thylacine fluids, where sufficiently mature. It is anticipated that the underlying Aptian - Albian Eumeralla Formation contains similar source potential, and this is assumed to be the main source interval for the Waarre Formation Play, both for the Thylacine discovery, and regionally. The Eumeralla Formation was not penetrated at Thylacine-1.

2.3 Thermal Maturity

Rock-Eval Tmax values (Table 2) vary from 431 to 437°C for the extracted samples, over the sampled interval (1972 - 2695.5m). A Tmax value of c. 435°C is regarded as marking the entrance into the oil generative window, for Type III organic matter, and Late Cretaceous sediments in this well are clearly immature (Figure 5).

Vitrinite reflectance measurements were made on 14 samples from the interval 980-2695 m. One sample (1440-1450 m) yielded no vitrinite, but the remainder range from 0.44% Ro. in the Nirranda Group to 0.7% Ro. in the Lower Waarre Formation.

These two types of measurements are in general agreement that source rocks identified in the Waarre Formation are immature for oil generation in Thylacine-1. The VR profile is plotted in Figure 1, and suggests that the top of the "oil window" (0.7% Ro.) is intersected at about 2600 mRT at this location. However, the quality of the organic matter in Lower Waarre source rocks is insufficient for oil expulsion, and only minor oil staining within the source rocks is observed. Gas at Thylacine is not being sourced from *in situ* potential source rocks, but instead, by extrapolation, from sediments above 1.0 - 1.3% Ro, at depths in excess of 3500m. The source rocks are more likely to be Eumeralla Formation carbonaceous siltstones and coals, or more deeply buried Waarre and Flaxman Formations.

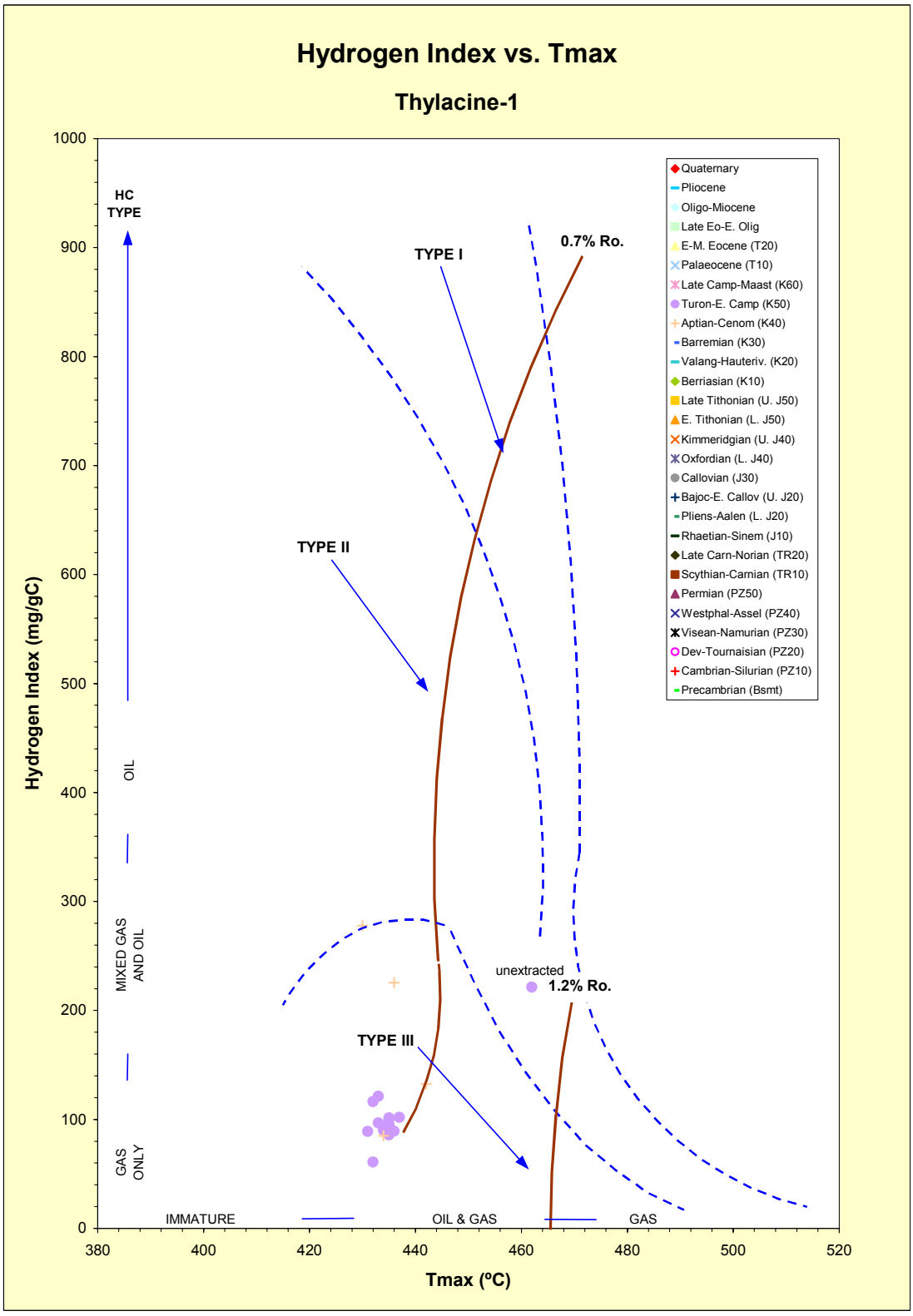

Figure 5: Hydrogen index vs. Tmax

Sample Details		Mean	Range	No of Readings	Sample Description
980-1000m	Rvmax	0.44	0.42-0.58	6	Rare lamalginite yellow to orange, rare liptodetrinite yellow to orange. (Argillaceous carbonate>calcareous claystone. Dom rare, I>L=V. All maceral groups rare. The most common rock type is a clay-rich coquina. One carbonate grain contains bitumens with reflectances in the range 1.77 to 1.98% and this may be a reworked population. Mineral fluorescence variable
Ctgs	RImax	1.18	0.66-2.32	15	
1170-1180m	Rvmax	0.43	0.33-0.57	25	Rare liptodetrinite yellowish orange to orange. (Siltstone>carbonaceous claystone>claystone >argillaceous carbonate. The carbonaceous claystone is transitional to shaly coal and consists of vitrinite>L>I. Dom abundant, V>L>I. Vitrinite abundant, liptinite sparse and inertinite rare. Mineral fluorescence weak dull orange to absent where organic matter is abundant, but strong fluorescence
Ctgs					
1440-1450m		-	-	-	Fluorescing liptinite absent. (Sandy siltstone. Dom absent. All maceral groups absent. Mineral fluorescence extremely weak to absent. Iron oxides abundant, mainly disseminated within clay matrix, but some larger grains of crystalline iron oxides. Pyrite absent.)
Ctgs				-	
1640-1650m	Rvmax	0.45	0.33-0.60	25	Sparse liptodetrinite orange. (Argillaceous siltstone. Dom abundant, I>V>>L. Inertinite abundant, vitrinite common, and liptinite sparse. Rare reworked coal/peat clasts, with vitrinite reflectance within the range of FGV. Mineral fluorescence pervasive moderate orange. Pyrite common.)
Ctgs	RImax	1.13	0.72-1.48	5	
1790-1800m	Rvmax	0.49	0.36-0.65	25	Sparse liptodetrinite orange. (Claystone>siltstone. Dom abundant, I>V>L. Inertinite abundant, vitrinite and liptinite sparse. Mineral fluorescence pervasive moderate orange. Pyrite abundant.)
Ctgs	RImax	0.97	0.78-1.10	6	
1972m	Rvmax	0.57	0.37-0.68	24	Sparse liptodetrinite orange, rare sporinite orange, rare cutinite orange to dull orange. (Claystone, carbonaceous. Dom abundant, I>L>V. Inertinite abundant, liptinite and vitrinite sparse. A high proportion of the inertinite is low reflecting, comprising both semifusinite and macrinite. Mineral fluorescence pervasive moderate orange. Pyrite common.)
SWC	RImax	0.84	0.76-0.94	9	
2089-2092m	Rvmax	0.56	0.39-0.67	18	Rare liptodetrinite orange. (Siltstone. Dom rare, I>V>L. Inertinite sparse, vitrinite and liptinite rare. The inertinite includes a high proportion of macrinite. Mineral fluorescence pervasive moderate orange. Iron oxides abundant but may represent a contaminant, or cavings. Pyrite common.)
Ctgs	RImax	1.13	0.86-1.45	11	
2258.5m	Rvmax	0.55	0.43-0.73	26	Sparse liptodetrinite yellowish orange to orange. (Siltstone> argillaceous siltstone. Dom abundant, I>V>L. Inertinite abundant, vitrinite and liptinite sparse. Mineral fluorescence pervasive to weakly patchy moderate to weak orange. Pyrite common.)
SWC	RImax	1.01	0.92-1.18	4	
2330-2335m	Rvmax	0.6	0.47-0.74	25	Sparse lamalginite yellow, sparse liptodetrinite yellow to orange.rare sporinite yellowish orange to orange. (Siltstone. Dom common, I>V>L. Rare oil or dead oil interstitial, yellow to yellowish orange. Strong fluorescence in the mounting resin suggesting oil has bled into the mounting medium. Mineral fluorescence patchy bright to moderate orange. Iron oxides abundant - mostly
Ctgs	RImax	1	0.92-1.08	2	
2449.2m	Rvmax	0.63	0.53-0.78	27	Sparse sporinite yellowish orange to orange, sparse liptodetrinite yellow to orange. (Argillaceous siltstone. Dom abundant, I>V>L. Inertinite and vitrinite abundant, liptinite sparse. Rare oil drops or dead oil yellowish orange to yellow, strong fluorescence from the mounting resin. Mineral fluorescence patchy bright to moderate orange. Pyrite common.)
SWC	RImax	0.96	-	1	
2597.2m	Rvmax	0.66	0.54-0.84	27	Sparse sporinite yellowish orange to orange, sparse liptodetrinite yellow to orange. (Silty claystone. Dom abundant, I>V>L. Inertinite and vitrinite abundant, liptinite sparse. Mineral fluorescence weakly patchy bright to moderate orange. Strong fluorescence from the mounting resin, presumably due to oil impregnation from the sample. Pyrite common.)
SWC					
2636.2	Rvmax	0.7	0.55-0.88	25	Sparse sporinite yellowish orange to orange, sparse cutinite orange to dull orange, rare liptodetrinite yellow to orange. (Siltstone, argillaceous. Dom abundant, I>V>L. Inertinite abundant, vitrinite common, liptinite sparse. Mineral fluorescence weakly patchy moderate to dull orange. Local brighter fluorescence associated with rare oil drops or inclusions of dead oil, yellow to
SWC					
2670-2690m	Rvmax	0.66	0.52-0.83	26	Sparse sporinite yellowish orange to orange, sparse liptodetrinite yellow to orange. (Siltstone. Dom abundant, I=V>L. Inertinite and vitrinite abundant, liptinite sparse. Mineral fluorescence weakly patchy bright to moderate orange. Strong fluorescence from the mounting resin, presumably due to oil impregnation from the sample. Iron oxides abundant, discrete grains,
Ctgs					
2695.2m	Rvmax	0.66	0.55-0.72	3	Rare liptodetrinite yellowish orange to orange. (Siltstone, calcareous. Dom rare, I>V>?L. All maceral groups rare and most could be from mud cake. Sparse bright yellow oil drops as inclusions within quartz grains. Mineral fluorescence patchy bright orange to very weak dull orange. Mounting resin, mostly weakly fluorescing but some brighter patches. Iron oxides common. Pyrite sparse.)

Table 3: Vitrinite reflectance data

3 Gas Characterisation

The following observations were made on gas recovered from MDT sample chambers collected in Thylacine-1 gas reservoir at 2053.8mRT and 2165.8mRT.

- Composition
  - 82% methane
  - 9% CO_2
  - 8% wet gases
  - 1% nitrogen
  - Only 0.1-0.2% pentanes plus
- CGR < 10
- Similar isotope profile to La Bella gases
- CO_2 origin in Type III organic matter

3.1 Gas Composition

ANALYSIS OF GAS COMPONENTS

THYLACINE-1, 2053.8m, PT-2065

GEOTECH

Compound	*Mol%*	*Mol Fraction*
methane	81.9	0.82
ethane	5.7	0.06
propane	1.6	0.02
i-butane	0.3	< 0.01
n-butane	0.5	< 0.01
i-pentane	0.1	< 0.01
n-pentane	0.1	< 0.01
C_6+	0.1	< 0.01
CO_2	8.6	0.09
O_2+Ar	<0.1	< 0.01
N_2	0.9	0.01

Table 4: Gas composition, Thylacine-1 2053.8 m

ANALYSIS OF GAS COMPONENTS

THYLACINE-1, 2165.8m, PT-1063

GEOTECH

Compound	*Mol%*	*Mol Fraction*
methane	82.2	0.82
ethane	5.1	0.05
propane	1.5	0.02
i-butane	0.2	< 0.01
n-butane	0.3	< 0.01
i-pentane	0.1	< 0.01
n-pentane	<0.1	< 0.01
C_6+	<0.1	< 0.01
CO_2	9.3	0.09
O_2+Ar	<0.1	< 0.01
N_2	1.1	0.01

Table 5: Gas composition, Thylacine-1 2165.8 m

3.2 Gas Isotope Analysis (CSIA)

Compound specific isotope analysis was carried out on the Thylacine-1 gas samples from 2053.8 mRT and 2166.8 mRT and compared to CSIA fingerprints of other gases from the Otway Basin in Figure 6.

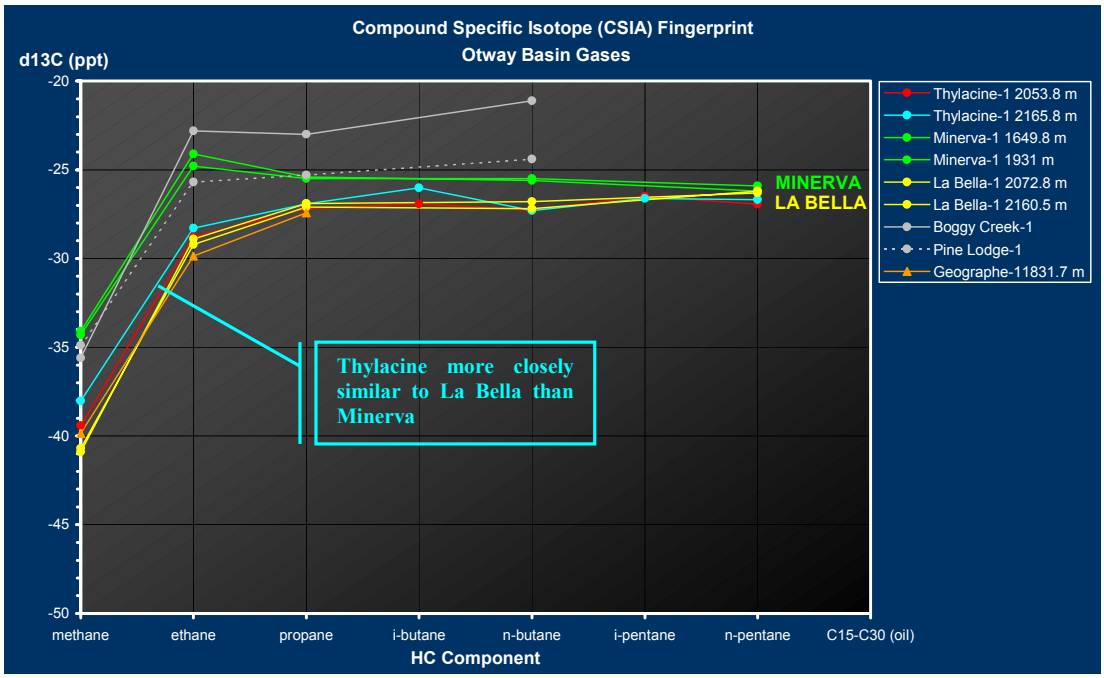

Figure 6: Gas CSIA profiles

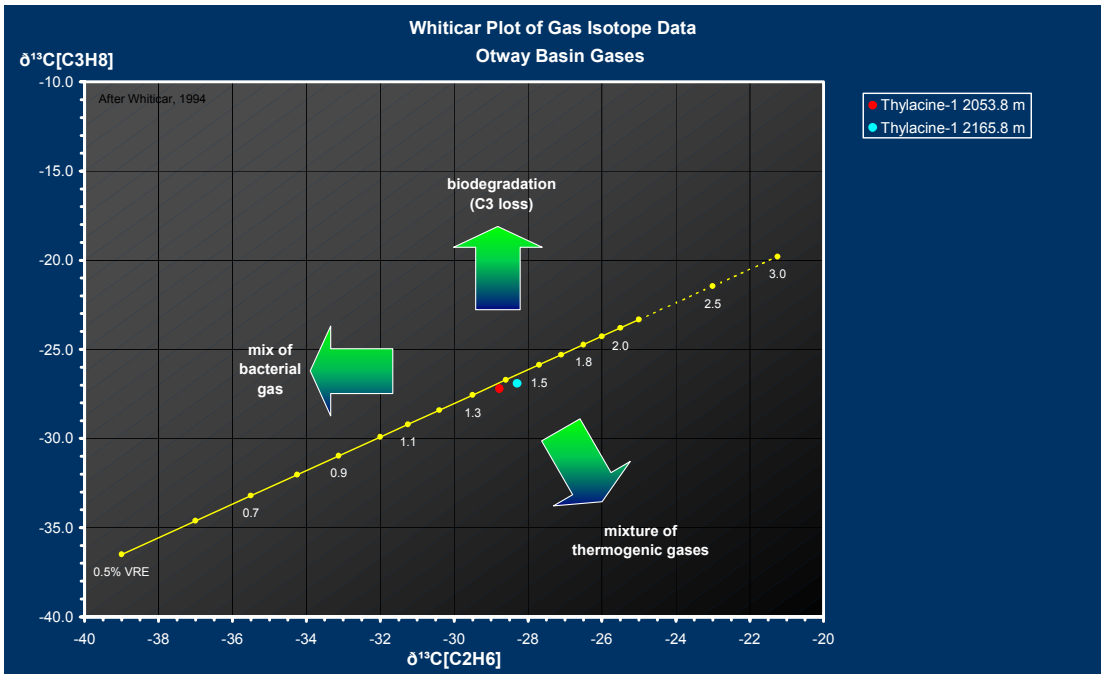

Figure 7: Whiticar plot of propane vs. ethane isotope values

The two Thylacine samples are similar, but not identical, with slight differences in isotopic composition suggesting they are isolated from one another by intraformational seals. They closely resemble samples from La Bella gas field, suggesting that the two fields are sourced by the same source interval, at a similar level of maturity. The area to the west of Thylacine could provide a common source kitchen to both fields.

A Whiticar plot of propane vs. ethane isotope values again reveals slight differences between the two fluids, though there is no indication of biodegradation, or mixing of different thermogenic gases (Figure 7). These fluids were possibly expelled at an equivalent vitrinite reflectance of about 1.4%.

3.3 CO_2 Isotope Analysis

Stable carbon isotope values from the CO_2 fall between -9 and -10 ppt, and do not correlate closely with data from onshore Otway gas fields (Figure 8). The Thylacine data suggests a diagenetic origin in Type III organic matter.

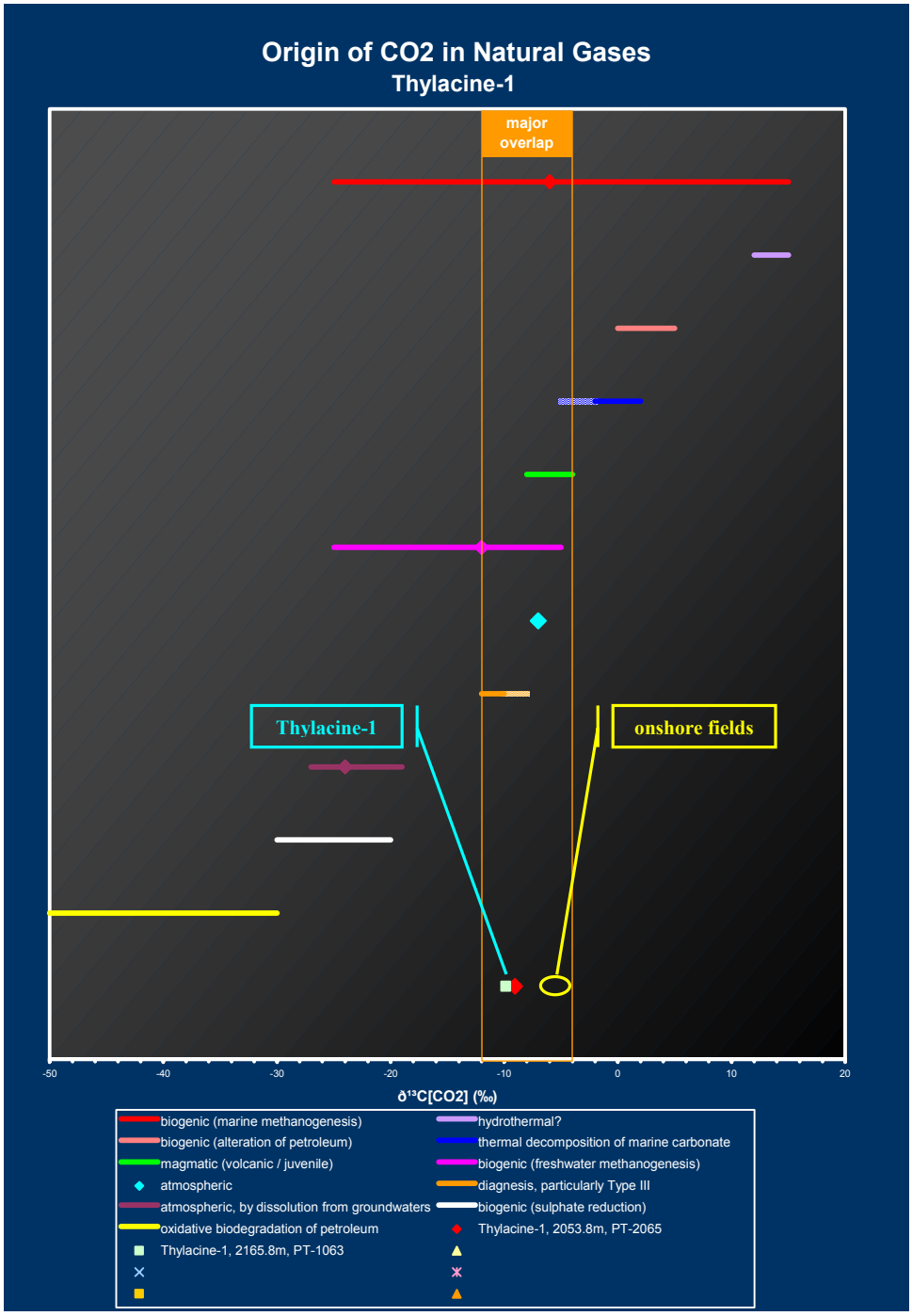

Figure 8: Origin of CO2 in natural gases

4 Condensate Characterisation

Condensates were analysed from MDT sample chambers collected in Thylacine-1 gas reservoir. These samples were obtained by cold trapping of gas samples at 2053.8mRT and 2165.8mRT and display a relatively aromatic bulk composition, with 82-86% saturated compounds, 12-16% aromatics and 2% non-hydrocarbon (NSO) components.

4.1 Whole-Oil GC Analysis

Whole-oil GC data are presented in Figure 9. These confirm that the Thylacine condensates are relatively napthenic-aromatic in composition, and that the most abundant component is methylcyclohexane. This is also indicated by Thompson's light hydrocarbon indices, which plot on the aromatic curve in Figure 10.

Some contamination by mud additive alkenes is evident, especially in the deeper sample. The paraffin distribution is largely biased towards lighter compounds, though waxy C15+ paraffins are also present. The aromatic composition of these condensates, in association with high Pristane/Phytane and Pristane/nC_{17} ratios suggest a coaly terrigenous source facies.

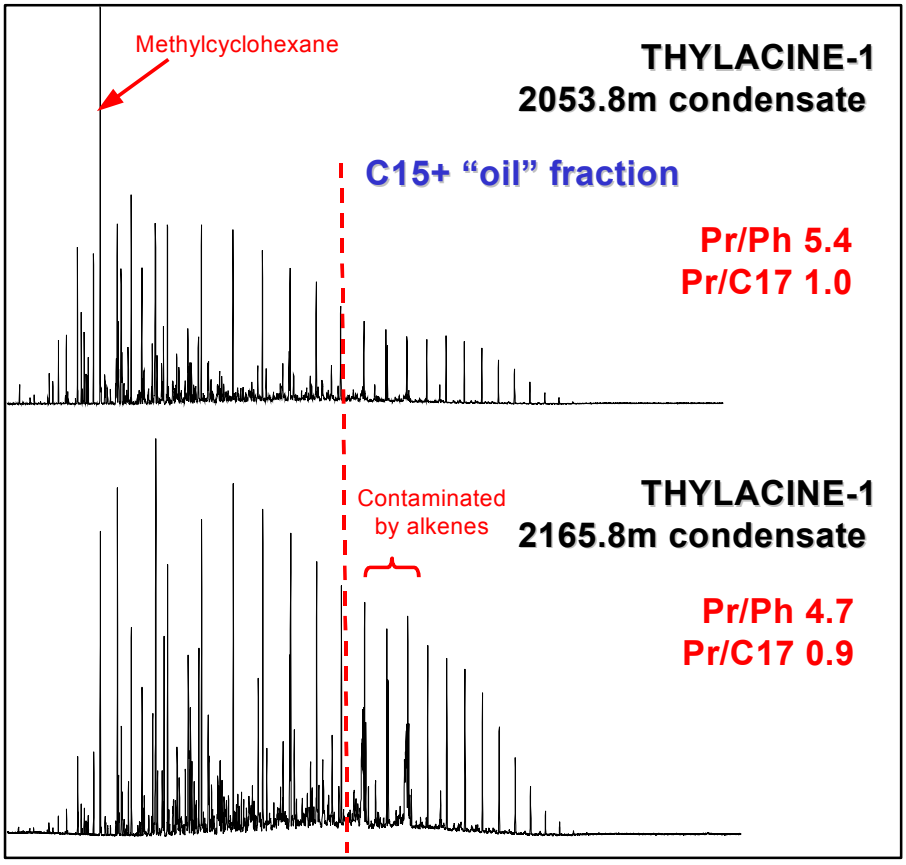

Figure 9: Comparison of GC profiles, Thylacine-1 condensates

Heptane indices suggest that the condensate samples are "mature", i.e. were expelled together with gas within the "gas window". There is a significant difference in heptane indices between the two condensates, suggesting they are similar, but not identical fluids, and supporting CSIA data in suggesting compartmentalisation.

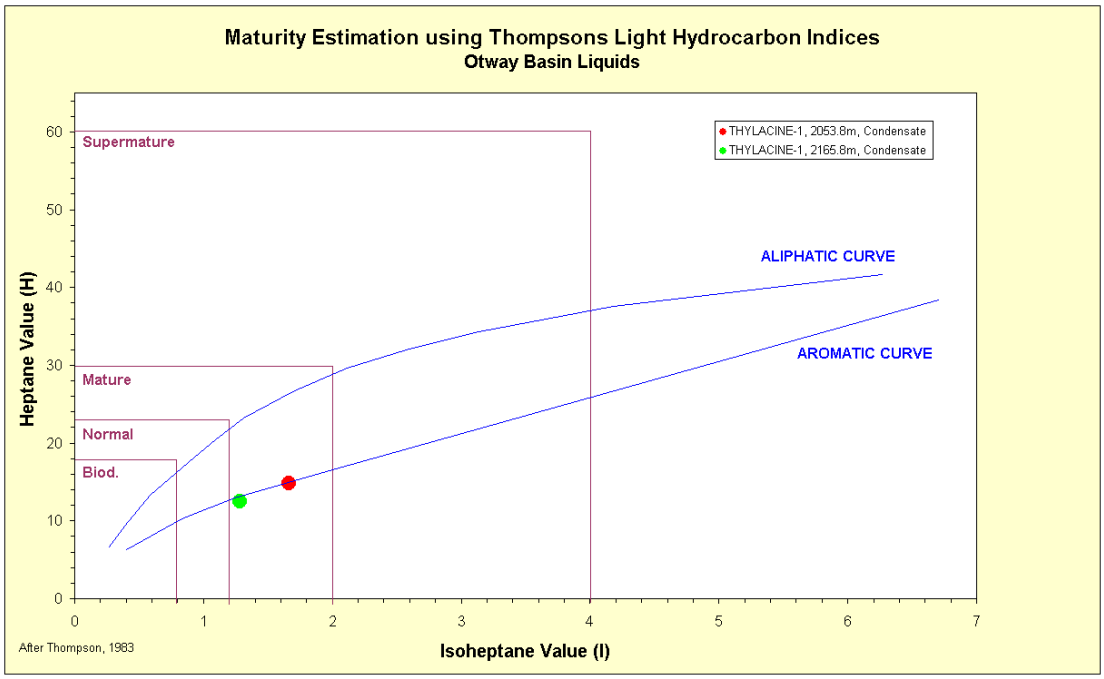

Figure 10: Thompson plot of light hydrocarbon indices

4.2 Biomarker and Compound Specific Isotope (CSIA) Data

GC-MS biomarker profiles for terpanes and steranes are presented in Figure 11 and Figure 12. These are virtually identical. Biomarker content of the Thylacine-1 condensates is very low, consistent with advanced maturity, and both figures reveal a low signal to noise ratio. The terpane profile is strongly dominated by tricyclics, especially C19 - C20 forms, consistent with expulsion from a highly mature, coaly terrestrial source kerogen.

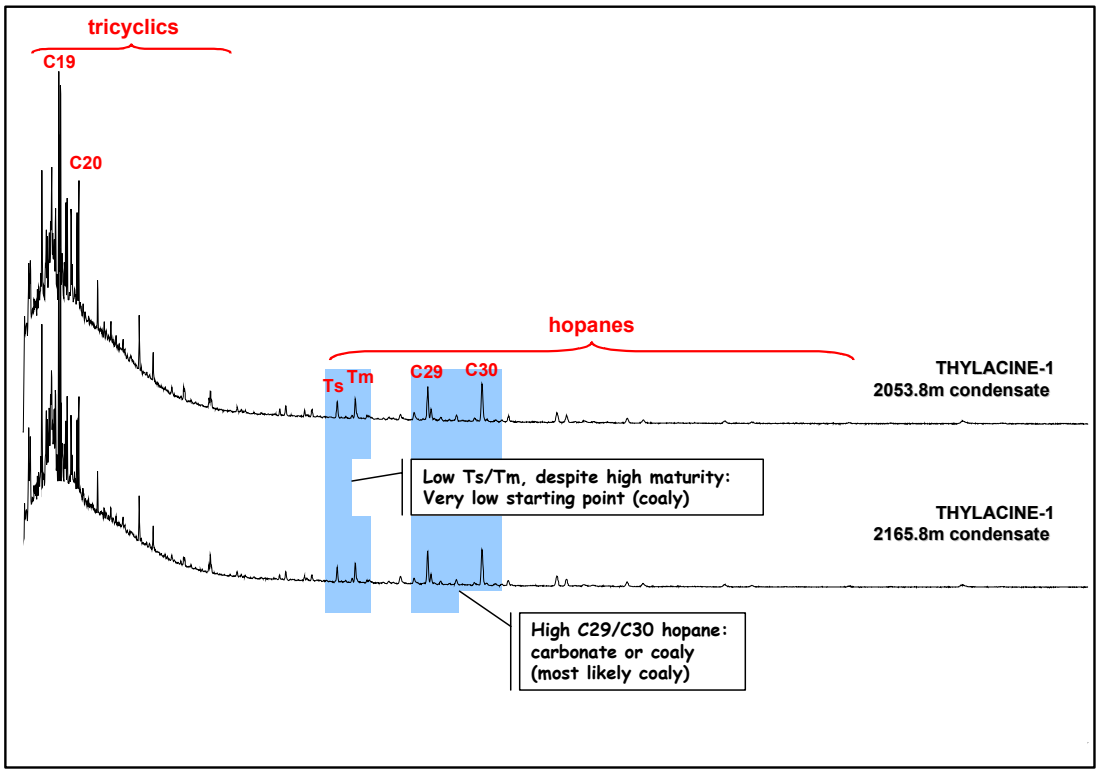

Figure 11: Comparison of GC-MS m/z 191 (terpane) profiles, Thylacine condensates

Another indication of a coaly organofacies is the low Ts/Tm ratio, despite the high maturity of these fluids. This suggests that the ratio had a low starting point, in keeping with the source being coaly. The high C29/C30 hopane ratio again suggests that the source rock was coaly, which is very much in line with the assumption that terrestrial organic matter within the Eumeralla and Lower Waarre Formation is the origin of Thylacine gas and condensate.

The sterane biomarker profiles in Figure 12 again display an excellent correlation. They are strongly dominated by pregnanes and diasteranes, consistent with a clastic source facies at high maturity. Sub equal C27/C29 diasterane content may indicate a mixture of marine and terrestrial kerogen, which could indicate a Waarre type shallow marine and embayment facies.

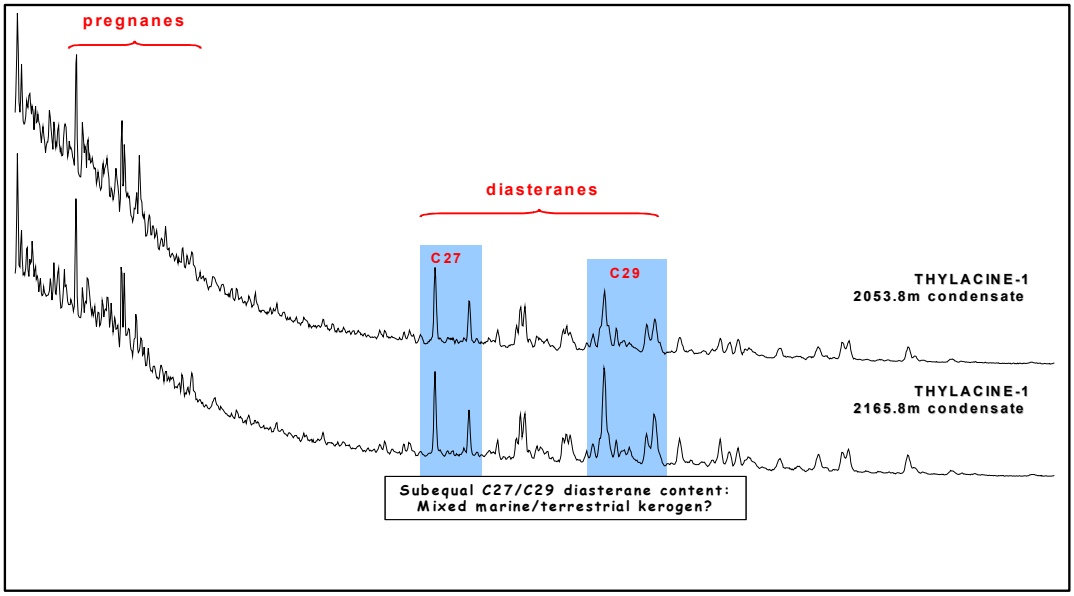

Figure 12: Comparison of GC-MS m/z 217 (sterane) profiles, Thylacine condensates

The carbon isotope composition of individual paraffins in the two condensate samples from Thylacine-1 is essentially the same, within experimental error (Figure 13). This confirms an identical source facies for the two samples.

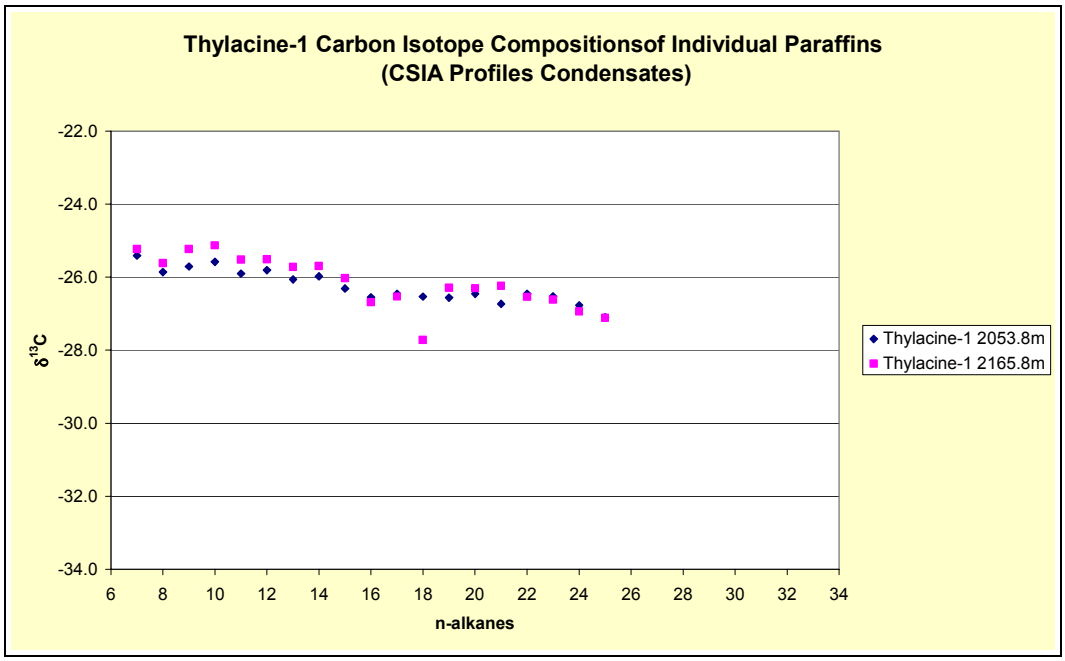

Figure 13: CSIA profiles, Thylacine condensates

5 Oil Show Evaluation

5.1 GC and Biomarker Analysis

Sandstones at several locations within the Upper Waarre Formation, displayed good fluorescence and cut. These "shows" were subjected to extraction/LC, SCAN GC-MS whole extract and sats. gas chromatography, and compared with extracts from the mud, to eliminate contamination from mud additives.

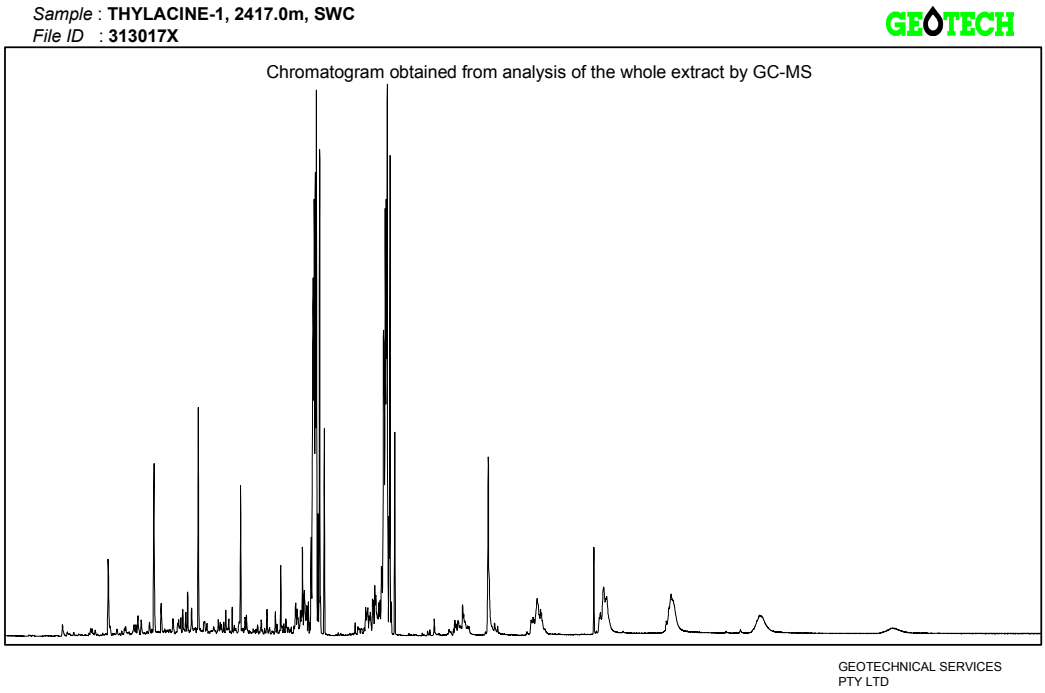

Figure 14: Whole extract GC, show at 2417 m

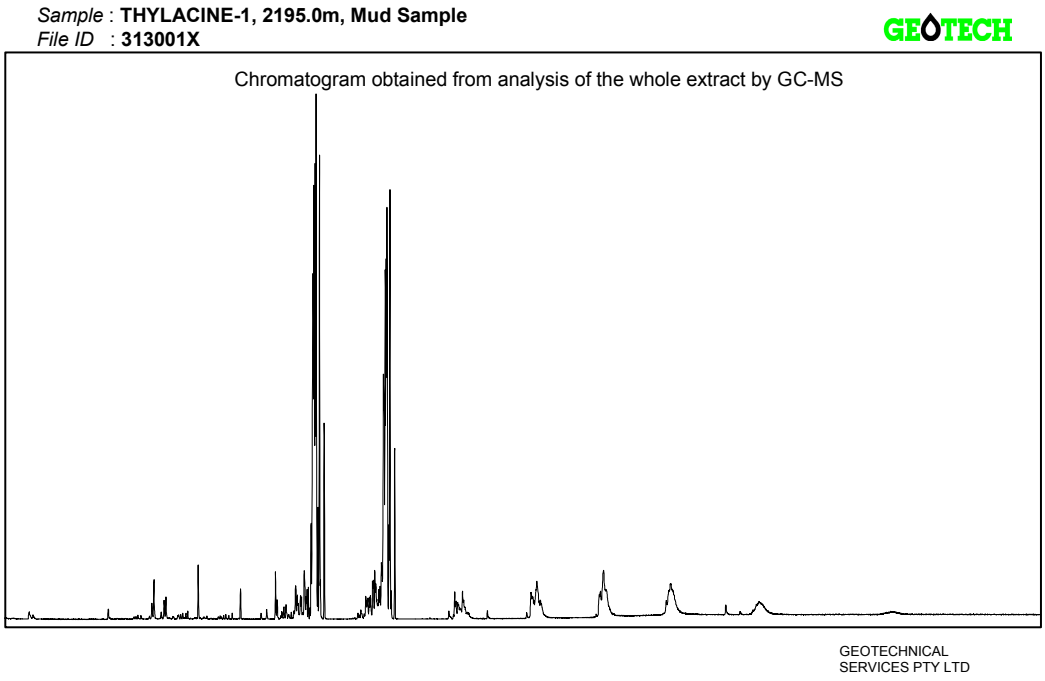

Figure 15: Whole extract GC, mud sample at 2195 m

An example of a whole extract GC from a show at 2417 mRT is displayed in Figure 14. This is dominated by glycols and alkenes, and displays a very similar profile to the mud extract from 2195 mRT (Figure 15), though contains a higher proportion of light paraffins. When alkenes are removed from the isolated saturated hydrocarbon fraction, these light paraffins assume the appearance of a very light condensate, peaking at nC13 (Figure 16).

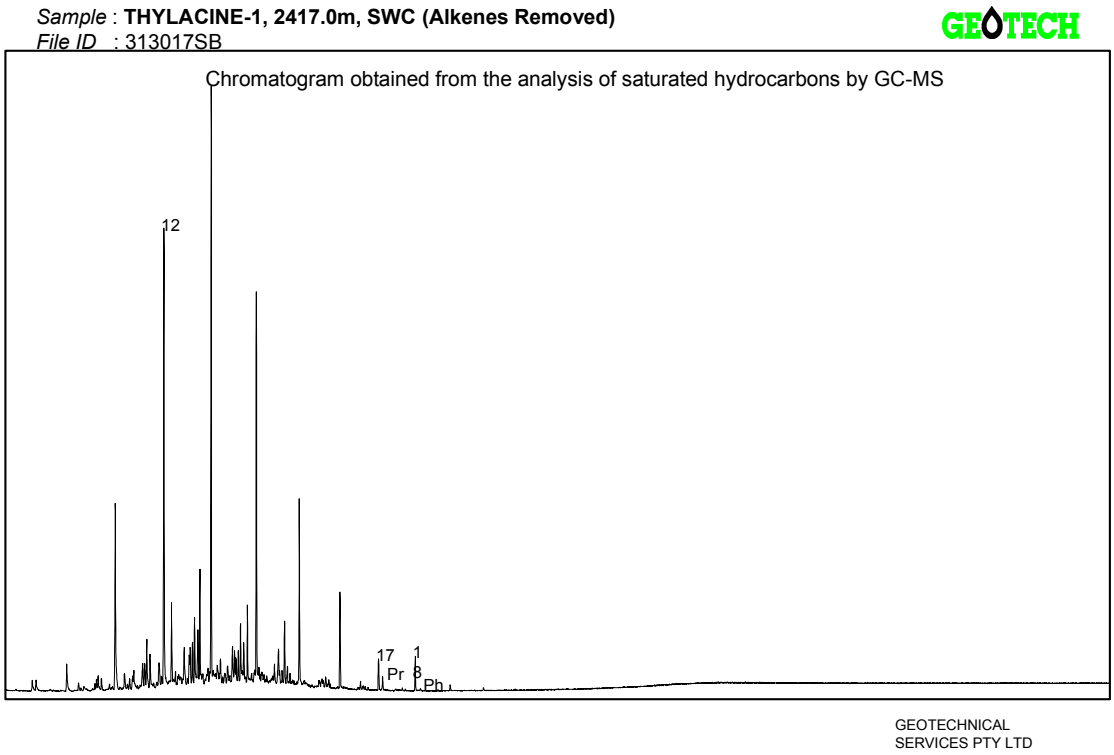

Figure 16: Whole extract GC (alkenes removed), show at 2417 m

This extraction and characterisation process was also applied to samples from 2536 mRT and 2438 mRT and results are compared in Figure 17. The oil from these shows also has a very light paraffin distribution, though there is also evidence of residual alkenes from mud contamination in the chromatograms. The high Pr/Ph ratio (4.8 - 7.5) is similar to, or slightly higher than the Thylacine condensates.

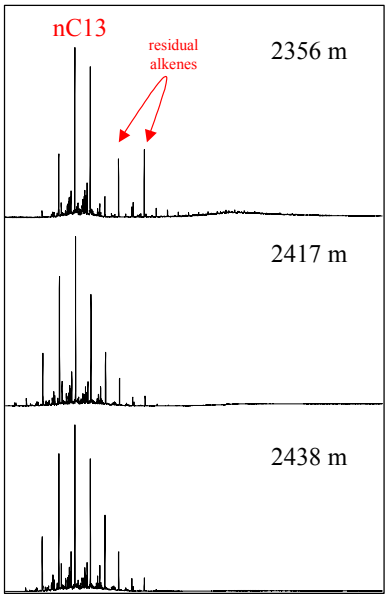

Figure 17: Comparison of GC data (alkenes removed), shows from SWC

GC-MS biomarker analysis was performed on the show at 2417 m. Terpane and sterane profiles, in conjunction with GC data suggest a mature, coaly terrigenous source rock, although the shows appear to be less mature than condensates recovered from MDT samples, with significantly lower tricyclic/pentacyclic terpane, pregnane/sterane and diasterane/sterane ratios.

The shows in these Upper and Lower Waarre sandstones confirm that charge has moved through these sands to the main reservoirs in the Thylacine gas field.

Despite lower maturity, the similarity of the oil shows to the condensates suggests that the charge all came from a mature coaly, terrigenous source rock, probably carbonaceous material in the underlying Lower Waarre and Eumeralla Formations.

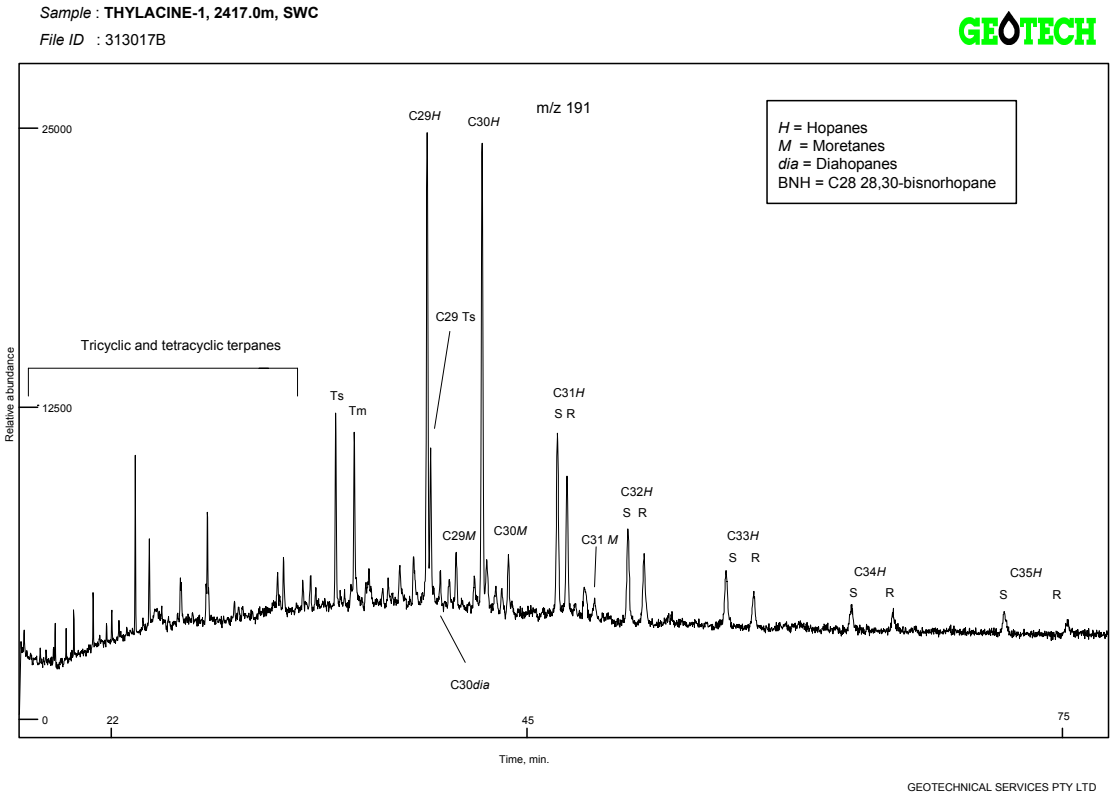

Figure 18: GC-MS m/z 191 (terpane) profile, show at 2417 m

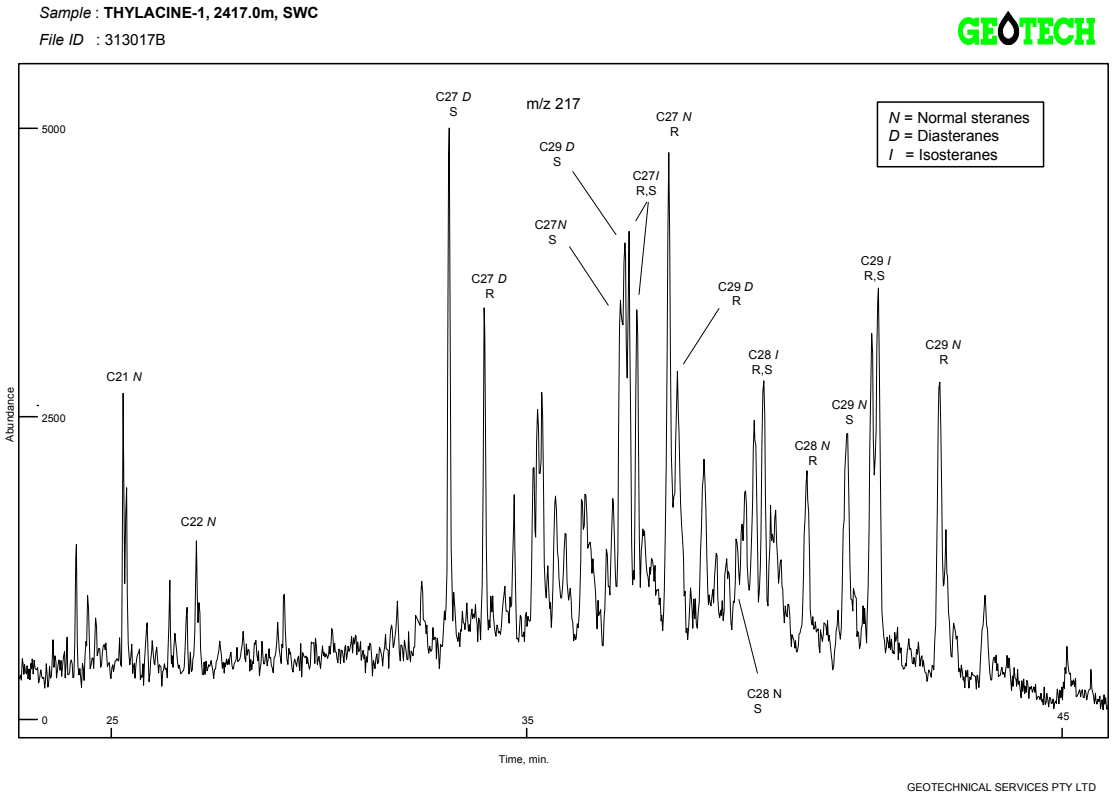

Figure 19: GC-MS m/z 217 (sterane) profile, show at 2417 m

Figure 16 shows the mapped drainage cell at top porosity for the Thylacine structure, with the seismic amplitudes displayed as a colour-filled grid. The expected drainage pattern, drawn as arrows interpreted from the structural contouring, has been confirmed by the areas of high amplitude (coloured red, yellow and green) related to gas fill.

It can be seen from the isoreflectance contours (at top Eumeralla Formation), that the Eumeralla and Lower Waarre reach the approximate thermal maturity of the Thylacine fluids (1.3 - 1.4% VRE) in the Thylacine drainage cell. This is immediately adjacent to the La Bella drainage cell, and accounts for the similarity between the hydrocarbons in the two wells. The base of the Eumeralla source rock within the drainage cell is estimated to be reaching vitrinite reflectance equivalents of 2.8% VRE, well beyond the maturity of the source rocks that generated the hydrocarbons currently trapped in Thylacine-1.

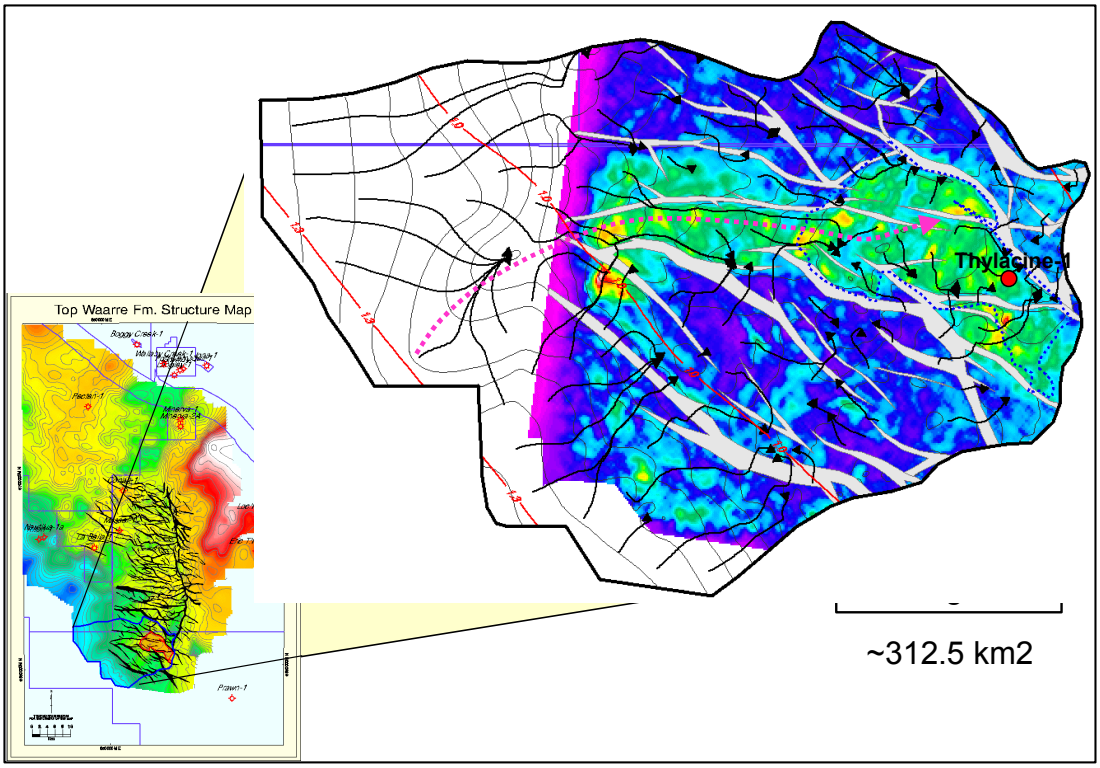

Figure 20: Thylacine Drainage Cell

6 Thylacine HTGC Wax Analysis

Two condensate samples (combined reservoir fluid from Thylacine-1 MDT samples 6, TS5702 and 7, TS5601 (2236.8 mRT), and a separator sample (dead condensate) from Thylacine-2 DST-2, (2296-2302 mRT)) were subjected to wax analysis by High Temperature Gas Chromatography (HTGC). Basic fluid properties (%water, API, %S, specific gravity and density) were also determined for the separator sample (Table 6). These results were used to evaluate whether the Thylacine gas discovery has potential wax precipitation problems.

The dead condensate from Thylacine-2 displayed a rapid decrease in higher n-paraffin content above n-C_{20}. The derived cloud point was -3°C and the derived pour point was <-17°C. The distribution of the light normal paraffins (n-C_{25} to n-C_{35}) in the Thylacine-1 combined reservoir fluid was almost identical to that of the Thylacine-2 separator sample, which validated the quality of the latter.

Both fluids exhibited a rapid decline in the concentration of normal alkanes above nC_{20}. In the separator sample, heavier normal alkanes are present in very low quantities (Figure 21). Assuming that all fluids in the reservoir have the same wax properties as the ones investigated in this study, the low calculated cloud point and pour point temperatures indicate that under normal operating conditions (lowest pipeline T~ 4°C) there is no risk for wax precipitation from the Thylacine fluid during production.

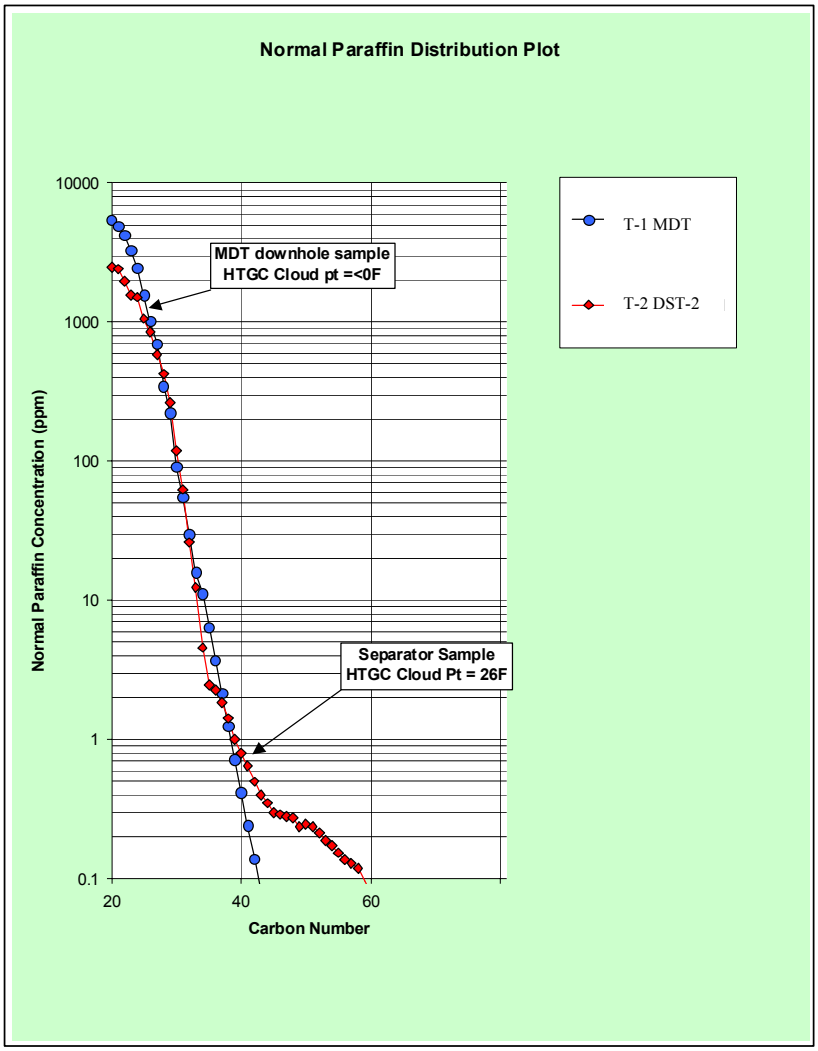

Figure 21: Paraffin distribution plot from HTGC analysis

SAM #	Well #	Type	T_{res} (°C)	P_{res} (psi)	API	%water	%S	Spec. Gravity	Density (g cm^{-3})
AUS-O-32	Thylacine-2	separator	89	3280	44	0.03	0.0092	0.8072	0.8064
AUS-O-33	Thylacine-1	reservoir	insufficient sample						

Table 6: Thylacine condensate bulk properties

APPENDIX 4
PALYNOLOGICAL REPORT

PALYNOLOGY OF

THYLACINE-1

OFFSHORE OTWAY BASIN, AUSTRALIA

BY

ROGER MORGAN

for **WOODSIDE ENERGY LTD** **NOVEMBER 2001**

REF: OTW.THYLACINE1 REPORT

PALYNOLOGY OF

THYLACINE-1

OFFSHORE OTWAY BASIN, AUSTRALIA

CONTENTS **PAGE**

1 SUMMARY

1170/80 m (cutts) : ***D. heterophlycta* Zone** : Middle Eocene : shelfal marine : immature

1230/40 m (cutts) – 1300/10 m (cutts) : ***P. aperopolus* Zone** : Early Eocene : nearshore marine : immature

1360/70 m (cutts) : ***K. edwardsii* Zone** : Early Eocene : very nearshore marine : immature

1380/90 m (cutts) : ***K. thompsonae-W. ornatum* Zones** : Early Eocene : nearshore marine : immature

1400/10 m (cutts) – 1470/80 m (cutts) **: *M. druggii* Zone** (1400/10 m – 1440/50 m upper subzone, 1460/70 m – 1470/80 m lower subzone); *F. longus* (upper) Zone : Maastrichtian : nearshore to shelfal marine : immature

1480/90 m (cutts) – 1490/1500 m (cutts) : ***I. pellucidum* Zone**; *F. longus* (lower) Zone: Maastrichtian : nearshore marine : immature

1540/50 m (cutts) : ***I. korojonense* Zone**; *T. lillei* Zone: Maastrichtian-Campanian : very nearshore marine : immature

1590/1600 m (cutts) : ***X. australis* (upper) Zone**; *N. senectus* (upper) Zone : Campanian : ?marginal marine : immature

1640/50 m (cutts) – 1866.7 m (swc) : ***X. australis* (lower) Zone** (1640/50 m lower d, 1690/1700 m lower c, 1740/50 – 1790/1800 m lower b, 1866.7 m lower a); *N. senectus* (upper) Zone : Campanian : nearshore marine : immature

1931.3 m (swc) : ***N. aceras* (upper) Zone**; *N. senectus* Zone : Campanian : nearshore marine : immature

1972.0 m (swc) : ***N. aceras* (middle) Zone**; *N. senectus* Zone : Campanian : shelfal marine : immature

1988.0 m (swc) **: *N. aceras* (lower) Zone** ; ?*N. senectus* Zone : Campanian : shelfal marine : immature

2027.0 m (swc) – 2040.0 m (swc) : ***I. cretaceum* (upper) Zone** (2027.0 m upper b, 2040.0 m upper a); *T. apoxyexinus* (upper) Zone : Santonian : shelfal marine : immature

2044.0 m (swc) – 2076.0 m (swc) : ***I. cretaceum* (lower) Zone** (2044.0 m lower b, 2076.0 m lower a); *T. apoxyexinus* (middle) Zone : Santonian : nearshore to shelfal marine : marginally mature

2090.0 m (swc) – 2131.5 m (swc) : ***O. porifera* (upper) Zone**; *T. apoxyexinus* (middle) Zone : Santonian : nearshore marine : marginally mature

2168.37 m (core) – 2295.0 m (swc) : ***P. infusorioides* (upper) Zone** (2168.37 m – 2191.82 m upper c, 2193.07 m – 2203.40 m upper b, 2246.5 m – 2295.0 m upper a); *T. apoxyexinus* (lower) Zone : Turonian : nearshore to marginal marine : marginally mature

2334.8 m (swc) – 2397.7 m (swc) : ***P. infusorioides* (middle) Zone** (part middle b-c); *P. mawsonii* (upper) Zone: Turonian : marginal marine : marginally mature

2425.7 m (swc) – 2501.5 m (swc) **: *P. infusorioides* (middle) Zone** (2425.7 m part middle b-c, 2449.0 m – 2501.5 middle a); *P. mawsonii* (lower) Zone : Turonian : marginal marine to non-marine : marginally mature

2571.0 m (swc) – 2667.5 m (swc) : ***P. infusorioides* (lower) Zone** (2571.0 m – 2636.2 m lower c, 2667.5 m lower b); *P. mawsonii* (lower) Zone : Turonian : nearshore to marginal marine : marginally mature

2 INTRODUCTION

A total of 48 samples (18 cuttings, 25 sidewall cores and 15 core samples) have been studied from **Thylacine-1** for Woodside Energy Ltd. The zonation used for the Tertiary is based on the spore-pollen zonation of Stover and Partridge (1973) and the dinoflagellate zonation of Partridge (1976) both since modified by Alan Partridge and available in published form as summarised in Figure 1. The zonation used for the Cretaceous is based on the scheme of Helby, Morgan and Partridge (1987), revised and refined using Otway Basin cuttings by Morgan (1992, 1994) and herein, and summarised in Figure 2. Alan Partridge has also revised this zonation in unpublished studies and published it as an outline table in Partridge (1997). His summary figure from Partridge (1998) is shown as Figure 3. The two schemes are easily reconciled as in Figure 4. The main difference is different usage for the base of the *T. apoxyexinus* Zone. A summary of the palynological details for each sample is presented on Table 1.

All informal species names are shown in quotation marks and listed in Section 5 with informal authorship. Names are given in full when first mentioned in the text, but only the genus initial and full species name is given when subsequently mentioned.

Maturity data were generated in the form of Spore Colour Index, and are plotted on Figure 5 Maturity Profile: Thylacine-1. The oil and gas windows on Figure 5 follow the general consensus of geochemical literature. The oil window corresponds to spore colours of light-mid brown (Staplin Spore Colour Index of 2.7) to dark brown (3.6), equivalent to vitrinite reflectance values of 0.6% to 1.3%. Geochemists argue variations on kerogen type, basin type and basin history. The maturity interpretation is thus open to reinterpretation using the basic colour observations as raw data. However, the range of interpretation philosophies is not great, and probably would not move the oil window by more than 200 m.

Raw palynological data are included in Appendix 1. The data are based on a 100+ specimen count in cuttings and a 250+ count in swcs and core from which an indication of marine microplankton to terrestrial palynomorph proportions can be derived. The microplankton percentages are listed in Table 1, which also summarizes other palynological details. Environmental assessments are derived from the palynomorph counts using content and diversity of saline taxa (dinoflagellates and spiny acritarchs), other microplankton (mostly freshwater algae), and terrestrial spores and pollen. The criteria for these assessments are defined in Table 1. However, dinoflagellate content and diversity in the Otway Basin are lower than might be expected from other data sources, especially sedimentology in the offshore marine shales. It may be that dinoflagellate productivity is suppressed by

lowered salinity or restricted oceanic circulation caused by the enclosed nature of a long narrow marine gulf. Environments interpreted here may therefore underestimate marine influence in this section with environments really being more marine than interpreted here. In running text, frequency of taxa is discussed in the following intervals: Very rare = <1%, Rare = 1-3%, Frequent = 4-10%, Common = 11-29%, Abundant = 30-49%, Super-abundant = 50-100%.

TABLE 1: SUMMARY PALYNOLOGICAL DATA, THYLACINE-1

RT= 25 m

LOG DEPTH [mbRT]	CORE DEPTH [mbRT]	SAMPLE TYPE	ORGANIC YIELD *1	MICROFOSSIL YIELD	PRESERVATION *2	PERCENTAGE				DIVERSITY *3		DINOFLAGELLATE ZONE/SUBZONE	SPORE-POLLEN ZONE/SUBZONE	ENVIRONMENT *4
						MICROPLANKTON			SPORE-POLLEN	MICROPLANKTON	SPORE-POLLEN			
						DINOFLAG.	SPINY AC.	OTHER ALGAE						
1170/80		CUTTS	0.286	FAIR	3 + GOOD	36	2	7	55	HIGH	HIGH	D. HETEROPHLYCTA	?N. ASPERUS, ?LOWER	SHELFAL
1230/40		CUTTS	0.018	LEAN	3 = GOOD	25	2	9	63	HIGH	HIGH		P. ASPEROPOLUS	NEARSHORE
1300/10		CUTTS	0.045	LEAN	3 = GOOD	7	4	19	70	MODERATE	HIGH		P. ASPEROPOLUS	VERY NEARSHORE
1360/70		CUTTS	0.039	LEAN	3 = GOOD	18	0	9	73	MODERATE	MODERATE	K. EDWARDSII		NEARSHORE
1380/90		CUTTS	0.032	LEAN	3 = GOOD	17	0	10	72	MODERATE	MODERATE	K. THOMPSONAE-W. ORNATUM		NEARSHORE
1400/10		CUTTS	0.025	GOOD	3 = GOOD	31	27	2	41	HIGH	HIGH	M. DRUGGII, UPPER	F. LONGUS, UPPER	SHELFAL
1420/30		CUTTS	0.032	GOOD	3 = GOOD	18	29	1	52	MODERATE	HIGH	M. DRUGGII, UPPER	F. LONGUS, UPPER	SHELFAL
1440/50		CUTTS	0.025	GOOD	3 = GOOD	22	29	2	47	MODERATE	HIGH	M. DRUGGII, UPPER	F. LONGUS, UPPER	SHELFAL
1460/70		CUTTS	0.045	GOOD	3 = GOOD	21	4	3	72	MODERATE	HIGH	M. DRUGGII, LOWER	F. LONGUS, UPPER	NEARSHORE
1470/80		CUTTS	0.019	GOOD	3 = GOOD	15	4	9	72	MODERATE	HIGH	M. DRUGGII, LOWER	F. LONGUS, UPPER	NEARSHORE
1480/90		CUTTS	0.025	GOOD	3 = GOOD	17	0	5	78	HIGH	VERY HIGH	I. PELLUCIDUM	F. LONGUS, LOWER	NEARSHORE
1490/1500		CUTTS	0.066	GOOD	3 = GOOD	9	1	4	86	MODERATE	VERY HIGH	I. PELLUCIDUM	F. LONGUS, LOWER	NEARSHORE
1540/50		CUTTS	0.019	GOOD	3 = GOOD	5	0	13	82	LOW	VERY HIGH	I. KOROJONENSE	T. LILLEI	VERY NEARSHORE
1590/1600		CUTTS	0.092	FAIR	3 = GOOD	1	0	2	95	LOW	VERY HIGH	X. AUSTRALIS, UPPER	N. SENECTUS, UPPER	VERY NEARSHORE
1640/50		CUTTS	0.019	FAIR	3 = GOOD	30	0	11	59	LOW	HIGH	X. AUSTRALIS, LOWER d	N. SENECTUS, UPPER	NEARSHORE
1690/1700		CUTTS	0.006	FAIR	3 = GOOD	55	0	4	41	LOW	MODERATE	X. AUSTRALIS, LOWER c	N. SENECTUS, UPPER	SHELFAL
1740/50		CUTTS	0.039	FAIR	3 = GOOD	28	0	2	69	LOW	HIGH	X. AUSTRALIS, LOWER b	N. SENECTUS, UPPER	NEARSHORE
1790/1800		CUTTS	0.095	FAIR	3 = GOOD	25	1	1	73	MODERATE	HIGH	X. AUSTRALIS, LOWER b	N. SENECTUS, UPPER	NEARSHORE
1866.70		SWC 60	0.043	FAIR	3 = GOOD	24	0	9	67	MODERATE	VERY HIGH	X. AUSTRALIS, LOWER a	N. SENECTUS, UPPER	NEARSHORE
1931.30		SWC 58	0.112	GOOD	3 = GOOD	16	0	1	82	MODERATE	VERY HIGH	N. ACERAS, UPPER	N. SENECTUS	NEARSHORE
1972.00		SWC 57	0.105	GOOD	3 = GOOD	36	0	1	64	MODERATE	VERY HIGH	N. ACERAS, MIDDLE	N. SENECTUS	SHELFAL
1988.00		SWC 56	0.128	GOOD	3 = GOOD	36	0	3	61	MODERATE	HIGH	N. ACERAS, LOWER	?N. SENECTUS	SHELFAL
2027.00		SWC 55	0.142	GOOD	3 = GOOD	35	0	1	64	MODERATE	HIGH	I. CRETACEUM, UPPER b	T. APOXYEXINUS, UPPER	SHELFAL
2040.00		SWC 54	0.083	GOOD	3 = GOOD	34	0	1	64	HIGH	HIGH	I. CRETACEUM, UPPER a	T. APOXYEXINUS, UPPER	SHELFAL
2044.00		SWC 53	0.066	GOOD	3 = GOOD	50	0	7	43	HIGH	HIGH	I. CRETACEUM, LOWER b	T. APOXYEXINUS, MIDDLE	SHELFAL
2076.00		SWC 50	0.060	GOOD	3 = GOOD	16	2	1	81	MODERATE	HIGH	I. CRETACEUM, LOWER a	T. APOXYEXINUS, MIDDLE	NEARSHORE
2090.00		SWC 49	0.065	GOOD	3 = GOOD	12	2	4	83	MODERATE	HIGH	O. PORIFERA, UPPER	T. APOXYEXINUS, MIDDLE	NEARSHORE
2115.00		SWC 47	0.058	GOOD	3 = GOOD	18	2	2	78	MODERATE	HIGH	O. PORIFERA, UPPER	T. APOXYEXINUS, MIDDLE	NEARSHORE
2131.50		SWC 45	0.068	GOOD	3 = GOOD	22	1	1	76	MODERATE	HIGH	O. PORIFERA, UPPER	T. APOXYEXINUS, MIDDLE	NEARSHORE
2168.37	2165.00	CC	0.042	FAIR	3 = GOOD	23	0	4	72	MODERATE	HIGH	P. INFUSORIOIDES, UPPER c	T. APOXYEXINUS, LOWER	NEARSHORE
2169.87	2166.50	CC	0.134	FAIR	3 = GOOD	6	1	3	90	MODERATE	HIGH	P. INFUSORIOIDES, UPPER c	T. APOXYEXINUS, LOWER	VERY NEARSHORE
2172.37	2169.00	CC	0.098	FAIR	3 = GOOD	12	0	11	77	MODERATE	HIGH	P. INFUSORIOIDES, UPPER c	T. APOXYEXINUS, LOWER	VERY NEARSHORE
2178.37	2175.00	CC	0.200	FAIR	3 = GOOD	6	0	7	87	LOW	HIGH	P. INFUSORIOIDES, UPPER c	T. APOXYEXINUS, LOWER	MARGINAL
2180.44	2177.37	CC	0.126	FAIR	3 = GOOD	4	0	2	94	LOW	HIGH	P. INFUSORIOIDES, UPPER c	T. APOXYEXINUS, LOWER	MARGINAL
2183.74	2180.67	CC	0.078	FAIR	3 = GOOD	9	0	2	89	MODERATE	HIGH	P. INFUSORIOIDES, UPPER c	T. APOXYEXINUS, LOWER	VERY NEARSHORE
2189.52	2186.45	CC	0.191	FAIR	3 = GOOD	5	2	0	94	LOW	HIGH	P. INFUSORIOIDES, UPPER c	T. APOXYEXINUS, LOWER	MARGINAL
2191.82	2188.75	CC	0.094	FAIR	3 = GOOD	3	0	5	91	LOW	HIGH	P. INFUSORIOIDES, UPPER c	T. APOXYEXINUS, LOWER	MARGINAL
2193.07	2190.00	CC	0.093	FAIR	3 = GOOD	13	2	1	83	MODERATE	HIGH	P. INFUSORIOIDES, UPPER b	T. APOXYEXINUS, LOWER	NEARSHORE
2194.98	2191.91	CC	0.130	FAIR	3 = GOOD	9	1	1	89	MODERATE	HIGH	P. INFUSORIOIDES, UPPER b	T. APOXYEXINUS, LOWER	VERY NEARSHORE
2197.51	2194.40	CC	0.150	FAIR	3 = GOOD	7	2	0	91	MODERATE	HIGH	P. INFUSORIOIDES, UPPER b	T. APOXYEXINUS, LOWER	VERY NEARSHORE
2198.34	2195.23	CC	0.083	FAIR	3 = GOOD	8	0	4	88	MODERATE	VERY HIGH	P. INFUSORIOIDES, UPPER b	T. APOXYEXINUS, LOWER	VERY NEARSHORE
2200.11	2197.00	CC	0.086	FAIR	3 = GOOD	12	0	4	83	MODERATE	HIGH	P. INFUSORIOIDES, UPPER b	T. APOXYEXINUS, LOWER	NEARSHORE
2202.66	2199.55	CC	0.093	FAIR	3 = GOOD	12	2	8	78	MODERATE	HIGH	P. INFUSORIOIDES, UPPER b	T. APOXYEXINUS, LOWER	NEARSHORE
2203.40	2200.29	CC	0.091	FAIR	3 = GOOD	24	1	5	70	HIGH	HIGH	P. INFUSORIOIDES, UPPER b	T. APOXYEXINUS, LOWER	NEARSHORE
2246.50		SWC 38	0.049	GOOD	3 = GOOD	46	0	12	42	HIGH	HIGH	P. INFUSORIOIDES, UPPER a	T. APOXYEXINUS, LOWER	SHELFAL
2272.50		SWC 35	0.093	GOOD	3 = GOOD	16	0	5	79	MODERATE	HIGH	P. INFUSORIOIDES, UPPER a	T. APOXYEXINUS, LOWER	NEARSHORE
2295.00		SWC 32	0.070	GOOD	3 = GOOD	31	0	9	60	MODERATE	HIGH	P. INFUSORIOIDES, UPPER a	T. APOXYEXINUS, LOWER	NEARSHORE
2334.80		SWC 28	0.054	GOOD	3 = GOOD	1	0	9	89	LOW	VERY HIGH	P. INFUSORIOIDES, MIDDLE b-c	P. MAWSONII, UPPER	MARGINAL
2384.00		SWC 26	0.183	GOOD	3 = GOOD	5	1	8	86	MODERATE	HIGH	P. INFUSORIOIDES, MIDDLE b-c	P. MAWSONII, UPPER	VERY NEARSHORE
2397.70		SWC 25	0.245	FAIR	3 = GOOD	2	1	4	92	LOW	HIGH	P. INFUSORIOIDES, MIDDLE b-c	P. MAWSONII, UPPER	MARGINAL

LOG DEPTH [mbRT]	CORE DEPTH [mbRT]	SAMPLE TYPE	ORGANIC YIELD *1	MICROFOSSIL YIELD	PRESERVATION *2	PERCENTAGE				DIVERSITY *3		DINOFLAGELLATE ZONE/SUBZONE	SPORE-POLLEN ZONE/SUBZONE	ENVIRONMENT *4
						MICROPLANKTON			SPORE-POLLEN	MICROPLANKTON	SPORE-POLLEN			
						DINOFLAG.	SPINY AC.	OTHER ALGAE						
2425.70		SWC 22	0.123	FAIR	3 = GOOD	0	0	2	97	EX LOW	VERY HIGH	P. INFUSORIOIDES, MIDDLE b-c	P. MAWSONII, LOWER	NON-MARINE
2449.00		SWC 19	0.150	FAIR	3 = GOOD	3	0	10	87	LOW	VERY HIGH	P. INFUSORIOIDES, MIDDLE a	P. MAWSONII, LOWER	MARGINAL
2501.50		SWC 17	0.064	FAIR	3 = GOOD	1	0	8	91	EX LOW	VERY HIGH	P. INFUSORIOIDES, MIDDLE a	P. MAWSONII, LOWER	MARGINAL
2571.00		SWC 13	0.085	FAIR	3 = GOOD	5	0	3	92	LOW	VERY HIGH	P. INFUSORIOIDES, LOWER c	P. MAWSONII, LOWER	VERY NEARSHORE
2597.00		SWC 10	0.101	FAIR	3 = GOOD	7	0	3	90	MODERATE	VERY HIGH	P. INFUSORIOIDES, LOWER c	P. MAWSONII, LOWER	VERY NEARSHORE
2620.50		SWC 7	0.121	FAIR	3 = GOOD	1	0	2	96	EX LOW	HIGH	P. INFUSORIOIDES, LOWER c	P. MAWSONII, LOWER	MARGINAL
2636.20		SWC 5	0.080	FAIR	3 = GOOD	0	0	3	96	EX LOW	VERY HIGH	P. INFUSORIOIDES, LOWER c	P. MAWSONII, LOWER	NON-MARINE
2667.50		SWC 3	0.111	FAIR	3 = GOOD	9	0	4	87	MODERATE	VERY HIGH	P. INFUSORIOIDES, LOWER b	P. MAWSONII, LOWER	VERY NEARSHORE

*1 ORGANIC YLD=VOL(cc)/WGHT(g)	*2 NOTE:PRESERVATION	*3 DIVERSITY	
<0.01 : EXTREMELY LOW	(FRAGMENTATION INDEX)	V HIGH	30+ SPECIES
0.01 - 0.10 : LOW	1 = SUPERB	HIGH	20-29 SPECIES
0.1 - 0.5 : MODERATE	2 = EXCELLENT	MOD	10-19 SPECIES
>0.5 : HIGH	3 = GOOD	LOW	5-9 SPECIES
	4 = FAIR	EX LOW	1-4 SPECIES
	5 = POOR		

**** ENVIRONMENTS HEREIN MAY UNDERESTIMATE MARINE INFLUENCE, AS DINOFLAGELLATE PRODUCTIVITY SEEMS DEPRESSED IN THE OTWAY BASIN LATE CRETACEOUS.**

*4 ENVIRONMENTS	DINOFLAGELLATE CONTENT %	DINOFLAGELLATE DIVERSITY	FRESHWATER ALGAE CONTENT%
OFFSHORE MARINE	67 to 100	VERY HIGH	LOW
SHELFAL MARINE	34 to 66	HIGH	"
NEARSHORE MARINE	11 to 33	MODERATE	"
VERY NEARSHORE MARINE	5 to 10	MODERATE-LOW	"
MARGINAL MARINE	<1 to 4	LOW-VERY LOW	"
BRACKISH	0, SPINY ACRITARCHS ONLY	EXTREMELY LOW	"
NON-MARINE (UNDIFF)	0, NO SPINY ACRITARCHS	NIL	LOW <3
NON-MARINE (LACUSTRINE)	0, NO SPINY ACRITARCHS	NIL	MODERATE 3-10+

TABLE 2: SUMMARY OF SAMPLE LITHOLOGIES, THYLACINE-1
RT= 25 m

LOG DEPTH [mbRT]	CORE DEPTH [mbRT]	SAMPLE TYPE	RECOVERY [mm]	LITHOLOGY
1170/80		CUTTS		DK GY-BRN SLTST
1230/40		CUTTS		DK GY ARG SST & SLTST
1300/10		CUTTS		DK GY ARG SST & SLTST
1360/70		CUTTS		DK GY SLTST
1380/90		CUTTS		MED-LT GY ARG SST & SLTST
1400/10		CUTTS		MED BRN ARG SST & SLTST
1420/30		CUTTS		DK RED BRN ARG SLTST
1440/50		CUTTS		DK RED BRN ARG SLTST
1460/70		CUTTS		DK GRY SLTST
1470/80		CUTTS		DK GRY SLTST
1480/90		CUTTS		DK GRY SLTST
1490/1500		CUTTS		DK GRY SLTST
1540/50		CUTTS		DK GRY SLTST
1590/1600		CUTTS		DK GRY SLTST
1640/50		CUTTS		DK GRY SLTST
1690/1700		CUTTS		MED-DK GRY SST & SLTST
1740/50		CUTTS		DK GRY SLTST
1790/1800		CUTTS		DK GRY-BLK SLTST
1866.70		SWC 60	20.00	DK GN GY CLYST
1931.30		SWC 58	22.00	DK GN GY CLYST
1972.00		SWC 57	20.00	DK GN GY CLYST
1988.00		SWC 56	23.00	DK GN GY ARG SLTST
2027.00		SWC 55	24.00	DK GN GY ARG SLTST
2040.00		SWC 54	21.00	DK GY SLTST
2044.00		SWC 53	20.00	DK GY SLTST
2076.00		SWC 50	19.00	GY ARG SLTST, RARE COAL, TR GLAUCONITE
2090.00		SWC 49	20.00	GN GY ARG SLTST, RARE COAL
2115.00		SWC 47	21.00	GY ARG SLTST, RARE COAL
2131.50		SWC 45	18.00	GY ARG SLTST, RARE COAL, TR GLAUCONITE
2168.37	2165.00	CC		MED GY SLTST/F. SST, HIGHLY BIOTURB
2169.87	2166.50	CC		DK GY SLTST, F. LAM
2172.37	2169.00	CC		DK GY SLTST, F. LAM
2178.37	2175.00	CC		DK GY SLTST, F. LAM
2180.44	2177.37	CC		DK GY SLTST, F. LAM
2183.74	2180.67	CC		DK GY SLTST, F. LAM; INTERBEDDED F. LAM SST
2189.52	2186.45	CC		DK GY SLTST, F. LAM
2191.82	2188.75	CC		DK GY SLTST/SST, BIOTURB. NOTE: CLEAN OFF DRILLING MUD
2193.07	2190.00	CC		DK GY SLTST
2194.98	2191.91	CC		DK GY SLTST
2197.51	2194.40	CC		DK GY SLTST, F. LAM
2198.34	2195.23	CC		DK GY SLTST, F. LAM, BIOTURB.
2200.11	2197.00	CC		DK GY SLTST/F. SST, COARSELY BIOTURB.
2202.66	2199.55	CC		DK GY SLTST, F. LAM
2203.40	2200.29	CC		DK GY SLTST/SST, BIOTURB.
2246.50		SWC 38	19.00	DK GY ARG SLTST, RARE COAL
2272.50		SWC 35	17.00	DK GY SLTST, FREQUENT COAL
2295.00		SWC 32	18.00	GY SLTST, RARE COAL
2334.80		SWC 28	12.00	DK GY ARG SLTST, FREQUENT COAL
2384.00		SWC 26	20.00	DK GY ARG SLTST, FREQUENT COAL
2397.70		SWC 25	19.00	DK GY ARG SLTST, FREQUENT COAL
2425.70		SWC 22	21.00	DK GY ARG SLTST, FREQUENT COAL
2449.00		SWC 19	22.00	DK GY SLTST, FREQUENT COAL
2501.50		SWC 17	18.00	GY ARG SST, RARE COAL
2571.00		SWC 13	15.00	GY ARG SST, RARE COAL, TR CALCITE
2597.00		SWC 10	18.00	GY ARG SLTST, FREQUENT COAL
2620.50		SWC 7	16.00	GY SLTST, RARE COAL
2636.20		SWC 5	17.00	GY ARG SST, RARE COAL, TR CALCITE
2667.50		SWC 3	20.00	GY ARG SLTST, FREQUENT COAL

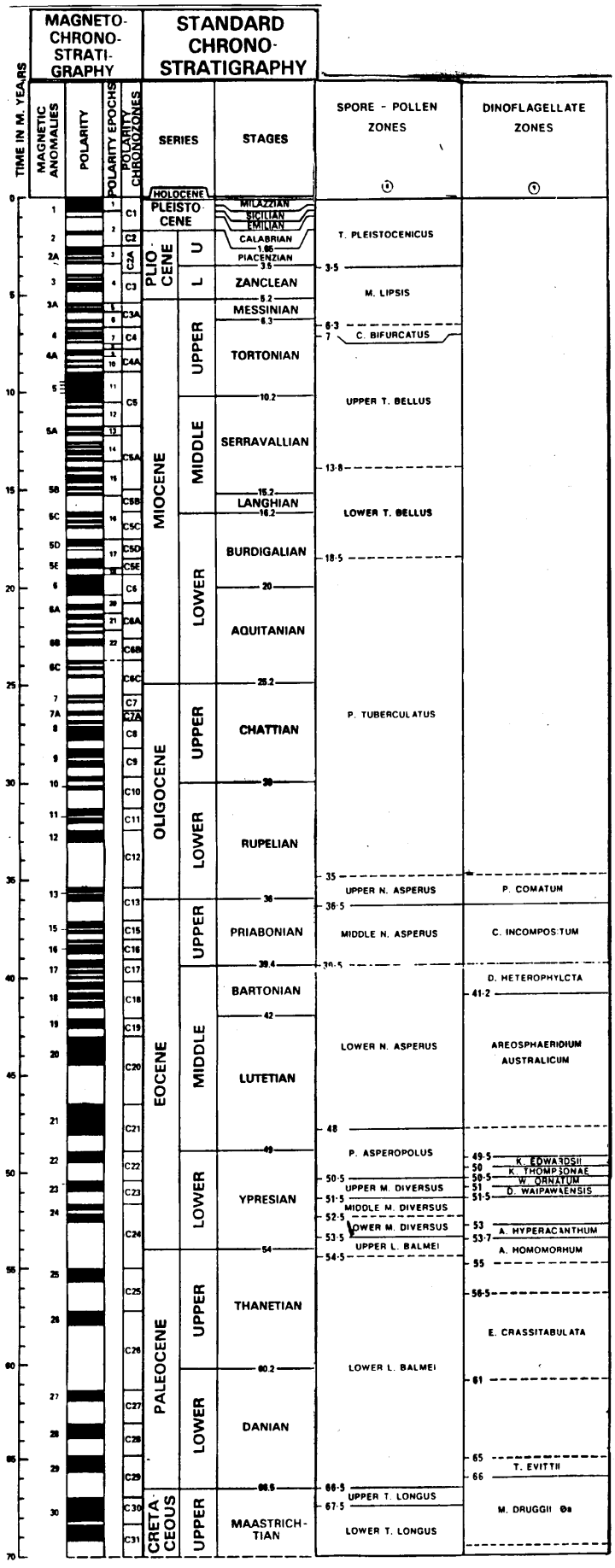

FIGURE 1 **TERTIARY ZONATION SCHEME (Partridge 1976 and pers. comm. using time scale of Haq et al)**

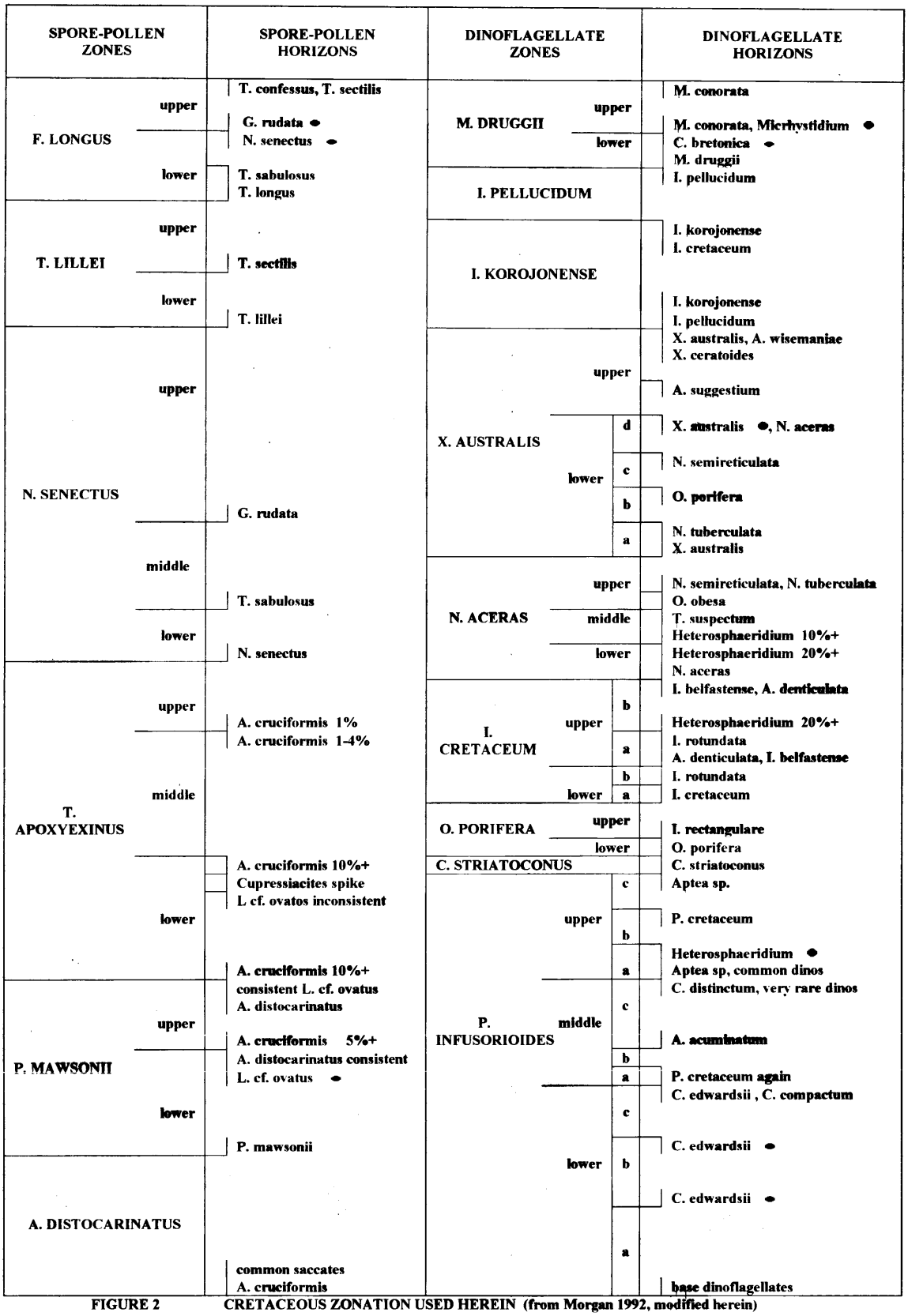

FIGURE 2 CRETACEOUS ZONATION USED HEREIN (from Morgan 1992, modified herein)

● = frequent (4-10%) ● = common (11-30%)

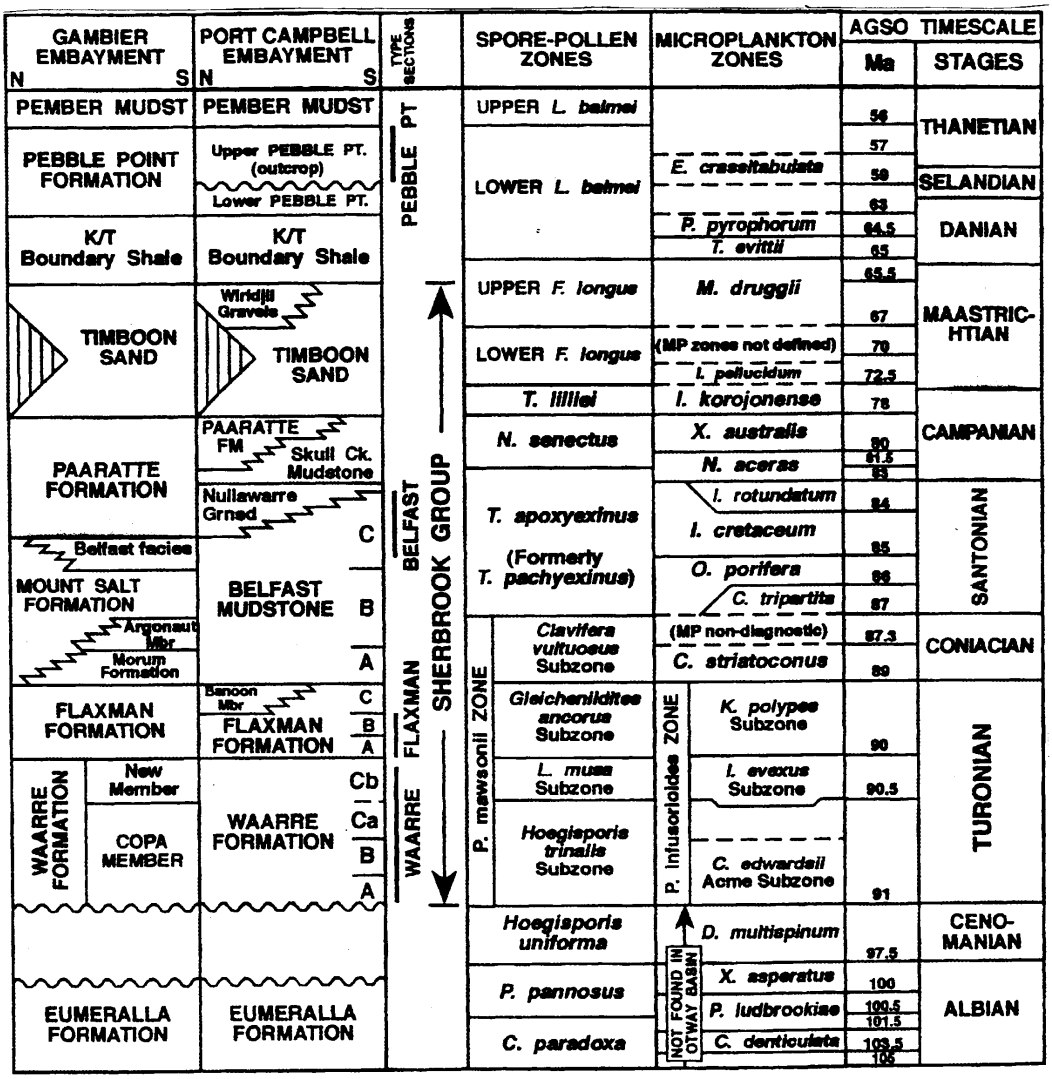

Figure 3 : **Revised Sherbrook Group stratigraphy and palynological timescale. (from Partridge 1998)**

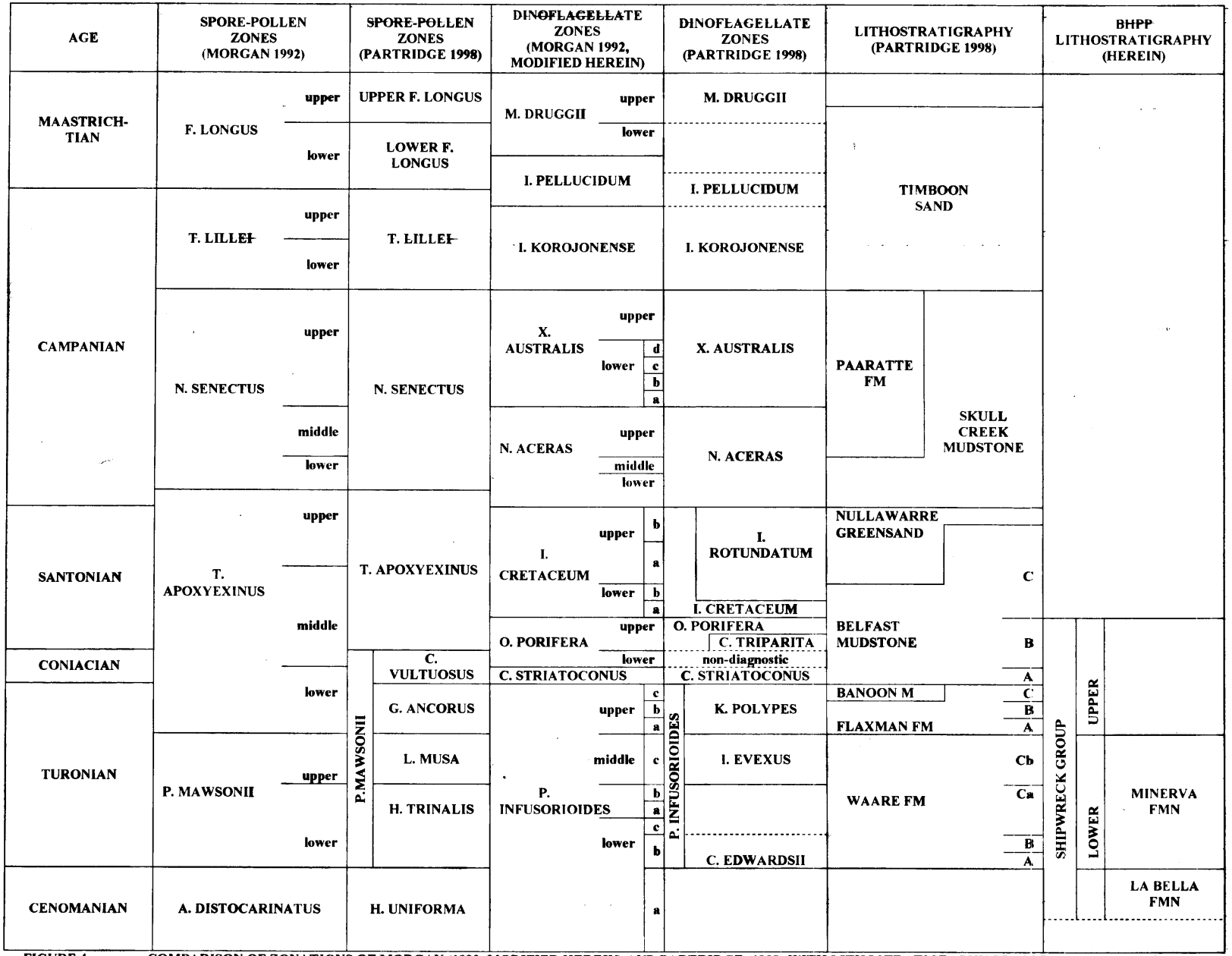

FIGURE 4 COMPARISON OF ZONATIONS OF MORGAN (1992, MODIFIED HEREIN) AND PARTRIDGE (1998) WITH LITHOSTRATIGRAPHY FROM PARTRIDGE (1998)

FIGURE 5 MATURITY PROFILE : THYLACINE-1

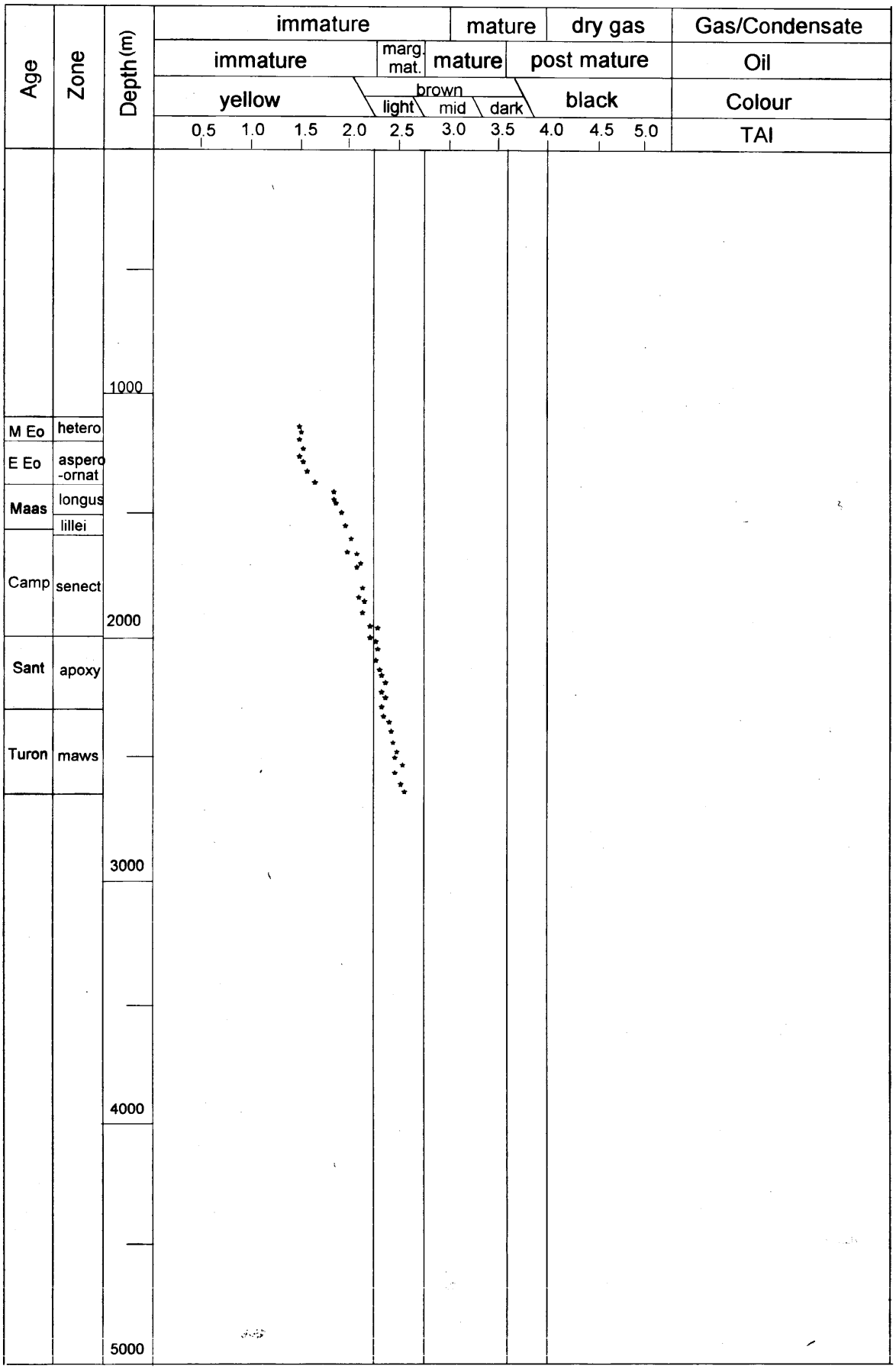

3 PALYNOSTRATIGRAPHY

3.1 1170/80 m (cutts) : *D. heterophlycta* Zone, shelfal marine

Assignment to the *Deflandra heterophlycta* Dinoflagellate Zone is indicated by the presence of *D. heterophlycta* and *Tritonites tricornus*. Other rare taxa supporting the assignment include *Areosphaeridium multicornutum, Corrudinium incompositum, Phthanoperidinium comatum* and *Systematophora placacantha*. No elements are obviously caved. *Diconodinium pusillum* is obviously reworked from the Cretaceous. Amongst the microplankton, *Spiniferites ramosus* is common, with frequent *Botryococcus* sp*., Operculodinium centrocarpum* and *P. comatum*.

Spores and pollen are also common, with the dominance of *Nothofagidites* spp. including *N. deminutus* and *N. falcata* indicating the *N. asperus* Spore-pollen Zone. The associated dinoflagellates indicate the *N. asperus* (lower) Zone which is consistent with the absence of *Triorites magnificus* (the *N. asperus* (middle) Zone indicator). Of the spore-pollen, common are *N. deminutus* and *Nothofagidites emarcidus* with frequent *Dilwynites granulatus, Laevigatosporites ovatus, Malvacipollis subtilis* and *Phyllocladidites mawsonii*.

Shelfal marine environments are indicated by the slight dominance of diverse spores and pollen over the diverse microplankton.

Yellow spore colours indicate immaturity for hydrocarbons.

3.2 1230/40 m (cutts) – 1300/10 m (cutts) : *P. asperopolus* Zone, nearshore marine

This interval marks a major kerogen change to abundant amorphous organic matter (AOM), massively diluting recognisable palynomorphs and so decreasing confidence in zonal assignments. Thus, although markers for the *D. heterophlycta* Zone and *A. australicum* Zone are seen, they are considered caved into the upper part of the *P. asperopolus* Spore-pollen Zone.

Dinoflagellates are subordinate and include markers for the *D. heterophlycta* Zone (*D. heterophlycta, P. comatum, S. placacantha*) and *A. australicum* Zone (*A. multicornutum, Achilleodinium biformoides*). New elements downhole include robust *Cordosphaeridium inodes* and *C. gracilis* at 1230/40 m and youngest *Homotriblium tasmaniense* at 1300/10 m. Frequent microplankton are *S. ramosus,*

O. centrocarpum and *Botryococcus* sp. at 1230/40 m but they may be caved, and common *Botryococcus* sp. at 1300/10 m.

Assignment to the *P. asperopolus* Spore-pollen Zone is indicated at the top by the downhole increase in *Haloragacidites harrisii* at 1230/40 m (the so called "harrisii reversal" of Stover and Partridge 1973), and youngest *Intratriporopollenites notabilis* at 1300/10 m, and at the base by oldest *Proteacidites asperopolus* at 1230/40 m and dinoflagellate data in underlying samples. Amongst the spore-pollen, *Nothofagidites* are still common at 1230/40 m but are probably partly caved. Common is *Dilwynites granulatus* with frequent *Cyathidites minor, H. harrisii, N. deminutus, N. emarcidus* and *Podosporites microsaccatus*. Rare elements include *Cupanieidites orthteichus, I. notabilis* (1300/10 m), *Kuylisporites waterbolkii* (1230/40 m), *N. falcata* (1230/40 m), *P. asperopolus* (1230/40 m) and *Proteacidites pachypolus* (both samples).

Nearshore marine environments are suggested by the dominant and diverse spores and pollen, frequent freshwater algae, and subordinate (at 1230/40 m) to minor (at 1300/10 m) dinoflagellates, many of which appear caved. Anoxic bottom conditions are indicated by the abundant AOM.

Yellow spore colours indicate immaturity for hydrocarbons.

3.3 1360/70 m (cutts) : *K. edwardsii* Zone, very nearshore marine

Continued abundant AOM dilutes recognisable palynomorphs. However, several specimens of the distinctive *Kisselovia edwardsii* indicate the *K. edwardsii* Dinoflagellate Zone of Partridge (1976). Assignment is confirmed by frequent *H. tasmaniense* and rare *Cassidium fragile* and *Deflandrea truncata*. Common is *Botryococcus* sp. with frequent *H. tasmaniense* and consistent *S. ramosus*. Robust *C. inodes* are rare elements.

Spores and pollen are dominant but zonal taxa rare due to the dilution by abundant AOM. Common is *H. harrisii* with frequent *Cyathidites minor, D. granulatus, Microcachryidites antarcticus, Nothofagidites emarcidus* and *Proteacidites* spp. Rare elements include *C. orthoteichus* and *Santalumidites cainozoicus* indicating the *M. diversus* (upper) Zone or younger zones. Spore-pollen zonal assignment is not clear, but the dinoflagellate zone is normally seen within the *P. asperopolus* Spore-pollen Zone.

Very nearshore marine environments are indicated by the low content of low diversity dinoflagellates, common freshwater algae and dominant and diverse spores and pollen.

Yellow spore colours indicate immaturity for hydrocarbons.

3.4 1380/90 m (cutts) : *K. thompsonae-W. ornatum* Zones, nearshore marine

Continued abundant AOM dilutes the recognisable palynomorphs. Rare *H. tasmaniense* indicates assignment to the *Kisselovia thompsonae-Dracodinium waipawaense* Dinoflagellate Zones interval with rare *Kisselovia coleothrypta* and *Wetzeliella articulata* indicating the *K. thompsonae* to *Wilsonidium ornatum* Dinoflagellate Zones interval. Common is *Botryococcus* sp. and frequent is *S. ramosus.* Other elements are rare and include robust *C. inodes*.

Spores and pollen are rare, diluted by the abundant AOM and zonal assignment is poorly based. However, these dinoflagellate zones are normally seen with the *P. asperopolus* Zone to *M. diversus* Zone, Upper Subzone interval. Common are *H. harrisii* and *Podosporites microsaccatus* with frequent *Cyathidites minor, D. granulatus, F. similis, Lygistepollenites florinii, M. antarcticus* and *Proteacidites* spp. However, rare *Malvacipollis diversus* and *S. cainozoicus* suggest the *M. diversus* (upper) Zone.

Nearshore marine environments are indicated by the low content of low diversity dinoflagellates, common freshwater algae and dominant and diverse spores and pollen.

Yellow spore colours indicate immaturity for hydrocarbons.

3.5 1400/10 m (cutts) - 1470/80 m (cutts) : *M. druggii* Zone, *F. longus* (upper) Zone, nearshore to shelfal marine

Inertinite is dominant in marked contrast to the AOM above. Assignment to the spore pollen unit is indicated at the top by youngest *Tricolpites waipawaensis* and *Triporopollenites sectilis* and at the base by oldest common *Gambierina rudata*. Youngest *Forcipites sabulosus* at 1470/80 m suggests the lower subzone, but may be reworked. Common are *Proteacidites* spp. with *G. rudata* common at 1460/70 m (cutts) and 1470/80 m (cutts) and frequent above. Other frequent taxa include *Falcisporites similis* and *Stereisporites antiquasporites*. Other key rare elements include *Stereisporites punctatus* (down to 1440/50 m), *Nothofagidites endurus,*

Nothofagidites senectus, Lygistepollenites balmei, Gambierina edwardsii, Quadraplanus brossus (1420/30 m only), *Tetracolporites verrucosus* (1460/70 m only) and *Forcipites longus* (1470/80 m only).

Microplankton are subordinate to co-dominant. Zonal assignment is indicated at the top by youngest *Manumiella druggii* and at the base by oldest *M. druggii* without older markers. *Micrhystridium* spp. are abundant in the upper part (1400/10 m - 1440/50 m) with rare *Canninginopsis bretonica* and frequent in the lower part (1460/70 m-1470/80 m) with frequent *C. bretonica*. Youngest *Canninginopsis "foveobretonica"* occurs at 1460/70 m and oldest *Alisocysta circumtabulata* occurs at 1420/30 m. Common to frequent throughout is *Manumiella conorata* with frequent to abundant *Micrhystridium* spp., frequent to rare *C. bretonica* and frequent *S. ramosus*. Rare elements include *Areoligera senonensis* and *M. druggii*. The interval can be subdivided as below.

upper subzone = *M. druggii* and *M. coronata* with abundant *Micrhystridium* spp. (1400/10 m – 1440/50 m)

lower subzone = top frequent *C. bretonica* above older markers (1460/70 m – 1470/80 m)

The following events have further potential for detailed event correlation and the future erection of finer subdivisions.

1400/10 m	: top *G. rudata* frequent, *Micrhystridium* spp. abundant
1420/30 m	: base *A. circumtabulatum*
1440/50 m	: base abundant *Micrhystridium* spp., base *T. punctatus*
1460/70 m	: top *C. "foveobretonica"*, frequent *C. bretonica*, common *G. rudata*
	: base frequent *M. conorata* (?caved below this point)
1470/80 m	: base common *G. rudata*
	: top *F. sabulosus*

Environments appear to be initially nearshore (subordinate moderate diversity microplankton, dominant and diverse spore-pollen), becoming more offshore (co-dominant moderately diverse microplankton with co-dominant diverse spore-pollen).

Yellow spore colours indicate immaturity for hydrocarbons.

3.6 1480/90 m (cutts) – 1490/1500 m (cutts) : *I. pellucidum* Zone, *F. longus* (lower) Zone, nearshore marine

Inertinite is dominant. Assignment to the spore-pollen subzone is indicated at the top by the downhole increase of *Nothofagidites* spp., youngest consistent *T. sabulosus* and the downhole decrease of *G. rudata.* At the base, assignment is on oldest *Gambierina edwardsii* (1490/1500 m), supported by oldest *T. sectilis* (1490/1500 m) and *T. waipawaensis* (1480/90 m). Very common are *Proteacidites* spp. with frequent *C. minor*, *Dictyophyllidites harrisii, D. granulatus, F. similis, M. antarcticus, P. microsaccatus, R. austroclavatidites* and *S. antiquasporites*. Rare elements include *G. edwardsii, G. rudata, N. endurus, N. senectus, Tricolpites confessus, T. lillei* and *T. sectilis*. Permian and Triassic reworking is rare but persistent.

Amongst the minor dinoflagellates, assignment is indicated at the top by youngest *Isabelidinium pellucidum* and at the base by the absence of older markers. Other youngest occurrences coincident with the zone top include *Cribroperidinium "polyacanthum", Nummus* spp., *Spinidinium echinoidea* and *Odontochitina* spp. Other rare elements include *Acanthaulax wilsonii, Ceratiopsis diebellii* (1480/90 m), *C. bretonica* (probably caved) and *M. conorata* (single specimen at 1480/90 m considered caved). *Botryococcus* sp. and *A. senonensis* are the most frequent microplankton.

Nearshore marine environments are indicated by the low content of moderate diversity dinoflagellates and the dominant and diverse spores and pollen.

Yellow spore colours indicate immaturity for hydrocarbons.

3.7 1540/50 m (cutts) : *I. korojonense* Zone, *T. lillei* Zone, very nearshore marine

Vitrinite and inertinite are dominant. Assignment to the spore-pollen zone is indicated by oldest *T. lillei* without younger markers. Common is *F. similis* in contrast to the very common *Proteacidites* spp. seen above. Frequent are *Ceratosporites equalis, Cyathidites australis, D. granulatus* and *Proteacidites* spp. Also frequent is Permian and Triassic reworking, suggesting lowstand conditions with significant clastic input from an eroded hinterland. Rare elements include *G. rudata, N. endurus, N. senectus, Forcipites stiplatus, Peninsulapollis gillii, F. sabulosus* and *T. lillei.*

Dinoflagellates are extremely scarce but zonal assignment is indicated by youngest *Isabelidinium cretaceum* without older markers. *Botryococcus* sp. is frequent. All dinoflagellates are rare.

Very nearshore marine environments are indicated by the rare low diversity dinoflagellates and dominant and diverse spores and pollen.

Yellow spore colours indicate immaturity for hydrocarbons.

3.8 1590/1600 m (cutts) : *X. australis* (upper) Zone, *N. senectus* (upper) Zone, ?marginal marine

Inertinite is dominant. Spore-pollen zonal assignment is indicated at the top by the absence of younger indicators (and a downhole influx of *N. senectus*) and at the base by the presence of *G. rudata* which occurs in and below this interval. Common are *Proteacidites* spp. and *C. minor* with frequent *Gleicheniidites* spp., *N. senectus* and *P. microsaccatus*. Rare elements include *A. cruciformis, G. rudata, N. endurus, T. confessus, P. gillii* and *F. sabulosus*. Minor Permian reworking was seen.

Dinoflagellate zonal assignment is indicated at the top by youngest *Xenikoon australis* and youngest *Xenascus ceratoides* and at the base by the absence of older markers. Dinoflagellates are very rare.

Marginal marine environments are suggested by extremely rare very low diversity dinoflagellates and dominant, diverse spore-pollen. However, the dominance of inertinite and absence of plant debris suggests more offshore marine environments.

Yellow to light brown spore colours indicate immaturity for hydrocarbons.

3.9 1640/50 m (cutts) – 1866.7 m (swc) : *X. australis* (lower) Zone, *N. senectus* (upper) Zone, nearshore marine

Inertinite is dominant. Spore-pollen zonal assignment is indicated at the top by the absence of younger markers and at the base by oldest *G. rudata*. Common are *F. similis* and *Proteacidites* spp. with frequent *C. minor, D. harrisii* and *M. antarcticus*. Rare elements include *A. cruciformis, G. rudata, N. endurus, N. senectus, T. confessus, P. gillii, F. stiplatus* and *F. sabulosus*. Minor Permian reworking was seen.

Dinoflagellate zonal assignment is indicated at the top by youngest *Nelsoniella aceras* and youngest common *X. australis* and at the base by oldest *X. australis*. Notably, at 1866.7 m (swc), youngest *Nelsoniella tuberculata* occurs with common *X. australis* and in cuttings this top-range has been used in the past to approximate top *N. aceras* Zone. Hence a slight miscorrelation will occur when comparing cuttings based data with swc based data (with top *N. aceras* Zone being picked slightly higher in the cuttings data by including the *X. australis* (lower a) Zone in the underlying *N. aceras* Zone, and slightly lower in the swc based data by including this Subzone in the overlying *X. australis* Zone).

Common to abundant throughout is *X. australis*. At 1690/1700 m, only *N. aceras* is common and *N. semireticulatum* is frequent. At 1866.7 m (swc) only, *H. "solida"* and *Escharisphaeridia* spp. are frequent. Otherwise all dinoflagellates are rare and include *Heterosphaeridium "solida", Maduradinium pentagonum* and below 1740/50 m, *Exochosphaeridium phragmites, Odontochina* spp., *Oligosphaeridium* spp. and *S. ramosus.*

Within the interval, the following subzones can be identified.

lower d subzone = top *N. aceras* above older markers (1640/50 m)
lower c subzone = top *Nelsoniella semireticulata* above older markers (1690/1700 m)
lower b subzone = top *Odontochitina porifera* above older markers (1740/50 – 1790/1800 m)
lower a subzone = top *N. tuberculata* with abundant *X. australis* (1866.7 m swc)

Within this interval, markers with high potential for detailed correlation include:

1640/50 m	: top *N. aceras*
1690/1700 m	: top *Nelsoniella semireticulata*
	: marked acme *N. aceras* and *N. semireticulata*
1740/50 m	: top *Odontochitina porifera*
	: top increase dinoflagellate diversity
1790/1800 m	: top *P. infusorioides*
1866.7 m (swc)	: top *N. tuberculata* with abundant *X. australis*
	: top frequent *H. "solida"*

Nearshore to shelfal marine environments are indicated by subordinate moderate diversity dinoflagellates and dominant and diverse spore-pollen.

Yellow to light brown spore colours indicate immaturity for hydrocarbons.

3.10 1931.3 m (swc) : *N. aceras* (upper) Zone, *N. senectus* Zone, nearshore marine

Inertinite is dominant. Spore-pollen sub-zonal assignment is not possible due to scarcity of the key species. This may be caused by increased distance from shore with the key, small angiosperm pollen not being carried or transported offshore in sufficient numbers. From the associated dinoflagellate zone, the *N. senectus* (middle) Zone would be expected.

Common are *F. similis* and *Proteacidites* spp. with frequent *C. minor, D. harrisii* and *D. granulatus*. Rare elements include *T. confessus* and *P. gillii*. Rare Permian and Triassic reworking were seen.

Dinoflagellate zonal assignment is clear. Assignment at the top is on the absence of younger markers especially *X. australis*, confirmed by youngest *N. tuberculata* (seen at 1866.0 m swc above). Youngest *Trithyrodinium "marshallii"* occurs here. Assignment at the base is on the absence of older markers (especially *Odontochitina "obesa"* seen below). Frequent is *H. "solida"* with consistent *Oligosphaeridium pulcherrimum* and *Palaeohystrichophora infusorioides*. Rare elements include *Callaiosphaeridium asymmetricum, N. aceras* and *T. "marshallii"*.

Nearshore marine environments are indicated by the subordinant and moderately diverse dinoflagellates and dominant and diverse spores and pollen.

Yellow to light brown spore colours indicate immaturity for hydrocarbons.

3.11 1972.0 m (swc) : *N. aceras* (middle) Zone, *N. senectus* Zone, shelfal marine

Inertinite is dominant. Spore-pollen sub-zonal assignment is not possible due to scarcity of the key species. From the associated dinoflagellate zone, the *N. senectus* (lower) Zone would be expected. The presence of oldest *F. stiplatus* confirms the *N. senectus* Zone, but subzonal assignment is not possible. Common is *F. similis* with frequent *C. minor, D. harrisii, D. granulatus, Proteacidites* spp. and *Retitriletes austroclavatidites*. Rare taxa include *T. confessus* and *P. gillii*.

Dinoflagellate zonal assignment is indicated at the top by youngest common (10%+) *H. "solida",* confirmed by youngest *O. "obesa"* and at the base by the absence of older markers. Common are *H. "solida"* and *N. aceras*, with frequent *O. "obesa"* making a very distinctive horizon for correlation. Consistent are *Odontochinta operculata, S. ramosus* and *T. "marshallii"*. Rare elements include *Gillinia hymenophora, O. porifera* and *P. infusorioides*.

Shelfal marine environments are indicated by the co-dominant moderately diverse dinoflagellates and highly diverse spores and pollen.

Yellow to light brown spore colours indicate immaturity for hydrocarbons.

3.12 1988.0 m (swc) : *N. aceras* (lower) Zone, ?*N. senectus* Zone, shelfal marine

Inertinite is dominant. Spore-pollen zonal assignment is not possible due to scarcity of the key species. The associated dinoflagellate zone indicates the *N. senectus* (lower) Zone would be expected. Common is *F. similis* with frequent *D. harrisii* and *M. antarcticus.* Rare elements include *Australopollis obscurus, Clavifera triplex* and *Phimopollenites pannosus*.

Dinoflagellate zonal assignment is indicated at the top by youngest very common (20%+) *H. "solida"* coincident with youngest *Chatangiella victoriensis* and at the base by the absence of older markers. Very common is *H. "solida"* with consistent *Botryococcus* sp., *N. aceras, O. porifera* and *S. ramosus*. Rare elements include *P. infusorioides* and *T. "marshallii"*.

Shelfal marine environments are indicated by the co-dominant moderately diverse dinoflagellates and highly diverse spores and pollen.

Yellow to light brown spore colours indicate immaturity for hydrocarbons.

3.13 2027.0 m (swc) – 2040.0 m (swc) : *I. cretaceum* (upper) Zone, *T. apoxyexinus* (upper) Zone, shelfal marine

Inertinite is dominant. Spore-pollen zonal assignment is not confident due to scarcity of the zonal *Nothofagidites* spp. in the overlying section. This interval does contain <1% *A. cruciformis* and so conforms to the subzone criteria. Common are *C. minor* (2040.0 m swc), *D. granulatus* (2027.0 m swc) and *F. similis* (both samples).

Frequent are *M. antarcticus* and *Proteacidites* spp. Rare elements include *A. cruciformis* and *Tricolporites apoxyexinus* (2040.0 m swc) only. *Proteacidites* spp. are near 5% in this interval and always 1% or less beneath.

Dinoflagellate zonal assignment is indicated at the top by youngest *Isabelidinium belfastense "belfastense"* coincident with youngest *Amphidadema denticulata, Circulodinium "solida"* and *Trthyrodinium "thick reticulate"* and at the base by oldest *Amphidiadema denticulata*.

Within this interval, the following subzones can be identified.

upper b subzone= top *I. belfastense "belfastense"* above older markers (2027.0 m swc)
upper a subzone= top *I. belfastense "rotundata"* above oldest *A. denticulata* (2040.0m swc)

Within the interval, markers with high potential for detailed correlation include:

2027.0 m (swc) : top *I. belfastense "belfastense"*
: oldest *H. solida* 20%+
: *A. denticulata* very consistent
2040.0 m (swc) : top *I. belfastense "rotundata"*
: frequent *O. operculata* and *T. "marshallii"*

At 2027.0 m (swc), some probable *N. aceras* specimens occur. This is at variance with previous experience. These specimens may be closely related New Zealand forms or mud contamination of these swcs. However they may represent a new subzone of range overlap between *I. belfastense belfastense* and *N. aceras* but until this feature is seen again, it will not be incorporated into the zonation. Common to very common is *H. "solida"*. At 2027.0 m (swc), *A. denticulata* is very consistent. At 2040.0 m (swc), *O. operculata* and *T. "marshallii"* are frequent. *T. "thick reticulate"* is consistent in both samples. Rare in both samples are *C. victoriensis, Hystrichodinium pulchrum, Nummus s*p. and *O. porifera*.

Shelfal marine environments are indicated by the co-dominant moderately diverse dinoflagellates and highly diverse spores and pollen.

Yellow to light brown spore colours indicate immaturity for hydrocarbons.

3.14 2044.0 m (swc) – 2076.0 m (swc) : *I. cretaceum* (lower) Zone, *T. apoxyexinus* (middle) Zone, nearshore to shelfal marine

Inertinite is dominant. Spore-pollen assignment is of low confidence due to the bland nature of this interval and the scarcity of the zonal markers in the overlying section. *A. cruciformis* is 1-4%, consistent with the *T. apoxyexinus* (middle) Zone. Frequent to common are *C. minor* and *F. similis* with frequent *D. granulatus* and *O. wellmanii*. Rare elements include *A. cruciformis, A. obscurus, C. triplex* and *P. mawsonii.*

Dinoflagellate zonal assignment is indicated at the top by the absence of younger markers and at the base by oldest *I. cretaceum*, coincident with oldest *Trithyrodinium glabra* and other thick *Trithyrodinium* spp.

The two samples are quite different and the interval can be subdivided.

Within the interval, the following subzones can be recognised:

lower b subzone = base *I. belfastense* beneath younger markers (2044.0 m swc)
lower a subzone = base *I. cretaceum* beneath younger markers (2076.0 m swc)

Within the interval, markers with high potential for detailed correlation include:

2044.0 m (swc) : base *I. belfastense "rotundata"*
: acmes *O. operculata* (6%), *T. glabra* (9%), other *Trithyrodinium* spp.
: *Odontochitina "triangulata"* present
: acme *H. "solida"* (10%)
2076.0 m (swc) : base *I. cretaceum*
: less *H. "solida"* (4%)
: base *T. glabra*

In both samples frequent to common is *H. "solida"* with frequent *Botryococcus* sp. and consistent *Trithyrodinium* spp.

Nearshore (2076.0 m swc) to shelfal (2044.0 m swc) marine environments are indicated by the subordinate to co-dominant moderately diverse dinoflagellates and dominant to co-dominant moderately diverse spore-pollen.

Light brown spore colours indicate marginal maturity for oil but immaturity for gas/condensate.

3.15 2090.0 m (swc) – 2131.5 m (swc) : *O. porifera* (upper) Zone, *T. apoxyexinus* (middle) Zone, nearshore marine

Inertinite is dominant. Spore-pollen zonal assignment is indicated by *A. cruciformis* at 4-5% at the top, without older markers. Common are *C. minor* and *F. similis* with frequent *A. cruciformis, D. granulatus, M. antarcticus* and *V. pallidus*. Rare elements include *Proteacidites* spp. which are virtually not seen below this interval.

Dinoflagellate zonal assignment is indicated at the top by the absence of younger markers concident with the downhole influx of *Isabelidinium rectangulare* and at the base by oldest *I. rectangulare*, here coincident with oldest *C. victoriensis* and *T. "marshallii"*. No dinoflagellates are common. Frequent are *Heterosphaeridium* spp. with consistent *Botryococcus* sp., *C. victoriensis, I. rectangulare* and *T. "marshallii"*. Very rare elements include *G. hymenophora* and *Dinogymnium acuminatum*.

Nearshore marine environments are indicated by the dominant and diverse spores and pollen and subordinate moderately diverse dinoflagellates.

Light brown spore colours indicate marginal maturity for oil but immaturity for gas/condensate.

3.16 2168.37 m (core) – 2295.0 m (swc) : *P. infusorioides* (upper) Zone, *T. apoxyexinus* (lower) Zone, nearshore to marginal marine

Vitrinite, cuticle and inertinite are all very common, in contrast to the inertinite dominated assemblages above. Assignment to the spore-pollen zone is indicated by maximum content of *A. cruciformis*. *A. cruciformis* is less common here than in many other wells in the basin and this interval can be defined by *A. cruciformis* >5%, while elsewhere it has been defined by *A. cruciformis* >10%. Common are *Cupressiacites* spp. (at the top), *A. cruciformis, D. granulatus, D." pusillum", F. similis* and *M. antarcticus*. Frequent are *C. minor, D. harrisii, R. austroclavatidites* and *V. pallidus*. Rare elements throughout include inconsistent *Laevigatosporites* cf. *ovatus* and *Gleicheniidites* sp. (thick). Occasional specimens of *Appendicisporites distocarinatus* seen in 4 out of 18 samples are considered reworked. The upper part

(2168.37 m core – 2169.87 m core) contain a peak of *Cupressacites* (15-23%) which is seen in other wells. Permian and occasionally Triassic reworking are minor components.

Dinoflagellate zonal assignment is indicated at the top by youngest *Aptea* sp. coincident with youngest *Kiokanosium polypes* and at the base by oldest *Aptea* sp. The upper part (2168.37 m core – 2203.40 m core) is totally dominated by plant debris with rare dinoflagellates. *K. polypes, Circulodinium "solida", Cribroperidinium* sp. and *Heterosphaeridium heteracanthum* are the most consistent. The lower part (2246.5 m swc – 2295.0 m swc) is dominated by plant cuticle and is much more marine, with common to very common *H. heteracanthum* and frequent *Botryococcus* sp. and *C. "solida"*. Consistent are *Aptea* sp., *Cribroperidinium* sp., *K. polypes, O. operculata* and *P. infusorioides*. The following dinoflagellate subdivisions can be recognised.

upper c subzone = *Aptea* sp. above youngest *P. cretaceum* (168.37 m – 2191.82 m)
upper b subzone = *P. cretaceum* above *Heterosphaeridium* acme (2193.07 m – 2203.40 m)
upper a subzone = *Heterosphaeridium* acme above base *Aptea* sp. (2246.5 m – 2295.0 m)

Within the interval, the following events have further potential for event stratigraphy and detailed local intra-reservoir correlation.

2168.37 m (core)	: top *Cupressiacites* acme (15%)
	: top *Aptea* sp., *K. polpes*
	: *C. "solida"* (5%), *K. polypes* (4%), *P. infusorioides* (4%) acmes
	: dinoflagellate peak (20%+)
2169.87 m (core)	: base *Cupressiacites* acme (23%)
2172.37 m (core)	: *Aptea* sp. acme (5%), less dinoflagellates
	: top inconsistent *L.* cf. *ovatus*
2178.37 m (core)	: less dinoflagellates
2189.52 m (core)	: top *D." pusillum"* acme (20%+)
	: *Dilwynites* acme (40%)
2193.07 m (core)	: top *P. cretaceum*
2197.51 m (core)	: base *D. pusillum* acme (20%+)
2200.11 m (core)	: top *P. infusorioides* influx (2%)
2203.43 m (core)	: top increased dinoflagellates (20%)

2246.5 m (swc) : dinoflagellate acme (40%), *H. heteracanthum* acme (30%)
2295.0 m (swc) : base common dinoflagellates (10%+), base *Aptea* sp.

Environments are marine throughout, but show a nearshore initially transgressive trend to a marine maximum at 2246.5 m (swc), then a regressive trend to very nearshore to marginal marine above. This is indicated by moderate and increasing dinoflagellate content and diversity up to 2246.5 m (swc), then a sharp decrease in both content and diversity above. Spores and pollen are common and diverse throughout.

Light brown spore colours indicate marginal maturity for oil but immaturity for gas/condensate.

3.17 2334.8 m (swc) – 2397.7 m (swc) : *P. infusorioides* (middle) Zone, *P. mawsonii* (upper) Zone, marginal marine

Massive plant debris dominates these assemblages with inertinite and vitrinite dominant. Spore-pollen zonal assignment is indicated at the top on the absence of younger markers (coincident with top consistent *L.* cf. *ovatus* and inconsistent *A. distocarinatus*) and at the base on consistent *P. mawsonii* above older markers (especially consistent *A. distocarinatus*, and a downhole influx of *L.* cf. *ovatus)*. Previously, an Upper Subzone was distinguished containing 5%+ *A. cruciformis*, above consistent *A. distocarinatus*. This critereon has proved unworkable herein as *A. cruciformis* is absent, presumably excluded by facies. The interval described here is considered indentical in time duration but is not crisply defined. Common pollen include *D. granulatus, Dilwynites" pusillum", F. similis* and *M. antarcticus* with the spore *D. harrisii* frequent to common. At 2397.7 m (swc), spores (especially *D. harrisii*) become more common. In this interval, *A. distocarinatus* is very rare (1 specimen in 3 slides) with *L.* cf. *ovatus* 2-3%, up from <1% above. *Liliacidites kaitangataensis* first occurs downhole at 2384.0 m but is inconsistent beneath. Permian reworking is frequent at 2334.8 m (swc).

Events with possible significance for detailed correlation include:

2334.8 m (swc) : acme *M. antarcticus* (12%), Permian reworking frequent (4%)
2384.0 m (swc) : acme *D. "pusillum"* (11%)
: top *L. kaitangataensis*
2397.7 m (swc) : acme *D. harrisii* (29%)

The *P. infusorioides* (middle) Zone can be subdivided into:

middle c subzone = base *Aptea* sp. to base *Alterbia acuminatum*
middle b subzone = base *A. acuminatum* to top *P. cretaceum* re-appearance
middle a subzone = top *P. cretaceum* re-appearance to top *Cribroperidinium edwardsii*

Dinoflagellate zonal assignment of this interval is negatively based, on the absence of distinctive markers seen both above and below, and so all these samples are assigned to the middle b-c subzone. In fact, dinoflagellates are extremely rare with a very limited assemblage including not much more than *Circulodinium deflandrei, K. polypes, Nummus* spp. and *S. ramosus*. *Botryococcus* sp. is frequent.

Marginally marine to very nearshore marine environments are indicated by the totally dominant and highly diverse spores and pollen and extremely rare low diversity dinoflagellates.

Light brown spore colours indicate marginal maturity for oil but immaturity for gas/condensate.

3.18 2425.7 m (swc) – 2501.5 m (swc) : *P. infusorioides* (middle) Zone, *P. mawsonii* (lower) Zone, marginal marine to non-marine

Plant debris is dominant, comprising mostly vitrinite and inertinite. Spore-pollen zonal assignment is indicated at the top by a downhole influx of *A. distocarinatus* (consistent, from very rare above) and *L.* cf. *ovatus* (frequent 5%, from rare 2% above) and at the base by *P. mawsonii* to and beyond the interval base. Spore diversity appears higher in this interval and *Hoegisporis "trinalis"* is an extremely rare and intermittent element. *D." pusillum"* becomes common downhole at 2501.5 m (swc) and remains common to the base of the well. Common taxa are *D. harrisii, D. granulatus, F. similis* and *M. antarcticus*.

Events with possible significance for detailed correlation include:

2425.7 m (swc) : acme *D. harrisii* (17%)
: non-marine
2449.0 m (swc) : increasing *D. "pusillum"* (9%)
2501.5 m (swc) : top common *D. "pusillum"* (15%)

Dinoflagellate zonal assignment is negatively based, on the absence of distinctive markers above and below. In fact, the sample at 2425.7 m (swc) is non-marine, totally lacking saline markers and has correlative potential. Rare dinoflagellates occur at 2449.0 m including a renewed top-range of *P. cretaceum*. These provide the following subzones.

middle b-c subzone = non-descript or no dinoflagellates below *Aptea* sp. and above *P. cretaceum* (2334.8 m – 2425.7 m)

middle a subzone = top *P. cretaceum* re-appearance above youngest *C. edwardsii* (2449.0 m – 2501.5 m)

Environments are marginally marine (2449.0 m swc and 2501.5 m swc) with extremely rare low diversity dinoflagellates amongst abundant and diverse spores and pollen. At 2425.7 m (swc) non-marine environments are indicated by the total absence of saline markers, and minor freshwater algae suggest fluvial rather than lacustrine sediments. This horizon may correlate with non-marine horizons seen at the top of the *P. mawsonii* (lower) Zone elsewhere.

Light brown spore colours indicate marginal maturity for oil but immaturity for gas/condensate.

3.19 2571.0 m (swc) – 2667.5 m (swc) : *P. infusorioides* (lower) Zone, *P. mawsonii* (lower), nearshore to marginal marine

Plant debris is dominant, comprising mostly inertinite and vitrinite. Spore-pollen zonal assignment is indicated at the top by continued consistent *A. distocarinatus* and rare *H. "trinalis"*, confirmed by continued common *D." pusillum"* and here coincident with a distinctive downhole return of *A. cruciformis.* Assignment is indicated at the base by oldest *P. mawsonii*. At 2571.0 m (swc) only, a distinctive spike of 4% *Corollina torosa* occurs. Common are *D. harrisii, D. granulatus, D. "pusillum", F. similis* and *M. antarcticus* with frequent *A. australis, C. minor* and *V. pallidus*. Rare but consistent species include *A. cruciformis, A. distocarinatus* and *L.* cf. *ovatus*, with *H. "trinalis"* extremely rare and inconsistent.

Dinoflagellate zonal assignment is indicated by youngest *Cribroperidinium edwardsii* (coincident with youngest consistent *Cyclonephelium compactum* and a downhole return of *Chlamydophorella nyei*) at the top and persistent *C. edwardsii* and other dinoflagellates to the base. Three further subdivisions can be recognised in this subzone as below.

lower c subzone = top *C. edwardsii* down to the sample above acme *C. edwardsii* (2571.0 m (swc) – 2636.2 m (swc))

All the dinoflagellates are very rare with the most consistent being *C. nyei, C. edwardsii, C. compactum, H. heteracanthum, K. polypes, O. complex, P. cretaceum* and *S. ramosus*. The freshwater algae *Botryococcus* sp. is consistent but never frequent. At 2636.2 m (swc), no marine microplankton were seen.

lower b subzone = acme *C. edwardsii* (usually seen in a lithologically distinctive massive shale usually about 20 m thick) (2667.5 m swc)

Dinoflagellates are still minor, but much more common than above and below *C. edwardsii* is still rare, but 10-15 specimens occur on every slide, in contrast to the 1-2 specimens over 3 slides above and below. Dinoflagellate diversity is higher in this interval, but still only moderate with the taxa listed above more frequent.

lower a subzone = beneath acme *C. edwardsii* to base dinoflagellates (base marine section) (not seen here)

Events with possible significance for detailed correlation include:

2571.0 m (swc) : acme *M. antarcticus* (14%)
2597.0 m (swc) : acme *D. harrisii* (16%); marine peak (7% dinoflagellates)
2620.5 m (swc) : repeat acme *M. antarcticus* (16%)
2036.2 m (swc) : repeat acme *M. antarcticus* (15%); non-marine
2667.5 m (swc) : rare *M. antarcticus* (3%); acme *C. edwardsii* (consistent), marine peak (9% dinoflagellates)

Environments are very nearshore marine (low content of moderately diverse dinoflagellates) in the lower b subzone to marginal marine (very low content of low diversity dinoflagellates) to non-marine in the lower c subzone. Spores and pollen are dominant and highly diverse.

Light brown spore colours indicate marginal maturity for oil but immaturity for gas/condensate.

4 REFERENCES

Helby, R., Morgan, R., & Partridge, A.D., (1987) A palynological zonation of the Australian Mesozoic. Mem. Assoc. Aust. Palaeontol. 4, 1-94.

Marshall, N.G., (1984) Late Cretaceous dinoflagellates from the Perth Basin, Western Australia. Unpubl. Ph.D. thesis, U.W.A.

Morgan, R.P., (1992) Overview of new cuttings based Late Cretaceous correlations, Otway Basin, Australia. Unpubl. rept. for BHPP

Morgan, R.P., (1994) Palynology of BHPP Minerva-2A, Offshore Otway Basin, Victoria, Australia. Unpubl. rept. for BHPP

Partridge, A.D., (1976) The geological expression of eustacy in the Early Tertiary of the Gippsland Basin. APEA Journal 16 (1), 73-79

Partridge, A.D., (1997) New Upper Cretaceous palynology of the Sherbrook Group, Otway Basin. In Victoria Supplement PESA News April/May p. 9

Partridge, A.D., (1998) Biostratigraphy and interpreted stratigraphy of Champion-1 and Conan-1 from open file basic data. Unpubl. rept. Biostrata 1998/02

Stover, L.E., and Partridge, A.D., (1973) Tertiary and Late Cretaceous spores and pollen from the Gippsland Basin, southeastern Australia. Proc. Roy. Soc. Vic. 85, 237-286

5 UNPUBLISHED NAMES

Dinoflagellates

Aptea sp	Morgan (?=*V. gryphus* sensu Partridge)
Canninginopsis "foveobretconica"	Morgan
Cauca sp.	Morgan
Circulodinium "solida"	Morgan
Cladopyxidium "goodmanii"	Marshall (1984)
Cribroperidinium "polyacanthum"	Marshall (1984)
Cribroperidinium sp.	Morgan
Heterosphaeridium "minutum"	Morgan
Heterosphaeridium "solida"	Morgan
Isabelidinium belfastense "belfastense"	Marshall (1984)
Isabelidinium belfastense "rotundata"	Marshall (1984)
Isabelidinium rectangulare "contractum"	Marshall (1984)
Isabelidinium rectangulare "diversum"	Marshall (1984)
Isabelidinium rectangulare "rectangulare"	Marshall (1984)
Microdinium "triangularis"	Morgan, herein
Odontochitina "indistincta"	Marshall (1984)
Odontochitina "obesa"	Morgan
Odontochitina "triangulata"	Marshall (1984)
Senoniasphaera "obscondita"	Marshall (1984)
Trithyrodinium "thick reticulate"	Morgan
Trithyrodinium "marshallii"	Morgan

Spores and Pollen

Cicatricosisporites "radialis"	Morgan
Concavissimisporites "wellmanii"	Morgan
Convolutispora "magnifica"	Morgan
Dilwynites "pusillum"	Partridge
Gleicheniidites sp. (thick)	Morgan (?=*G. "ancorus"* Partridge)
Hoegisporis "trinalis"	Morgan (?=*H. "trinalis"* Partridge)
Kuylisporites "zipperi"	Morgan
Laevigatosporites cf. *ovatus*	Morgan (?=*L. musa* Partridge)
Perotriletes "baldii"	Morgan
Phyllocladidites "eunuchus"	Morgan

"old" vs "new" P. infusorioides subdivisions

<table>
<tr><th>"old"</th><th colspan="2">"new"</th><th colspan="3">Partridge</th></tr>
<tr><td rowspan="3">uppermost</td><td rowspan="3">upper</td><td>c</td><td rowspan="3">K. polypes</td><td rowspan="3">Flaxmans</td><td rowspan="3"></td></tr>
<tr><td>b</td></tr>
<tr><td>a</td></tr>
<tr><td>upper</td><td rowspan="2">middle</td><td>c</td><td>I. evexa</td><td rowspan="3">Waare</td><td>Cb</td></tr>
<tr><td>middle</td><td>b</td><td rowspan="2"></td><td rowspan="3">Ca
– – –
B</td></tr>
<tr><td></td><td>a</td></tr>
<tr><td>lower</td><td rowspan="2">lower</td><td>c</td><td rowspan="2"></td></tr>
<tr><td>lowermost</td><td>b</td><td>C. edwardsii</td><td rowspan="2"></td></tr>
<tr><td></td><td>a</td><td></td><td>A</td></tr>
</table>

Well Name : THYLACINE-1 CRETACEOUS
Operator : WOODSIDE ENERGY LTD
Interval : 1400.00m - 2667.50m
Scale : 1:2000

THYLACINE-1 CRETACEOUS Interpretive Version
Style : TL Biostratigraphic Histogram
Author : RPM
Date : 15th December 2005

Palynology Distribution Chart

Morgan Palaeo Associates
South Australia

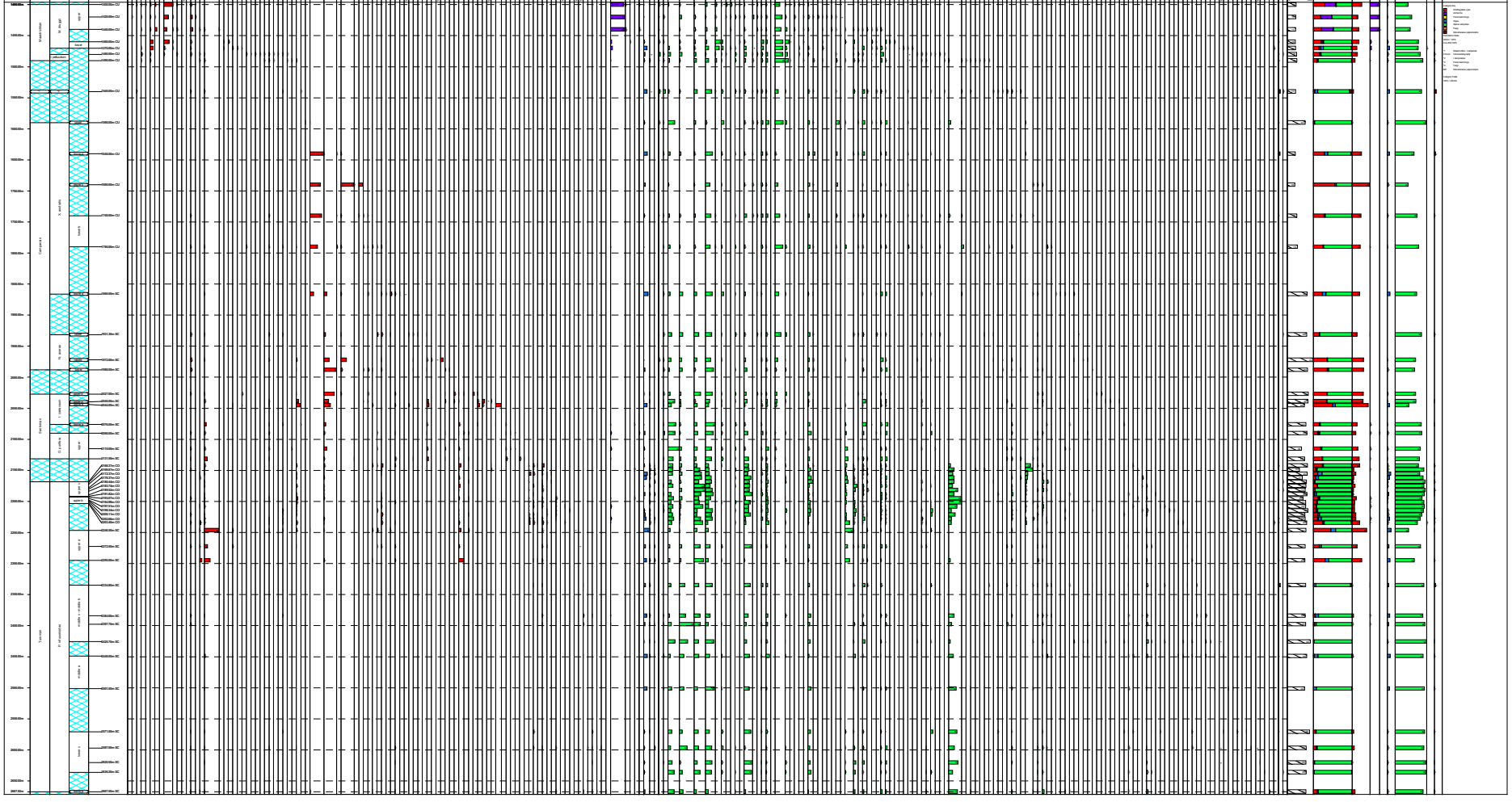

Well Name	: THYLACINE-1 TERTIARY
Operator	: WOODSIDE ENERGY LTD
Interval	: 1170.00m - 1380.00m
Scale	: 1:2000

THYLACINE-1 TERTIARY Interpretive Version
Style : % Abundance Histogram
Author : RPM
Date : 19-December-2001
Palynology Distribution Chart

Morgan Palaeo Associates
South Australia

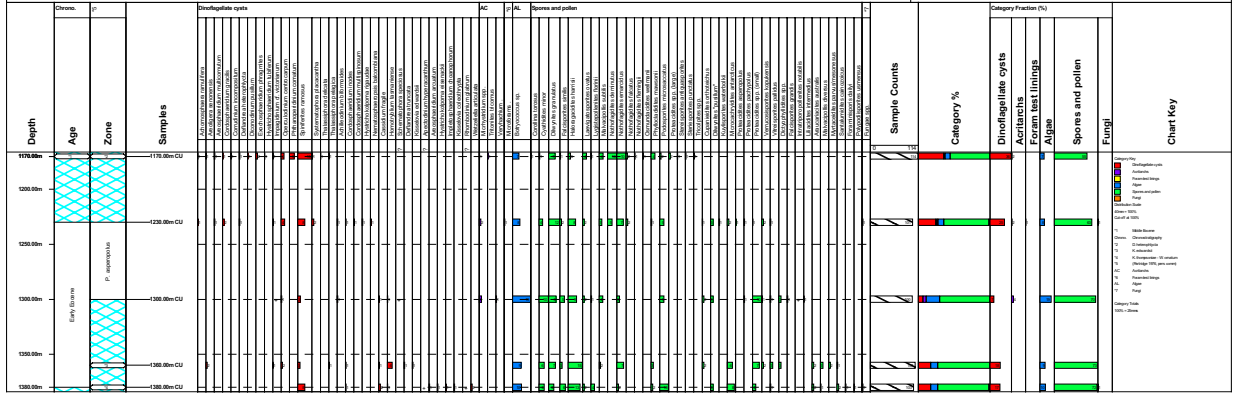

APPENDIX 5
MICROPALAEONTOLOGY REPORT

MICROPALAEONTOLOGICAL ANALYSIS

THYLACINE-1 (780 – 1150 mKB)

PERMIT T-30-P, OTWAY BASIN

FOR

WOODSIDE ENERGY LTD

J.P. REXILIUS
S.L. POWELL

OCTOBER, 2001

ISC BIOSTRAT

73 RULE STREET
NORTH FREMANTLE
WESTERN AUSTRALIA
PHONE 08-94308460 FAX 08-94308465

C O N T E N T S

I. SUMMARY

Thylacine-1 was drilled in offshore petroleum permit T-30-P, Otway Basin. Ditch cuttings samples from the interval 780m to 1150m have been examined for foraminifera and calcareous nannoplankton. A summary of the biostratigraphic breakdown of the respective microfossil groups and environment subdivision is given below:-

Benthonic Foraminiferal Subdivision

Depth Range (m)	**Zone**	**Age**
780 - 1150	indeterminate	indeterminate

Planktonic Foraminiferal Subdivision

Depth Range (m)	**Zone**	**Age**
780 - 790	H1	early Early Miocene
850 - 1110	H1 / H2	early Early Miocene - late Late Oligocene
1140 - 1150	indeterminate	indeterminate

Calcareous Nannoplankton Subdivision

Depth Range (m)	**Zone**	**Age**
780 - 790	CN1a	early Early Miocene
850 - 1010	CP19b	late - mid Late Oligocene
1050 - 1060	CP19a	early Late - late Early Oligocene
1100 - 1110	CP19a / CP18	late - mid Early Oligocene
1140 - 1150	indeterminate	indeterminate

Integrated Biostratigraphic Subdivision

Depth Range (m)	**Zone**	**Age**
780 - 790	H1, CN1a	early Early Miocene
850 - 1010	H1 / H2, CP19b	late - mid Late Oligocene
1050 - 1060	H1 / H2, CP19a	early Late - late Early Oligocene
1100 - 1110	H1 / H2, CP19a / CP18	late - mid Early Oligocene
1140 - 1150	indeterminate	indeterminate

Environment Subdivision

Depth Range (m)	**Environment**
780 – 790 to 940 – 960 inclusive	upper bathyal
1000 - 1010	outer neritic – upper bathyal
1050 - 1060	outer neritic
1100 - 1110	outer neritic – upper bathyal
1140 - 1150	undifferentiated marine

II. INTRODUCTION

A total of 8 ditch cuttings samples from the interval 780m to 1150m in Thylacine-1 have been examined for foraminifera and calcareous nannoplankton.

Fossil assemblages identified in the well section are shown in Appendix No. 2. A summary of results for each sample are shown in Appendix No. 1.

III. BIOSTRATIGRAPHIC ANALYSIS

The planktonic foraminiferal letter scheme of Taylor (unpublished) and the CN/CP calcareous nannoplankton letter scheme of Okada & Bukry (1980) are used for biostratigraphic control.

Other studies consulted include those of Jenkins (1985) and Perch-Nielsen (1985).

The Cenozoic Time Scale is after Berggren et al. (1995).

A. Benthonic Foraminiferal Subdivision

780m-1150m : Indeterminate

The samples in the interval lack age-diagnostic benthonic foraminiferal taxa.

B. Planktonic Foraminiferal Subdivision

780m-790m : Zone H1 (early Early Miocene)

The occurrence of *Globoquadrina dehiscens* s.s. and *Globigerina woodi connecta*, and the lack of *Globoquadrina dehiscens* s.l., indicates assignment to Zone H1.

850m-1110m : Zones H1/H2 (early Early Miocene-late Late Oligocene)

The association of *Globigerina woodi connecta, Globigerina woodi woodi, Globoquadrina dehiscens* s.l., *Globigerina euapertura* and *Globigerina ciperoensis*, and the lack of *Globoquadrina dehiscens* s.s., is consistent with a correlation to Zones H1 and H2.

1140-1150m : Indeterminate

The sample lacks in-situ age-diagnostic planktonic foraminiferal taxa.

C. Calcareous Nannoplankton Subdivision

780m-790m : Zone CN1a (early Early Miocene)

Zonal assignment is based on the occurrence of *Cyclicargolithus abisectus* and the lack of *Dictyococcites bisectus*.

850m-1010m : Zone CP19b (late-mid Late Oligocene)

The association of *Cyclicargolithus abisectus* and *Dictyococcites bisectus*, and lack of *Chiasmolithus altus*, is consistent with a correlation to Zone CP19b.

1050m-1060m : Zone CP19a (early Late-late Early Oligocene)

Assignment to Zone CP19a is based on the association of *Chiasmolithus altus, Cyclicargolithus abisectus* and *Dictyococcites bisectus*, and lack of older index taxa.

1100m-1110m : Zones CP19a lower/CP18 (late-mid Early Oligocene)

The nannoplankton assemblage includes *Helicosphaera compacta* and frequent numbers of *Cyclicargolithus abisectus*, and on this basis is assigned to Zones CP19a lower and CP18.

1140m-1150m : Indeterminate

The nannoplankton assemblage lacks age-diagnostic taxa.

D. Integrated Biostratigraphic Subdivision

780m-790m : Zones H1, CN1a (early Early Miocene)

Nannoplankton taxa provide biostratigraphic control.

850m-1010m : Zones H1/H2, CP19b (late-mid Late Oligocene)

Zonal assignment is based primarily on nannoplankton taxa.

1050m-1060m : Zones H1/H2, CP19a (early Late-late Early Oligocene)

Again zonal assignment is based primarily on nannoplankton taxa.

1100m-1110m : Zones H1/H2, CP19a lower/CP18 (late-mid Early Oligocene)

Again zonal assignment is based primarily on nannoplankton taxa.

1140m-1150m : Indeterminate

The cuttings sample lacks age-diagnostic in-situ calcareous microfossil taxa.

IV. ENVIRONMENT OF DEPOSITION

Bathymetric estimates are based on experience of Gippsland Basin/Northwest Shelf foraminiferal biofacies.

780-790m to 940-960m inclusive : Upper bathyal

The calcareous silty claystones and calcareous claystones in the interval are interpreted to have been deposited in an upper bathyal setting. Bathymetrically significant benthonic taxa include: *Cyclammina cancellata* (frequent from 850m to 960m), *Cyclammina* spp. (rare-frequent), *Planulina costata* (single-rare from 850m to 960m) and *Pullenia bulloides* (rare-frequent).

1000m-1010m : Outer neritic-upper bathyal

The calcareous claystone cuttings sample contains a rich outer neritic to upper bathyal benthonic foraminiferal fauna. The following environmentally diagnostic benthonic taxa are represented: *Cyclammina cancellata* (single), *Pullenia bulloides* (rare), smooth *Bathysiphon* spp. (single) and large *Cibicides* taxa.

1050m-1060m : Outer neritic

The calcareous claystone cuttings sample contains a benthonic foraminiferal assemblage that includes *Pullenia bulloides* (rare) and lacks upper bathyal taxa. Deposition in an outer neritic environment is envisaged.

1100m-1110m : Outer neritic-upper bathyal

The calcareous claystone cuttings sample contains a rich outer neritic to upper bathyal benthonic foraminiferal fauna. The following environmentally diagnostic benthonic taxa are represented: *Planulina costata* (single), *Planulina* aff. *wuellerstorfi* (single), smooth *Bathysiphon* spp. (single) and *Pullenia bulloides* (rare).

1140m-1150m : Undifferentiated marine

The in-situ facies comprises micritic limestone. The foraminiferal fauna is dominated by caved taxa from overlying calcareous claystone facies. No definitive environmental assessment is possible.

V. REFERENCES

BERGGREN, W.A., KENT, D.V., SWISHER, C.C. III & Aubry, M.P., 1995. A revised Cenozoic geochronology and chronostratigraphy, In: *Geochronology, time scales and global correlations* (eds W.A. Berggren, D.V. Kent, M.P. Aubry and J. Hardenbol), *SEPM Special Publication*, 54: 129-212.

JENKINS, D.G, 1985. Southern mid-latitude Paleocene to Holocene planktic foraminifera. In : BOLLI, H.M., SAUNDERS, J.B. & PERCH-NIELSEN, K. (Editors). *Plankton Stratigraphy*. Cambridge Univ. Press, Chapter 7 : 263-282.

OKADA, H., & BUKRY, D., 1980. Supplementary modification and introduction of code numbers to the low-latitude coccolith zonation (Bukry, 1973; 1975). *Marine Micropaleontology*., 5(3): 321-325.

PERCH-NIELSEN, K. 1985. Cenozoic calcareous nannofossils. In : BOLLI, H.M., SAUNDERS, J.B. & PERCH-NIELSEN, K. (Editors). *Plankton Stratigraphy*. Cambridge Univ. Press, Chapter 11: 427-554.

TAYLOR, D.J., (in prep.). Observed Gippsland Biostratographic biostratographic sequences of planktonic foraminiferal assemblages.

Appendix No. 1 : Summary of micropalaeontological sample analysis, Tertiary section, Thylacine-1.

DEPTH (m)	SAMPLE TYPE	* LITHOLOGY	FORAM YIELD	FORAM PRESERV.	FORAM DIVERSITY	NANNO YIELD	NANNO PRESERV.	NANNO DIVERSITY	PLANK FORAM %	BENTH FORAM %	FORAM ZONE	NANNO ZONE	FORAM / NANNO ZONE	AGE	ENVIRONMENT
780 - 790	DC	medium grey calcareous silty claystone, abundant bioclastic debris.	high	poor	high	high	moderate	moderate - high	30	70	H1	CN1a	H1, CN1a	early Early Miocene	upper bathyal
850 - 860	DC	light grey calcareous silty claystone.	high	good	high	high	moderate - good	moderate - high	40	60	H1 / H2	CP19b	H1 / H2, CP19b	late - mid Late Oligocene	upper bathyal
890 - 900	DC	medium grey calcareous claystone.	high	good	high	high	moderate - good	moderate - high	40	60	H1 / H2	CP19b	H1 / H2, CP19b	late - mid Late Oligocene	upper bathyal
940 - 960	DC	medium grey calcareous claystone.	high	good	high	high	moderate - good	moderate - high	45	55	H1 / H2	CP19b	H1 / H2, CP19b	late - mid Late Oligocene	upper bathyal
1000 - 1010	DC	light grey calcareous claystone.	high	moderate - good	high	high	moderate	moderate - high	40	60	H1 / H2	CP19b	H1 / H2, CP19b	late - mid Late Oligocene	outer neritic - upper bathyal
1050 - 1060	DC	light - medium grey calcareous claystone.	high	good	high	high	moderate - good	moderate	60	40	H1 / H2	CP19a	H1 / H2, CP19a	early Late - late Early Oligocene	outer neritic
1100 - 1110	DC	medium grey calcareous claystone.	high	good	high	high	moderate	moderate - high	65	35	H1 / H2	CP19a lower / CP18	H2 / H1, CP19a lower / CP18	late -mid Early Oligocene	outer neritic - upper bathyal
1140 - 1150	DC	off white - light grey micritic limestone with frequent glauconite grains. Common medium grey calcareous claystone [caved].	low	good - poor	moderate	low - moderate	moderate	low - moderate	no data	no data	indet. [only caved taxa].	indet.	indet.	indet.	undiff. marine

* lithology based on processed foraminiferal residue.

ISC BIOSTRAT

Appendix No. 2 : Micropalaeontological distribution chart, Thylacine-1. Page 1 of 3.

TAXA / DEPTH (m)	780 - 790 DC	850 - 860 DC	890 - 900 DC	940 - 960 DC	1000 - 1010 DC	1050 - 1060 DC	1100 - 1110 DC	1140 - 1150 DC
BENTHONIC FORAMINIFERA								
Globocassidulina subglobosa	c	a	a	a	a	a	a	c
Cibicides mediocris	c	c	c	c	a	c	c	c
Lenticulina spp.	c	a	a	a	c	c	f	r
Cibicides spp.	c	f	f	a	a	a	a	c
Gyroidinoides zealandica	f	r	f	r	r	r	r	s
Cassidulina delicata	f	r	r	r				
Indeterminate Nodosarids	f	c	c	c	c	f	c	r
Cibicides subhaidingeri	r	r	r		r			
Fissurina spp.	r	f	f	f	f	f	r	s
Sphaeroidina bulloides	r	c	c	a	c	c	a	s
Eponides lornensis	r	r						
Indeterminate agglutinate debris	r	f	r	f	r	f	r	
Gaudryina spp.	r	r	r	f	s	r	r	s
Anomalina aff. inversa	r	f	f	f	f	r	r	s
Pullenia bulloides	r	r	f	f	r	r	f	
Vagocibicides maoria	r		s	s	s			
Glandulina spp.	r	r	r	r	r	r	s	s
Haplophragmoides spp. (smooth)	r	r	s	s		s		
Cyclammina spp.	r	f	f	r		s		
Uvigerina miozea	r		s					
Bathysiphon spp. (smooth)	r	r	s	f	s		s	
Indeterminate Miliolids	r	r	r	r	s	r		s
Cibicides pseudoconvexus	r			s		s	s	
Cerobertina bartrumi	r	r	r	r	r	r		
Triloculina spp.	r	r	f	f	s	s	r	
Bulimina costata	r					r	r	
Gyroidinoides subzealandica	s	r	r	r	r	f	f	r
Lagena spp.	s	r	r	f	r	r	f	
Angulogenerina costornata	s							
Pseudonodosaria laevigata	s	s	s	s		r	r	
Vaginulina elegans	s	r	r			s		
Haeuslerrella decepta	s	r	s	r	s	s		
Pyrulina fusiformis	s	r	s					
Ammobaculites clifdenensis	s			s				
Lingulina semilineata	s							
Triloculina brochita	s	s						
Amphicoryna scalaris	s	s		s		s		
Cibicidoides mexicanus	s	s						
Cassidulina laevigata	s							
Pullenia quinqueloba	s	s	r	r	s	s	r	
Cyclammina cancellata		f	f	f	s			
Arenodosaria antipoda		r	r	r				
Anomalina nonionoides		r	s		r			
Anomalina/Anomalinoides spp.		r	f	f	f	f	c	r
Guttalina problema		r	s	r	r	r	s	s
Pyrgo spp.		r	r	s				
Quinqueloculina spp.		r	r	r	r	r	s	s
Ammodiscus spp.		r	s	s				
Anomalina macraglabra		r	f	r	f		r	
Dentalina spp.		r	r	r	r	r	r	
Brizalina/Bolivina spp.		r	r	r	r	r	r	s
Bathysiphon spp. (fi)		s	s					
Lenticulina peregrina		s						

s = single, r = rare, f = frequent, c = common, a = abundant, fi = fine grained agglutinated.

Appendix No. 2 : Micropalaeontological distribution chart, Thylacine-1. Page 2 of 3.

TAXA / DEPTH (m)	780 - 790 DC	850 - 860 DC	890 - 900 DC	940 - 960 DC	1000 - 1010 DC	1050 - 1060 DC	1100 - 1110 DC	1140 - 1150 DC
Marginulinopsis hydropica		s		r	s			
Mississippina concentrica		s	r		s	s		
Notorotalia dorreeni		s	r	r	s	s		
Planulina costata		s	r	r			s	
Pleurostomella spp.		s						
Siphonina australis		s	r	r	f	f	r	s
Textularia pseudomiozea		s						
Discorotalia tenuissima		s						
Quadrimorphina laevigata		s		s				
Heronallenia lingulata		s			s			
Globocassidulina oblonga		s	r	r	r	f	a	r
Indeterminate Buliminids			r	f	f	r	f	s
Astrononion spp.			r	f	f	f	f	r
Cibicides mundulus			r				r	
Alabamina tenuimarginata			r	r				
Francesina advena			r	r	r	s		s
Gaudryina midwayensis			r			r		
Discopulvinulina scoposs			s	r				
Epistominella cassidulinoides			s	r	f	r	r	s
Pyrgo sarsi			s					
Quinqueloculina spp. (large size, finely striate)			s					
Ehrenbergina pacifica			s					
Cibicides cygnorum			s	r	r		s	s
Siphouvigerina canariensis			s	r		s		
Textularia spp.			s	r	s			
Bulimina aff. striata				r	s		r	
Cribrostomoides bradyi				s				
Trifarina bradyi				r	f	f	f	s
Stilostomella spp.				r	s		s	
Pyrgo murrhina				s				
Vaginulina spp.				s				
Guttulina spp.						r	s	
Textularia semicarinata						r		
Cibicides semiperforatus							r	
Haplophragmoides spp. (fi)							s	
Planulina aff. wuellerstorfi							s	
PLANKTONIC FORAMINIFERA								
Globigerina spp.	c	a	a	a	a	a	a	c
Globigerina bulloides	f	c	c	a	c	a	a	c
Globorotalia nana	f	f	r	c	a	c	a	f
Globorotalia bella	r	r	r	r	r	r	f	s
Globigerina brazieri	r	c	f	r	s	s	r	
Globigerina woodi connecta		s	f	r	r	f	f	r
Globoqudrina dehiscens s.s.	r							
Globorotalia mayeri	r		s		s			s
Catapsydrax unicavus	r							
Globigerina euapertura	r	f	c	a	c	a	a	f
Globorotalia obesa	r	f	f	c	c	f	r	
Globigerina woodi woodi	s	r	r	r	s	s	r	s
Globorotalia opima group		f	f	c	c	f	c	r
Globoqudrina dehiscens s.l.		r	r	r	s	s	s	s
Globorotalia semivera		r	s	r	r	f	f	s
Globigerina ciperoensis		r	r	c	r	f	f	

s = single, r = rare, f = frequent, c = common, a = abundant, fi = fine grained agglutinated.

Appendix No. 2 : Micropalaeontological distribution chart, Thylacine-1. Page 3 of 3.

TAXA / DEPTH (m)	780 - 790 DC	850 - 860 DC	890 - 900 DC	940 - 960 DC	1000 - 1010 DC	1050 - 1060 DC	1100 - 1110 DC	1140 - 1150 DC
Catapsydrax dissimilis		s		r	s		r	
Cassigerinella chipolensis		s	r	s				
Globigerina sellii			s	r		s		s
Globorotaloides testarugosa				r	r	s		
CALCAREOUS NANNOPLANKTON								
Coccolithus pelagicus	f	f	f	f	f	f	f	f
Sphenolithus moriformis	a	a	a	a	a	a	c	f
Cyclicargolithus abisectus	f	f	f	c	f	c	f	f
Cyclicargolithus floridanus	a	a	a	a	a	a	a	c
Calcidiscus praemacintyrei	s							
Braarudosphaera bigelowii	c	c		c	f	f	f	r
Micrantholithus fornicatus	r	f	f	r	r		r	
Discoaster deflandre	f	r	f	r	r	f	s	
Coronocyclus nitescens	s	r		s			s	
Coccolithus miopelagicus	r	f	r	r	r	r		
Helicosphaera euphratis	r	r	f	r	r		r	
Reticulofenestra haqii	r							
Pontosphaera multipora	s	s	r	r	r			s
Helicosphaera spp.	s			s	s			
Micrantholithus spp.	s		s	s	s		s	
Dictyococcites bisectus		c	c	c	f	c	c	
Zygrhablithus bijugatus		f	c	c	f	r	f	f
Helicosphaera aff. compacta		s		s	s			
Micrantholithus attenuatus		r					s	
Helicosphaera perch-nielseniae		r						
Pontosphaera spp.		r	r		r			s
Pontosphaera plana		s		s		s		
Reticulofenestra sp. 1			r				s	
Helicosphaera recta					r	s		
Sphenolithus ciperoensis					s			
Rhabdosphaera spp.					s			
Chiasmolithus altus						r	r	
Triquetrorhabdulus carinatus						s		
Reticulofenestra lockeri							r	
Reticulofenestra sp. 2							r	
Helicosphaera compacta							s	
OTHER SKELETAL MATERIAL								
Bryozoan fragments	a	f	r	r	r			r
Echinoid debris	c	f	f	f	f	r	r	
Ostracods	f	r	r	f	r	f	f	
Gastropod debris		s	s	s		s		

s = single, r = rare, f = frequent, c = common, a = abundant, fi = fine grained agglutinated.

MICROPALAEONTOLOGICAL ANALYSIS

THYLACINE-1 (2165 – 2200.3 mKB)

PERMIT T-30-P, OTWAY BASIN

FOR

WOODSIDE ENERGY LTD

J.P. REXILIUS

JULY, 2001

ISC BIOSTRAT

73 RULE STREET
NORTH FREMANTLE
WESTERN AUSTRALIA
PHONE 08-94308460 FAX 08-94308465

C O N T E N T S

I. SUMMARY

Thylacine-1 was drilled in offshore petroleum permit T-30-P, Otway Basin. A total of 15 core samples were screened for their foraminiferal content. Only 3 samples yielded foraminifera and these were examined in detail for palaeoenvironment determination. A summary of the foraminiferal breakdown and environment subdivision is given below:-

Benthonic Foraminiferal Subdivision

Depth Range (m)	Zone	Age
2165.00 – 2166.50	not studied	
2169.00	indeterminate	indeterminate
2175.00 – 2188.75	not studied	
2190.00 – 2191.91	indeterminate	indeterminate
2194.40 – 2200.29	not studied	

Planktonic Foraminiferal Subdivision

Depth Range (m)	Zone	Age
2165.00 – 2166.50	not studied	
2169.00	indeterminate	indeterminate
2175.00 – 2188.75	not studied	
2190.00 – 2191.91	indeterminate	indeterminate
2194.40 – 2200.29	not studied	

Environment Subdivision

Depth Range (m)	Environment
2165.00 – 2166.50	not studied
2169.00	undifferentiated marine
2175.00 – 2188.75	not studied
2190.00	undifferentiated marine
2191.91	estuarine / undifferentiated marine
2194.40 – 2200.29	not studied

II. INTRODUCTION

A total of 15 core samples were screened for their foraminiferal content. Only 3 samples yielded foraminifera and these were examined in detail for palaeoenvironment determination.

Fossil assemblages identified in the well section are shown in Appendix No. 2. A summary of results for each sample is shown in Appendix No. 1.

III. BIOSTRATIGRAPHIC ANALYSIS

A. Benthonic Foraminiferal Subdivision

2165.00m-2166.50m : Not studied

2169.00m : Indeterminate

The sample lacks age-diagnostic benthonic foraminiferal taxa.

2175.00m-2188.75m : Not studied

2190.00m-2191.91m : Indeterminate

The core sample at 2190.00m is barren of benthonic foraminiferal taxa. The core sample at 2191.91m lacks age-diagnostic benthonic foraminiferal taxa.

2194.40m-2200.29m : Not studied

B. Planktonic Foraminiferal Subdivision

2165.00m-2166.50m : Not studied

2169.00m : Indeterminate

The sample is barren of planktonic foraminiferal taxa.

2175.00m-2188.75m : Not studied

2190.00m-2191.91m : Indeterminate

The core sample at 2190.00m contains a specimen of *Hedbergella* spp. which ranges from Maastrichtian to Barremian. The core sample at 2191.91m is barren of planktonic foraminifera.

2194.40m-2200.29m : Not studied

IV. ENVIRONMENT OF DEPOSITION

2165.00m-2166.50m : Not studied

2169.00m : Undifferentiated marine

The core sample comprises claystone with minor sandstone and very rare grains of fine grained glauconite in the sandstone facies. The very impoverished benthonic foraminiferal fauna includes smooth *Haplophragmoides* spp. (single) and smooth indeterminate agglutinates (single). A definitive environment interpretion is not possible. The occurrence of glauconite suggests deposition in a marine setting.

2175.00m-2188.75m : Not studied

2190.00m : Undifferentiated marine

The core sample consists of claystone with very minor sandstone. The sample lacks benthonic foraminiferal taxa but does contain a specimen of the planktonic foraminiferal taxon *Hedbergella* spp. A definitive environment interpretion is not possible. The occurrence of *Hedbergella* spp. suggests deposition in a marine setting.

2191.91m : Estuarine/undifferentiated marine

The slightly silty claystone core sample contains a very impoverished benthonic foraminiferal fauna which includes smooth ? *Haplophragmoides* spp. (single) and smooth indeterminate agglutinates (single). The agglutinated benthonic foraminiferal fauna is interpreted to have been deposited in an estuarine to undifferentiated marine setting. No glauconite was recorded in the sample.

2194.40m-2200.29m : Not studied

Appendix No. 1 : Summary of micropalaeontological sample analysis, Thylacine-1.

JULY, 2001.

DEPTH (m)	SAMPLE TYPE	* LITHOLOGY	FORAM YIELD	FORAM PRESERV.	FORAM DIVERSITY	ENVIRONMENT	COMMENTS
2165	CORE	argillaceous siltstone / fine grained sandstone.	barren [screening]	no data	no data	not studied	
2166.5	CORE	claystone	barren [screening]	no data	no data	not studied	
2169	CORE	claystone, minor sandstone, very rare fine grained glauconite in sandstone facies..	very low	poor	very low	undiff. marine	*Haplophragmoides* spp. (single), indeterminate agglutinates spp. (smooth), Very rare glauconite in sandstone facies.
2175	CORE	dominantly claystone	barren [screening]	no data	no data	not studied	
2177.37	CORE	claystone	barren [screening]	no data	no data	not studied	
2180.67	CORE	sandstone & claystone	barren [screening]	no data	no data	not studied	
2186.45	CORE	slightly silty claystone	barren [screening]	no data	no data	not studied	
2188.75	CORE	claystone / argillaceous sandstone	barren [screening]	no data	no data	not studied	
2190	CORE	claystone, very minor sandstone.	very low	poor	very low	undiff. marine	*Hedbergella* spp. (single - planktonic).
2191.91	CORE	slightly silty claystone	very low	poor	very low	estuarine / undiff. marine	? *Haplophragmoides* spp. (single), indeterminate agglutinates spp. (smooth).
2194.4	CORE	claystone / sandstone	barren [screening]	no data	no data	not studied	
2195.23	CORE	claystone / siltstone	barren [screening]	no data	no data	not studied	
2197	CORE	claystone / siltstone	barren [screening]	no data	no data	not studied	
2199.55	CORE	claystone / siltstone	barren [screening]	no data	no data	not studied	
2200.29	CORE	claystone / siltstone / fine grained sandstone.	barren [screening]	no data	no data	not studied	

* lithology based on processed foram residue.

ISC BIOSTRAT

Appendix No. 2 : Micropalaeontological distribution chart, Thylacine-1.

TAXA / DEPTH (m)	2165.00 CORE	2166.50 CORE	2169.00 CORE	2175.00 CORE	2177.37 CORE	2180.67 CORE	2186.45 CORE	2188.75 CORE	2190.00 CORE	2191.91 CORE	2194.40 CORE	2195.23 CORE	2197.00 CORE	2199.55 CORE	2200.29 CORE
BENTHONIC FORAMINIFERA	B	B		B	B	B	B	B			B	B	B	B	B
AGGLUTINATES															
Haplophragmoides spp. (smooth)			s												
Indeterminate agglutinates (smooth)			s							s					
? Haplophragmoides spp. (smooth)										s					
PLANKTONIC FORAMINIFERA															
Hedbergella spp.									s						
OTHER SKELETAL MATERIAL	B	B	B	B	B	B	B	B	B	B	B	B	B	B	B
OTHER DATA															
Glauconite			r					r							

s = single, r = rare, B= barren.

APPENDIX 6
PETROLOGY REPORT

RESERVOIR SOLUTIONS PTY LTD
LEVEL 2, 2 PARK RD, MILTON, 4064, QLD
PO BOX 2089, MILTON, 4064, QLD
ABN 27 088 995 073

PETROLOGY, DIAGENESIS AND RESERVOIR QUALITY OF SAMPLES FROM THYLACINE-1, T/30P

Julian C. Baker PhD

A report to:

Woodside Energy Ltd.
1 Adelaide Terrace
Perth WA 6000

12 December, 2001

C O N T E N T S

C O N T E N T S cont.

Page

FIGURES

TABLES

APPENDICES

EXECUTIVE SUMMARY

A petrological study was carried out on thirty-two core, msct and swc samples from 2050.0 - 2575.0m in Thylacine-1. Analytical techniques used were thin-section analysis, quantitative bulk rock/clay fraction X-ray diffraction analysis and scanning electron microscopy.

Sandstones are litharenites, sublitharenites and quartzarenites in which framework grains are mainly quartz and also include K-feldspar, metamorphic rock fragments, mica, organics and accessory heavy minerals. Compositional maturity generally increases with depth, with quartz increasing downward below 2143.6m at the expense of clay, rock fragments, feldspar and siderite. Two samples (M5, SWC #25) are mudrocks, one of which (M5) is extensively replaced by siderite.

Between 2050.0m and 2173.40m, sandstones are fine to medium grained and moderately-well to well sorted. Below this interval, sorting and grain size fluctuate widely. Sorting generally decreases with increasing grain size, although there is wide scatter in the grain size data for upper medium and coarse grained sandstones.

Sandstones are derived from a continental provenance dominated by low grade metasedimentary and granitic rocks and which also included siliciclastics and volcanics.

Minor detrital clay is concentrated along thin laminae and forms patchy matrix. Most sandstones lack detrital clay. Authigenic clay ranges up to 25.9% and is mainly kaolinite that occurs where micaceous/argillaceous grains have completely altered. Authigenic illite is associated with altered and compactionally deformed micaceous/argillaceous rock fragments. Expandable clay minerals are absent.

The main diagenetic effects besides authigenic clay formation are grain contact dissolution/microstylolitisation, labile grain (mainly K-feldspar) dissolution, ductile grain/authigenic clay compaction, cementation by quartz overgrowths, and cementation/replacement by ferroan carbonate and rare calcite.

Porosity reduction is mainly the result of authigenic clay formation, ductile grain/clay compaction, grain contact dissolution/microstylolitisation and quartz overgrowth cementation.

Visible porosity ranges up to 18.6% and generally decreases with increasing clay + metamorphic rock fragment content. Visible porosity could not be accurately measured for some of the sidewall core samples due to the effects of severe impact damage. Visible porosity is accounted for by variable proportions of primary intergranular pores and secondary intergranular, intragranular and mouldic labile grain dissolution pores.

Reservoir quality is mainly controlled by the content of clay (mostly authigenic kaolinite) and, of less importance, metamorphic rock fragments. Clay + metamorphic rock fragment content is only moderately correlated with grain size, and there is wide variation in sorting. Consequently, grain size and permeability are only moderately correlated. Carbonate has little influence on permeability.

1. INTRODUCTION

A petrological study was carried out on thirteen core samples, twelve msct samples and seven swc samples from between 2050.0m and 2575.0m in Thylacine-1, T/30P in order to provide information on texture, mineralogy, diagenesis and controls on reservoir quality. The study was carried out following a reconnaissance SEM study of six core samples from the same interval, which was done to provide preliminary information on clay mineralogy, distribution and habit. SEM images acquired during this reconnaissance study are included in this report. A list of sample depths, analyses performed and routine core analyses carried out by Core Laboratories Australia Pty Ltd is given in Table 1.

2. ANALYTICAL PROGRAM

2.1 THIN-SECTION ANALYSIS

Thin-sections were cut in kerosene and impregnated with blue dyed epoxy resin to assist in porosity recognition. Carbonate-bearing thin-sections were stained with Alizarin red-S and potassium ferricyanide to aid carbonate identification. Mineral composition and visible porosity were determined by a count of 400 points in all thin-sections, and grain size and sorting of all thin-sections were determined by measuring the long dimension of 100 point-counted quartz grains. From the grain size measurements, mean grain size and sorting (ϕ standard deviation, Trask) were calculated. Photomicrographs were taken of each thin-section to illustrate texture, composition, clay distribution, diagenetic effects and porosity.

2.2 X-RAY DIFFRACTION ANALYSIS

Bulk-rock X-ray diffraction (XRD) analysis was carried out on all thirteen core samples in order to quantify mineral abundance. The XRD analysis used a finely ground whole rock powder sample and the SIROQUANT processing technique was used to calculate mineral abundance.

Qualitative fine-fraction XRD analysis was carried out on three core samples (#5, #62, #83) in order to precisely identify clay mineralogy. The fine fraction was separated from each sample by disaggregation and settling in distilled water and was air dried on glass discs to produce oriented specimens for XRD analysis. Samples were analysed in air dried condition and also following treatment with ethylene glycol.

2.3 SCANNING ELECTRON MICROSCOPY

Scanning electron microscopy (SEM) was carried out on freshly broken surfaces of all core samples to provide information on clay distribution and porosity characteristics. An energy dispersive spectrometer (EDS) attached to the SEM provided qualitative elemental data on clays and carbonate cements.

TABLE 1. ANALYSES PERFORMED

Sample #	Depth (m)	Sample type	PETROLOGICAL ANALYSES						CORE ANALYSES		
			MA	GSA	XRDb	XRDf	SEM	PM	Por (%)*	Perm (md)* †	GD (g/cc)
M1	2050.0	msct	X	X	-	-	-	X	16.9	1.72	2.72
M2	2053.0	msct	X	X	-	-	-	X	19.7	17.5	2.67
M3	2055.0	msct	X	X	-	-	-	X	19.6	13.7	2.68
M4	2066.3	msct	X	X	-	-	-	X	21.3	46.3	2.65
M5	2076.5	msct	X	X	-	-	-	X	10.7	0.030	3.06
M6	2092.2	msct	X	X	-	-	-	X	23.0	45.2	2.67
M7	2094.0	msct	X	X	-	-	-	X	20.8	13.9	2.76
M8	2133.0	msct	X	X	-	-	-	X	19.7	3.77	2.68
M9	2139.1	msct	X	X	-	-	-	X	16.1	0.814	2.68
M10	2143.6	msct	X	X	-	-	-	X	20.8	24.7	2.65
M12	2165.9	msct	X	X	-	-	-	X	23.0	1590	2.65
5	2166.81	core	X	X	X	X	X	X	17.8	6.66	2.64
-	2170.40	core	-	-	-	-	X	-	-	-	-
14	2171.19	core	X	X	X	-	X	X	21.8	99.5	2.66
22	2173.40	core	X	X	X	-	X	X	11.7	0.483	2.69
24	2173.83	core	X	X	X	-	X	X	18.5	1240	2.66
25	2174.10	core	X	X	X	-	X	X	13.2	3.27	2.68
28	2174.80	core	X	X	X	-	X	X	20.9	3430	2.65
-	2180.06	core	-	-	-	-	X	-	-	-	-
46	2180.10	core	X	X	X	-	X	X	23.2	4710	2.65
55	2182.92	core	X	X	X	-	X	X	17.7	109	2.66
-	2184.76	core	-	-	-	-	X	-	-	-	-
62	2184.89	core	X	X	X	X	X	X	15.2	127	2.65
67	2186.60	core	X	X	X	-	X	X	17.0	1.93	2.75
69	2187.10	core	X	X	X	-	X	X	20.1	22.1	2.68
-	2187.22	core	-	-	-	-	X	-	-	-	-
-	2188.61	core	-	-	-	-	X	-	-	-	-
80	2192.71	core	X	X	X	-	X	X	21.1	524	2.66
-	2192.93	core	-	-	-	-	X	-	-	-	-
83	2193.59	core	X	X	X	X	X	X	18.4	251	2.66
M13	2230.0	msct	X	X	-	-	-	X	19.5	40.1	2.65
SWC 37	2255.5	swc	X	X	-	-	-	X	-	-	-
SWC 34	2277.0	swc	X	X	-	-	-	X	-	-	-
SWC 31	2306.0	swc	X	X	-	-	-	X	-	-	-
SWC 25	2397.7	swc	X	X	-	-	-	X	-	-	-
SWC 23	2417.0	swc	X	X	-	-	-	X	-	-	-
SWC 20	2437.5	swc	X	X	-	-	-	X	-	-	-
SWC 12	2575.0	swc	X	X	-	-	-	X	-	-	-

MA = modal analysis GSA = grain size analysis XRDb = bulk-rock X-ray diffraction analysis XRDf = fine-fraction X-ray diffraction analysis SEM = scanning electron microscopy PM = photomicroscopy

* ambient † air

3. TEXTURE

Lithology and texture are given in Table 2, a grain size comparison table is included in Appendix 1, and grain size frequency curves are given in Appendix 2.

Excluding M5 and SWC #25, samples are grain supported sandstones with a wide sorting and grain size range. M5 is a sideritised, arenaceous mudrock, and SWC #25 is a well compacted mudrock with very thin, silty/sandy laminae. M5 and SWC #25 are not considered further in this section.

Between 2050.0m and 2173.40m, sandstones are fine to medium grained and moderately-well to well sorted. Below this interval, sorting and grain size fluctuate widely, with sandstones between 2173.83m and 2575.0m being poorly to well sorted and fine to coarse grained (Fig. 1).

Sorting generally decreases with increasing grain size (R^2 = -0.611), with nearly all sandstones with a grain size less than 0.35mm (>1.5ϕ) being well sorted and all sandstones with a grain size greater than 0.35mm (<1.5ϕ) being poorly to moderately-well sorted (Fig. 2). The negative correlation between grain size and sorting is weakened by wide scatter in the data for sandstones with a grain size greater than 0.35mm.

Fine argillaceous/micaceous/carbonaceous laminae, some of which are replaced by siderite and ankerite, and patchy detrital clay matrix are included in a few samples (M1, M4, M6, M7, M13, #5, SWCs #12 & #37). Localised argillaceous patches and wispy laminae in #69 appear to be compacted argillaceous intraclasts. Fine microstylolitic seams and microstylolitic grain contacts are common in #22 and #25. The two poorly sorted sandstones (#25, #62) include scattered granules and pebbles up to 14mm long. Sample #28 is a clean, thickly laminated, coarse grained sandstone in which laminae are defined by grain size variations. Sample #55 includes sporadic, poorly defined, thin, fine grained laminae. The majority of sandstones are massive and contain little or no detrital clay.

SWCs #20, #23, #31 and #34, which are clean, medium to coarse grained quartzose sandstones, have undergone almost complete textural reorganisation due to sidewall coring impact.

Ignoring quartz overgrowths and the effects of grain contact dissolution, most quartz grains are subangular to subrounded.

TABLE 2. LITHOLOGY AND TEXTURE

Sample #	Depth (m)	Lithology	GRAIN SIZE			SORTING		
			ϕ	mm	Class	Trask	ϕSD	Class
M1	2050.0	Sandstone	2.02	0.25	medium	1.20	0.39	well
M2	2053.0	Sandstone	1.81	0.28	medium	1.21	0.44	well
M3	2055.0	Sandstone	1.85	0.28	medium	1.22	0.43	well
M4	2066.3	Sandstone	1.91	0.27	medium	1.21	0.41	well
M5	2076.5	Sid mrk	2.67	0.16	fine	1.39	0.74	moderate
M6	2092.2	Sandstone	1.71	0.31	medium	1.20	0.37	well
M7	2094.0	Sandstone	2.25	0.21	fine	1.13	0.35	well
M8	2133.0	Sandstone	2.14	0.23	fine	1.18	0.38	well
M9	2139.1	Sandstone	2.31	0.20	fine	1.22	0.40	well
M10	2143.6	Sandstone	1.77	0.29	medium	1.28	0.56	mod-well
M12	2165.9	Sandstone	1.07	0.48	medium	1.32	0.66	mod-well
5	2166.81	Sandstone	2.01	0.25	medium	1.18	0.36	well
14	2171.19	Sandstone	2.29	0.20	fine	1.20	0.46	well
22	2173.40	Sandstone	1.97	0.25	medium	1.22	0.42	well
24	2173.83	Sandstone	0.90	0.54	coarse	1.24	0.62	mod-well
25	2174.10	Sandstone	1.41	0.38	medium	1.67	1.02	poor
28	2174.80	Sandstone	0.33	0.79	coarse	1.40	0.67	mod-well
46	2180.10	Sandstone	0.89	0.54	coarse	1.24	0.55	mod-well
55	2182.92	Sandstone	0.92	0.53	coarse	1.50	0.85	moderate
62	2184.89	Peb sst	0.09	0.94	coarse	1.92	1.09	poor
67	2186.60	Sandstone	2.15	0.23	fine	1.20	0.40	well
69	2187.10	Sandstone	1.60	0.33	medium	1.28	0.48	well
80	2192.71	Sandstone	1.66	0.32	medium	1.17	0.44	well
83	2193.59	Sandstone	1.38	0.38	medium	1.43	0.82	moderate
M13	2230.0	Lam sst	2.15	0.23	fine	1.15	0.38	well
SWC 37	2255.5	Lam sst	2.47	0.18	fine	1.19	0.39	well
SWC 34	2277.0	Sandstone	1.59	0.33	medium	1.22	0.41	well
SWC 31	2306.0	Sandstone	0.87	0.55	coarse	1.30	0.78	moderate
SWC 25	2397.7	Lam mrk	4.24	0.05	coarse silt	1.18	0.43	well
SWC 23	2417.0	Sandstone	0.03	0.98	coarse	1.55	0.82	moderate
SWC 20	2437.5	Sandstone	0.77	0.59	coarse	1.29	0.61	mod-well
SWC 12	2575.0	Sandstone	2.63	0.16	fine	1.21	0.37	well

Sid mrk = sideritised arenaceous mudrock Peb sst = pebbly sandstone Lam sst = sandstone with argillaceous laminae
Lam mrk = mudrock with silty/sandy laminae

SORTING (ϕSD)

Class	*ϕ Standard Deviation*
very well sorted	<0.35
well sorted	0.35-<0.50
moderately well sorted	0.50-<0.71
moderately sorted	0.71-1.00
poorly sorted	>1.00

FIGURE 1. GRAIN SIZE/DEPTH CROSS-PLOT

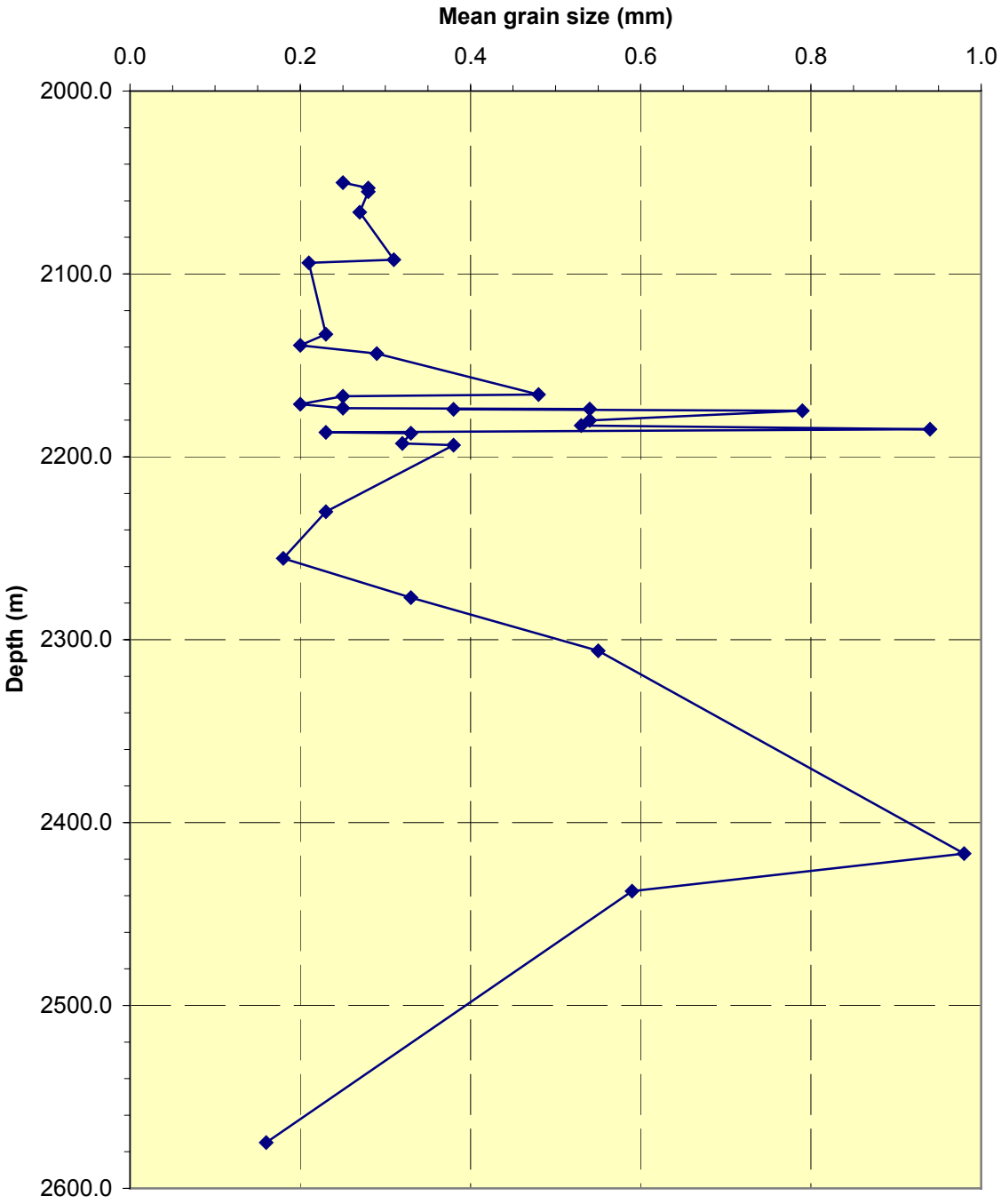

FIGURE 2. GRAIN SIZE/SORTING CROSS-PLOT

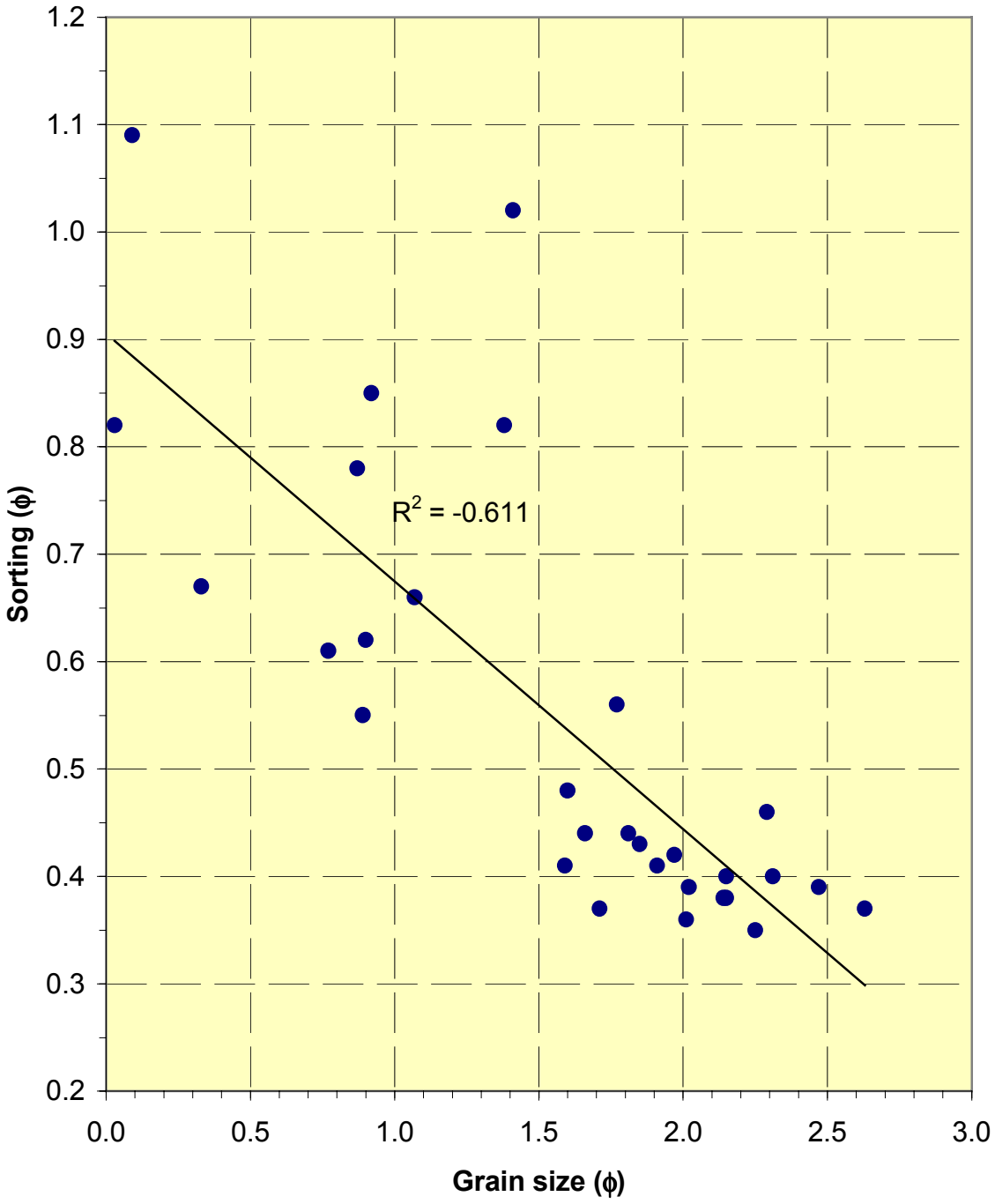

4. THIN-SECTION COMPOSITION

Thin-section composition and QFR ratios are shown in Table 3, and QFR ratios are plotted in Figure 3. Data summary sheets, brief thin-section descriptions and annotated photomicrographs for each sample are presented in Appendix 4. A key to plates in Appendix 4 is given on p. 33.

M5 is a sideritic mudrock in which scattered silt- and sand-sized siliciclastic grains (quartz, K-feldspar, quartzose/micaceous rock fragments, mica, heavy minerals), terrestrial organic fragments and rare glauconite grains are supported by detrital clay matrix that has been extensively replaced by microcrystalline siderite. SWC #25 is a well compacted, thinly laminated mudrock composed mainly of detrital clay and fine, locally pyritic, organic fragments and in which laminae are defined by concentrations of silt- and sand-sized siliciclastic grains. These two samples are not considered further in this section.

Sandstones from 2050.0 - 2143.6m are lithic-rich sublitharenites and litharenites, sandstones from 2165.9 - 2187.10m are quartz/lithic-rich sublitharenites, litharenites and quartzarenites, and sandstones from 2192.71 - 2575.0m are quartz-rich sublitharenites and quartzarenites (Fig. 3). Accordingly, compositional maturity generally increases with depth, but fluctuates between 2165.9m and 2187.10m. Framework grains are mainly quartz and also include K-feldspar, metamorphic rock fragments, mica, organics and accessory heavy minerals.

Between 2050.0m and 2143.6m, detrital quartz content ranges from 38.2% to 49.3% (mean = 44.6%), whereas between 2165.9m and 2187.10m, detrital quartz content varies from 43.3% to 69.5%. Between 2192.71m and 2575.0m, detrital quartz content is consistently high (61.5-80.5%), except where the sandstones are fine grained and include argillaceous/sideritic laminae (M13, SWCs #12 & #37). Figure 4 shows the general trend of increasing detrital quartz at the expense of clay, rock fragments, feldspar and siderite with increasing depth below 2143.6m.

Figure 5 shows that there is a moderate (R^2 = 0.474) positive correlation between quartz content and grain size for the sandstone msct and core samples. The sidewall core samples are not grouped with the msct and core samples in Figure 5 because they have anomalously high quartz contents for their grain size due to the effects of impact damage and, in the case of SWC #37, an anomalously low quartz content due to the presence of abundant siderite.

Most quartz is monocrystalline, even in the coarser sandstones. Quartz types include recrystallised metamorphic quartz, metaquartzite and plutonic quartz. Metamorphic quartz locally includes oriented phyllosilicates, and granitic quartz rarely contains K-feldspar intergrowths. Quartz grains are commonly enveloped by thin syntaxial quartz overgrowths and have welded (including microstylolitic) grain contacts that are the result of grain contact dissolution. Quartz overgrowth content ranges up to 7.6% and is mainly less than 5%.

Feldspar content ranges from 0% to 5.1% and decreases below 2187.10m, where it does not exceed 2.5% (Fig. 4). Feldspar is fresh to slightly altered granitic K-feldspar (orthoclase, microcline, microperthite) that is commonly etched or partly dissolved.

Rock fragment content ranges from 0% to 23.6% and, like feldspar content, decreases below 2187.10m, where it does not exceed 4.3% (Fig. 4). Most lithic grains are low grade metasedimentary rock fragments that include quartz/mica schist, illitic meta-argillite, phyllite, and mica/illite-bearing quartzite. Mica/illite-rich metamorphic rock fragments, which dominate over mica/illite-poor metamorphic rock fragments, are commonly compactionally

TABLE 3. THIN-SECTION COMPOSITION AND QFR RATIOS

Sample #	M1	M2	M3	M4	M5	M6	M7	M8	M9	M10	M12
Depth (m)	2050.0	2053.0	2055.0	2066.3	2076.5	2092.2	2094.0	2133.0	2139.1	2143.6	2165.9
Qtz (mono)	35.4	43.6	40.6	41.9	16.0	40.3	41.6	39.9	34.0	44.4	65.5
Qtz (poly)	4.3	3.3	4.8	4.3	3.0	5.8	3.5	4.5	4.2	4.9	4.0
Qtz og	0.3	3.8	2.7	2.9	-	3.1	4.3	2.3	2.5	4.8	4.3
Chert	1.0	1.3	1.9	1.1	0.3	3.4	1.0	1.5	2.2	1.3	-
K-feldspar	5.0	3.0	4.4	3.5	1.0	3.0	3.5	3.5	4.6	1.3	-
Plagioclase	-	-	-	-	-	-	-	-	-	-	-
VRF	0.7	1.1	1.0	1.5	-	0.8	1.0	1.4	2.2	1.2	0.3
GRF	0.3	-	-	-	-	-	-	-	-	-	-
MRF	8.3	6.9	8.3	8.8	2.5	8.5	7.8	9.2	14.1	11.5	1.8
SRF	2.0	2.3	1.6	2.0	0.8	1.5	1.3	2.7	3.1	1.0	0.3
Mica	0.8	0.3	0.3	0.5	-	-	0.3	-	0.3	-	-
Heavy min	-	-	-	0.3	-	-	0.3	0.3	-	0.3	-
Organics	1.6	0.7	0.4	0.3	3.5	0.3	0.7	0.3	1.8	0.3	-
Pyrite	-	-	-	-	-	0.3	-	0.3	1.4	-	0.5
Leucoxene	-	0.3	0.3	-	-	-	0.3	-	0.7	-	-
Sid (pf)	-	-	-	-	1.1	1.2	4.0	3.8	0.7	-	-
Sid (rpl)	8.0	4.0	6.7	0.8	56.6	0.3	5.8	5.6	6.1	-	-
Ank (pf)	0.7	-	-	-	-	4.8	-	-	-	-	-
Ank (rpl)	3.6	1.3	2.6	-	0.3	3.7	0.3	0.3	-	-	-
Cal (pf)	-	-	-	5.2	-	-	-	-	-	-	-
Cal (rpl)	-	-	-	1.1	-	-	-	-	-	-	-
Glauconite	-	-	-	-	-	-	-	-	-	-	-
AKa (pf)	9.2	4.2	5.0	-	-	3.3	7.1	6.4	2.1	6.8	1.1
AKa (rpl)	14.7	10.6	11.5	11.5	1.8	5.7	8.4	10.7	15.8	9.0	4.9
AIllite (pf)	0.3	0.4	0.4	-	-	-	-	-	-	-	-
AIllite (rpl)	1.7	2.4	1.5	0.7	-	0.8	1.0	1.3	1.6	0.7	-
Detrital clay	0.3	-	-	2.8	9.0	0.3	-	-	-	-	-
PP (inter)	0.3	3.0	1.6	3.7	-	5.1	2.4	1.2	0.3	4.7	9.3
SP (inter)	-	5.0	1.8	4.0	-	5.3	3.3	1.5	-	6.6	8.0
SP (mouldic)	1.5	1.8	1.9	1.8	3.8	1.8	1.0	2.3	2.0	0.5	-
SP (intra)	-	0.7	0.7	1.3	0.3	0.7	1.1	1.0	0.3	0.7	-
Q	75.5	79.9	76.6	76.1	81.8	79.2	78.7	74.1	63.9	78.9	96.9
F	9.2	4.6	6.7	5.3	4.2	4.5	5.5	5.4	6.8	1.9	0.0
R	15.3	15.5	16.7	18.6	14.0	16.3	15.8	20.5	29.3	19.2	3.1

Qtz (mono) = monocrystalline quartz Qtz (poly) = polycrystalline quartz Qtz og = quartz overgrowths VRF = volcanic rock fragments GRF = granitic rock fragments MRF = metamorphic rock fragments SRF = sedimentary rock fragments Heavy min = heavy minerals Sid (pf) = pore-filling siderite Sid (rpl) = replacement siderite Ank (pf) = pore-filling ankerite Ank (rpl) = replacement ankerite Cal (pf) = pore-filling calcite Cal (rpl) = replacement calcite AKa (pf) = pore-filling authigenic kaolinite AKa (rpl) = replacement authigenic kaolinite AIllite (pf) = pore-filling authigenic illitic clay AIllite (rpl) = replacement authigenic illitic clay PP (inter) = visible primary intergranular porosity SP (inter) = visible secondary intergranular porosity SP (mouldic) = visible secondary mouldic porosity SP (intra) = visible secondary intragranular porosity

Q = quartz + chert F = feldspar R = rock fragments

TABLE 3. THIN-SECTION COMPOSITION AND QFR RATIOS cont.

Sample #	5	14	22	24	25	28	46	55	62	67	69
Depth (m)	2166.81	2171.19	2173.40	2173.83	2174.10	2174.80	2180.10	2182.92	2184.89	2186.60	2187.10
Qtz (mono)	42.9	58.8	50.1	62.8	55.2	63.3	59.6	55.1	53.7	39.4	40.9
Qtz (poly)	5.6	2.8	4.4	3.6	5.4	3.9	3.4	4.3	10.0	3.9	4.0
Qtz og	2.9	5.3	1.8	7.6	0.7	7.3	5.8	2.3	3.7	2.0	2.4
Chert	1.5	0.7	1.3	-	0.7	-	-	0.7	0.8	2.6	1.0
K-feldspar	1.2	2.5	3.8	1.1	3.4	2.3	2.3	3.4	2.5	4.8	5.1
Plagioclase	-	-	-	-	-	-	-	-	-	-	-
VRF	0.5	0.3	0.7	0.3	0.7	-	0.3	0.6	0.5	2.0	1.6
GRF	-	-	-	-	-	-	0.3	-	0.3	0.3	-
MRF	13.5	6.5	15.0	2.8	15.8	1.3	4.0	10.0	4.0	12.5	19.1
SRF	1.3	0.3	1.3	-	1.0	-	-	0.3	0.9	0.9	2.9
Mica	-	0.3	-	-	0.3	-	-	-	-	-	0.3
Heavy min	0.3	-	0.3	-	-	-	-	-	-	-	-
Organics	-	-	0.3	-	1.4	-	-	0.9	-	-	-
Pyrite	0.5	-	-	-	-	-	0.3	-	1.8	0.3	-
Leucoxene	-	-	-	-	-	-	-	-	-	-	-
Sid (pf)	-	-	-	-	-	-	-	-	-	-	-
Sid (rpl)	-	0.3	1.3	-	2.3	-	-	3.0	7.5	11.3	1.9
Ank (pf)	-	-	-	-	-	-	-	-	-	-	-
Ank (rpl)	-	-	-	-	-	-	-	-	-	-	0.5
Cal (pf)	-	-	-	-	-	-	-	-	-	-	-
Cal (rpl)	-	-	-	-	-	-	-	-	-	-	-
Glauconite	-	-	-	-	-	-	-	-	-	-	-
AKa (pf)	5.6	4.8	5.2	2.0	1.1	0.5	0.5	2.1	1.0	4.8	5.9
AKa (rpl)	11.3	8.0	11.5	5.8	7.8	3.9	4.9	8.6	5.3	11.8	10.3
AIllite (pf)	-	-	-	-	-	-	-	-	-	0.3	-
AIllite (rpl)	0.7	0.7	1.7	-	1.2	-	-	0.7	0.7	2.1	-
Detrital clay	5.8	-	1.0	-	0.7	-	-	0.3	-	-	-
PP (inter)	0.8	2.3	-	8.2	0.3	11.0	11.8	3.4	2.8	-	1.4
SP (inter)	1.2	2.1	-	5.1	-	5.8	6.5	4.0	4.5	-	2.4
SP (mouldic)	4.4	4.0	0.3	-	2.0	-	-	-	-	1.0	0.3
SP (intra)	-	0.3	-	0.7	-	0.7	0.3	0.3	-	-	-
Q	76.3	87.6	73.5	94.6	74.8	95.4	90.9	81.4	89.2	70.0	62.8
F	1.7	3.2	4.8	1.4	4.1	2.9	3.0	4.4	3.3	7.0	6.6
R	22.0	9.2	21.7	4.0	21.1	1.7	6.1	14.2	7.5	23.0	30.6

Qtz (mono) = monocrystalline quartz Qtz (poly) = polycrystalline quartz Qtz og = quartz overgrowths VRF = volcanic rock fragments GRF = granitic rock fragments MRF = metamorphic rock fragments SRF = sedimentary rock fragments Heavy min = heavy minerals Sid (pf) = pore-filling siderite Sid (rpl) = replacement siderite Ank (pf) = pore-filling ankerite Ank (rpl) = replacement ankerite Cal (pf) = pore-filling calcite Cal (rpl) = replacement calcite AKa (pf) = pore-filling authigenic kaolinite AKa (rpl) = replacement authigenic kaolinite AIllite (pf) = pore-filling authigenic illitic clay AIllite (rpl) = replacement authigenic illitic clay PP (inter) = visible primary intergranular porosity SP (inter) = visible secondary intergranular porosity SP (mouldic) = visible secondary mouldic porosity SP (intra) = visible secondary intragranular porosity

Q = quartz + chert F = feldspar R = rock fragments

TABLE 3. THIN-SECTION COMPOSITION AND QFR RATIOS cont.

Sample #	80	83	M13	37	34	31	25	23	20	12
Depth (m)	2192.71	2193.59	2230.0	2255.5	2277.0	2306.0	2397.7	2417.0	2437.5	2575.0
Qtz (mono)	59.5	63.5	41.0	26.0	75.4	74.2	2.2	74.8	77.1	57.5
Qtz (poly)	2.0	2.1	3.0	0.8	2.6	2.5	0.3	3.1	3.4	1.0
Qtz og	6.5	6.3	4.8	-	3.0	2.1	-	1.1	1.4	2.5
Chert	0.5	0.3	-	-	-	-	-	-	-	-
K-feldspar	1.8	2.5	1.3	0.3	-	0.3	-	-	-	0.5
Plagioclase	-	-	-	-	-	-	-	-	-	-
VRF	0.5	0.5	0.4	-	-	-	-	-	-	-
GRF	-		-	-	-	-	-	-	-	-
MRF	3.8	2.1	2.5	0.3	0.3	0.3	0.3	-	-	0.7
SRF	-	-	-	-	-	0.3	-	-	-	-
Mica	0.3	-	0.5	0.3	-	-	0.7	-	0.3	0.7
Heavy min	-	-	-	-	-	-	-	-	-	0.3
Organics	-	-	5.0	9.2	-	-	13.0	-	-	3.0
Pyrite	0.3	0.8	2.5	3.6	-	1.0	1.8	1.6	-	-
Leucoxene	-	-	-	-	-	-	0.7	-	-	-
Sid (pf)	-	-	-	5.2	-	-	-	-	-	-
Sid (rpl)	-	-	6.5	47.8	-	-	1.7	-	-	1.8
Ank (pf)	0.5	0.5	-	-	-	-	-	-	-	-
Ank (rpl)	-	-	-	-	-	-	-	-	-	4.5
Cal (pf)	-	-	-	-	-	-	-	-	-	-
Cal (rpl)	-	-	-	-	-	-	-	-	-	-
Glauconite	-	-	-	-	-	-	-	-	-	-
AKa (pf)	2.8	2.5	1.7	2.0	2.0	1.4	-	2.0	1.1	6.0
AKa (rpl)	4.2	4.5	4.3	3.2	2.8	3.1	-	3.2	3.1	12.9
AIllite (pf)	-	-	-	-	-	-	-	-	-	1.0
AIllite (rpl)	-	-	0.3	0.8	0.3	0.7	-	0.7	0.7	3.3
Detrital clay	-	-	13.8	-	-	-	79.3	-	-	4.3
PP (inter)	11.3	8.0	5.8	-	13.6	14.1	-	13.5	12.9	-
SP (inter)	5.1	5.7	5.6	-	-	-	-	-	-	-
SP (mouldic)	-	-	0.3	0.5	-	-	-	-	-	-
SP (intra)	0.9	0.7	0.7	-	-	-	-	-	-	-
Q	91.8	93.4	92.0	97.8	99.6	98.8	-	100.0	100.0	98.1
F	2.4	3.2	2.5	1.1	0.0	0.4	-	0.0	0.0	0.8
R	5.8	3.4	5.5	1.1	0.4	0.8	-	0.0	0.0	1.1

Qtz (mono) = monocrystalline quartz Qtz (poly) = polycrystalline quartz Qtz og = quartz overgrowths VRF = volcanic rock fragments GRF = granitic rock fragments MRF = metamorphic rock fragments SRF = sedimentary rock fragments Heavy min = heavy minerals Sid (pf) = pore-filling siderite Sid (rpl) = replacement siderite Ank (pf) = pore-filling ankerite Ank (rpl) = replacement ankerite Cal (pf) = pore-filling calcite Cal (rpl) = replacement calcite AKa (pf) = pore-filling authigenic kaolinite AKa (rpl) = replacement authigenic kaolinite AIllite (pf) = pore-filling authigenic illitic clay AIllite (rpl) = replacement authigenic illitic clay PP (inter) = visible primary intergranular porosity SP (inter) = visible secondary intergranular porosity SP (mouldic) = visible secondary mouldic porosity SP (intra) = visible secondary intragranular porosity

Q = quartz + chert F = feldspar R = rock fragments

FIGURE 3. QFR COMPOSITIONS

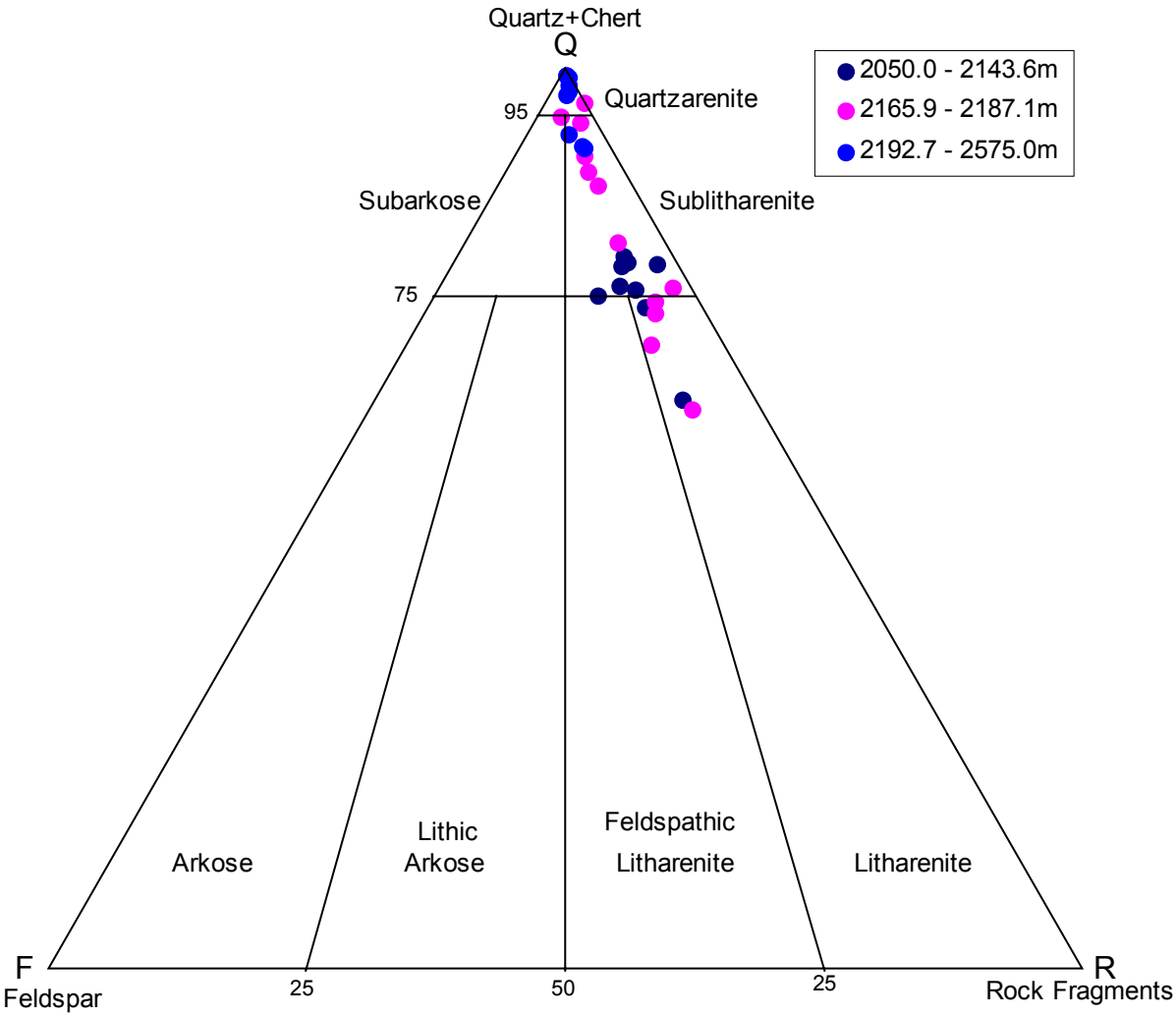

FIGURE 4. THIN-SECTION COMPOSITION/DEPTH CROSS-PLOT

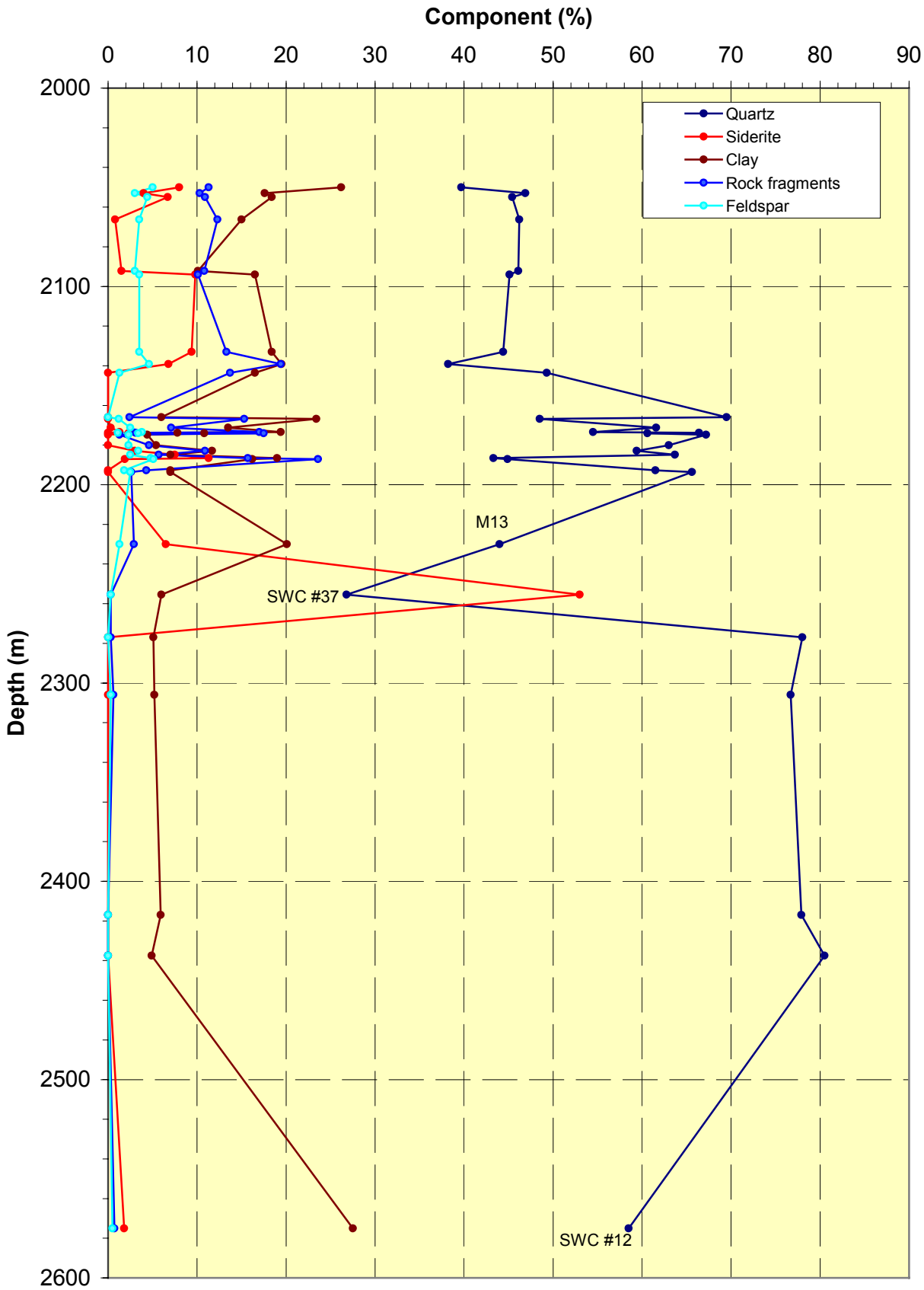

FIGURE 5. THIN-SECTION COMPOSITION/GRAIN SIZE CROSS-PLOT

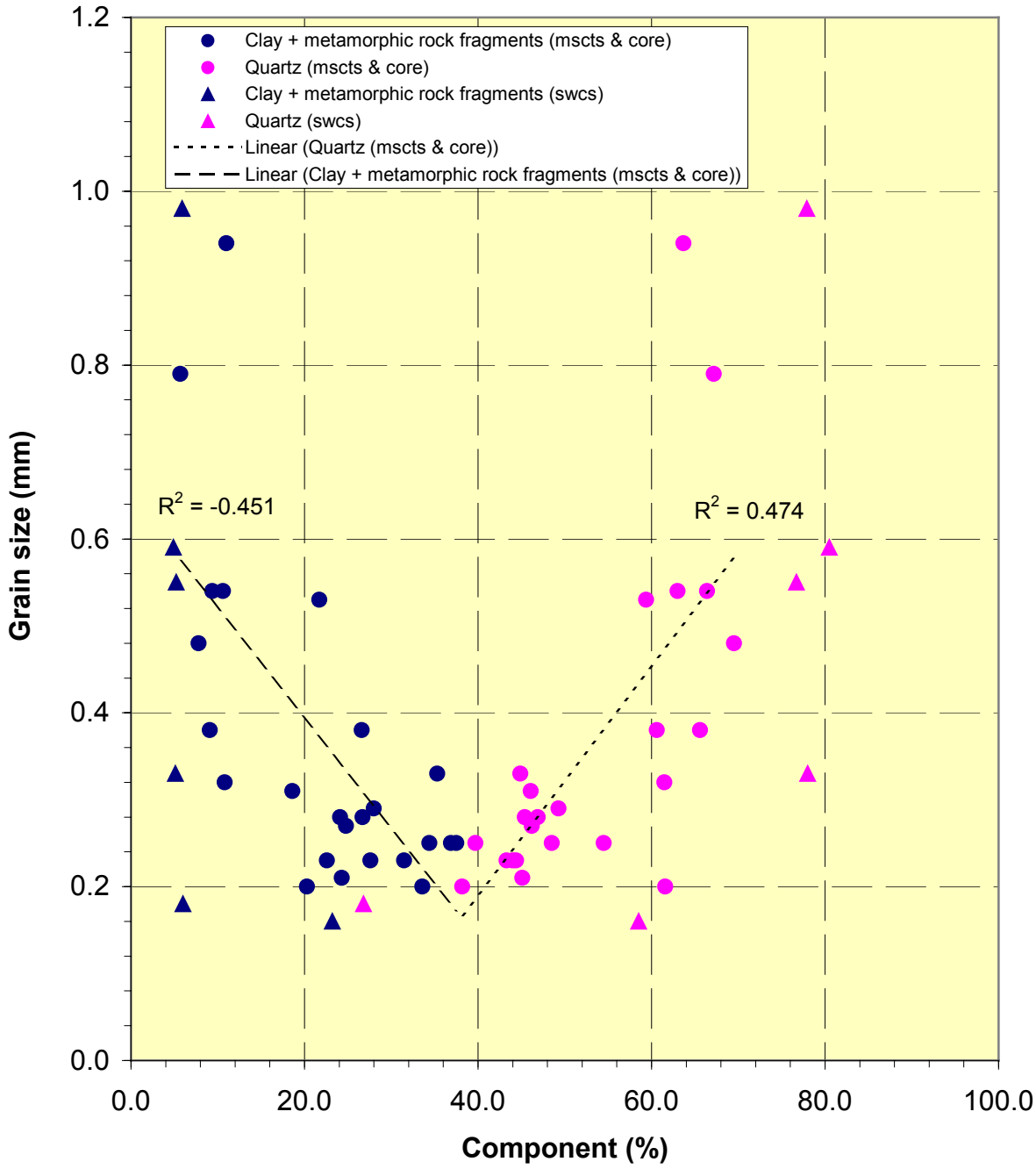

deformed between adjacent rigid grains and partly altered to illite and kaolinite. Other lithic grains include sedimentary rock fragments (mudrock, argillaceous siltstone), felsic volcanic rock fragments (composed mainly of cherty/chalcedonic/microcrystalline quartz) and rare granitic rock fragments (intergrown quartz and K-feldspar). Chert content does not exceed 3.4% and is consistently less than 1.0% below 2187.10m.

Other framework grains include muscovite, biotite, terrestrial organic fragments, rare reworked glauconite peloids (only above 2143.6m) and accessory heavy minerals (tourmaline, zircon, monazite, garnet, leucoxene). Biotite grains, which were common at the time of accumulation, have mainly altered to kaolinite and been replaced by siderite. Organic fragments are commonly concentrated with clay and mica along laminae.

Sandstones are derived from a continental provenance dominated by low grade metasedimentary and granitic rocks and which also included siliciclastics and volcanics.

Monazite grains are rimmed by radiogenically immobilised bitumen in M3, #5, #14 and #80.

M13 contains 13.8% detrital clay that is concentrated along irregular laminae up to 6mm thick. In the other samples, detrital clay does not exceed 5.8% and is mainly concentrated along thin laminae and forms patchy matrix. Most sandstones lack detrital clay.

Authigenic clay ranges up to 25.9% and is mainly kaolinite that occurs where micaceous/argillaceous rock fragments, mica and, less commonly, feldspar have altered. Muscovite grains are locally partly altered to kaolinite, and mica-like kaolinite grains occur where biotite has altered. Illitic remnants of micaceous precursor grains are locally associated with authigenic kaolinite, and minor authigenic illite is associated with partly altered and compactionally deformed micaceous/argillaceous metamorphic rock fragments. Figure 4 shows the variation of authigenic clay + detrital clay with depth.

Figure 5 shows that there is a moderate (R^2 = -0.451) negative correlation between authigenic clay + detrital clay + metamorphic rock fragment content and grain size for the sandstone msct and core samples.

Carbonate is mainly siderite, the content of which peaks at 53.0% in SWC #37 (Fig. 4), where microcrystalline siderite replaces coarse mica flakes and detrital clay that are concentrated with organic fragments along closely spaced laminae. In the other sandstones, siderite does not exceed 11.3%, is less than 2% below 2255.5m, and mainly forms large finely-crystalline and microcrystalline patches that replace altered biotite flakes, micaceous/argillaceous metamorphic rock fragments, clay and argillaceous sedimentary rock fragments (intraclasts). In M6, microcrystalline siderite also rims framework grains within localised areas, and in M7, siderite forms 50-150µm, disseminated/clustered rhombic crystals that fill pores and replace labile grains.

Ankerite ranges up to 8.5% and exceeds 1% only in M1, M2, M3, M6 and SWC #12, where it forms scattered, coarsely-crystalline patches and fine rhombic crystals that fill pores (particularly in M6) and replace framework grains and clay.

Calcite forms scattered poikilotopic cement/replacement patches at 2066.3m (M4).

Fine pyrite is locally associated with organic fragments and detrital clay.

Visible porosity ranges from 0% to 18.6% and generally decreases with increasing clay + metamorphic rock fragment content (see Fig. 10). Visible porosity could not be accurately measured for the clean sandstone sidewall core samples (SWCs #20, #23, #31, #34) due to the effects of severe impact damage. Visible porosity is accounted for by variable proportions of primary intergranular pores and secondary intergranular, intragranular and mouldic pores that have formed by partial to complete dissolution of labile grains (mainly K-feldspar).

5. X-RAY DIFFRACTION ANALYSES

Quantitative bulk-rock XRD analyses were carried out on all thirteen core samples, and fine fraction XRD analyses were carried out on three core samples (#5, #62, #83). Annotated XRD traces are given in Appendix 3.

Quantitative XRD analyses complement the thin-section analyses but cannot be compared directly. This is because thin-section clay and siderite components include microporosity, and therefore total thin-section clay and siderite are elevated relative to other grain types. In addition, XRD analyses do not include visible porosity. Therefore, in the case of those sandstones that contain significant visible porosity, component abundances as determined by XRD analysis will be higher than those determined by thin-section analysis. Finally, the thin-section rock fragment and clay components include quartz, K-feldspar, mica, kaolinite and illite that are recorded as these phases by XRD.

Quantitative XRD analyses (Table 4) accord with the thin-section analyses by showing that the sandstones are dominated by quartz (71.6-93.3%) and also contain variable amounts of kaolinite (4.3-19.5%) and siderite (0-13.6%) as well as minor K-feldspar (1.2-5.0%), illite/mica (0.3-4.4%), pyrite (0-1.3%) and ankerite (0-0.5%). Kaolinite dominates over illite/mica in all samples. Quartz varies mainly according to clay content (Fig. 6), with some variation in quartz content also being due to the presence of significant amounts of siderite in #62 and #67.

Fine-fraction XRD analyses (Table 5) indicate that the only clay minerals in the core samples are kaolinite (dominant) and discrete illite.

TABLE 4. BULK-ROCK XRD ANALYSES

Sample #	Depth (m)	Qtz	KF	PF	Ka	I/M	Sid	Ank	Pyr
5	2166.81	75.2	2.2	-	19.5	2.9	0.2	-	-
14	2171.19	84.1	2.0	-	11.0	1.7	1.2	-	-
22	2173.40	71.6	4.0	-	19.3	3.8	1.3	-	-
24	2173.83	90.5	2.2	-	5.0	0.3	2.0	-	-
25	2174.10	82.2	2.5	-	11.7	2.3	1.3	-	-
28	2174.80	93.3	1.2	-	5.1	0.3	0.1	-	-
46	2180.10	92.9	2.2	-	4.3	0.5	0.1	-	-
55	2182.92	87.9	2.7	-	7.5	1.2	0.7	-	-
62	2184.89	82.6	2.5	-	5.3	0.8	7.5	-	1.3
67	2186.60	60.5	5.0	-	16.4	4.4	13.6	-	0.1
69	2187.10	76.3	4.4	-	14.6	3.3	1.4	-	-
80	2192.71	90.0	2.4	-	6.5	0.8	-	0.3	-
83	2193.59	88.8	2.4	-	7.1	0.6	0.2	0.5	0.4

Qtz = quartz KF = K-feldspar PF = plagioclase Ka = kaolinite I/M = illite/mica Sid = siderite Ank = ankerite Pyr = pyrite

TABLE 5. CLAY MINERALOGY

Sample #	Depth (m)	Ka	I/M	I/S	Sm	Chl
5	2166.81	A	m	-	-	-
62	2184.89	A	m	-	-	-
83	2193.59	A	m	-	-	-

Ka = kaolinite I/M = illite/mica I/S = mixed-layer illite/smectite Sm = smectite Chl = chlorite

A = abundant M = major m = minor T = trace

FIGURE 6. XRD QUARTZ/CLAY CROSS-PLOT (CORE SAMPLES)

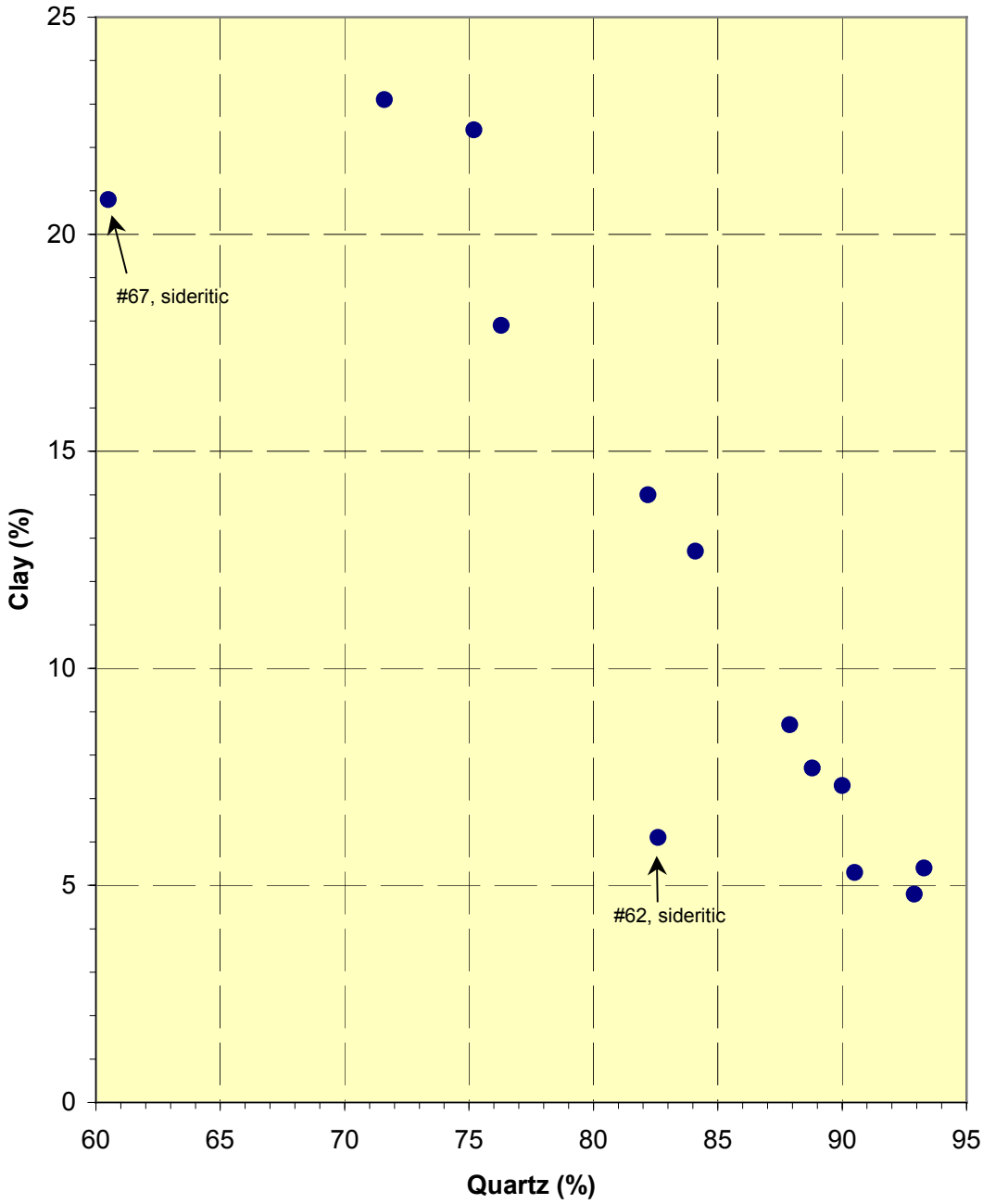

6. DIAGENESIS

In the sideritised mudrock sample (M5), detrital clay matrix has been extensively replaced by early-diagenetic microcrystalline siderite and there has been later labile grain dissolution to form scattered secondary mouldic pores (Plate 5). The laminated mudrock (SWC #25) is well compacted and contains minor microcrystalline siderite replacement. M5 and SWC #25 are not considered further in this section.

The main diagenetic processes that have affected the sandstones are grain contact dissolution, labile grain dissolution, authigenic clay formation, ductile grain/authigenic clay compaction, quartz overgrowth cementation and carbonate cementation/replacement.

Grain contact dissolution has increased framework grain packing density by producing long, embayed and sutured grain contacts between most juxtaposed quartz grains, quartzose/illitic rock fragments and feldspar grains (Plates 4, 6, 7, 36). Advanced grain contact dissolution and microstylolitisation have occurred within localised argillaceous areas and also throughout much of #22 and #25 (Plates 18, 22), where grain contact dissolution was promoted by the presence of thin illitic clay films between grains.

K-feldspar grains have partly to completely dissolved to form common secondary intergranular pores (Plates 7, 10, 45), intragranular pores (Plates 6, 7; Plate 31, Fig. 1) and, in the less macroporous samples (e.g. M1), mouldic pores (Plates 1, 6, 9, 16, 18, 22). A few microcrystalline quartzose rock fragments have also partly dissolved to form intragranular pores. Secondary K-feldspar dissolution porosity makes up a large component of total macroporosity.

Most authigenic clay is kaolinite that forms scattered, grain-sized patches and patchy pseudomatrix that occur where micaceous/argillaceous rock fragments, mica and feldspar have completely altered (Plates 1, 11, 20; Plate 21, Fig. 2; Plate 26, Fig. 2; Plate 33, Fig. 1; Plate 36; Plate 39, Fig. 2). Muscovite grains are locally partly altered to kaolinite, and mica-like kaolinite grains occur where biotite has altered. The other authigenic clay is illite, which is mainly associated with partly altered and compactionally deformed micaceous/argillaceous metamorphic rock fragments (Plate 23, Fig. 2; Plate 31, Fig. 2; Plate 38, Fig. 2). Total authigenic clay content ranges up to 25.9% and is weakly (R^2 = -0.387) negatively correlated with grain size.

Micaceous/illitic metamorphic rock fragments, argillaceous sedimentary rock fragments, mica and authigenic clay are commonly compactionally deformed (Plates 3, 6, 8, 9, 16, 24, 34, 36), locally to form pseudomatrix, particularly in the more lithic labile samples, which were susceptible to physical compaction and authigenic clay formation on account of their high content of micaceous/argillaceous grains at the time of accumulation. Some organic fragments are also compactionally deformed.

Quartz overgrowth cement content ranges up to 7.6% and is mainly less than 5%. Although common, quartz overgrowths are only thinly developed on quartz grain surfaces and thus only partly occlude all available intergranular space (Plates 6, 10, 22, 24; Plate 25, Fig. 2; Plates 28, 40, 45), except in the fine grained sandstones (Plate 17, Fig. 1), where quartz overgrowths commonly totally fill intergranular spaces to form triple point grain junctions. In many areas, quartz overgrowth development has been inhibited by the presence of compacted ductile grains and authigenic clay.

Siderite is common above 2277.0m, where it does not exceed 11.3%, except at 2255.5m (SWC #37), where siderite content peaks at 53% (Fig. 4). In SWC #37, micaceous laminae and detrital clay are largely replaced by microcrystalline siderite (Plate 46). Elsewhere, siderite mainly forms large finely-crystalline and microcrystalline patches that replace altered biotite flakes, micaceous/argillaceous metamorphic rock fragments, clay and argillaceous intraclasts (Plates 8, 9, 22, 34). Grain-rimming microcrystalline siderite also occurs within localised areas in M6, and siderite forms 50-150µm, disseminated/clustered rhombic crystals that fill pores and replace labile grains in M7 (Plate 7). Patchy coarsely-crystalline ankerite and fine ankerite rhombs occupy intergranular pores and replace framework grains and clay in a few samples (Plates 1, 34, 43, 52), and patchy, poikilotopic calcite occupies intergranular pores and replaces framework grains in M4 (Plate 4).

Minor authigenic minerals include fine framboidal pyrite and anatase.

The interpreted paragenetic history of the sandstones is shown in Figure 7. Siderite completely rims compacted grains in M6, indicating that siderite predates compaction. Siderite is enclosed by and thus predates calcite, ankerite and quartz overgrowths. Pyrite is included within later formed siderite, ankerite and quartz overgrowths. Calcite and ankerite replace and thus postdate authigenic kaolinite. Authigenic kaolinite and illite are engulfed by quartz overgrowths (Plate 19, Fig. 2, Plate 23, Fig. 2; Plate 26, Fig. 2), indicating that authigenic clay predates quartz overgrowths. Calcite and ankerite encase quartz grains that, unlike quartz grains in non-carbonate cemented areas, lack quartz overgrowths (Plate 43), indicating that calcite and ankerite predate quartz overgrowths. Calcite and ankerite also encase quartz grains with welded grain contacts resulting from grain contact dissolution, indicating that calcite and ankerite postdate grain contact dissolution. Secondary K-feldspar dissolution pores are bordered by authigenic kaolinite (Plate 12), siderite, calcite and ankerite, indicating that K-feldspar dissolution postdates authigenic kaolinite, siderite, calcite and ankerite. Grain contact dissolution has occurred between quartz grains and now-dissolved K-feldspar grains, indicating that K-feldspar dissolution also postdates grain contact dissolution. Grain contact dissolution has also occurred between quartz grains and kaolinitised micaceous grains, suggesting that kaolinitisation of micaceous grains occurred after grain contact dissolution. Quartz overgrowths have developed inside secondary K-feldspar dissolution pores (Plate 22), indicating that at least some quartz overgrowth cementation postdates K-feldspar dissolution. Quartz overgrowth cementation appears to be the latest diagenetic event.

FIGURE 7. DIAGENETIC PARAGENESIS*

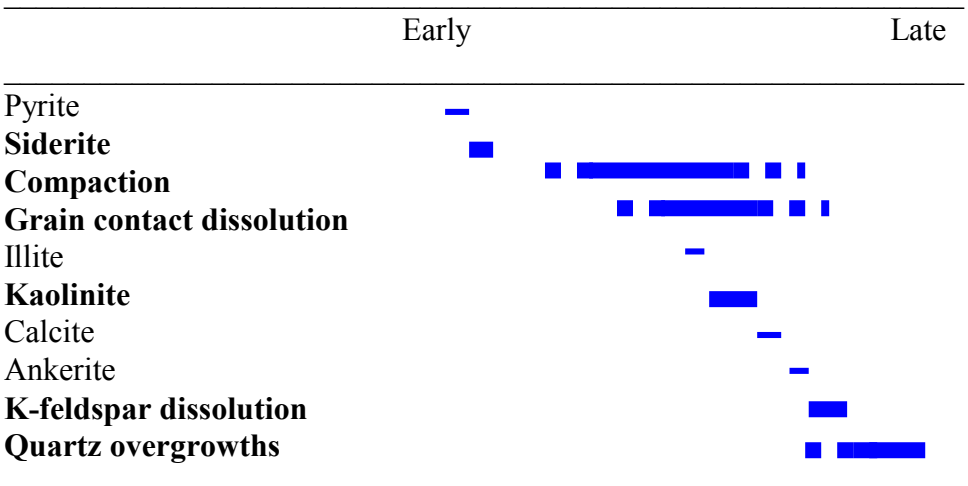

* main diagenetic effects in bold

7. RESERVOIR QUALITY

Routine core analyses for the twenty-five msct and core samples are given in Table 1 and plotted in Figure 8. Figure 8 also includes routine core analyses for one hundred and fifteen core samples from between 2165.10m and 2200.40m that were not petrologically analysed. The plot shows that measured porosity ranges from 4.6% to 24.4% and permeability ranges from 0.001md to 7500md and that measured porosity and permeability are strongly (R^2 = 0.711) correlated. Figure 8 also shows that the petrologically-analysed msct and core samples cover most of the porosity and permeability range in the cored section.

The least porous and permeable of the petrologically-analysed msct and core samples is M5 (Fig. 8), which is one of the two mudrock samples included in this study. The other mudrock sample (SWC #25) would probably have an even lower porosity and permeability than M5 given that, unlike M5, it is totally microporous. M5 and SWC #25 are not considered further in this section.

The other twenty-four petrologically-analysed msct and core samples are sandstones that have a measured porosity between 11.7% and 23.2% and permeability between 0.483md and 4710md (Fig. 8).

Figure 9 shows that there is a strong (R^2 = 0.819) positive correlation between visible macroporosity and permeability. This trend is expected given that visible porosity is conducive to permeability. Visible porosity is accounted for by variable proportions of primary intergranular pores and secondary intergranular, intragranular and, in the less macroporous samples, mouldic pores that have formed mainly by partial to complete dissolution of K-feldspar grains.

Figure 10 shows that there is a strong (R^2 = -0.733) negative correlation (excluding #25 and #62) between detrital clay + authigenic clay + metamorphic rock fragment content and visible porosity. The correlation would be weakened by including #25 and #62, which have anomalously low visible porosity for their clay + metamorphic rock fragment content on account of being poorly sorted and, in the case of #25, having undergone advanced grain contact dissolution.

With sandstone visible porosity being positively correlated to permeability (Fig. 9) and with clay + metamorphic rock fragment content being negatively correlated with visible porosity (Fig. 10), clay + metamorphic rock fragment content should be negatively correlated to permeability. Figure 11 confirms that there is in fact a strong (R^2 = -0.820) negative correlation between clay + metamorphic rock fragment content and permeability, indicating that permeability variation within the reservoir sandstones is due mainly to differences in detrital clay + authigenic clay + metamorphic rock fragment content. Metamorphic rock fragments influence permeability on account of being largely micaceous/argillaceous and thus prone to compactional deformation and dispersion, commonly to form pseudomatrix.

Permeability is more influenced by clay content than by metamorphic rock fragment content, with clay content being strongly (R^2 = -0.704) correlated with permeability and metamorphic rock fragment content being moderately (R^2 = -0.573) correlated with permeability.

With authigenic kaolinite being the dominant clay, the negative correlation between clay and permeability reflects a moderate (R^2 = -0.686) negative correlation between authigenic kaolinite and permeability. This correlation is improved (R^2 = -0.787) if two samples (#22,

FIGURE 8. POROSITY/PERMEABILITY CROSS-PLOT

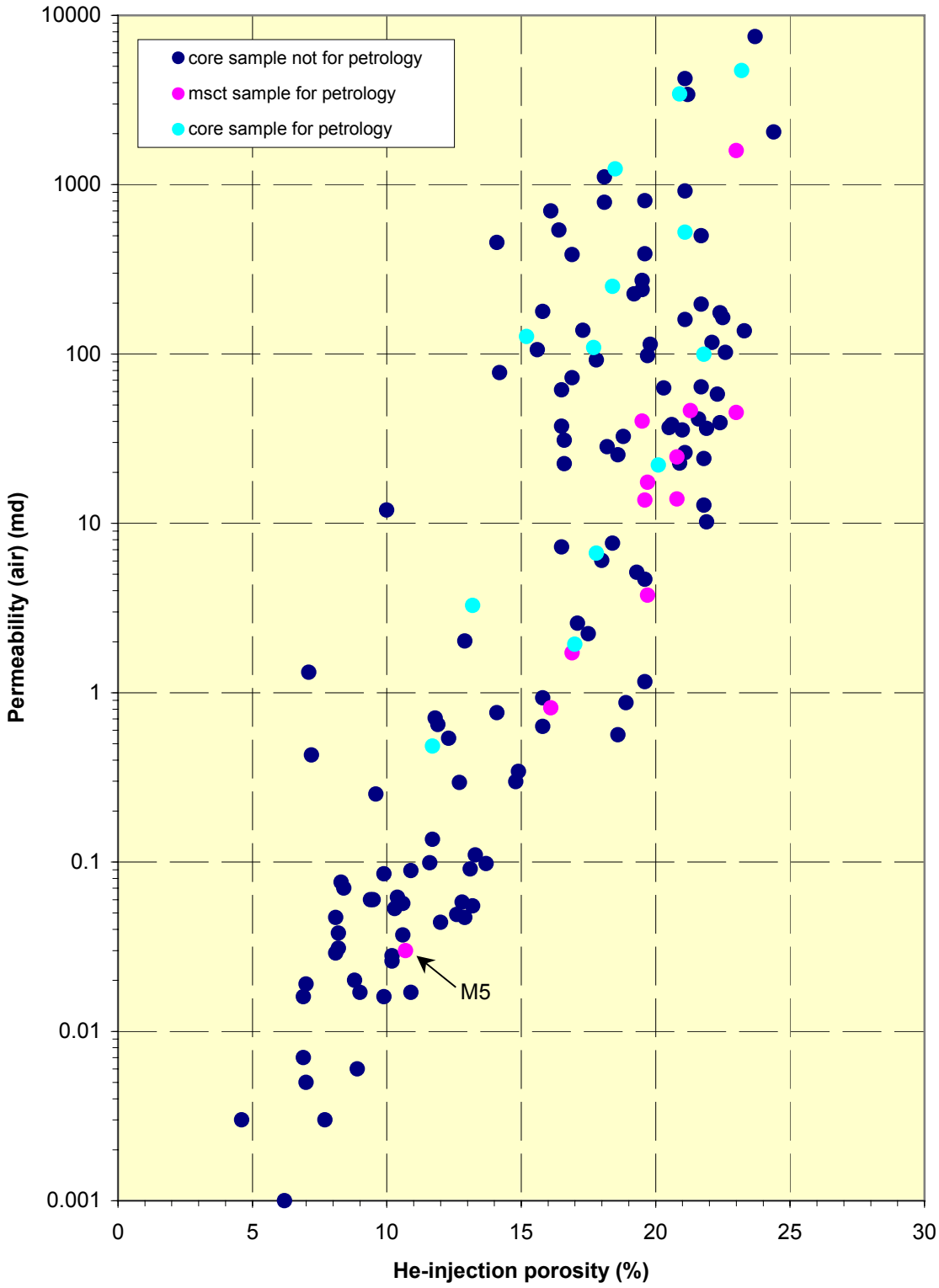

FIGURE 9. VISIBLE POROSITY/PERMEABILITY CROSS-PLOT

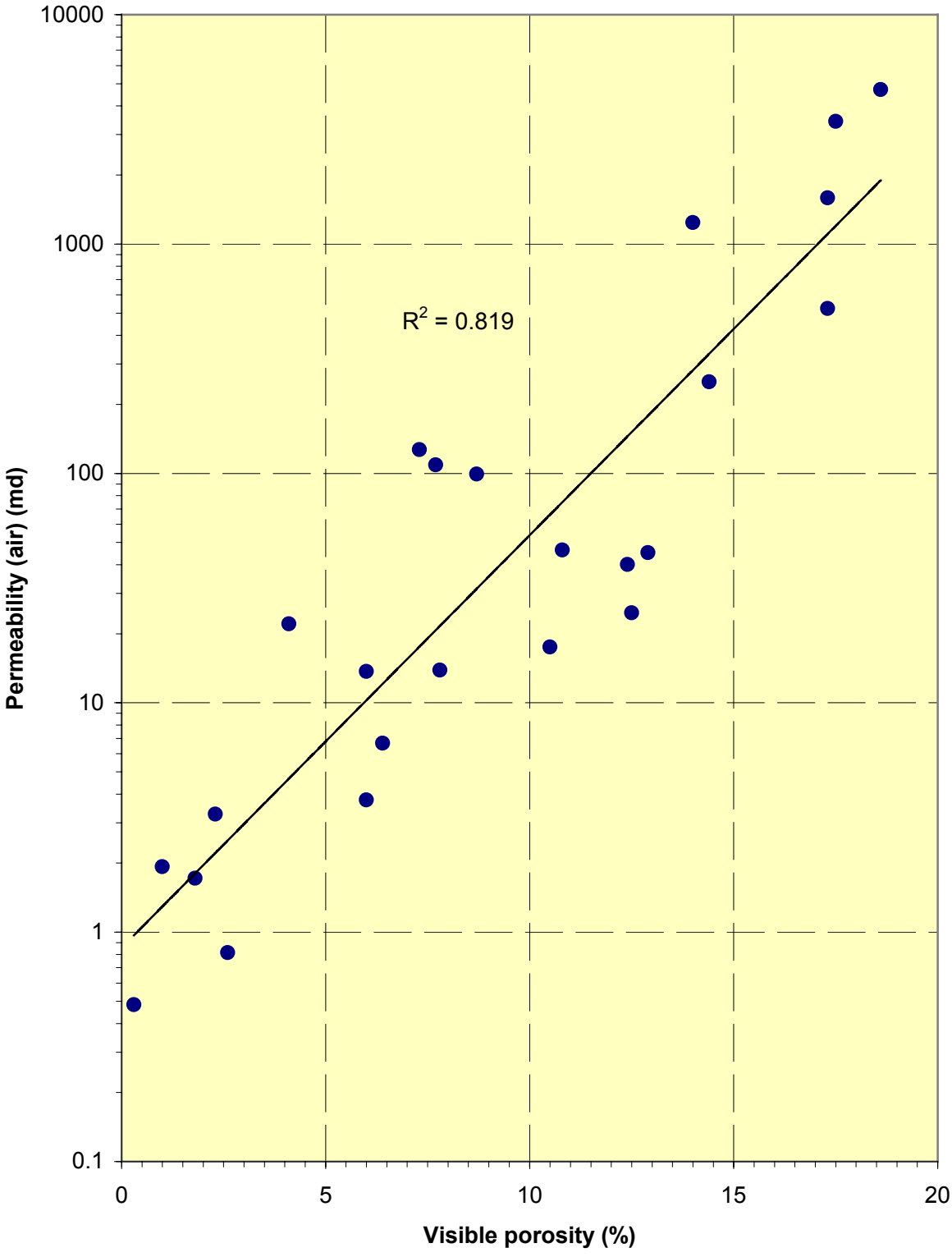

FIGURE 10. CLAY + METAMORPHIC ROCK FRAGMENTS/VISIBLE POROSITY CROSS-PLOT

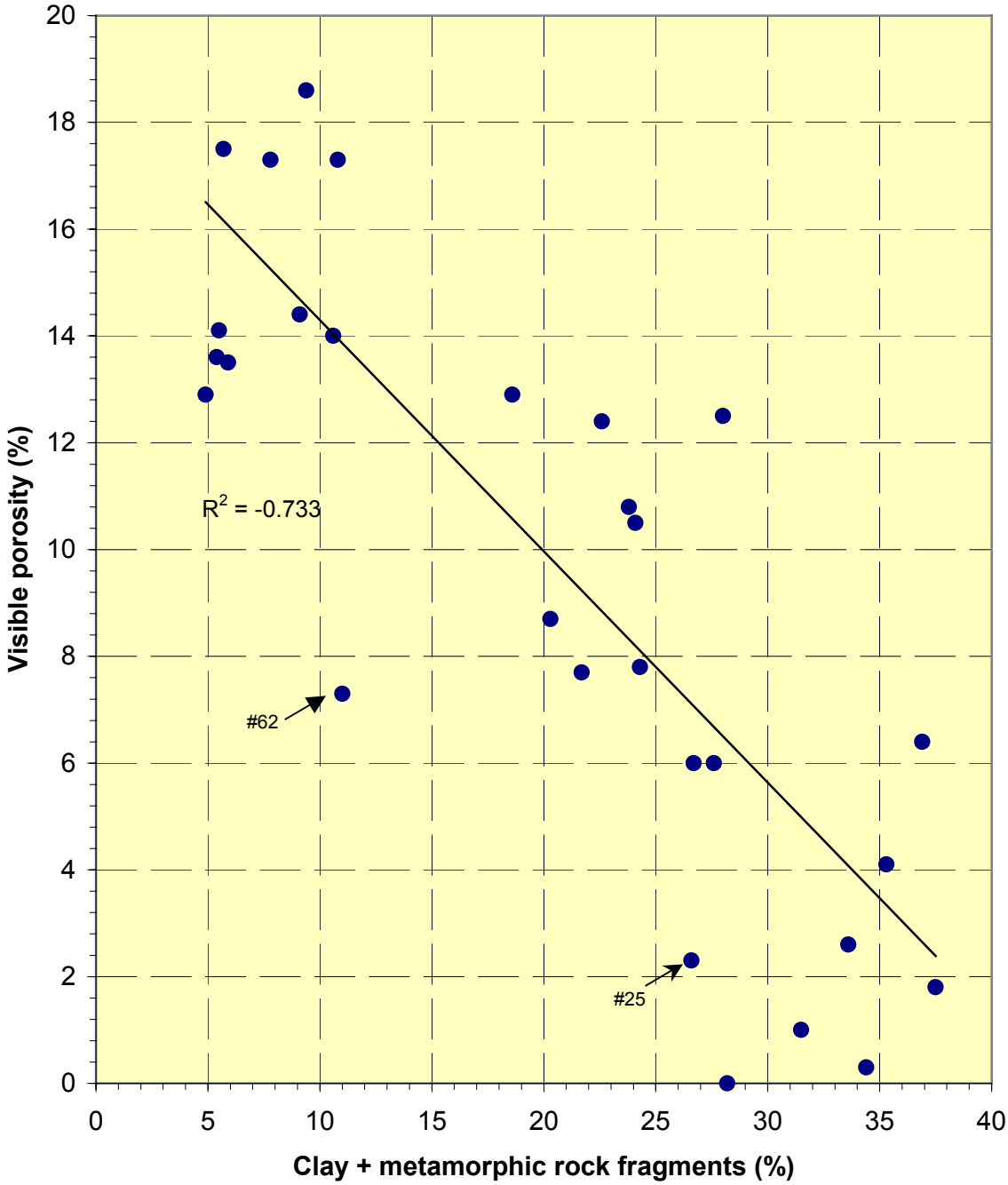

FIGURE 11. CLAY + METAMORPHIC ROCK FRAGMENTS/PERMEABILITY CROSS-PLOT

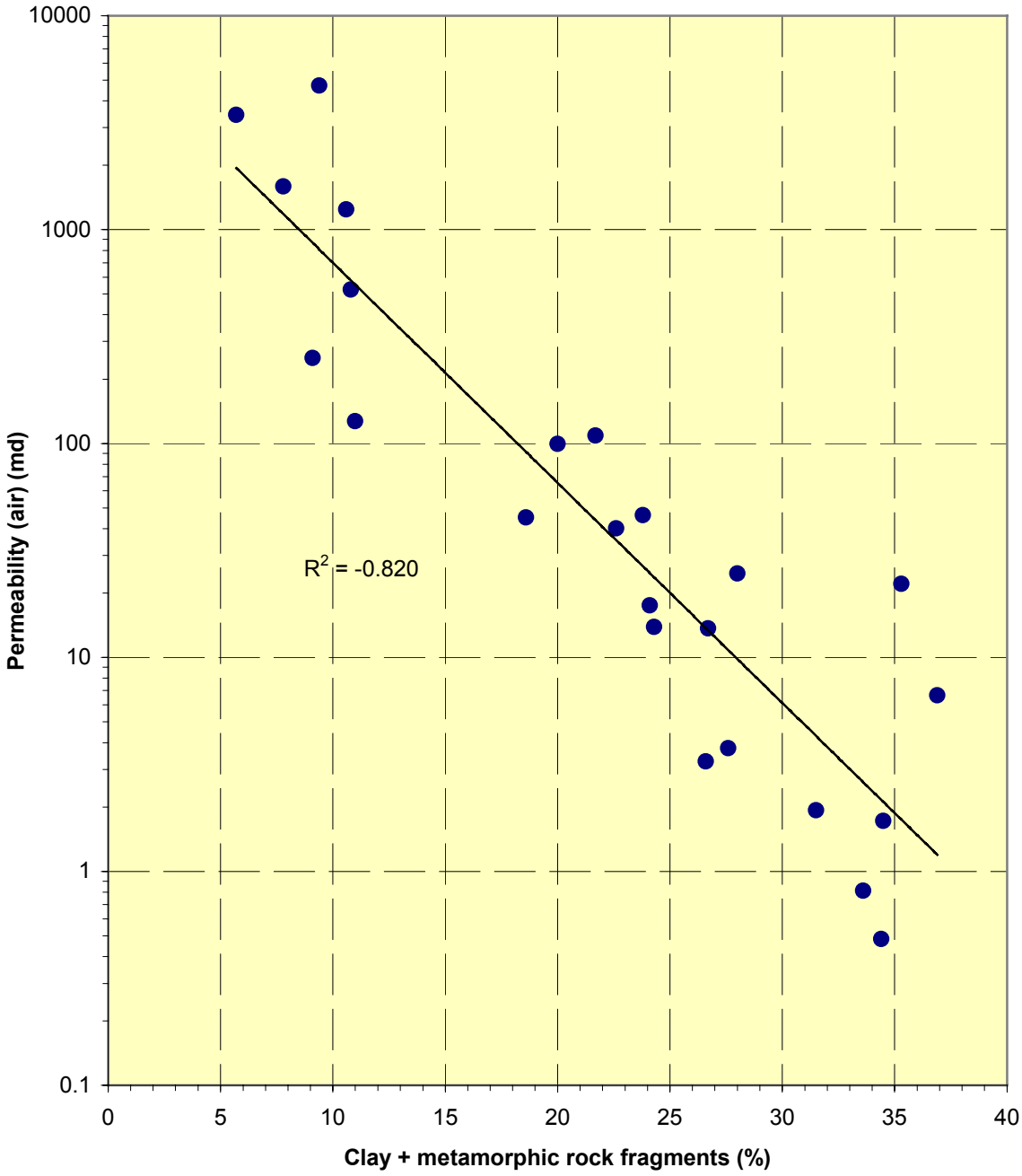

#25) that have anomalously low permeability for their kaolinite content on account of having undergone advanced grain contact dissolution and microstylolitisation are excluded from the plot (Fig. 12).

Clay + metamorphic rock fragment content generally decreases with increasing quartz content (Figs. 4 & 5), hence the strong negative correlation between clay + metamorphic rock fragment content and permeability (Fig. 11) is mirrored by a strong (R^2 = 0.838) positive correlation between quartz content and permeability (Fig. 13). The trendline in Figure 13 excludes two samples (#22, #25) that have anomalously low permeability for their quartz content on account of having undergone advanced grain contact dissolution and microstylolitisation.

There is a moderate (R^2 = -0.451) negative correlation between total clay + metamorphic rock fragment content and grain size (Fig. 5). Accordingly, given that there is a strong negative correlation between clay + metamorphic rock fragment and permeability (Fig. 11), there should be a positive correlation between grain size and permeability.

Figure 14 shows that there is in fact a positive correlation between grain size and permeability, but the correlation is only modest (R^2 = 0.485) Sorting ranges from well to poor, hence, given that intrinsic porosity and permeability decrease with decreasing sorting, it appears that the control of grain size on permeability is being largely masked by the wide range of sorting coupled with the fact that the correlation between clay + metamorphic rock fragment content and grain size is only moderate (Fig. 5).

In summary, permeability variation between the msct and core sandstone samples is mainly due to differences in the amount of clay (particularly authigenic kaolinite) and, of less importance, metamorphic rock fragments. Clay + metamorphic rock fragment content is only moderately correlated with grain size, and there is wide variation in sorting. As a result, grain size and permeability are only moderately correlated. Carbonate has little influence on permeability.

Two of the sandstone sidewall core samples (SWCs #37, #12) would have very low permeability on account of being fine grained and containing little or no macroporosity due to grain contact dissolution and extensive pore filling by siderite, authigenic kaolinite and, in SWC #12, quartz overgrowths, ankerite and detrital clay. The other four sidewall core samples (SWCs #20, #23, #31, #34) are clean, medium to coarse grained quartzose sandstones in which original texture and porosity characteristics have been almost completely obliterated by the effects of sidewall coring impact. In accord with the trends between composition and permeability shown in Figures 11 and 13, indications are that these four sandstones originally contained abundant macroporosity and had moderate to high permeability prior to sidewall coring, despite porosity reduction by grain contact dissolution, quartz overgrowth cementation and authigenic clay formation.

Figure 15 shows the relationship between siderite content and grain density.

Reservoir quality is briefly described for each sample in Appendix 4.

FIGURE 12. AUTHIGENIC KAOLINITE/PERMEABILITY CROSS-PLOT

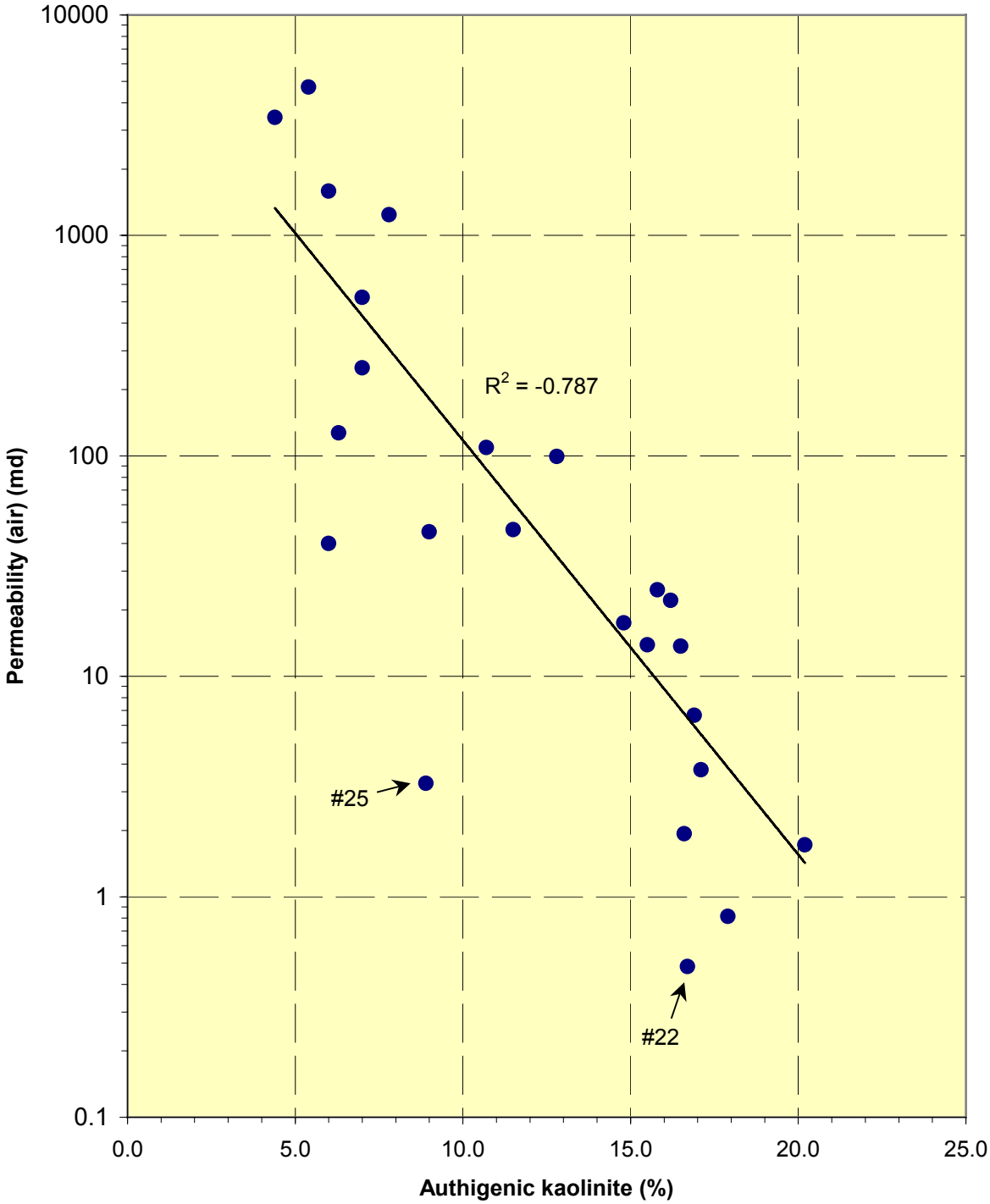

FIGURE 13. QUARTZ/PERMEABILITY CROSS-PLOT

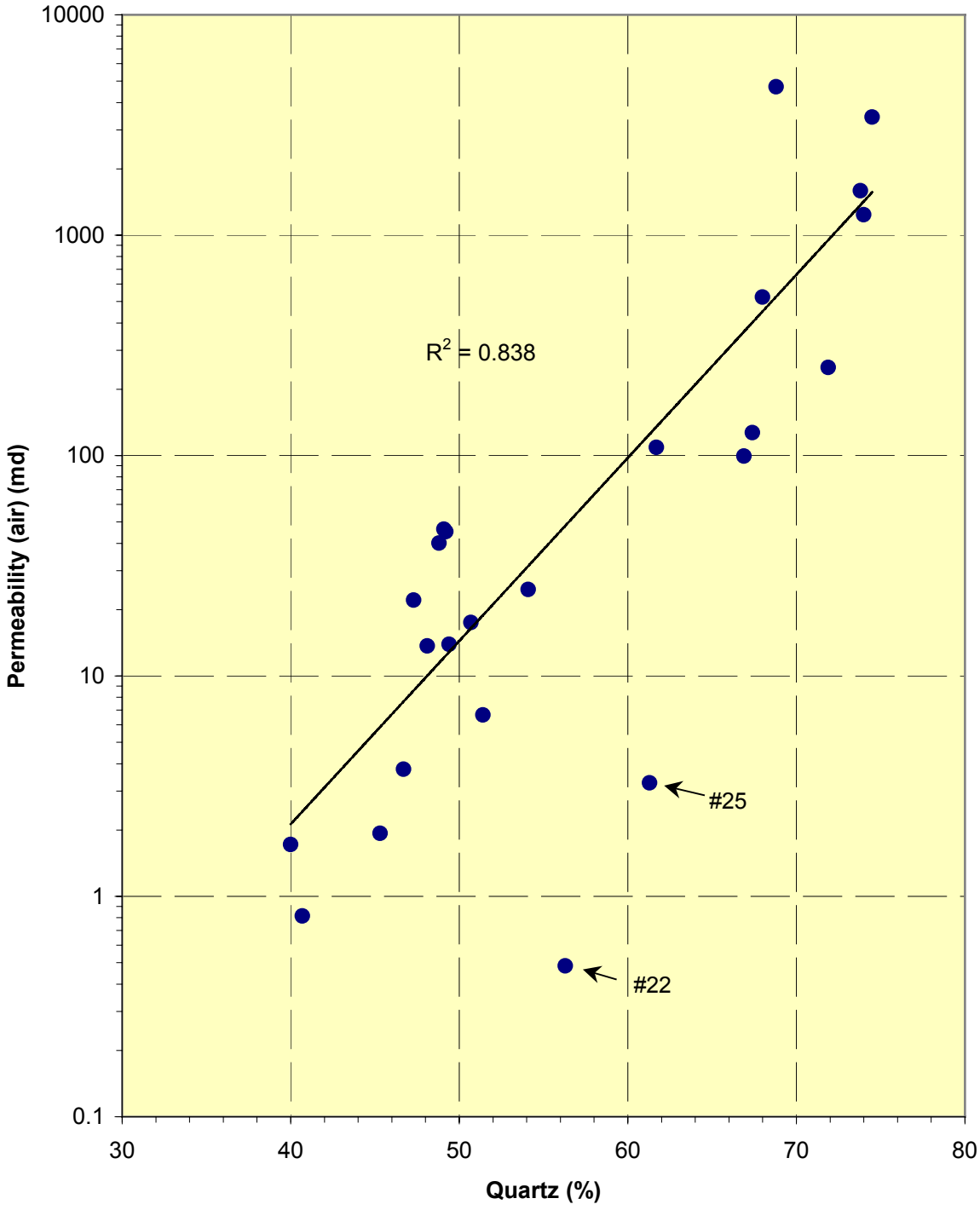

FIGURE 14. MEAN GRAIN SIZE/PERMEABILITY CROSS-PLOT

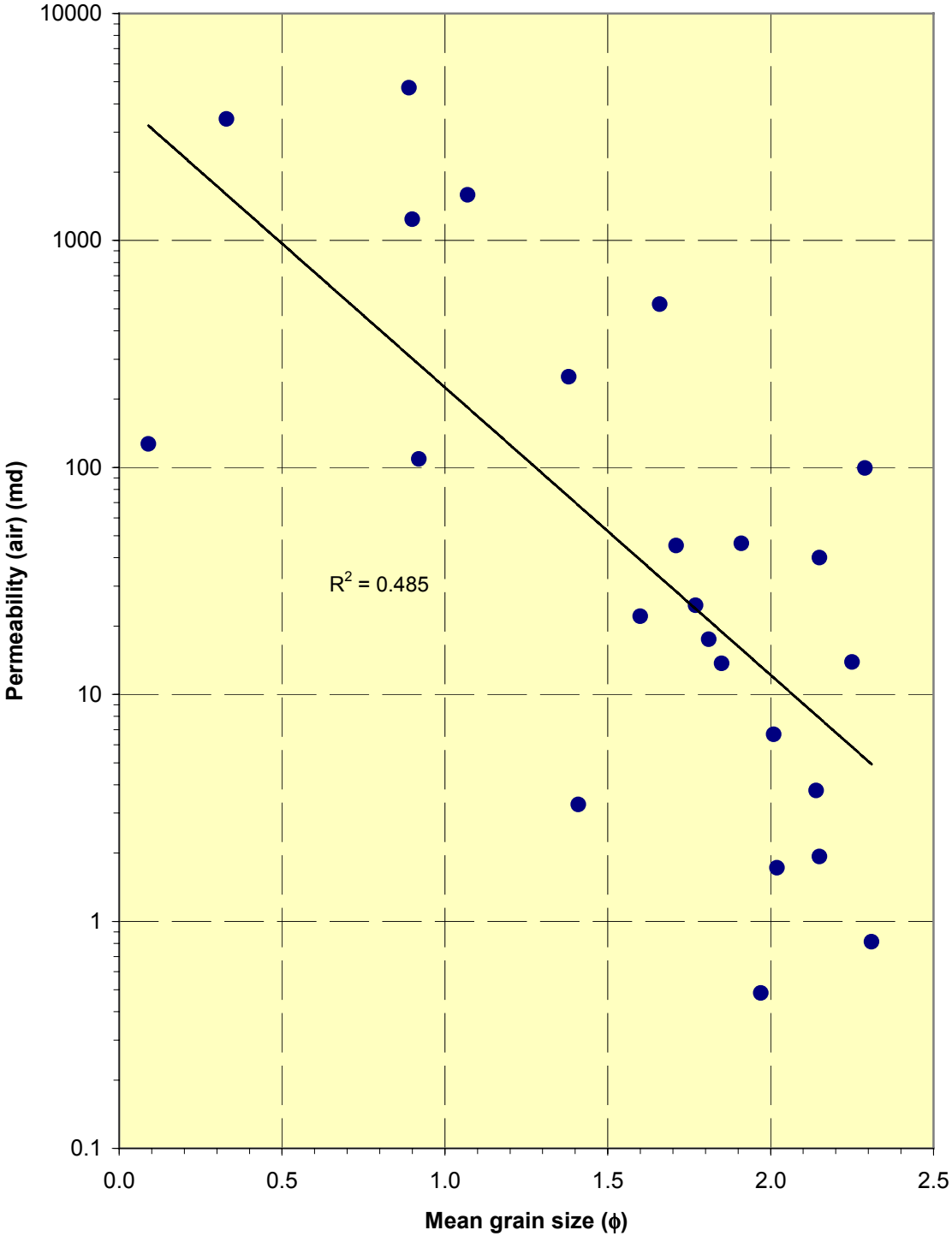

FIGURE 15. SIDERITE/GRAIN DENSITY CROSS-PLOT

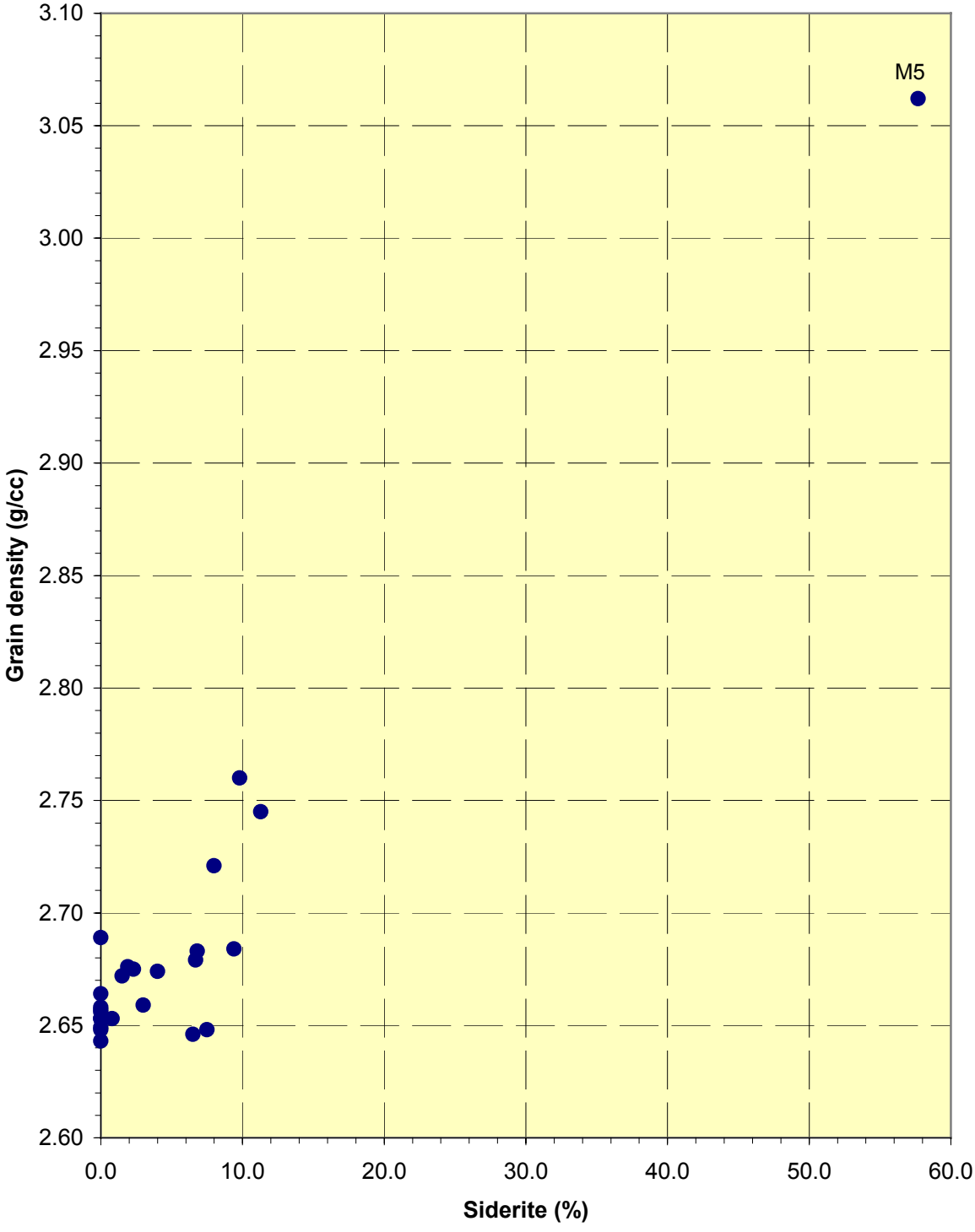

8. SUMMARY AND CONCLUSIONS

- Samples from 2050.0 - 2575.0m in Thylacine-1 are litharenites, sublitharenites and quartzarenites in which framework grains are mainly quartz and also include K-feldspar, metamorphic rock fragments, mica, organics and accessory heavy minerals. Compositional maturity generally increases with depth, with quartz increasing downward below 2143.6m at the expense of clay, rock fragments, feldspar and siderite. Two samples (M5, SWC #25) are mudrocks, one of which (M5) is extensively replaced by siderite.

- Between 2050.0m and 2173.40m, sandstones are fine to medium grained and moderately-well to well sorted. Below this interval, sorting and grain size fluctuate widely, with sandstones between 2173.83m and 2575.0m being poorly to well sorted and fine to coarse grained. Sorting generally decreases with increasing grain size, although there is wide scatter in the grain size data for upper medium and coarse grained sandstones.

- Sandstones are derived from a continental provenance dominated by low grade metasedimentary rocks and granitic rocks and which also included siliciclastics and volcanics.

- M13 contains 13.8% detrital clay, whereas the other sandstones contain less than 5.9% detrital clay, most of which is concentrated along thin laminae and forms patchy matrix. Most sandstones lack detrital clay.

- Authigenic clay ranges up to 25.9% and is mainly kaolinite that occurs where labile grains have altered. Illitic remnants of micaceous precursor grains are locally associated with authigenic kaolinite, and minor authigenic illite is associated with partly altered and compactionally deformed micaceous/argillaceous metamorphic rock fragments. All clay detected in the sandstones by XRD is kaolinite and minor illite.

- Diagenetic effects in the sandstones besides authigenic clay formation include grain contact dissolution/microstylolitisation, labile grain (mainly K-feldspar) dissolution, ductile grain/authigenic clay compaction, cementation by quartz overgrowths, and cementation/replacement by siderite, ankerite and rare calcite.

- Porosity reduction in the sandstones is mainly the result of authigenic clay formation, ductile grain/clay compaction, grain contact dissolution/microstylolitisation and quartz overgrowth cementation.

- Visible porosity ranges up to 18.6% and generally decreases with increasing clay + metamorphic rock fragment content. Visible porosity could not be accurately measured for the clean sandstone sidewall core samples (SWCs #20, #23, #31, #34) due to the effects of severe impact damage. Visible porosity is accounted for by variable proportions of primary intergranular pores and secondary intergranular, intragranular and mouldic labile grain dissolution pores.

- Reservoir quality is mainly controlled by the content of clay (mostly authigenic kaolinite) and, of less importance, metamorphic rock fragments. Clay + metamorphic rock fragment content is only moderately correlated with grain size, and there is wide variation in sorting. Consequently, grain size and permeability are only moderately correlated. Carbonate has little influence on permeability.

KEY TO PLATES IN APPENDIX 4

Sample #	Depth (m)	Plate #
M1	2050.0	1
M2	2053.0	2
M3	2055.0	3
M4	2066.3	4
M5	2076.5	5
M6	2092.2	6
M7	2094.0	7
M8	2133.0	8
M9	2139.1	9
M10	2143.6	10
M12	2165.9	11,12
5	2166.81	13, 14*
-	2170.40	15*
14	2171.19	16, 17*
22	2173.40	18, 19*
24	2173.83	20, 21*
25	2174.10	22, 23*
28	2174.80	24, 25*
-	2180.06	26*
46	2180.10	27, 28*
55	2182.92	29, 30*
-	2184.76	31*
62	2184.89	32, 33*
67	2186.60	34, 35*
69	2187.10	36, 37*
-	2187.22	38*
-	2188.61	39*
80	2192.71	40, 41*
-	2192.93	42*
83	2193.59	43, 44*
M13	2230.0	45
SWC 37	2255.5	46
SWC 34	2277.0	47
SWC 31	2306.0	48
SWC 25	2397.7	49
SWC 23	2417.0	50
SWC 20	2437.5	51
SWC 12	2575.0	52

* SEM micrographs

APPENDIX 1. GRAIN SIZE COMPARISON TABLE

Millimetres	Microns	Phi (ϕ)	Wentworth Size Class
4096		-12	
1024		-10	Boulder (-8 to -12)
256		- 8	
			Cobble (-6 to -8)
64		- 6	
16		- 4	Pebble (-2 to -6)
4		- 2	
3.36		- 1.75	
2.83		- 1.5	Granule
2.38		- 1.25	
2.00		**- 1.0**	
1.68		- 0.75	
1.41		- 0.5	Very coarse sand
1.19		- 0.25	
1.00		0.0	
0.84		0.25	
0.71		0.5	Coarse sand
0.59		0.75	
1/2 --- 0.50	500	1.0	
0.42	420	1.25	
0.35	350	1.5	Medium sand
0.30	300	1.75	
1/4 --- 0.25	250	2.0	
0.210	210	2.25	
0.177	177	2.5	Fine sand
0.149	149	2.75	
1/8 --- 0.125	125	3.0	
0.105	105	3.25	
0.088	88	3.5	Very fine sand
0.074	74	3.75	
1/16 -- **0.0625**	**62.5**	**4.0**	
0.053	53	4.25	
0.044	44	4.5	Coarse silt
0.037	37	4.75	
1/32 -- 0.031	31	5.0	
			Medium silt
1/64 -- 0.0156	15.6	6.0	
			Fine silt
1/128 - 0.0078	7.8	7.0	
			Very fine silt
1/256 - 0.0039	3.9	8.0	
0.0020	2.0	9.0	
0.00098	0.98	10.0	Clay
0.00049	0.49	11.0	

APPENDIX 2.

GRAIN SIZE FREQUENCY CURVES

MGS = mean grain size

0-1ϕ = coarse sand; 1-2ϕ = medium sand; 2-3ϕ = fine sand;
3-4ϕ = very fine sand; 4-5ϕ = coarse silt

Sorting (ϕSD)

Class	*ϕ Standard Deviation*
very well sorted	<0.35
well sorted	0.35-<0.50
moderately well sorted	0.50-<0.71
moderately sorted	0.71-1.00
poorly sorted	>1.00+

2050.0m – 2092.2m

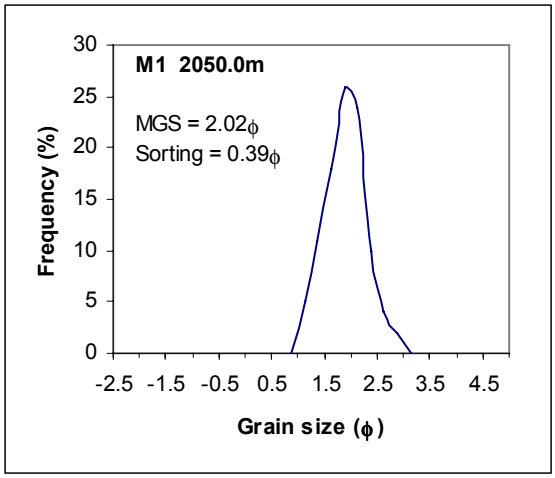

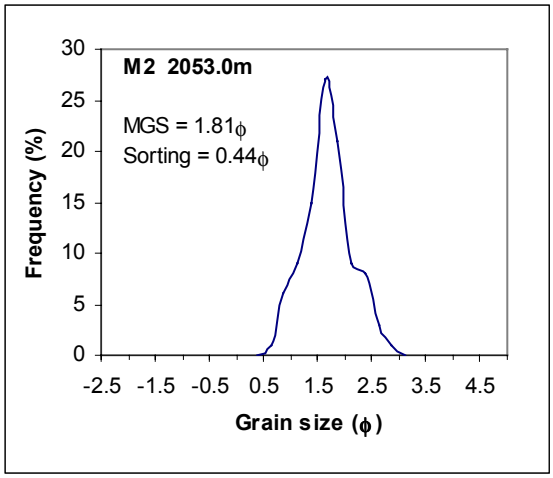

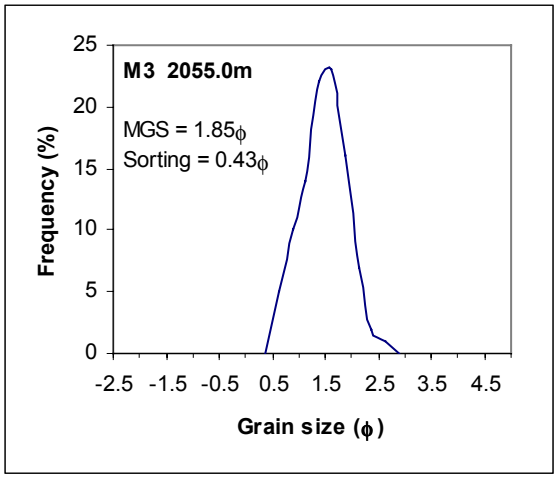

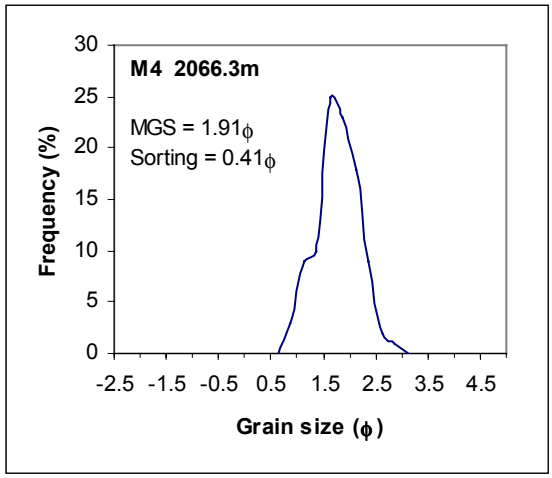

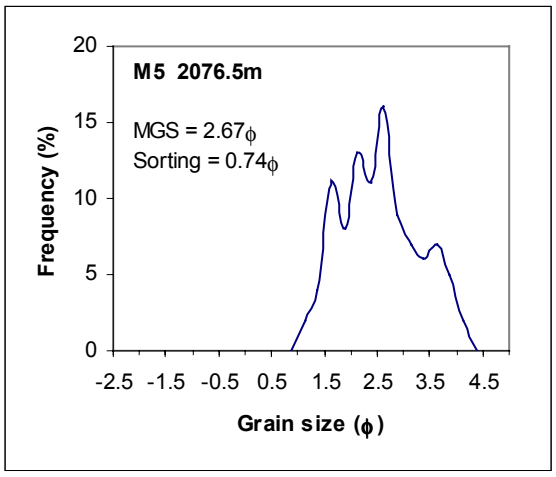

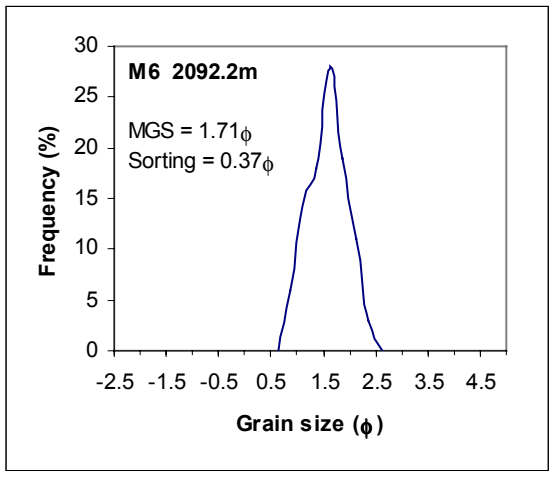

2094.0m – 2166.81m

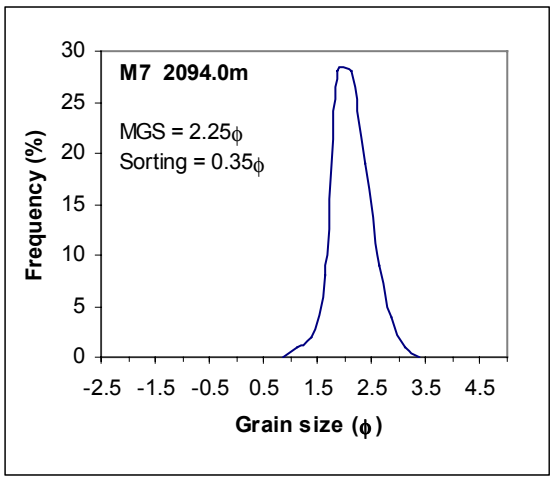

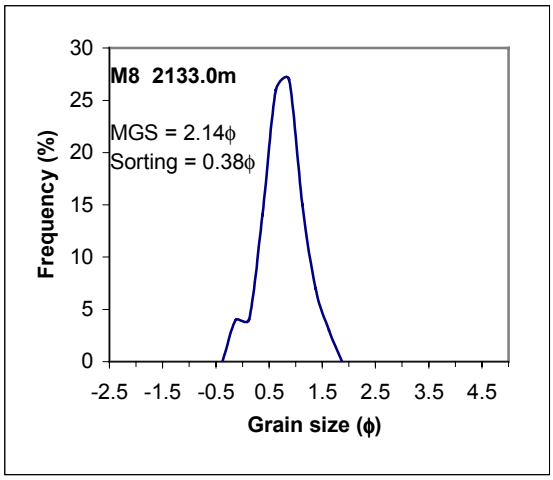

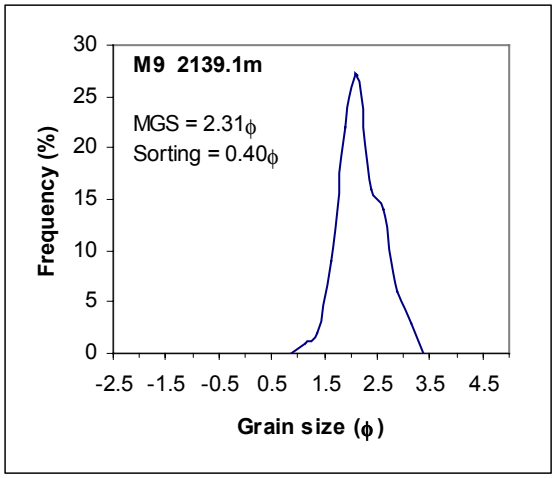

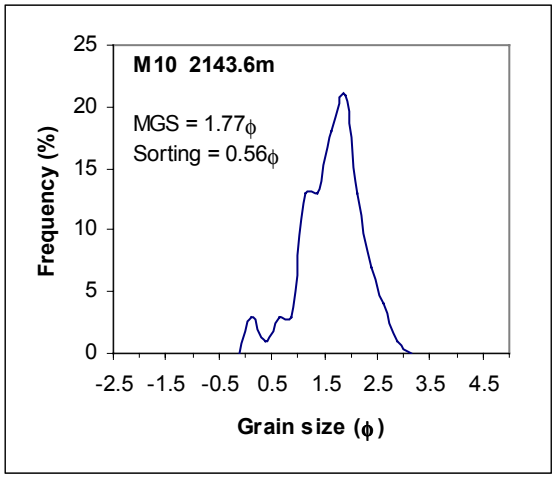

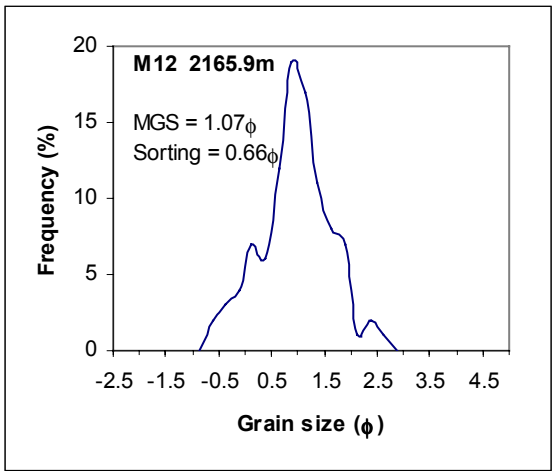

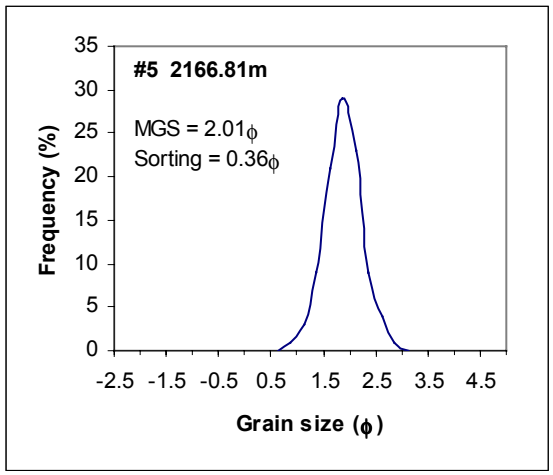

2171.19m – 2180.10m

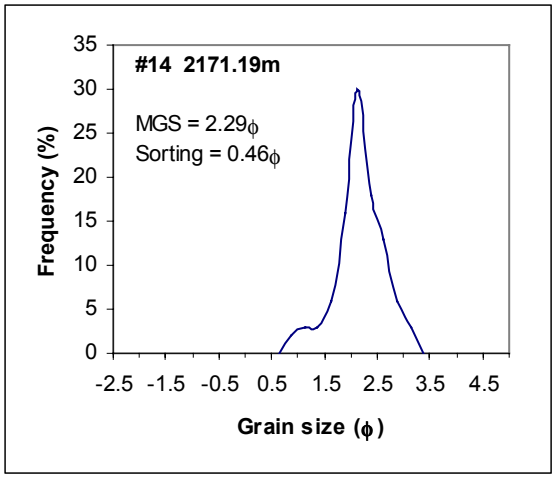

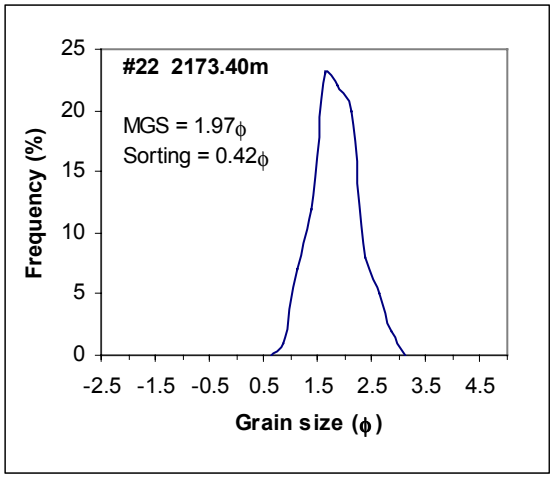

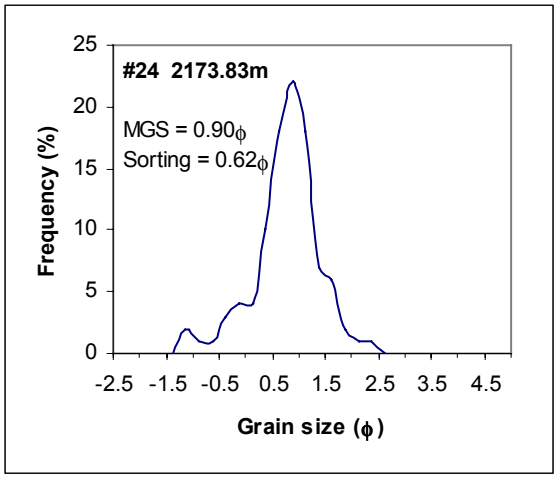

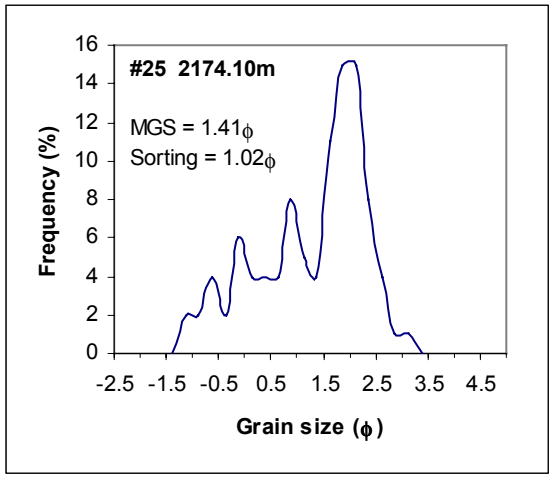

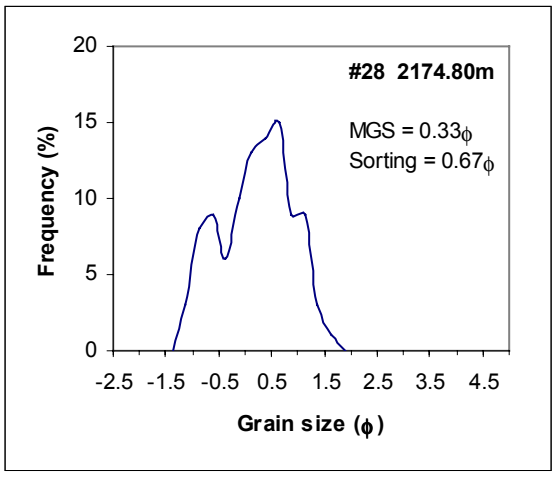

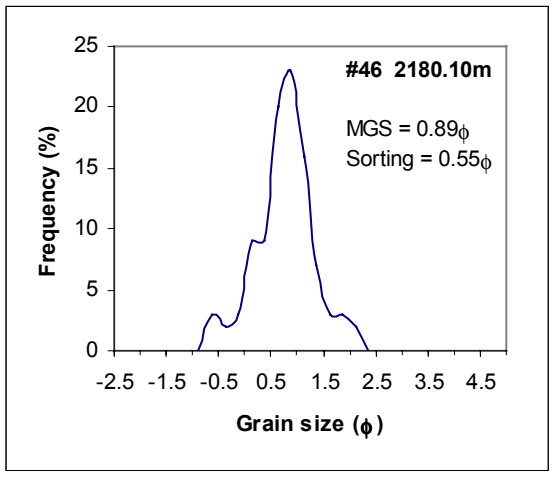

2182.92m – 2193.59m

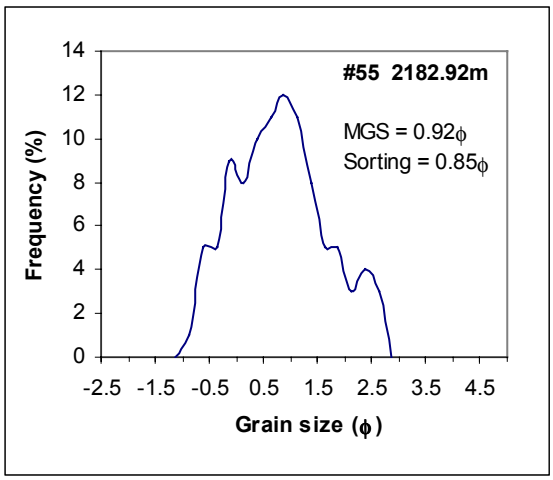

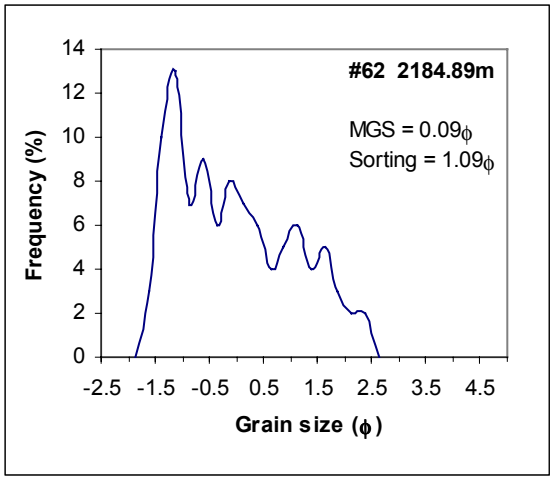

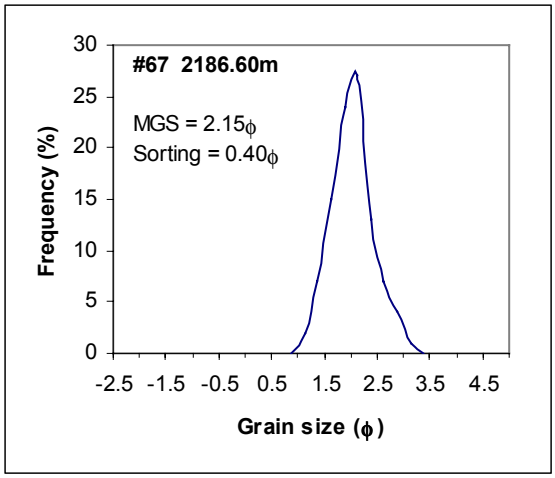

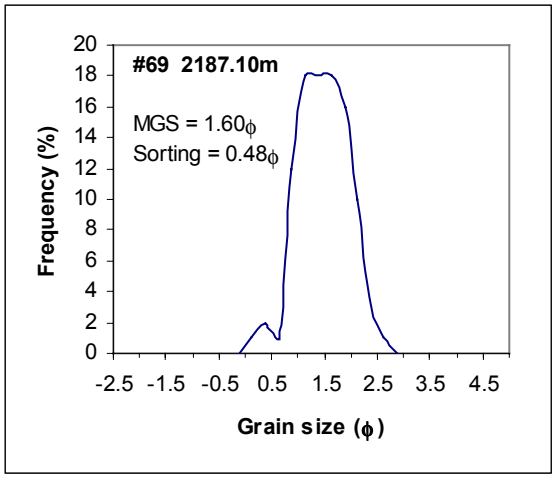

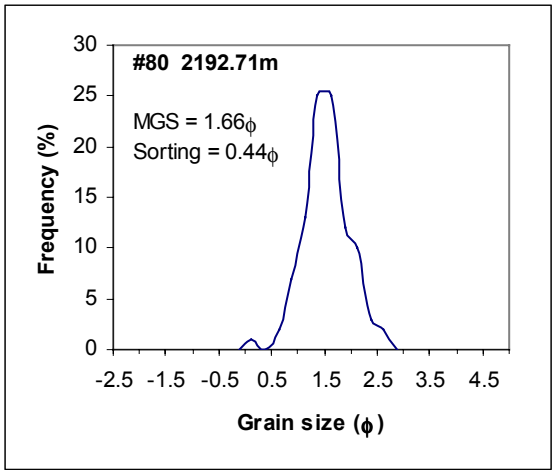

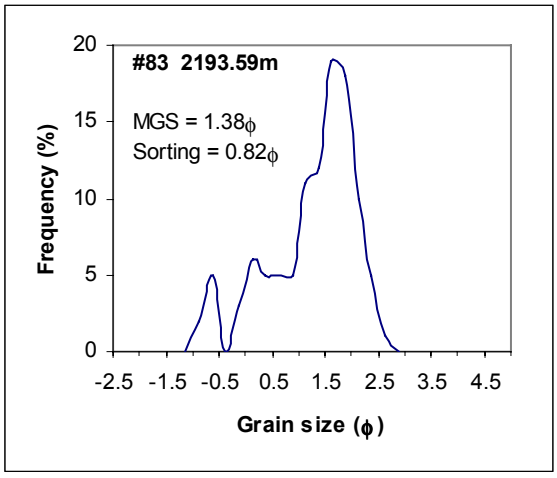

2230.0m – 2417.0m

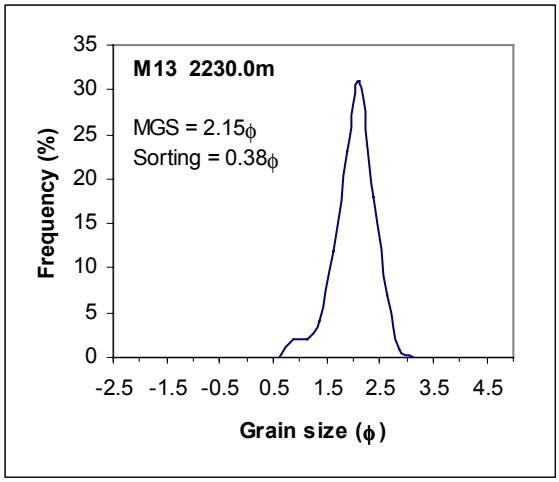

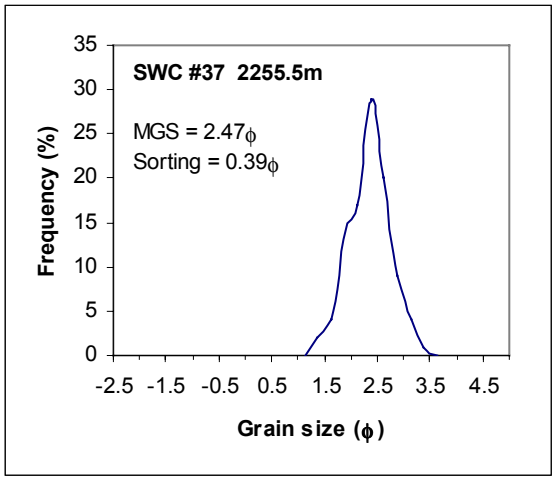

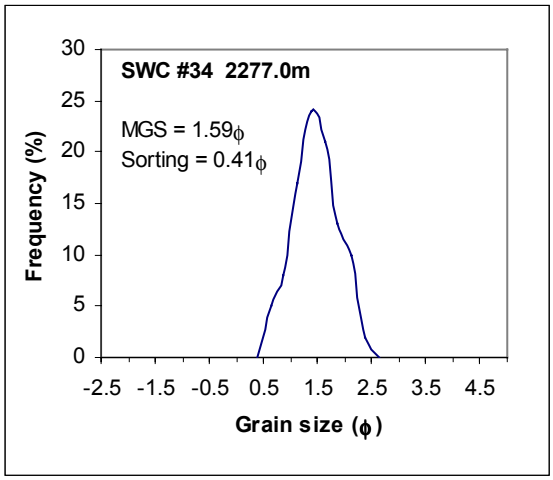

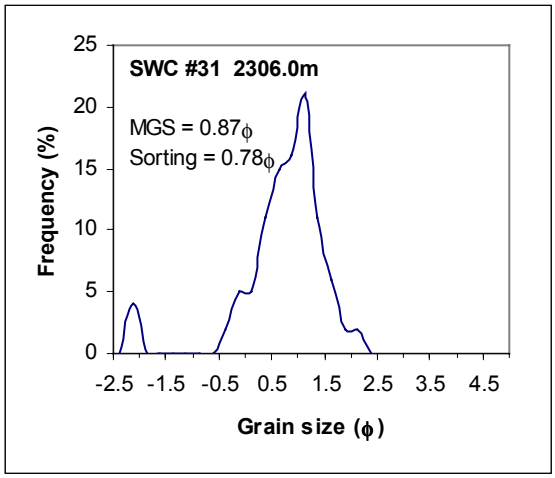

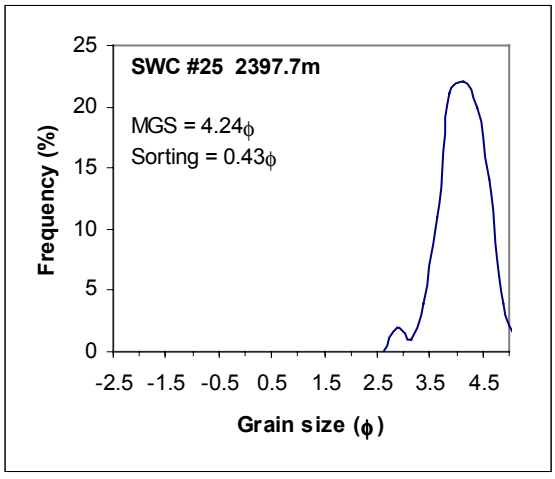

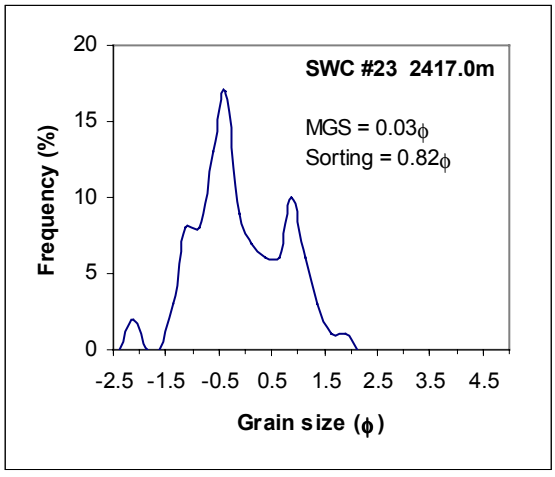

2437.5m – 2575.0m

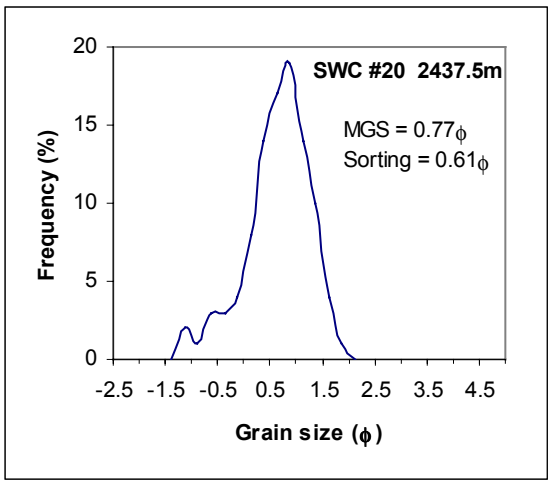

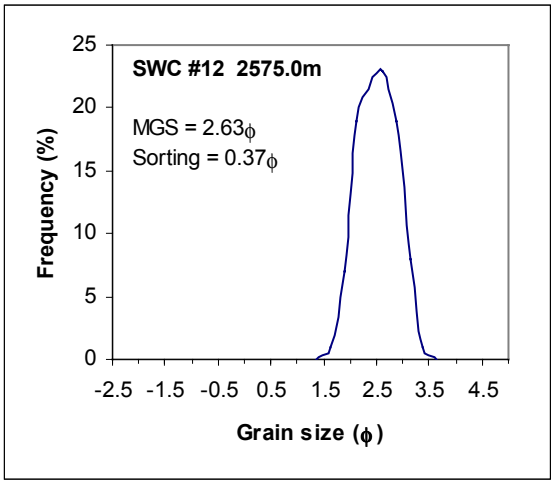

APPENDIX 3.

X-RAY DIFFRACTOGRAMS

Key to abbreviations:

An = ankerite

I = illite/mica

K = kaolinite

KCl = potassium chloride (contaminant)

KF = K-feldspar

Py = pyrite

Q = quartz

S = siderite

#5 2166.81m
Bulk rock

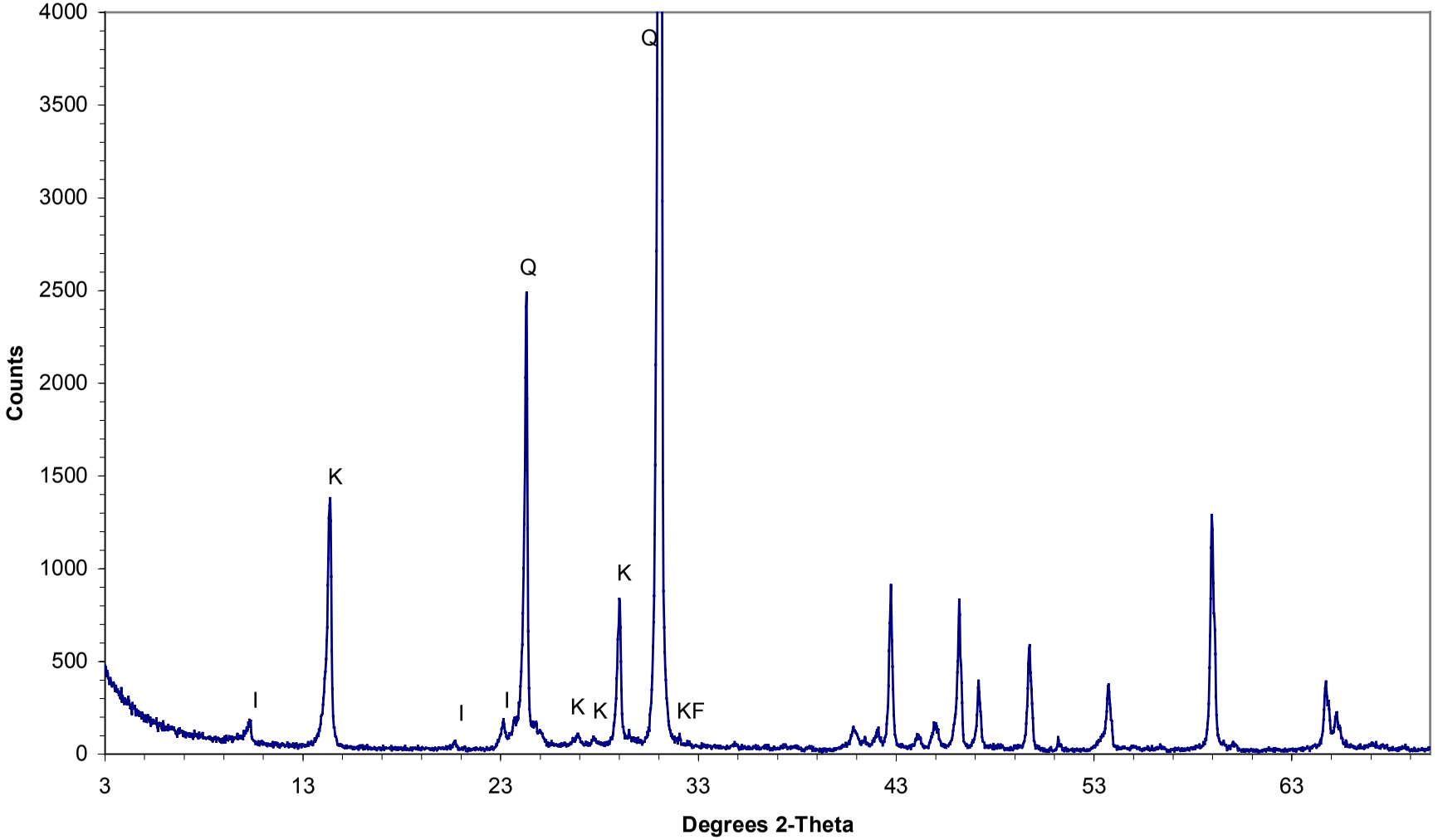

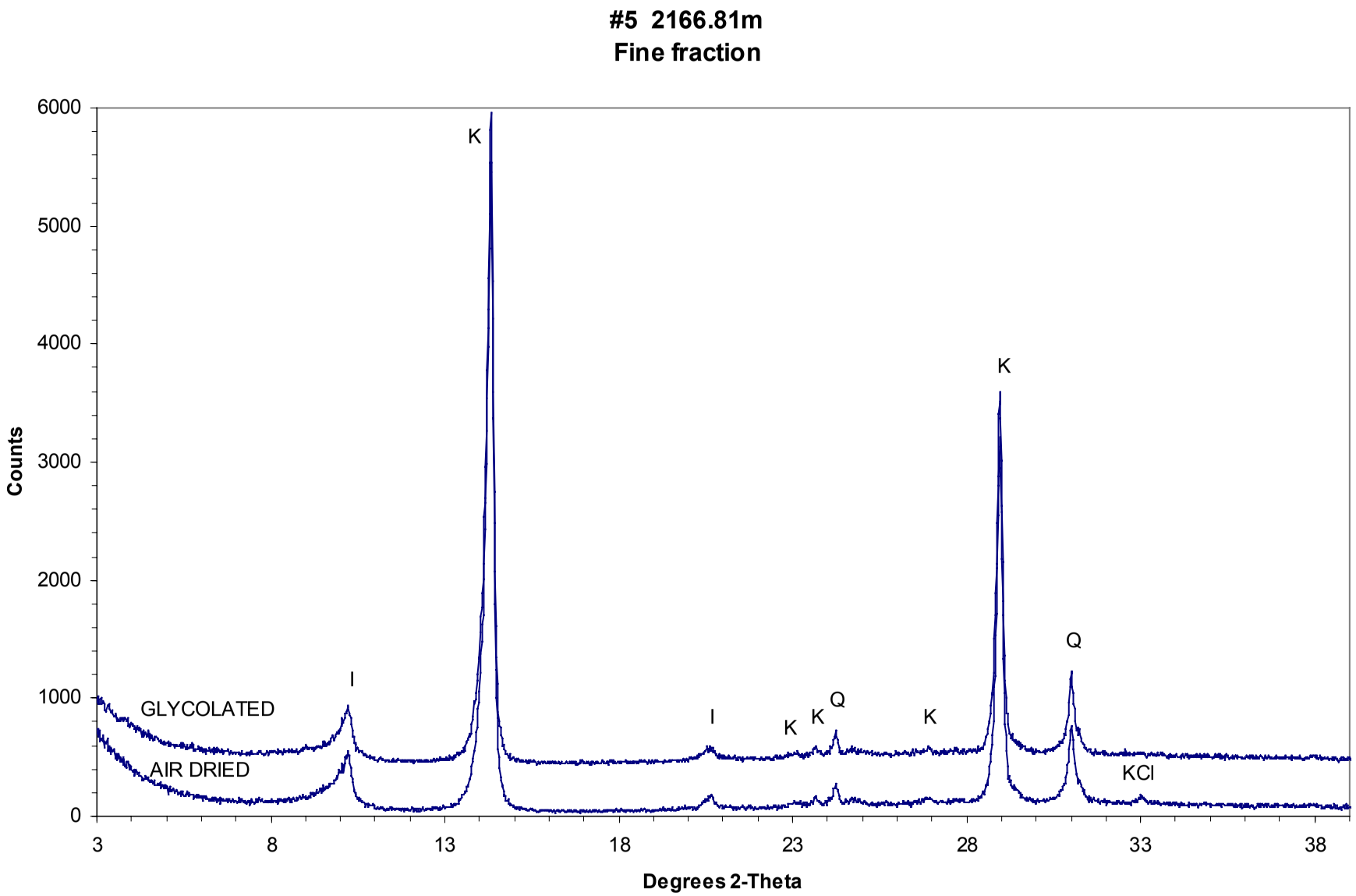
#5 2166.81m
Fine fraction
Counts
Degrees 2-Theta
GLYCOLATED
AIR DRIED
KCl
K
I
Q
6000
5000
4000
3000
2000
1000
0
3
8
13
18
23
28
33
38

#14 2171.19m
Bulk rock

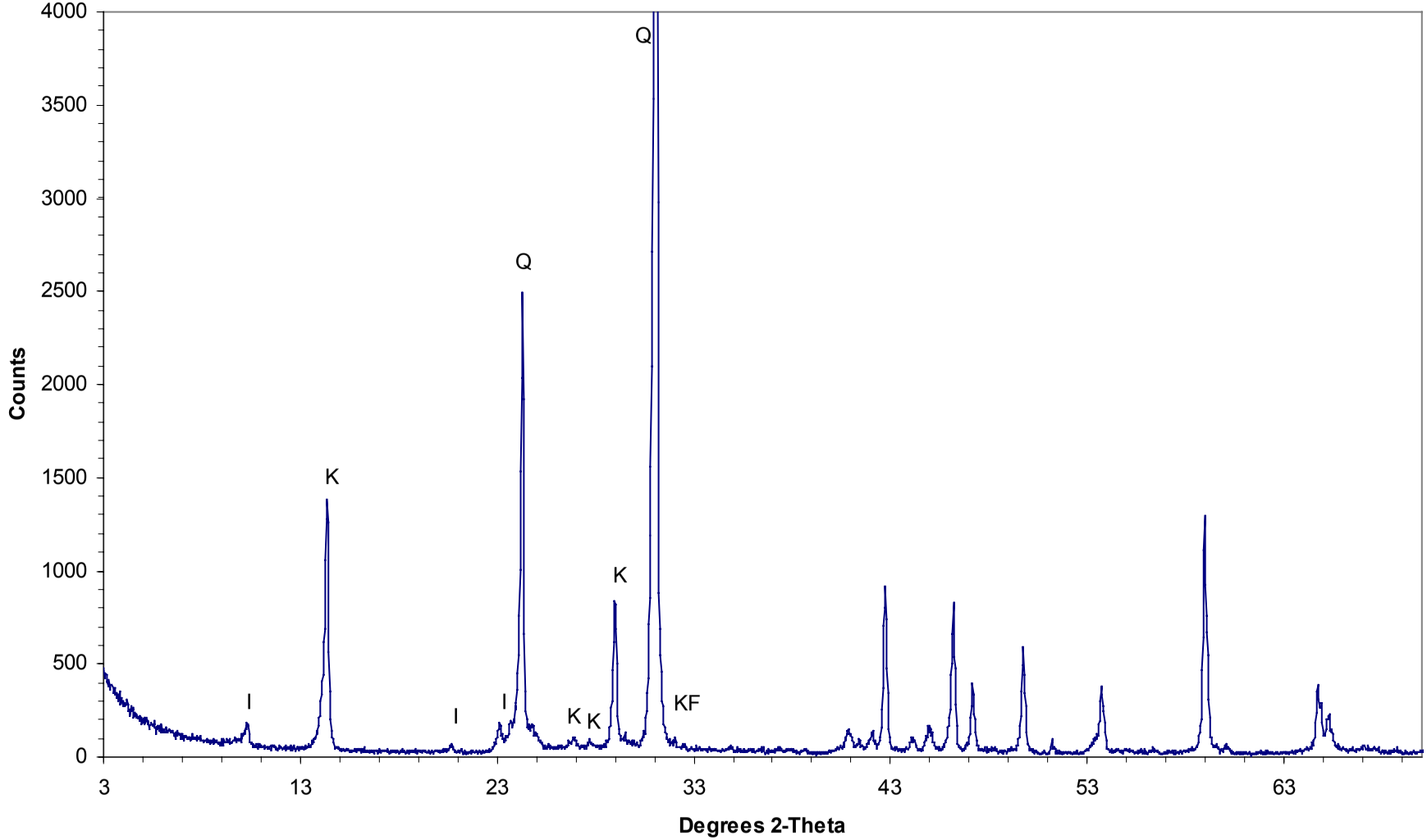

#22 2173.40m
Bulk rock

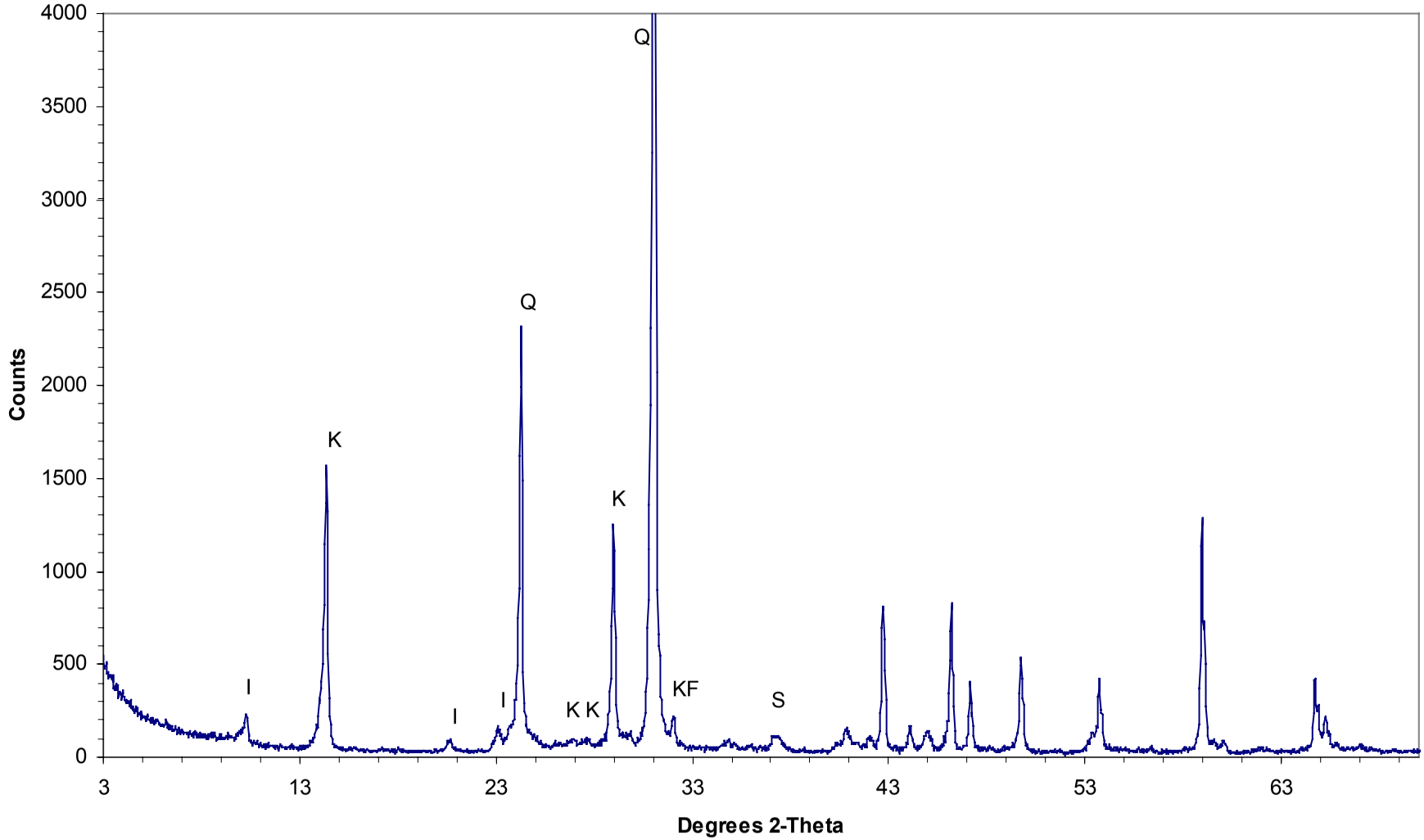

#24 2173.83m
Bulk rock

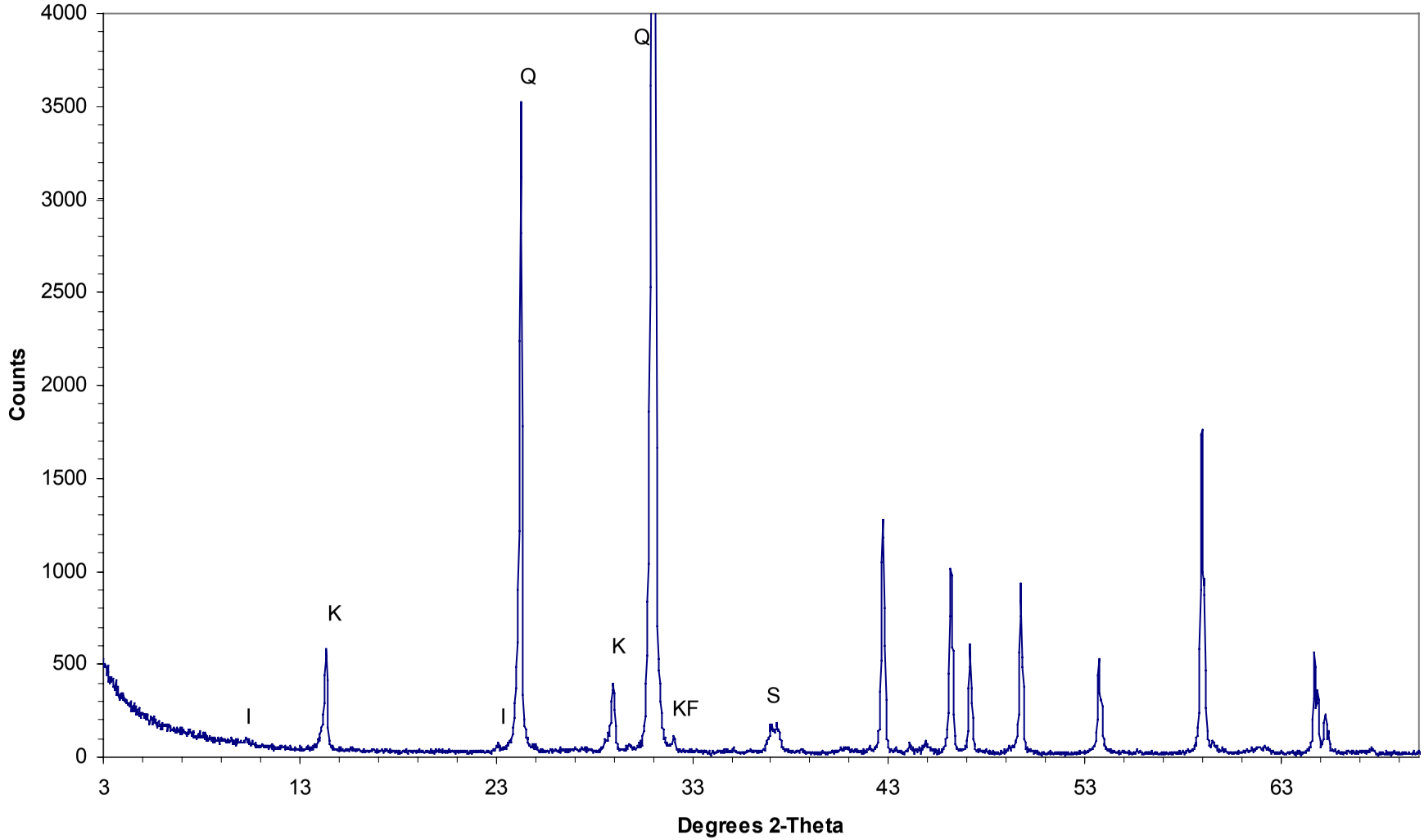

#25 2174.10m
Bulk rock

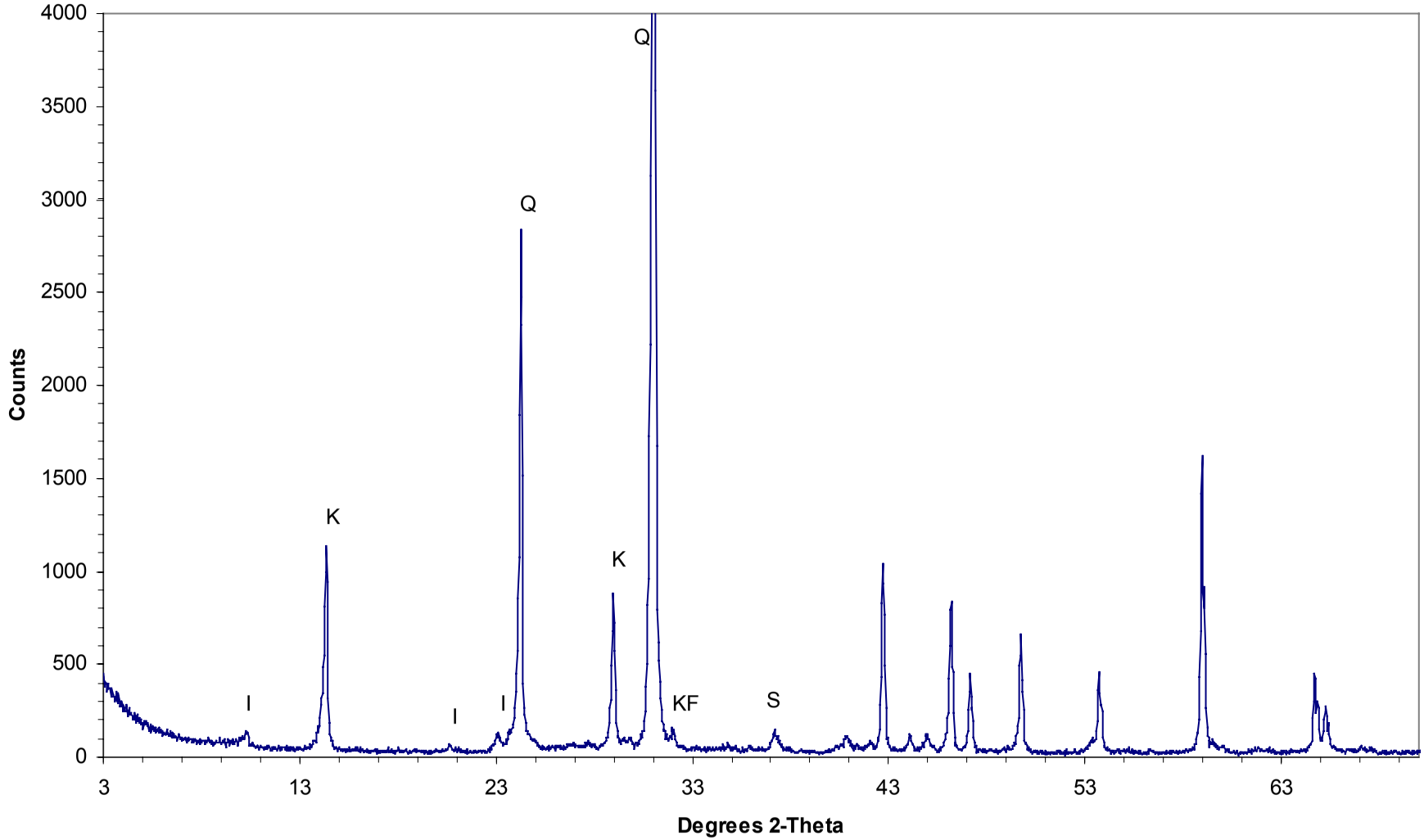

#28 2174.80m
Bulk rock

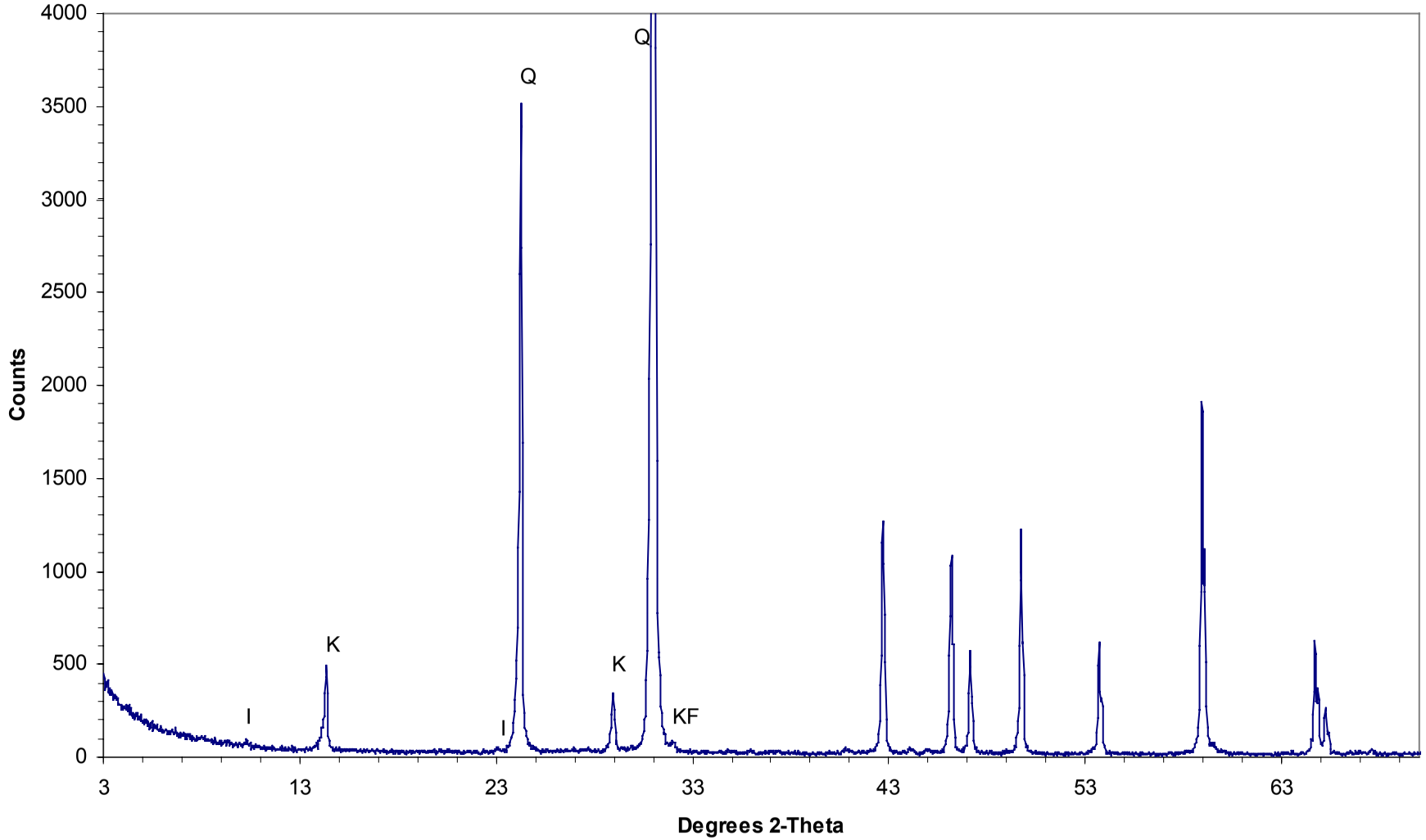

#46 2180.10m
Bulk rock

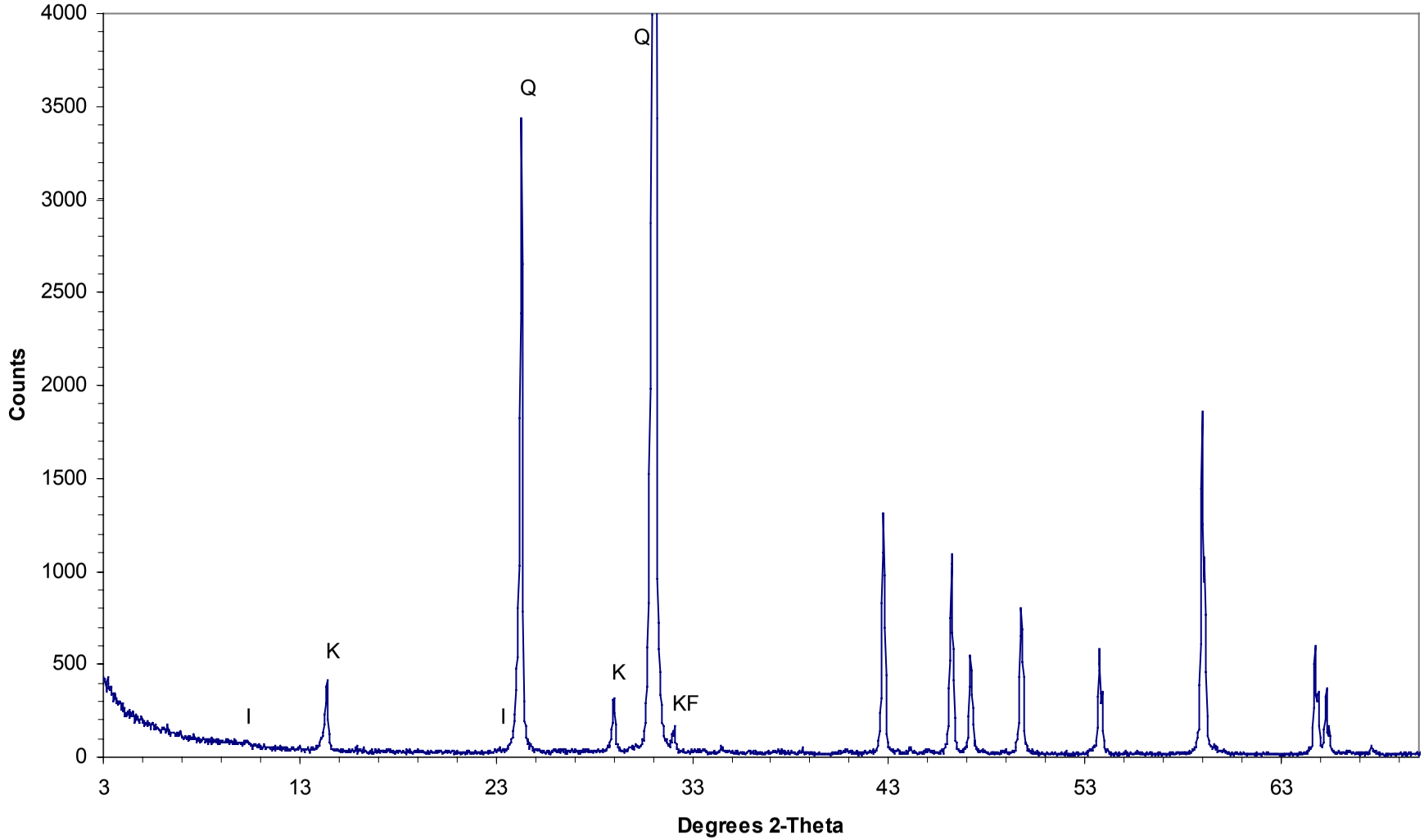

#55 2182.92m
Bulk rock

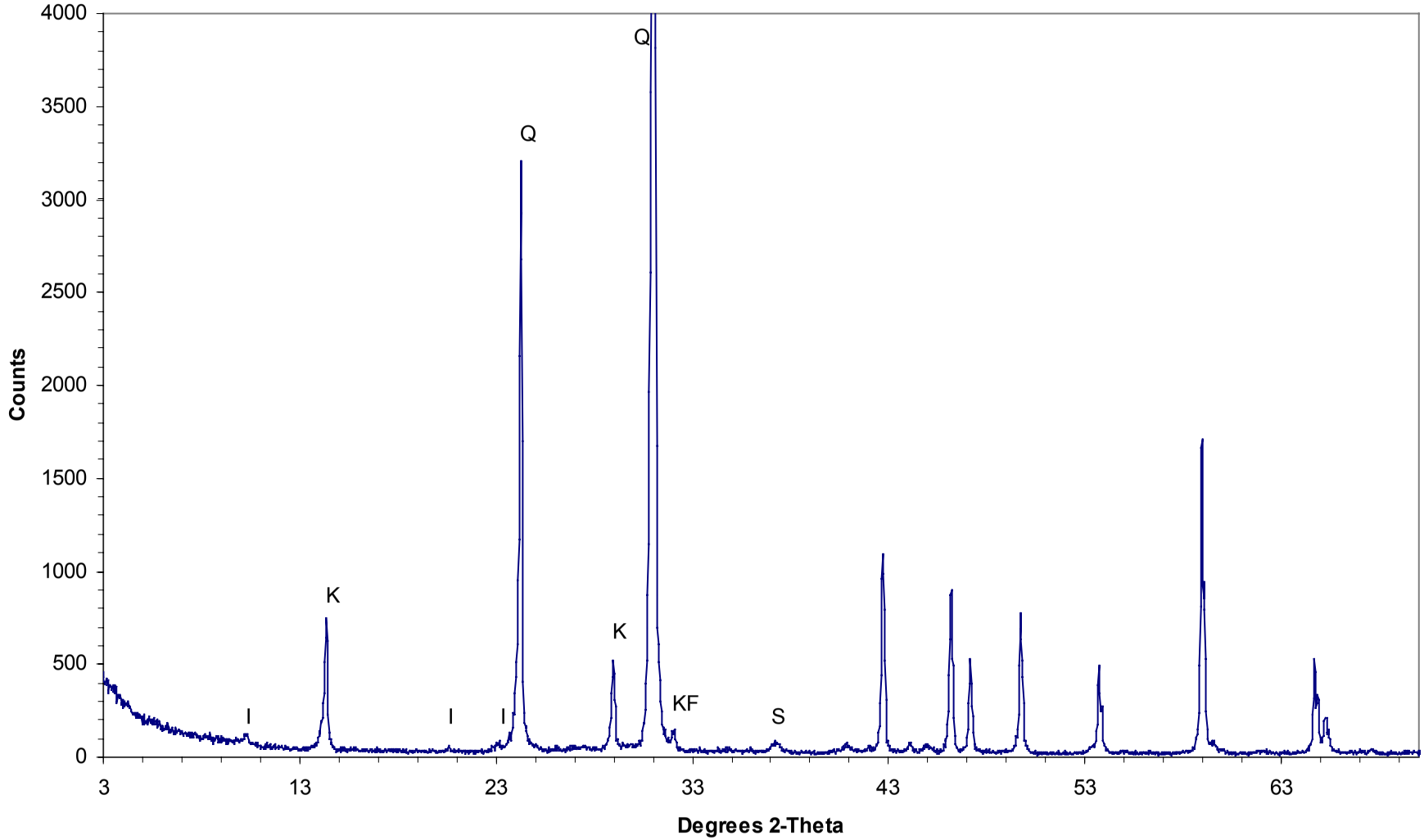

#62 2184.89m
Bulk rock

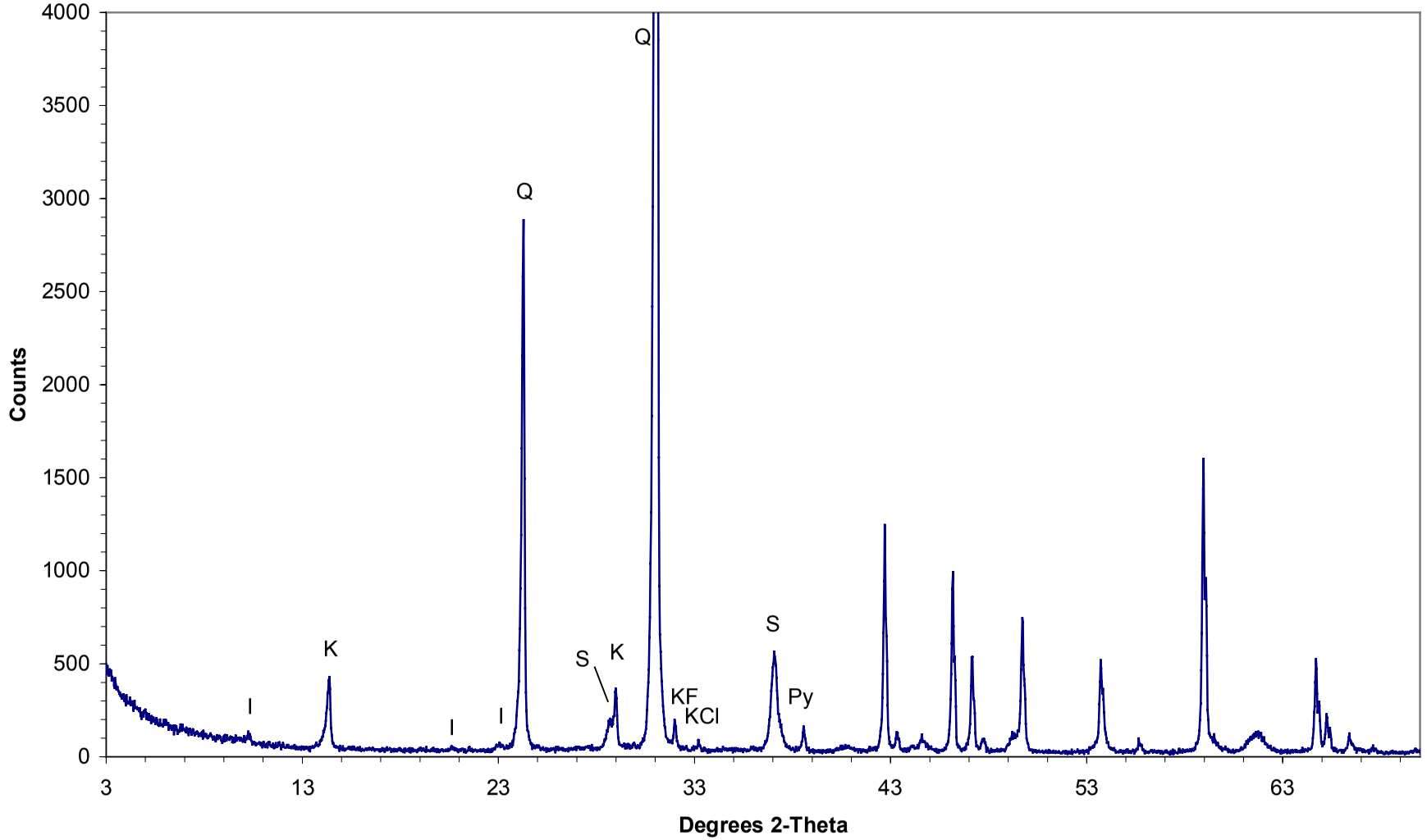

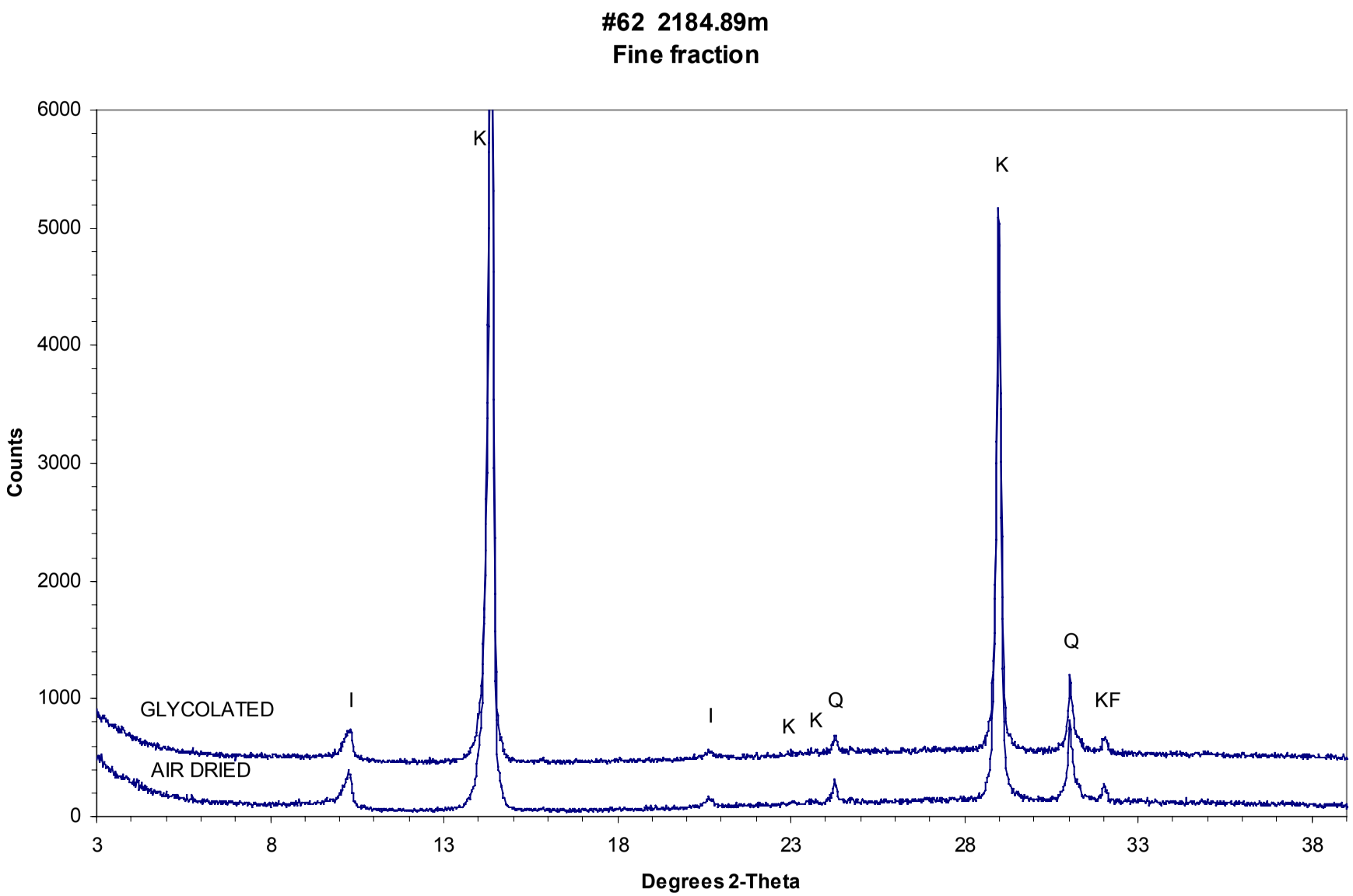
#62 2184.89m
Fine fraction
Counts
6000
5000
4000
3000
2000
1000
0
3
8
13
18
23
28
33
38
Degrees 2-Theta
GLYCOLATED
AIR DRIED
K
K
I
I
K
K
Q
Q
KF

#67 2186.60m
Bulk rock

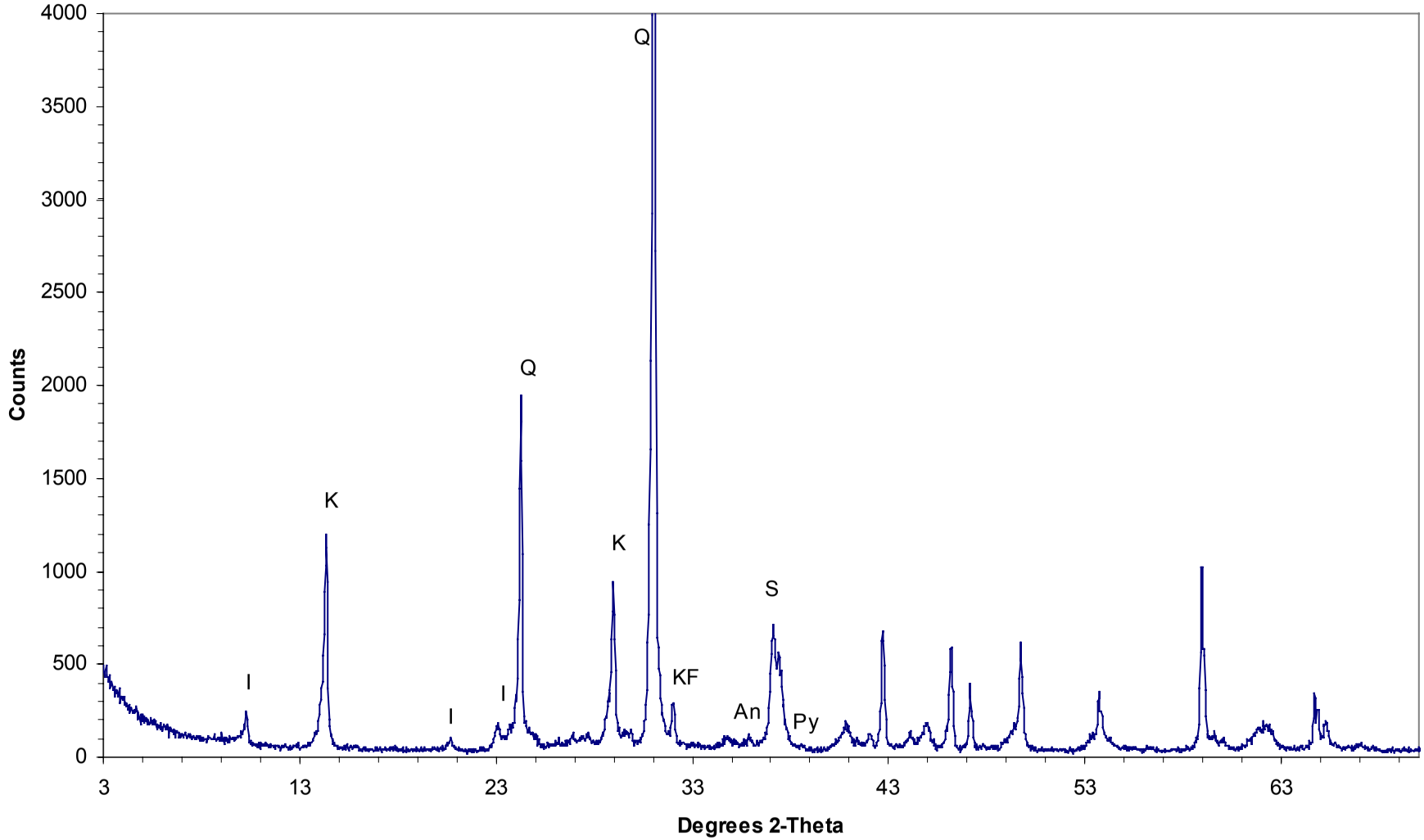

#69 2187.10m
Bulk rock

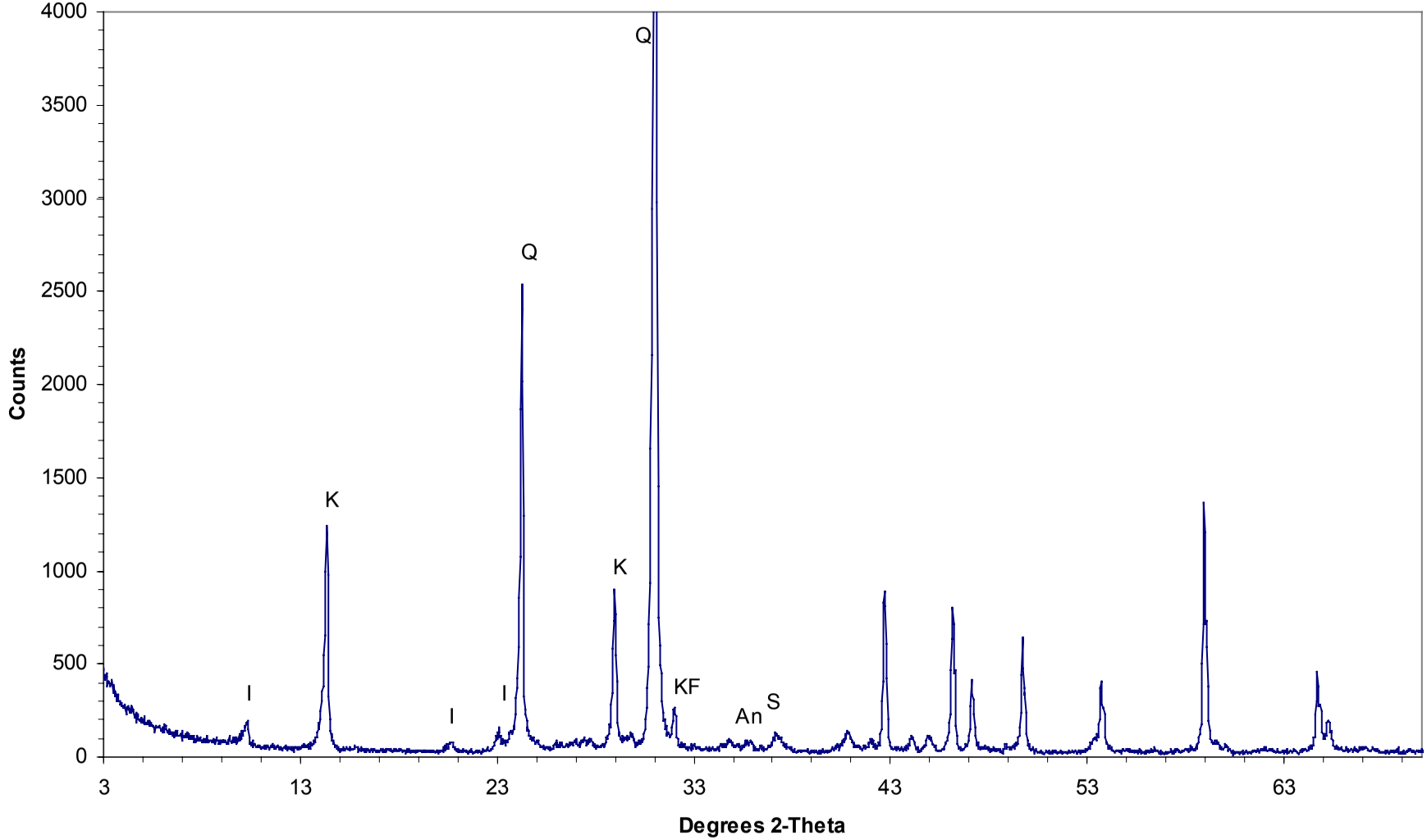

#80 2192.71m
Bulk rock

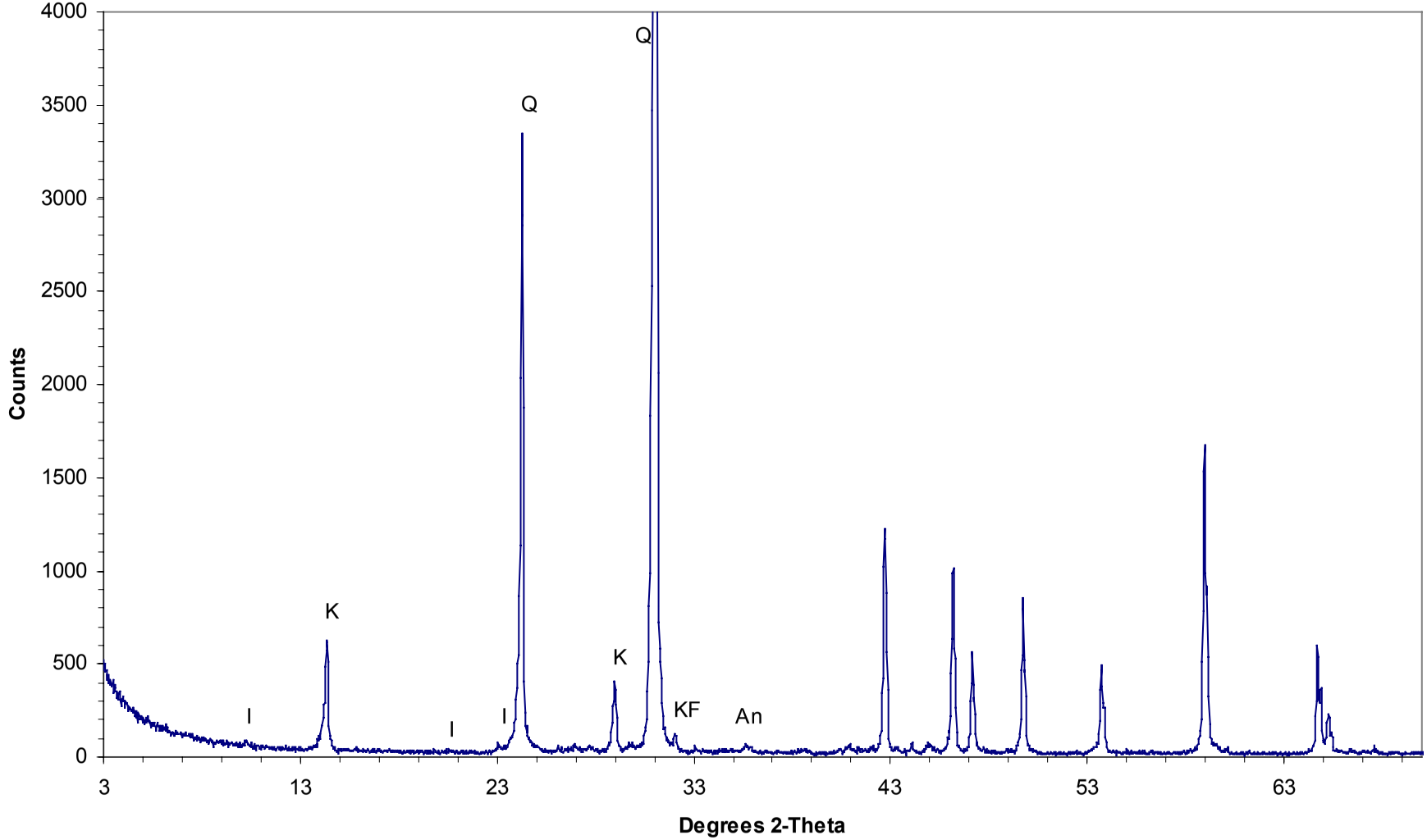

#83 2193.59m
Bulk rock

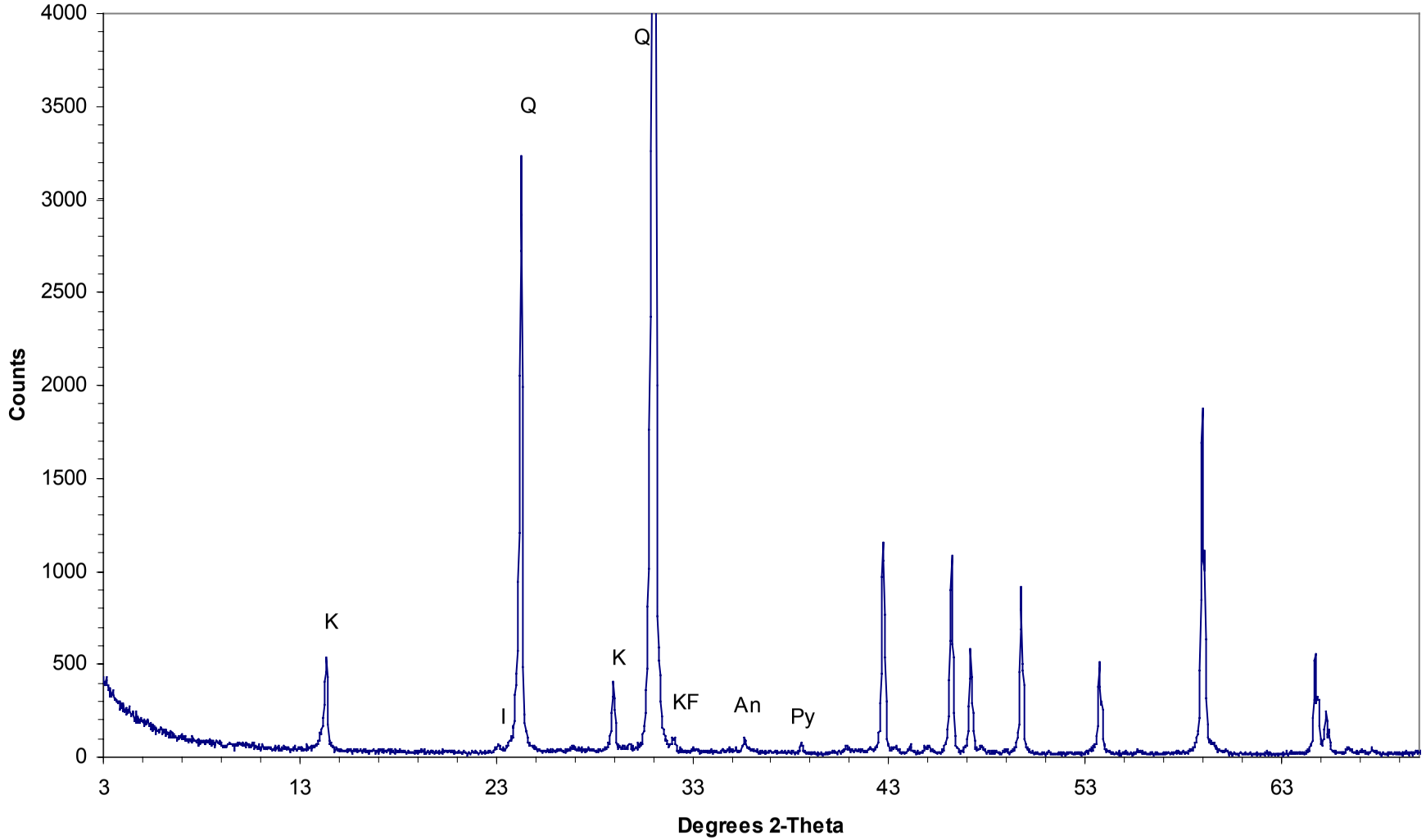

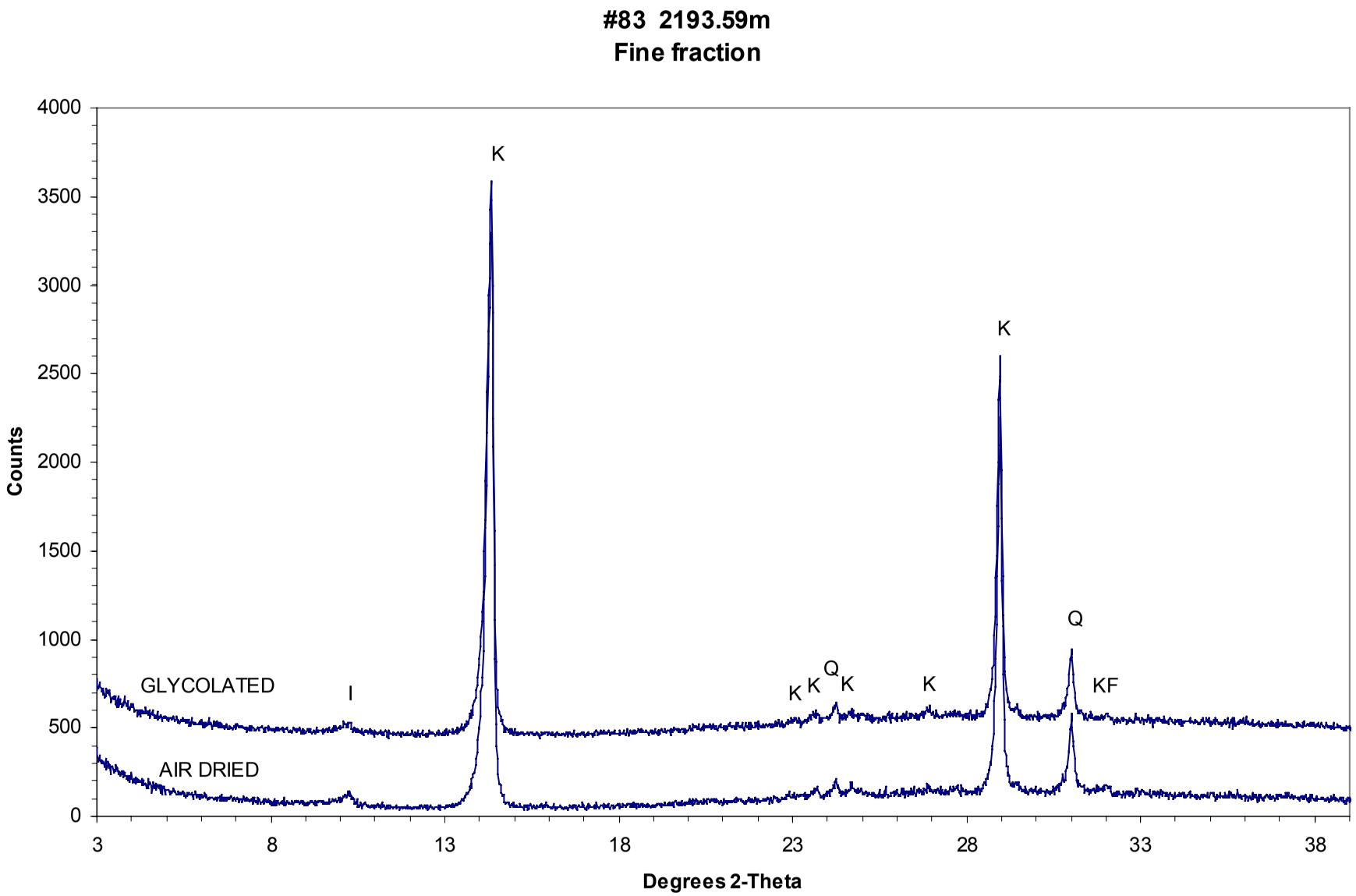
#83 2193.59m
Fine fraction
Counts
Degrees 2-Theta
GLYCOLATED
AIR DRIED
K
I
K K Q K
K
K
Q
KF
4000
3500
3000
2500
2000
1500
1000
500
0
3
8
13
18
23
28
33
38

APPENDIX 4.

PHOTOMICROGRAPHS

PLATE 1: M1 2050.0m

Rock classification: Sublitharenite

Texture:

Sedimentary structures:	Single, 4mm-thick sideritic lamination; otherwise massive
Sorting:	Well
Average grain size:	0.25mm (medium sand)
Roundness:	Angular-subrounded
Texture:	Grain supported
Packing /grain contacts:	Moderate/long, embayed, sutured
Macropore types:	Secondary mouldic porosity (dominant), secondary intragranular porosity, primary intergranular porosity
Core analyses:	Por. = 16.9%, Perm. = 1.72md, GD = 2.72g/cc

Composition:

Quartz (monocrystalline)	35.4%	Siderite (replacement)	8.0%
Quartz (polycrystalline)	4.3%	Ankerite (pore filling)	0.7%
Quartz overgrowths	0.3%	Ankerite (replacement)	3.6%
Chert	1.0%	Authigenic kaolinite (pf)	9.2%
K-feldspar	5.0%	Authigenic kaolinite (rpl)	14.7%
Volcanic rock fragments	0.7%	Authigenic illite (pore filling)	0.3%
Granitic rock fragments	0.3%	Authigenic illite (replacement)	1.7%
Metamorphic rock fragments	8.3%	Detrital clay	0.3%
Sedimentary rock fragments	2.0%	Primary porosity (intergranular)	0.3%
Mica	0.8%	Secondary porosity (mouldic)	1.5%
Organics	1.6%		

Comments: This sublitharenite was highly susceptible to authigenic clay formation and compaction on account of containing abundant micaceous/argillaceous rock fragments at the time of accumulation. Primary intergranular porosity has been almost completely eliminated by authigenic clay (kaolinite, illite) formation, ductile grain/authigenic clay compaction to form pseudomatrix, grain contact dissolution, and cementation by patchy ankerite and localised quartz overgrowths. A lamination is defined by patches of densely intergrown, finely-crystalline siderite up to 1.7mm long that replace coarse, altered biotite flakes. Scattered mouldic secondary pores occur where labile grains (mainly feldspar) have dissolved. The sample is mainly microporous and consequently has low permeability.

PLATE 1: M1 2050.0m

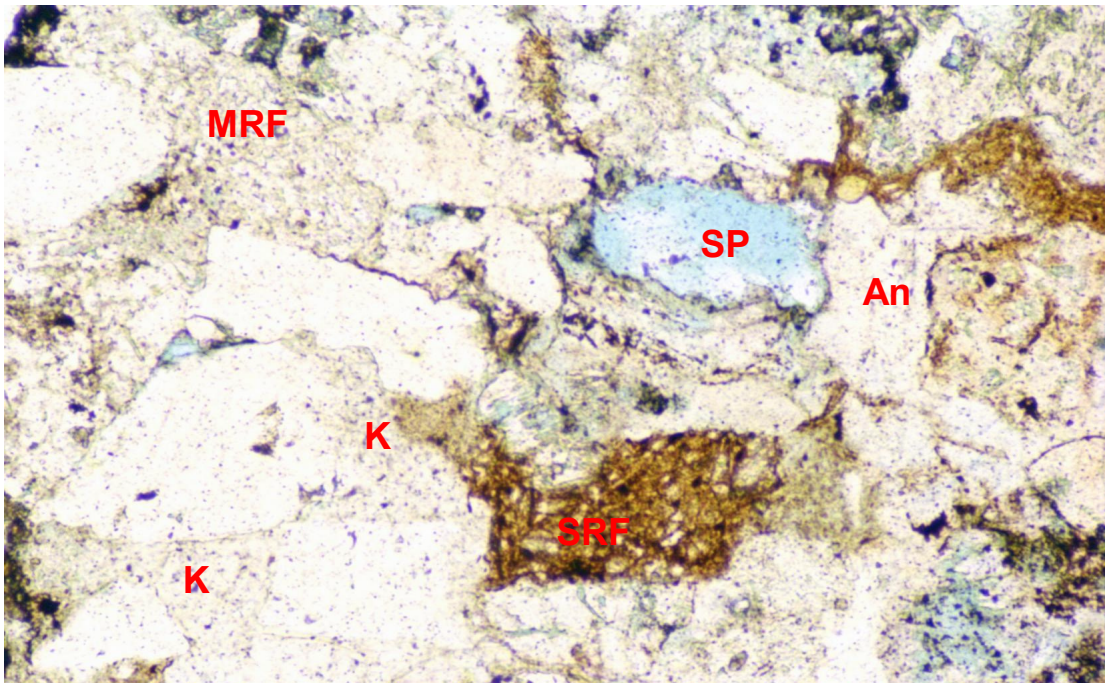

FIGURE 1 Plane polarised light
FIGURE 2 Crossed polarisers

0.2mm

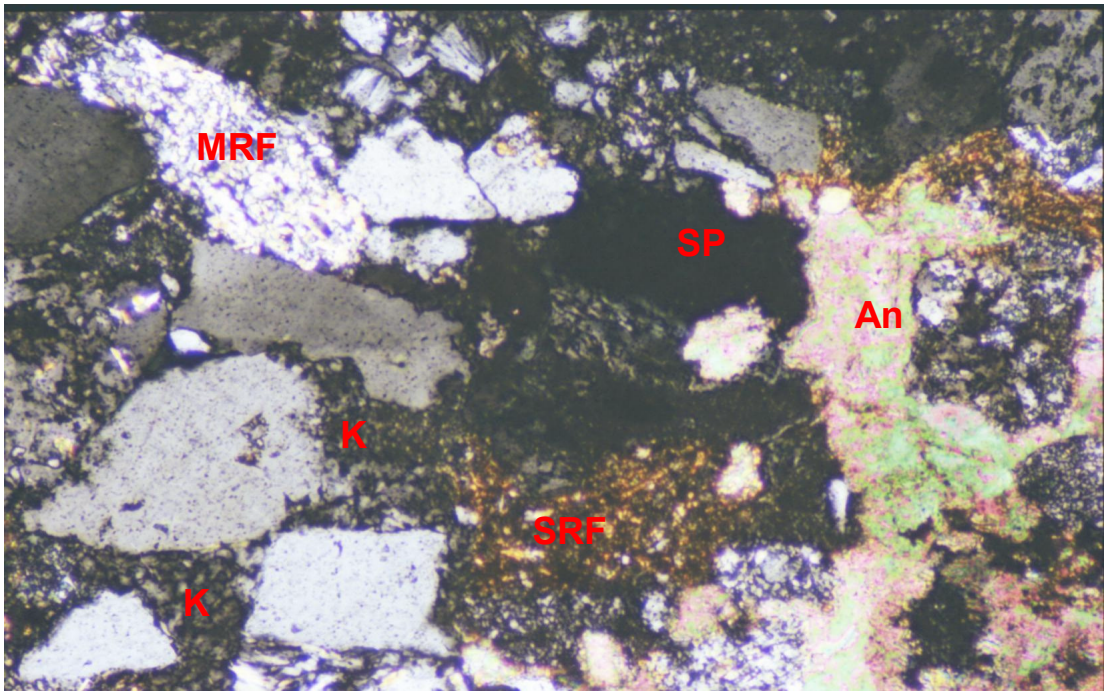

Intergranular porosity has been almost completely eliminated by authigenic kaolinite (K) formation, compaction of authigenic kaolinite, argillaceous sedimentary rock fragments (SRF) and micaceous metamorphic rock fragments (MRF), and patchy, coarsely-crystalline ankerite (An) cementation. Visible porosity is mainly accounted for by widely scattered, hence poorly interconnected secondary mouldic pores (SP) that have formed by labile grain dissolution.

PLATE 2: M2 2053.0m

Rock classification: Sublitharenite

Texture:

Sedimentary structures: Massive

Sorting: Well

Average grain size: 0.28mm (medium sand)

Roundness: Subangular-subrounded

Texture: Grain supported

Packing /grain contacts: Moderate/long, embayed, sutured

Macropore types: Primary intergranular porosity, secondary intergranular porosity, secondary mouldic porosity, secondary intragranular porosity

Core analyses: Por. = 19.7%, Perm. = 17.5md, GD = 2.67g/cc

Composition:

Quartz (monocrystalline)	43.6%	Siderite (replacement)	4.0%
Quartz (polycrystalline)	3.3%	Ankerite (replacement)	1.3%
Quartz overgrowths	3.8%	Authigenic kaolinite (pf)	4.2%
Chert	1.3%	Authigenic kaolinite (rpl)	10.6%
K-feldspar	3.0%	Authigenic illite (pore filling)	0.4%
Volcanic rock fragments	1.1%	Authigenic illite (replacement)	2.4%
Metamorphic rock fragments	6.9%	Primary porosity (intergranular)	3.0%
Sedimentary rock fragments	2.3%	Secondary porosity (intergran)	5.0%
Mica	0.3%	Secondary porosity (mouldic)	1.8%
Organics	0.7%	Secondary porosity (intragran)	0.7%
Leucoxene	0.3%		

Comments: This sample contains more quartz than the previous sample and consequently has significantly more primary intergranular porosity. Quartz overgrowths are common between juxtaposed quartz grains, but generally only partly occlude all available intergranular space. Primary porosity is supplemented by common secondary pores that occur where labile grains (mainly K-feldspar) have partly to completely dissolved. Significant porosity reduction has resulted mainly from authigenic kaolinite formation, ductile grain/authigenic clay compaction, and localised grain contact dissolution and quartz overgrowth cementation.

PLATE 2: M2 2053.0m

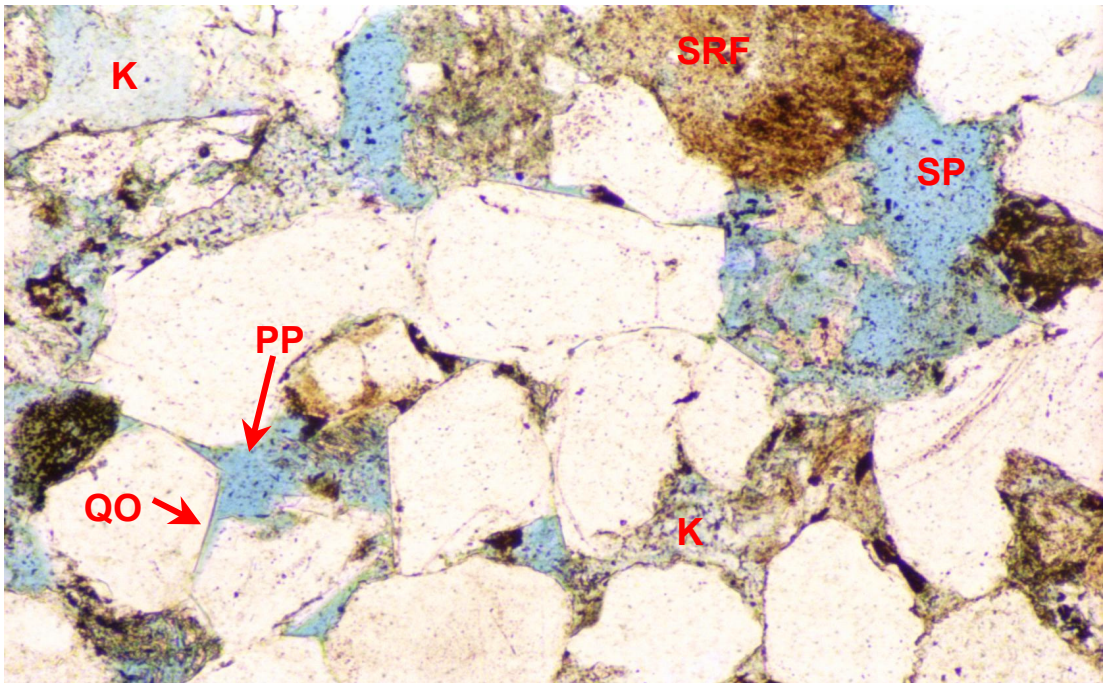

FIGURE 1 Plane polarised light
FIGURE 2 Crossed polarisers

0.2mm

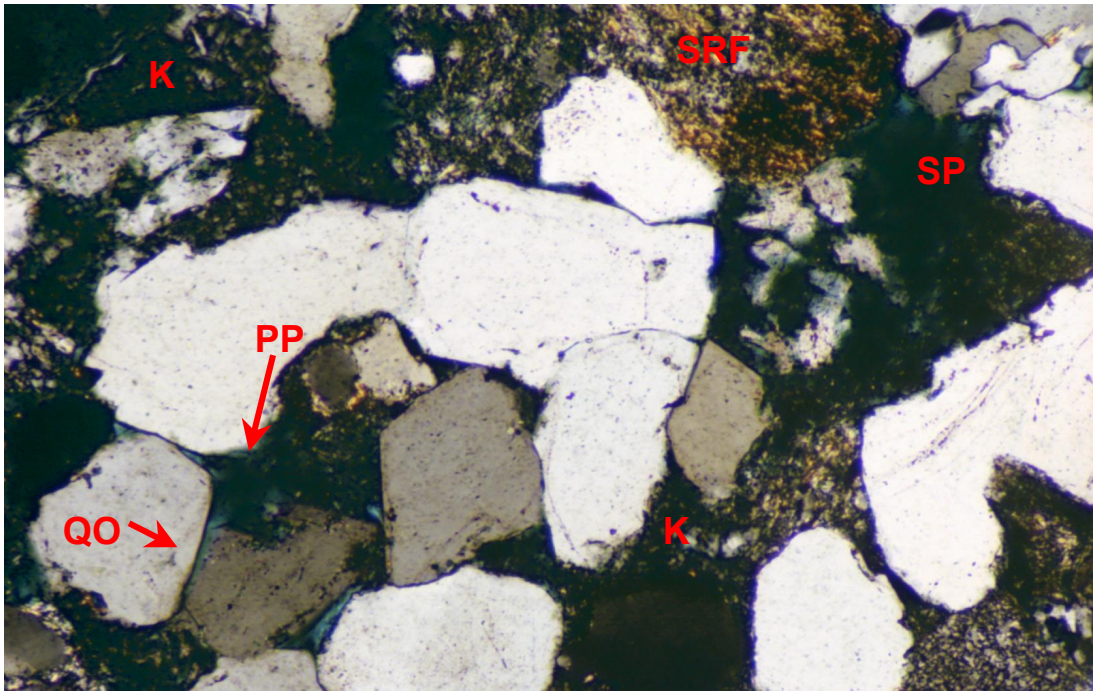

Good primary intergranular porosity (PP) is preserved between juxtaposed quartz grains, despite cementation by quartz overgrowths (QO). An oversized secondary pore (SP) occurs where a K-feldspar grain has largely dissolved. Microporous authigenic kaolinite (K) pseudomatrix is the altered remnant of compacted micaceous/argillaceous grains. An argillaceous sedimentary rock fragment (SRF) is also marked.

PLATE 3: M3 2055.0m

Rock classification: Sublitharenite

Texture:

Sedimentary structures: Massive

Sorting: Well

Average grain size: 0.28mm (medium sand)

Roundness: Subangular-subrounded

Texture: Grain supported

Packing /grain contacts: Moderate/long, embayed, microstylolitic

Grain coating: 3% (fine siderite)

Macropore types: Primary intergranular porosity, secondary intergranular porosity, secondary mouldic porosity, secondary intragranular porosity

Core analyses: Por. = 19.6%, Perm. = 13.7md, GD = 2.68g/cc

Composition:

Quartz (monocrystalline)	40.6%	Siderite (replacement)	6.7%
Quartz (polycrystalline)	4.8%	Ankerite (replacement)	2.6%
Quartz overgrowths	2.7%	Authigenic kaolinite (pf)	5.0%
Chert	1.9%	Authigenic kaolinite (rpl)	11.5%
K-feldspar	4.4%	Authigenic illite (pore filling)	0.4%
Volcanic rock fragments	1.0%	Authigenic illite (replacement)	1.5%
Metamorphic rock fragments	8.3%	Primary porosity (intergranular)	1.6%
Sedimentary rock fragments	1.6%	Secondary porosity (intergran)	1.8%
Mica	0.3%	Secondary porosity (mouldic)	1.9%
Organics	0.4%	Secondary porosity (intragran)	0.7%
Leucoxene	0.3%		

Comments: Intergranular porosity in this sublitharenite has been largely eliminated by authigenic kaolinite formation, ductile grain/authigenic clay compaction, and localised grain contact dissolution and quartz overgrowth cementation. Minor primary intergranular porosity is supplemented by scattered secondary pores that are the result of labile grain dissolution. Pore throats are largely chocked by authigenic clay, compacted ductile grains and fine siderite, hence permeability is relatively low.

PLATE 3: M3 2055.0m

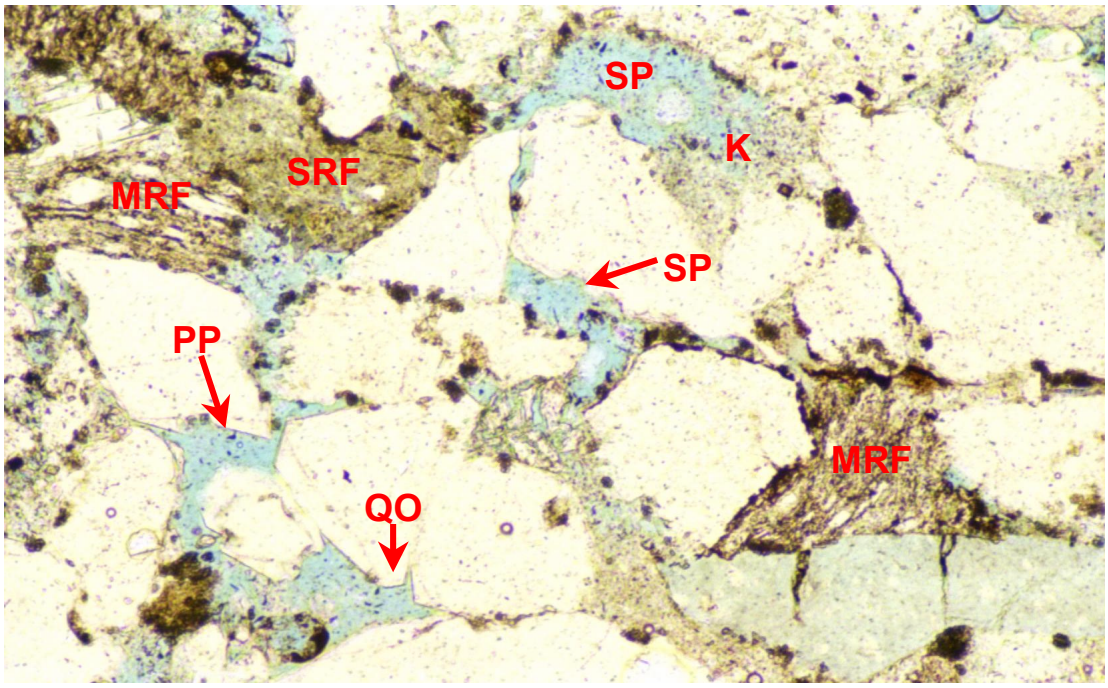

FIGURE 1 Plane polarised light
FIGURE 2 Crossed polarisers

0.2mm

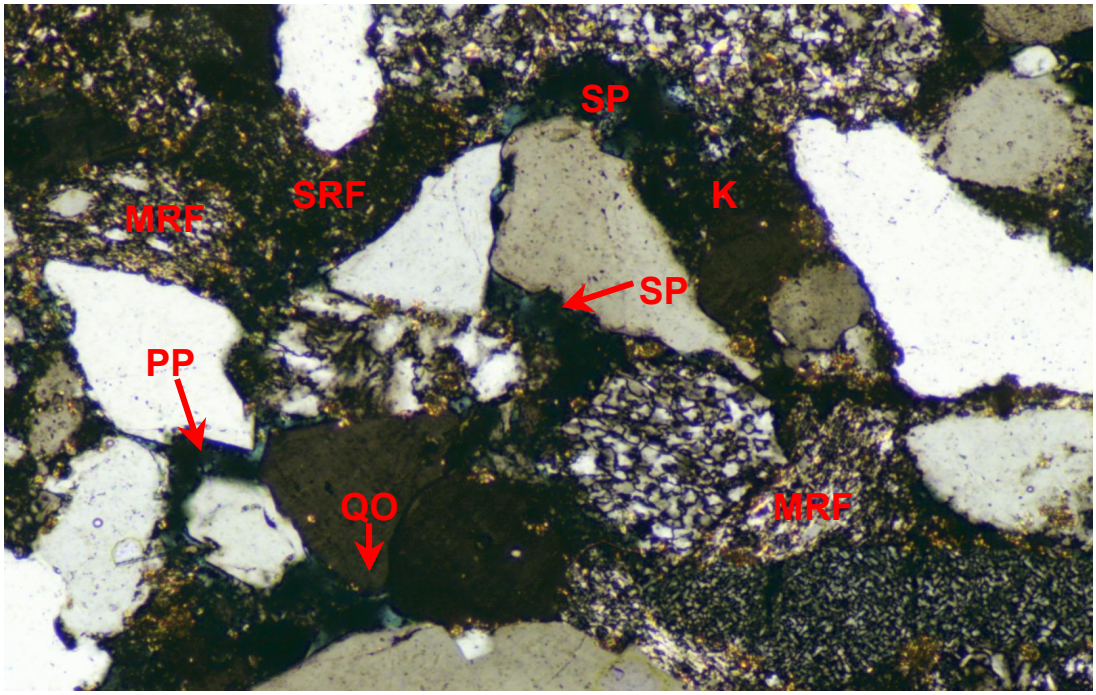

Localised primary porosity (PP) is preserved between juxtaposed, quartz overgrowth (QO)-cemented quartz grains, and secondary pores (SP) have formed by labile grain dissolution. Intergranular porosity has been largely eliminated by the compactional deformation of metasedimentary rock fragments (MRF) and argillaceous sedimentary rock fragments (SRF). One secondary pore is partly filled by authigenic kaolinite (K).

PLATE 4: M4 2066.3m

Rock classification: Sublitharenite

Texture:

Sedimentary structures:	Localised wispy patches of clay matrix; otherwise massive
Sorting:	Well
Average grain size:	0.27mm (medium sand)
Roundness:	Subangular-subrounded
Texture:	Grain supported
Packing /grain contacts:	Moderate/long, embayed
Macropore types:	Primary intergranular porosity, secondary intergranular porosity, secondary mouldic porosity, secondary intragranular porosity
Core analyses:	Por. = 21.3%, Perm. = 46.3md, GD = 2.65g/cc

Composition:

Quartz (monocrystalline)	41.9%	Siderite (replacement)	0.8%
Quartz (polycrystalline)	4.3%	Calcite (pore filling)	5.2%
Quartz overgrowths	2.9%	Calcite (replacement)	1.1%
Chert	1.1%	Authigenic kaolinite (rpl)	11.5%
K-feldspar	3.5%	Authigenic illite (replacement)	0.7%
Volcanic rock fragments	1.5%	Detrital clay	2.8%
Metamorphic rock fragments	8.8%	Primary porosity (intergranular)	3.7%
Sedimentary rock fragments	2.0%	Secondary porosity (intergran)	4.0%
Mica	0.5%	Secondary porosity (mouldic)	1.8%
Heavy minerals	0.3%	Secondary porosity (intragran)	1.3%
Organics	0.3%		

Comments: Significant intergranular porosity reduction is the result of localised quartz overgrowth and patchy, coarsely-crystalline/poikilotopic calcite cementation, authigenic clay formation, ductile grain/authigenic clay compaction and grain contact dissolution. However, the sandstone still contains common primary intergranular pores that provide fair interconnection for scattered secondary pores that have formed by partial to complete dissolution of K-feldspar and labile rock fragments.

PLATE 4: M4 2066.3m

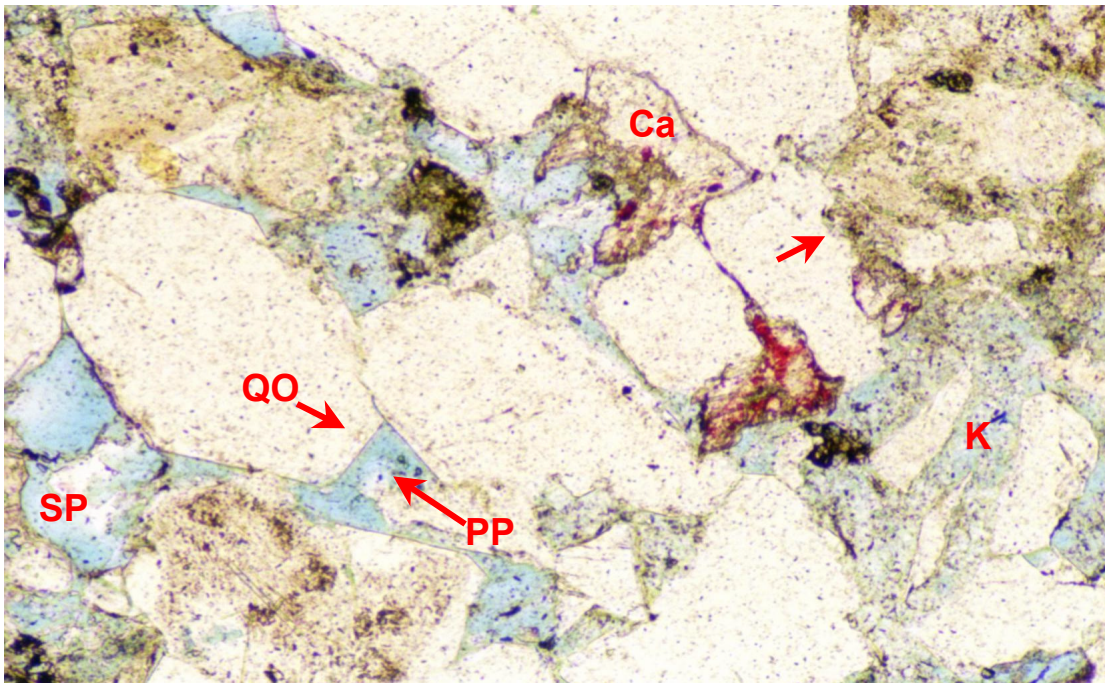

FIGURE 1 Plane polarised light
FIGURE 2 Crossed polarisers

0.2mm

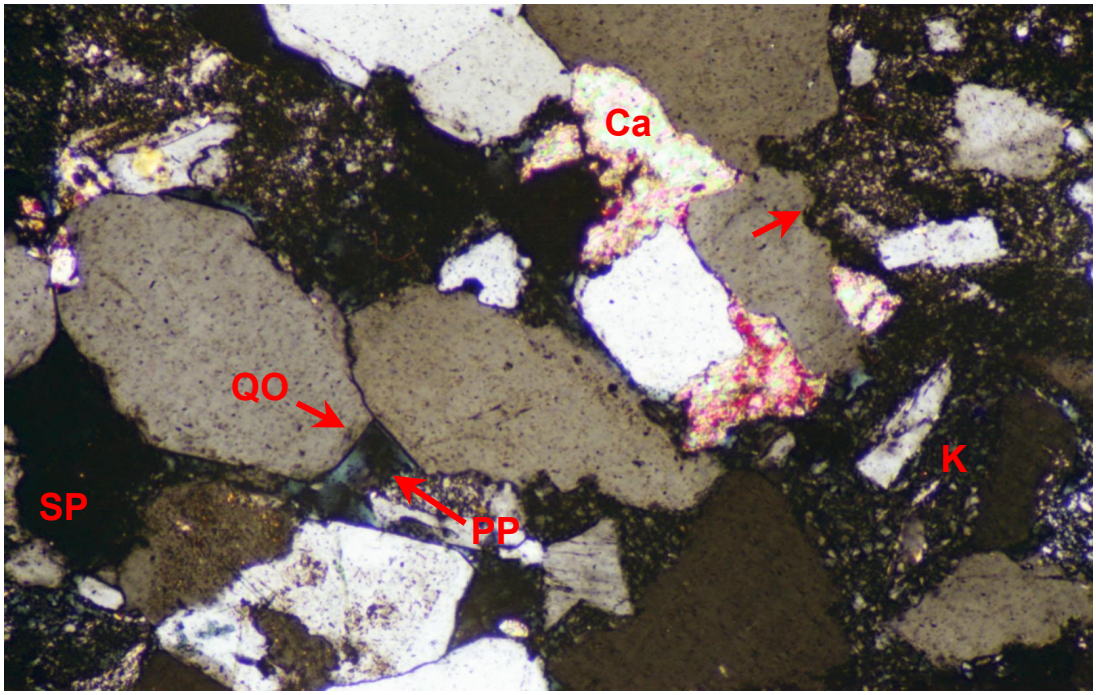

Intergranular porosity has been reduced in this sublitharenite by localised quartz overgrowth (QO) and patchy, coarsely-crystalline calcite (Ca) (stained red) cementation and also by pore filling by microporous authigenic kaolinite (K) and grain welding by grain contact dissolution (arrow). However, primary intergranular pores (PP) are commonly preserved between groups of quartz grains, and there are scattered secondary pores (SP) that have formed by K-feldspar dissolution.

PLATE 5: M5 2076.5m

Rock classification: Sideritised arenaceous mudrock

Texture:

Sedimentary structures: Sandy burrows

Sorting: Moderate

Average grain size: 0.16mm (fine sand)

Roundness: Angular-subrounded

Texture: Cement/matrix supported

Packing /grain contacts: Open/point, long

Macropore types: Secondary mouldic porosity, secondary intragranular porosity

Core analyses: Por. = 10.7%, Perm. = 0.030md, GD = 3.06g/cc

Composition:

Quartz (monocrystalline)	16.0%	Siderite (pore filling)	1.1%
Quartz (polycrystalline)	3.0%	Siderite (replacement)	56.6%
Chert	0.3%	Ankerite (replacement)	0.3%
K-feldspar	1.0%	Authigenic kaolinite (rpl)	1.8%
Metamorphic rock fragments	2.5%	Detrital clay	9.0%
Sedimentary rock fragments	0.8%	Secondary porosity (mouldic)	3.8%
Organics	3.5%	Secondary porosity (intragran)	0.3%

Comments: The detrital clay component of this bioturbated arenaceous mudrock has been extensively replaced by finely-crystalline siderite. Intergranular porosity is lacking due to the presence of widespread sideritised clay matrix, which is sufficiently abundant in most areas to support grains. Most porosity is accounted for by scattered secondary mouldic pores that have formed by feldspar and labile rock fragment dissolution. Although common, the secondary pores are isolated from one another by tight, siderite-cemented mudrock and thus have little or no interconnectivity. High grain density reflects the presence of abundant siderite.

PLATE 5: M5 2076.5m

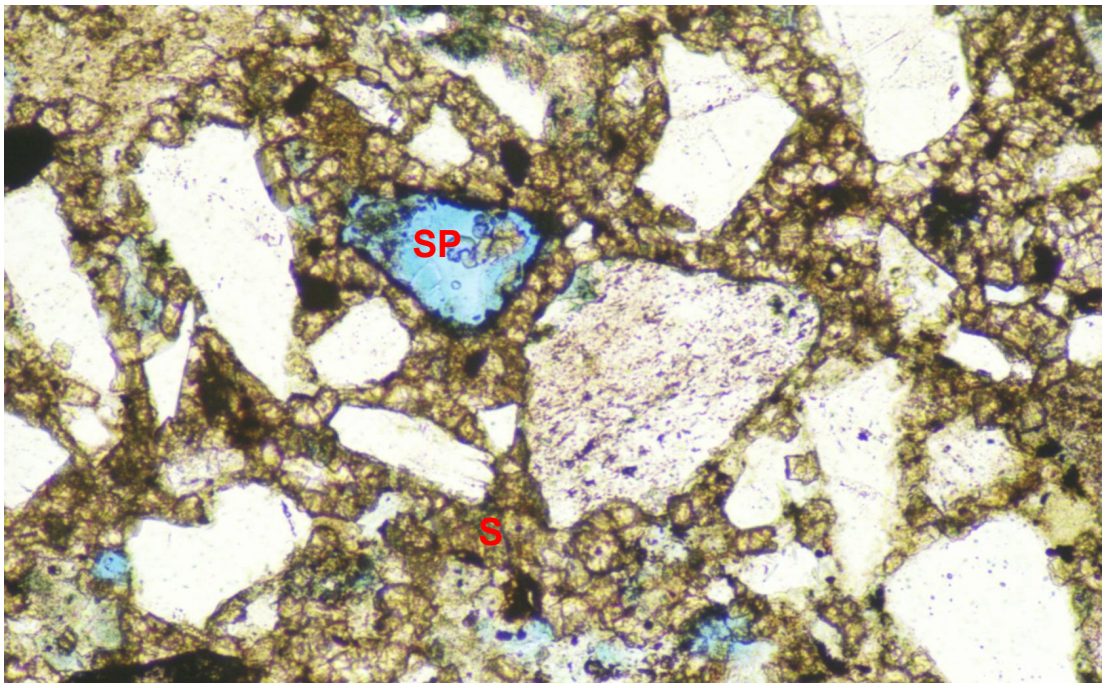

FIGURE 1 Plane polarised light
FIGURE 2 Crossed polarisers

0.2mm

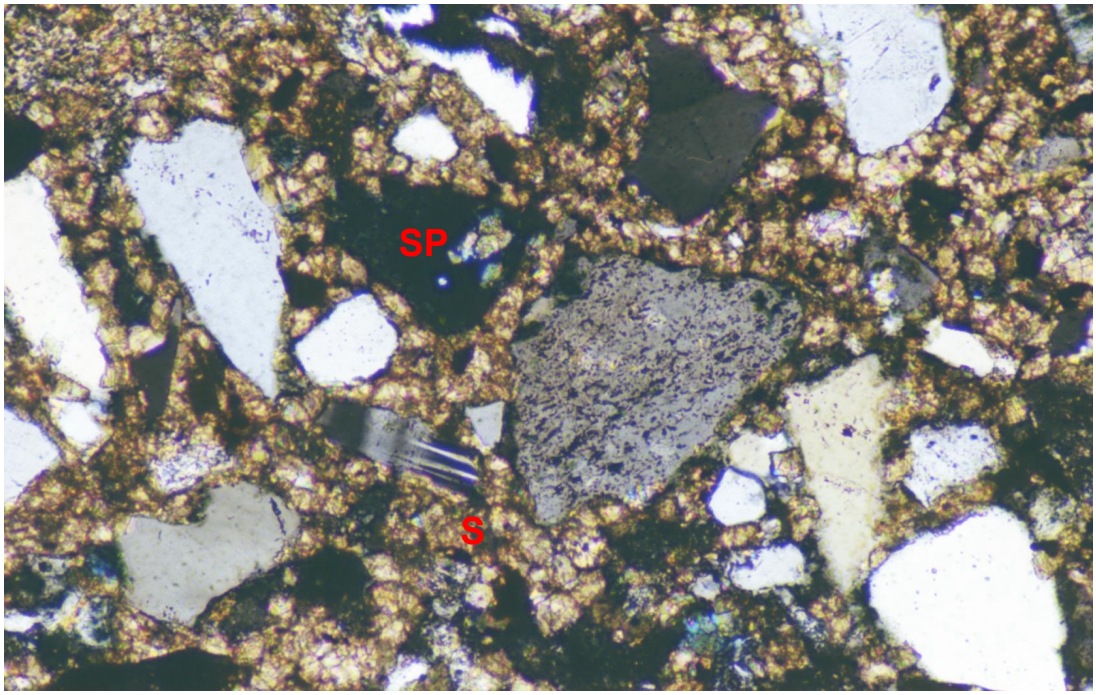

Intergranular spaces are filled by finely-crystalline siderite (S) that has replaced grain-supporting detrital clay matrix. A secondary mouldic pore (SP) occurs where a K-feldspar grain has dissolved subsequent to siderite cementation. The presence of such pores does not enhance reservoir quality.

PLATE 6: M6 2092.2m

Rock classification: Sublitharenite

Texture:

Sedimentary structures:	Single, ankeritised, argillaceous/pyritic lamination; otherwise massive
Sorting:	Well
Average grain size:	0.31mm (medium sand)
Roundness:	Subangular-subrounded
Texture:	Grain supported
Packing /grain contacts:	Moderate/long, embayed, sutured
Grain coating:	<1% (fine siderite continuously coats grains in one small area)
Macropore types:	Primary intergranular porosity, secondary intergranular porosity, secondary mouldic porosity, secondary intragranular porosity
Core analyses:	Por. = 23.0%, Perm. = 45.2md, GD = 2.67g/cc

Composition:

Quartz (monocrystalline)	40.3%	Siderite (replacement)	0.3%
Quartz (polycrystalline)	5.8%	Ankerite (pore filling)	4.8%
Quartz overgrowths	3.1%	Ankerite (replacement)	3.7%
Chert	3.4%	Authigenic kaolinite (pf)	3.3%
K-feldspar	3.0%	Authigenic kaolinite (rpl)	5.7%
Volcanic rock fragments	0.8%	Authigenic illite (replacement)	0.8%
Metamorphic rock fragments	8.5%	Detrital clay	0.3%
Sedimentary rock fragments	1.5%	Primary porosity (intergranular)	5.1%
Organics	0.3%	Secondary porosity (intergran)	5.3%
Pyrite	0.3%	Secondary porosity (mouldic)	1.8%
Siderite (pore filling)	1.2%	Secondary porosity (intragran)	0.7%

Comments: Moderate primary intergranular porosity is supplemented by common secondary pores that occur where labile grains (mainly K-feldspar) have partly to completely dissolved. Porosity reduction is mainly the result of authigenic kaolinite formation, ductile grain/authigenic clay compaction, grain contact dissolution and cementation by localised quartz overgrowths and patchy, coarsely-crystalline ankerite. Within localised areas, these diagenetic effects have largely eliminated intergranular porosity, but macropores are still sufficiently common throughout the sand to be conducive to moderate permeability.

PLATE 6: M6 2092.2m

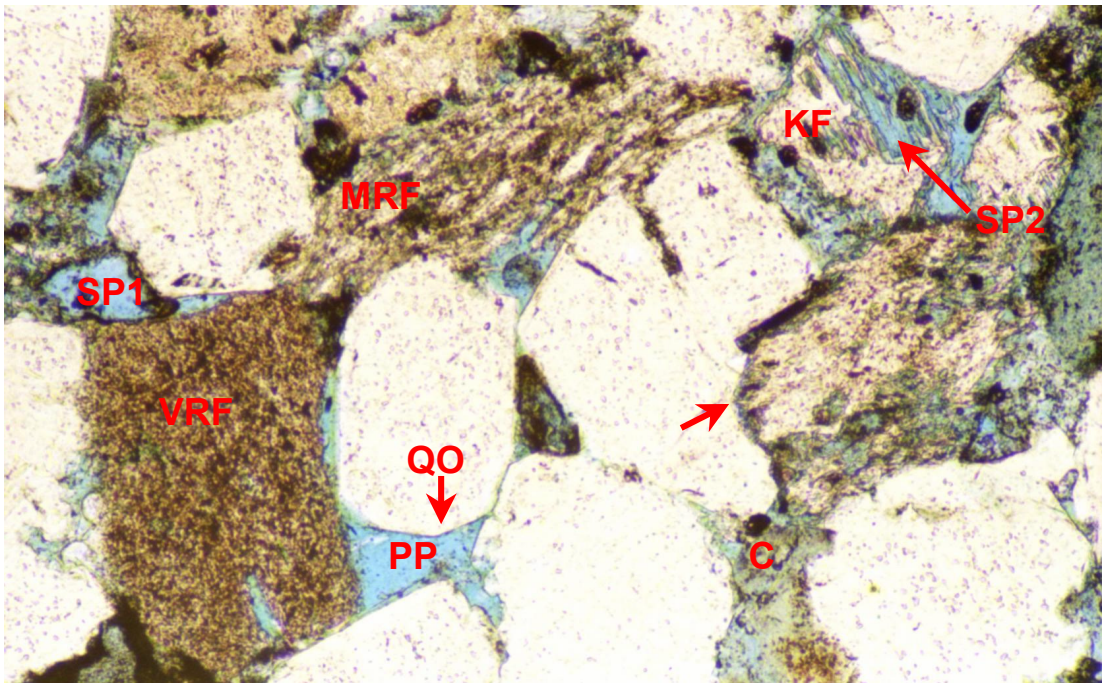

FIGURE 1 Plane polarised light
FIGURE 2 Crossed polarisers

0.2mm

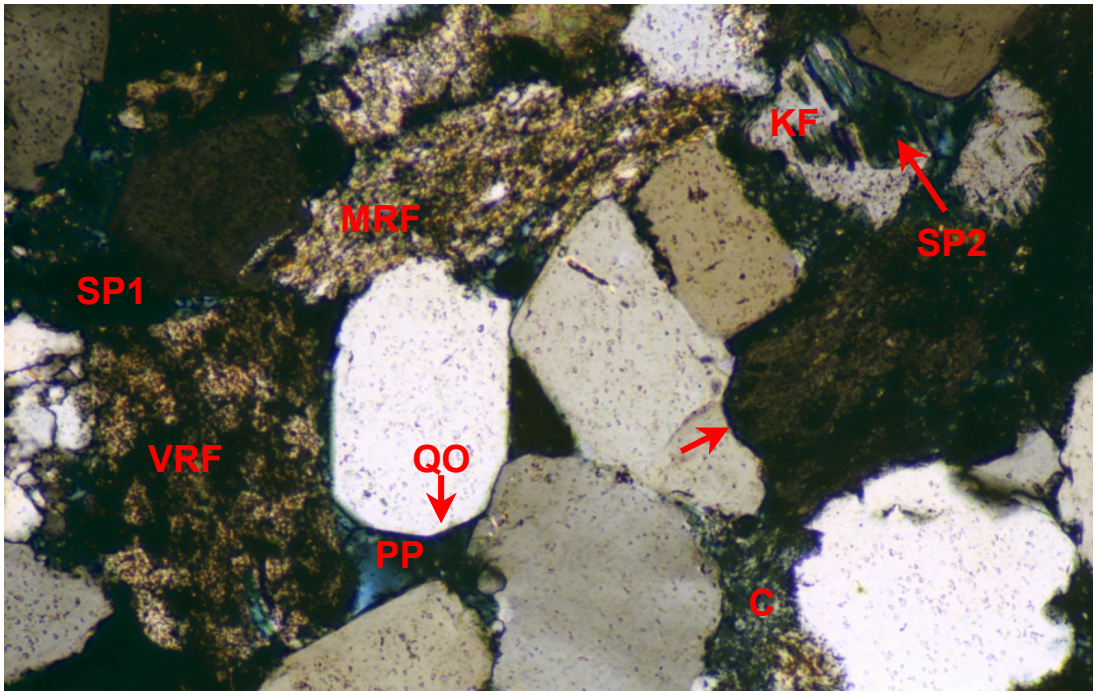

This sublitharenite contains moderate amounts of primary intergranular porosity (PP), despite porosity reduction by quartz overgrowth (QO) cementation, grain contact dissolution (arrow) and compaction of metasedimentary rock fragments (MRF) and authigenic clay (C). Primary porosity is supplemented by secondary mouldic porosity (SP1) and secondary intragranular porosity (SP2) that have formed by K-feldspar (KF) dissolution. An altered felsic volcanic rock fragment (VRF) is also marked.

PLATE 7: M7 2094.0m

Rock classification: Sublitharenite

Texture:

Sedimentary structures:	Single, irregular, argillaceous lamination; otherwise massive
Sorting:	Well
Average grain size:	0.21mm (fine sand)
Roundness:	Subangular-subrounded
Texture:	Grain supported
Packing /grain contacts:	Moderate/long, embayed
Macropore types:	Primary intergranular porosity, secondary intergranular porosity, secondary mouldic porosity, secondary intragranular porosity
Core analyses:	Por. = 20.8%, Perm. = 13.9md, GD = 2.76g/cc

Composition:

Quartz (monocrystalline)	41.6%	Leucoxene	0.3%
Quartz (polycrystalline)	3.5%	Siderite (pore filling)	4.0%
Quartz overgrowths	4.3%	Siderite (replacement)	5.8%
Chert	1.0%	Ankerite (replacement)	0.3%
K-feldspar	3.5%	Authigenic kaolinite (pf)	7.1%
Volcanic rock fragments	1.0%	Authigenic kaolinite (rpl)	8.4%
Metamorphic rock fragments	7.8%	Authigenic illite (replacement)	1.0%
Sedimentary rock fragments	1.3%	Primary porosity (intergranular)	2.4%
Mica	0.3%	Secondary porosity (intergran)	3.3%
Heavy minerals	0.3%	Secondary porosity (mouldic)	1.0%
Organics	0.7%	Secondary porosity (intragran)	1.1%

Comments: Intergranular spaces are commonly occupied by authigenic kaolinite, single/clustered, fine siderite rhombs and compacted ductile grains, and there has been further porosity loss by quartz overgrowth cementation, grain contact dissolution and pore filling by localised detrital clay matrix. Except within an argillaceous lamination, the sandstone still contains common primary and secondary macropores, but, with many pore throats being choked by authigenic clay and siderite, permeability remains relatively low.

PLATE 7: M7 2094.0m

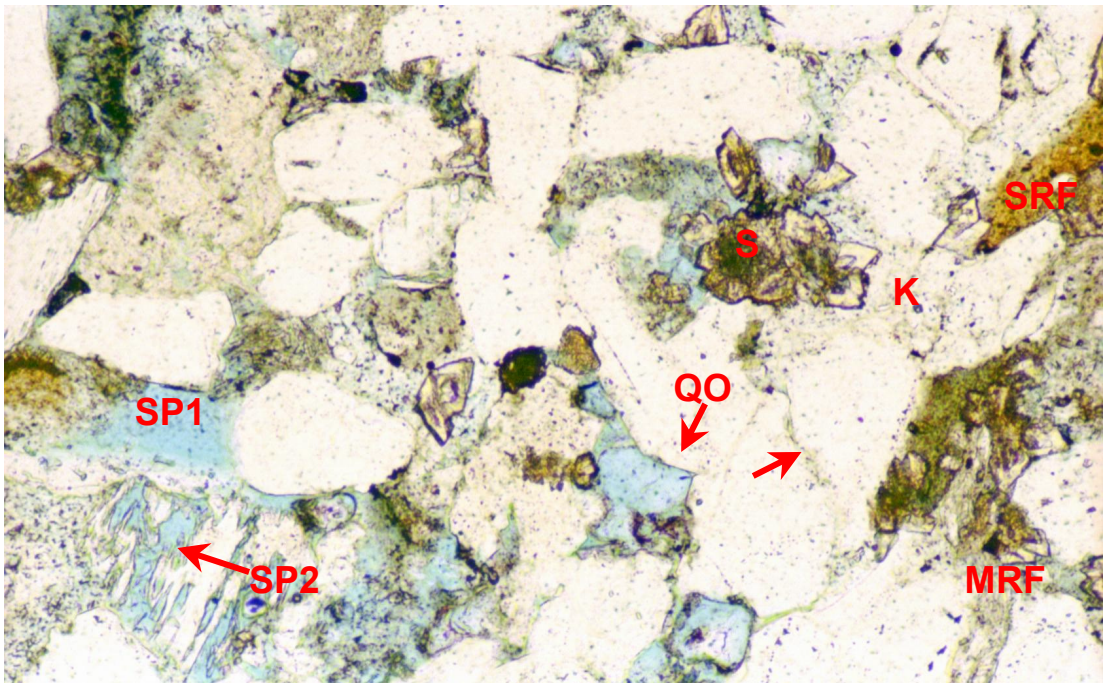

FIGURE 1 Plane polarised light
FIGURE 2 Crossed polarisers

0.2mm

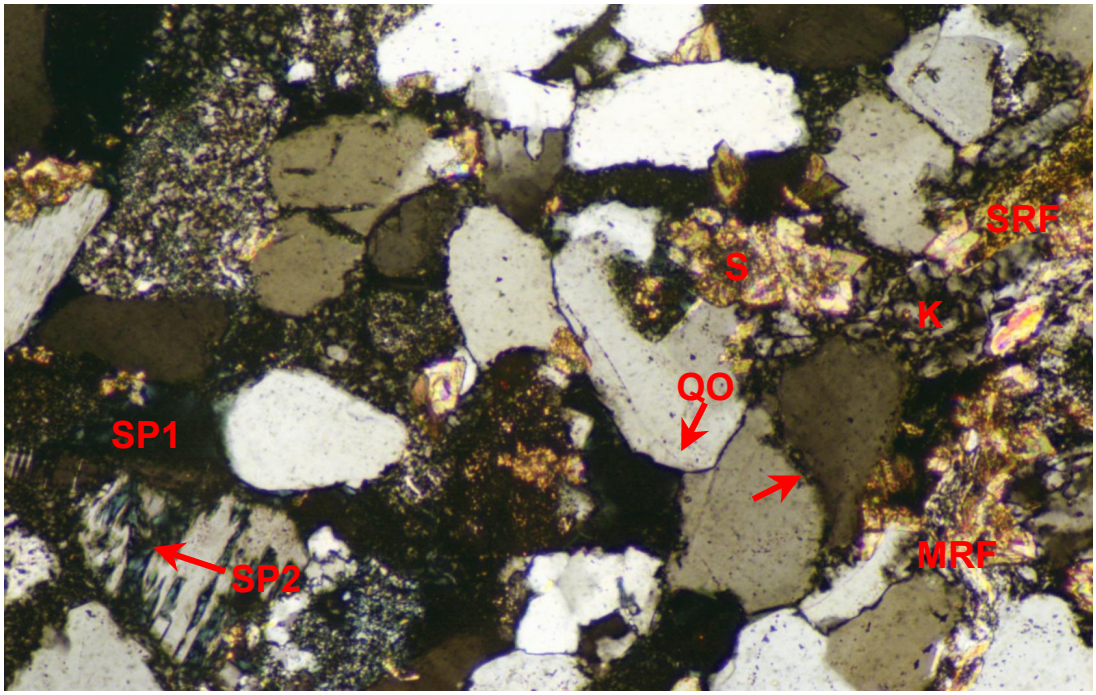

Fine grained sublitharenite in which intergranular porosity has been largely reduced by grain contact dissolution (arrow), quartz overgrowth (QO) and rhombic siderite (S) cementation, authigenic kaolinite (K) formation, and compaction of argillaceous sedimentary rock fragments (SRF) and micaceous metamorphic rock fragments (MRF). Secondary intergranular pores (SP1) occur where labile grains have dissolved, and secondary intragranular porosity (SP2) is associated with the skeletal remains of a partly dissolved K-feldspar grain.

PLATE 8: M8 2133.0m

Rock classification: Litharenite

Texture:

Sedimentary structures: Massive

Sorting: Well

Average grain size: 0.23mm (fine sand)

Roundness: Angular-subrounded

Texture: Grain supported

Packing /grain contacts: Moderate/long, embayed

Macropore types: Secondary intergranular porosity, primary intergranular porosity, secondary mouldic porosity, secondary intragranular porosity

Core analyses: Por. = 19.7%, Perm. = 3.77md, GD = 2.68g/cc

Composition:

Quartz (monocrystalline)	39.9%	Siderite (pore filling)	3.8%
Quartz (polycrystalline)	4.5%	Siderite (replacement)	5.6%
Quartz overgrowths	2.3%	Ankerite (replacement)	0.3%
Chert	1.5%	Authigenic kaolinite (pf)	6.4%
K-feldspar	3.5%	Authigenic kaolinite (rpl)	10.7%
Volcanic rock fragments	1.4%	Authigenic illite (replacement)	1.3%
Metamorphic rock fragments	9.2%	Primary porosity (intergranular)	1.2%
Sedimentary rock fragments	2.7%	Secondary porosity (intergran)	1.5%
Heavy minerals	0.3%	Secondary porosity (mouldic)	2.3%
Organics	0.3%	Secondary porosity (intragran)	1.0%
Pyrite	0.3%		

Comments: Primary intergranular porosity has been severely reduced by authigenic kaolinite formation, compaction of authigenic clay and ductile grains, grain contact dissolution, and siderite and quartz overgrowth cementation. Secondary labile grain dissolution pores are common, but, with most intergranular spaces being filled by authigenic kaolinite, fine siderite and compacted ductile grains, permeability is low.

PLATE 8: M8 2133.0m

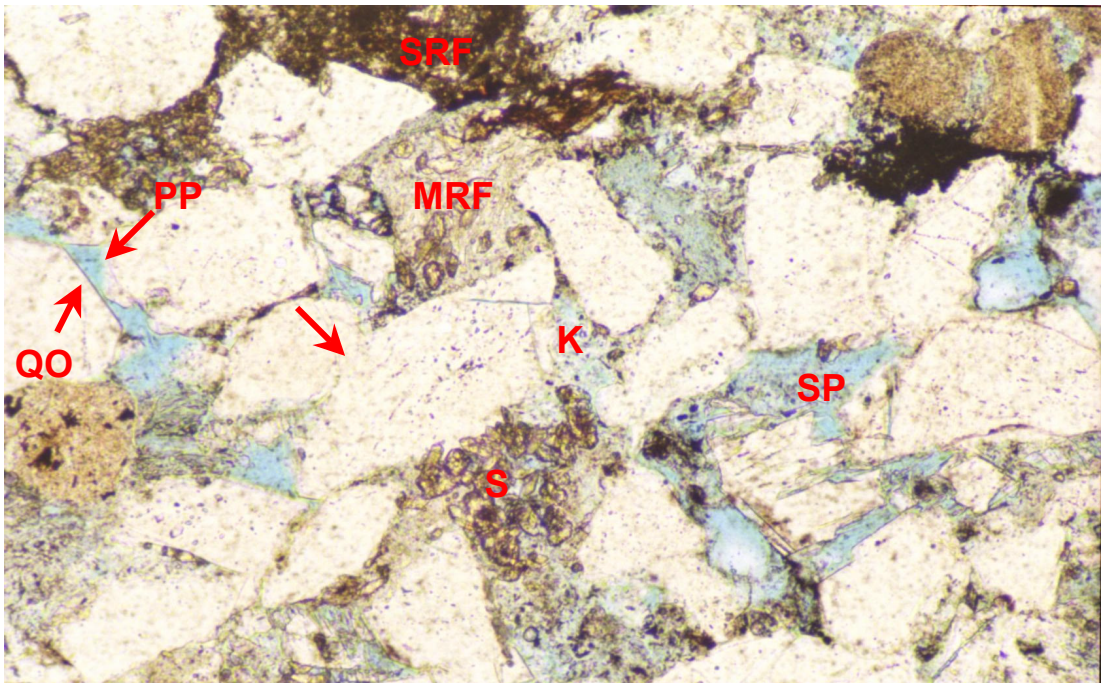

FIGURE 1 Plane polarised light
FIGURE 2 Crossed polarisers

0.2mm

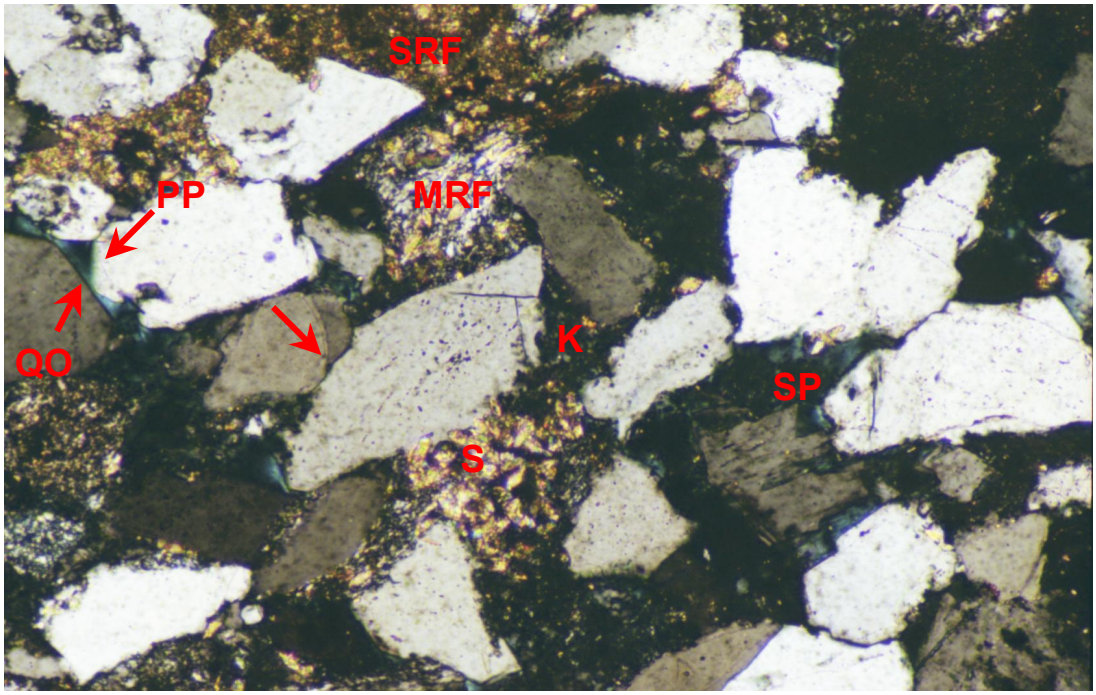

Intergranular spaces are largely filled by authigenic kaolinite (K) and fine siderite (S), and there has been further porosity loss by quartz overgrowth (QO) cementation, grain contact dissolution (arrow) and compaction of argillaceous sedimentary rock fragments (SRF) and altered micaceous metamorphic rock fragments (MRF). Primary intergranular pores (PP) and secondary K-feldspar dissolution pores (SP) are not sufficiently common throughout the sand to be well interconnected.

PLATE 9: M9 2139.1m

Rock classification: Litharenite

Texture:

Sedimentary structures: Massive

Sorting: Well

Average grain size: 0.20mm (fine sand)

Roundness: Angular-subrounded

Texture: Grain supported

Packing /grain contacts: Moderate/long, embayed

Macropore types: Secondary intergranular porosity, primary intergranular porosity, secondary mouldic porosity, secondary intragranular porosity

Core analyses: Por. = 16.1%, Perm. = 0.814md, GD = 2.68g/cc

Composition:

Quartz (monocrystalline)	34.0%	Pyrite	1.4%
Quartz (polycrystalline)	4.2%	Leucoxene	0.7%
Quartz overgrowths	2.5%	Siderite (pore filling)	0.7%
Chert	2.2%	Siderite (replacement)	6.1%
K-feldspar	4.6%	Authigenic kaolinite (pf)	2.1%
Volcanic rock fragments	2.2%	Authigenic kaolinite (rpl)	15.8%
Metamorphic rock fragments	14.1%	Authigenic illite (replacement)	1.6%
Sedimentary rock fragments	3.1%	Primary porosity (intergranular)	0.3%
Mica	0.3%	Secondary porosity (mouldic)	2.0%
Organics	1.8%	Secondary porosity (intragran)	0.3%

Comments: Like M1, this litharenite was highly susceptible to authigenic clay formation and compaction on account of containing abundant micaceous/argillaceous rock fragments at the time of accumulation. Primary intergranular porosity has been almost completely eliminated by authigenic clay (kaolinite, illite) formation, ductile grain/authigenic clay compaction to form pseudomatrix, grain contact dissolution, and cementation by localised quartz overgrowths. Scattered mouldic secondary pores occur where labile grains (mainly feldspar) have dissolved. The sample is mainly microporous and consequently has very low permeability.

PLATE 9: M9 2139.1m

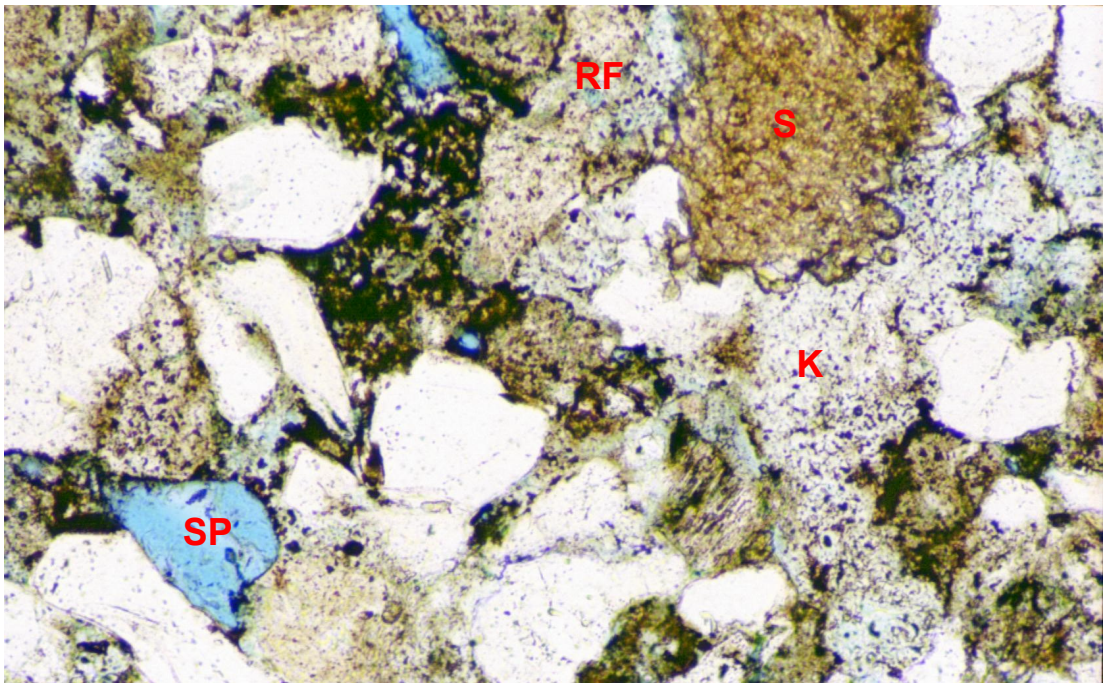

FIGURE 1 Plane polarised light
FIGURE 2 Crossed polarisers

0.2mm

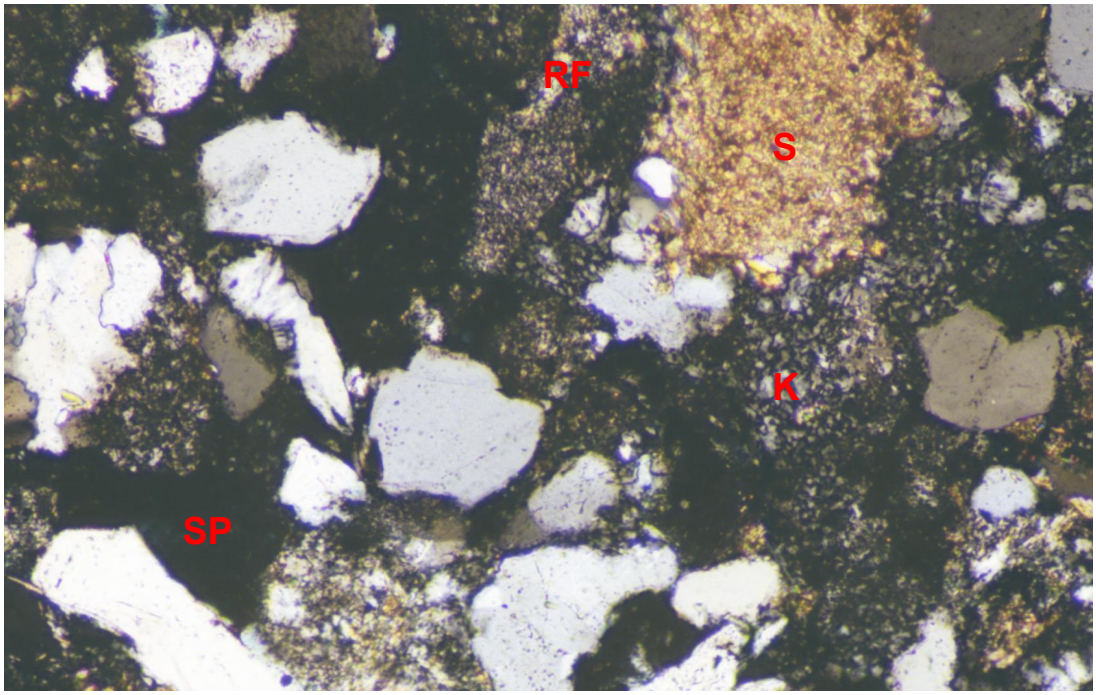

Intergranular porosity has been eliminated by authigenic kaolinite formation (K) and by compaction of micaceous/argillaceous rock fragments (RF) and authigenic clay. Secondary mouldic pores (SP) have little or no interconnectivity. A patch of finely-crystalline siderite (S) has replaced an altered biotite grain.

PLATE 10: M10 2143.6m

Rock classification: Sublitharenite

Texture:

Sedimentary structures:	Massive
Sorting:	Moderately-well
Average grain size:	0.29mm (medium sand)
Roundness:	Subangular-subrounded
Texture:	Grain supported
Packing /grain contacts:	Moderate/long, embayed
Macropore types:	Primary intergranular porosity, secondary intergranular porosity, secondary mouldic porosity, secondary intragranular porosity
Core analyses:	Por. = 20.8%, Perm. = 24.7md, GD = 2.65g/cc

Composition:

Quartz (monocrystalline)	44.4%	Organics	0.3%
Quartz (polycrystalline)	4.9%	Authigenic kaolinite (pf)	6.8%
Quartz overgrowths	4.8%	Authigenic kaolinite (rpl)	9.0%
Chert	1.3%	Authigenic illite (replacement)	0.7%
K-feldspar	1.3%	Primary porosity (intergranular)	4.7%
Volcanic rock fragments	1.2%	Secondary porosity (intergran)	6.6%
Metamorphic rock fragments	11.5%	Secondary porosity (mouldic)	0.5%
Sedimentary rock fragments	1.0%	Secondary porosity (intragran)	0.7%
Heavy minerals	0.3%		

Comments: Moderate primary intergranular porosity is supplemented by common secondary pores that occur where labile grains (mainly feldspar) have partly to completely dissolved. Porosity reduction is mainly the result of authigenic kaolinite formation, ductile grain/authigenic clay compaction, grain contact dissolution and quartz overgrowth cementation. Within localised areas, all intergranular spaces are filled by kaolinitic pseudomatrix, hence, despite the presence of common macropores, permeability is only modest.

PLATE 10: M10 2143.6m

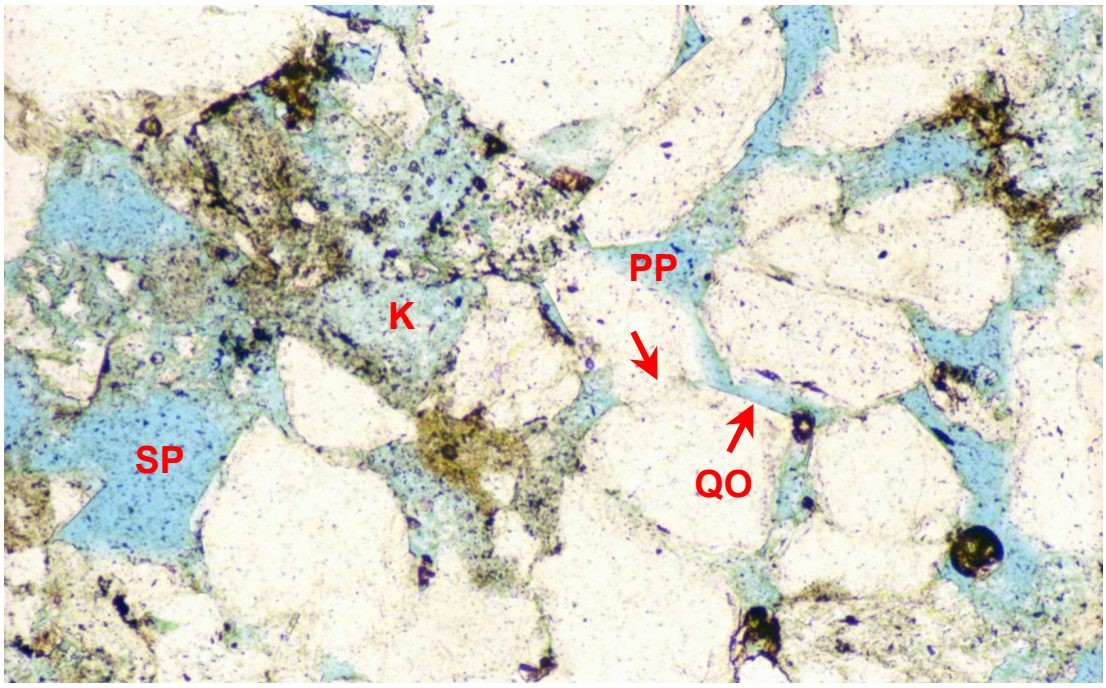

FIGURE 1 Plane polarised light
FIGURE 2 Crossed polarisers

0.2mm

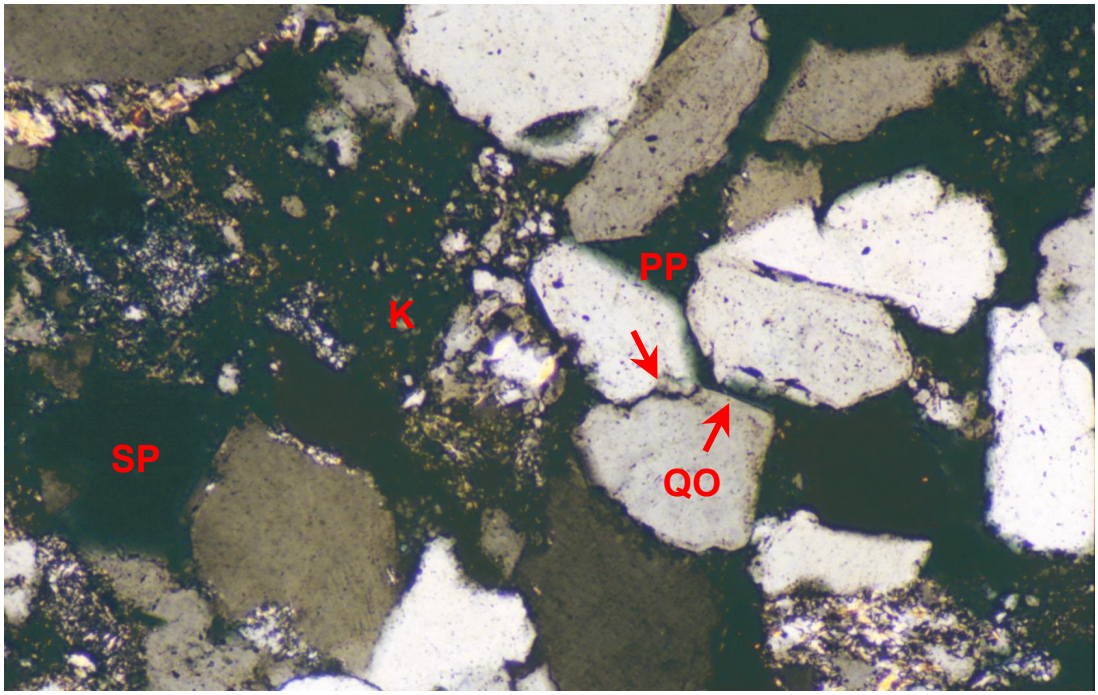

This sublitharenite contains modest primary intergranular porosity (PP), particularly where there are juxtaposed quartz grains, despite porosity reduction by authigenic kaolinite pseudomatrix (K) formation, quartz overgrowth (QO) cementation and grain contact dissolution (arrow). Primary porosity is supplemented by common oversized secondary intergranular pores (SP) that occur where K-feldspar grains have dissolved. However, within localised areas (outside of field of view), all intergranular areas are filled by authigenic kaolinite pseudomatrix, which significantly reduces permeability.

PLATE 11: M12 2165.9m

Rock classification: Quartzarenite

Texture:

Sedimentary structures:	Massive
Sorting:	Moderately-well
Average grain size:	0.48mm (medium sand)
Roundness:	Subangular-rounded
Texture:	Grain supported
Packing /grain contacts:	Moderate/long, embayed
Macropore types:	Primary intergranular porosity, secondary intergranular porosity
Core analyses:	Por. = 23.0%, Perm. = 1590md, GD = 2.65g/cc

Composition:

Quartz (monocrystalline)	65.5%	Pyrite	0.5%
Quartz (polycrystalline)	4.0%	Authigenic kaolinite (pf)	1.1%
Quartz overgrowths	4.3%	Authigenic kaolinite (rpl)	4.9%
Volcanic rock fragments	0.3%	Primary porosity (intergranular)	9.3%
Metamorphic rock fragments	1.8%	Secondary porosity (intergran)	8.0%
Sedimentary rock fragments	0.3%		

Comments: Despite porosity reduction by quartz overgrowth cementation, grain contact dissolution, authigenic kaolinite formation and ductile grain/authigenic clay compaction, this quartzarenite contains abundant clean primary intergranular porosity that is supplemented by common secondary intergranular pores that occur where labile grains have completely dissolved. The sandstone was far less susceptible to authigenic clay formation and ductile grain compaction than the previous samples on account of its high quartz content at the time of accumulation. Macropores are evenly distributed throughout most of the sandstone, hence are well interconnected.

PLATE 11: M12 2165.9m

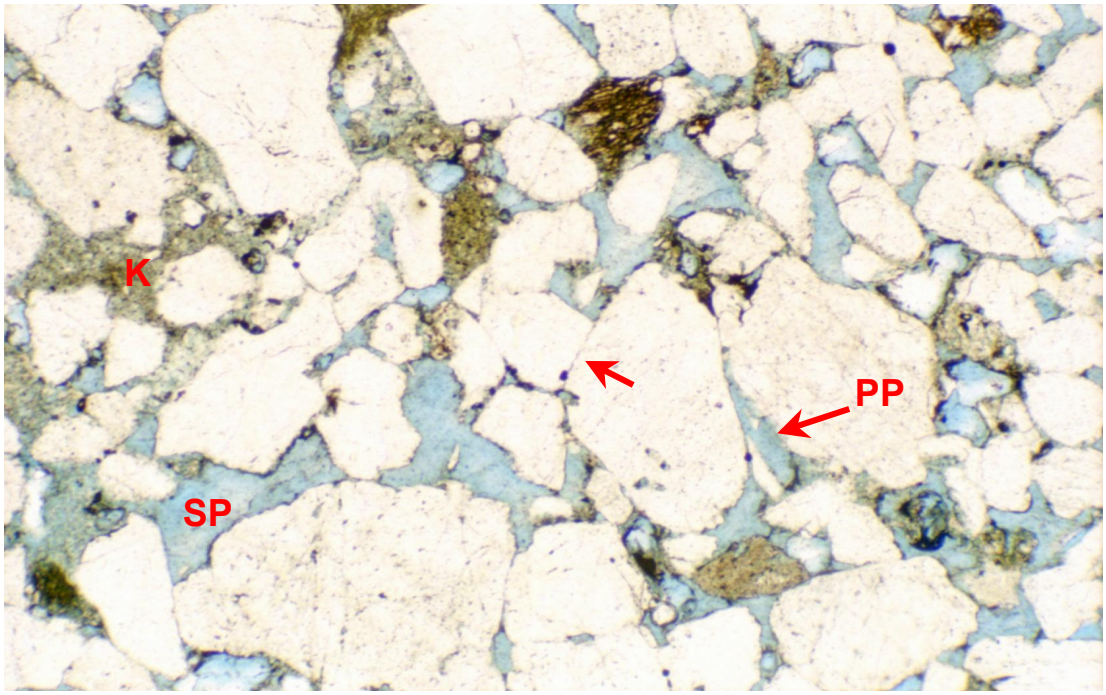

FIGURE 1 Plane polarised light
FIGURE 2 Crossed polarisers

0.4mm

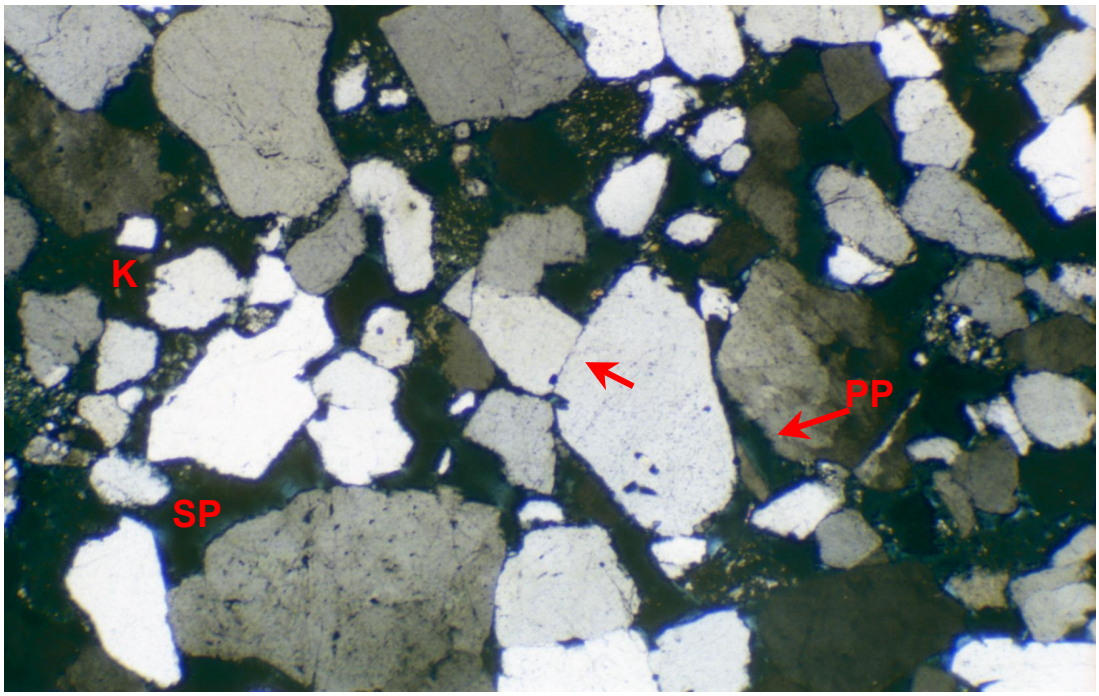

This quartzarenite contains a system of clean, well interconnected primary (PP) and secondary (SP) intergranular pores. Porosity loss is mainly the result of minor grain welding by grain contact dissolution (arrow) and the compactional deformation of argillaceous/micaceous rock fragments to form localised kaolinitic pseudomatrix (K). Quartz overgrowths are too small to be visible in the micrographs.

PLATE 12: M12 2165.9m cont.

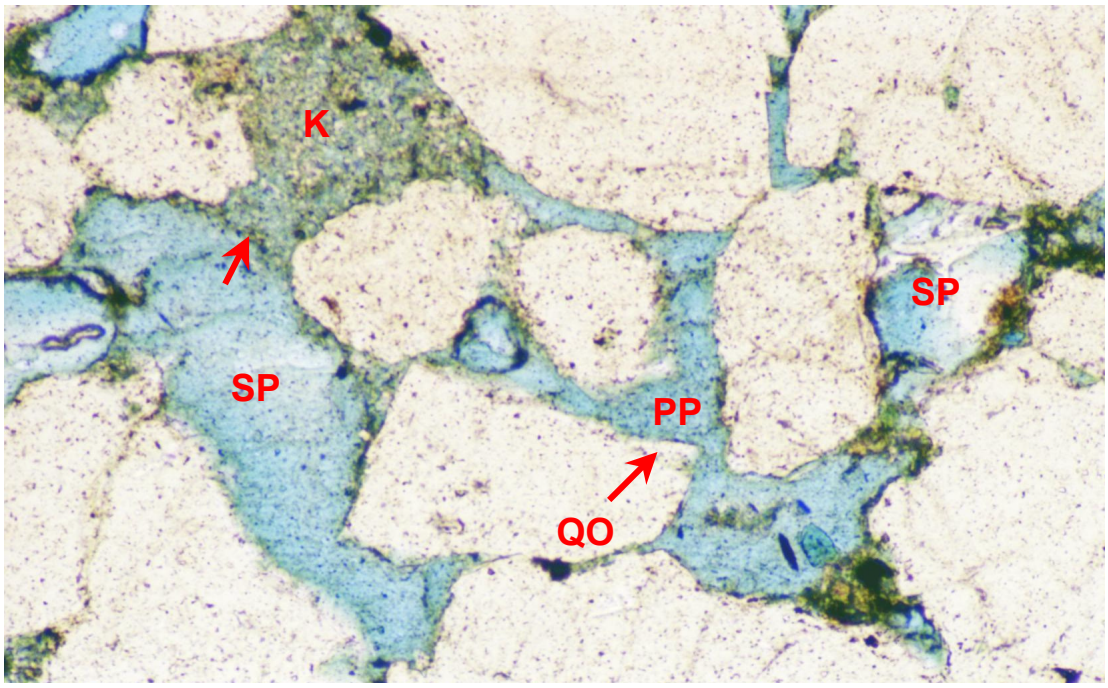

FIGURE 1 Plane polarised light
FIGURE 2 Crossed polarisers

0.2mm

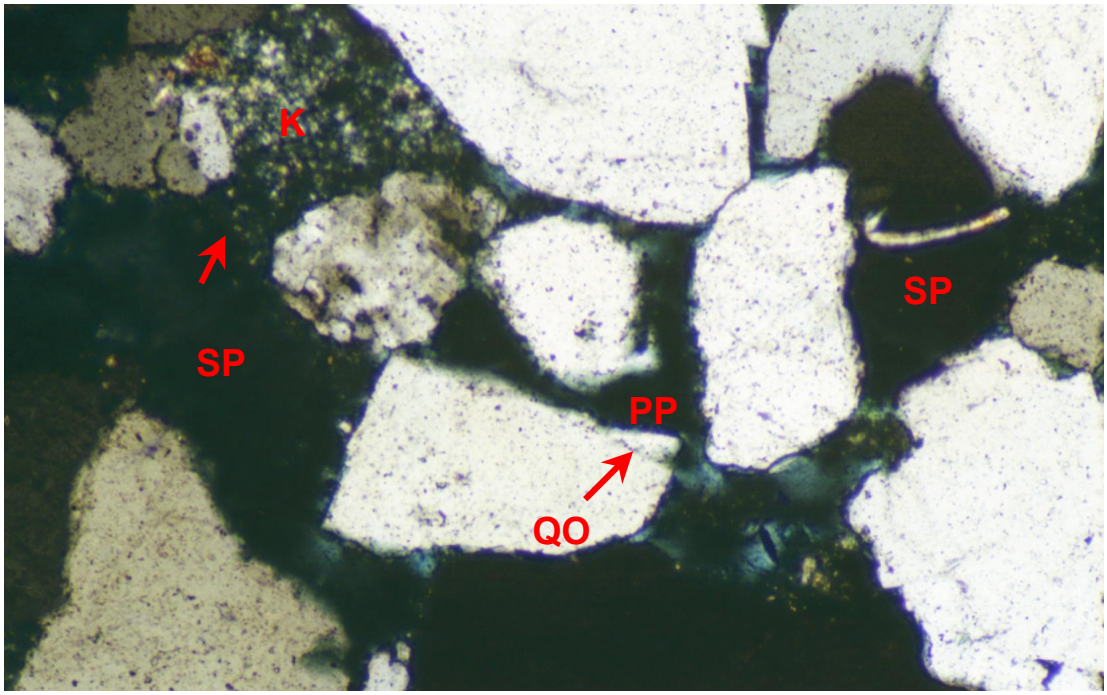

Representative area in which abundant, clean primary (PP) and secondary (SP) intergranular porosity is preserved between poorly quartz overgrowth (QO)-cemented quartz framework grains. An isolated patch of microporous kaolinite (K) partly borders (arrow) an earlier formed secondary pore.

PLATE 13: #5 2166.81m

Rock classification: Sublitharenite

Texture:

Sedimentary structures: Patchy detrital clay; single, 2mm-thick sideritic lamination

Sorting: Well

Average grain size: 0.25mm (medium sand)

Roundness: Subangular-subrounded

Texture: Grain supported

Packing /grain contacts: Moderate/long, embayed, sutured

Macropore types: Secondary mouldic porosity, primary intergranular porosity, secondary intergranular porosity

Core analyses: Por. = 17.8%, Perm. = 6.66md, GD = 2.64g/cc

Composition:

Quartz (monocrystalline)	42.9%	Pyrite	0.5%
Quartz (polycrystalline)	5.6%	Authigenic kaolinite (pf)	5.6%
Quartz overgrowths	2.9%	Authigenic kaolinite (rpl)	11.3%
Chert	1.5%	Authigenic illite (replacement)	0.7%
K-feldspar	1.2%	Detrital clay	5.8%
Volcanic rock fragments	0.5%	Primary porosity (intergranular)	0.8%
Metamorphic rock fragments	13.5%	Secondary porosity (intergran)	1.2%
Sedimentary rock fragments	1.3%	Secondary porosity (mouldic)	4.4%
Heavy minerals	0.3%		

Comments: Most intergranular porosity in this sublitharenite has been eliminated by authigenic kaolinite formation, ductile grain/authigenic clay compaction, grain contact dissolution (including microstylolitisation), quartz overgrowth cementation and localised pore filling by detrital clay matrix. Macroporosity is mainly accounted for by scattered secondary pores that are the result of labile grain dissolution. Pore throats between macropores are largely chocked by clay, compacted ductile grains and quartz overgrowths, hence permeability is relatively low.

PLATE 13: #5 2166.81m

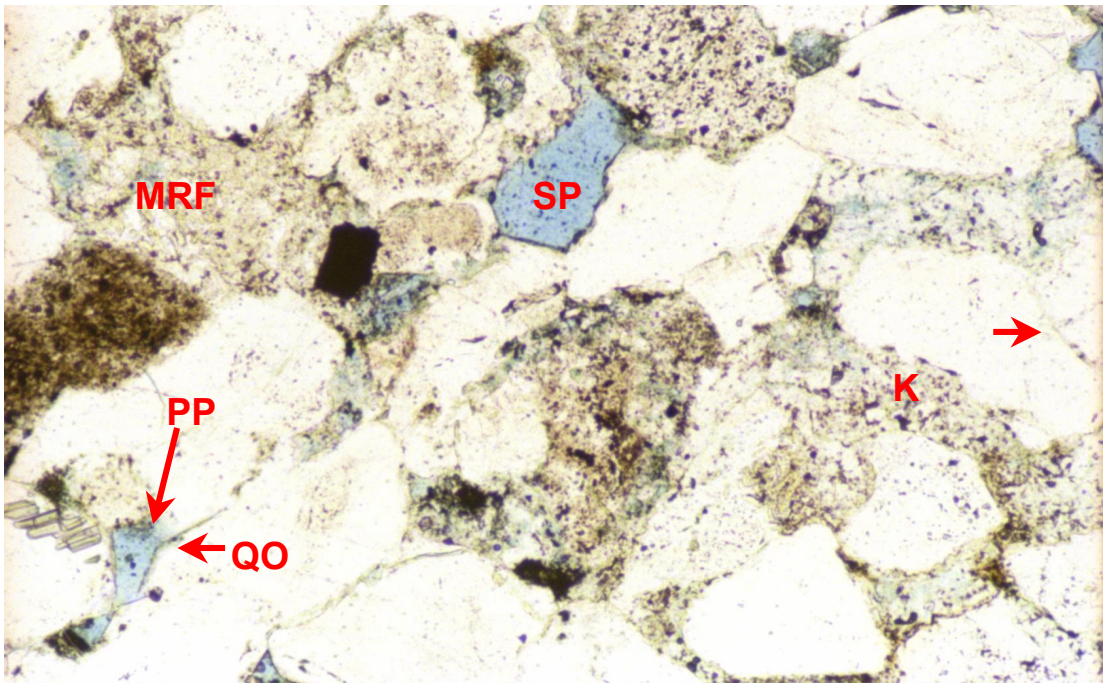

FIGURE 1 Plane polarised light
FIGURE 2 Crossed polarisers

0.2mm

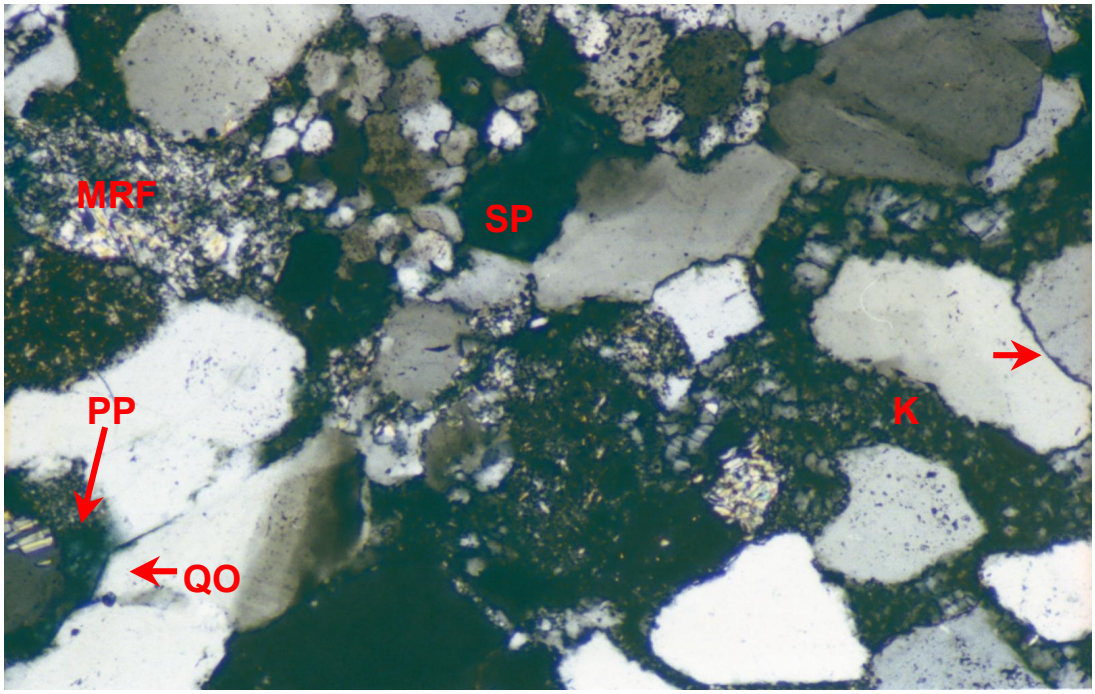

Isolated, hence poorly interconnected primary pores (PP) and secondary mouldic pores (SP) occur in a sublitharenite in which intergranular porosity has been largely eliminated by authigenic kaolinite (K) formation, compaction of micaceous metamorphic rock fragments (MRF) and authigenic clay, and by localised quartz overgrowth (QO) cementation.

PLATE 14: #5 2166.81m cont.

FIGURE 1

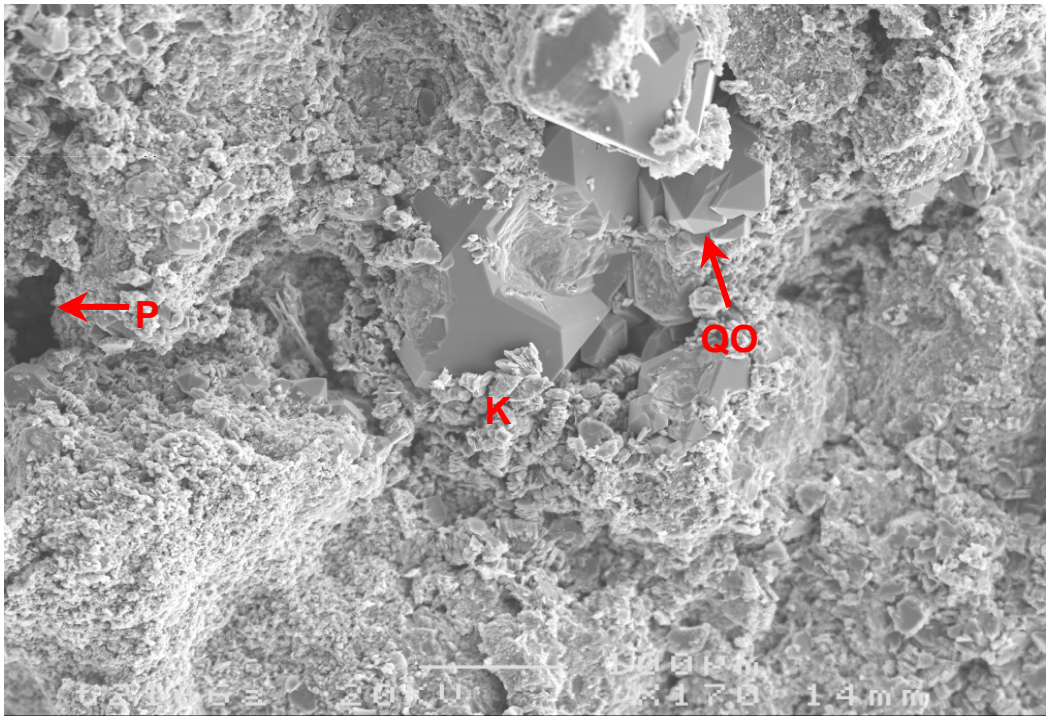

SEM micrograph showing a representative area in which intergranular areas are almost entirely filled by authigenic kaolinite (K) and quartz overgrowth cement (QO). An isolated macropore (P) would be poorly connected to any macropores in the vicinity.

FIGURE 2

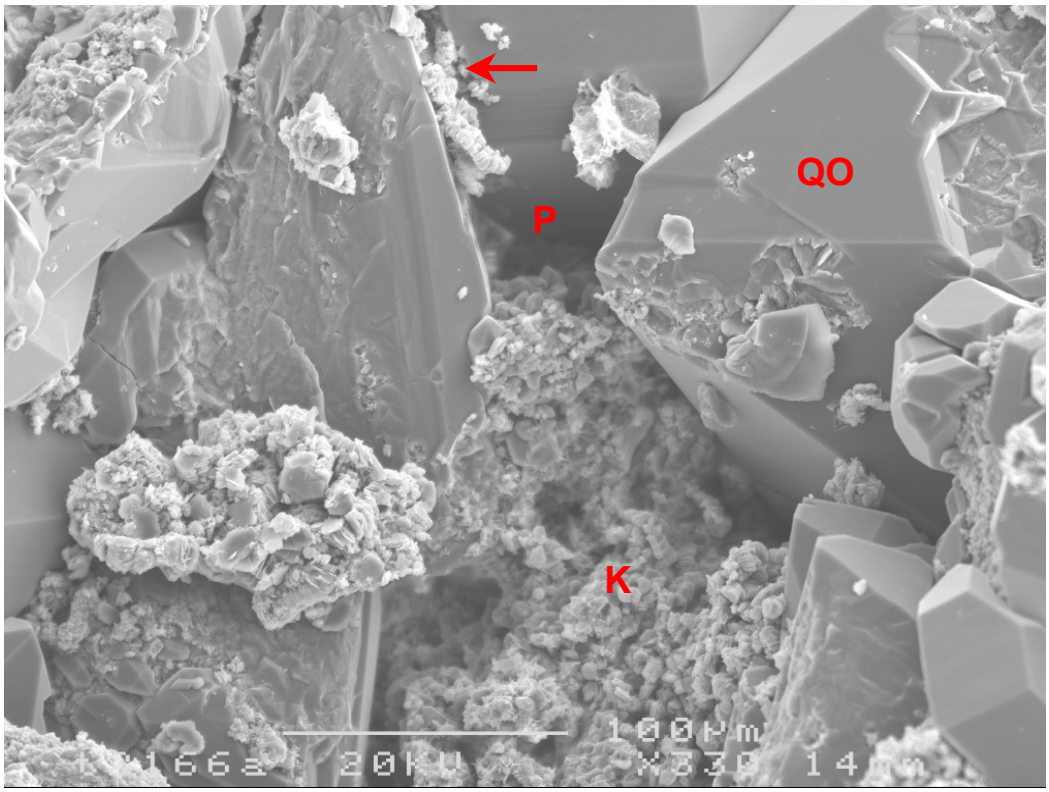

An intergranular pore (P) is largely filled by quartz overgrowths (QO) and authigenic kaolinite (K) that is the compacted and altered remnant of a micaceous grain. Quartz overgrowths enclose (arrow) some of the earlier formed kaolinite.

PLATE 15: 2170.40m (reconnaissance SEM study sample)

FIGURE 1

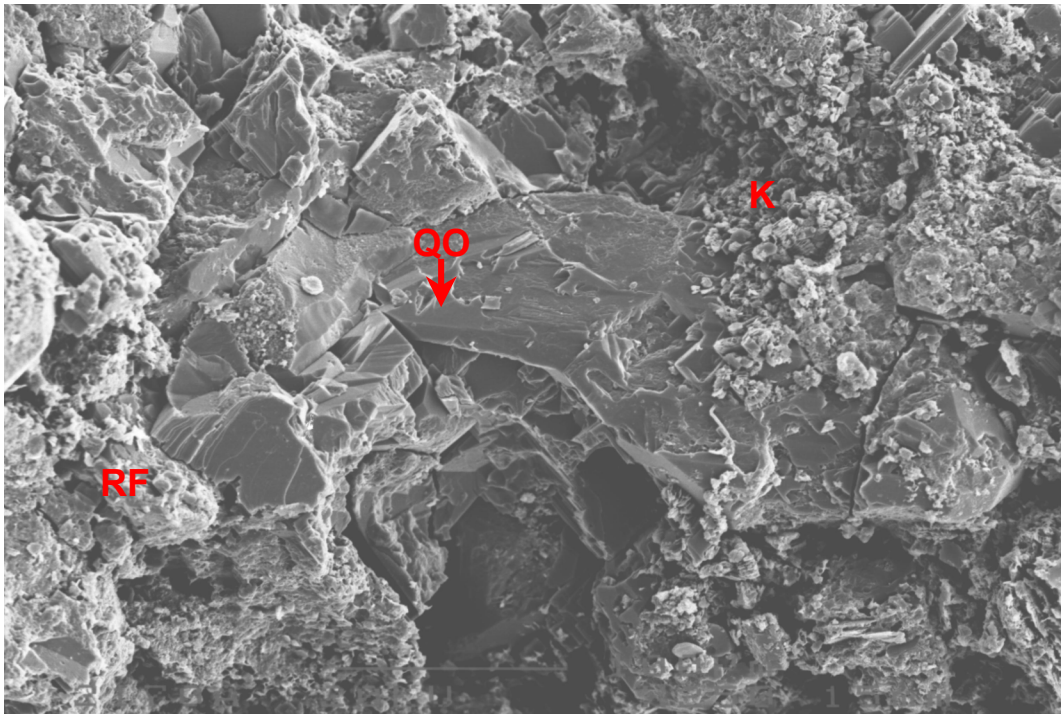

Representative area of a low porosity sandstone in which intergranular areas are filled by compacted micaceous rock fragments (RF), authigenic kaolinite (K) and quartz overgrowths (QO).

FIGURE 2

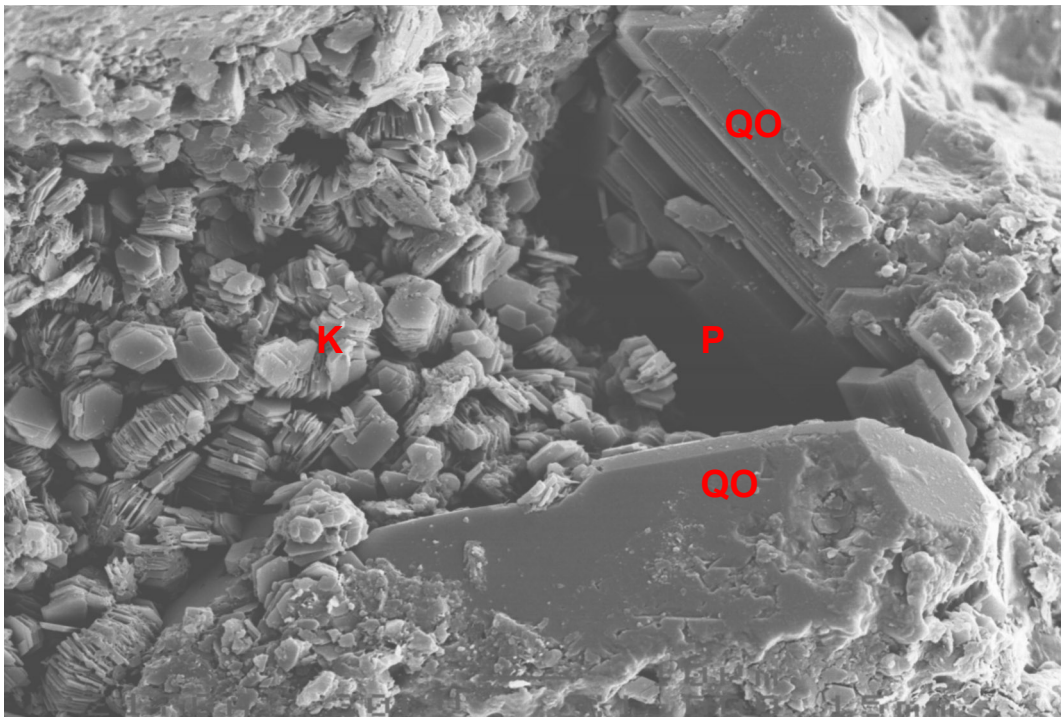

Clay in the sandstone is overwhelmingly dominated by authigenic kaolinite (K) that has formed by labile grain alteration. In the field of view, authigenic kaolinite largely fills an intergranular pore (P) that is partly bounded by quartz overgrowths (QO).

PLATE 16: #14 2171.19m

Rock classification: Sublitharenite

Texture:

Sedimentary structures: Massive

Sorting: Well

Average grain size: 0.20mm (fine sand)

Roundness: Subangular-subrounded

Texture: Grain supported

Packing /grain contacts: Moderate/long, embayed

Macropore types: Secondary mouldic porosity, secondary intergranular porosity, primary intergranular porosity, secondary intragranular porosity

Core analyses: Por. = 21.8%, Perm. = 99.5md, GD = 2.66g/cc

Composition:

Quartz (monocrystalline)	58.8%	Siderite (replacement)	0.3%
Quartz (polycrystalline)	2.8%	Authigenic kaolinite (pf)	4.8%
Quartz overgrowths	5.3%	Authigenic kaolinite (rpl)	8.0%
Chert	0.7%	Authigenic illite (replacement)	0.7%
K-feldspar	2.5%	Primary porosity (intergranular)	2.3%
Volcanic rock fragments	0.3%	Secondary porosity (intergran)	2.1%
Metamorphic rock fragments	6.5%	Secondary porosity (mouldic)	4.0%
Sedimentary rock fragments	0.3%	Secondary porosity (intragran)	0.3%
Mica	0.3%		

Comments: Intergranular porosity has been largely eliminated by the effects of grain contact dissolution, quartz overgrowth cementation, authigenic clay formation and ductile micaceous grain/authigenic clay compaction. Triple point grain junctions and patches of kaolinitic pseudomatrix are common. However, there are common secondary mouldic and intergranular pores that have formed by labile grain dissolution, which, together with minor primary intergranular porosity, results in moderately good permeability.

PLATE 16: #14 2171.19m

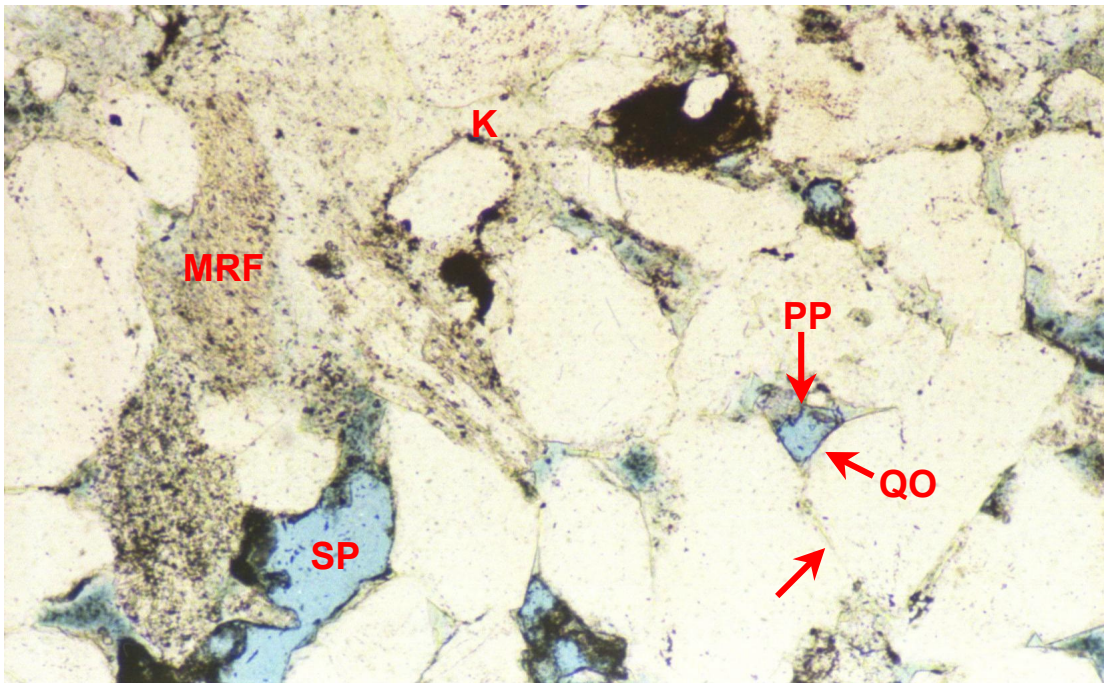

FIGURE 1 Plane polarised light
FIGURE 2 Crossed polarisers

0.2mm

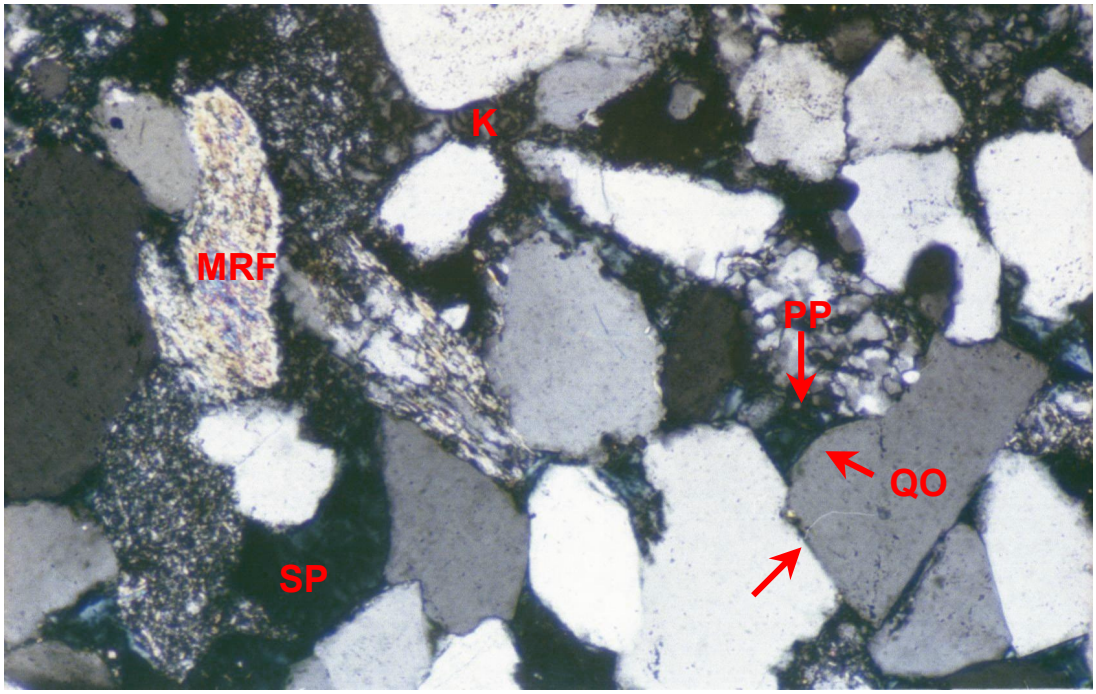

Macroporosity in this sample is largely accounted for by secondary mouldic pores (SP) that mark the locations of labile grains that have dissolved. Small primary intergranular pores (PP) occur where quartz overgrowth (QO) cementation and grain contact dissolution (arrow) have not completely eliminated intergranular space between juxtaposed quartzose grains. In many areas, intergranular porosity has been completely eliminated by authigenic kaolinite (K) formation and by compaction of micaceous metamorphic rock fragments (MRF) and authigenic clay.

PLATE 17: #14 2171.19m cont.

FIGURE 1

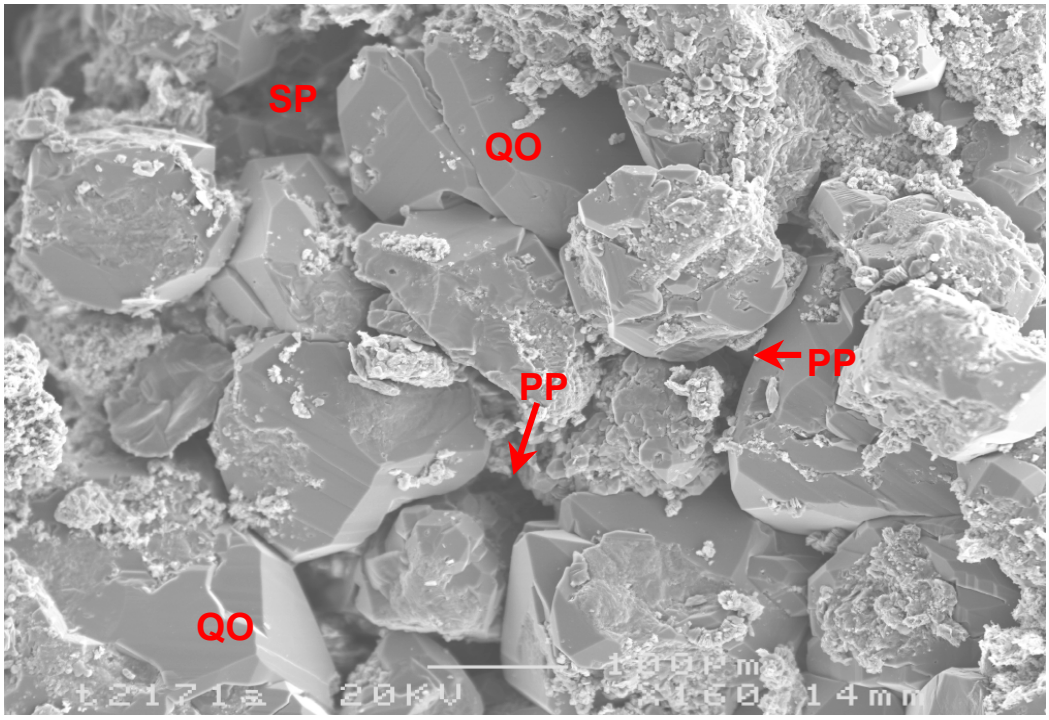

Small primary intergranular pores (PP) that are preserved between quartzose framework grains provide connection for common secondary labile grain dissolution pores (SP). Quartz overgrowths (QO) are only thinly developed, but are effective in reducing intergranular porosity due to the fine grain size.

FIGURE 2

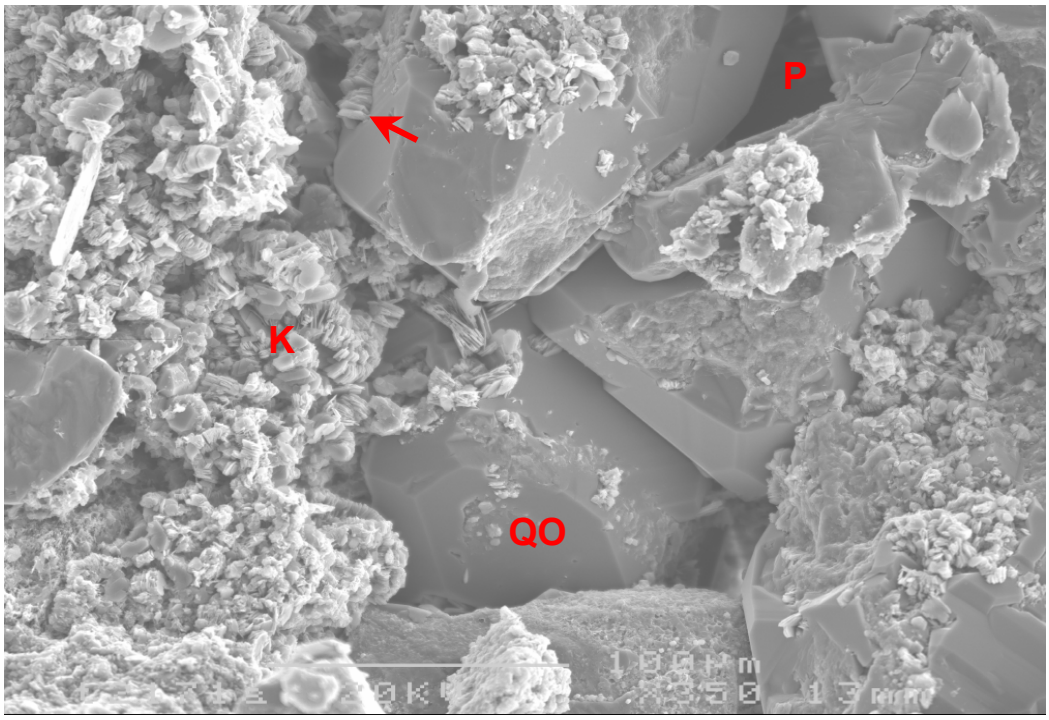

Intergranular porosity (P) reduction is largely the result of authigenic kaolinite (K) formation/compaction and cementation by quartz overgrowths (QO). Kaolinite is engulfed (arrow) by the later formed quartz overgrowths.

PLATE 18: #22 2173.40m

Rock classification: Litharenite

Texture:

Sedimentary structures: Massive

Sorting: Well

Average grain size: 0.25mm (medium sand)

Roundness: Subangular-subrounded

Texture: Grain supported

Packing /grain contacts: Moderate to tight/long, embayed, sutured/microstylolitic

Macropore types: Rare secondary mouldic porosity

Core analyses: Por. = 11.7%, Perm. = 0.483md, GD = 2.69g/cc

Composition:

Quartz (monocrystalline)	50.1%	Heavy minerals	0.3%
Quartz (polycrystalline)	4.4%	Organics	0.3%
Quartz overgrowths	1.8%	Siderite (replacement)	1.3%
Chert	1.3%	Authigenic kaolinite (pf)	5.2%
K-feldspar	3.8%	Authigenic kaolinite (rpl)	11.5%
Volcanic rock fragments	0.7%	Authigenic illite (replacement)	1.7%
Metamorphic rock fragments	15.0%	Detrital clay	1.0%
Sedimentary rock fragments	1.3%	Secondary porosity (mouldic)	0.3%

Comments: This litharenite was highly susceptible to authigenic clay formation and compaction on account of containing abundant micaceous/argillaceous rock fragments at the time of accumulation. Primary intergranular porosity has been almost completely eliminated by authigenic clay (kaolinite, illite) formation, ductile grain/authigenic clay compaction to form pseudomatrix, grain contact dissolution/microstylolitisation, and localised cementation by quartz overgrowths. Common microstylolitic seams and microstylolitic grain contacts, the formation of which was promoted by thin illite clay films, result in tight grain packing. Scattered mouldic secondary pores occur where labile grains (mainly K-feldspar) have dissolved. The sample is mainly microporous and consequently has low permeability.

PLATE 18: #22 2173.40m

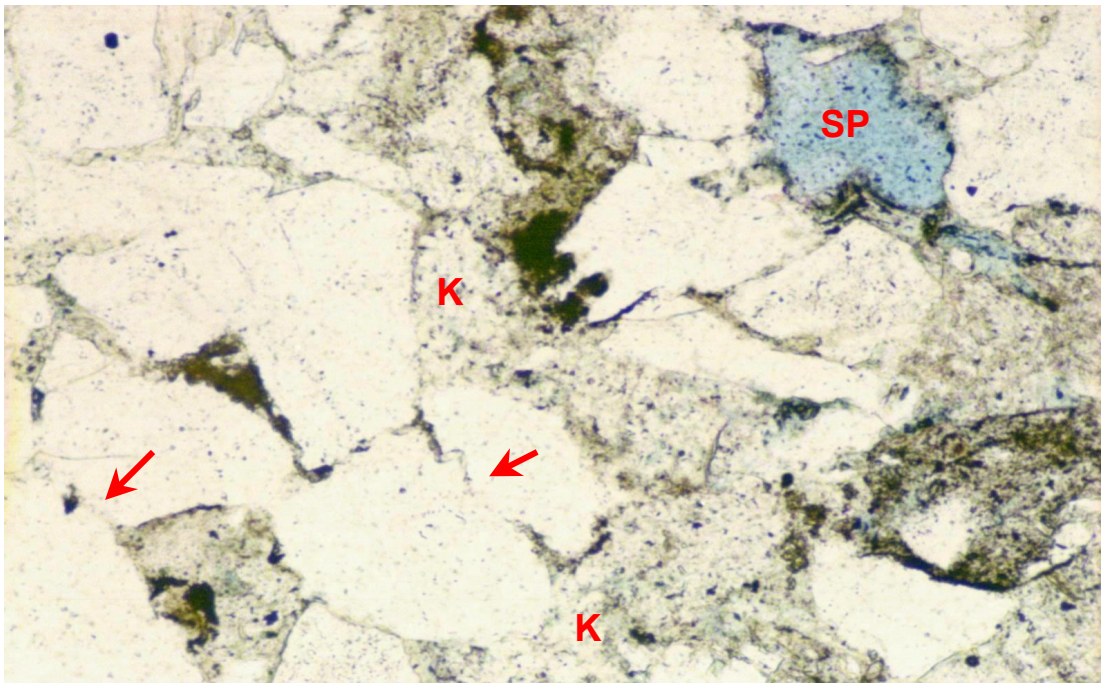

FIGURE 1 Plane polarised light
FIGURE 2 Crossed polarisers

0.2mm

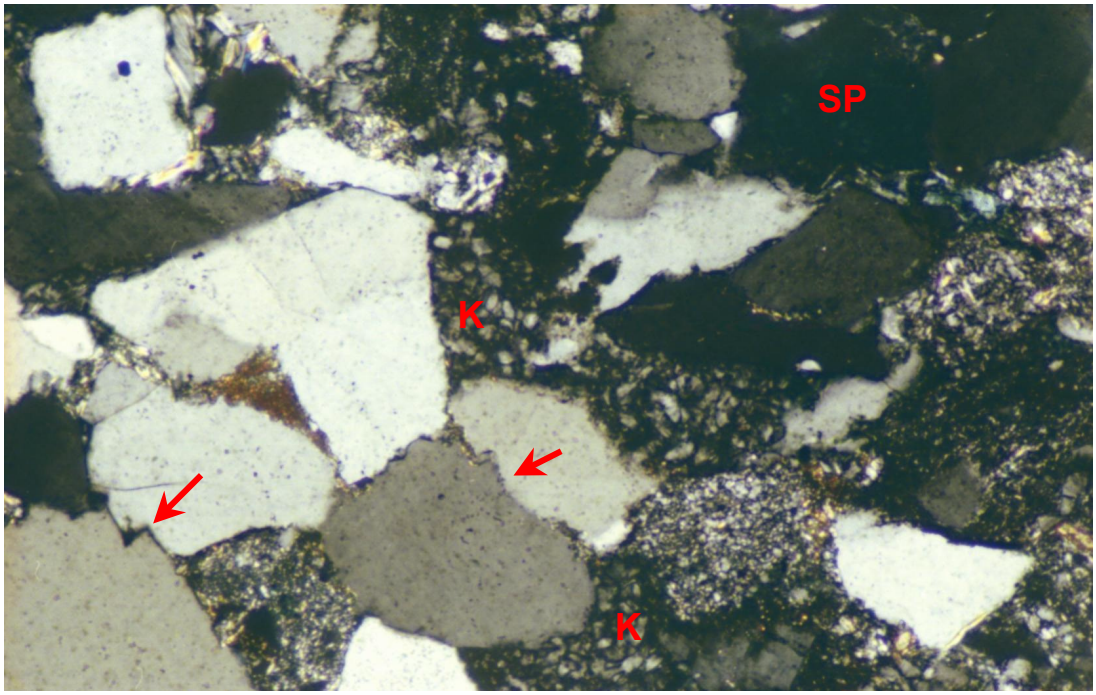

An isolated secondary mouldic pore (SP) occurs in a sandstone in which intergranular porosity has been eliminated by grain contact dissolution/microstylolitisation (arrows) and authigenic kaolinite (K) formation.

PLATE 19: #22 2173.40m cont.

FIGURE 1

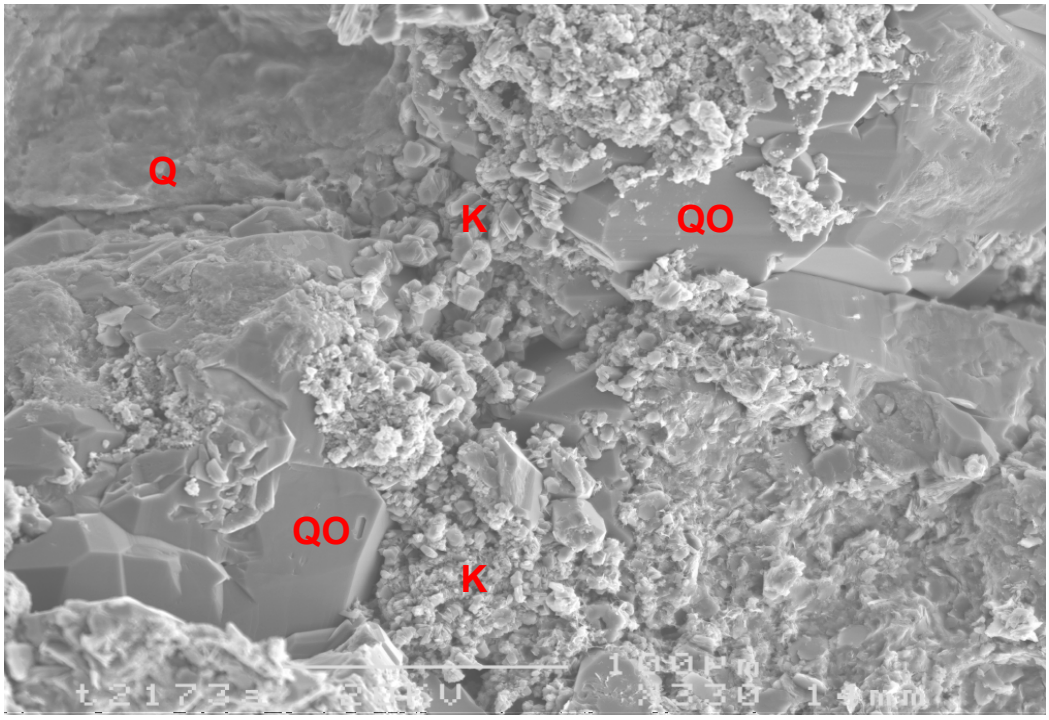

Tight sandstone in which intergranular areas between chemically compacted quartz grains (Q) are filled by authigenic kaolinite (K) and localised quartz overgrowth cement (QO). The kaolinite is the altered and compacted remnant of a micaceous rock fragment.

FIGURE 2

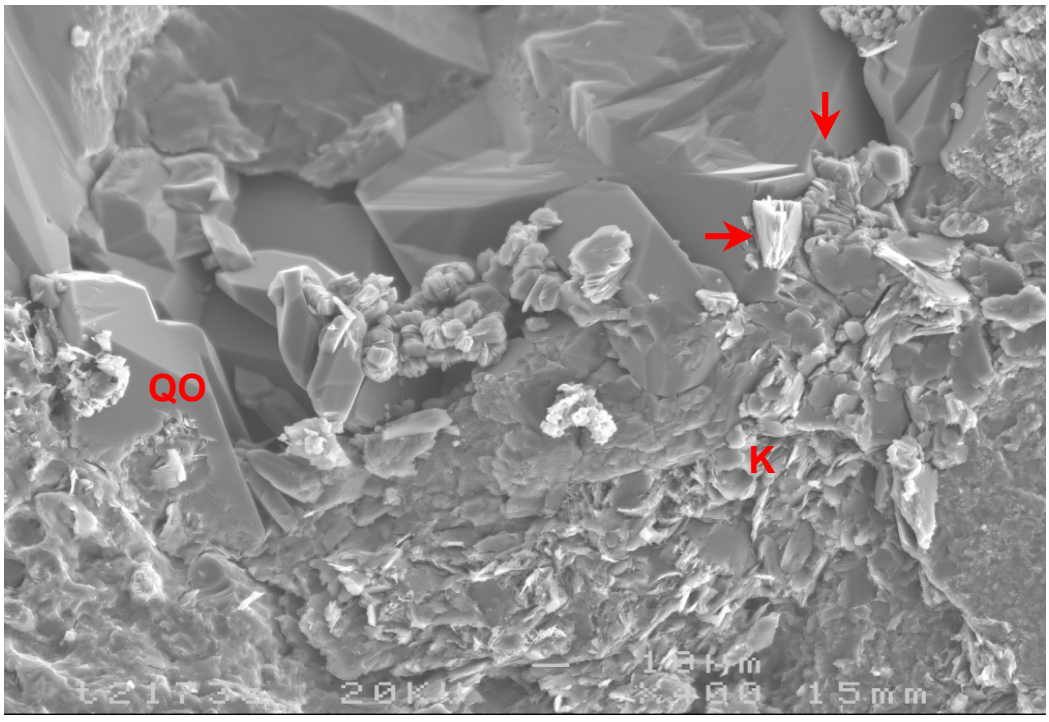

Intergranular porosity has been eliminated by quartz overgrowth (QO) cementation and the compactional deformation of a kaolinitised micaceous rock fragment (K). Quartz overgrowths enclose (arrows) earlier formed kaolinite. The sandstone contains negligible intergranular porosity and consequently has very low (0.483md) permeability.

PLATE 20: #24 2173.83m

Rock classification: Sublitharenite

Texture:

Sedimentary structures:	Massive
Sorting:	Moderately-well
Average grain size:	0.54mm (coarse sand)
Roundness:	Subangular-subrounded
Texture:	Grain supported
Packing /grain contacts:	Moderate/long, embayed
Macropore types:	Primary intergranular porosity, secondary intergranular porosity, secondary intragranular porosity
Core analyses:	Por. = 18.5%, Perm. = 1240md, GD = 2.66g/cc

Composition:

Quartz (monocrystalline)	62.8%	Authigenic kaolinite (pf)	2.0%
Quartz (polycrystalline)	3.6%	Authigenic kaolinite (rpl)	5.8%
Quartz overgrowths	7.6%	Primary porosity (intergranular)	8.2%
K-feldspar	1.1%	Secondary porosity (intergran)	5.1%
Volcanic rock fragments	0.3%	Secondary porosity (intragran)	0.7%
Metamorphic rock fragments	2.8%		

Comments: This sandstone is coarse grained and relatively quartzose and therefore contains abundant primary intergranular porosity, despite porosity reduction by grain contact dissolution, quartz overgrowth cementation, authigenic kaolinite formation and ductile grain/authigenic clay compaction to form localised kaolinitic pseudomatrix. Primary porosity is supplemented by scattered secondary intergranular pores that are the result of K-feldspar dissolution. Macropores are generally evenly distributed, hence are well interconnected.

PLATE 20: #24 2173.83m

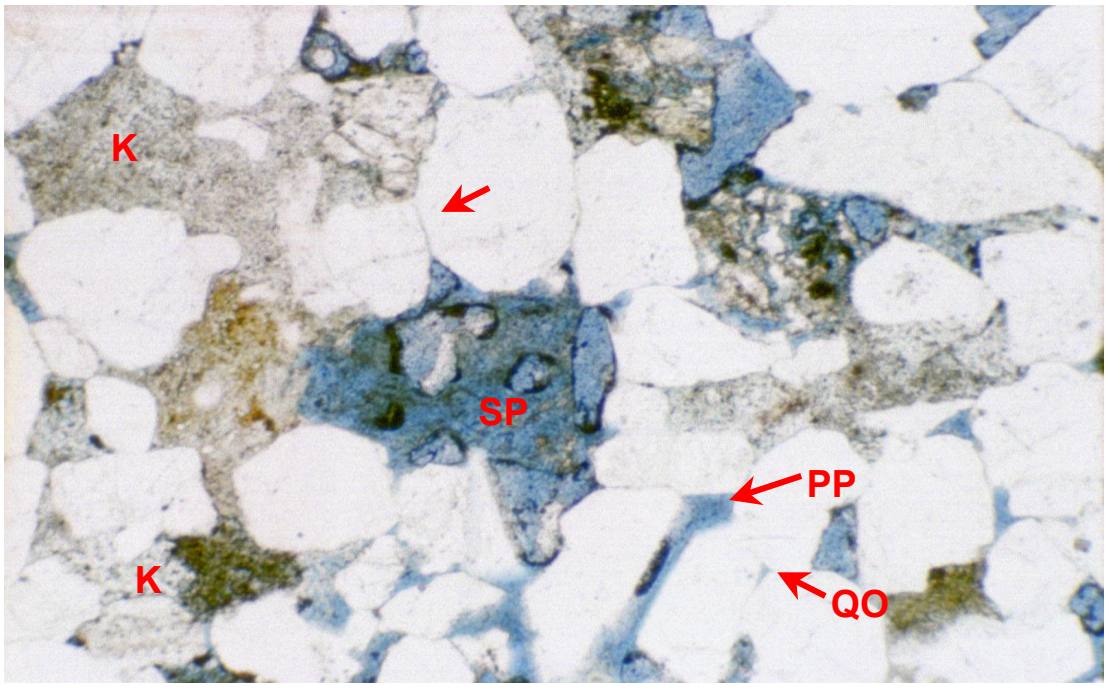

FIGURE 1 Plane polarised light
FIGURE 2 Crossed polarisers

0.4mm

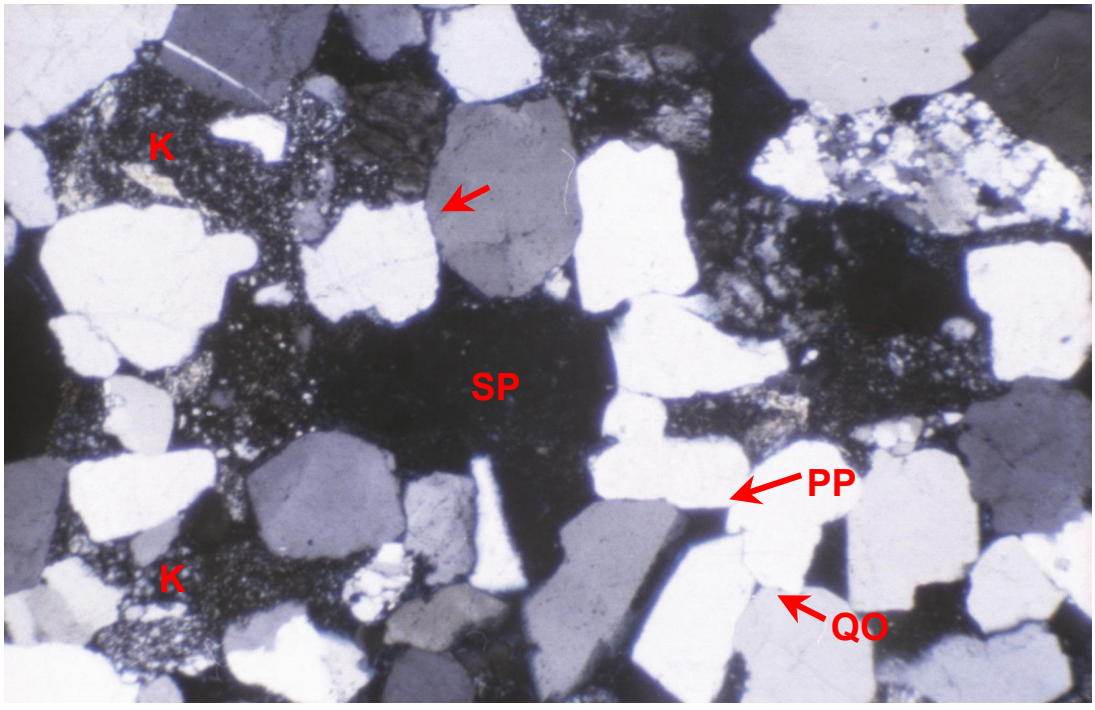

High permeability reflects the presence of abundant, evenly distributed primary intergranular pores (PP) that provide connection for scattered secondary pores (SP) that occur where K-feldspar grains have partly to completely dissolved. Good porosity is preserved despite the porosity-reducing effects of grain contact dissolution (arrow), quartz overgrowth (QO) cementation and kaolinite pseudomatrix (K) formation.

PLATE 21: #24 2173.83m cont.

FIGURE 1

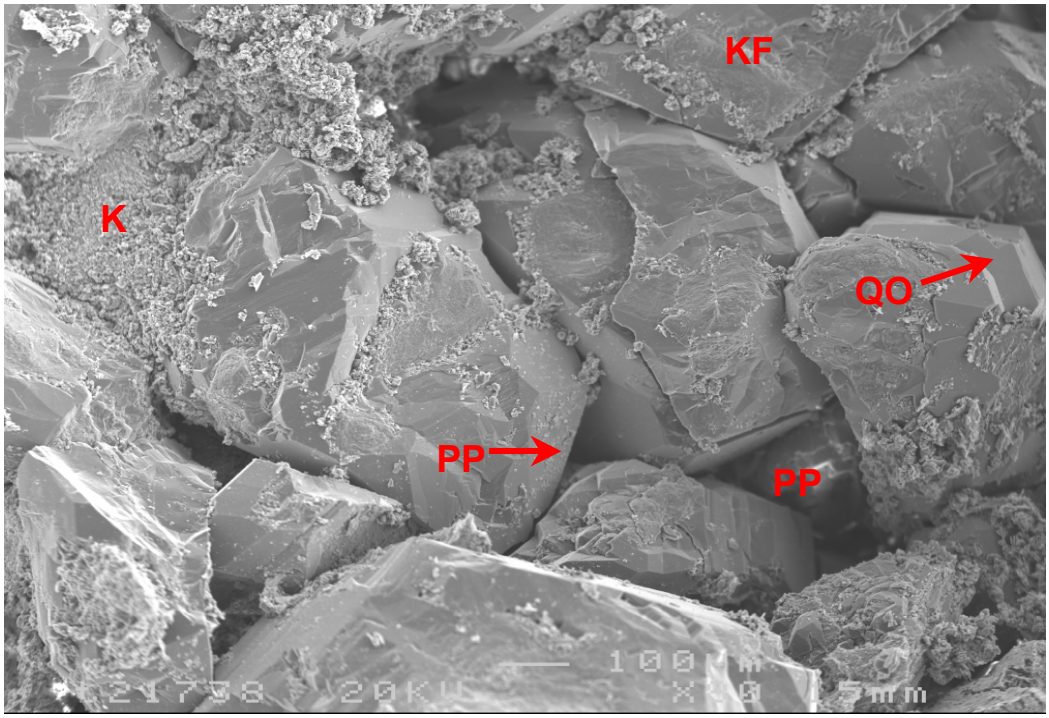

Despite porosity reduction by quartz overgrowth (QO) cementation and localised kaolinite pseudomatrix (K) formation, this sandstone contains common primary intergranular pores (PP). A K-feldspar grain (KF) is also marked.

FIGURE 2

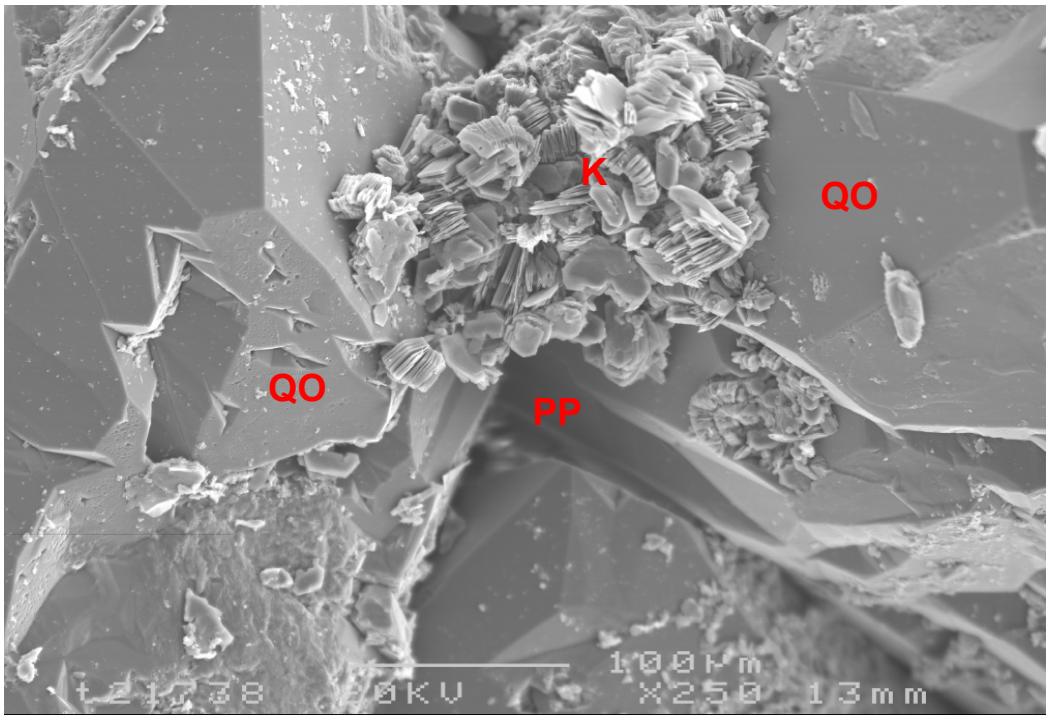

This SEM micrograph shows typical authigenic kaolinite (K) that has formed by alteration of a micaceous grain. The kaolinite partly occupies a primary intergranular pore (PP) that is bounded by quartz overgrowths (QO). Between most quartz grains, quartz overgrowths only partly occupy all available intergranular space.

PLATE 22: #25 2174.10m

Rock classification: Litharenite

Texture:

Sedimentary structures:	Sporadic fine microstylolitic laminae; otherwise massive
Sorting:	Poor
Average grain size:	0.38mm (medium sand)
Roundness:	Subangular-subrounded
Texture:	Grain supported
Packing /grain contacts:	Moderate to tight/long, embayed, sutured/microstylolitic
Macropore types:	Secondary mouldic porosity; very minor primary intergranular porosity
Core analyses:	Por. = 13.2%, Perm. = 3.27md, GD = 2.68g/cc

Composition:

Quartz (monocrystalline)	55.2%	Organics	1.4%
Quartz (polycrystalline)	5.4%	Siderite (replacement)	2.3%
Quartz overgrowths	0.7%	Authigenic kaolinite (pf)	1.1%
Chert	0.7%	Authigenic kaolinite (rpl)	7.8%
K-feldspar	3.4%	Authigenic illite (replacement)	1.2%
Volcanic rock fragments	0.7%	Detrital clay	0.7%
Metamorphic rock fragments	15.8%	Primary porosity (intergranular)	0.3%
Sedimentary rock fragments	1.0%	Secondary porosity (mouldic)	2.0%
Mica	0.3%		

Comments: Intergranular porosity in this litharenite has been almost completely eliminated by ductile grain/authigenic clay compaction, authigenic kaolinite formation, grain contact dissolution/microstylolitisation and very minor quartz overgrowth cementation. The sample includes sporadic tight stylolitic laminae along which there are concentrations of organic fragments and detrital clay, and there are also common microstylolitic grain contacts, the formation of which was promoted by thin illite clay films. Microcrystalline siderite replaces altered micaceous grains and argillaceous intraclasts. Most macroporosity is accounted for by widely scattered, hence poorly interconnected secondary mouldic pores that are the result of K-feldspar grain dissolution. Pore throats are largely chocked by authigenic clay, compacted ductile grains, quartz overgrowths and fine siderite, hence permeability is low.

PLATE 22: #25 2174.10m

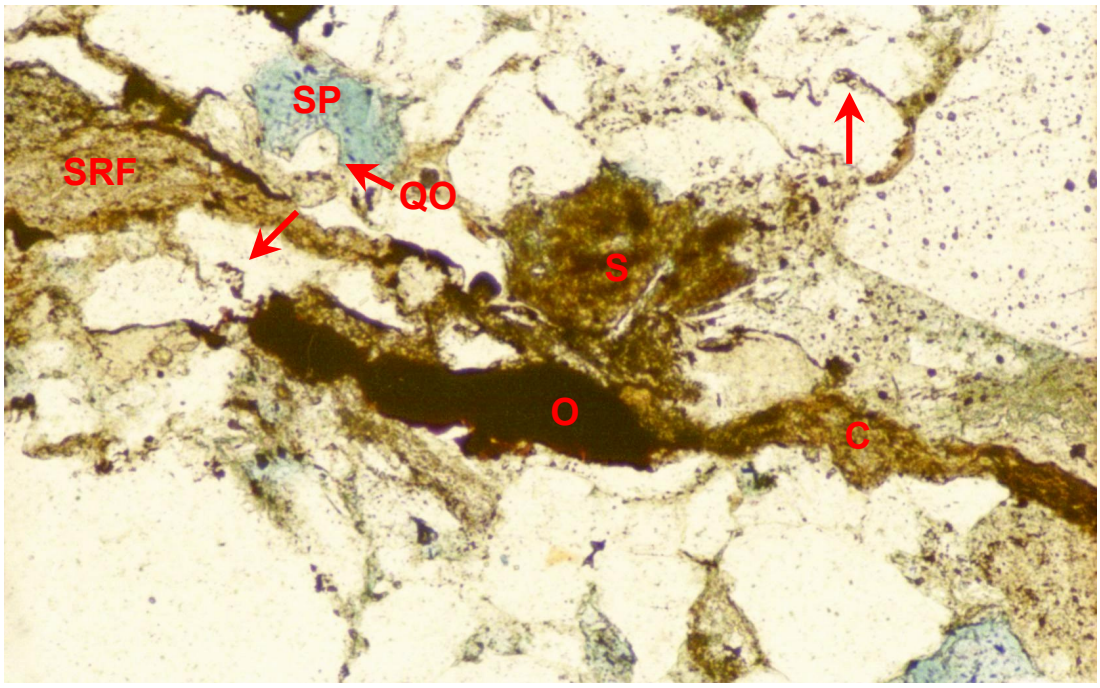

FIGURE 1 Plane polarised light

FIGURE 2 Crossed polarisers

0.2mm

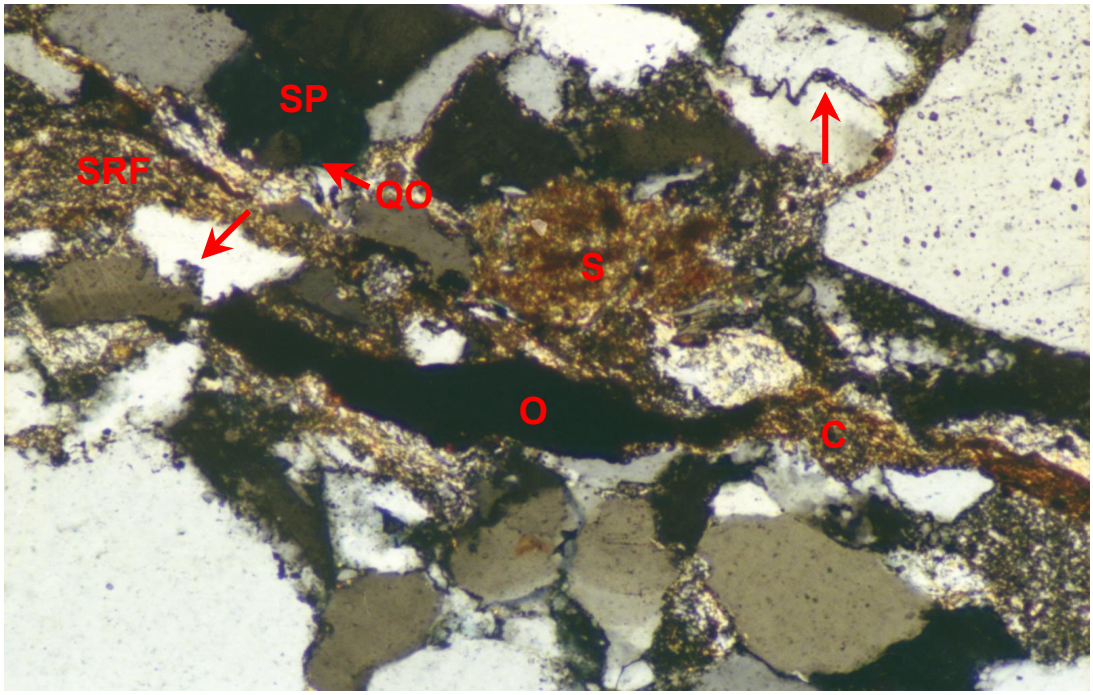

Intergranular porosity has been eliminated by microstylolitisation (arrows), the compaction of argillaceous sedimentary rock fragments (SRF) and organics (O), and pore filling by detrital clay (C). One altered micaceous grain is replaced by microcrystalline siderite (S). Most porosity in the sample is accounted for by isolated secondary mouldic pores (SP). A quartz overgrowth (QO) has developed inside the marked secondary pore, indicating that at least some quartz overgrowths postdate secondary porosity formation.

PLATE 23: #25 2174.10m cont.

FIGURE 1

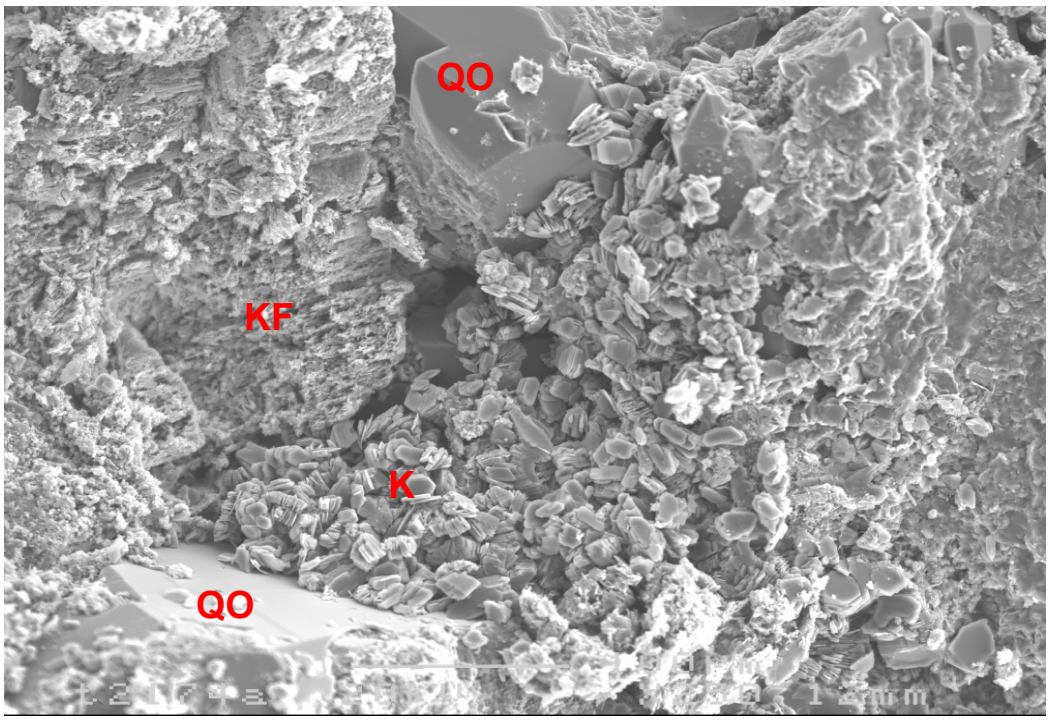

An intergranular space between quartz grains and a corroded K-feldspar grain (KF) is filled by authigenic kaolinite (K) and poorly developed quartz overgrowths (QO).

FIGURE 2

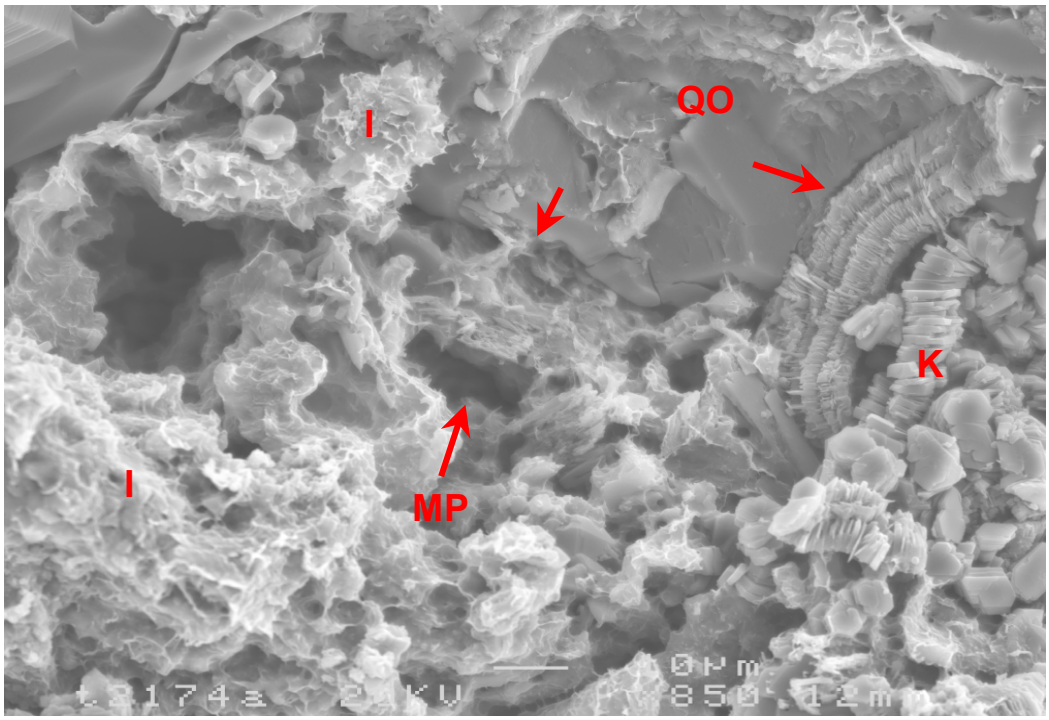

Clay in the sample is mainly authigenic kaolinite (K) and subordinate illite (I) that have formed by partial to complete alteration of labile micaceous/argillaceous grains. The clay is highly microporous (MP) and is enclosed (arrows) by a later formed quartz overgrowth (QO). Low permeability largely reflects the common occurrence of authigenic clay within intergranular spaces.

PLATE 24: #28 2174.80m

Rock classification: Quartzarenite

Texture:

Sedimentary structures:	Thickly laminated – laminae defined by grain size variations
Sorting:	Moderately-well
Average grain size:	0.79mm (coarse sand)
Roundness:	Subangular-subrounded
Texture:	Grain supported
Packing /grain contacts:	Moderate/long, embayed
Macropore types:	Primary intergranular porosity, secondary intergranular porosity, secondary intragranular porosity
Core analyses:	Por. = 20.9%, Perm. = 3430md, GD = 2.65g/cc

Composition:

Quartz (monocrystalline)	63.3%	Authigenic kaolinite (pf)	0.5%
Quartz (polycrystalline)	3.9%	Authigenic kaolinite (rpl)	3.9%
Quartz overgrowths	7.3%	Primary porosity (intergranular)	11.0%
K-feldspar	2.3%	Secondary porosity (intergran)	5.8%
Metamorphic rock fragments	1.3%	Secondary porosity (intragran)	0.7%

Comments: This sandstone is coarse grained and relatively quartzose and therefore contains abundant primary intergranular porosity, despite porosity reduction by grain contact dissolution, quartz overgrowth cementation, minor authigenic kaolinite formation and minor ductile grain/authigenic clay compaction to form localised kaolinitic pseudomatrix. Primary porosity is supplemented by scattered secondary intergranular and intragranular pores that are the result of K-feldspar dissolution. Macropores are evenly distributed, hence are well interconnected.

PLATE 24: #28 2174.80m

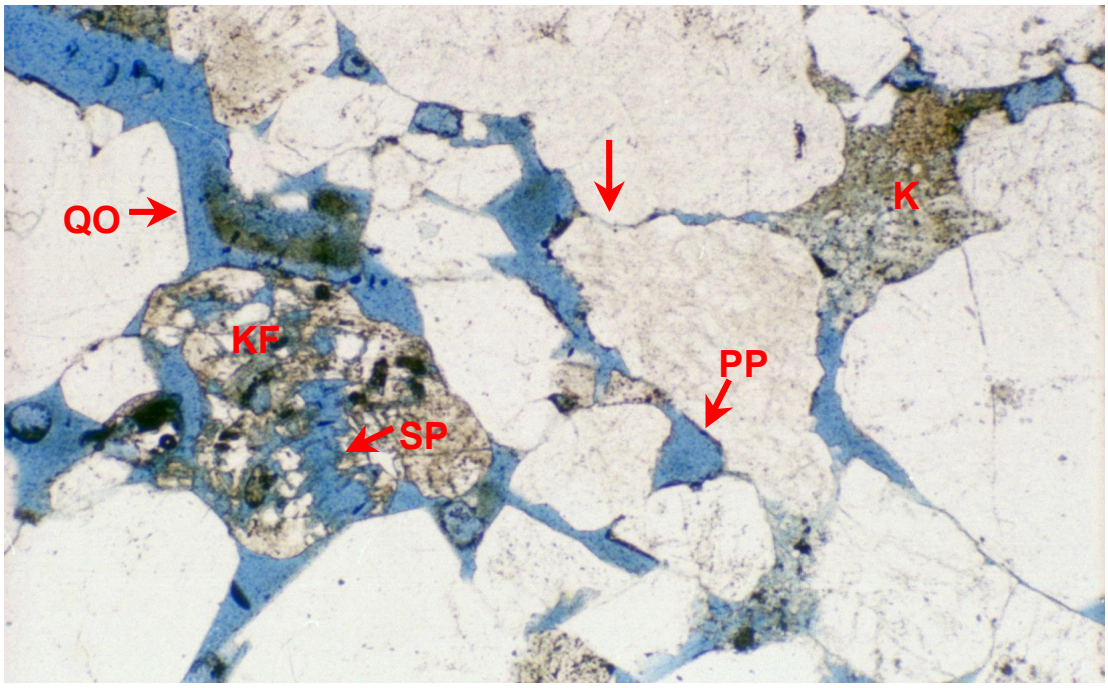

FIGURE 1 Plane polarised light

FIGURE 2 Crossed polarisers

0.4mm

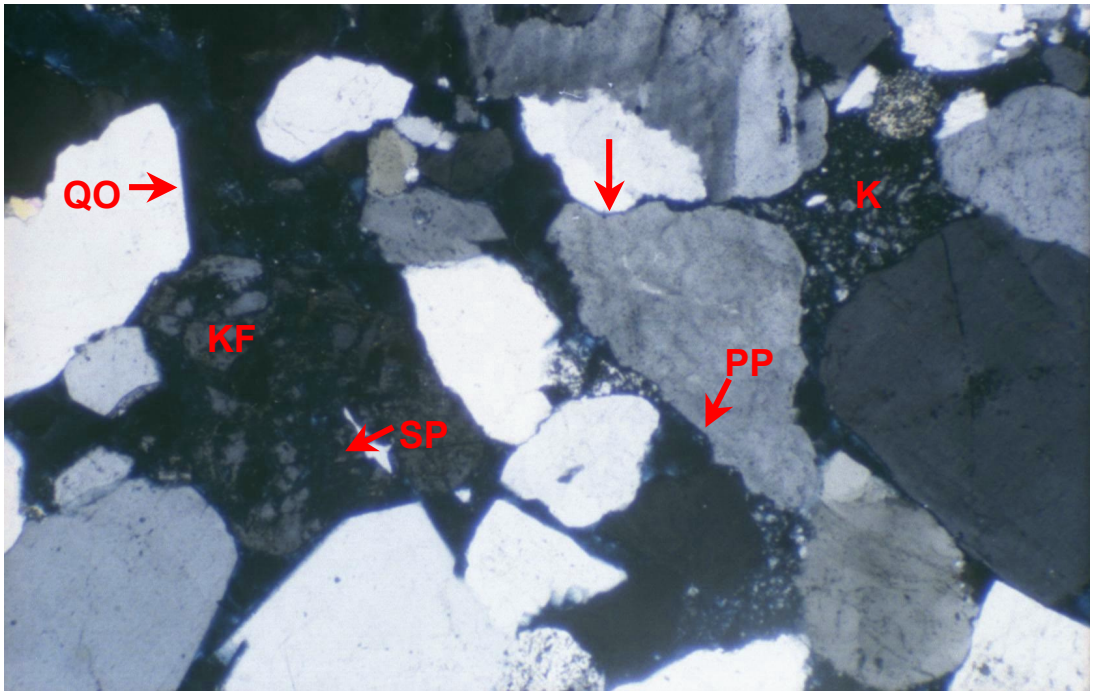

Abundant, clean, evenly distributed primary intergranular porosity (PP) is supplemented by secondary porosity (SP) that is associated with a partly dissolved, granitic K-feldspar (KF) grain. Minor porosity reduction is the result of grain contact dissolution (arrow), quartz overgrowth (QO) cementation and compaction of a kaolinitised labile grain (K).

PLATE 25: #28 2174.80m cont.

FIGURE 1

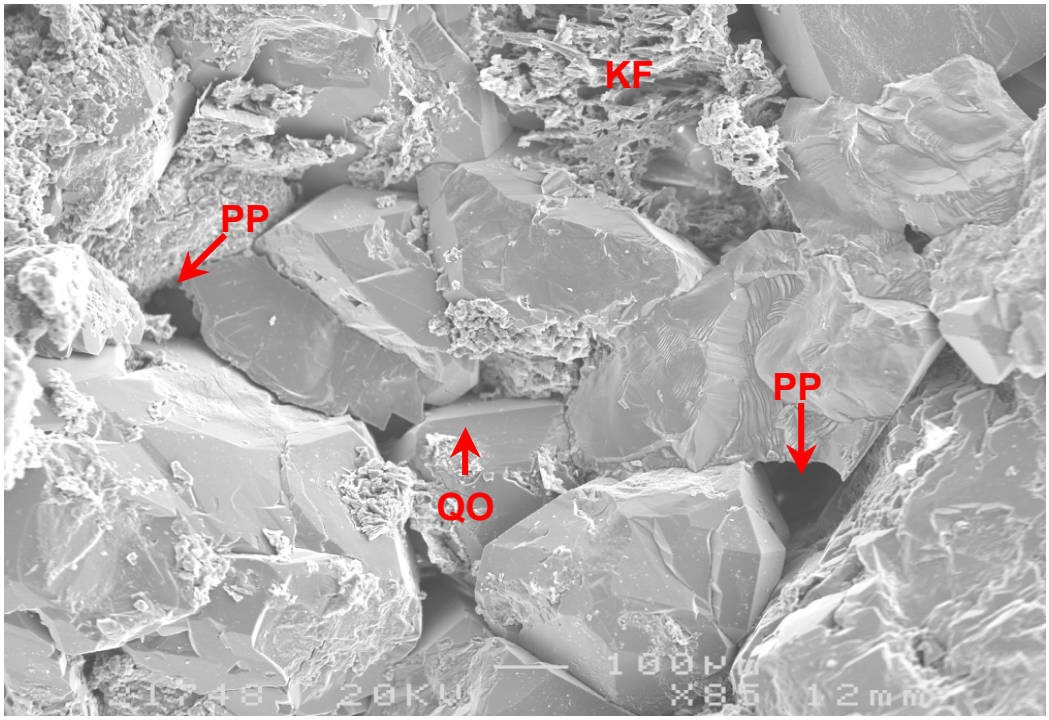

Clean, well interconnected primary intergranular pores (PP) are preserved between quartz grains and a corroded K-feldspar grain (KF). Quartz overgrowths (QO) only occupy a small portion of total available intergranular space between most grains.

FIGURE 2

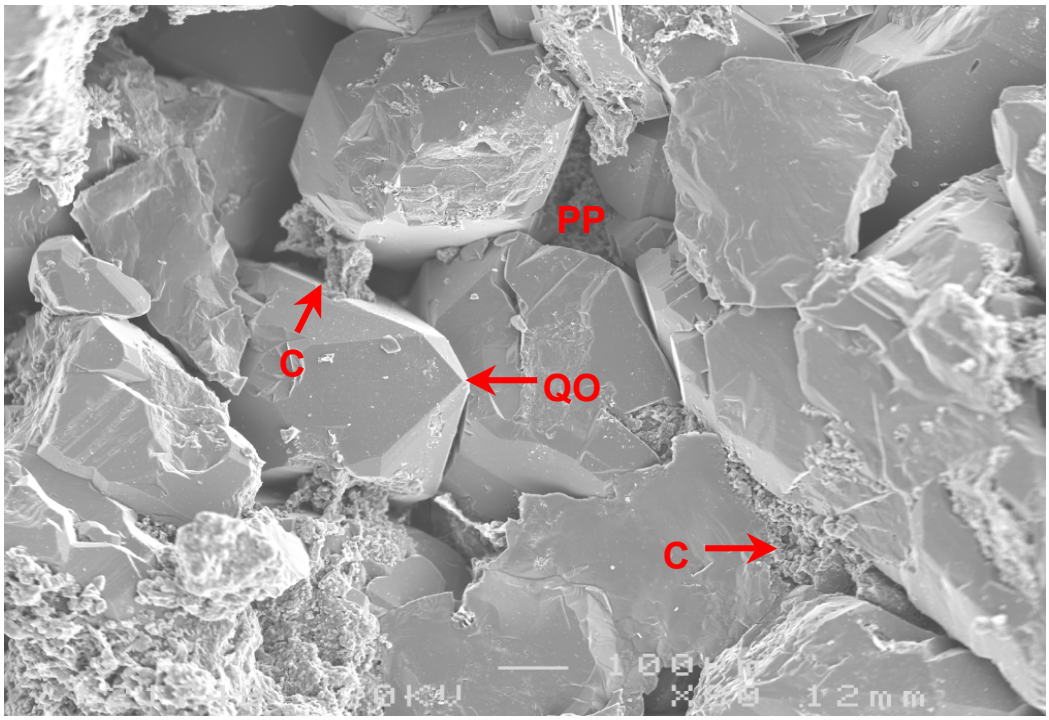

Preservation of abundant primary intergranular porosity (PP) reflects the quartzose and coarse grained character of the sandstone. Quartz overgrowths (QO) are common, but only partly occlude intergranular spaces. Intergranular spaces locally contain authigenic clay (C) that is the altered remnant of labile grains.

PLATE 26: 2180.06m (reconnaissance SEM study sample)

FIGURE 1

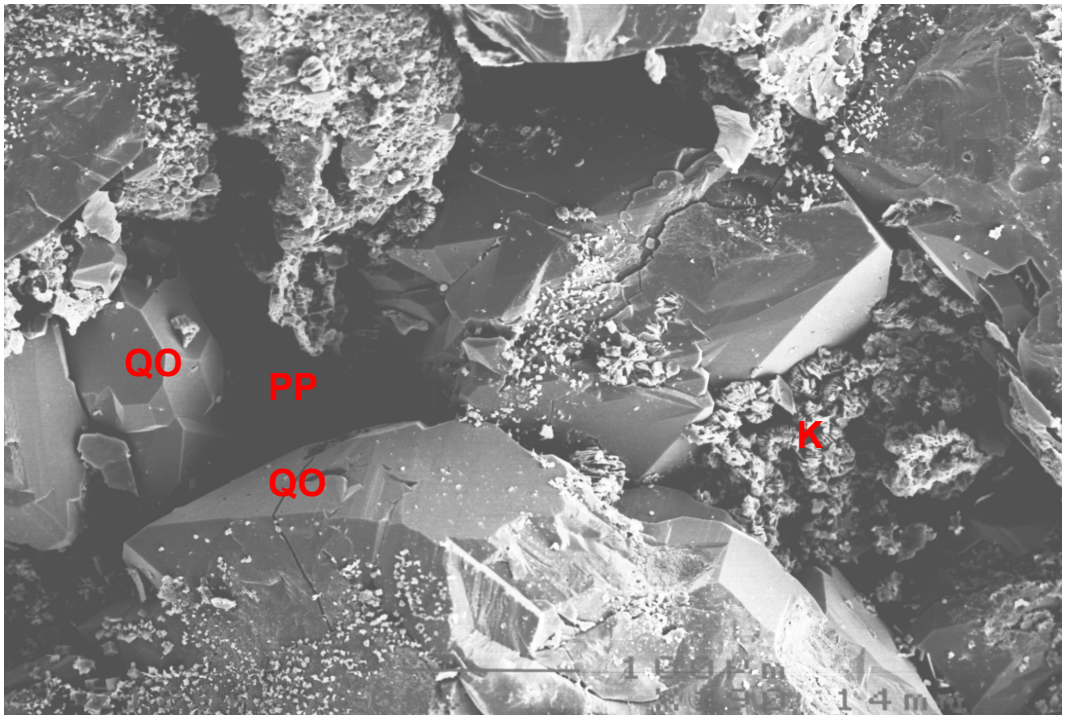

Quartz overgrowths (QO) partly occupy a clean primary intergranular pore (PP). An adjacent intergranular area is largely filled by loosely packed authigenic kaolinite (K) that is the altered remnant of a micaceous grain.

FIGURE 2

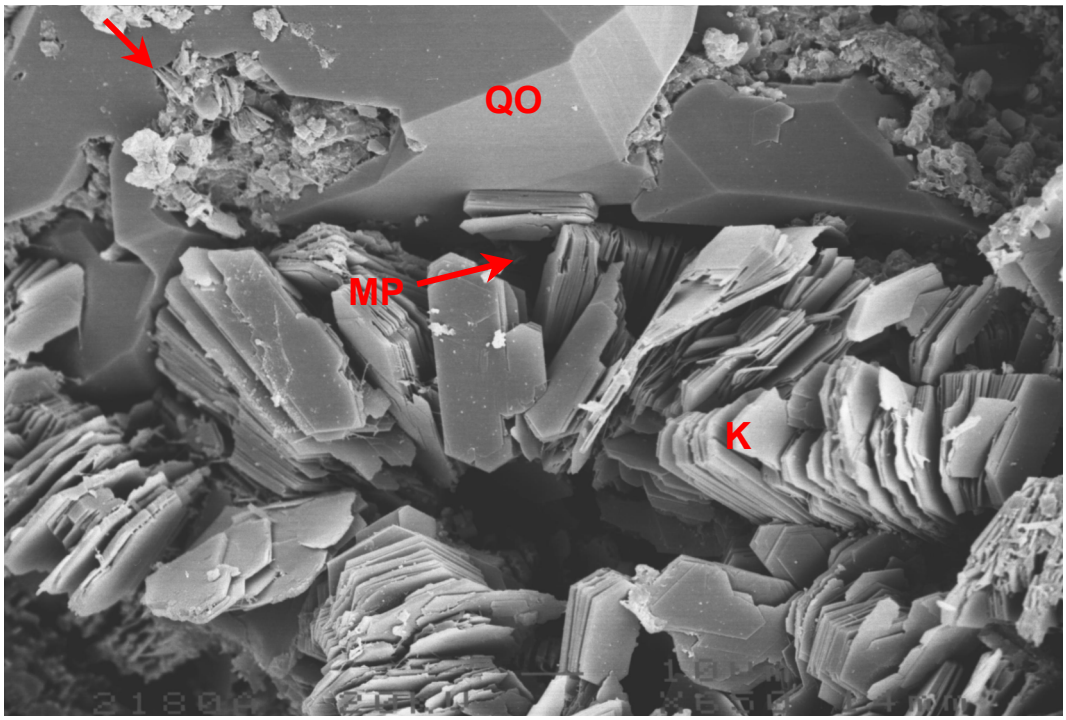

Detail of typical authigenic kaolinite (K) and associated microporosity (MP) that occur where a micaceous grain has altered. Kaolinite is enclosed (arrow) by a later formed quartz overgrowth (QO). Most clay in the sandstone is authigenic kaolinite.

PLATE 27: #46 2180.10m

Rock classification: Sublitharenite

Texture:

Sedimentary structures:	Massive
Sorting:	Moderately-well
Average grain size:	0.54mm (coarse sand)
Roundness:	Subangular-subrounded
Texture:	Grain supported
Packing /grain contacts:	Moderate/long, embayed
Macropore types:	Primary intergranular porosity, secondary intergranular porosity, secondary intragranular porosity
Core analyses:	Por. = 23.2%, Perm. = 4710md, GD = 2.65g/cc

Composition:

Quartz (monocrystalline)	59.6%	Pyrite	0.3%
Quartz (polycrystalline)	3.4%	Authigenic kaolinite (pf)	0.5%
Quartz overgrowths	5.8 %	Authigenic kaolinite (rpl)	4.9%
K-feldspar	2.3%	Primary porosity (intergranular)	11.8%
Volcanic rock fragments	0.3%	Secondary porosity (intergran)	6.5%
Granitic rock fragments	0.3%	Secondary porosity (intragran)	0.3%
Metamorphic rock fragments	4.0%		

Comments: This sandstone is the most permeable of the sample suite. Like the previous sample, it is coarse grained and relatively quartzose and therefore contains abundant primary intergranular porosity, despite porosity reduction by grain contact dissolution, quartz overgrowth cementation, authigenic kaolinite formation and ductile grain/authigenic clay compaction to form localised kaolinitic pseudomatrix. Primary porosity is supplemented by scattered secondary intergranular pores that are the result of K-feldspar dissolution. Macropores are generally evenly distributed, hence are well interconnected.

PLATE 27: #46 2180.10m

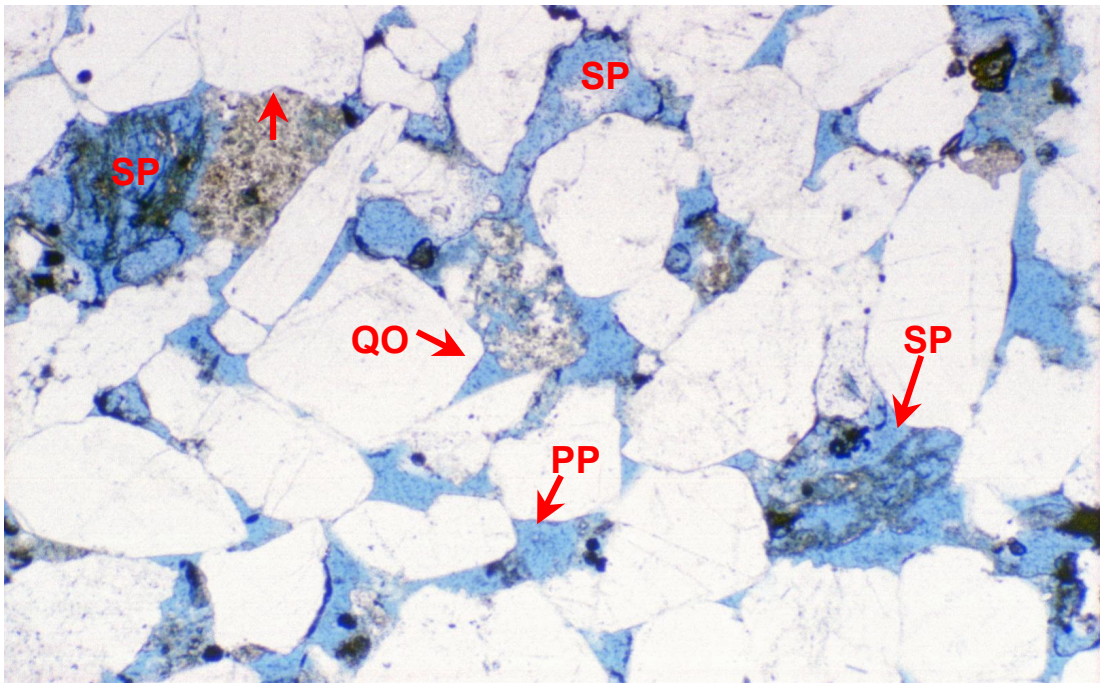

FIGURE 1 Plane polarised light
FIGURE 2 Crossed polarisers

0.4mm

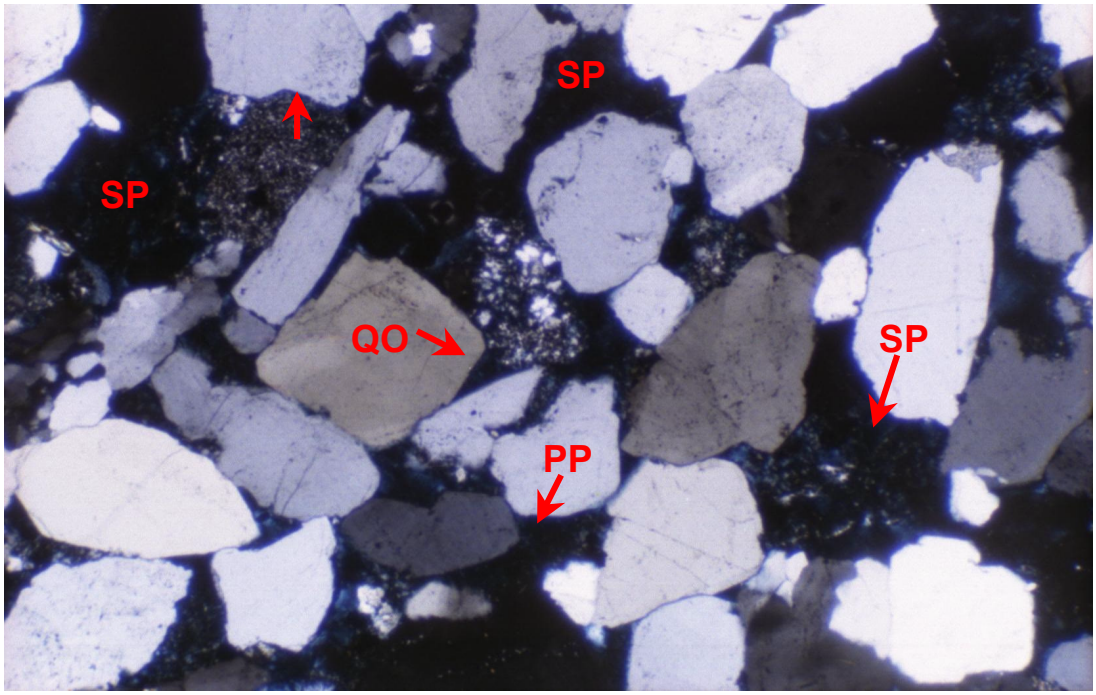

Abundant, clean, evenly distributed, primary intergranular porosity (PP) is supplemented by secondary porosity (SP) that occurs where K-feldspar grains have largely or completely dissolved. Minor porosity reduction is the result of grain contact dissolution (arrow) and quartz overgrowth (QO) cementation.

PLATE 28: #46 2180.10m cont.

FIGURE 1

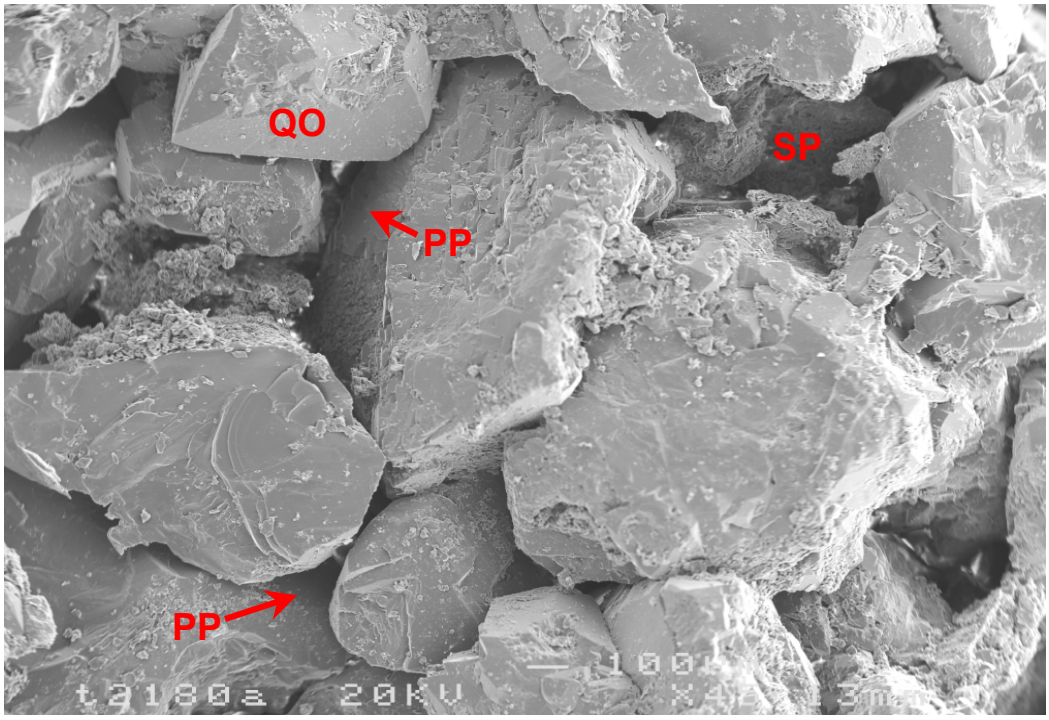

High permeability reflects the presence of abundant, clean primary intergranular porosity (PP) and secondary labile grain dissolution porosity (SP). Quartz overgrowths (QO) are thinly developed and thus occlude only a small portion of intergranular spaces.

FIGURE 2

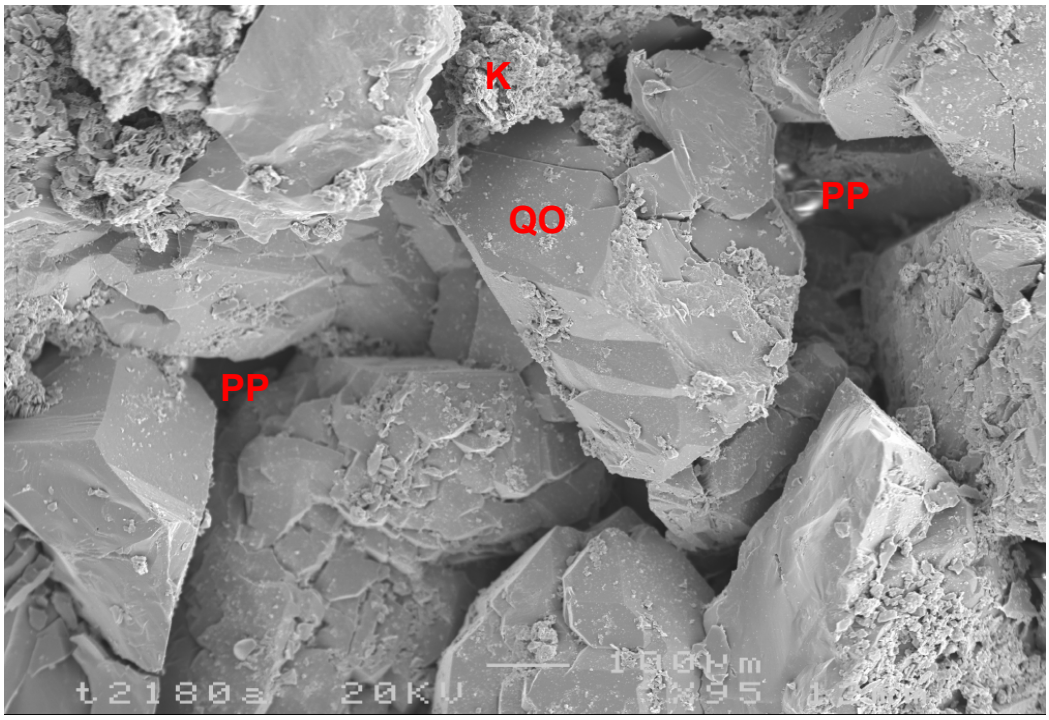

Large clean primary intergranular pores (PP) are preserved between juxtaposed quartz grains, despite cementation by quartz overgrowths (QO). Kaolinitic remnants of compacted and altered labile grains (K) that occur between some quartz grains have little impact on reservoir quality.

PLATE 29: #55 2182.92m

Rock classification: Sublitharenite

Texture:

Sedimentary structures:	Sporadic, poorly defined, thin, fine grained laminae
Sorting:	Moderate
Average grain size:	0.53mm (coarse sand)
Roundness:	Subangular-subrounded
Texture:	Grain supported
Packing /grain contacts:	Moderate/long, embayed, sutured/microstylolitic
Macropore types:	Primary intergranular porosity, secondary intergranular porosity, secondary intragranular porosity
Core analyses:	Por. = 17.7%, Perm. = 109md, GD = 2.66g/cc

Composition:

Quartz (monocrystalline)	55.1%	Siderite (replacement)	3.0%
Quartz (polycrystalline)	4.3%	Authigenic kaolinite (pf)	2.1%
Quartz overgrowths	2.3%	Authigenic kaolinite (rpl)	8.6%
Chert	0.7%	Authigenic illite (replacement)	0.7%
K-feldspar	3.4%	Detrital clay	0.3%
Volcanic rock fragments	0.6%	Primary porosity (intergranular)	3.4%
Metamorphic rock fragments	10.0%	Secondary porosity (intergran)	4.0%
Sedimentary rock fragments	0.3%	Secondary porosity (intragran)	0.3%
Organics	0.9%		

Comments: Despite being coarse grained, this sample contains only minor primary intergranular porosity due to the porosity reducing effects of authigenic clay formation, ductile grain/authigenic clay compaction, grain contact dissolution and quartz overgrowth cementation. However, there are common secondary intergranular pores that have formed by K-feldspar dissolution. The sample was relatively lithic labile at the time of accumulation on account of containing significant amounts of fine to medium sand-sized grains, and was thus prone to authigenic clay formation and compaction. Some altered micaceous grains are replaced by microcrystalline siderite. Finer parts of the sample contain little or no intergranular porosity due to authigenic clay formation and compaction. With many pores and pore throats being filled by authigenic clay, compacted ductile grains and quartz overgrowths, permeability is only moderate.

PLATE 29: #55 2182.92m

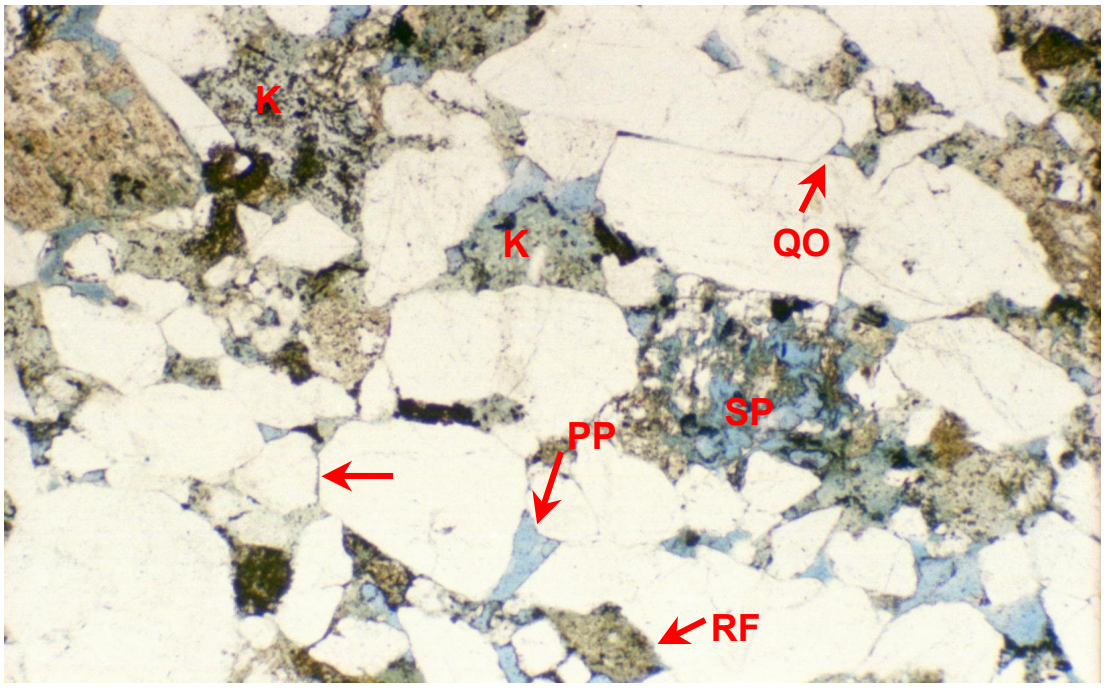

FIGURE 1 Plane polarised light
FIGURE 2 Crossed polarisers

0.4mm

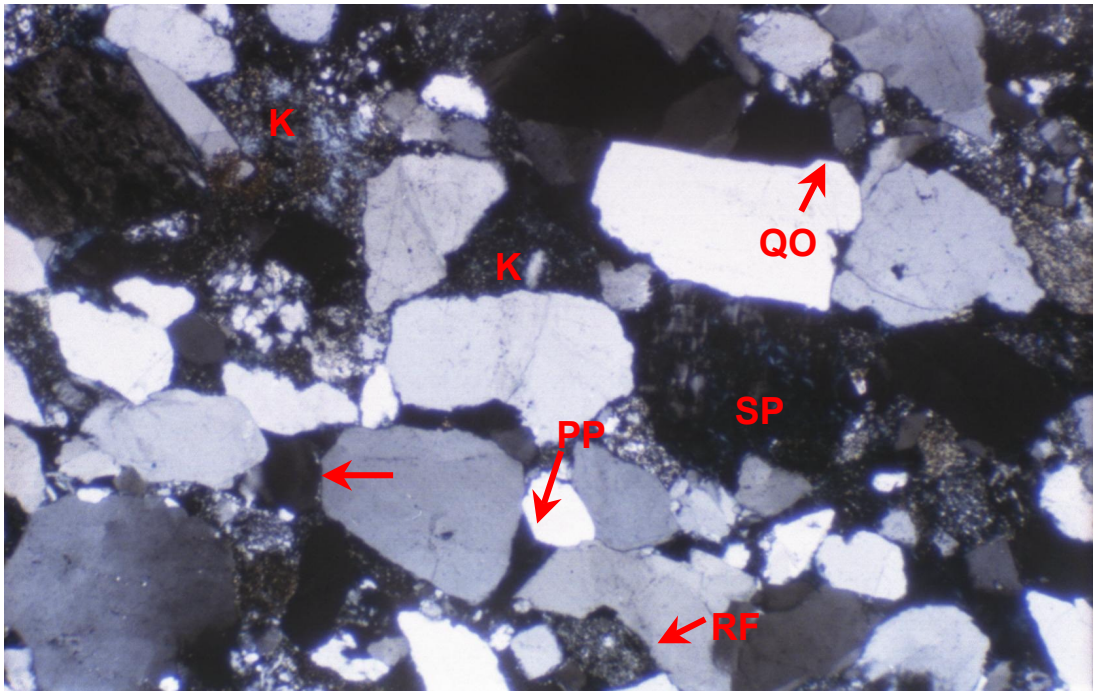

Connection between primary intergranular pores (PP) and secondary K-feldspar dissolution pores (SP) is significantly reduced by the effects of authigenic kaolinite (K) formation, compaction of argillaceous rock fragments (RF), grain contact dissolution (arrow) and quartz overgrowth (QO) cementation.

PLATE 30: #55 2182.92m

FIGURE 1

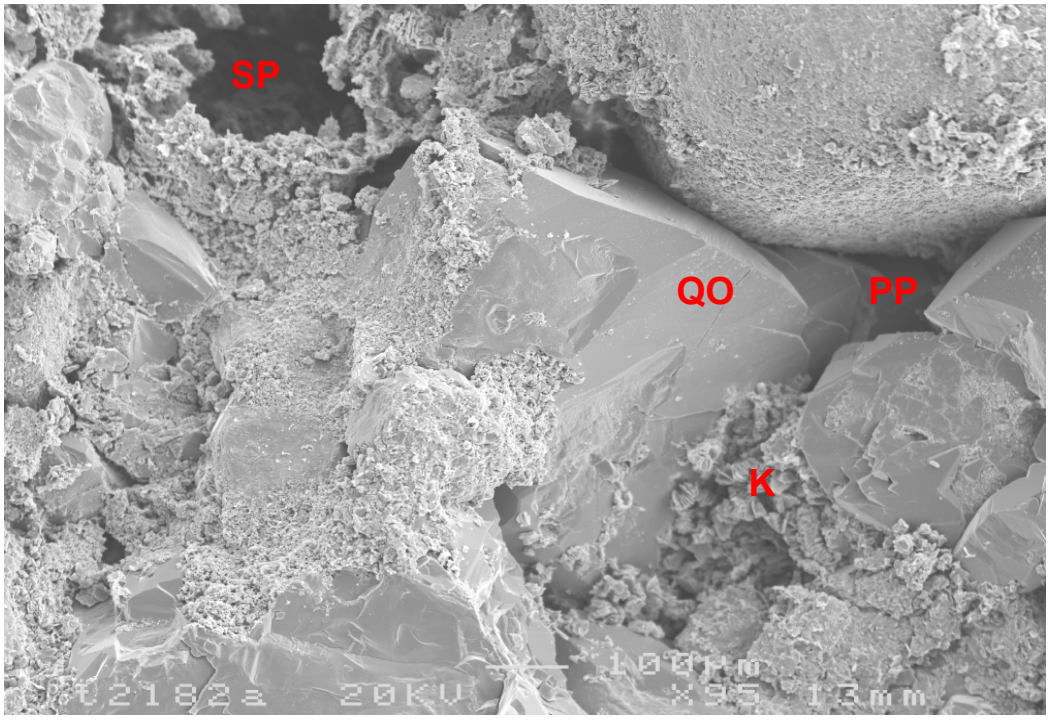

With many intergranular spaces being filled by authigenic kaolinite (K) and quartz overgrowths (QO), primary intergranular pores (PP) and secondary labile grain dissolution pores (SP) are not uniformly distributed and thus do not have a high degree of connectivity throughout the sandstone.

FIGURE 2

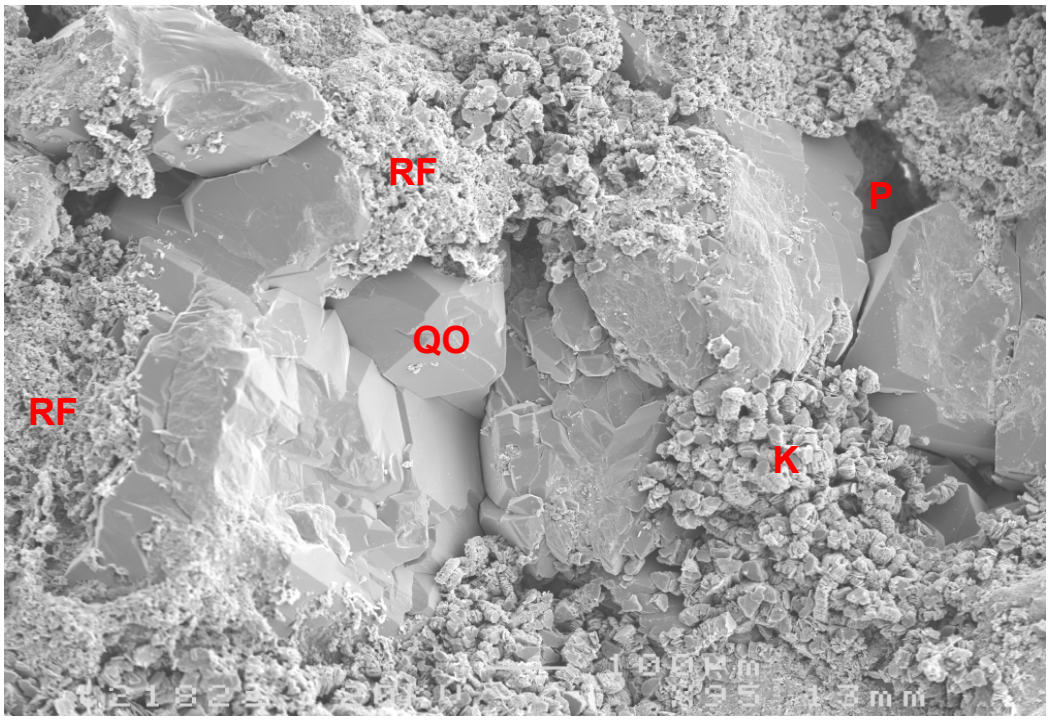

Within some parts of the sample, intergranular porosity (P) has been almost entirely eliminated by the compactional deformation of variably altered, ductile rock fragments (RF) and by authigenic kaolinite (K) formation and quartz overgrowth cementation (QO).

PLATE 31: 2184.76m (reconnaissance SEM study sample)

FIGURE 1

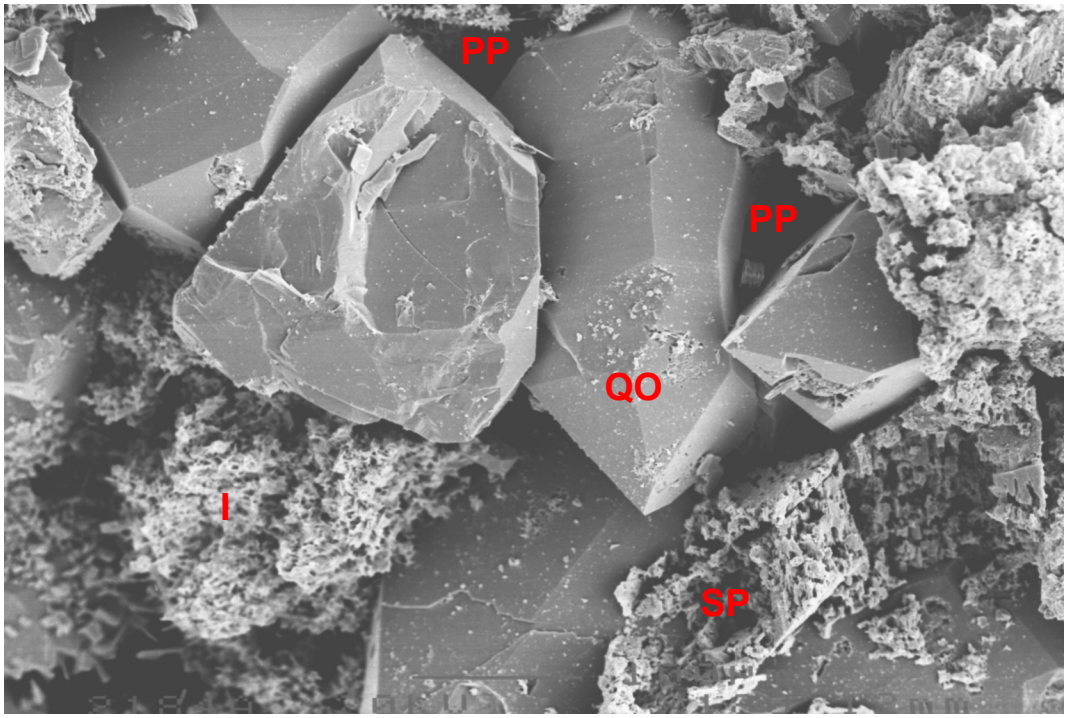

Good, clean primary intergranular porosity (PP) is preserved between adjacent quartz grains, despite cementation by quartz overgrowths (QO). Secondary intragranular porosity (SP) is associated with a partly dissolved K-feldspar grain (KF). The illitic remnants (I) of an altered micaceous rock fragment are also marked.

FIGURE 2

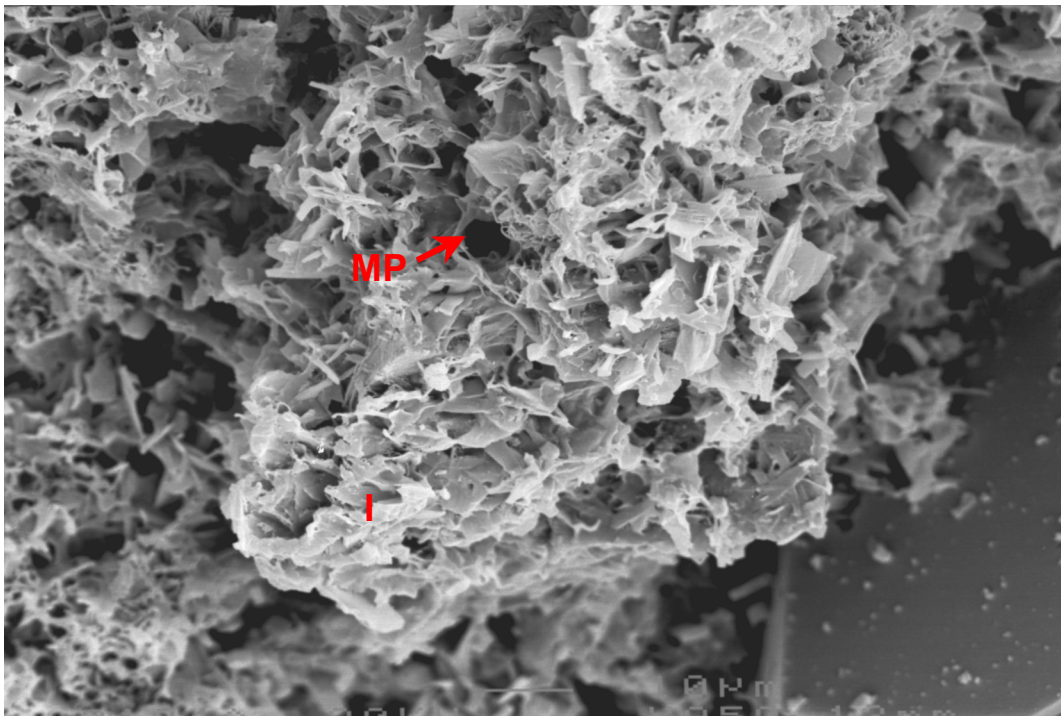

Detail of typical authigenic illite (I) and associated microporosity (MP). Authigenic illite in the sandstone tends to form discrete, grain-sized patches that mark the location of micaceous/argillaceous grains that have altered.

PLATE 32: #62 2184.89m

Rock classification: Sublitharenite

Texture:

Sedimentary structures:	Massive; scattered pebbles up to 14mm long
Sorting:	Poor
Average grain size:	0.94mm (coarse sand)
Roundness:	Subangular-subrounded
Texture:	Grain supported
Packing /grain contacts:	Moderate/long, embayed, sutured/microstylolitic
Macropore types:	Primary intergranular porosity, secondary intergranular porosity, secondary intragranular porosity
Core analyses:	Por. = 15.2%, Perm. = 127md, GD = 2.65g/cc

Composition:

Quartz (monocrystalline)	53.7%	Sedimentary rock fragments	0.9%
Quartz (polycrystalline)	10.0%	Pyrite	1.8%
Quartz overgrowths	3.7%	Siderite (replacement)	7.5%
Chert	0.8%	Authigenic kaolinite (pf)	1.0%
K-feldspar	2.5%	Authigenic kaolinite (rpl)	5.3%
Volcanic rock fragments	0.5%	Authigenic illite (replacement)	0.7%
Granitic rock fragments	0.3%	Primary porosity (intergranular)	2.8%
Metamorphic rock fragments	4.0%	Secondary porosity (intergran)	4.5%

Comments: Low permeability for the grain size is the result of poor sorting and the inclusion of common labile rock fragments within the finer parts of the sandstone, the presence of which has led to significant intergranular porosity loss by authigenic clay formation and ductile grain/authigenic clay compaction. Further porosity loss is the result of grain contact dissolution and quartz overgrowth cementation. Minor primary intergranular porosity is supplemented by common secondary intergranular pores that are the result of K-feldspar dissolution. The sample includes a 14mm long argillaceous intraclast that is replaced by siderite and minor pyrite. With many pores and pore throats being filled by authigenic clay, compacted ductile grains and quartz overgrowths, permeability is only moderate.

PLATE 32: #62 2184.89m

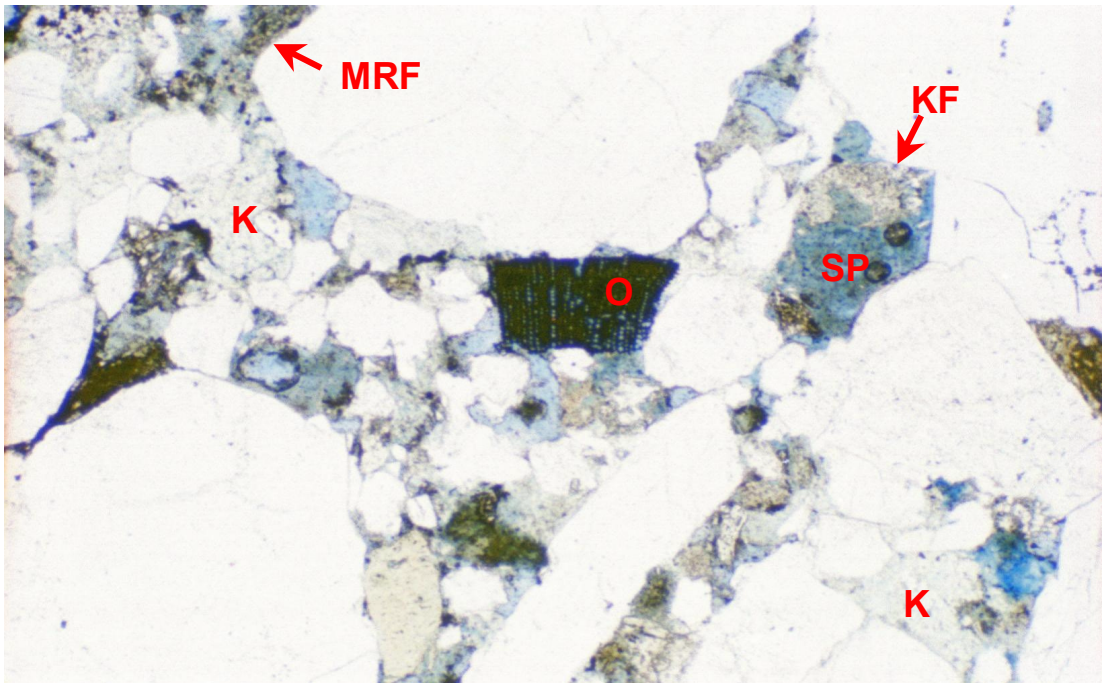

FIGURE 1 Plane polarised light
FIGURE 2 Crossed polarisers

0.4mm

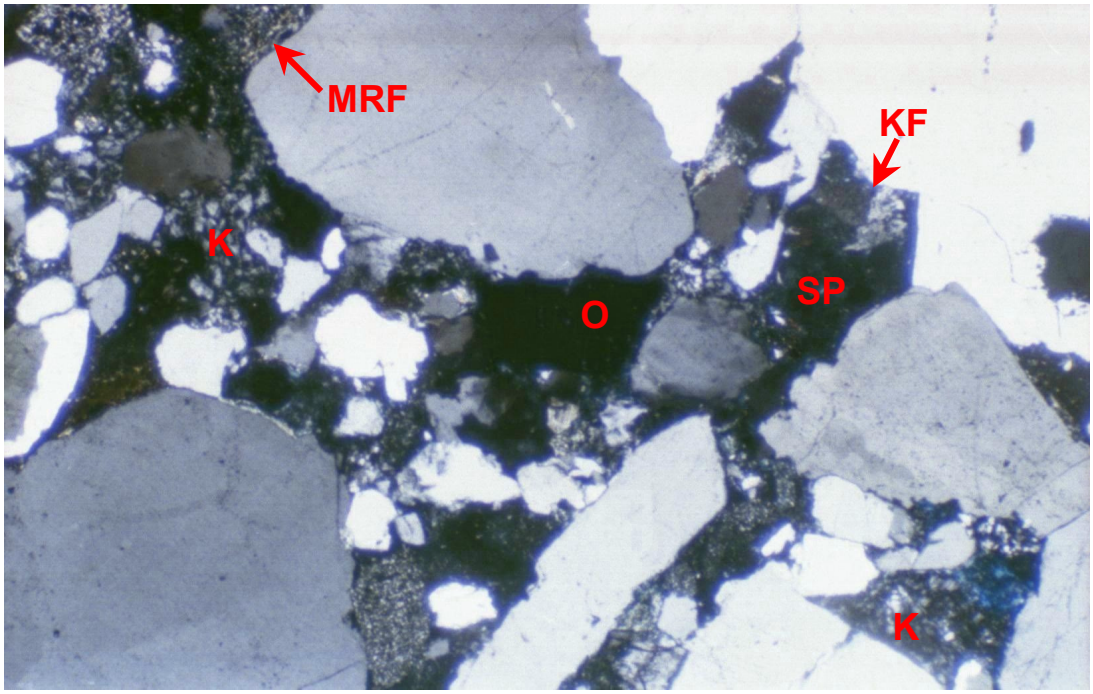

Poorly sorted sandstone in which there has been significant intergranular porosity reduction within finer grained areas due to authigenic kaolinite (K) formation and compaction of illitic metamorphic rock fragments (MRF). Secondary pores (SP) occur where K-feldspar grains (KF) have partly to completely dissolved. An organic fragment (O) with well preserved cellular structure is also marked.

PLATE 33: #62 2184.89m cont.

FIGURE 1

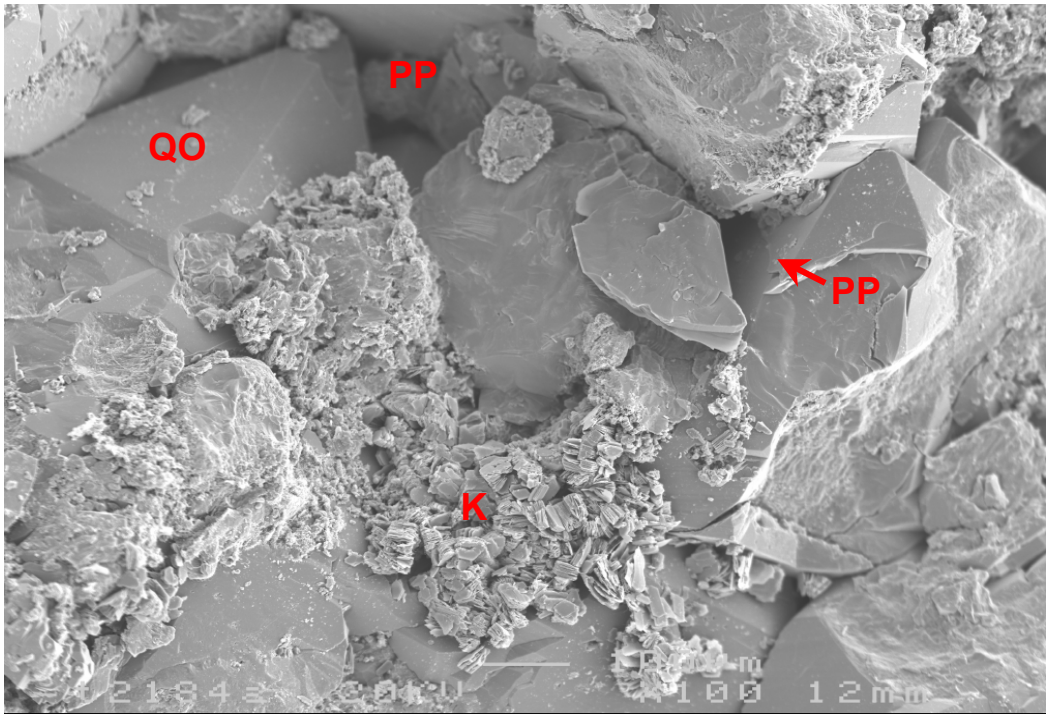

A micaceous metamorphic rock fragment has compactionally deformed and altered to kaolinite (K). Elsewhere, primary intergranular pores (PP) are partly filled by quartz overgrowths (QO). Connectivity between macropores is severely reduced by the presence of authigenic kaolinite in many intergranular spaces.

FIGURE 2

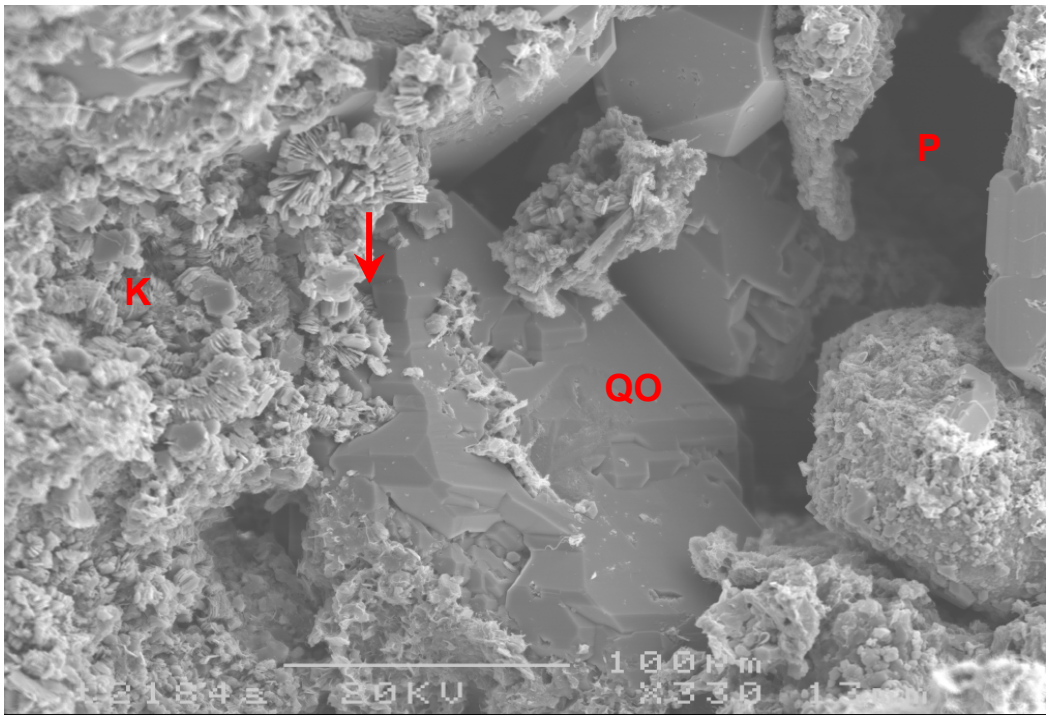

Intergranular pores (P) are preserved between juxtaposed quartz grains, despite cementation by quartz overgrowths (QO). An adjacent intergranular space is filled by authigenic kaolinite (K) that is the altered remnant of a compacted micaceous grain. The presence of the kaolinite would reduce connectivity between the marked pore and any macropores in the vicinity. Quartz overgrowths enclose (arrow) earlier formed authigenic kaolinite.

PLATE 34: #67 2186.60m

Rock classification: Litharenite

Texture:

Sedimentary structures: Sporadic faint laminae defined by concentrations of sideritised mica flakes; otherwise massive

Sorting: Well

Average grain size: 0.23mm (fine sand)

Roundness: Angular-subrounded

Texture: Grain supported

Packing /grain contacts: Moderate/long, embayed

Macropore types: Secondary mouldic porosity, rare primary intergranular porosity

Core analyses: Por. = 17.0%, Perm. = 1.93md, GD = 2.75g/cc

Composition:

Quartz (monocrystalline)	39.4%	Sedimentary rock fragments	0.9%
Quartz (polycrystalline)	3.9%	Pyrite	0.3%
Quartz overgrowths	2.0%	Siderite (replacement)	11.3%
Chert	2.6%	Authigenic kaolinite (pf)	4.8%
K-feldspar	4.8%	Authigenic kaolinite (rpl)	11.8%
Volcanic rock fragments	2.0%	Authigenic illite (pore filling)	0.3%
Granitic rock fragments	0.3%	Authigenic illite (replacement)	2.1%
Metamorphic rock fragments	12.5%	Secondary porosity (mouldic)	1.0%

Comments: This litharenite was susceptible to authigenic clay formation and compaction on account of containing abundant micaceous/argillaceous rock fragments at the time of accumulation. Primary intergranular porosity has been almost completely eliminated by authigenic clay (kaolinite, illite) formation, ductile grain/authigenic clay compaction, grain contact dissolution, and cementation by localised quartz overgrowths. Widely scattered secondary mouldic pores occur where K-feldspar has dissolved. Micaceous/illitic grains are commonly replaced by microcrystalline and finely-crystalline siderite, and widely scattered, fine ankerite rhombs replace clay. The sample is mainly microporous and consequently has low permeability.

PLATE 34: #67 2186.60m

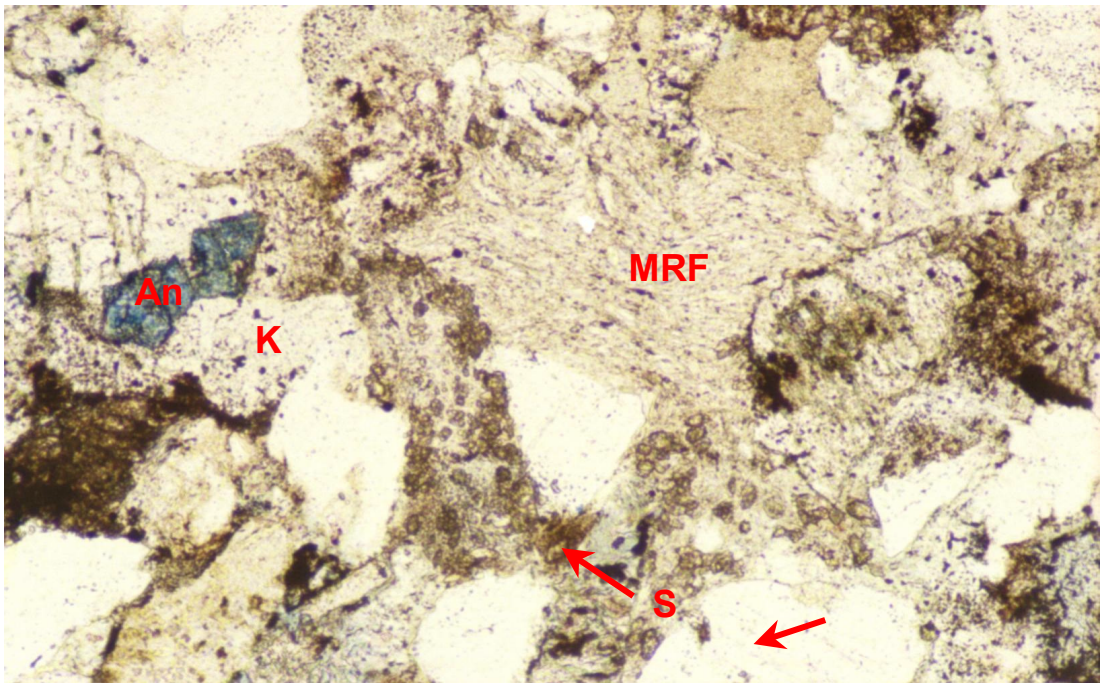

FIGURE 1 Plane polarised light
FIGURE 2 Crossed polarisers

0.2mm

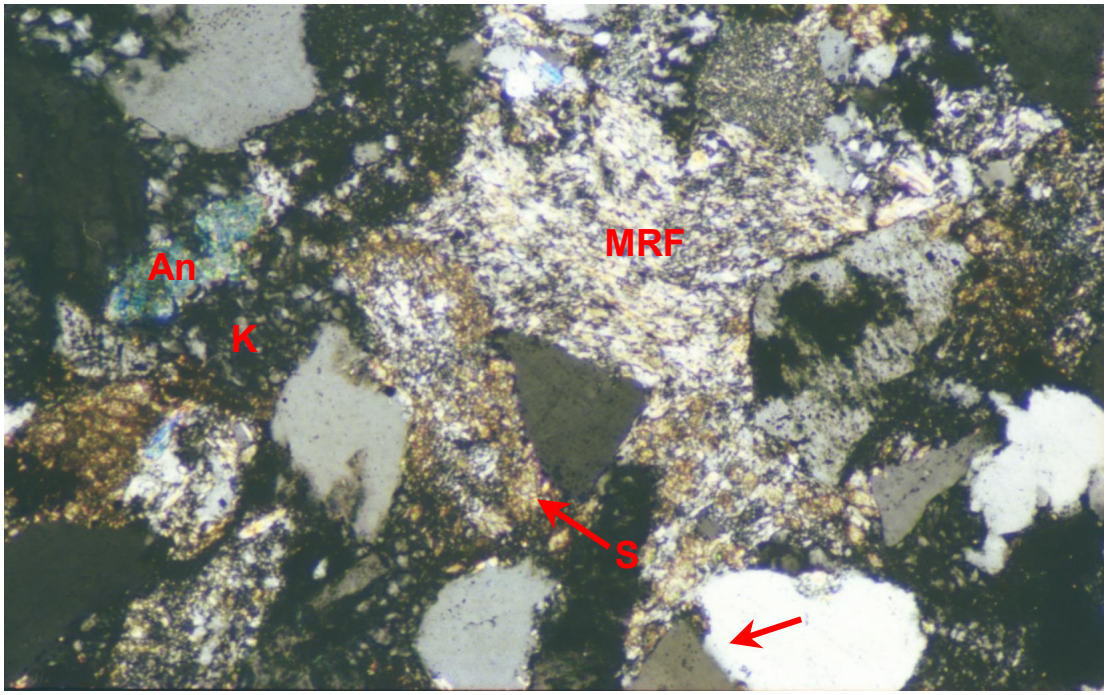

Intergranular porosity has been completely eliminated by compaction of micaceous metamorphic rock fragments (MRF), authigenic kaolinite (K) formation and grain welding by grain contact dissolution (arrow). Fine siderite (S) commonly replaces micaceous/illitic grains, and fine ankerite rhombs (An) (stained blue) locally replace clay.

PLATE 35: #67 2186.60m cont.

FIGURE 1

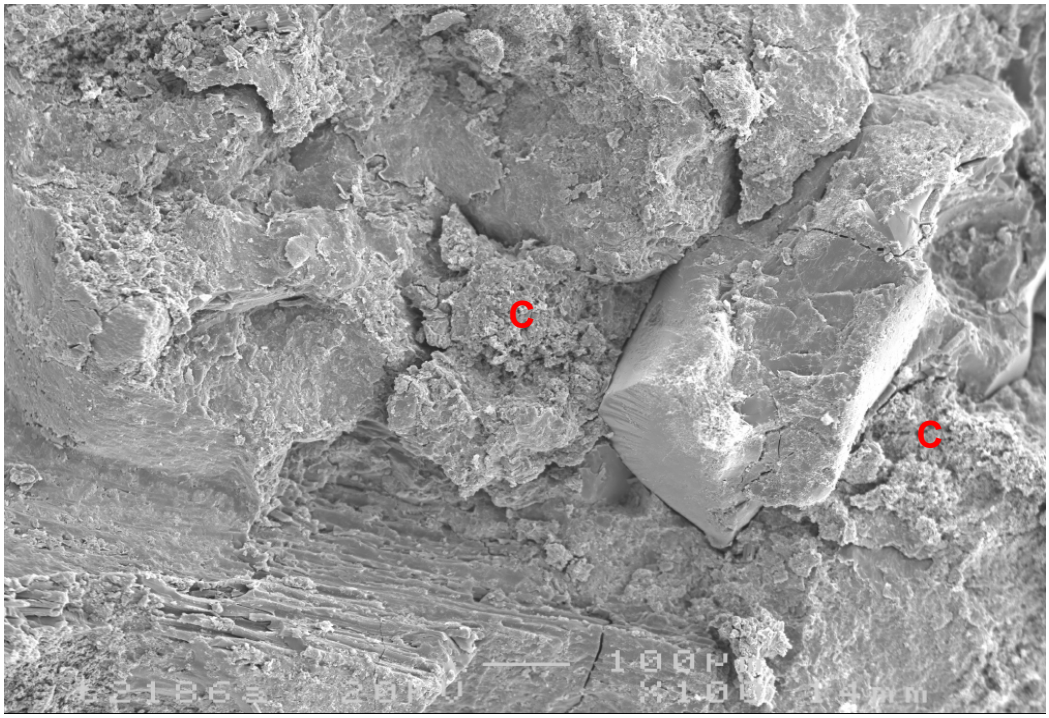

Representative area in which all intergranular areas are filled by compacted ductile rock fragments and clay (C).

FIGURE 2

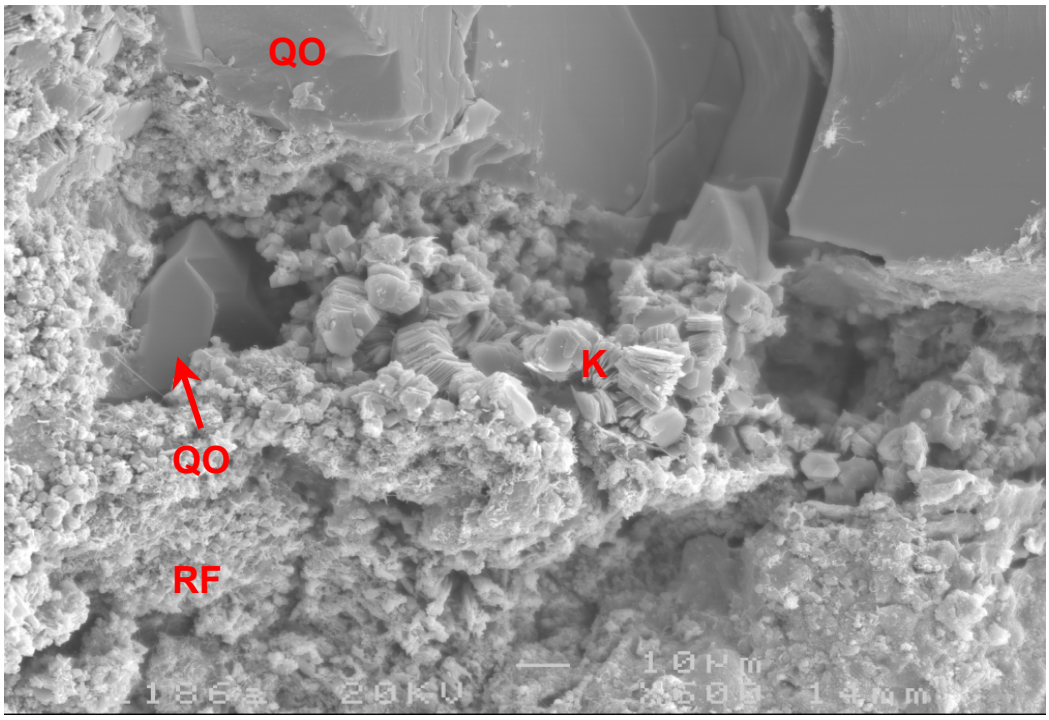

Detail of a typical intergranular area that is filled by authigenic kaolinite (K) and later formed quartz overgrowths (QO). The kaolinite is the altered remnant of a compacted micaceous/illitic rock fragment (RF). Low permeability largely reflects the abundance of compacted rock fragments and authigenic clay in the sample.

PLATE 36: #69 2187.10m

Rock classification: Litharenite

Texture:

Sedimentary structures:	Localised compacted clay patches and wisps (probably intraclasts); otherwise massive
Sorting:	Well
Average grain size:	0.33mm (medium sand)
Roundness:	Subangular-subrounded
Texture:	Grain supported
Packing /grain contacts:	Moderate/long, embayed, sutured
Macropore types:	Primary intergranular porosity, secondary intergranular porosity, secondary mouldic porosity, secondary intragranular porosity
Core analyses:	Por. = 20.1%, Perm. = 22.1md, GD = 2.68g/cc

Composition:

Quartz (monocrystalline)	40.9%	Mica	0.3%
Quartz (polycrystalline)	4.0%	Siderite (replacement)	1.9%
Quartz overgrowths	2.4%	Ankerite (replacement)	0.5%
Chert	1.0%	Authigenic kaolinite (pf)	5.9%
K-feldspar	5.1%	Authigenic kaolinite (rpl)	10.3%
Volcanic rock fragments	1.6%	Primary porosity (intergranular)	1.4%
Metamorphic rock fragments	19.1%	Secondary porosity (intergran)	2.4%
Sedimentary rock fragments	2.9%	Secondary porosity (mouldic)	0.3%

Comments: Intergranular porosity in this litharenite has been largely eliminated by authigenic kaolinite formation, ductile grain/authigenic clay compaction, grain contact dissolution and quartz overgrowth cementation. Minor primary intergranular porosity is supplemented by scattered secondary pores that are the result of K-feldspar dissolution. Pore throats are largely chocked by authigenic clay, compacted ductile grains and quartz overgrowths, hence permeability is relatively low.

PLATE 36: #69 2187.10m

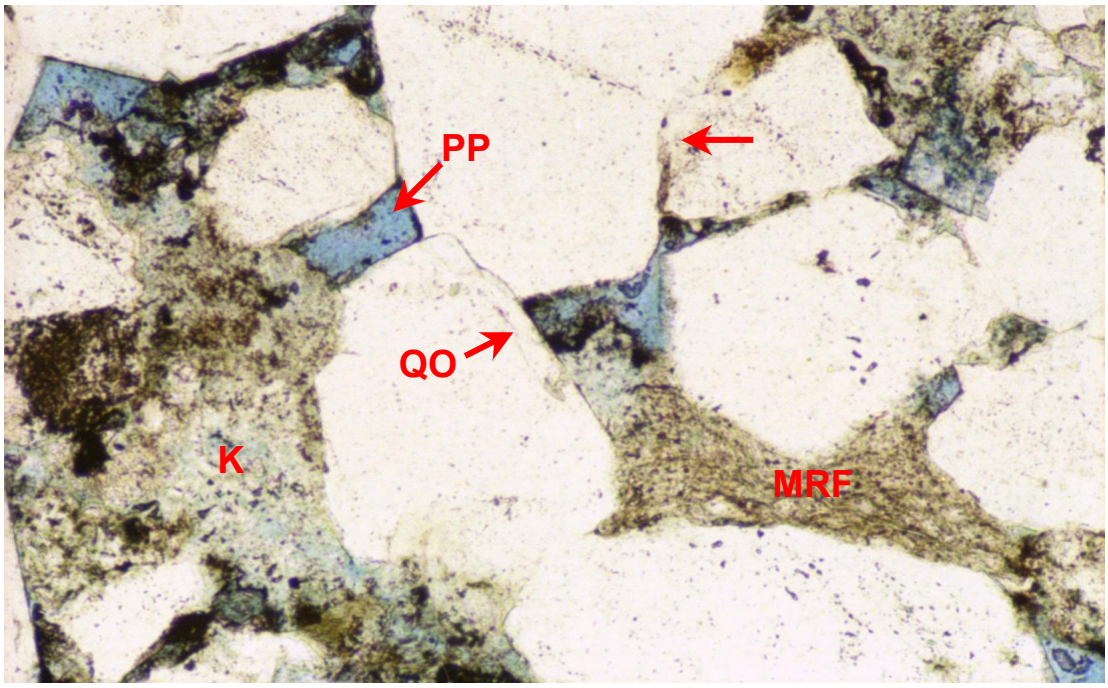

FIGURE 1 Plane polarised light
FIGURE 2 Crossed polarisers

0.2mm

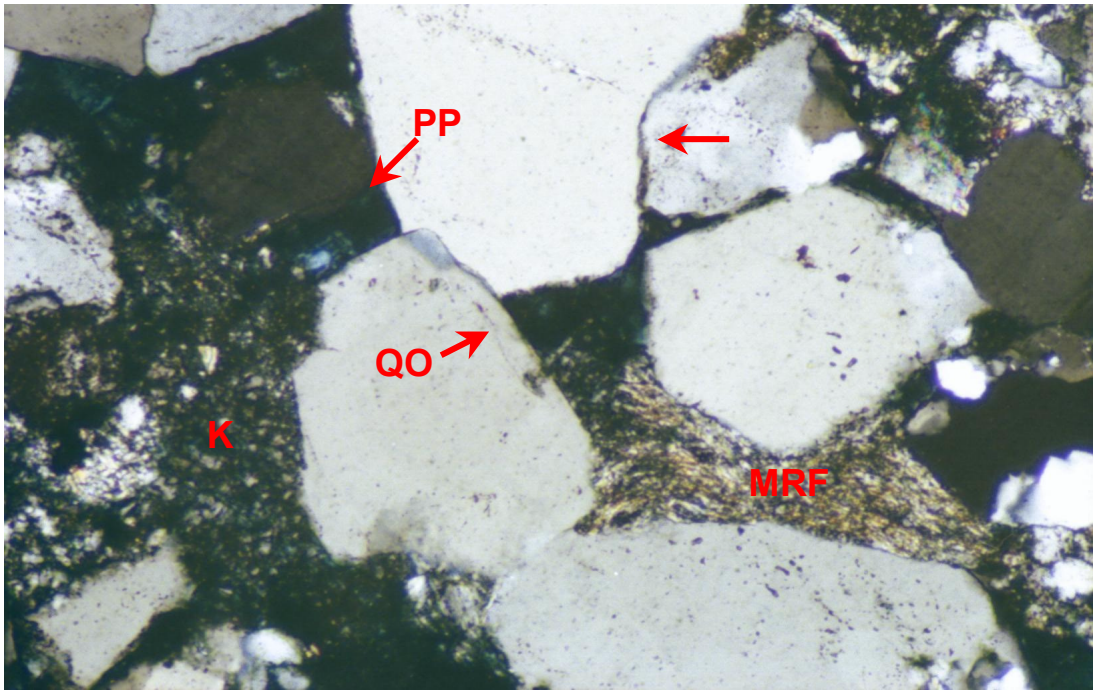

Although primary intergranular pores (PP) are preserved between some juxtaposed quartz grains, permeability is low due to extensive porosity reduction by authigenic kaolinite (K) formation, the compactional deformation of micaceous/illitic metamorphic rock fragments (MRF), quartz overgrowth (QO) cementation and grain contact dissolution (arrow).

PLATE 37: #69 2187.10m cont.

FIGURE 1

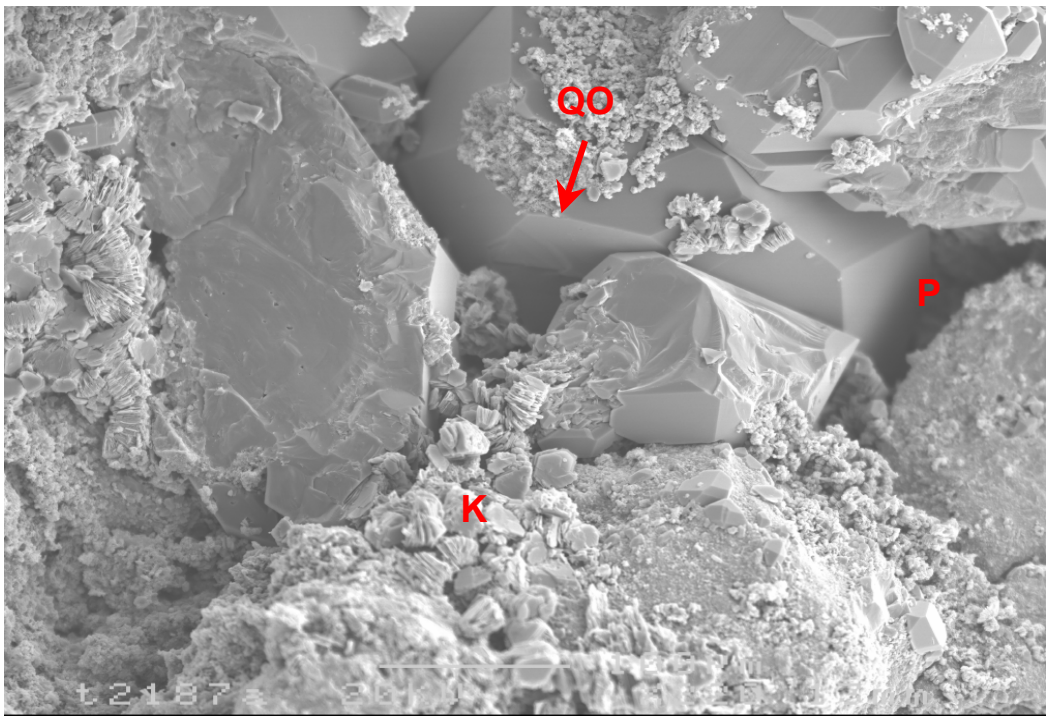

Intergranular pores (P) are largely filled by authigenic kaolinite (K) and quartz overgrowths (QO).

FIGURE 2

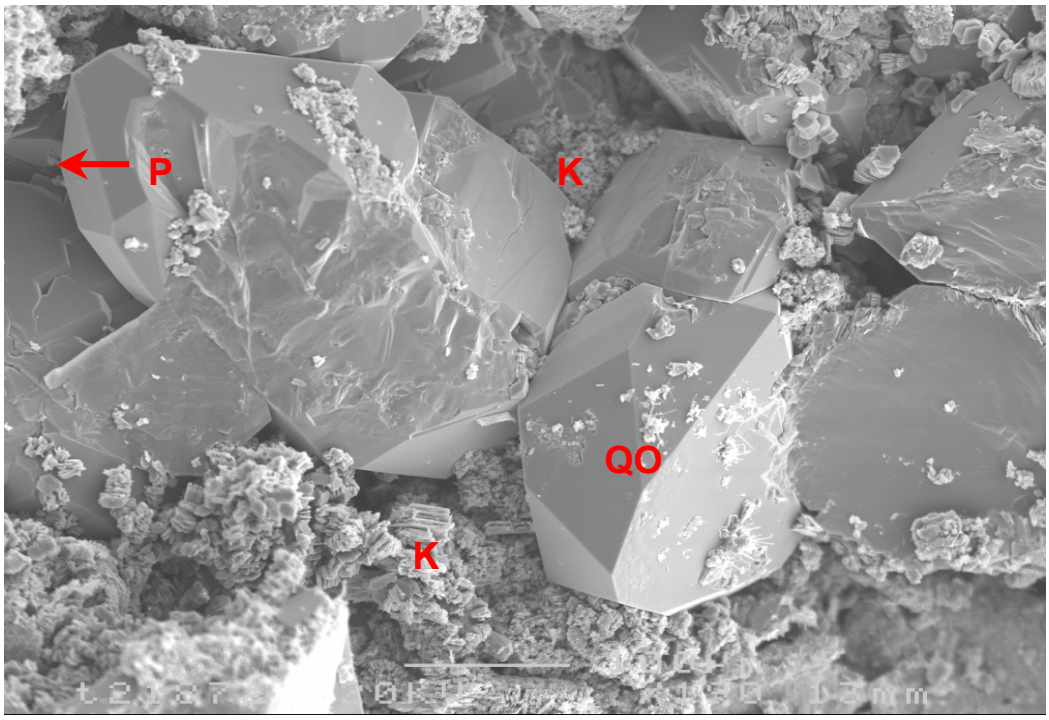

Low permeability (22.1md) largely reflects the presence of authigenic kaolinite within many intergranular areas. Porosity has also been reduced by quartz overgrowth (QO) cementation. Primary pores (PP) are preserved where quartz overgrowths have not filled all available intergranular space.

PLATE 38: 2187.22m (reconnaissance SEM study sample)

FIGURE 1

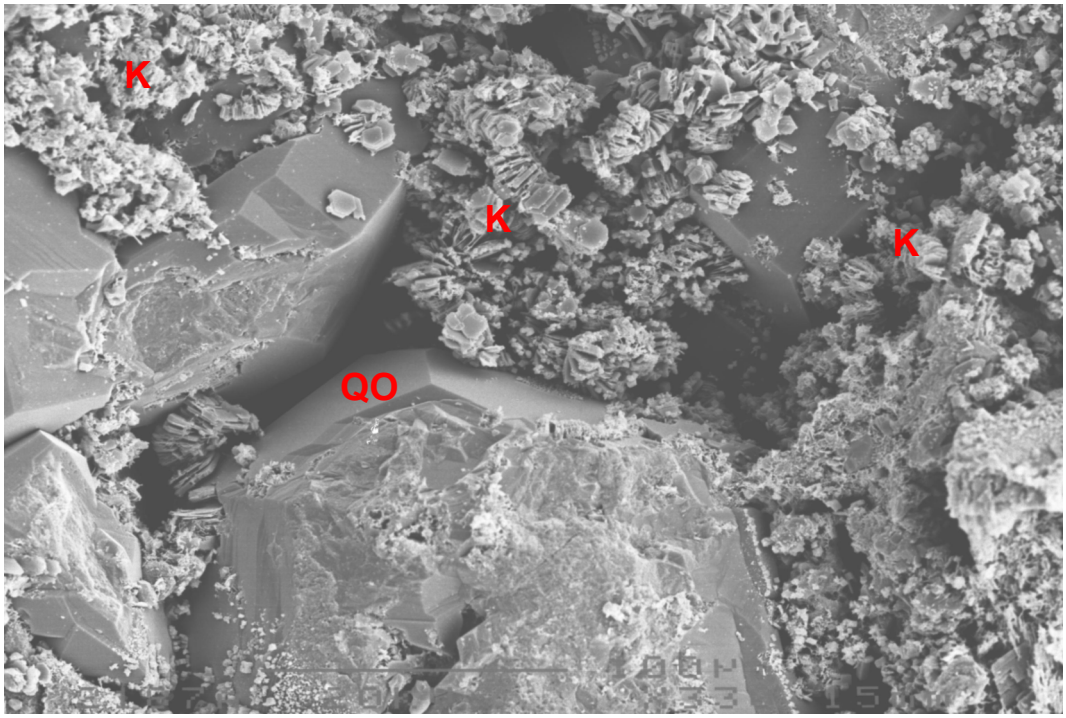

Porosity reduction in this sandstone is largely the result of pore filling by authigenic kaolinite (K). Quartz overgrowths (QO) are thinly developed and thus only partly occlude all available intergranular space.

FIGURE 2

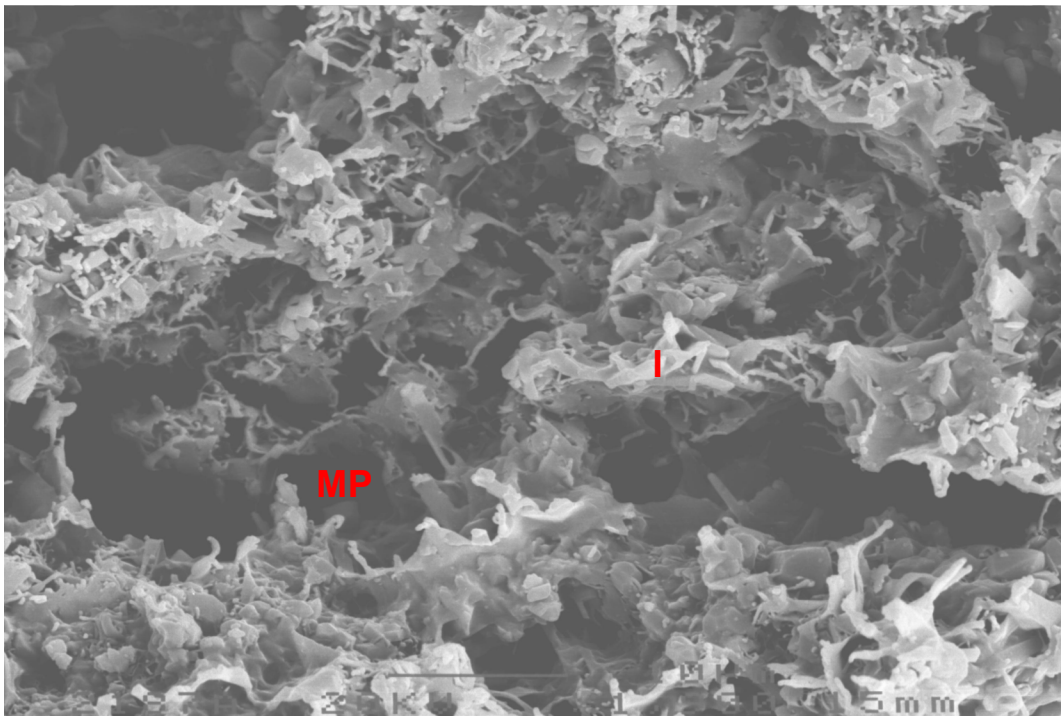

An isolated, microporous (MP) patch of authigenic illite (I) occurs where a micaceous rock fragment has altered.

PLATE 39: 2188.61m (reconnaissance SEM study sample)

FIGURE 1

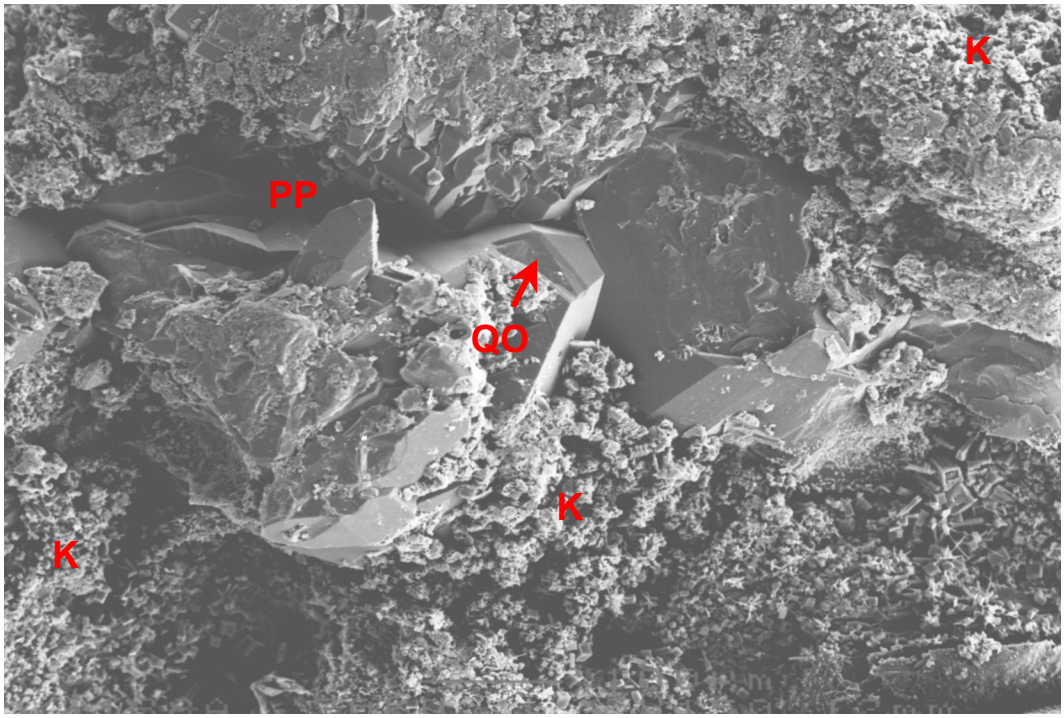

A primary intergranular pore (PP) is preserved between adjacent quartz overgrowth (QO)-cemented quartz grains. Elsewhere, intergranular porosity has been severely reduced by authigenic clay formation and compaction to form kaolinitic pseudomatrix (K).

FIGURE 2

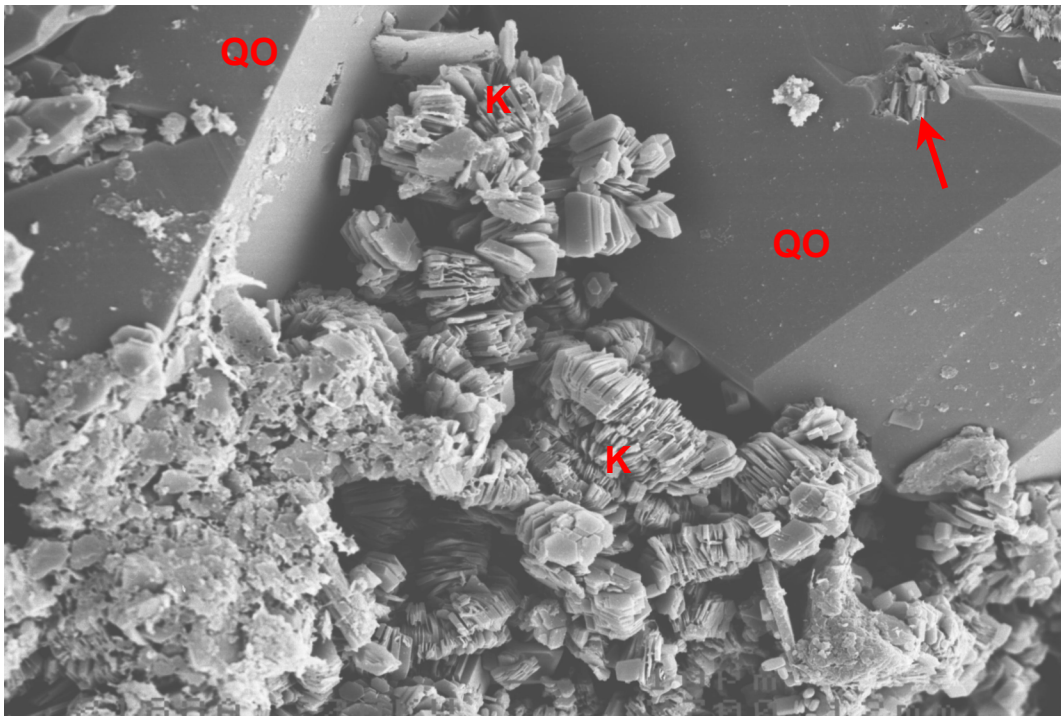

Authigenic kaolinite (K) fills an intergranular area between two quartz overgrowths (QO) that precipitated subsequent to kaolinite formation (as shown by the presence of kaolinite plates included within the overgrowths - arrow). Intergranular spaces in the sample are commonly occupied by authigenic kaolinite that has formed by alteration of compacted micaceous/argillaceous grains.

PLATE 40: #80 2192.71m

Rock classification: Sublitharenite

Texture:

Sedimentary structures:	Massive
Sorting:	Well
Average grain size:	0.32mm (medium sand)
Roundness:	Subangular-subrounded
Texture:	Grain supported
Packing /grain contacts:	Moderate/long, embayed
Macropore types:	Primary intergranular porosity, secondary intergranular porosity, secondary intragranular porosity
Core analyses:	Por. = 21.1%, Perm. = 524md, GD = 2.66g/cc

Composition:

Quartz (monocrystalline)	59.5%	Pyrite	0.3%
Quartz (polycrystalline)	2.0%	Ankerite (pore filling)	0.5%
Quartz overgrowths	6.5%	Authigenic kaolinite (pf)	2.8%
Chert	0.5%	Authigenic kaolinite (rpl)	4.2%
K-feldspar	1.8%	Primary porosity (intergranular)	11.3%
Volcanic rock fragments	0.5%	Secondary porosity (intergran)	5.1%
Metamorphic rock fragments	3.8%	Secondary porosity (intragran)	0.9%
Mica	0.3%		

Comments: This sample is enriched in quartz and consequently contains abundant clean primary intergranular porosity. Quartz overgrowths are common but generally only partly occlude all available intergranular space. Primary porosity is supplemented by scattered secondary pores that occur where K-feldspar has partly to completely dissolved. Porosity reduction has resulted mainly from quartz overgrowth cementation, grain contact dissolution, authigenic kaolinite formation, ductile grain/authigenic clay compaction, grain contact dissolution and minor ankerite cementation. Macropores are evenly distributed, hence are well interconnected.

PLATE 40: #80 2192.71m

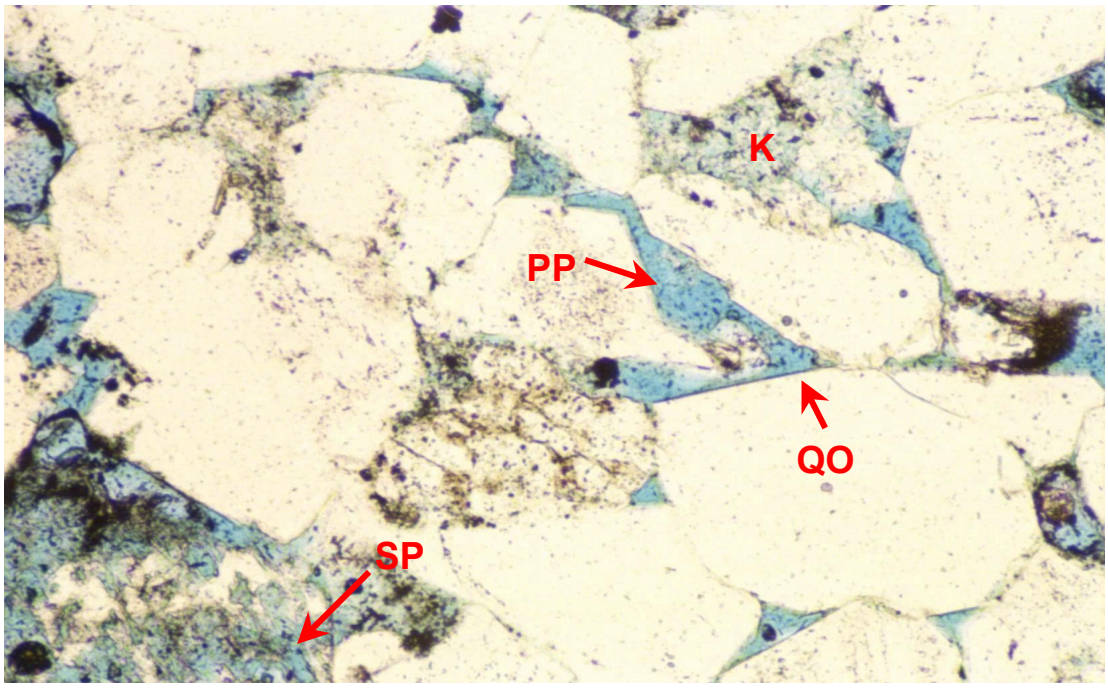

FIGURE 1 Plane polarised light
FIGURE 2 Crossed polarisers

0.2mm

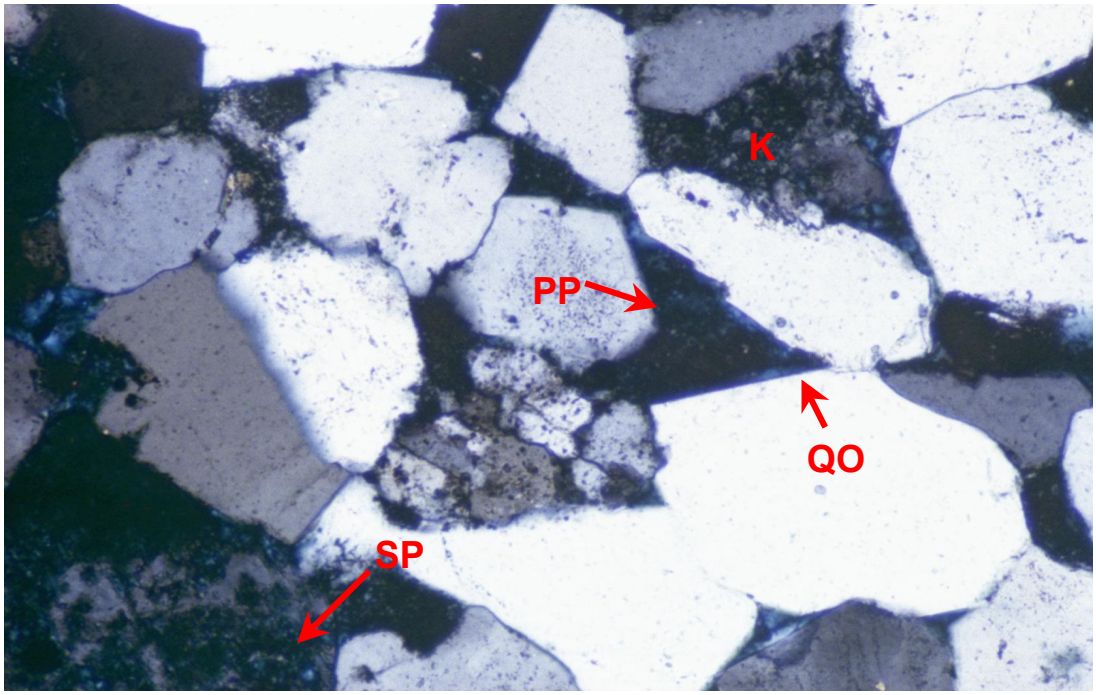

This sandstone is relatively quartzose and was thus far less susceptible to authigenic kaolinite (K) formation and ductile grain/clay compaction than the more lithic labile sandstone samples (e.g., previous sample). Consequently, the sandstone contains abundant primary intergranular porosity (PP), which provides good connection for scattered secondary pores (SP) that have formed by partial to complete dissolution of K-feldspar. Quartz overgrowths (QO) are common, but only partly occlude intergranular spaces.

PLATE 41: #80 2192.71m cont.

FIGURE 1

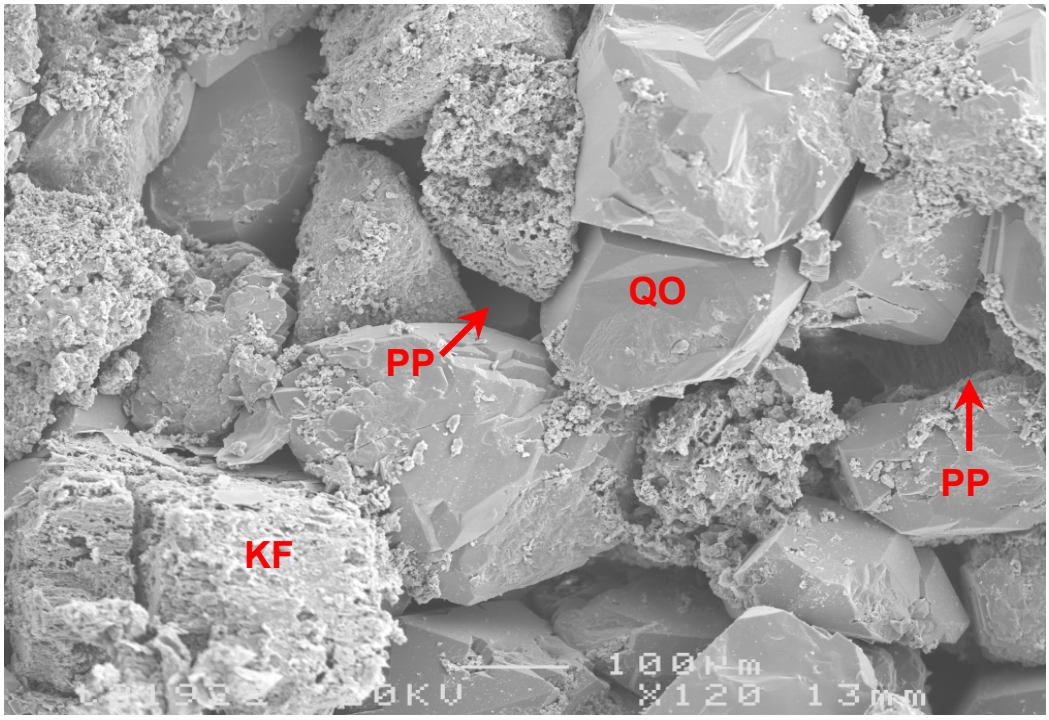

Primary intergranular pores (PP) are preserved between most grains, despite cementation by quartz overgrowths (QO). Preservation of abundant intergranular porosity reflects the quartzose character of the sandstone. A corroded K-feldspar grain (KF) is also marked.

FIGURE 2

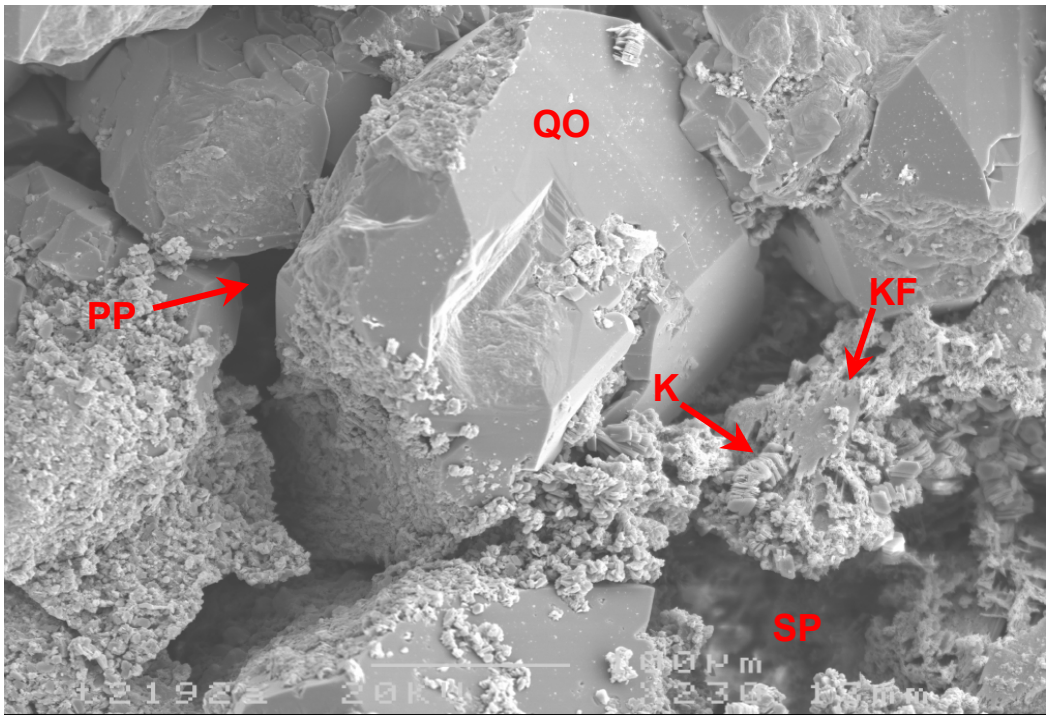

Clean, primary intergranular pores (PP) provide connection for scattered secondary pores (SP) that occur where K-feldspar has partly to completely dissolved. In addition to unaltered remnants of the pore precursor K-feldspar grain (KF), the marked secondary pore contains authigenic kaolinite (K) that has formed by alteration of the K-feldspar grain. Quartz overgrowths (QO) partly occlude intergranular pores.

PLATE 42: 2192.93m (reconnaissance SEM study sample)

FIGURE 1

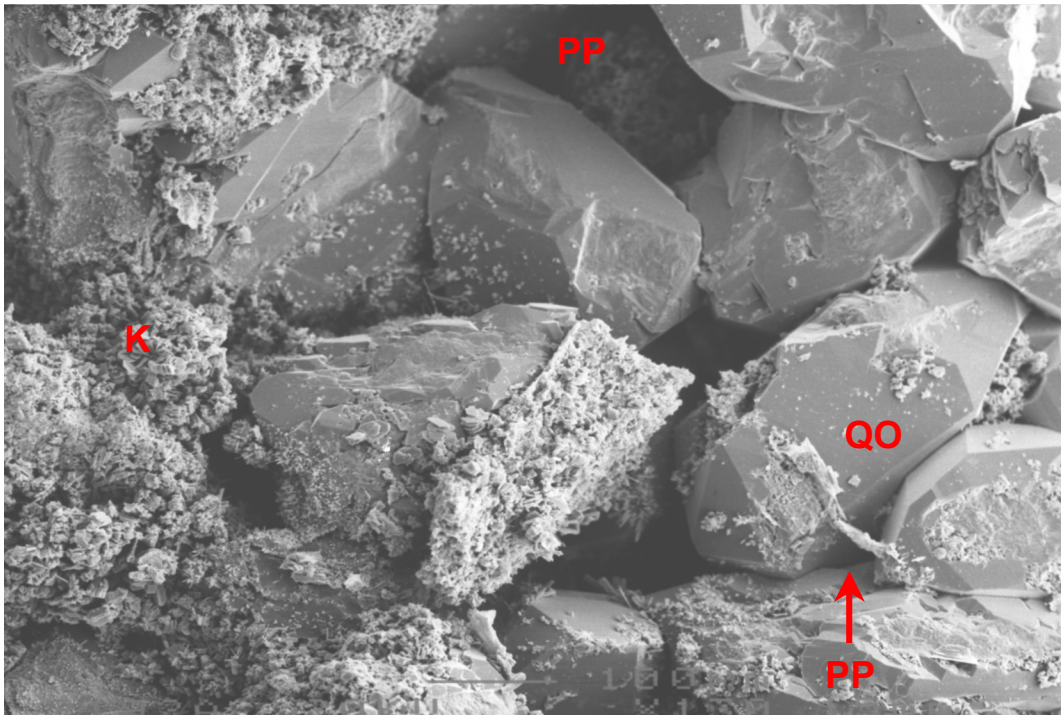

Good primary intergranular porosity (PP) is preserved between juxtaposed quartz grains, despite cementation by quartz overgrowths (QO). Elsewhere, labile micaceous/argillaceous rock fragments have altered to kaolinite (K) that effectively fills intergranular spaces.

FIGURE 2

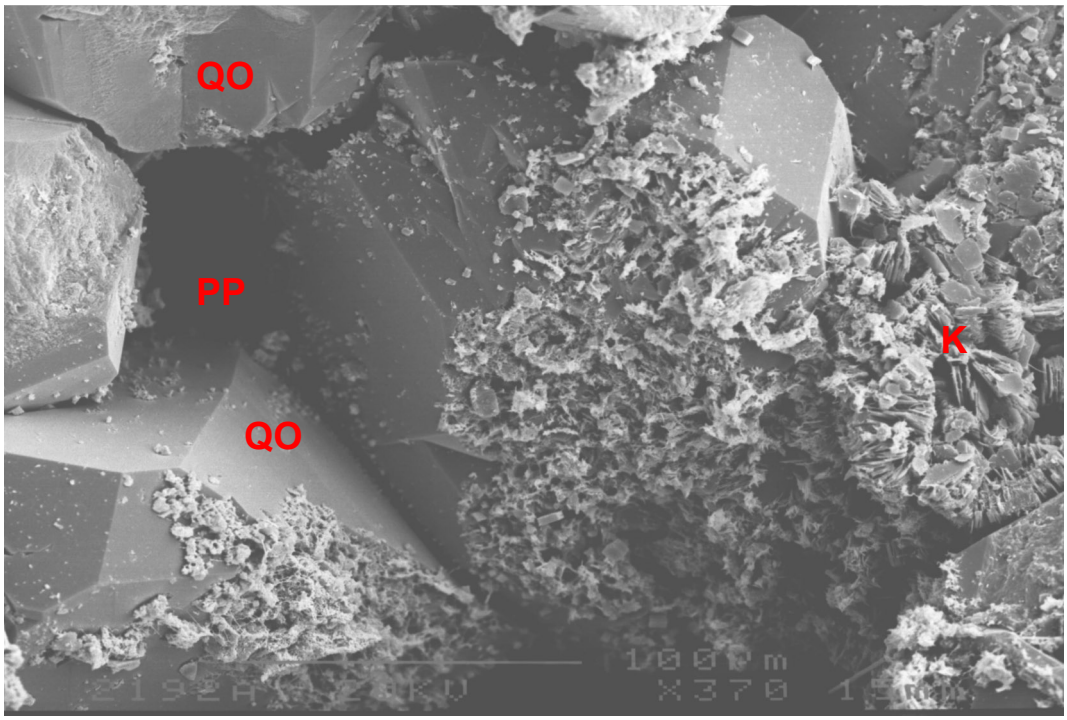

A primary intergranular pore (PP) is bounded by thinly developed quartz overgrowths (QO), and an adjacent intergranular space is filled with authigenic kaolinite (K) that is the altered remnant of a micaceous grain. Porosity reduction in the sandstone is largely due to pore filling by authigenic kaolinite.

PLATE 43: #83 2193.59m

Rock classification: Sublitharenite

Texture:

Sedimentary structures:	Massive
Sorting:	Moderate
Average grain size:	0.38mm (medium sand)
Roundness:	Subangular-subrounded
Texture:	Grain supported
Packing /grain contacts:	Moderate/long, embayed
Macropore types:	Primary intergranular porosity, secondary intergranular porosity, secondary intragranular porosity
Core analyses:	Por. = 18.4%, Perm. = 251md, GD = 2.66g/cc

Composition:

Quartz (monocrystalline)	63.5%	Pyrite	0.8%
Quartz (polycrystalline)	2.1%	Ankerite (pore filling)	0.5%
Quartz overgrowths	6.3%	Authigenic kaolinite (pf)	2.5%
Chert	0.3%	Authigenic kaolinite (rpl)	4.5%
K-feldspar	2.5%	Primary porosity (intergranular)	8.0%
Volcanic rock fragments	0.5%	Secondary porosity (intergran)	5.7%
Metamorphic rock fragments	2.1%	Secondary porosity (intragran)	0.7%

Comments: Like the previous sample, this sandstone is relatively quartzose and thus contains abundant clean primary intergranular porosity, which is supplemented by scattered secondary pores that occur where K-feldspar has partly to completely dissolved. Porosity reduction has resulted mainly from quartz overgrowth cementation, grain contact dissolution, authigenic kaolinite formation/compaction and minor ankerite cementation. Although authigenic kaolinite fills some pores and pore throats, macropores are generally clean and evenly distributed, hence are well interconnected.

PLATE 43: #83 2193.59m

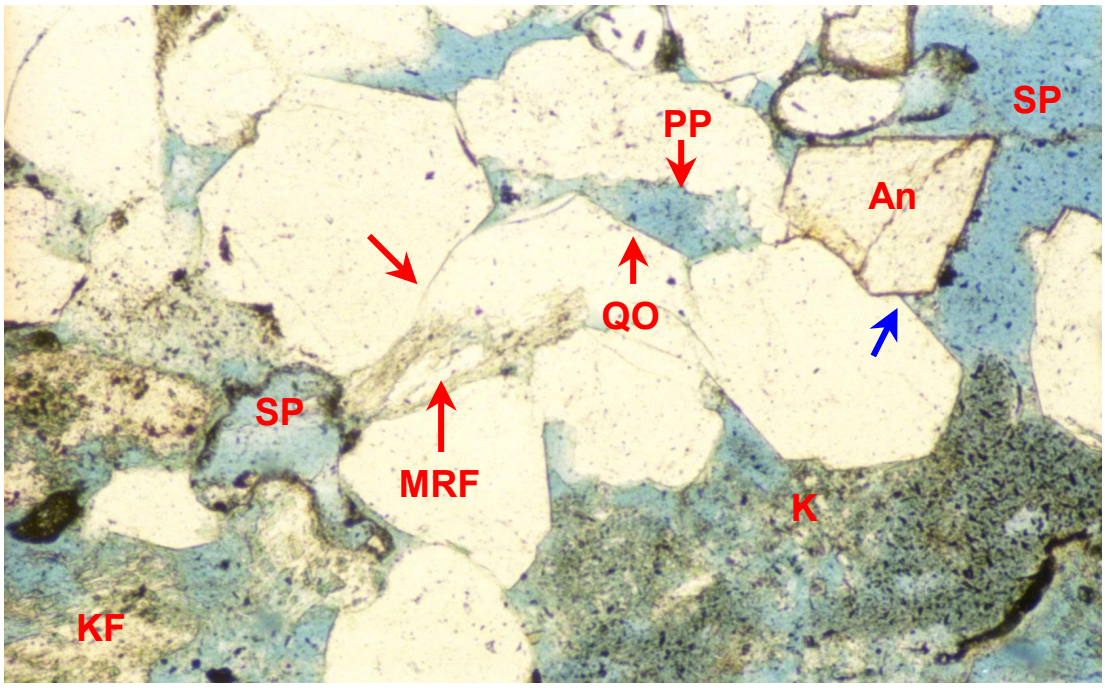

FIGURE 1 Plane polarised light
FIGURE 2 Crossed polarisers

0.2mm

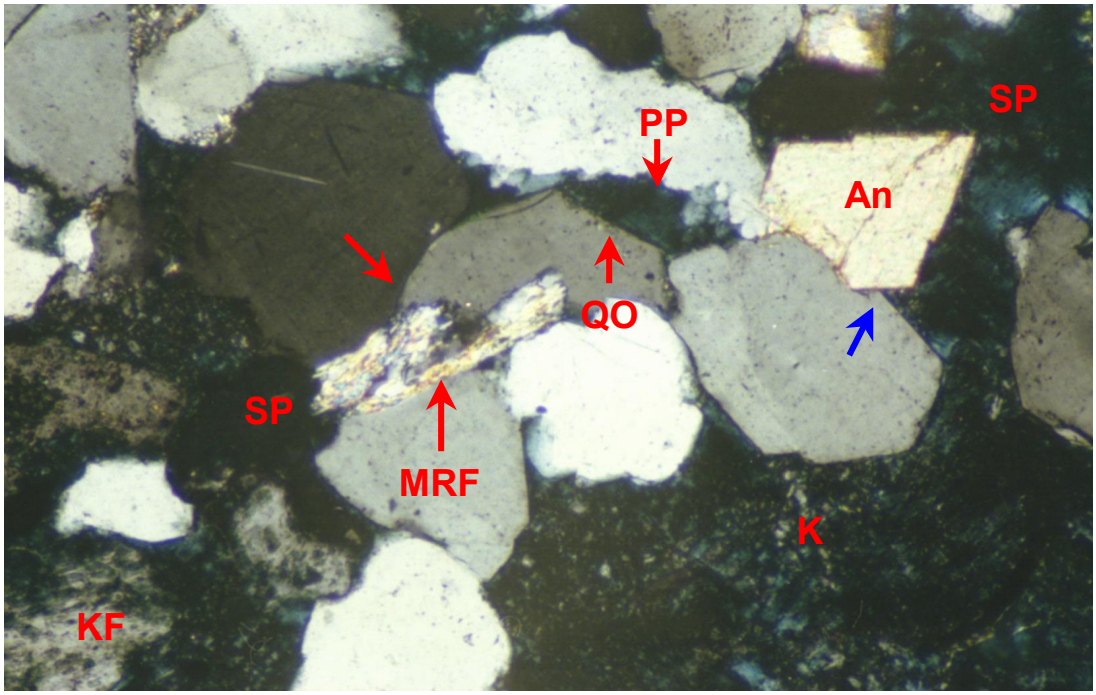

This quartzose sandstone contains a system of well interconnected primary intergranular pores (PP) and secondary K-feldspar (KF) dissolution pores (SP), despite porosity reduction by quartz overgrowth (QO) cementation, grain contact dissolution (red arrow) and the precipitation of rhombic ankerite crystals (An) within some pore spaces. The sandstone originally contained few micaceous metamorphic rock fragments (MRF), hence was not prone to significant physical compaction and authigenic kaolinite (K) formation. Ankerite has inhibited development of a quartz overgrowth (blue arrow), indicating that quartz overgrowths postdate ankerite.

PLATE 44: #83 2193.59m cont.

FIGURE 1

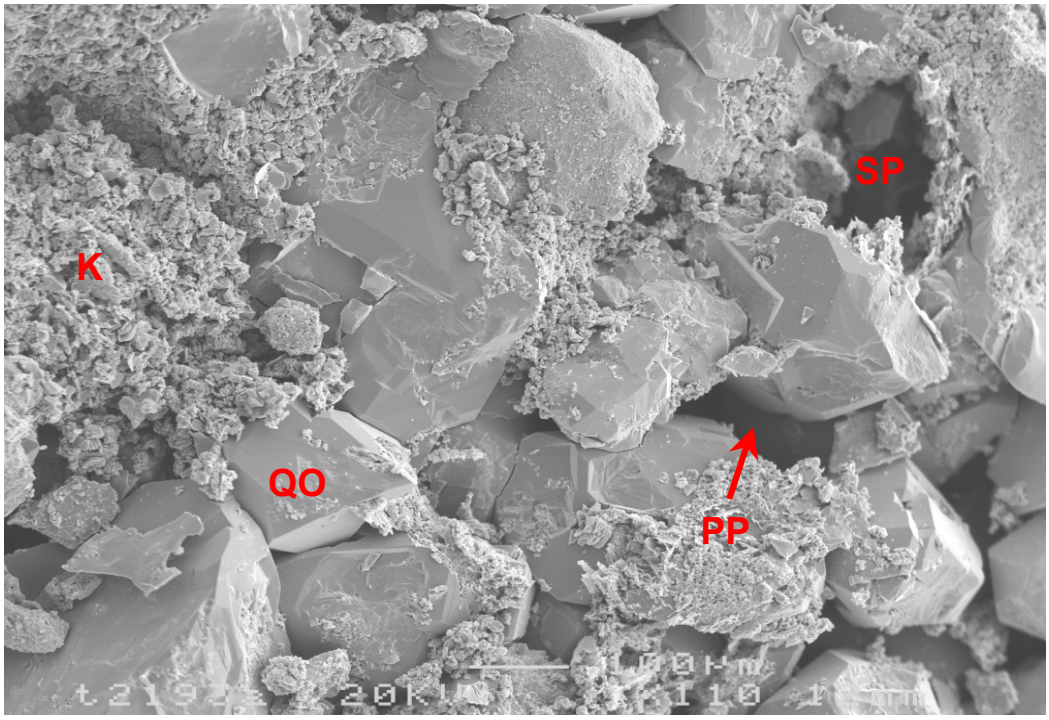

In this area, porosity has been reduced by quartz overgrowth (QO) cementation and localised authigenic kaolinite (K) formation by labile grain alteration. However, the sandstone still contains a system of well interconnected primary intergranular pores (PP) and secondary grain dissolution pores (SP).

FIGURE 2

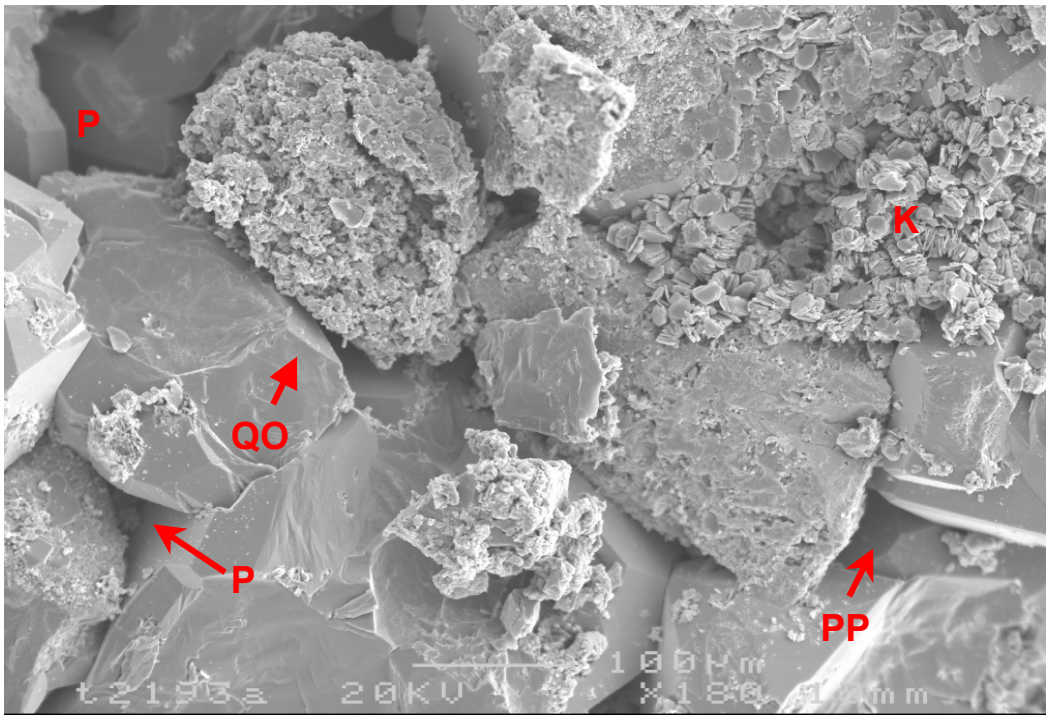

Authigenic kaolinite (K) forms scattered patches that mark the locations of labile grains that have altered. Where clay is absent, intergranular porosity (P) has been reduced by cementation by quartz overgrowths (QO), most of which only partly occlude intergranular spaces.

PLATE 45: M13 2230.0m

Rock classification: Sublitharenite

Texture:

Sedimentary structures:	Irregular argillaceous laminae up to 6mm thick
Sorting:	Well
Average grain size:	0.23mm (fine sand)
Roundness:	Subangular-subrounded
Texture:	Grain supported
Packing /grain contacts:	Moderate/long, embayed, sutured/microstylolitic
Macropore types:	Primary intergranular porosity, secondary intergranular porosity, secondary mouldic porosity, secondary intragranular porosity
Core analyses:	Por. = 19.5%, Perm. = 40.1md, GD = 2.65g/cc

Composition:

Quartz (monocrystalline)	41.0%	Siderite (replacement)	6.5%
Quartz (polycrystalline)	3.0%	Authigenic kaolinite (pf)	1.7%
Quartz overgrowths	4.8%	Authigenic kaolinite (rpl)	4.3%
K-feldspar	1.3%	Authigenic illite (replacement)	0.3%
Volcanic rock fragments	0.4%	Detrital clay	13.8%
Metamorphic rock fragments	2.5%	Primary porosity (intergranular)	5.8%
Mica	0.5%	Secondary porosity (intergran)	5.6%
Organics	5.0%	Secondary porosity (mouldic)	0.3%
Pyrite	2.5%	Secondary porosity (intragran)	0.7%

Comments: Widely-spaced (up to 1cm), irregular argillaceous laminae up to 6mm thick are partly replaced by microcrystalline siderite and contain abundant pyritic organic fragments. The thinnest laminae are stylolitic. Laminae are separated by fine grained sandstone that is relatively clean and quartzose. Despite porosity reduction by quartz overgrowth cementation, grain contact dissolution and authigenic kaolinite formation, the sandstone contains abundant primary intergranular porosity that would provide good interconnection for common oversized secondary intergranular pores that are mainly the result of K-feldspar dissolution. Argillaceous/carbonaceous laminae would significantly impact reservoir quality, but the sample is still sufficiently macroporous to be moderately permeable.

PLATE 45: M13 2230.0m

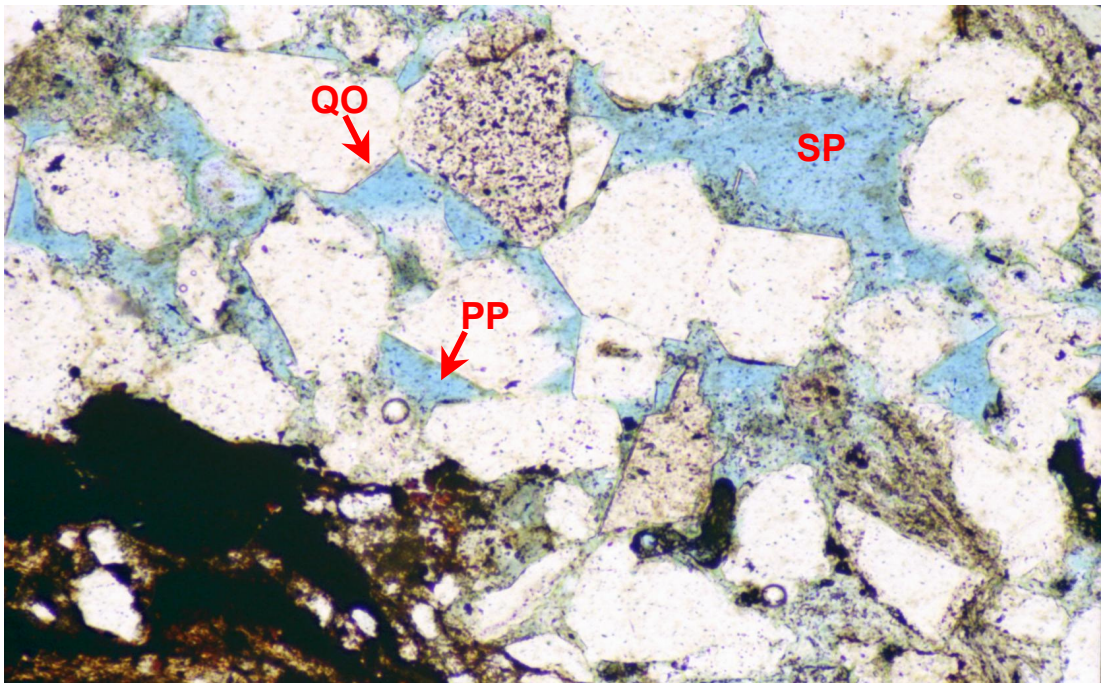

FIGURE 1 Plane polarised light

FIGURE 2 Crossed polarisers

0.2mm

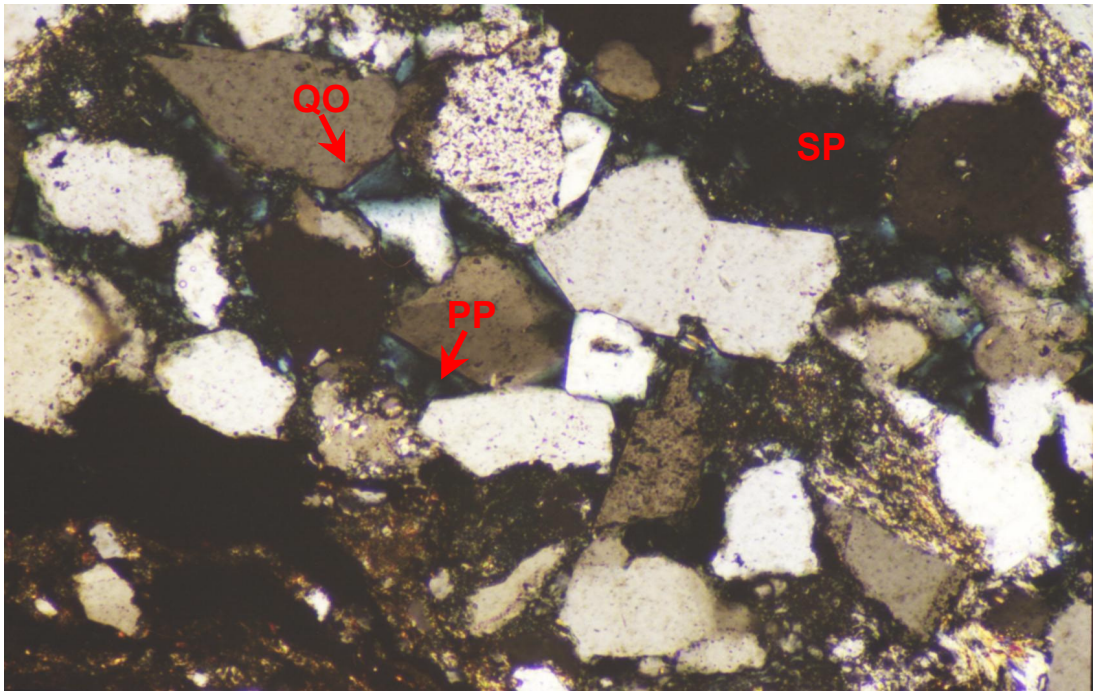

Contact between an argillaceous/carbonaceous lamination (lower left) and clean sandstone that contains abundant primary (PP) and secondary (SP) intergranular porosity. Quartz overgrowths (QO) are common within the clean sandstone, but only partly occlude intergranular pores.

PLATE 46: SWC #37 2255.5m

Rock classification: Quartzarenite

Texture:

Sedimentary structures:	Common sideritic/carbonaceous laminae up to 2mm thick
Sorting:	Well
Average grain size:	0.18mm (fine sand)
Roundness:	Angular-subrounded
Texture:	Grain supported; siderite supported within laminae
Packing /grain contacts:	Moderate/long, embayed
Macropore types:	Secondary mouldic porosity

Composition:

Quartz (monocrystalline)	26.0%	Siderite (pore filling)	5.2%
Quartz (polycrystalline)	0.8%	Siderite (replacement)	47.8%
K-feldspar	0.3%	Authigenic kaolinite (pf)	2.0%
Metamorphic rock fragments	0.3%	Authigenic kaolinite (rpl)	3.2%
Mica	0.3%	Authigenic illite (replacement)	0.8%
Organics	9.2%	Secondary porosity (mouldic)	0.5%
Pyrite	3.6%		

Comments: Laminae are defined by concentrations of siderite, fine pyritic organic fragments and pyrite. Siderite within laminae commonly forms microcrystalline patches up to 1mm long that replace altered biotite flakes that were originally abundant along laminae. Microcrystalline siderite also replaces detrital clay matrix within argillaceous areas. Intervening sandstone is almost entirely microporous due to extensive pore filling by authigenic kaolinite pseudomatrix and microcrystalline siderite cement. Negligible permeability.

PLATE 46: SWC #37 2255.5m

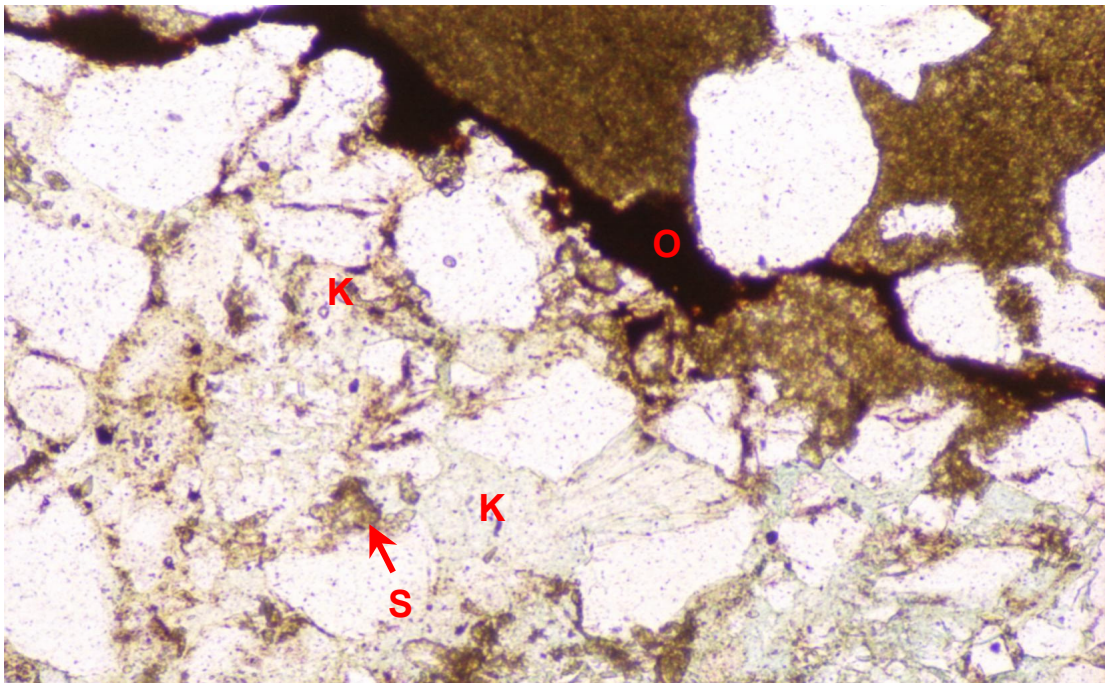

FIGURE 1 Plane polarised light
FIGURE 2 Crossed polarisers

0.2mm

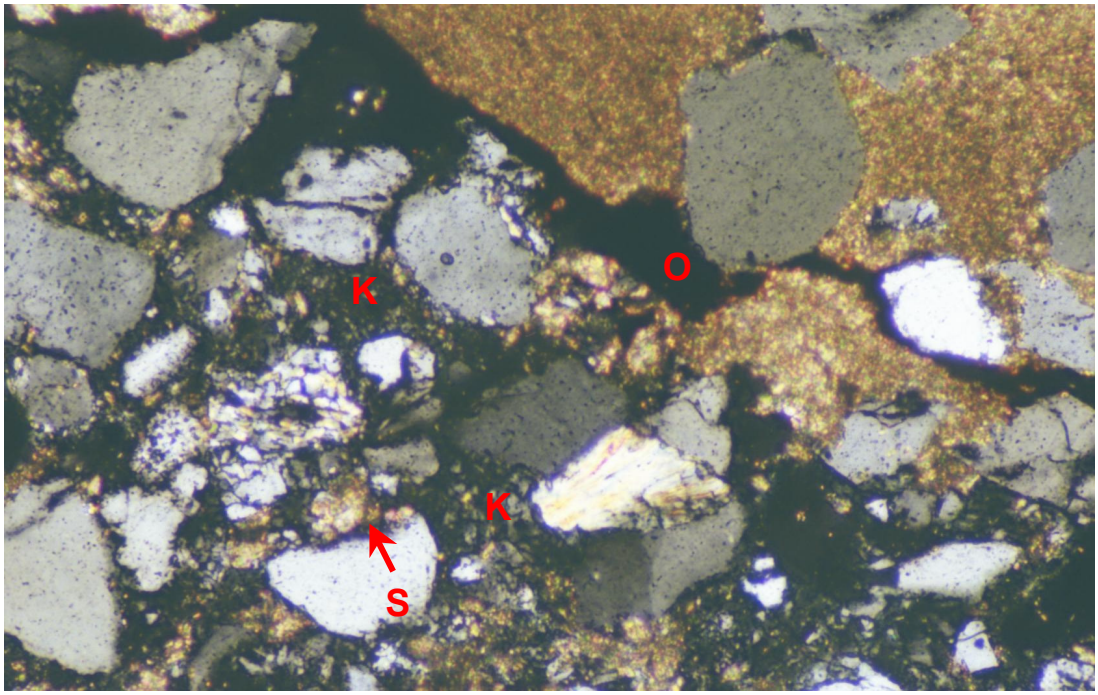

Contact between a tight sideritic lamination (upper right) and microporous sandstone in which all intergranular areas are occupied by authigenic kaolinite (K) and fine siderite (S). A compacted pyritic organic fragment (O) is associated with the sideritic lamination.

PLATE 47: SWC #34 2277.0m

Rock classification: Quartzarenite

Texture:

Sedimentary structures:	Massive
Sorting:	Well
Average grain size:	0.33mm (medium sand)
Roundness:	Subangular-subrounded
Texture:	Grain supported; severely impact damaged
Packing /grain contacts:	Moderate/long, embayed
Macropore types:	Primary intergranular porosity, ?secondary intergranular porosity

Composition:

Quartz (monocrystalline)	75.4%	Authigenic kaolinite (pf)	2.0%
Quartz (polycrystalline)	2.6%	Authigenic kaolinite (rpl)	2.8%
Quartz overgrowths	3.0%	Authigenic illite (replacement)	0.3%
Metamorphic rock fragments	0.3%	Primary porosity (intergranular)	13.6%

Comments: This sample consists of loose quartz grains and fragments of pulverised sandstone that are the remains of a quartzarenite that probably contained good primary intergranular porosity, despite porosity reduction by grain contact dissolution, minor quartz overgrowth cementation and localised pore filling by authigenic kaolinite and illite. All porosity was recorded as primary intergranular porosity during point counting, but the sample probably also contained secondary intergranular porosity. Visible porosity could not be accurately measured and characterised due to complete impact-induced textural reorganisation.

PLATE 47: SWC #34 2277.0m

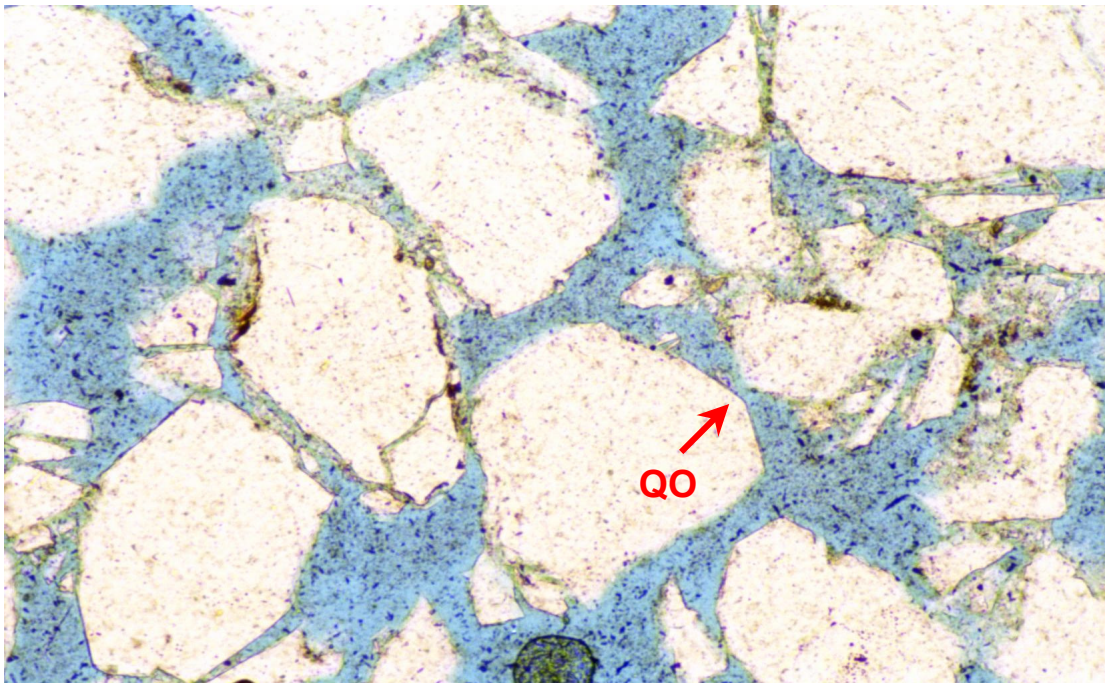

FIGURE 1 Plane polarised light
FIGURE 2 Crossed polarisers

0.2mm

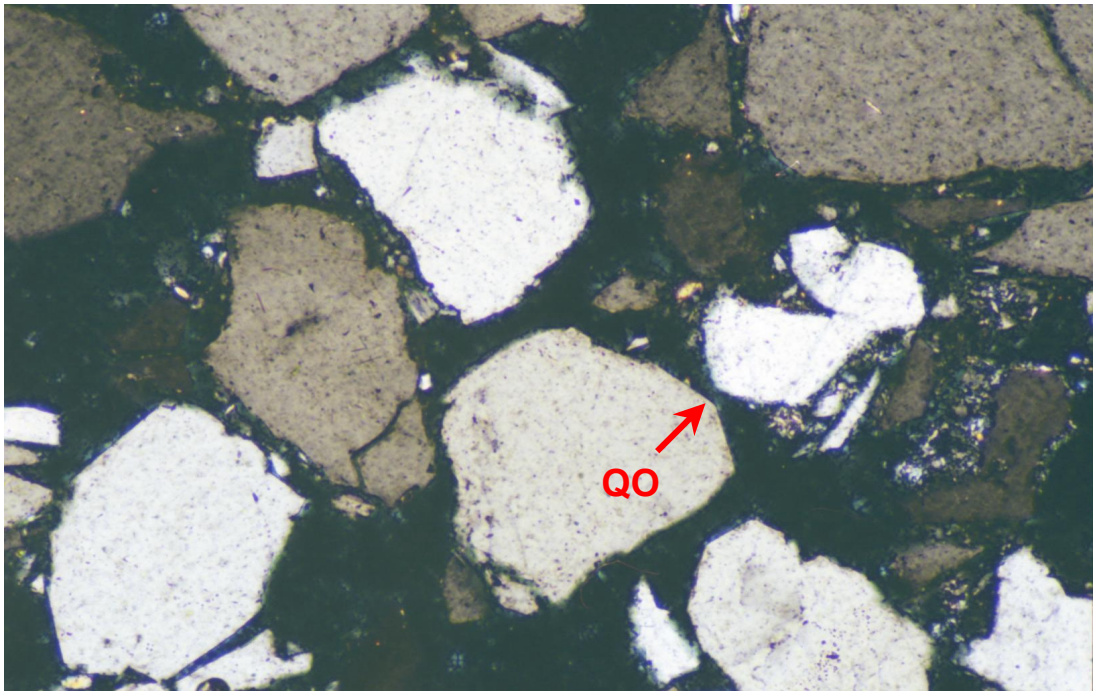

Loose quartz grains are the remains of a quartzarenite that was severely impact damaged during coring. The quartzarenite most likely contained good intergranular porosity. Thin, euhedral quartz overgrowths (QO) would have only partly occluded intergranular spaces.

PLATE 48: SWC #31 2306.0m

Rock classification: Quartzarenite

Texture:

Sedimentary structures:	Massive
Sorting:	Moderate
Average grain size:	0.55mm (coarse sand)
Roundness:	Subangular-subrounded
Texture:	Grain supported; severely impact damaged
Packing /grain contacts:	Moderate/long, embayed
Macropore types:	Primary intergranular porosity, ?secondary intergranular porosity

Composition:

Quartz (monocrystalline)	74.2%	Pyrite	1.0%
Quartz (polycrystalline)	2.5%	Authigenic kaolinite (pf)	1.4%
Quartz overgrowths	2.1%	Authigenic kaolinite (rpl)	3.1%
K-feldspar	0.3%	Authigenic illite (replacement)	0.7%
Metamorphic rock fragments	0.3%	Primary porosity (intergranular)	14.1%
Sedimentary rock fragments	0.3%		

Comments: This quartzarenite is severely impact damaged, but includes small areas in which original porosity characteristics have not been totally obliterated by sidewall coring. Within these areas, there has been porosity reduction by grain contact dissolution, minor quartz overgrowth cementation and localised pore filling by authigenic kaolinite, illite and pyrite. However, clean intergranular pores are common, and consequently the sample most likely had good permeability prior to sidewall coring. Visible porosity could not be accurately measured and characterised due to almost complete impact-induced textural reorganisation.

PLATE 48: SWC #31 2306.0m

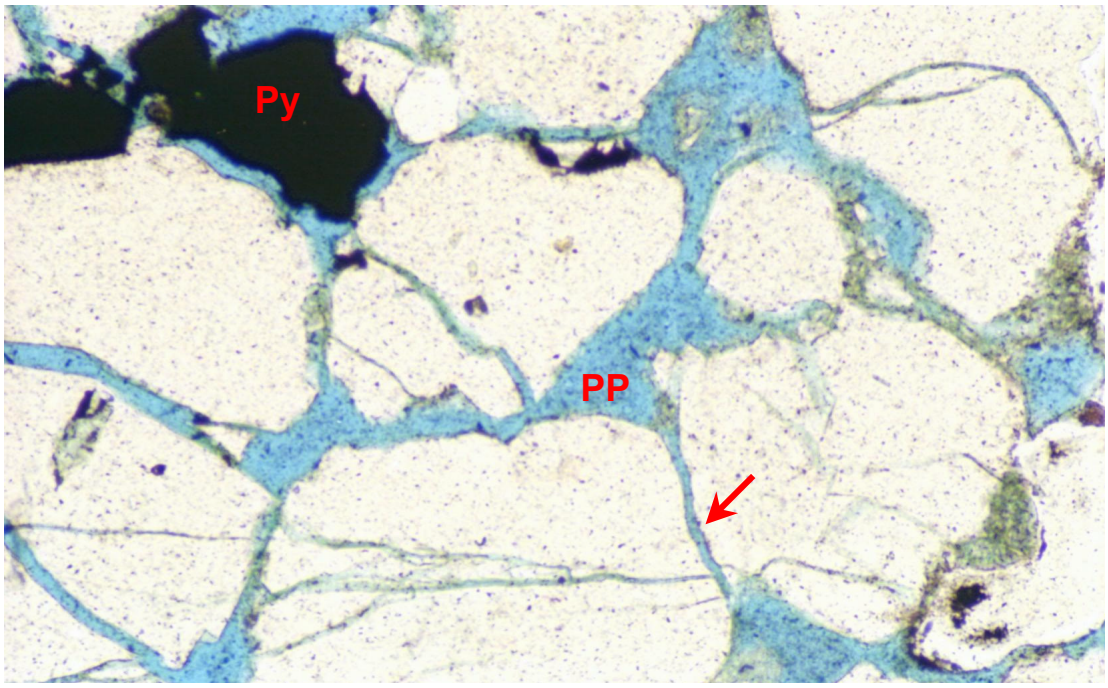

FIGURE 1 Plane polarised light
FIGURE 2 Crossed polarisers

0.2mm

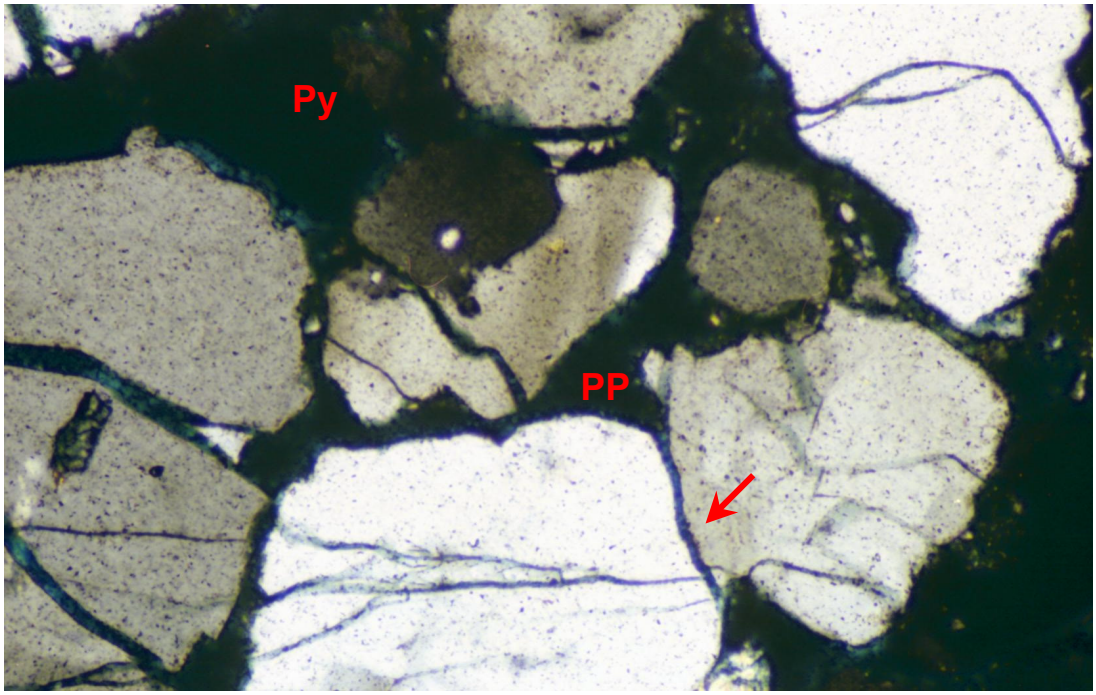

These micrographs show part of the sample in which original porosity characteristics have not been totally eliminated by sidewall coring. Despite grain welding by grain contact dissolution (arrow) and localised pore filling by pyrite cement (Py), the sandstone appears to have contained abundant primary intergranular porosity (PP) prior to sidewall coring. Framework grains are fractured due to sidewall coring impact.

PLATE 49: SWC #25 2397.7m

Rock classification: Laminated mudrock

Texture:

Sedimentary structures:	Thin silty/sandy laminae
Sorting:	Well (within silty laminae)
Average grain size:	0.05mm (coarse silt) (silty laminae)
Roundness:	Angular-subrounded
Texture:	Mainly matrix supported
Macropore types:	No macroporosity

Composition:

Quartz (monocrystalline)	2.2%	Pyrite	1.8%
Quartz (polycrystalline)	0.3%	Leucoxene	0.7%
Metamorphic rock fragments	0.3%	Siderite (replacement)	1.7%
Mica	0.7%	Detrital clay	79.3%
Organics	13.0%		

Comments: This sample is a laminated, well compacted mudrock composed mainly of detrital clay and fine, locally pyritic, organic fragments. The mudrock is totally microporous.

PLATE 49: SWC #25 2397.7m

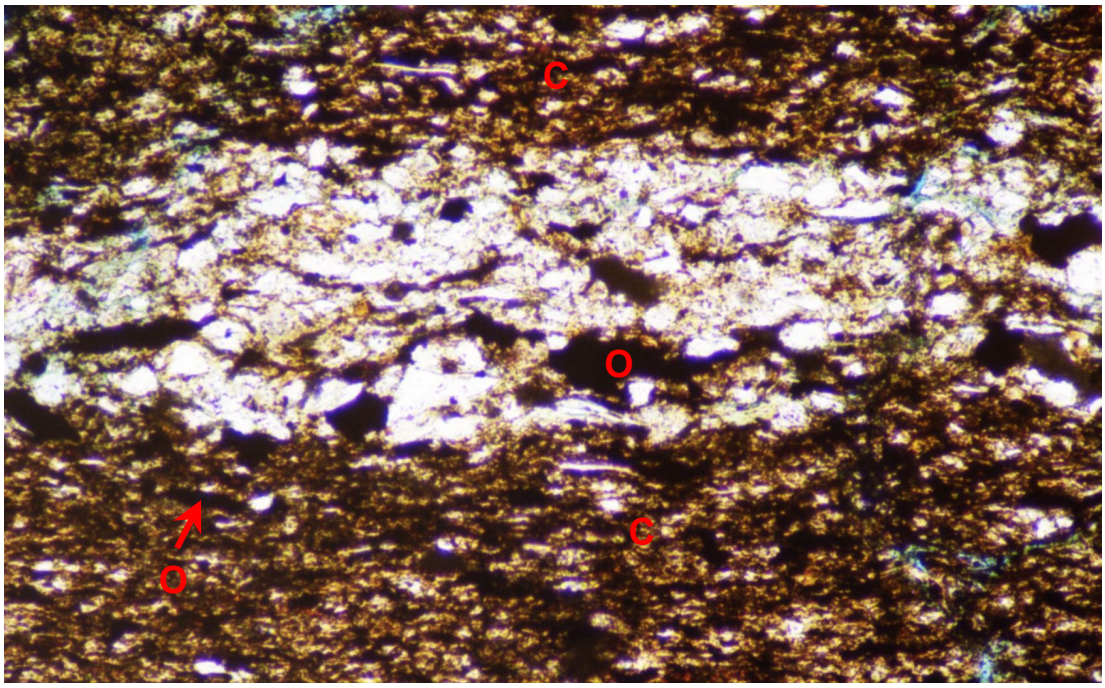

FIGURE 1 Plane polarised light
FIGURE 2 Crossed polarisers

0.2mm

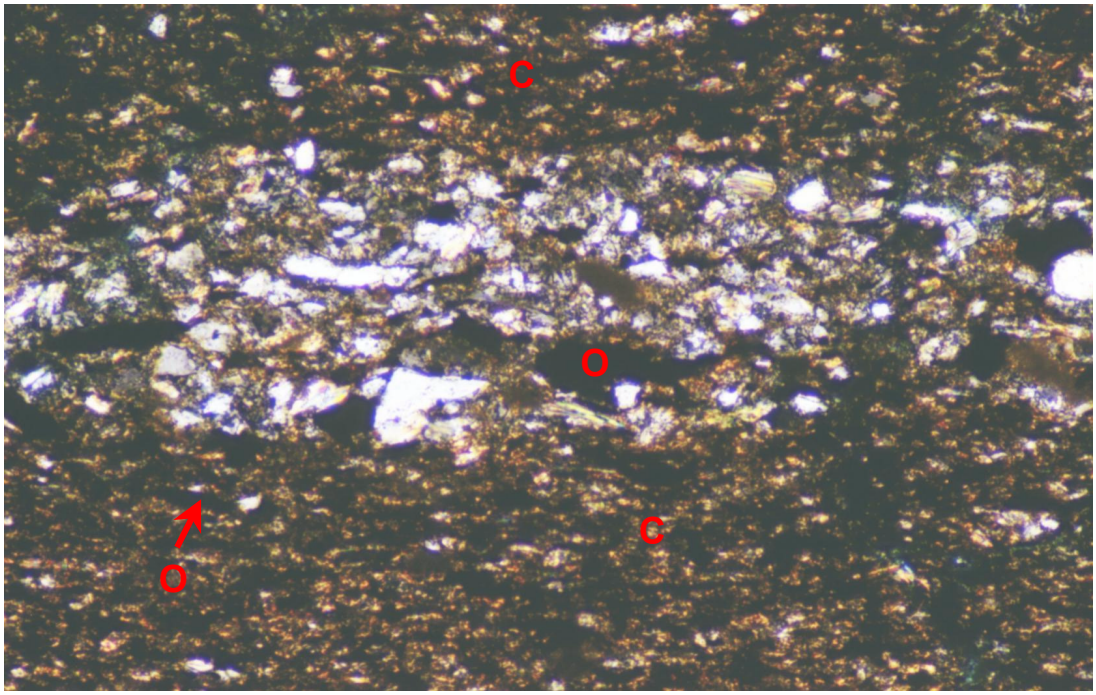

A silty lamination is included in a microporous mudrock that is composed mainly of detrital clay matrix (C) and fine organic fragments (O).

PLATE 50: SWC #23 2417.0m

Rock classification: Quartzarenite

Texture:

Sedimentary structures:	Massive
Sorting:	Moderate
Average grain size:	0.98mm (coarse sand)
Roundness:	Subangular-subrounded
Texture:	Grain supported; severely impact damaged
Packing /grain contacts:	Moderate/long, embayed
Macropore types:	Primary intergranular porosity, ?secondary intergranular porosity

Composition:

Quartz (monocrystalline)	74.8%	Authigenic kaolinite (pf)	2.0%
Quartz (polycrystalline)	3.1%	Authigenic kaolinite (rpl)	3.2%
Quartz overgrowths	1.1%	Authigenic illite (replacement)	0.7%
Pyrite	1.6%	Primary porosity (intergranular)	13.5%

Comments: This sample consists of loose quartz grains and fragments of pulverised sandstone that are the remains of a coarse grained quartzarenite that probably contained good primary intergranular porosity, despite porosity reduction by grain contact dissolution, minor quartz overgrowth cementation and localised pore filling by authigenic kaolinite, illite and pyrite. All porosity was recorded as primary intergranular porosity during point counting, but the sample probably also contained secondary intergranular porosity. Visible porosity could not be accurately measured and characterised due to complete impact-induced textural reorganisation.

PLATE 50: SWC #23 2417.0m

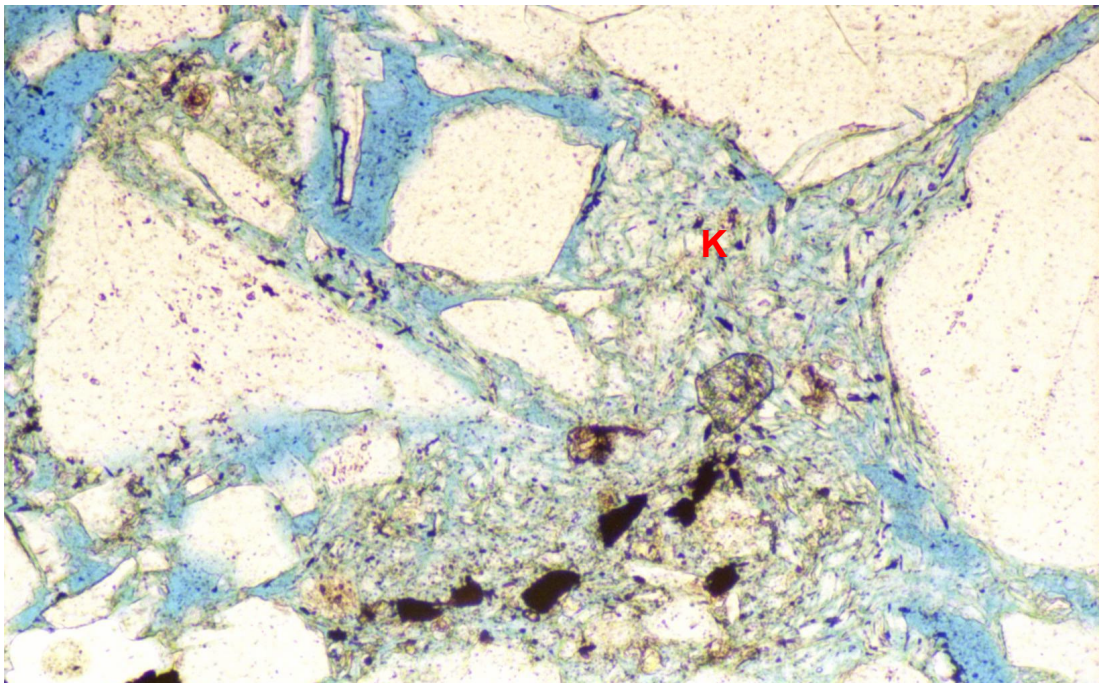

FIGURE 1 Plane polarised light

FIGURE 2 Crossed polarisers

0.2mm

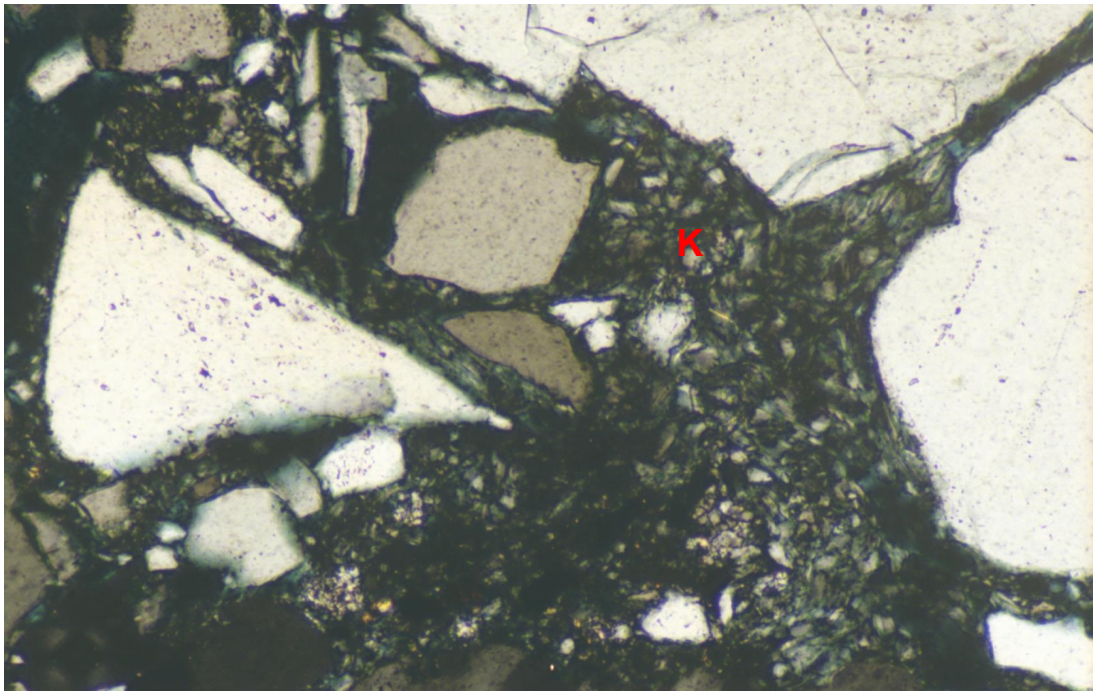

In this severely impact damaged, coarse grained quartzarenite, porosity had been reduced by micaceous grain alteration to kaolinite (K). However, the quartzarenite probably contained good intergranular porosity prior to sidewall coring.

PLATE 51: SWC #20 2437.5m

Rock classification: Quartzarenite

Texture:

Sedimentary structures:	Massive
Sorting:	Moderately-well
Average grain size:	0.59mm (coarse sand)
Roundness:	Subangular-subrounded
Texture:	Grain supported; severely impact damaged
Packing /grain contacts:	Moderate/long, embayed
Macropore types:	Primary intergranular porosity, ?secondary intergranular porosity

Composition:

Quartz (monocrystalline)	77.1%	Authigenic kaolinite (pf)	1.1%
Quartz (polycrystalline)	3.4%	Authigenic kaolinite (rpl)	3.1%
Quartz overgrowths	1.4%	Authigenic illite (replacement)	0.7%
Mica	0.3%	Primary porosity (intergranular)	12.9%

Comments: This quartzarenite is severely impact damaged, but includes rare, very small (three or four grains) intact sandstone fragments. Within these sandstone fragments, there are intergranular pores that indicate that the sample contained moderate to good intergranular porosity prior to sidewall coring. Porosity reduction has resulted from grain contact dissolution, minor quartz overgrowth cementation and localised pore filling by authigenic kaolinite, illite and rare finely-crystalline siderite. Visible porosity could not be accurately measured and characterised due to almost complete impact-induced textural reorganisation.

PLATE 51: SWC #20 2437.5m

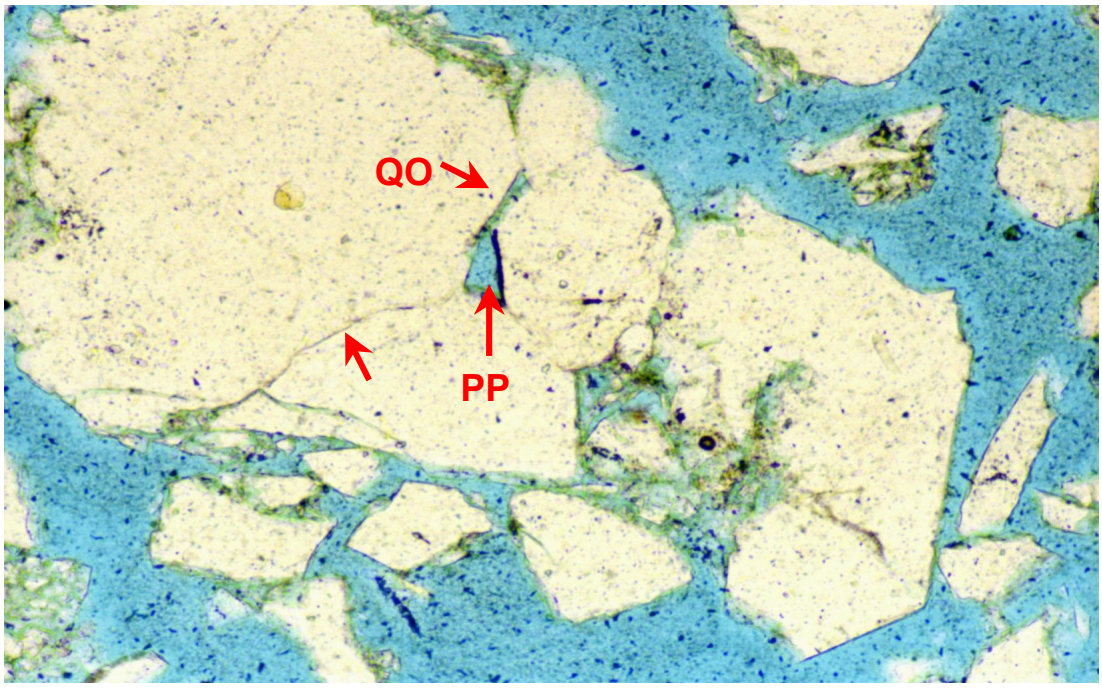

FIGURE 1 Plane polarised light
FIGURE 2 Crossed polarisers

0.2mm

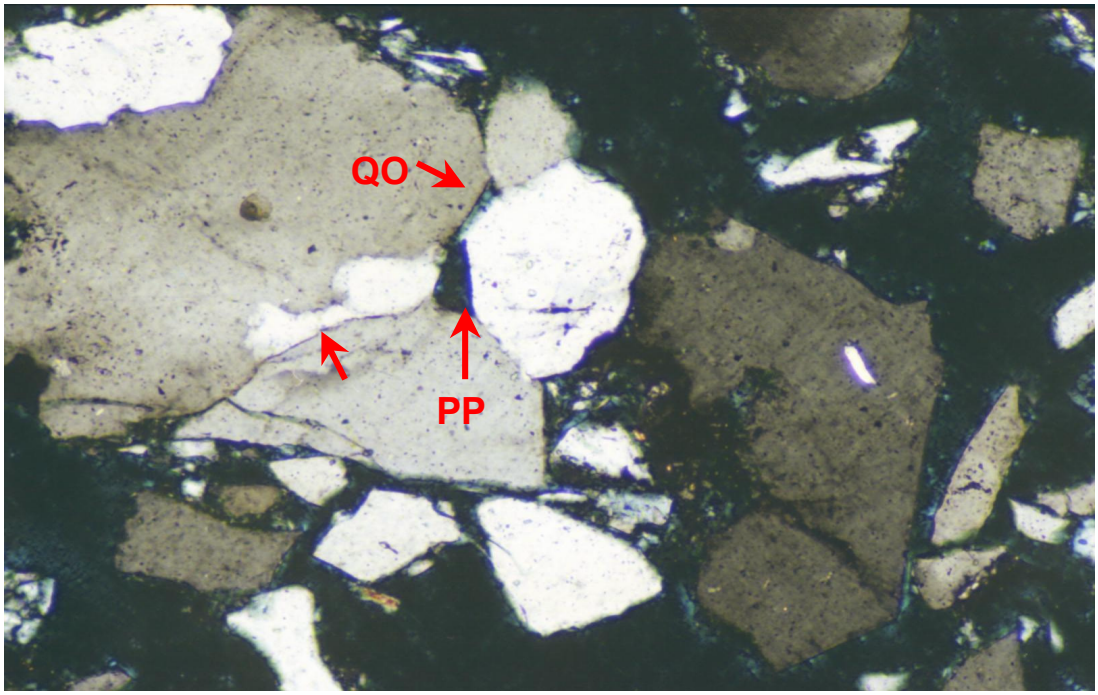

The presence of a primary intergranular pore (PP) within a small, intact quartzarenite fragment indicates that the sample contained at least moderate intergranular porosity prior to sidewall coring, despite porosity reduction by grain contact dissolution (arrow) and quartz overgrowth (QO) cementation.

PLATE 52: SWC #12 2575.0m

Rock classification: Quartzarenite

Texture:

Sedimentary structures:	Thin, argillaceous/carbonaceous laminae
Sorting:	Well
Average grain size:	0.16mm (fine sand)
Roundness:	Subangular-subrounded
Texture:	Grain supported
Packing /grain contacts:	Moderate/long, embayed
Macropore types:	Rare secondary mouldic porosity

Composition:

Quartz (monocrystalline)	57.5%	Siderite (replacement)	1.8%
Quartz (polycrystalline)	1.0%	Ankerite (replacement)	4.5%
Quartz overgrowths	2.5%	Authigenic kaolinite (pf)	6.0%
K-feldspar	0.5%	Authigenic kaolinite (rpl)	12.9%
Metamorphic rock fragments	0.7%	Authigenic illite (pore filling)	1.0%
Mica	0.7%	Authigenic illite (replacement)	3.3%
Heavy minerals	0.3%	Detrital clay	4.3%
Organics	3.0%		

Comments: Intergranular porosity is lacking in this impact damaged, but partly intact sandstone largely due to pore filling by authigenic clay (kaolinite, illite) that has formed by alteration of compacted micaceous grains. Porosity reduction is also the result of grain contact dissolution, quartz overgrowth and ankerite cementation, and pore filling by detrital clay and associated microcrystalline siderite (within argillaceous laminae). Quartz overgrowths fill all available intergranular space between juxtaposed quartz grains to form triple point grain junctions. Rare secondary mouldic pores occur where K-feldspar grains have dissolved. The sandstone is almost entirely microporous and thus would have very low permeability.

PLATE 52: SWC #12 2575.0m

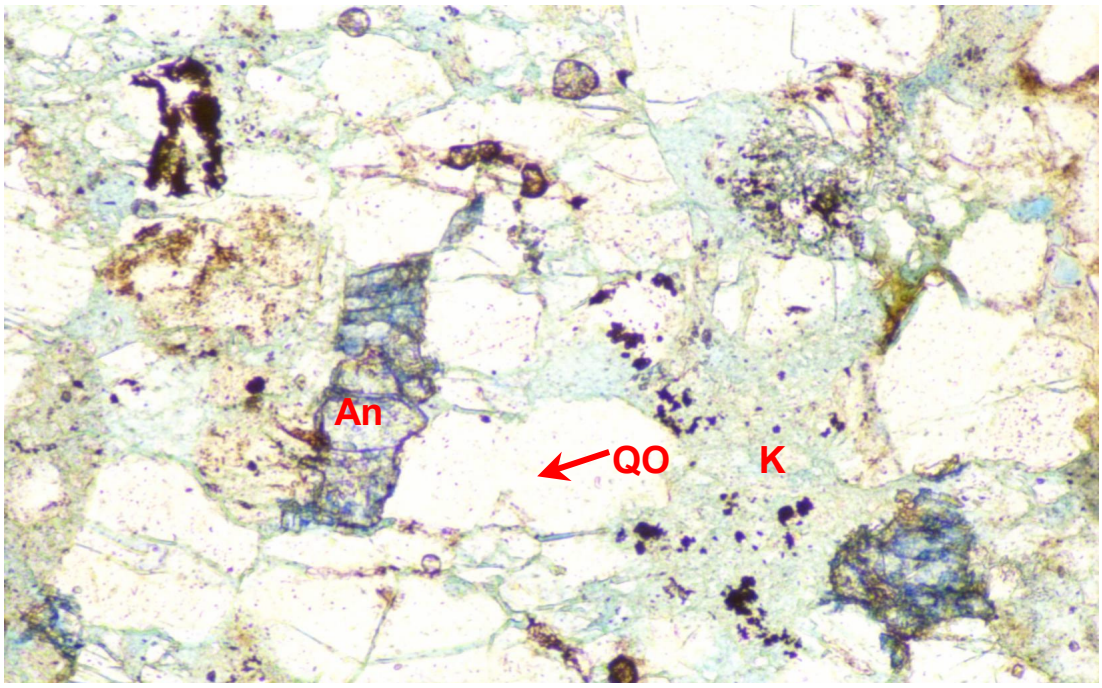

FIGURE 1 Plane polarised light
FIGURE 2 Crossed polarisers

0.2mm

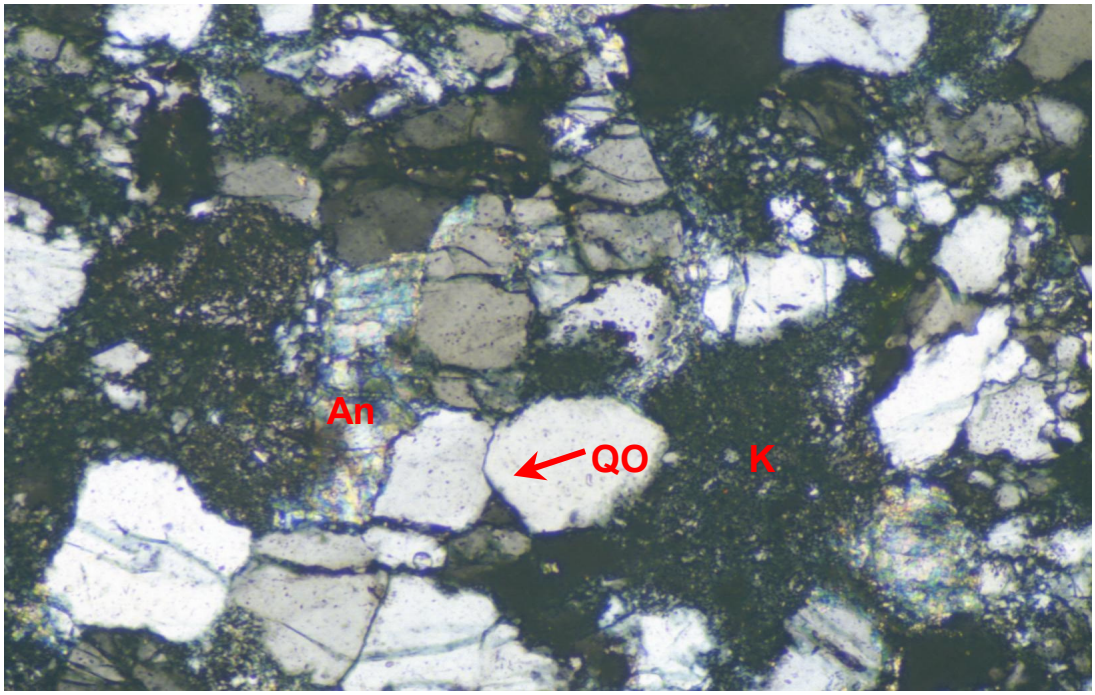

Intergranular porosity is lacking in this impact damaged, fine grained quartzarenite due to pore filling by highly microporous (as shown by blue hue) authigenic kaolinite (K) and cementation by quartz overgrowths (QO) and ankerite (An) (stained blue). Framework grains are fractured due to sidewall coring impact.

APPENDIX 7
CORE DESCRIPTION AND INTERPRETATION (SEDSTRAT PTY LTD)

DESCRIPTION AND INTERPRETATION OF THYLACINE-1 CONVENTIONAL CORE, T/30P, EASTERN OTWAY BASIN

A CONFIDENTIAL REPORT PREPARED FOR CORE LABORATORIES (PERTH) ON BEHALF OF WOODSIDE ENERGY LTD.

By

Peter A. Arditto

REPORT 2001/1
June, 2001

SEDSTRAT Pty Ltd
A.C.N. 090 428 247

CONTENTS

APPENDIX

I. FIGURES

1. SUMMARY

One 4 inch (10cm) diameter conventional core was recovered from the Turonian Flaxman Formation; core 1 was recovered over the interval 2165.00m - 2200.73m KB drillers depth. This interval comprised a siliciclastic succession (predominately quartz arenites with minor quartz-lithic intervals) of tidally-influenced distributary channel sandstones with minor mouth bar and crevasse splays, interbedded with interdistributary bay mudstones with minor storm wave-generated sandstones. A wireline log to drill depth correction of 3.04m (core depth high to log depth) was estimated by comparing the core gamma ray log to the wireline gamma ray log. A detailed lithological description and environmental interpretation of the cored succession is given in sections 3.1 and 3.2 of this report.

2. INTRODUCTION

Thylacine-1 was a wildcat exploration well drilled within the northeastern portion of T/30P, adjacent to the boundary of VIC/P43, within the eastern Otway Basin. The primary target was structural closure at the top of the Turonian Waarre Sandstone, sealed by Belfast Mudstone. The nearest well control is Prawn-A1, 27km to the southeast, and La Bella-1, 28km to the northwest within VIC/RL7. Core from the Waarre Formation in La Bella-1 was previously described and interpreted by Arditto (1999) and from Prawn-A1 by Arditto (2000). Peter Arditto, of SEDSTRAT Pty Ltd, was subcontracted by Core Laboratories on behalf of the client, Woodside Energy Ltd, to undertake a detailed lithological description and environmental interpretation of the conventional core recovered from Thylacine-1. This study was undertaken by the author over the period May 26 and 27 at the offices of Core Laboratories, 447 Belmont Avenue, Kewdale (Perth, W.A.). During this period lithological descriptions were recorded on A4 1:25 scale graphic core logs and these form the basis of this report. A brief presentation of the core interpretation was made by the author to Woodside staff on the afternoon of May 28 at the offices of Core Laboratories.

Lithological descriptions and environmental interpretations are followed by the A4 1:25 graphic log sheets, an A4 1:200 core gamma ray log and an A4 portion of 1:200 selected wireline log curves with the depth-corrected position of core 1 shown. Ichnofauna terminology used in this report is that of Pemberton (1992) and a summary of key ichnofauna identified in this study is given in section 5 of this report.

3. THYLACINE-1, CORE 1 (2165.00m – 2200.73m)

3.1 Lithological Description

The interval 2200.73m (base core 1) to 2200.45m is muddy sandstone to sandy mudstone with dispersed sub-angular quartz granules and pebbles up to 3mm by 5mm. It is internally homogeneous and the top is gradational into the overlying interval, with nodular siderite cement developed towards the top. The interval 2200.45m to 2194.77m is sandstone , very fine grained and very well sorted with good hummocky cross stratification (HCS) and sparsely burrowed by *Palaeophycus* and, more rarely, *Ophiomorpha*, alternating with sandy mudstone with common *Palaeophycus*, and more rarely *Terebellina*, burrows and sporadic wave oscillation

ripple laminations. An isolated sub-vertical burrow (?*Skolithos*), over 35cm long, penetrates a thick HCS sandstone unit in the lower half of the interval.

The interval 2194.77m to 2194.00m is sandstone, fine to medium grained and well sorted with load/flame structured basal contacts and lenticular-laminated to burrowed tops, alternating with mudstone, sparsely burrowed (small ?*Skolithos*) with minor starved ripple laminations and foundering features. The basal contact of this interval is highly incised with lag-lined 4cm relief topography (rounded quartz pebbles and rip up clasts up to 1cm). The interval 2194.00m to 2192.27m is sandstone, fine to medium, and up to very coarse grained and well to poorly sorted, being a composite interval of upward fining units separated by scour surfaces. Internally the interval is homogeneous to trough cross bedded or current ripple-laminated, with basal lags of quartz pebbles or rip up clasts and lenticular-laminated tops. Quartz overgrowths are developed (grains sparkle) but the sandstone retains very good visual porosity. The interval 2192.27m to 2192.00m is muddy sandstone, very fine grained with dispersed quartz granules and rounded pebbles up to 1cm in diameter. Internally it is lenticular-laminated with foundering features and bioturbated top.

The interval 2192.00m to 2189.88m is mudstone, moderately bioturbated with sporadic wave oscillation ripple laminations, with thin stringers of sandy siltstone with HCS and sparsely burrowed by *Anconichnus* near the base. The interval 2189.88m to 2188.60m is mudstone to muddy sandstone or sandstone, very fine grained, quartzose with minor lithics and clay matrix. Internally it is current ripple- to wave oscillation ripple-laminated with rare *Anconichnus* burrows. Minor carbonaceous drapes are disturbed by isolated foundering features.

The interval 2188.60m to 2186.98m is sandstone, fine to medium grained and well sorted with basal scour. The interval is predominately quartzose with minor lithics and clay matrix. It is internally homogeneous to trough cross bedded with minor lenticular laminations, dewatering features and scattered dark red brown sideritic mudstone rip up clasts up to 2cm by 4cm. The interval 2186.98m to 2185.60m is sandstone, fine up to fine to medium grained and well sorted, being a composite separated by scour surfaces and thin shale plugs. It is predominately quartzose with minor lithics and clay matrix. Internally it is planar-laminated to trough cross bedded or current ripple- and lenticular-laminated, with a mud-draped thin basal pebble lag sparsely burrowed by *Palaeophycus*.

The interval 2185.60m to 2184.25m is sandstone, very coarse to pebbly and poorly sorted. Internally it is homogeneous to trough cross bedded or planar-laminated with rare isolated lignite wood fragment (with clear growth rings) and sparse dark red brown sideritic mudstone rip up clasts up to 1cm by 4cm. The basal pebbly section (rounded quartz pebbles up to 1cm) contains lenticular mud drapes with sparse *Palaeophycus* burrows. The interval 2184.25m to 2183.08m is sandstone, fine grained, well sorted and predominately quartzose with minor lithics and clay cement. Internally it is trough cross bedded to planar- or current ripple-laminated with minor lenticular and flaser laminations, with and undulating basal scour surface. The interval 2183.08m to 2179.82m is sandstone, ranging from very coarse to pebbly, with sub-rounded quartz pebbles from 5mm to 10mm across, to medium to coarse grained and very poorly to poorly sorted, being composed of multiple stacked upward fining units separated by scour surfaces. Internally these units are trough cross bedded with

quartz pebble and mudstone rip up clast basal lags and lenticular-laminated tops. Minor carbonised plant debris and flattened stems occur in the lower half. Quartz overgrowths are well developed (grains sparkle) but sandstone retains very good visual porosity.

The interval 2179.82m to 2177.52m is sandstone, generally fine grained (up to medium grained and well sorted and predominately quartzose with minor lithics and clay cement. Internally it is current ripple-laminated with minor lenticular laminations and small scale trough cross bedding near the base. Some of the lenticular drapes are rich in carbonised plant debris. The sandstone retains moderate to good visual porosity. The interval 2177.52m to 2176.80m is sandstone, medium up to medium to coarse grained and moderately well sorted with lenticular laminations and foundering features, interbedded with shale and mudstone with starved current ripple laminations. The sandstone content and unit thickness generally increases upward.

The interval 2176.80m to 2172.30m is sandstone, ranging from very coarse to pebbly and very poorly sorted to fine grained and moderately well sorted, being composed of multiple stacked upward fining units separated by scour surfaces, lenticular laminations or thin shale plugs. Internally these units are trough cross bedded with minor rounded quartz pebble lags (up to 5mm diameter) and sub-rounded to angular dark red brown sideritic mudstone rip up clast lags (clasts ranging from 1cm to 3cm long). Quartz overgrowths are moderately well developed (grains sparkle) but the sandstone retains very good visual porosity. The interval 2172.30m to 2169.01m is sandstone, fine grained and very well sorted. Internally it is current ripple- to flaser- and lenticular-laminated with minor trough cross bedding and a number of zones of abundant *Palaeophycus* and *Planolites* burrows. Rare pyrite cement is developed along carbonaceous flaser laminations. Quartz overgrowths are moderately well developed (grains sparkle) but the sandstone retains good visual porosity.

The interval 2169.01m to 2167.02m is shale with starved current and wave oscillation ripple laminations, microfoundering features and rare *Teichichnus* and *Terebellina* burrows, interbedded with minor thin stringers of sandstone, very fine to fine grained and lenticular- to current ripple-laminated with rare HCS burrowed by *Anconichnus*. Rare load and flame features are associated with the basal contacts of the thin sandstones and there are rare occurrences of nodular pyrite and siderite cement. The interval 2167.02m to 2166.11m is shale with starved ripple and lenticular laminations with sparse *Teichichnus* burrows, grading upwards into sandstone, very fine to fine grained and up to fine to medium grained, well sorted with current ripple laminations, small scale trough cross bedding, rip up clasts and minor *Palaeophycus* burrows. It is a composite of four upward coarsening cycles. The interval 2166.11m to 2165.00m (top core 1) is muddy sandstone, fine to medium grained at the base to very fine grained at the top, very poorly sorted with a basal scour surface. Internally it is moderately to intensely burrowed to bioturbated by *Teichichnus* (sparse *Palaeophycus* near the base). Sparse quartz granules are scattered throughout.

3.2 Environmental Interpretation

Environmental interpretations given are based on lithological associations, primary sedimentary structures, ichnofauna associations and associated wireline log motifs

over and adjacent to the cored interval. Biostratigraphic data was not available at the time of this study. The interval 2200.73m to 2194.77m contains good elements of a tempestite succession with alternating storm wave deposition of hummocky cross stratified (HCS) very fine grained clean and sparsely burrowed sandstones rhythmically alternating with fair weather deposition of wave oscillation ripple-laminated to heavily burrowed mudstones. Such elements are common in a lower shoreface shelfal marine setting but the ichnofauna association present (common *Palaeophycus* with rare *Skolithos* in the sandstones and *Palaeophycus* with rare *Terebellina* in the mudstones) is more typical of brackish-water, rather than open marine lower shoreface, it is more likely that the succession was deposited within an outer interdistributary bay setting sufficiently broad to be storm wave-influenced. An interdistributary bay setting is also preferred in the light of the nature of the overlying succession (crevasse splays and distributary channels).

The interval 2194.77m to 2194.00m is composed of sandstone stringers with dewatering features (load and flame structures) alternating with sparsely burrowed mudstones with starved ripple laminations and foundering features. This is inferred to represent shallow subaqueous deposition within a crevasse splay setting. The basal contact for this interval is highly incised with a 4cm topographic relief infilled by a lag of quartz pebbles and mudstone rip up clasts up to 1cm). This appears to be a significant erosional boundary, cut by a high energy pulse but subsequently back filled by more quiescent splay deposition. This surface appears to represent a significant downward shift and may be a candidate for a regional sequence boundary. The interval 2194.00m to 2192.27m contains several upward fining relatively coarse grained sandstone units separated by scour surfaces, with basal pebble lags and lenticular-laminated tops and is interpreted as a stacked distributary channel succession. The uppermost 27cm of very fine grained muddy sandstone with dispersed (matrix-supported) quartz granules is interpreted as a probable transgressive surface.

The interval 2192.00m to 2189.88m is bioturbated mudstone with rare thin stringers of sandy siltstone with HCS and minor *Anconichnus* burrows and is interpreted as an interdistributary bay succession with minor storm wave influence. The interval 2189.88m to 2188.60m is composed of four mudstone to very fine grained muddy sandstone upward coarsening units, with wave oscillation ripple and lenticular laminations and disturbed by sparse burrows (including rare *Anconichnus*) and foundering features. This interval is interpreted as a distal crevasse splay succession. The interval 2188.60m to 2185.35m is composed of sandstone, fine to medium grained in the lower half and fine grained in the upper half. It is homogeneous to trough cross bedded or current ripple-laminated, with horizons of rip up clasts and is lenticular-laminated (rare thin mudstone plugs), with rare *Palaeophycus* burrows (brackish-water influence), in the upper half. These characteristics are interpreted to indicate the interval is a tidally-influenced, stacked, waning channel succession.

The interval 2185.35m to 2184.25m is very coarse to pebbly sandstone, with minor *Palaeophycus*-burrowed (brackish-water) lenticular mud drapes near the base and rare lignite wood fragments and carbonised plant stems towards the top. This is interpreted as a high energy , tidally-influenced distributary channel succession, with the overlying interval 2184.25m to 2183.08m of fine grained sandstone being interpreted as the waning cycle of this distributary channel succession. The interval

2183.08m to 2179.82m is of sandstone, ranging from very coarse to pebbly down to medium grained, being composed of multiple upward fining units, with basal scour surfaces and lenticular-laminated tops. This is interpreted as a stacked succession of high energy distributary channels, with the overlying interval 2179.82m to 2177.52m of fine grained and current ripple- to lenticular-laminated sandstone representing the waning channel succession. The interval 2177.52m to 2176.80m is interpreted as the crevasse splay component of the active channel to channel abandonment succession contained within the interval 2183.08m to 2176.80m.

The interval 2176.80m to 2172.30m is a composite sandstone interval, ranging from very coarse to pebbly down to fine grained representing a stacked succession of upward fining units separated by scour surfaces. These are trough cross bedded with basal rip up clast basal lags and lenticular-laminated tops. This interval is interpreted as succession of high energy distributary channels with possible minor tidal influence. The interval 2172.30m to 2169.01m is composed of relatively uniform fine grained and well sorted sandstone with rhythmical alternating zones of current ripple and flaser lamination or small scale trough cross bedding and concentrated *Palaeophycus* and *Planolites* burrows. Overall, these factors indicates continuous subaqueous deposition in brackish-water and the interval is interpreted as a tidally-influenced distributary mouth bar or possible tidal bar succession.

The interval 2169.01m to 2167.02m is predominately shale with starved ripple laminations, foundering features and rare *Teichichnus* and *Terebellina* burrows, alternating with minor thin stringers of current ripple- to lenticular-laminated sandstone, with rare HCS burrowed by *Anconichnus*, and minor load and flame features. This is interpreted as an interdistributary bay succession with minor storm wave influence. The interval 2167.02m to 2166.11m is a succession of upward coarsening units from shale, with starved ripple and lenticular laminations and sparse *Teichichnus* burrows, to very fine grained sandstone with current ripple and lenticular laminations, small scale trough cross bedding and rare *Palaeophycus* burrows. The ichnofauna indicate brackish-water and the interval is interpreted as an interdistributary bay crevasse splay succession. The interval 2166.11m to 2165.00m is an upward fining mudstone sandstone interval which is moderately to intensely burrowed to bioturbated with *Teichichnus* burrows (sparse *Palaeophycus* towards the base). Sparse quartz granules are scattered throughout and there is minor development of nodular siderite cement. This interval may represent the initiation of a transgressive phase of sedimentation although according to the wireline logs, it is immediately overlain by a thick, clean, sandstone package with a slightly upward fining gamma ray log motif. Although it is not possible to make a categoric statement on depositional environment for this interval, the presence of granule quartz scattered within throughout a highly burrowed muddy sandstone indicates it is likely to represent an abandoned estuarine distributary channel succession.

4. REFERENCES

ARDITTO, P.A., 1999*: Description and interpretation of selected core material from the lower Sherbrook Group, Otway Basin, Victoria.* A confidential report prepared by SEDSTRAT Pty Ltd on behalf of Boral Energy Resources Ltd, November 1999 (*Unpubl.*).

ARDITTO, P.A., 2000: *Description and interpretation of conventional core from the Late Cretaceous Sherbrook Group and Early Cretaceous Ptway Group in Prawn-A1, Otway Basin, T/30P (Tasmania).* A confidential report prepared for Origin Energy Resources Ltd, July 2000 (*Unpubl*.)

PEMBERTON, S.G., (ED), 1992: Applications of Ichnology to Petroleum Exploration; A Core Workshop. SEPM Core Workshop No. 17, Calgary, June 21, 1992. ISBN #0-918985-97-8.

5. SUMMARY OF ICHNOFAUNA

ANCONICHNUS

Description: Irregularly meandering, black-cored burrows with s pale halo of coarser silt. In cross-section, the burrows are elliptical to sub-circular, U-shaped in the longitudinal profile. Burrow structure is normally erratic, vermicularly tangled (Bromley, 1990), and often short in length. Extensive bioturbation tends to create a mottled fabric, obscuring most traces. In core, *Anconichnus* commonly appears as tiny dark pin-head sized spots (transverse section) or dark lines (longitudinal section), which may be discontinuous and surrounded by a pale silt halo.

Trophic Classification: Systematic feeding/grazing.

Environmental Considerations: *Anconichnus* ia a common element of the *Cruziana* and *Skolithos* ichnofacies on a normal marine shallow shelf and is often found as an opportunistic colonizer of storm-deposited sands. *Anconichnus* is associated with *Chondrites*, *Terebellina*, *Planolites* and other shallow tier trace fossils.

OPHIOMORPHA

Description: Simple to complex burrow systems distinctly lined with agglutinated pelletiodal sediment. Burrow lining is near smooth on the interior and densely to strongly mammalated or nodose on the exterior. Individual pellets or pellet masses may be discoid, ovoid, conical, mastoid bilobate or irregular in shape. Characteristics of the linings may vary within a similar composition to host rock but in some instances it may be filled actively with meniscate laminae. Branching is irregular and, where present, Y-shaped. At bifurcations the burrow become swollen.

Trophic Classification: Dwelling burrow of suspension-feeding shrimp.

Environmental Considerations: *Ophiomorpha* is commonly associated with the *Skolithos* ichnofacies and can be found in prolific numbers in marine shoreface environments. It is also found in brackish water, sandy substrates including estuaries and tidal shoals.

PALAEOPHYCUS

Description: Infrequently branch, distinctly lined, cylindrical, horizontal to inclined burrows in which the sediment fill typically is of the same lithology and texture as the

host stratum. Wall linings may be smooth, longitudinally striated or with transverse annuli.

Trophic Classification: Dwelling burrow of predaceous polychaete.

Environmental Considerations: *Palaeophycus* is associated with the *Skolithos* ichnofacies in both high and low energy shoreface envirobments and is commonly found with *Planolites* or *Macaronichnus*. It can also be found in episodic storm sands and brackish-water assemblages.

PLANOLITES

Description: Unlined, rarely branched, straight to tortuous, smooth to irregular walled or annulated burrows, circular to elliptical in cross-section, of variable dimensions and configurations. Fillings are essentially structureless, differing in lithology from the host rock.

Trophic Classification: Feeding burrow of deposit feeder.

Environmental Considerations: Found in virtually all environments from freshwater to deep marine.

SKOLITHOS

Description: Single entrance, cylindrical to sub cylindrical, straight to curved, vertical to sub vertical. Unbranched burrows that do not cross over or interpenetrate. The shafts are either lined or unlined with generally smooth walls, but may be annulated. The infill is typically structureless.

Trophic Classification: Dwelling burrow of suspension feeding vermiform organism.

Environmental Considerations: Lined species of *Skolithos* are generally associated with marine or brackish environments. It is an element of the *Skolithos* ichnofacies but, because *Skolithos* can be constructed by many different kinds of organisms, it is found in virtually every type of environment from marine to non-marine.

TEICHICHNUS

Description: *Teichichnus* appears in slabbed core sections as a vertical series of tightly packed concave-up or (more rarely) concave-down, crescentric laminae. Longitudinal sections show wavy, long laminae that usually merge upwards at the ends. It is formed by the upward migration of a horizontal to sub horizontal tunnel produced by an organism moving back and forth in the same vertical plane, probing the sediment for food.

Trophic Classification: Dwelling/feeding burrow of a deposit feeding organism.

Environmental Considerations: *Teichichnus* is commonly found in lower shoreface to offshore environments associated with *Cruziana* ichnofacies and is prevalent in low energy lagoon/bay settings characterised by brackish-water conditions. It is never associated with freshwater.

TEREBELLINA

Description: Sub cylindrical, vertical gently to strongly curved burrows with circular to elliptical cross sections. Diameters are highly variable and the tubes gradually taper distally. The lining is very distinct, ranges in thickness from 1.5mm to 5mm, is composed of either calcium carbonate or sand grains, and is more resistant to weathering than either the surrounding matrix or burrow fill. Material infilling the burrow is similar in composition to the host rock. In core, specimens generally appear to be horizontal due to the curvature of the tube.

Trophic Classification: Dwelling burrow of suspension feeding organism.

Environmental Considerations: *Terebellina* is commonly found in the distal *Cruziana* ichnofacies in offshore marine environments with special adaptation for constructing an open tube in argillaceous substrates. It is also found in fine grained brackish-water bay environments.

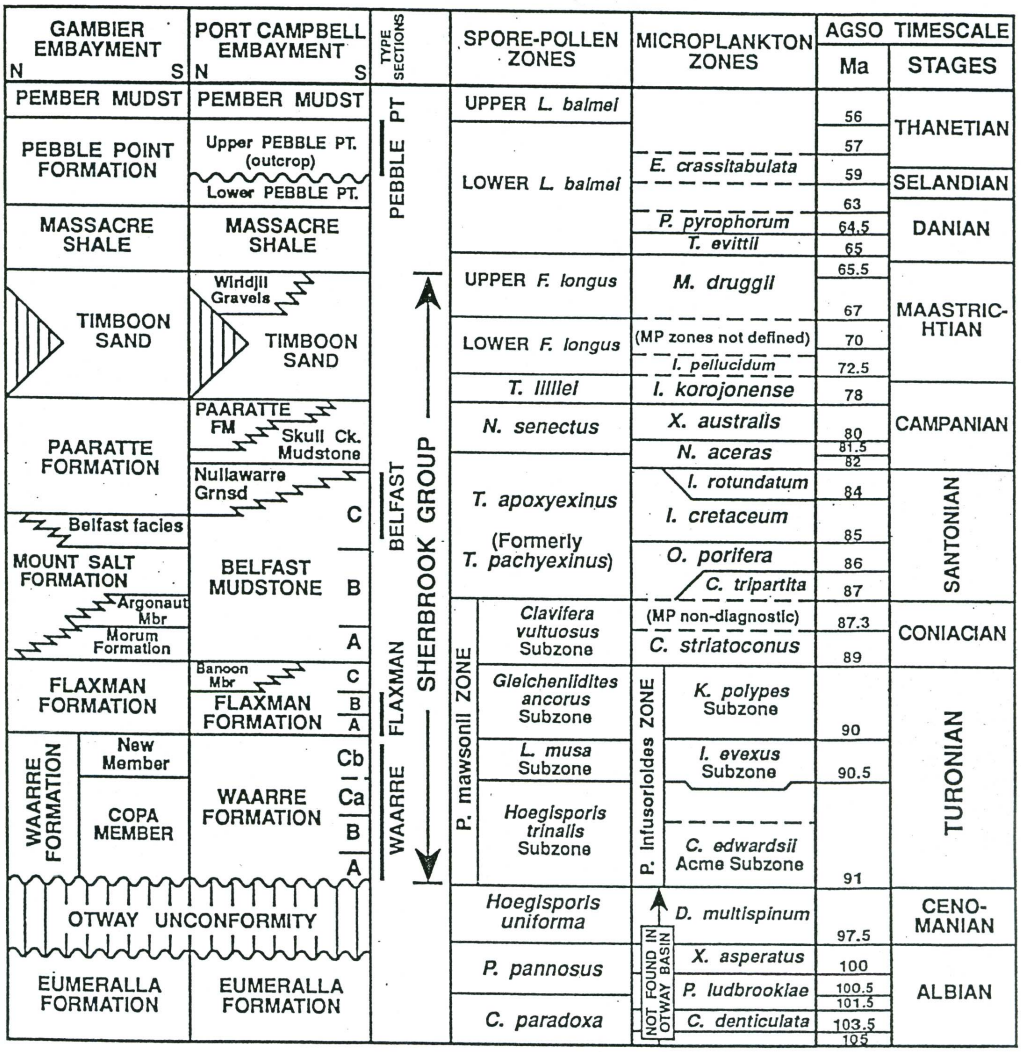

Revised Sherbrook Group stratigraphy and palynological timescale.
Prepared by Alan D. Partridge — January 1999 version.

COMPANY : WOODSIDE ENERGY LTD
WELL : THYLACINE -1
TOP DEPTH : 2165m - 2200.73m

SURFACE CORE GAMMA

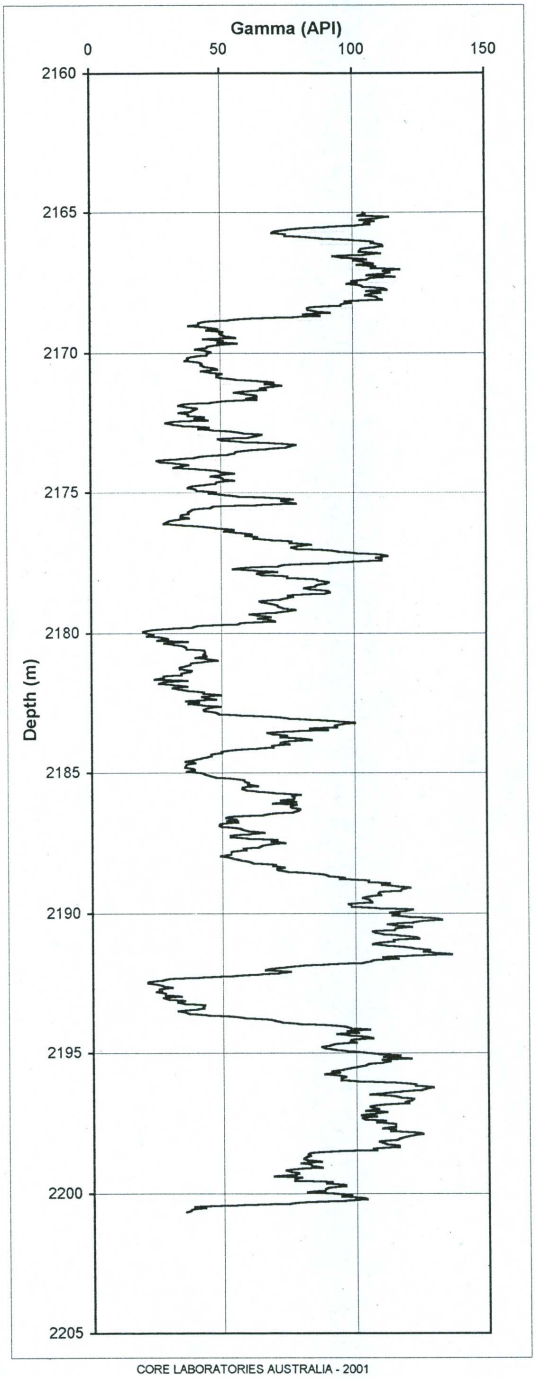

File : PRP-01025

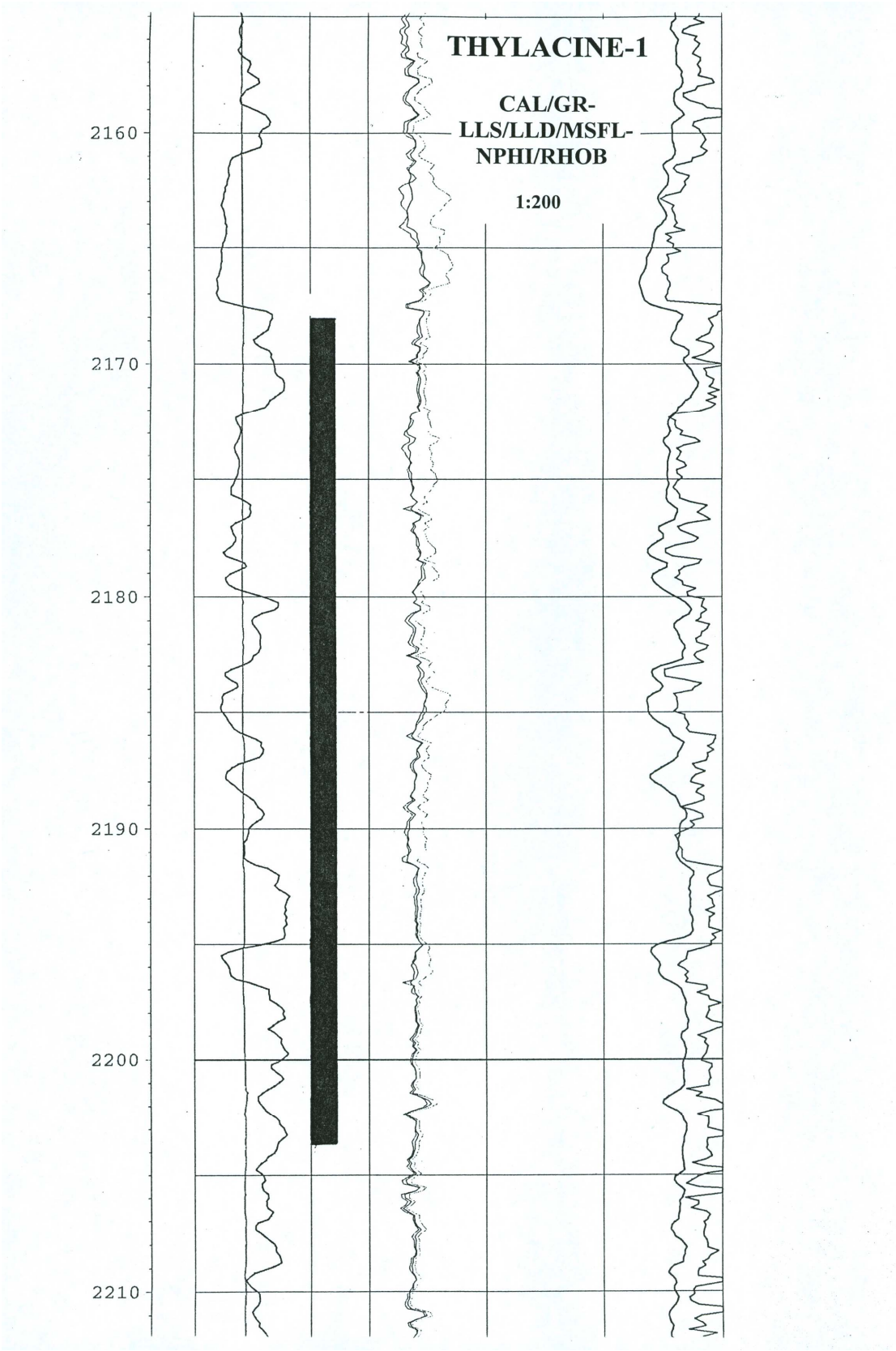
THYLACINE-1
CAL/GR-
LLS/LLD/MSFL-
NPHI/RHOB
1:200
2160
2170
2180
2190
2200
2210

THYLACINE - 1

WOODSIDE AUSTRALIAN ENERGY

PERMIT : T/30P	**DATE :** 26/05/01	**CORE NO. :** 1	**Page :** of
AUTHOR : P.A. Arditto	**JOB NO. :** 400-18120	**INTERVAL :** 2165.00m - 2200.73m	
RIG :		**CUT :**	
K.B. :	**W.D. :**	**CORE BARREL & MUD TYPE :**	

DEPTH (m)	LITHOLOGY	GRAIN SIZE (SILT, V.FINE, FINE, MEDIUM, COARSE, V.COARSE)	DEPOSITIIONAL ENVIRONMENT	SEDIMENTARY STRUCTURE	LITHOLOGICAL DESCRIPTION TOP CORE 1
2165 – 2166	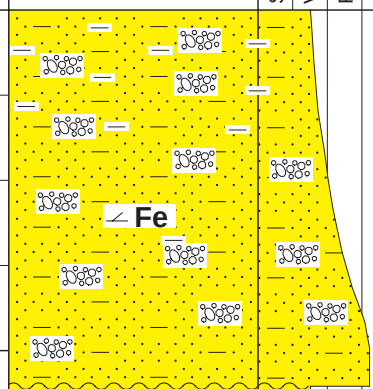		2166.11m to 2165.00m Abandoned Estuarine Distributary Channel Succession?	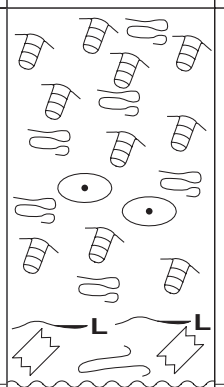	The interval 2166.11m to 2165.00m (top core 1) is muddy sandstone, fine to medium grained at the base to very fine grained at the top, very poorly sorted with a basal scour surface. Internally it is moderately to intensely burrowed to bioturbated by *Teichichnus* (sparse *Palaeophycus* near the base). Sparse quartz granules are scattered throughout.
2166 – 2167	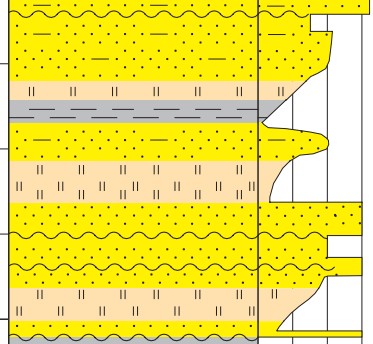	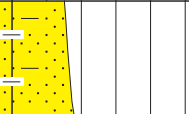	2167.02m to 2166.11m Interdistributary Bay Crevasse Splay Succession	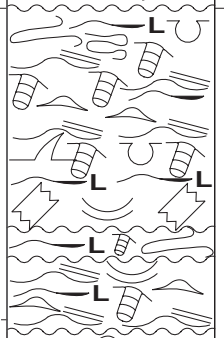	The interval 2167.02m to 2166.11m is shale with starved ripple and lenticular laminations with sparse *Teichichnus* burrows, grading upwards into sandstone, very fine to fine grained and up to fine to medium grained, well sorted with current ripple laminations, small scale trough cross bedding, rip up clasts and minor *Palaeophycus* burrows. It is a composite of four upward coarsening cycles.
2167 – 2169	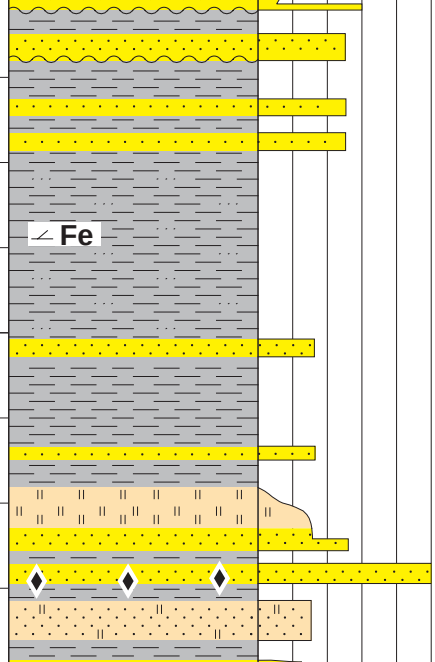	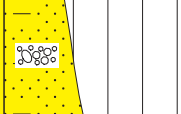	2169.01m to 2167.02m Interdistributary Bay Succession	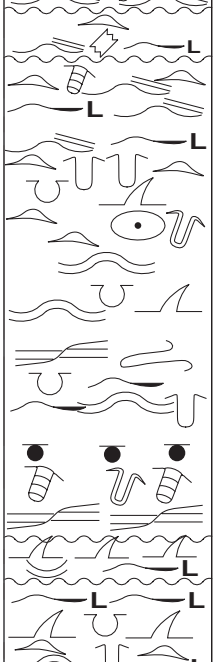	The interval 2169.01m to 2167.02m is shale with starved current and wave oscillation ripple laminations, microfoundering features and rare *Teichichnus* and *Terebellina* burrows, interbedded with minor thin stringers of sandstone, very fine to fine grained and lenticular- to current ripple-laminated with rare HCS burrowed by *Anconichnus*. Rare load and flame features are associated with the basal contacts of the thin sandstones and there are rare occurrences of nodular pyrite and siderite cement.
2169 –	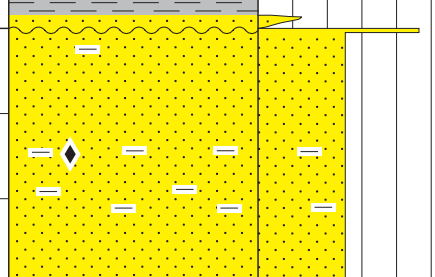	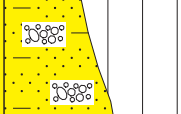		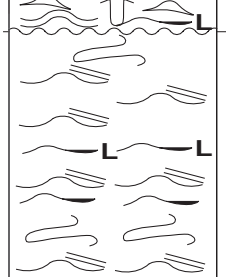	

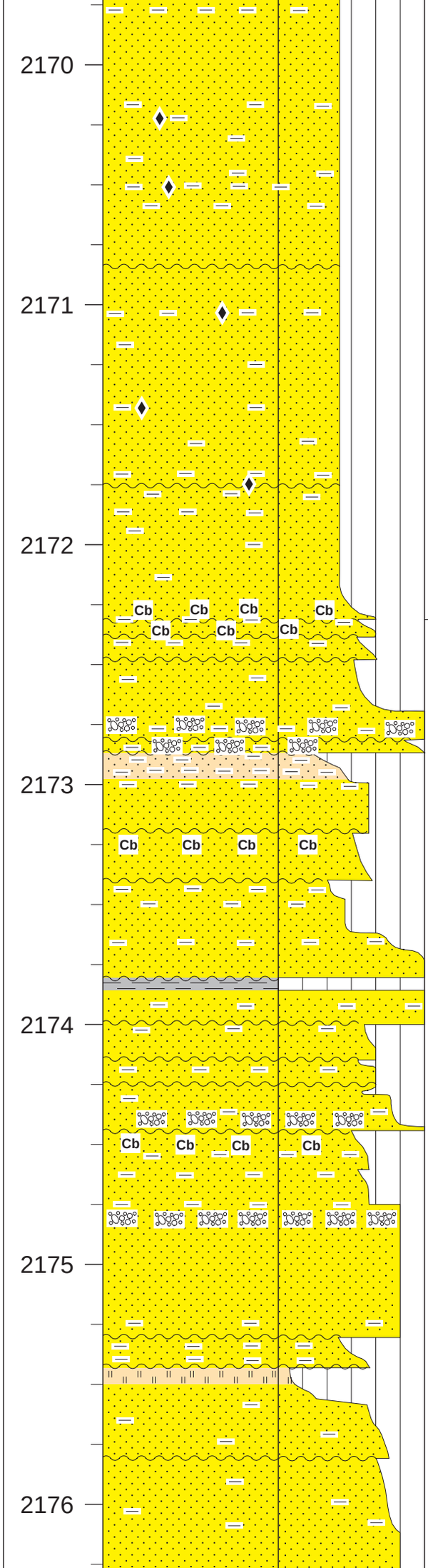

2172.30m to 2169.01m
Tidally-influenced
Distributary Mouth Bar
Succession

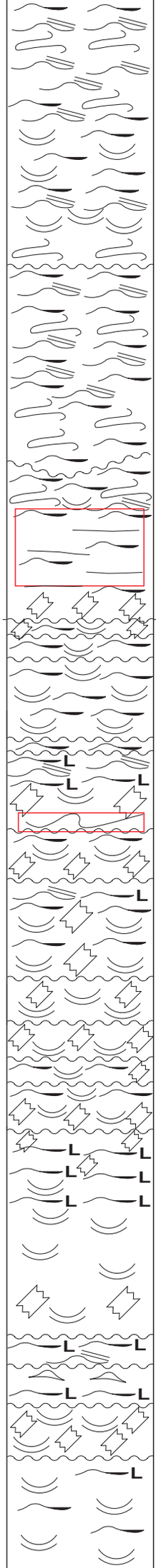

The interval 2172.30m to 2169.01m is sandstone, fine grained and very well sorted. Internally it is current ripple- to flaser- and lenticular-laminated with minor trough cross bedding and a number of zones of abundant *Palaeophycus* and *Planolites* burrows. Rare pyrite cement is developed along carbonaceous flaser laminations. Quartz overgrowths are moderately well developed (grains sparkle) but the sandstone retains good visual porosity.

2176.80m to 2172.30m
High Energy
Distributary Channels

The interval 2176.80m to 2172.30m is sandstone, ranging from very coarse to pebbly and very poorly sorted to fine grained and moderately well sorted, being composed of multiple stacked upward fining units separated by scour surfaces, lenticular laminations or thin shale plugs. Internally these units are trough cross bedded with minor rounded quartz pebble lags (up to 5mm diameter) and sub-rounded to angular dark red brown sideritic mudstone rip up clast lags (clasts ranging from 1cm to 3cm long). Quartz overgrowths are moderately well developed (grains sparkle) but the sandstone retains very good visual porosity.

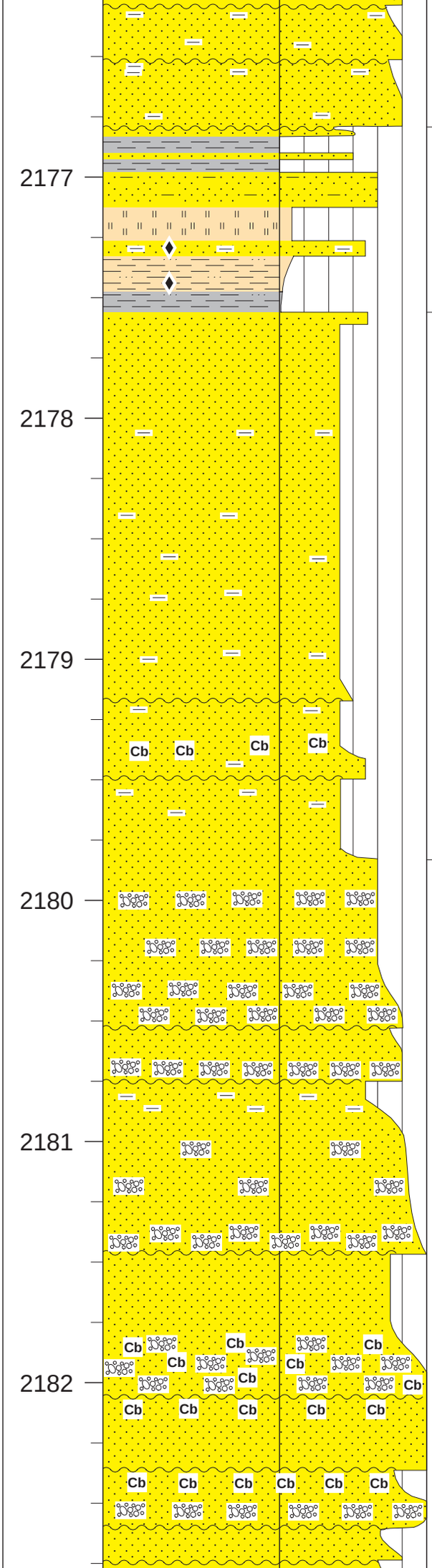

2177.52m to 2176.80m
Crevasse Splay

The interval 2177.52m to 2176.80m is sandstone, medium up to medium to coarse grained and moderately well sorted with lenticular laminations and foundering features, interbedded with shale and mudstone with starved current ripple laminations. The sandstone content and unit thickness generally increases upward.

2179.82m to 2177.52m
Waning Channel
Succession

The interval 2179.82m to 2177.52m is sandstone, generally fine grained (up to medium grained and well sorted and predominately quartzose with minor lithics and clay cement. Internally it is current ripple-laminated with minor lenticular laminations and small scale trough cross bedding near the base. Some of the lenticular drapes are rich in carbonised plant debris. The sandstone retains moderate to good visual porosity.

2183.08m to 2179.82m
High Energy
Distributary channels

The interval 2183.08m to 2179.82m is sandstone, ranging from very coarse to pebbly, with sub-rounded quartz pebbles from 5mm to 10mm across, to medium to coarse grained and very poorly to poorly sorted, being composed of multiple stacked upward fining units separated by scour surfaces. Internally these units are trough cross bedded with quartz pebble and mudstone rip up clast basal lags and lenticular-laminated tops. Minor carbonised plant debris and flattened stems occur in the lower half. Quartz overgrowths are well developed (grains sparkle) but sandstone retains very good visual porosity.

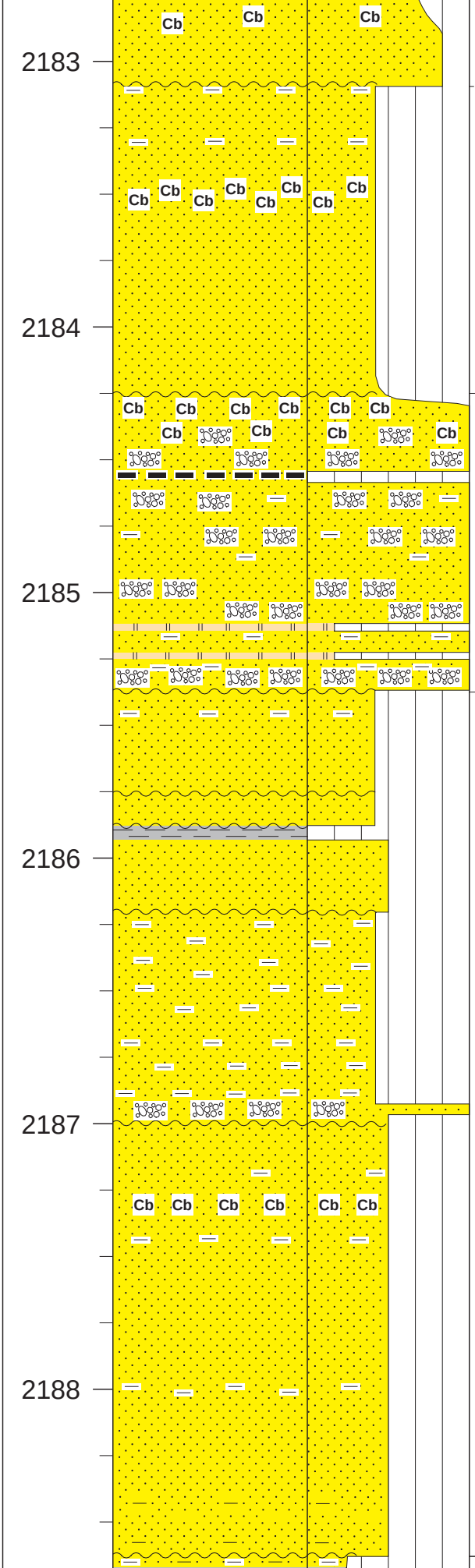

2184.25m to 2183.08m
Waning, Distributary
Channel Succession

2185.35m to 2184.25m
High Energy,
Tidally-influenced
Distributary Channel
Succession

2188.60m to 2185.35m
Tidally-influenced,
Waning Distributary
Channel Succession

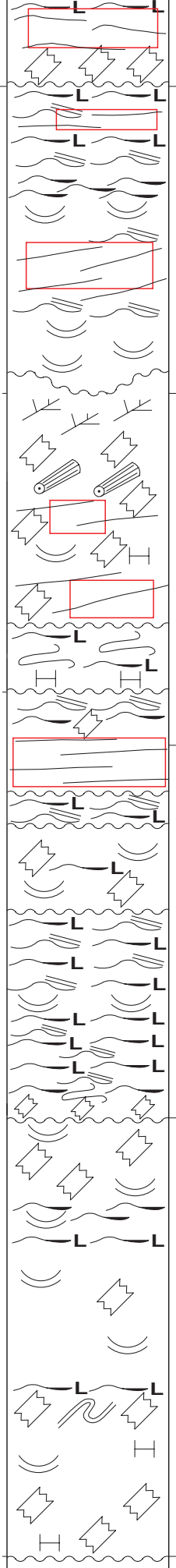

The interval 2184.25m to 2183.08m is sandstone, fine grained, well sorted and predominately quartzose with minor lithics and clay cement. Internally it is trough cross bedded to planar- or current ripple-laminated with minor lenticular and flaser laminations, with and undulating basal scour surface.

The interval 2185.60m to 2184.25m is sandstone, very coarse to pebbly and poorly sorted. Internally it is homogeneous to trough cross bedded or planar-laminated with rare isolated lignite wood fragment (with clear growth rings) and sparse dark red brown sideritic mudstone rip up clasts up to 1cm by 4cm. The basal pebbly section (rounded quartz pebbles up to 1cm) contains lenticular mud drapes with sparse *Palaeophycus* burrows.

The interval 2186.98m to 2185.60m is sandstone, fine up to fine to medium grained and well sorted, being a composite separated by scour surfaces and thin shale plugs. It is predominately quartzose with minor lithics and clay matrix. Internally it is planar-laminated to trough cross bedded or current ripple- and lenticular-laminated, with a mud-draped thin basal pebble lag sparsely burrowed by *Palaeophycus* .

The interval 2188.60m to 2186.98m is sandstone, fine to medium grained and well sorted with basal scour. The interval is predominately quartzose with minor lithics and clay matrix. It is internally homogeneous to trough cross bedded with minor lenticular laminations, dewatering features and scattered dark red brown sideritic mudstone rip up clasts up to 2cm by 4cm.

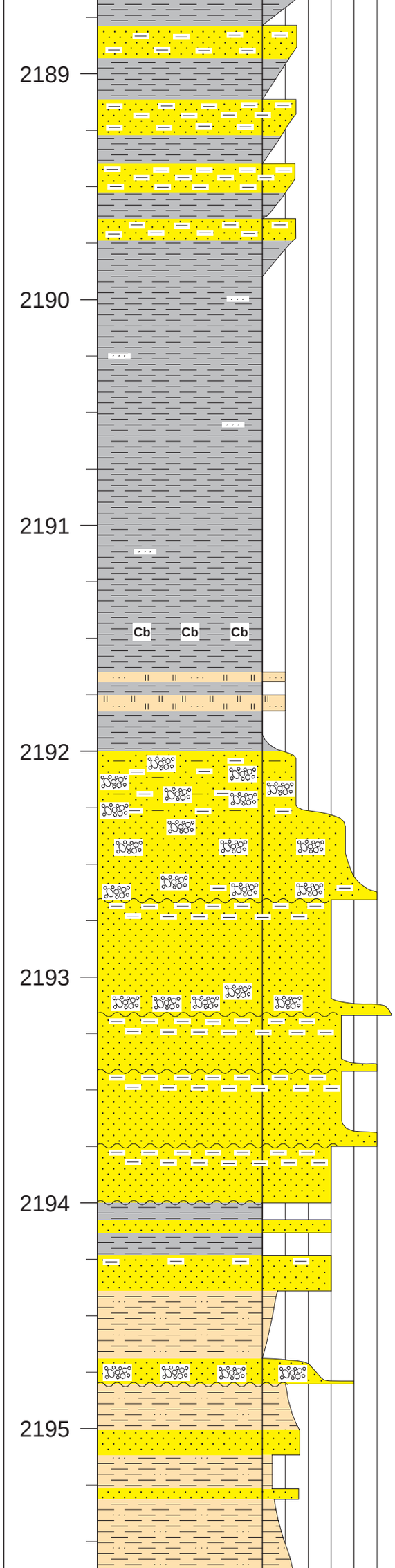

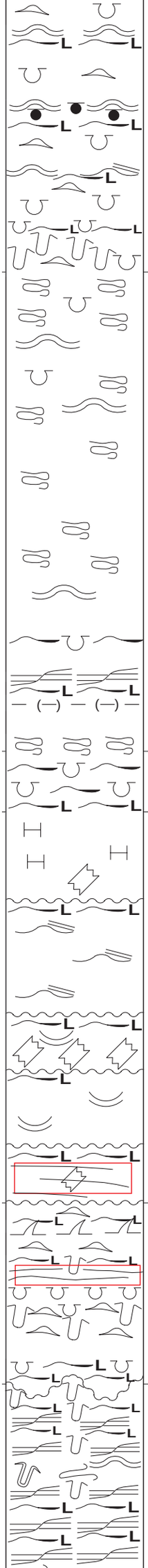

2189.88m to 2188.60m
Distal Crevasse
Splay Succession

The interval 2189.88m to 2188.60m is mudstone to muddy sandstone or sandstone, very fine grained, quartzose with minor lithics and clay matrix. Internally it is current ripple- to wave oscillation ripple-laminated with rare *Anconichnus* burrows. Minor carbonaceous drapes are disturbed by isolated foundering features.

2192.00m to 2189.88m
Interdistributary
Bay Succession

The interval 2192.00m to 2189.88m is mudstone, moderately bioturbated with sporadic wave oscillation ripple laminations, with thin stringers of sandy siltstone with HCS and sparsely burrowed by *Anconichnus* near the base.

2192.00m
Probable Transgressive
Surface

The interval 2192.27m to 2192.00m is muddy sandstone, very fine grained with dispersed quartz granules and rounded pebbles up to 1cm in diameter. Internally it is lenticular-laminated with foundering features and bioturbated top.

2194.00m to 2192.27m
Distributary Channel
Succession

The interval 2194.00m to 2192.27m is sandstone, fine to medium, and up to very coarse grained and well to poorly sorted, being a composite interval of upward fining units separated by scour surfaces. Internally the interval is homogeneous to trough cross bedded or current ripple-laminated, with basal lags of quartz pebbles or rip up clasts and lenticular-laminated tops. Quartz overgrowths are developed (grains sparkle) but the sandstone retains very good visual porosity.

2194.77m to 2194m
Crevasse Splay

2194.77m
Regional Sequence
Boundary?

The interval 2194.77m to 2194.00m is sandstone, fine to medium grained and well sorted with load/flame structured basal contacts and lenticular-laminated to burrowed tops, alternating with mudstone, sparsely burrowed (small ?*Skolithos*) with minor starved ripple laminations and foundering features. The basal contact of this interval is highly incised with lag-lined 4cm relief topography (rounded quartz pebbles and rip up clasts up to 1cm).

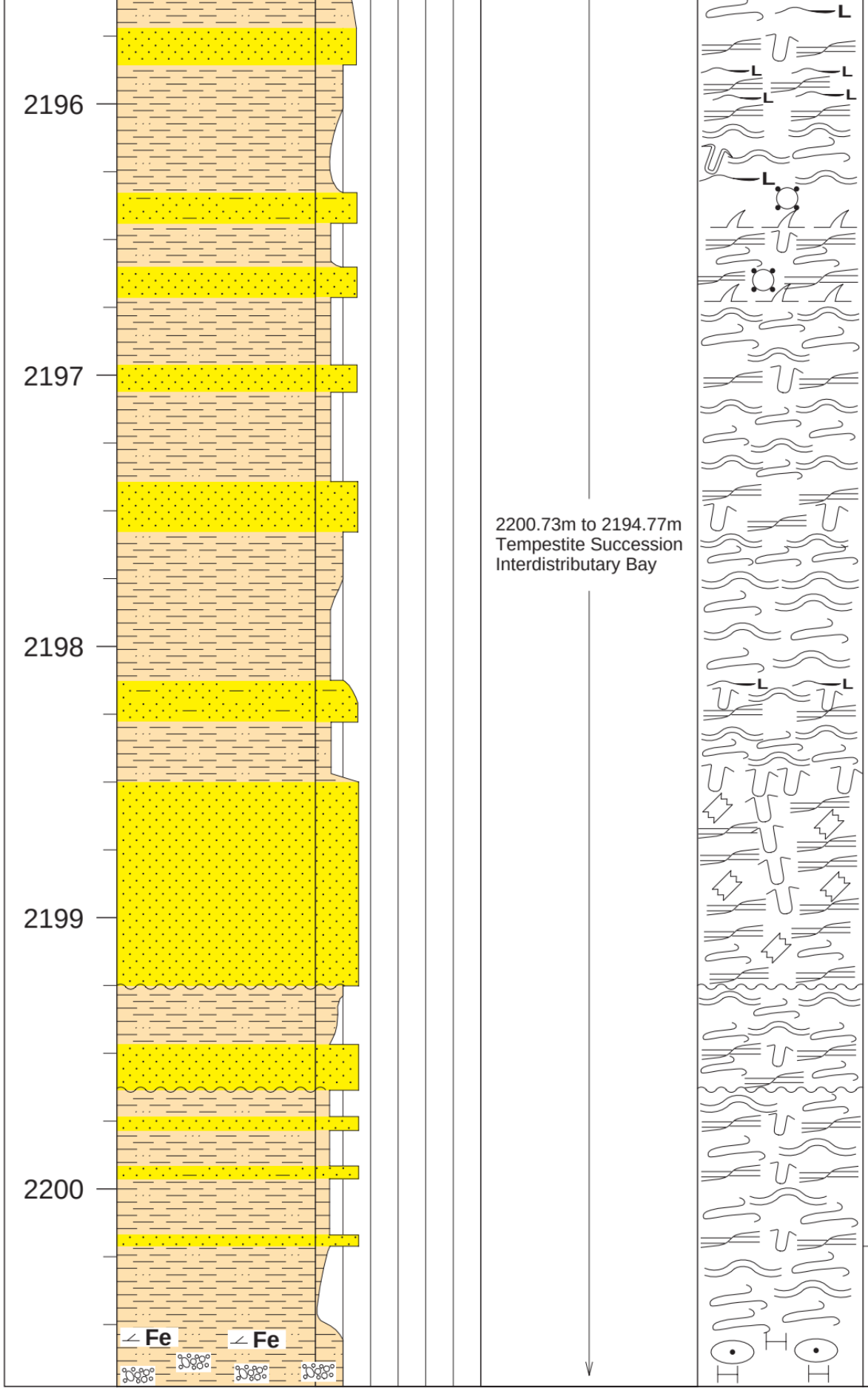

2200.73m to 2194.77m
Tempestite Succession
Interdistributary Bay

The interval 2200.45m to 2194.77m is sandstone , very fine grained and very well sorted with good hummocky cross stratification (HCS) and sparsely burrowed by *Palaeophycus* and, more rarely, *Ophiomorpha* , alternating with sandy mudstone with common *Palaeophycus* , and more rarely *Terebellina* , burrows and sporadic wave oscillation ripple laminations. An isolated sub-vertical burrow (?*Skolithos*), over 35cm long, penetrates a thick HCS sandstone unit in the lower half of the interval.

The interval 2200.73m (base core 1) to 2200.45m is muddy sandstone to sandy mudstone with dispersed sub-angular quartz granules and pebbles up to 3mm by 5mm. It is internally homogeneous and the top is gradational into the overlying interval, with nodular siderite cement developed towards the top.

APPENDIX 8
CORE DESCRIPTION AND INTERPRETATION (CORE LABORATORIES AUSTRALIA)

SEDIMENTOLOGY STUDY
WELL: THYLACINE-1

A Complimentary Report Prepared For:

WOODSIDE ENERGY LTD.

By:

Duncan Barr

June, 2001

EXECUTIVE SUMMARY

Core from Thylacine-1 consists mainly of sandstone with subordinate, heterolithically interbedded sandstone and claystone. Depositional environment is interpreted to have been estuarine-deltaic.

Sandstones range in grain size from very fine to very coarse grained, and vary from poorly to well sorted. Localised conglomerate layers are also observed.

Coarser grained, planar to trough cross-bedded sandstone is interpreted to have been deposited as high energy, tidally reworked estuarine channels, while ripple-laminated sandstone probably formed as tidally reworked bars. Evidence for bimodal current reversals is frequently observed in both the cross-bedded and rippled facies.

Most bioturbated heterolithics and claystones exhibit highly diverse trace fossil assemblages, indicating shallow, open marine influence. These beds are believed to have been deposited in a lower shoreface to offshore transition environment. Thin, very fine grained, laminated sandstones interbedded with the heterolithics are thought to represent storm sands.

The vertical successions of lithofacies and ichnofacies indicate that fluctuations in relative sea level have influenced sedimentation, and a number of important depositional surfaces, some of which may be laterally continuous, were observed in the core. These surfaces include a scoured hardground and several transgressive surfaces of erosion. The transgressive surfaces usually occur at the top of sandstone bodies, and are frequently accompanied by a thin, coarse to very coarse grained lag deposit.

The main control on reservoir quality appears to be grain size. Excellent reservoir quality is observed in the coarsest, cross-bedded facies (profile permeability locally reaches several darcies). Very fine to fine grained, laminated to rippled sandstones show poor to good reservoir quality. Calcite cementation has caused only minor, highly localised reduction in reservoir quality.

The sandstones are mostly well indurated, thus sanding potential is considered to be low. Fines migration is a potential production hazard, due to the presence of whitish clay matrix in some sandstones. Further insights into potential production problems would require petrographic study.

DISCUSSION

Introduction

The principle aim of this complimentary report is to demonstrate Core Laboratories Australia's sedimentological capability, and to provide an example of the AppleCore digital logging format (see Enclosure 1).

Approximately 36 metres of conventional core were recovered from Thylacine-1, a detailed description of which is provided in AppleCore format in Enclosure 1. AppleCore logs are readily convertible (without the need for scanning) to the main digital imaging formats, such as TIFF, JPEG, GIF and BMP, and can therefore be displayed and printed by a wide range of computer platforms. AppleCore can also output core log data in ASCII format, thus allowing the log to be translated for use in other applications.

Thylacine-1 core has already been described and discussed in detail by Peter Arditto of SedStrat Pty Ltd, and further in-depth discussion of the sedimentology is considered unnecessary. The text that follows therefore represents a summary of the main features observed.

Cored Interval

The following interval of core was recovered and described:

Core 1: 2165.00 m – 2200.56 m

Note: Description was carried out after full diameter samples had been removed from the core.

Sedimentology

Overview

The cored interval is believed to have been deposited in an estuarine-deltaic environment, and consists of a series of fine to very coarse grained sandstones interbedded with intervals of argillaceous heterolithics and very fine grained, laminated sandstone. The heterolithic intervals tend to be bioturbated (often intensely) while coarser grained sandstones are mostly barren of trace fossils. Very good to excellent visible porosity is exhibited by some of the coarse grained sandstone.

Lithofacies

A wide range of lithofacies were identified in the core (refer to Table 1 for comprehensive descriptions).

Sandstones can be subdivided into three main lithofacies:

- Cross-bedded, medium to very coarse grained sandstone (facies Sx)
- Ripple-laminated, fine grained sandstone (facies Sr)
- Horizontally-laminated, very fine to fine grained sandstone (facies Sl)

Facies Sx is interpreted to represent tidally reworked estuarine channel deposits. Facies Sr is thought to have formed as tidally reworked bars, possibly in slightly deeper water than facies Sx, either in a more distal, seaward position, or to the side of the main axis of channel deposition. Thin layers of very fine grained facies Sl represent storm sands deposited in a lower shoreface to proximal offshore environment.

The main argillaceous lithofacies are:

- Bioturbated heterolithics (facies Hb)
- Laminated heterolithics (facies Hl)
- Bioturbated claystone (facies Mb)

The bioturbated heterolithics (facies Hb) and claystone (facies Mb) exhibit intense bioturbation and mostly diverse trace fossil assemblages. These facies are therefore interpreted to represent relatively open, shallow marine deposits. They are interrupted by thin beds of laminated sandstone (facies Sl) that exhibit hummocky to swaly cross-stratification, and are considered to have formed as storm sands. The interbedded claystones and heterolithics are therefore thought to have formed during periods of fair-weather deposition.

Ichnofacies

Ichnofacies descriptions are provided in Table 2. A brief discussion is provided below:

Trace fossils are best developed in facies Hb and Mb. Bioturbation in these facies is generally intense with diverse ichnofauna (the *Planolites-Helminthopsis-Palaeophycus* Association; see Table 2), especially in facies Hb, which contains a wide range of both dwelling and grazing traces. This diversity suggests relatively unrestricted, open shallow marine conditions, possibly formed during periods of fair weather in a lower shoreface to offshore transition setting. Similar burrow types are observed in facies Mb, although grazing traces tend to dominate, indicating quieter, deeper water conditions consistent with a proximal offshore setting. The *Planolites-Helminthopsis-Palaeophycus* association is considered to be equivalent to the *Cruziana* ichnofacies (Pemberton et al, 1992).

The thin, laminated storm sands that are frequently associated with facies Hb and Mb exhibit common *Anconichnus*, *Palaeophycus* and *Ophiomorpha* traces. These traces are common features of storm deposits, and were formed by

colonisation of the tops of the sands by opportunistic burrowers shortly after deposition (Pemberton et al, 1992).

A few intensely bioturbated siltstone beds exhibit ichnofossil assemblages that are dominated by *Teichichnus* burrows (*Teichichnus* Association). Ichnofacies dominated by one burrow type are generally considered to reflect environmental restriction, possibly forming in brackish water environments. The *Teichichnus* Association may therefore indicate embayment.

Less bioturbated, laminated heterolithics usually exhibit a relatively sparse ichnofossil assemblage dominated by *Planolites* burrows (*Planolites* Association). The low diversity and low burrowing intensity of this ichnofacies suggest some form of environmental restriction (possibly due to brackish water) in combination with rapid sedimentation rate. Sedimentological structures – clay drapes, ripple and wave laminae – suggest the environment was likely to have been tidal.

Several fine grained sandstone beds exhibit intermittent zones of moderately intense *Palaeophycus* and possible *Macaronichnus* burrowing (*Palaeophycus* Association). This ichnofacies is considered to be equivalent to the *Skolithos* ichnofacies, and is thought to indicate an upper shoreface environment within the upper portions of tidally reworked estuarine bars.

Depositional Sequences and Surfaces

Deposition is interpreted to have been influenced by changes in relative sea level. Evidence for this is provided by the vertical succession of sediments, and by the presence of several important depositional surfaces.

The core can be subdivided into the following cycles:

1. 2200.56 – 2192.20 m

The lower half of this cycle consists of interbedded, bioturbated heterolithics and thin, very fine laminated sandstones of an interpreted storm-reworked offshore transition environment. These deposits are interrupted at 2194.5 m by an irregular, erosive surface that appears to have formed in a hardground. This surface is overlain by a series of fine to medium grained, tidally-influenced channels and tidal flats. The exact nature of the erosion surface is unclear, but it appears to represent a regressive surface, possibly caused by a minor reduction in sea-level.

The upper part of the cycle culminates at 2192.20 m in a medium to coarse grained sandstone that is truncated by a sharp, undulating surface. This surface is believed to represent a transgressive surface of erosion. It is overlain by a very argillaceous sandstone, containing chaotically arranged quartzose granules, which grades upwards into proximal offshore, bioturbated claystones.

2. 2192.20 m – 2169.00 m

The bioturbated, proximal offshore claystones at the base of this cycle give way at 2189.8 m to moderately bioturbated heterolithic beds of an interpreted offshore transition environment. These bioturbated heterolithics are overlain at 2188.6 m by a thick sequence of sandstones, locally interrupted by conglomerate beds and by clay drapes. This sequence of sandstones is interpreted to represent a series of stacked, tidally reworked estuarine channels and bars (see Plates 1A and 1B). The conglomerates represent high energy channel lags, while localised heterolithic beds (sandstone interbedded with clay drapes) represent tidal flats formed during periods of reduced sand influx.

The top of the cycle is marked by a 1 cm-thick layer of coarse grained sandstone (Plate 1C). This coarse layer is interpreted to represent a very thin, transgressive sand sheet, corresponding to a transgressive surface of erosion.

3. 2169.00 m – 2165.00 m

The basal half-metre of this interval consists of a series of thinly interbedded argillaceous sandstone, bioturbated claystone, laminated heterolithics and laminated sandstone. These deposits are thought to have formed during a period of transgression, marked by gradually increasing sea level, and culminating in a return to proximal offshore conditions. Maximum flooding is thought to have occurred within the bioturbated claystone at around 2168 m.

A sharp, erosive surface within the claystone at 2167.5 m is accompanied by a sudden change in ichnofossil assemblage, with the *Planolites-Helminthopsis-Palaeophycus* association giving way suddenly to the sparsely bioturbated *Planolites* association. This change in ichnofacies is very similar to the change seen at 2194.5 m (which is also related to an erosive surface), and is thought to be regressive, marking a shift from proximal offshore conditions to a more tidally-dominated setting.

Another surface that may have stratigraphic significance occurs at 2166.10 m. This surface is sharp and is overlain by a medium to coarse grained, heavily bioturbated sandstone. This sandstone represents a marked change in grain size (underlying sandstone layers are very fine to fine grained), but quickly grades upwards into argillaceous siltstone. The presence of rip-up clasts and chaotically arranged quartzose granules that appear to "float" within the sandstone's matrix indicate the deposit is likely to represent a transgressive lag. The surface at 2166.10 m is therefore thought to be a flooding surface.

Reservoir Quality

Reservoir quality is best developed in the cross-bedded facies (facies Sx). Visible porosity in this facies is very good to excellent, with unconfined profile permeability measurements commonly reaching several darcies (maximum profile permeability of 10 darcies was recorded in Sx sandstone at 2176.1 m). Clay-draped sandstone (facies Sd), ripple-laminated sandstone (Sr) and massive sandstone (Sm) show fair to good visible porosity. Profile permeability values in these facies mostly range from around 10 md to over 100 md.

Controls on Reservoir Quality

Within the sandstone facies, reservoir quality appears to be mainly controlled by grain size, with the coarsest grained sandstone generally showing the highest permeability. Cementation is rare, and is mainly confined to isolated pyrite nodules. However, a short interval of calcite-cemented sandstone occurs between 2170.2 and 2170.4 m, reducing visible porosity and profile permeability in this part of the core.

Diagenesis is also believed to have had an effect on reservoir quality. Most of the sandstone appears to have been partly cemented by quartz overgrowths, and possibly by authigenic kaolinite (whitish clay matrix is locally observed by hand lens). Detailed petrographic analysis (Thin Section, X-ray Diffraction and Scanning Electron Microscopy) would provide a more detailed understanding of both diagenetic and depositional controls on reservoir development.

Potential Production Problems

Most of the sandstone is moderately to strongly lithified; the potential for sand production is therefore thought to be low. Although several weakly consolidated zones exist, these zones occur in association with coring-induced fracturing and were probably weakened as a result of damage caused by coring.

The presence of whitish clay matrix within the fine grained ripple-laminated sandstone facies raises the possibility that fines migration might occur. In order to further investigate the potential for fines migration and other forms of fluid-rock interaction (such as clay swelling and acid sensitivity) detailed petrographic study would be required.

REFERENCE

Pemberton, S.G., Van Wagoner, J.C., and Wach, G.D., 1992, Ichnofacies of a wave-dominated shoreline, in Pemberton, S.G. (ed.), Applications of Ichnology to Petroleum Exploration, SEPM Core Workshop No. 17.

TABLE 1
DEPOSITIONAL LITHOFACIES DESCRIPTIONS

FACIES	DESCRIPTION	THICKNESS	DEPOSITIONAL ENVIRONMENT	RESERVOIR POTENTIAL
Sx	Cross-bedded to massive, lower medium to lower coarse, locally very coarse grained, poorly to moderately sorted sandstone. Decimetre scale planar to trough cross-bedding, locally showing current reversals and herringbone structure. Common rip-up clasts, occasional thin, very coarse grained graded laminae, minor clay drapes, carbonaceous layers. Generally barren of trace fossils. Associated with facies Sd.	Up to 2 m. Individual units approx. 20 cm to 0.5 m.	Very high energy, tidally reworked estuarine/deltaic channel. Herringbone structure indicates alternating current directions indicative of tides.	Variable. Fair to excellent visible porosity.
Sm	Massive, medium to coarse grained, moderately sorted sandstone with occasional clay drapes and rip-up clasts. Occasional decimetre scale planar to trough cross-bedding, bundled clay drapes. Barren of trace fossils. Associated with facies Sx and Sd.	Approx. 1 m.	High energy deposit. Tidally reworked estuarine/deltaic channel.	Good to very good visible porosity.
Sb	Intensely bioturbated, upper fine to lower medium grained sandstone. Burrows appear to be mainly *Planolites* and *Palaeophycus*.	Approx. 20 cm	Possible tidal sand flat. Minor facies, may relate to transgression that led to deposition of overlying bioturbated siltstone at top of core.	Poor. Interstitial clay reduces permeability.
Sd	Upper fine to lower medium grained, moderately well sorted sandstone with common clay drapes. Wave and current ripples observed in sandstone lenses between drapes. Clay rip-up clasts common. Sparsely bioturbated with *Planolites* burrows in clay drapes.	Up to 1 m.	Intermittent low to moderately high energy. Tidal sand flat or tidally reworked channel deposits.	Variable. Fair to good visible porosity.
Sl	Horizontally laminated, very fine to fine grained sandstone. Localised rip-up clasts, thin coaly and argillaceous laminae. Occasional water escape structures observed. Fine grained, thicker beds are usually unbioturbated, while thinner, very fine grained beds contain common *Anconichnus*, *Palaeophycus*, *Teichichnus*, and occasional *Ophiomorpha* and fugichnia (escape traces).	10 cm to 1 m.	Moderate energy. Thinner, very fine grained beds represent storm events. Thicker, fine grained beds may represent tidally reworked bars.	Mostly poor visible porosity.
Sr	Current-rippled, fine grained sandstone. Lamination ranges from horizontal to rippled. Ripples mainly formed by currents, locally showing climbing structure and current reversals. Oscillatory ripples noted locally. Also observed are thin clay drapes, layers of carbonaceous “coffee grounds”, occasional sideritised rip-up clasts, localised soft sediment deformation, graded laminae. Whitish clay matrix, possibly kaolinite, is observed locally.	Up to 3 m.	Moderate to high energy, tidally reworked estuarine bar. Probably deposited in deeper water than channel facies, possibly away from main channel axis. Climbing ripples and current reversals indicate strong tidal influence.	Fair visible porosity.

TABLE 1 (Continued)
DEPOSITIONAL LITHOFACIES DESCRIPTIONS

FACIES	DESCRIPTION	THICKNESS	DEPOSITIONAL ENVIRONMENT	RESERVOIR POTENTIAL
Gms & Gcs	Matrix-supported (Gms) and clast-supported (Gcs) conglomerate. Mainly consisting of sideritised claystone pebbles (large rip-up clasts) with common small quartzose pebbles and granules. Associated with Sx facies.	Less than 20 cm.	Estuarine channel lag.	Poor visible porosity.
Sarg	Very argillaceous, fine to medium grained sandstone to silty, sandy claystone. Moderately to poorly sorted. Heavily bioturbated (burrows include *Zoophycos*, *Planolites*, *Teichichnus* and localised *Thalassinoides*). Associated with Sm and Mb.	Less than 20 cm.	Transgressive sandstone/claystone. Generally occurs at top of sandstone cycles, or just above, and is overlain by bioturbated claystones (facies Mb).	Very poor visible porosity.
Hl & Ml	Sparsely bioturbated, laminated heterolithics (Hl) and claystone (Ml), consisting of thinly interbedded, very fine to fine sandstone and drape-like claystone or siltstone layers. Common starved ripples, current and wave ripples, occasional rip-up clasts. Bioturbation intensity varies from very low to moderate. Moderately bioturbated beds exhibit diverse trace fossil assemblage, including *Teichichnus*, *Planolites*, *Anconichnus*, *Rhizocorallium*, *Helminthopsis* and *Asterosoma*.	Successions up to 1 m. Individual sandstone lenses < 1cm to approx. 10 cm.	Low to moderate energy, tidally reworked deposits. Tidal mud and sand flats or tidally reworked interdistributary bay.	Generally poor, though individual sand lenses may show fair visible porosity.
Hb	Intensely bioturbated heterolithics, consisting of argillaceous sandstone to sandy, argillaceous siltstone. Interbedded with facies Sl, which locally shows swaly to hummocky cross-strat. Diverse ichnofauna include *Planolites*, *Palaeophycus*, *Teichichnus*, *Anconichnus* (in sandier layers), *Helminthopsis* (in argillaceous layers), occasional *Terebellina*, *Thalassinoides*, *Ophiomorpha*, *Siphonichnus*, Arenicolites, *Rhizocorallium*, *Asterosoma* and *Zoophycos*. Associated with facies Sl.	Successions up to 1.5 m.	Low energy shallow marine. Fair weather deposits of offshore transition to lower shoreface setting. Diverse trace fossil assemblage indicates Proximal *Cruziana* ichnofacies and relatively open marine conditions. Associated facies Sl represents storm sand deposition.	Poor visible porosity.
Mb	Intensely bioturbated, silty claystone with minor thin silty layers. Burrows include *Helminthopsis*/*Helminthoida*, *Planolites*, *Chondrites*, *Teichichnus*, *Zoophycos*, *Terebellina* and *Anconichnus*.	Up to 1.7 m.	Very low energy, proximal offshore muds. Diverse ichnofossil assemblage, dominated by grazing structures, is indicative of Distal *Cruziana* ichnofacies.	None.

TABLE 2
ICHNOFACIES DESCRIPTIONS

ICHNOFACIES	DESCRIPTION	DEPOSITIONAL ENVIRONMENT
Planolites-Helminthopsis-Palaeophycus Association	Ichnofacies characterised by intense bioturbation and diverse trace fossil assemblage. Mainly found in bioturbated mudstones and heterolithics (facies Hb and Mb) and interbedded laminated sandstones (facies Sl). Burrow types include *Planolites*, *Palaeophycus*, *Teichichnus*, *Anconichnus* (in sandier layers), *Helminthopsis* (in argillaceous layers), occasional *Terebellina*, *Thalassinoides*, *Ophiomorpha*, *Siphonichnus*, Arenicolites, *Rhizocorallium*, *Asterosoma* and *Zoophycos*.	Shallow marine fair-weather deposits with intermittent storm reworking. Equivalent to *Cruziana* ichnofacies. More argillaceous facies (Mb) contain higher incidence of dwelling burrows, indicating more distal, proximal offshore conditions than those of the heterolithics (Hb), which are interpreted to represent offshore transition to lower shoreface fair weather deposits.
Planolites Association	Characterised by sparse to moderate bioturbation, usually dominated by *Planolites* burrows. Generally occurs in laminated heterolithics (Hl) and claystone (Ml). Other burrow types include *Teichichnus*, *Planolites*, *Anconichnus*, *Rhizocorallium*, *Helminthopsis* and *Asterosoma*.	Tidal mud/sand flat or tidally reworked interdistributary bay. Equivalent to *Cruziana* ichnofacies, although low to moderate bioturbation intensity and reduced trace fossil diversity suggests either environmental restriction or rapid sedimentation rate.
Palaeophycus Association	Intermittent ichnofacies consisting of *Palaeophycus* and possible *Macaronichnus* burrows within sandstone. Confined to faintly but often moderately strongly bioturbated zones within fine grained, horizontally laminated to ripple laminated sandstones.	Upper shoreface, formed close to the surface of estuarine bars and shoals. Probably equivalent to *Skolithos* ichnofacies.
Teichichnus Association	Intensely bioturbated fabric within argillaceous siltstone, dominated by *Teichichnus* burrows. Other burrows include *Zoophycos*, *Rhizocorallium*, *Chondrites* and *Thalassinoides*.	Possible embayment. Dominance of *Teichichnus* indicates possible brackish water conditions.

DESCRIPTIONS OF SELECTED CORE PHOTOS

PLATE 1A
2175.06 m – 2175.42 m

Cross-Bedded Sandstone (Facies Sx) Overlying Laminated Heterolithics (Facies Hl)

The underlying heterolithics (facies Hl) consist of thinly interbedded sandstone layers and clay drapes (*Drapes*). Note the scoured erosion surface that marks the contact with overlying cross-bedded sandstone (facies Sx) at 2175.34 m (*Scour*). This particular unit of cross-bedded sandstone exhibits inverse grading at its base, coarsening up from upper medium grained to upper coarse grained by 2175.20 m. Note also the upwardly increasing dip angle of cross-bed laminae (*X-bed*) and the presence of rip-up clasts (*Rip-up*), which were probably derived from underlying clay drapes. Reservoir quality in Facies Sx is very good to excellent; profile permeability measurements at 2175.1 m and 2175.2 m returned values of 6710 md and 1960 md, respectively.

PLATE 1B
2170.31 m – 2170.68 m

Ripple-Laminated Sandstone (Facies Sr)

Fine grained, ripple-laminated sandstone is shown in this view. Sedimentary structures include wavy to planar, discontinuous horizontal lamination (*Pl Lam*) alternating with ripple lamination, some of which exhibits climbing structure (*CR*). Localised carbonaceous laminae (*Carb Lam*) and occasional pyrite nodules are also encountered (*Pyr*). Note the alternating lamination directions, indicative of tidal reworking.

PLATE 1C
2168.85 – 2169.23 m

Ripple Laminated Sandstone (Facies Sr) Overlain by Bioturbated Claystone (Facies Mb)

A layer of coarse grained sandstone marks the top of the ripple-laminated sandstone facies at 2169.01 m (*Lag*). This coarse grained layer is believed to have formed as a lag deposit, possibly in response to the transgression that led to deposition of the overlying claystone. Note the discontinuous carbonaceous lamination (*Carb*) and the clay-lined *Palaeophycus* burrow (*Pal*) in the sandstone. The overlying claystone (dark colouration) contains thin, bioturbated silty laminae and occasional quartzose granules (*Gran*). The presence of granules and very coarse sand within the claystone indicates probable transgressive reworking.

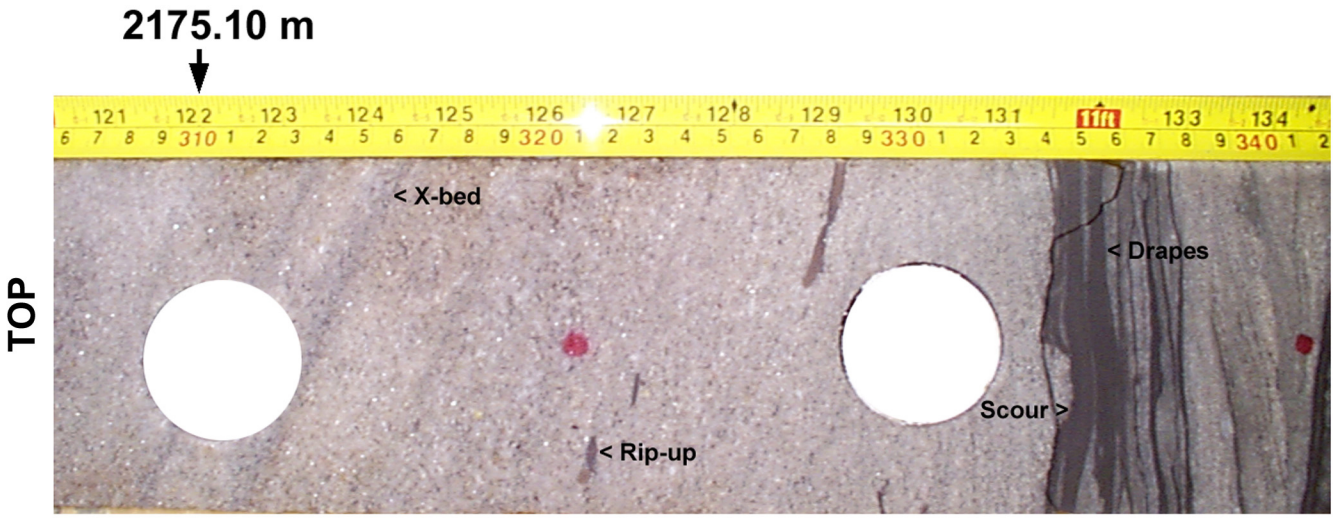

PLATE 1A

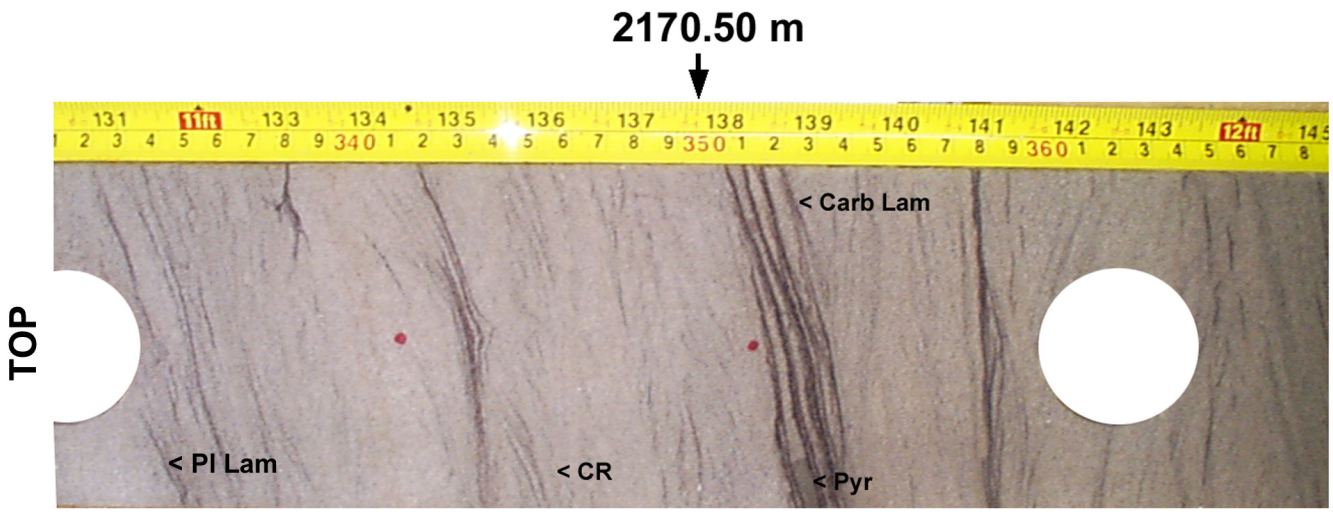

PLATE 1B

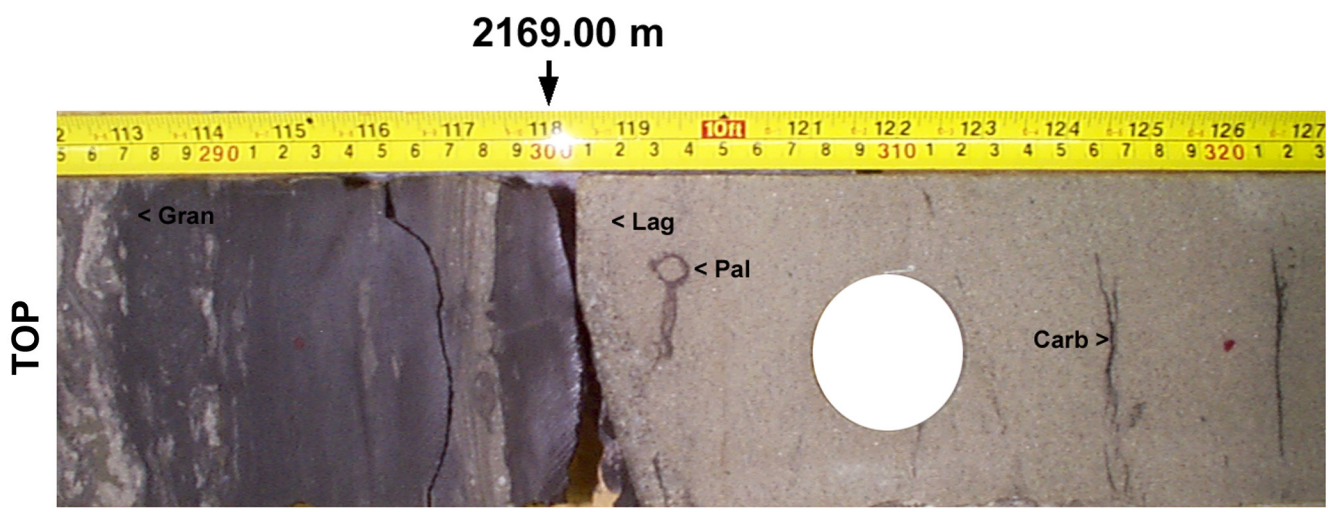

PLATE 1C

THYLACINE-1
WOODSIDE ENERGY LTD

Date logged: June 8, 2001
Logged by: Duncan Blair
Ground: 0.00 m KB: 0.00 m
Remarks: ICHNOFACIES IN FACIES ASSOCIATION COLUMN

SCALE 1:40

LEGEND

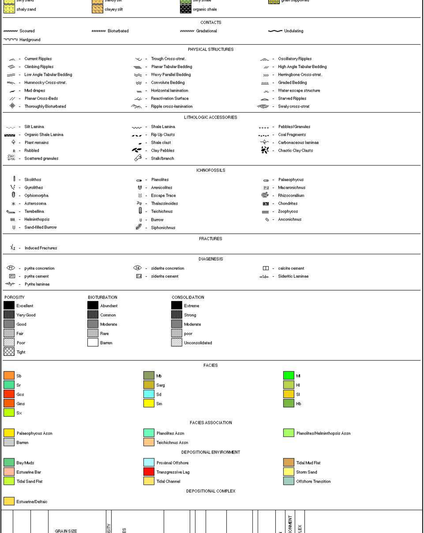

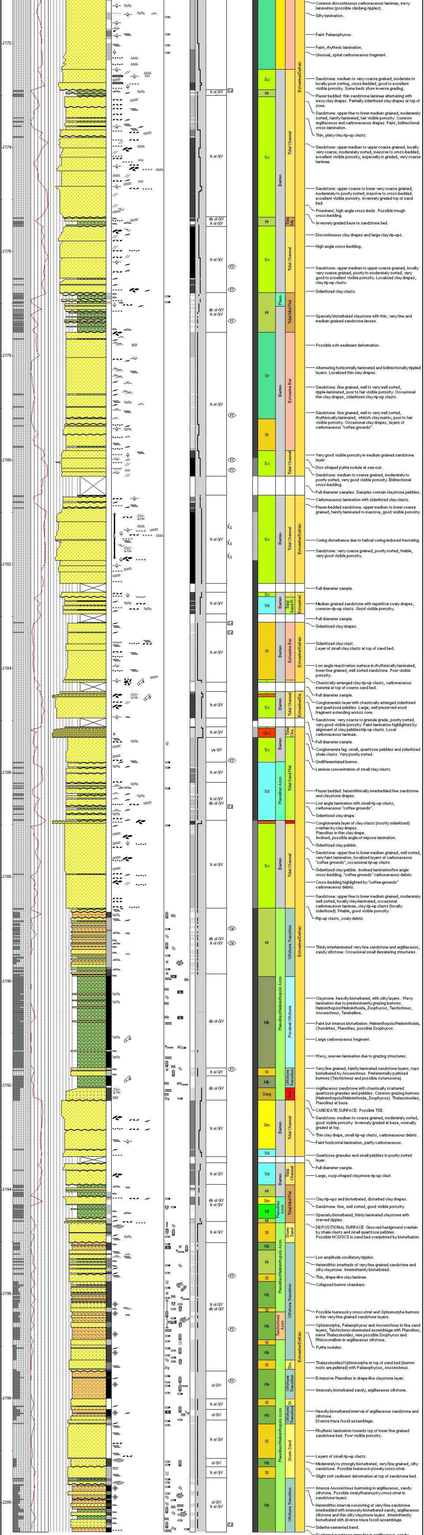

APPENDIX 9
SPECIAL CORE ANALYSIS

A Special Core Analysis Study Of Selected Samples From Well : THYLACINE - 1

Australia

Prepared for
WOODSIDE ENERGY LIMITED

September 2002

File: PRP-01025A

Rock Properties
Core Laboratories Australia Pty. Ltd.
Perth
Australia

9th September, 2002

WOODSIDE ENERGY LIMITED.
1 Adelaide Terrace
PERTH, Western Australia, 6000

Attention : Mr. Jon Kelly

Subject: Special Core Analysis.
Well : Thylacine - 1
File : PRP-01025A

Dear Jon,

Presented here are the final results of the special core analyses conducted on the selected core and sidewall (MSCT) samples from the well Thylacine – 1.

Thank you for the opportunity to have been of service to Woodside Energy Limited. If you have any questions regarding these results or if we can be of any further assistance please do not hesitate to contact us.

Yours sincerely,
CORE LABORATORIES

Ajit Singh
Supervisor - Rock Properties Perth

CONTENTS

SECTION 1
INTRODUCTION & SUMMARY

INTRODUCTION

This report contains the final results of the Special Core Analysis (SCAL) study performed on selected samples, core plugs and sidewall cores (MSCT) taken from the well Thylacine - 1. This study was initiated by Mr Jon Kelly of Woodside.

The test programme involved :

- Selection and visual inspection of samples for the study
- CT-scanning of selected samples
- Measurement / re-measurement of porosity, permeability, and grain density values
- Formation resistivity factor (FRF) analysis
- Formation resistivity index (RI) analysis
- Air-brine drainage capillary pressure by centrifuge
- Water-gas relative permeability by centrifuge
- Rock (pore volume) compressibility
- Additional core plugs drilled for mechanical strength tests (samples sent to CSIRO for rock strength analysis)

Thirteen core plug samples and five MSCT samples which had previously undergone routine core analysis constituted the original SCAL sample selection for electrical, capillary pressure and relative permeability analyses. Four additional duplicate samples were drilled from the core for rock (pore volume) compressibility tests (suffix “A”).

Four selected core plug samples were found to be unsuitable for analysis upon visual inspection and substitutes were subsequently re-selected. All samples then underwent CT-scanning to screen out any samples which exhibited heterogeneity. Each sample passed this phase of the screening procedure. A full list of samples which both finally underwent analysis and also which failed initial screening are listed in this SECTION 1 of this report. Please also refer to the routine core analysis report issued for this well (PRP-01025 September 2001).

A simulated formation brine of 13,500 ppm comprising 80% NaCl and 20% KCl was used during the SCAL studies conducted at Core Laboratories.

An additional eight samples were later drilled for mechanical strength tests and sent to CSIRO (see Appendix 2).

Trim ends and sample remnants for the thirteen samples which underwent electrical, capillary pressure and relative permeability tests were despatched to Julian Baker at Reservoir Solutions Limited for a petrographic study.

SUMMARY OF RESULTS

Electrical Properties

Cementation exponent “m” values, measured at net overburden pressure (NOBP), ranged between 1.79 to 2.01. The average “m” was 1.88. CEC corrected values of “m*” ranged between 1.93 and 2.34 with an average “m*” of 2.10. Resistivity index analysis yielded sample average saturation exponent “n” values ranging between 1.46 to 2.38. The average “n” was 1.97. CEC corrected values of “n*” ranged between 2.03 to 2.78 with an average “n*” of 2.36.

Cation exchange capacity (CEC) analyses were performed on all 13 core plug trim-ends and the MSCT samples by the wet chemistry method on crushed sample. The recorded CEC values ranged from 0.97 to 8.42 meq/100gm. For comparison purposes, CEC analysis was performed using the wet chemistry method on uncrushed sample-split trim-ends of 3 core plug samples. These data were compared to CEC data generated on crushed sample-split trim-ends from the same 3 core plugs and found to be fairly similar. The conclusion was, therefore, that crushing the samples did not lead to excessively high CEC values.

Capillary Pressure

Samples tested ranged from 0.483 md to 4710 md air permeability (Kair at ambient). At the maximum air-brine capillary pressure, the selected samples yielded immobile water saturation (Swi) values between 9.1 and 38.8 percent pore volume (% PV). For most samples the requested maximum air-brine capillary pressure of 200 psi was attained. Due to shorter sample lengths, the maximum attainable capillary pressure for samples #24, #28 and #46 was 100 psi, with the 200 psi point being extrapolated using the Table-Curve programme. The data indicate a strong trend of immobile water saturation as a function of air permeability.

The MSCT samples were exposed to the maximum air-brine capillary pressure of 500 psi.

Air-brine capillary pressure measurements were repeated for six samples using an overburden centrifuge at 1910 psi. Up to the maximum attainable air-brine capillary pressure of 100 psi, the six samples yielded very similar values of water saturation to those recorded at ambient (zero) overburden pressure. The comparison therefore indicated that the ambient capillary pressure data do not need to be adjusted for the effects of overburden pressure – as one would expect for well-indurated samples.

Relative permeability analyses.

Water-gas relative permeability analysis (end-point) by centrifuge were conducted on all thirteen core plug samples following the air-brine capillary pressure analyses. Residual gas saturations from centrifuge water-gas relative permeability (representing a reservoir displacement mechanism dominated by capillary / gravity forces) ranged from 3.5% to 14.9%.

Although traditional comparative parameters such as Kair versus Sgr and Sgi versus Sgr do not exhibit strong trends, Kair versus gas recovery % pore volume does indicate a good trend. This plot is included in SECTION 4.

Rock (pore volume) compressibility.

Rock (pore volume) compressibility tests conducted on 4 samples indicated compressibility (uniaxial loading) values ranging from 2.40 X 10^{-6} to 6.28 X 10^{-6} pv/pv/psi at the maximum confining stress of 3,800 psi. As would be expected, the higher the porosity and permeability values of the samples, the larger the degree of compressibility exhibited through the range of pressure utilised in the tests.

COMPANY : WOODSIDE ENERGY LIMITED
WELL : THYLACINE - 1

POROSITY, PERMEABILITY AND GRAIN DENSITY
(Ambient & Overburden)

SAMPLE NUMBER	DEPTH (m)	Ambient			NOB PRESSURE				GRAIN DENSITY (g/cc)	Screening Pass/Fail (P/F)	
		PERMEABILITY		POROSITY (%)	NOBP (psi)	PERMEABILITY		POROSITY (%)		Visual	CT
		Kinf (md)	Kair (md)			Kinf (md)	Kair (md)				
MSCT-2	2053.00	15.2	17.4	20.3	1700	14.3	16.5	19.3	2.668	P	P
MSCT-3	2055.00	11.6	13.5	19.9	1700	11.0	12.7	19.3	2.677	P	P
MSCT-6	2092.20	36.5	42.8	23.2	1760	34.5	40.7	22.5	2.672	P	P
MSCT-7	2094.00	11.1	12.9	21.1	1760	10.5	12.2	20.5	2.769	P	P
MSCT-10	2143.60	22.0	24.9	20.8	1840	20.8	23.4	20.3	2.654	P	P
5	2166.81	5.41	6.66	17.8	1910	4.65	5.75	17.3	2.643	P	P
14	2171.19	93.3	99.5	21.8	1910	88.8	94.7	21.4	2.664	P	P
14A	2171.24	42.7	46.5	19.9	1910	*	*	*	2.665	P	P
22	2173.40	0.351	0.483	11.7	1910	0.188	0.298	11.3	2.689	P	P
22A	2173.34	0.111	0.198	10.4	1910	*	*	*	2.691	P	P
24	2173.83	1060	1240	18.5	1910	995	1150	18.0	2.657	P	P
25	2174.10	2.65	3.27	13.2	1910	2.14	2.67	12.8	2.675	P	P
26	2174.36	19.6	22.5	16.6	1910	17.8	20.4	16.2	2.701	F-replaced by #55	NA
28	2174.80	2910	3430	20.9	1910	2570	3170	20.2	2.653	P	P
46	2180.10	4670	4710	23.2	1910	3370	3980	22.5	2.648	P	P
46A	2180.14	2230	2650	22.7	1910	*	*	*	2.652	P	P
49	2181.02	5240	7500	23.7	1910	3590	5380	21.5	2.650	F-replaced by #46	NA
54	2182.74	33.2	37.4	16.5	1910	27.1	30.7	16.0	2.670	F-replaced by #26	NA
55	2182.92	82.3	109	17.7	1910	73.6	97.2	17.1	2.659	P	P
60	2184.20	0.179	0.295	12.7	1910	0.110	0.193	12.2	2.685	F-replaced by #22	NA

POROSITY, PERMEABILITY AND GRAIN DENSITY
(Ambient & Overburden)

SAMPLE NUMBER	DEPTH (m)	Ambient			NOB PRESSURE				GRAIN DENSITY (g/cc)	Screening Pass/Fail (P/F)	
		PERMEABILITY		POROSITY (%)	NOBP (psi)	PERMEABILITY		POROSITY (%)			
		Kinf (md)	Kair (md)			Kinf (md)	Kair (md)			Visual	CT
62	2184.89	105	127	15.2	1910	92.8	111	14.6	2.648	P	P
62A	2184.76	163	192	12.4	1910	*	*	*	2.655	P	P
67	2186.60	1.50	1.93	17.0	1910	1.25	1.62	16.4	2.745	P	P
69	2187.10	19.6	22.1	20.1	1910	17.7	20.0	19.6	2.676	P	P
80	2192.71	515	524	21.1	1910	491	500	20.7	2.658	P	P
83	2193.59	240	251	18.4	1910	227	237	18.0	2.656	P	P

* Permeability and porosity at NOBP not measured on samples scheduled for rock compressibility tests.

NOTES

1. All selected samples with the exception of the 4 samples with "A" suffix, had previously undergone routine core analysis measurements.
2. The 4 samples with "A" suffix, drilled on 3/12/2001, were selected for rock (pore volume) compressibility tests.
3. Trimmed ends of all SCAL-selected samples (13 nos), with the exception of the "A" suffixed samples were sent to Reservoir Solutions Limited (Julian Baker) on

SECTION 2
ELECTRICAL PROPERTIES

Formation resistivity factor (FRF) at net overburden pressure (NOBP)

Sample no.	Depth (metres)	Grain Density gm/cc	CEC meq/100gm	K air (md)	AT NOBP					
					NOBP (psi)	Porosity (%)	FRF	FRF *	m	m*
MSCT2	2053.00	2.668	4.84	16.5	1700	19.3	21.46	37.01	1.86	2.20
MSCT3	2055.00	2.677	5.77	12.7	1700	19.3	22.67	42.34	1.90	2.28
MSCT7	2094.00	2.769	3.56	12.2	1760	20.5	20.25	30.66	1.90	2.16
MSCT10	2143.60	2.654	2.38	23.4	1840	20.3	17.80	23.72	1.81	1.99
5	2166.81	2.643	5.38	5.75	1910	17.3	29.29	51.40	1.92	2.25
14	2171.19	2.664	4.01	94.7	1910	21.4	17.70	25.40	1.86	2.10
22	2173.40	2.689	8.42	0.298	1910	11.3	55.55	165.08	1.84	2.34
24	2173.83	2.657	3.13 (1.47*)	1150	1910	18.0	25.43	30.45	1.89	1.99
25	2174.10	2.675	2.57	2.67	1910	12.8	42.58	64.73	1.82	2.03
28	2174.80	2.653	0.97	3170	1910	20.2	20.92	23.28	1.90	1.97
46	2180.10	2.648	1.48	3980	1910	22.5	15.51	17.82	1.84	1.93
55	2182.92	2.659	3.72 (3.66*)	97.2	1910	17.1	28.61	43.83	1.90	2.14
62	2184.89	2.648	3.14	111	1910	14.6	31.02	47.73	1.79	2.00
67	2186.60	2.745	4.01 (4.72*)	1.62	1910	16.4	25.55	41.45	1.79	2.06
69	2187.10	2.676	2.60	20.0	1910	19.6	24.33	31.99	1.96	2.13
80	2192.71	2.658	1.55	500	1910	20.7	23.57	27.72	2.01	2.11
83	2193.59	2.656	2.34	237	1910	18.0	25.61	33.64	1.89	2.05
							Average Cementation Exponent **		**1.88**	**2.10**

* CEC measured on uncrushed sample.

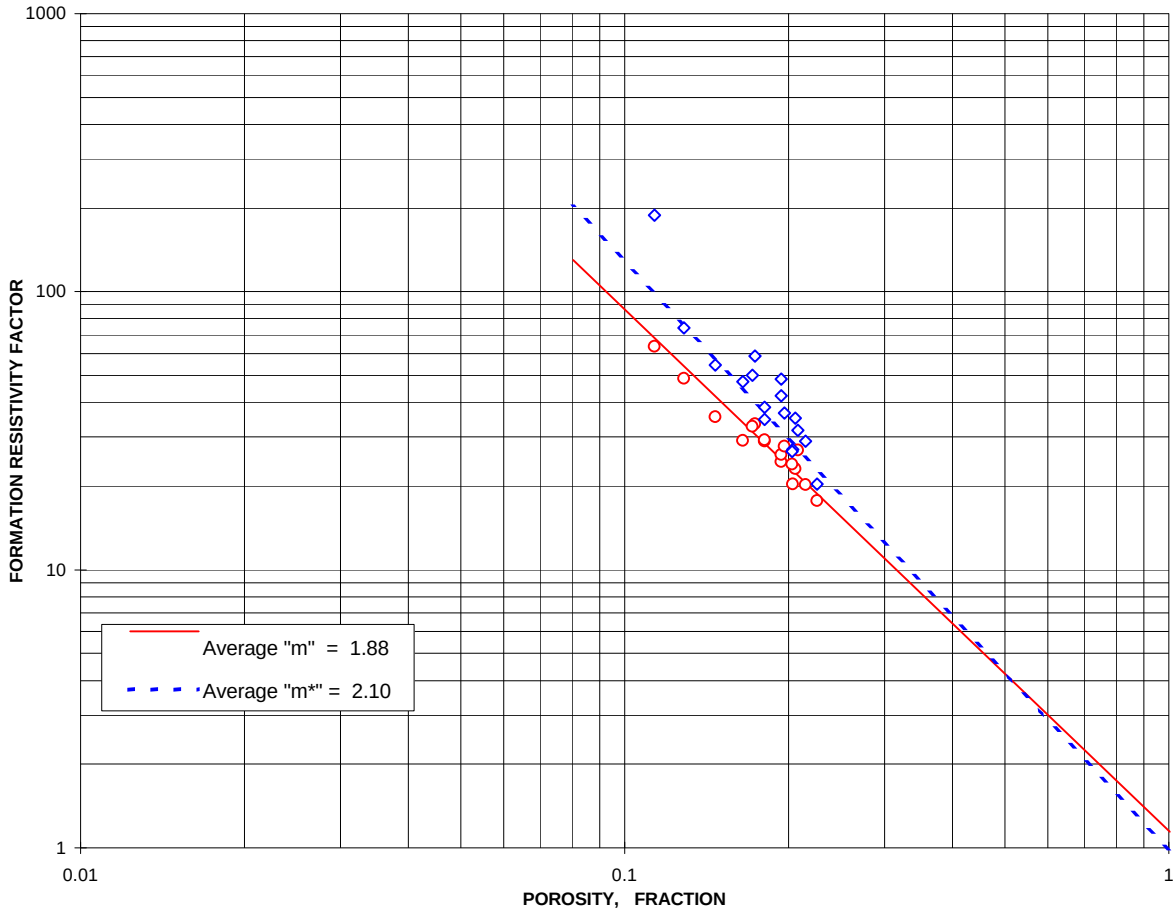

Composite Graph - Formation Resistivity Index at NOBP.

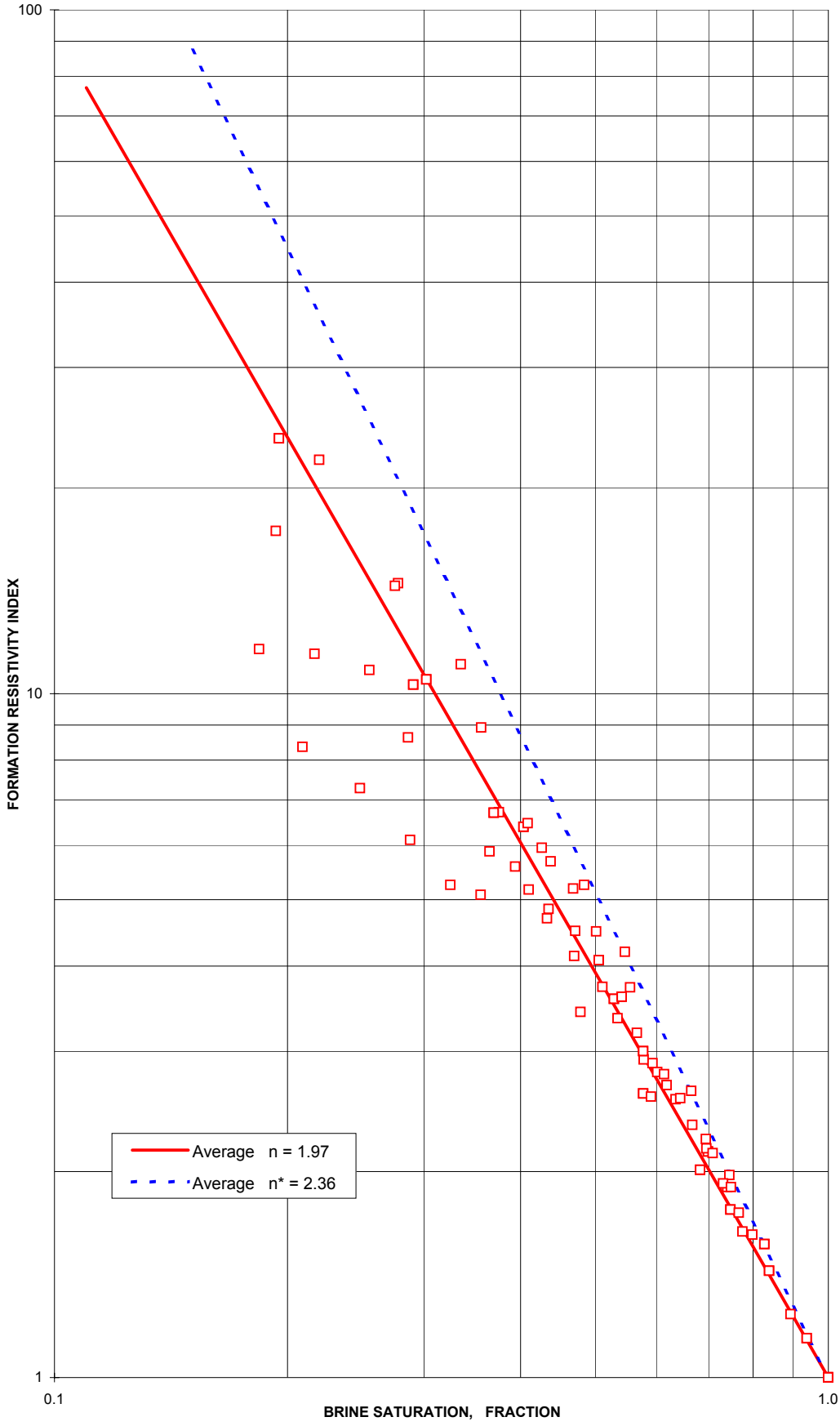

Formation resistivity index at NOBP - Composite Table.

(with simulated formation brine)

Sample no.	Depth (metres)	Grain density (gm/cc)	Determined at NOBP						
			NOBP (psi)	Perm. to air (md)	Porosity (%)	Brine saturation (%pv)	Resistivity index	Sat. Exp. n	Corrected Sat. Exp. n *
MSCT2	2053.00	2.668	1700	16.5	19.3	100.0	1.00	-	-
						60.1	2.80	2.02	2.50
						47.9	3.42	1.67	2.18
						35.6	5.08	1.57	2.12
						32.5	5.25	1.48	2.03
						28.8	6.11	1.46	2.03
						18.4	11.62	1.45	2.07
MSCT3	2055.00	2.677	1700	12.7	19.3	100.0	1.00	-	-
						56.6	3.19	2.04	2.57
						41.1	5.17	1.85	2.42
						28.6	8.62	1.72	2.34
						25.5	10.82	1.74	2.37
						19.3	17.30	1.73	2.39
MSCT7	2094.00	2.769	1760	12.2	20.5	100.0	1.00	-	-
						54.6	4.19	2.37	2.78
						48.4	5.25	2.28	2.71
						42.7	5.95	2.09	2.54
						37.6	6.70	1.94	2.40
						21.7	11.44	1.59	2.12
MSCT10	2143.60	2.654	1840	23.4	20.3	100.0	1.00	-	-
						66.6	2.62	2.37	2.66
						55.5	3.72	2.23	2.54
						47.1	4.49	2.00	2.32
						24.8	7.27	1.42	1.83
						20.9	8.35	1.36	1.78
5	2166.81	2.643	1910	5.75	17.3	100.0	1.00	-	-
						74.5	1.98	2.32	2.78
						69.5	2.23	2.21	2.68
						66.7	2.34	2.10	2.58
						57.8	2.91	1.95	2.45
						51.1	3.72	1.96	2.47
						39.4	5.58	1.85	2.39
14	2171.19	2.664	1910	94.7	21.4	100.0	1.00	-	-
						70.0	2.14	2.13	2.47
						57.6	3.00	1.99	2.36
						50.6	4.08	2.06	2.44
						40.4	6.38	2.04	2.45
						30.3	10.48	1.97	2.41
22	2173.40	2.689	1910	0.298	11.3	100.0	1.00	-	-
						93.8	1.14	2.06	2.73
						83.9	1.43	2.04	2.72
						74.8	1.76	1.95	2.64
						68.3	2.01	1.83	2.54
						57.6	2.60	1.73	2.46

Formation resistivity index at NOBP - Composite Table.

(with simulated formation brine)

Sample no.	Depth (metres)	Grain density (gm/cc)	Determined at NOBP						
			NOBP (psi)	Perm. to air (md)	Porosity (%)	Brine saturation (%pv)	Resistivity index	Sat. Exp. n	Corrected Sat. Exp. n *
24	2173.83	2.657	1910	1150	18.0	100.0	1.00	-	-
						82.8	1.57	2.38	2.56
						61.8	2.68	2.05	2.25
						52.8	3.58	2.00	2.21
						37.0	6.70	1.91	2.16
						29.1	10.31	1.89	2.16
						19.5	23.63	1.94	2.25
25	2174.10	2.675	1910	2.67	12.8	100.0	1.00	-	-
						89.4	1.24	1.91	2.26
						76.7	1.74	2.09	2.46
						69.6	2.16	2.13	2.52
						59.0	2.57	1.79	2.20
						54.1	3.60	2.08	2.50
28	2174.80	2.653	1910	3170	20.2	100.0	1.00	-	-
						74.1	1.90	2.14	2.25
						63.5	2.55	2.06	2.19
						46.8	5.19	2.17	2.31
						40.9	6.46	2.09	2.24
						19.3	30.07	2.07	2.29
46	2180.10	2.648	1910	3980	22.5	100.0	1.00	-	-
						67.3	2.55	2.37	2.52
						51.0	3.51	1.86	2.04
						31.4	11.46	2.10	2.32
						18.3	28.55	1.97	2.24
						13.8	47.74	1.96	2.26
55	2182.92	2.659	1910	97.2	17.1	100.0	1.00	-	-
						73.1	1.92	2.09	2.47
						64.4	2.56	2.14	2.53
						53.4	3.35	1.93	2.35
						43.6	4.84	1.90	2.34
						32.1	7.64	1.79	2.27
62	2184.89	2.648	1910	111	14.6	100.0	1.00	-	-
						73.9	2.00	2.30	2.68
						55.4	3.49	2.12	2.54
						49.0	4.04	1.95	2.39
						41.6	6.54	2.14	2.60
						24.0	16.27	1.96	2.48
67	2186.60	2.745	1910	1.62	16.4	100.0	1.00	-	-
						80.9	1.42	1.66	2.07
						73.9	1.75	1.84	2.26
						67.4	1.91	1.64	2.07
						61.0	2.29	1.67	2.12
						53.3	2.78	1.62	2.09

Formation resistivity index at NOBP - Composite Table.

(with simulated formation brine)

Sample no.	Depth (metres)	Grain density (gm/cc)	Determined at NOBP						
			NOBP (psi)	Perm. to air (md)	Porosity (%)	Brine saturation (%pv)	Resistivity index	Sat. Exp. n	Corrected Sat. Exp. n *
69	2187.10	2.676	1910	20.0	19.6	100.0	1.00	-	-
						77.5	1.63	1.93	2.19
						59.3	2.88	2.02	2.32
						47.0	4.13	1.88	2.20
						43.3	4.69	1.85	2.17
						36.5	5.87	1.76	2.10
80	2192.71	2.658	1910	500	20.7	100.0	1.00	-	-
						74.8	1.90	2.21	2.38
						61.3	2.77	2.09	2.27
						50.2	4.49	2.18	2.38
						35.6	8.92	2.12	2.35
						27.8	14.49	2.09	2.34
						22.0	21.97	2.04	2.32
83	2193.59	2.656	1910	237	18.0	100.0	1.00	-	-
						79.8	1.62	2.13	2.39
						70.9	2.13	2.20	2.47
						43.8	5.69	2.11	2.43
						33.5	11.03	2.20	2.55
						27.6	14.37	2.07	2.45
						Average Exponent		1.97	2.36

Formation resistivity index at 1700 psi NOBP.

(with simulated formation brine)

Sample no.	Depth (metres)	Grain density (gm/cc)	Determined at 1700 psi NOBP					
			Perm. to air (md)	Porosity (%)	Brine saturation (%pv)	Resistivity index	Sat. Exp. n	Corrected Sat. Exp. n *
MSCT2	2053.00	2.668	16.5	19.3	100.0	1.00	-	-
					60.1	2.80	2.02	2.50
					47.9	3.42	1.67	2.18
					35.6	5.08	1.57	2.12
					32.5	5.25	1.48	2.03
					28.8	6.11	1.46	2.03
					18.4	11.62	1.45	2.07
					Average Exponent		1.61	2.16

FRF at NOBP	21.46
CEC (meq / 100gm)	4.84
FRF * at NOBP	37.01
Rw at 25°C, ohm-m	0.4150

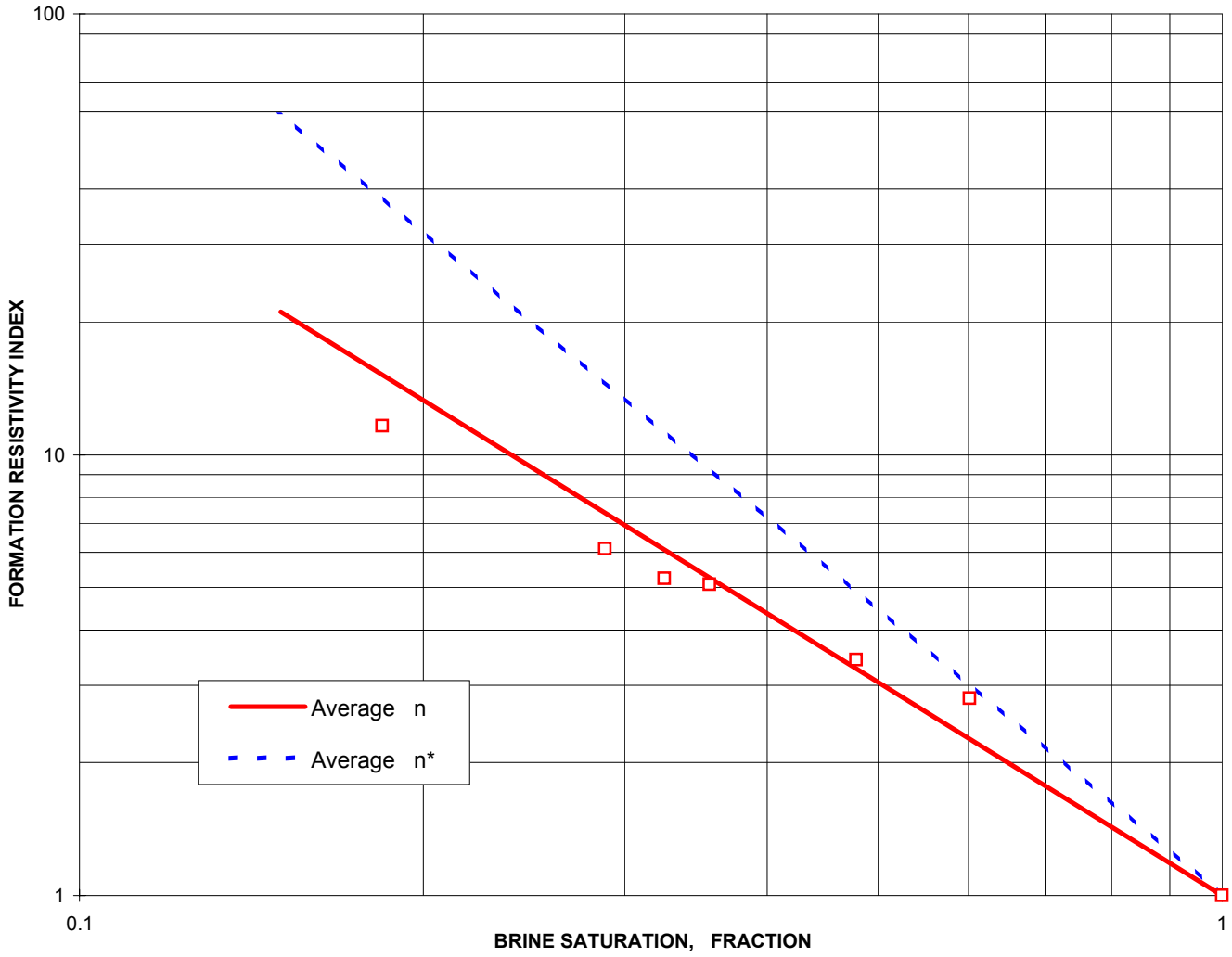

(with simulated formation brine)

Sample no.	Depth (metres)	Grain density (gm/cc)	Determined at 1700 psi NOBP					
			Perm. to air (md)	Porosity (%)	Brine saturation (%pv)	Resistivity index	Sat. Exp. n	Corrected Sat. Exp. n *
MSCT3	2055.00	2.677	12.7	19.3	100.0	1.00	-	-
					56.6	3.19	2.04	2.57
					41.1	5.17	1.85	2.42
					28.6	8.62	1.72	2.34
					25.5	10.82	1.74	2.37
					19.3	17.30	1.73	2.39
					Average Exponent		1.82	2.42

FRF at NOBP	22.67
CEC (meq / 100gm)	5.77
FRF * at NOBP	42.34
Rw at 25°C, ohm-m	0.4150

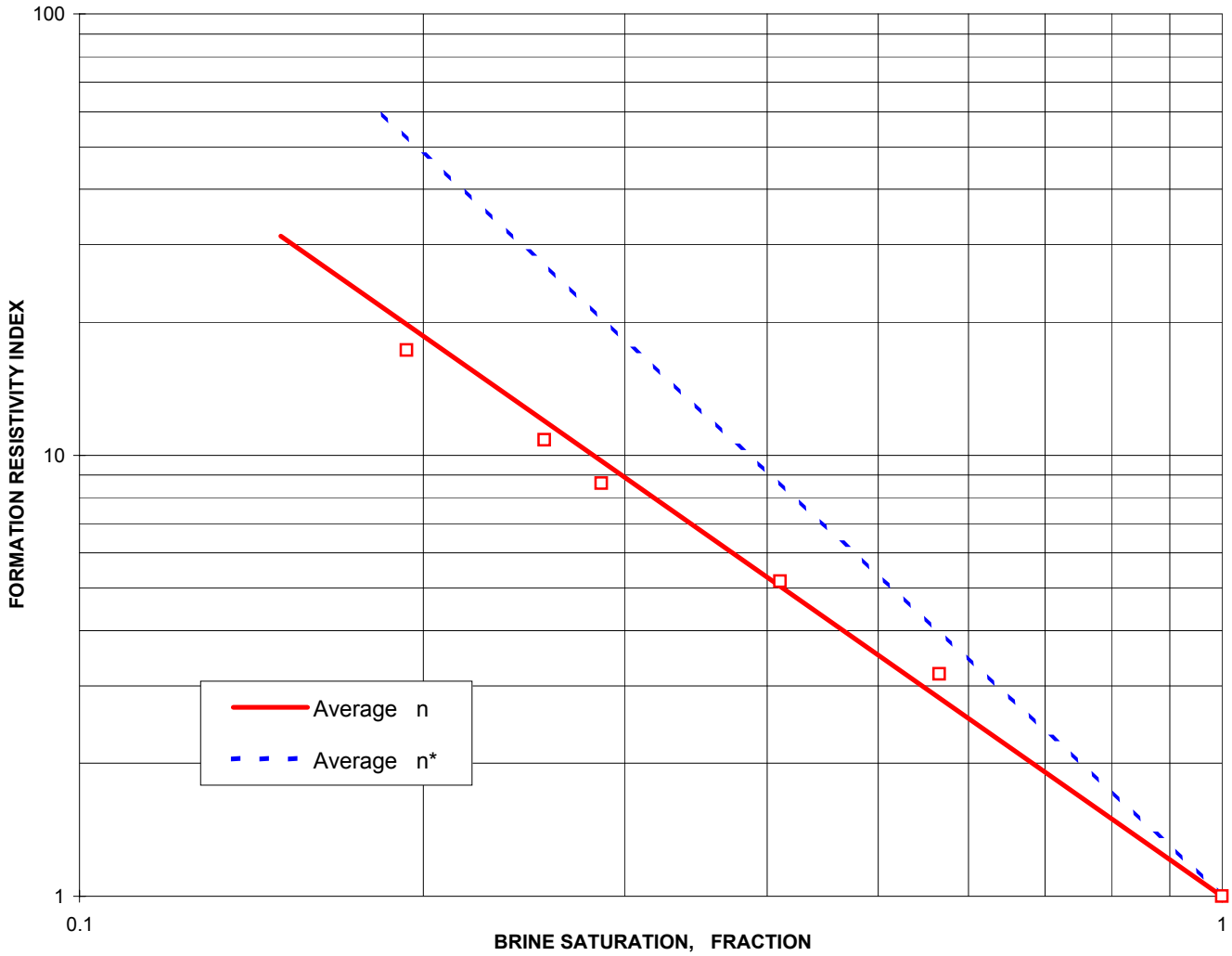

(with simulated formation brine)

Sample no.	Depth (metres)	Grain density (gm/cc)	Determined at 1760 psi NOBP					
			Perm. to air (md)	Porosity (%)	Brine saturation (%pv)	Resistivity index	Sat. Exp. n	Corrected Sat. Exp. n *
MSCT7	2094.00	2.769	12.2	20.5	100.0	1.00	-	-
					54.6	4.19	2.37	2.78
					48.4	5.25	2.28	2.71
					42.7	5.95	2.09	2.54
					37.6	6.70	1.94	2.40
					21.7	11.44	1.59	2.12
					Average Exponent		2.06	2.51

FRF at NOBP	20.25
CEC (meq / 100gm)	3.56
FRF * at NOBP	30.66
Rw at 25°C, ohm-m	0.4150

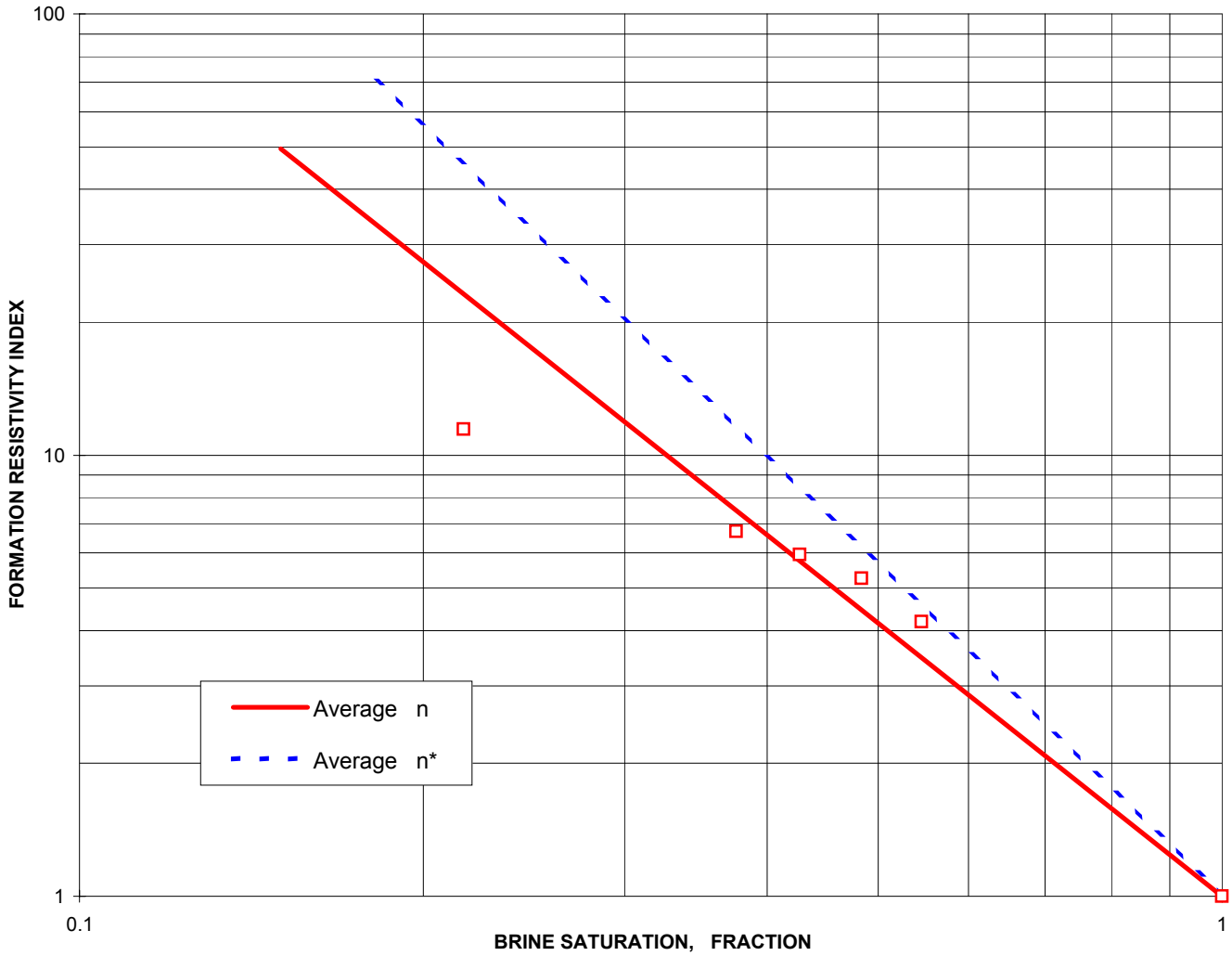

(with simulated formation brine)

Sample no.	Depth (metres)	Grain density (gm/cc)	Determined at 1840 psi NOBP					
			Perm. to air (md)	Porosity (%)	Brine saturation (%pv)	Resistivity index	Sat. Exp. n	Corrected Sat. Exp. n *
MSCT10	2143.60	2.654	23.4	20.3	100.0	1.00	-	-
					66.6	2.62	2.37	2.66
					55.5	3.72	2.23	2.54
					47.1	4.49	2.00	2.32
					24.8	7.27	1.42	1.83
					20.9	8.35	1.36	1.78
					Average Exponent		1.88	2.23

FRF at NOBP	17.80
CEC (meq / 100gm)	2.38
FRF * at NOBP	23.72
Rw at 25°C, ohm-m	0.4150

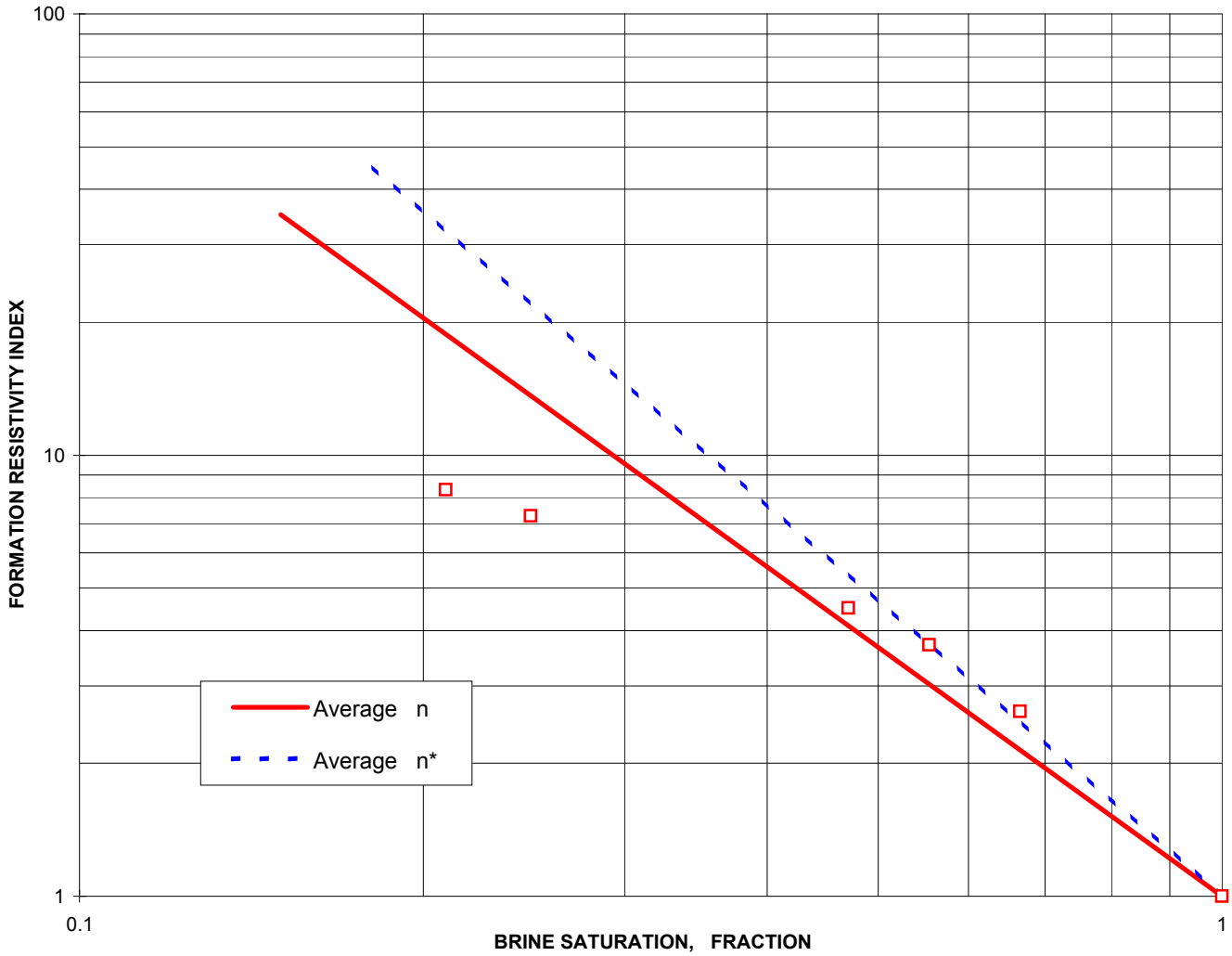

Formation resistivity index at 1910 psi NOBP.

(with simulated formation brine)

Sample no.	Depth (metres)	Grain density (gm/cc)	Determined at 1910 psi NOBP					
			Perm. to air (md)	Porosity (%)	Brine saturation (%pv)	Resistivity index	Sat. Exp. n	Corrected Sat. Exp. n *
5	2166.81	2.643	5.75	17.3	100.0	1.00	-	-
					74.5	1.98	2.32	2.78
					69.5	2.23	2.21	2.68
					66.7	2.34	2.10	2.58
					57.8	2.91	1.95	2.45
					51.1	3.72	1.96	2.47
					39.4	5.58	1.85	2.39
					Average Exponent		2.06	2.56

FRF at NOBP	29.29
CEC (meq / 100gm)	5.38
FRF * at NOBP	51.40
Rw at 25°C, ohm-m	0.4150

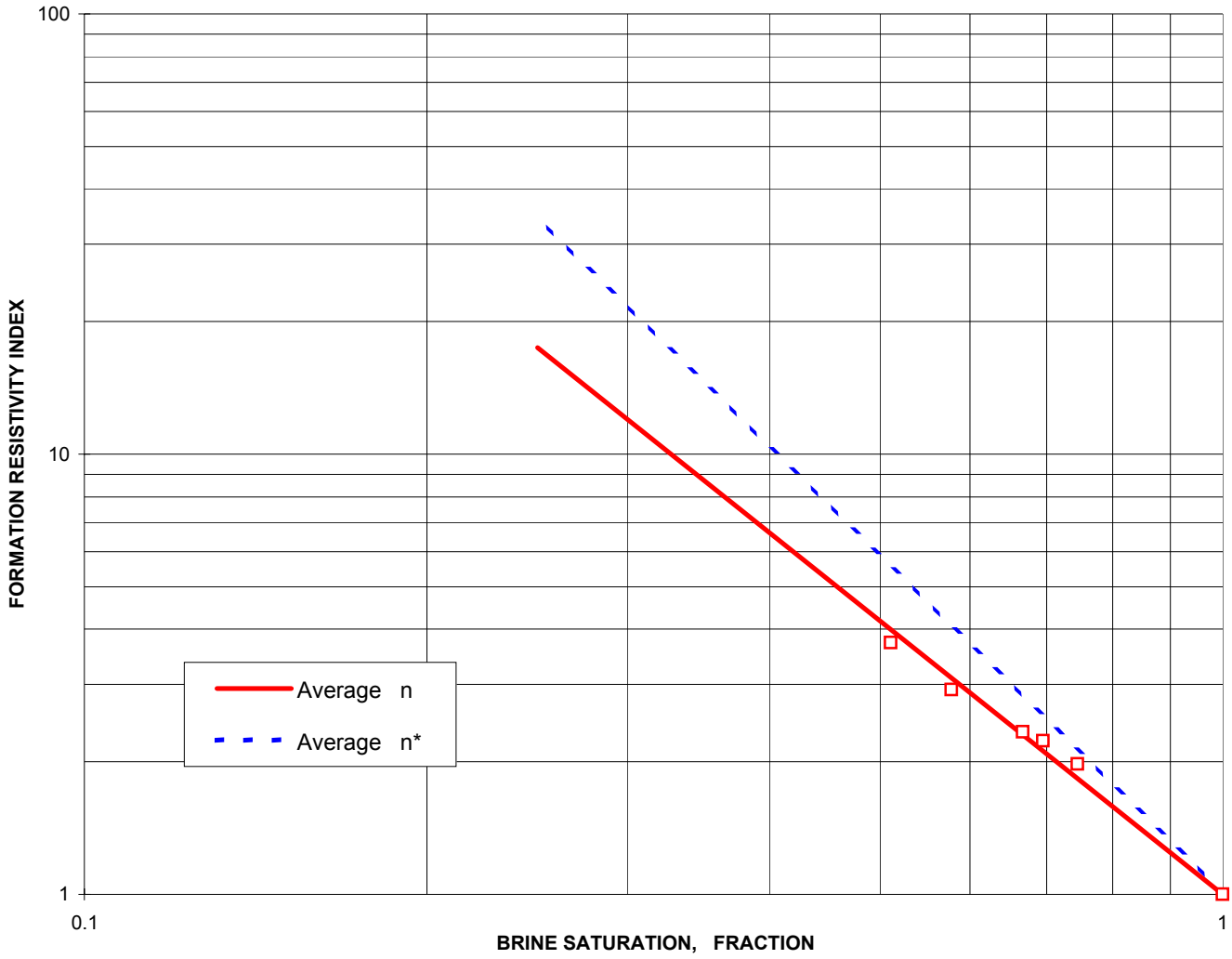

Formation resistivity index at 1910 psi NOBP.

(with simulated formation brine)

Sample no.	Depth (metres)	Grain density (gm/cc)	Determined at 1910 psi NOBP					
			Perm. to air (md)	Porosity (%)	Brine saturation (%pv)	Resistivity index	Sat. Exp. n	Corrected Sat. Exp. n *
14	2171.19	2.664	94.7	21.4	100.0	1.00	-	-
					70.0	2.14	2.13	2.47
					57.6	3.00	1.99	2.36
					50.6	4.08	2.06	2.44
					40.4	6.38	2.04	2.45
					30.3	10.48	1.97	2.41
					Average Exponent		2.04	2.43

FRF at NOBP	17.70
CEC (meq / 100gm)	4.01
FRF * at NOBP	25.40
Rw at 25°C, ohm-m	0.4150

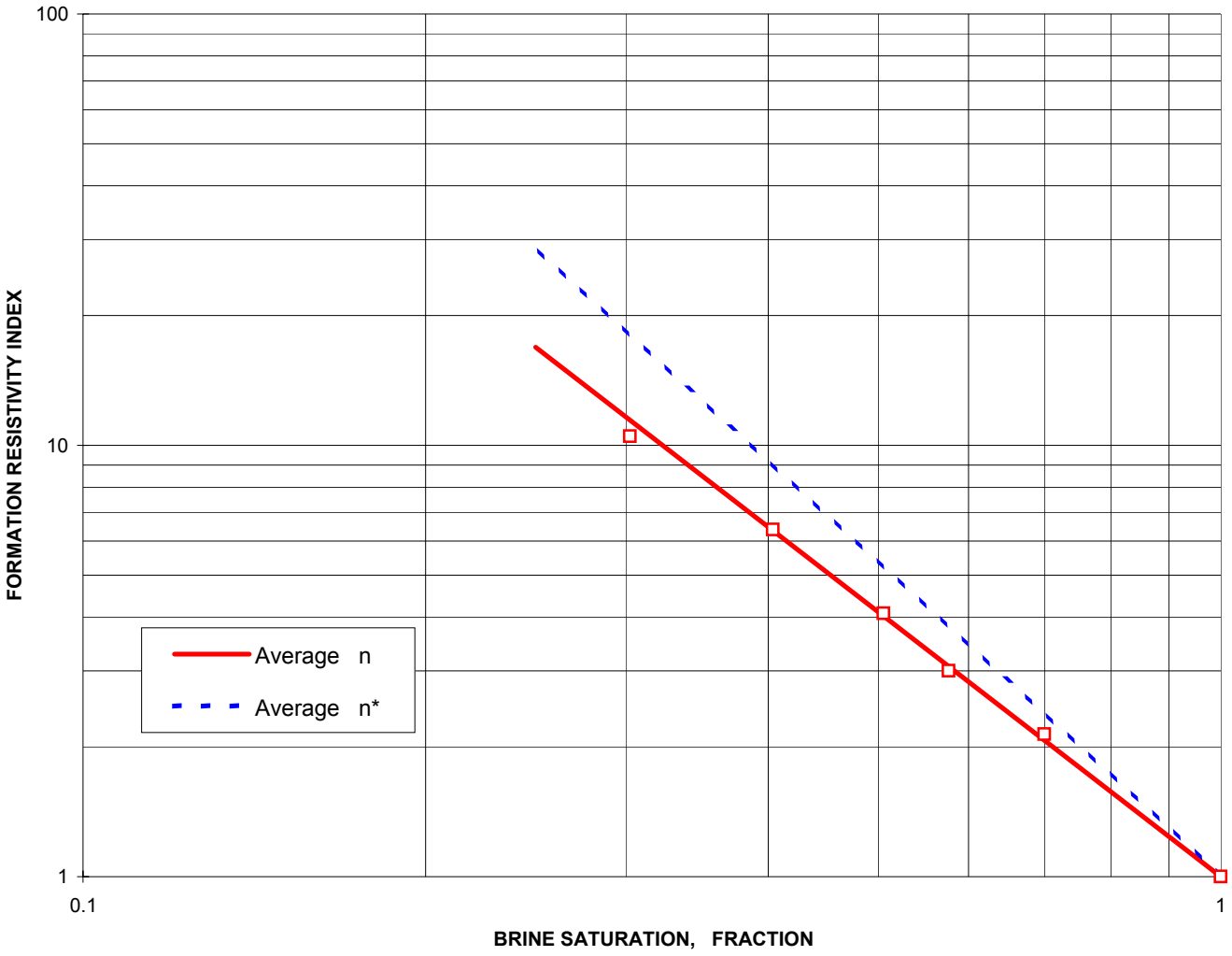

Formation resistivity index at 1910 psi NOBP.

(with simulated formation brine)

Sample no.	Depth (metres)	Grain density (gm/cc)	Determined at 1910 psi NOBP					
			Perm. to air (md)	Porosity (%)	Brine saturation (%pv)	Resistivity index	Sat. Exp. n	Corrected Sat. Exp. n *
22	2173.40	2.689	0.298	11.3	100.0	1.00	-	-
					93.8	1.14	2.06	2.73
					83.9	1.43	2.04	2.72
					74.8	1.76	1.95	2.64
					68.3	2.01	1.83	2.54
					57.6	2.60	1.73	2.46
					Average Exponent		1.92	2.62

FRF at NOBP	55.55
CEC (meq / 100gm)	8.42
FRF * at NOBP	165.08
Rw at 25°C, ohm-m	0.4150

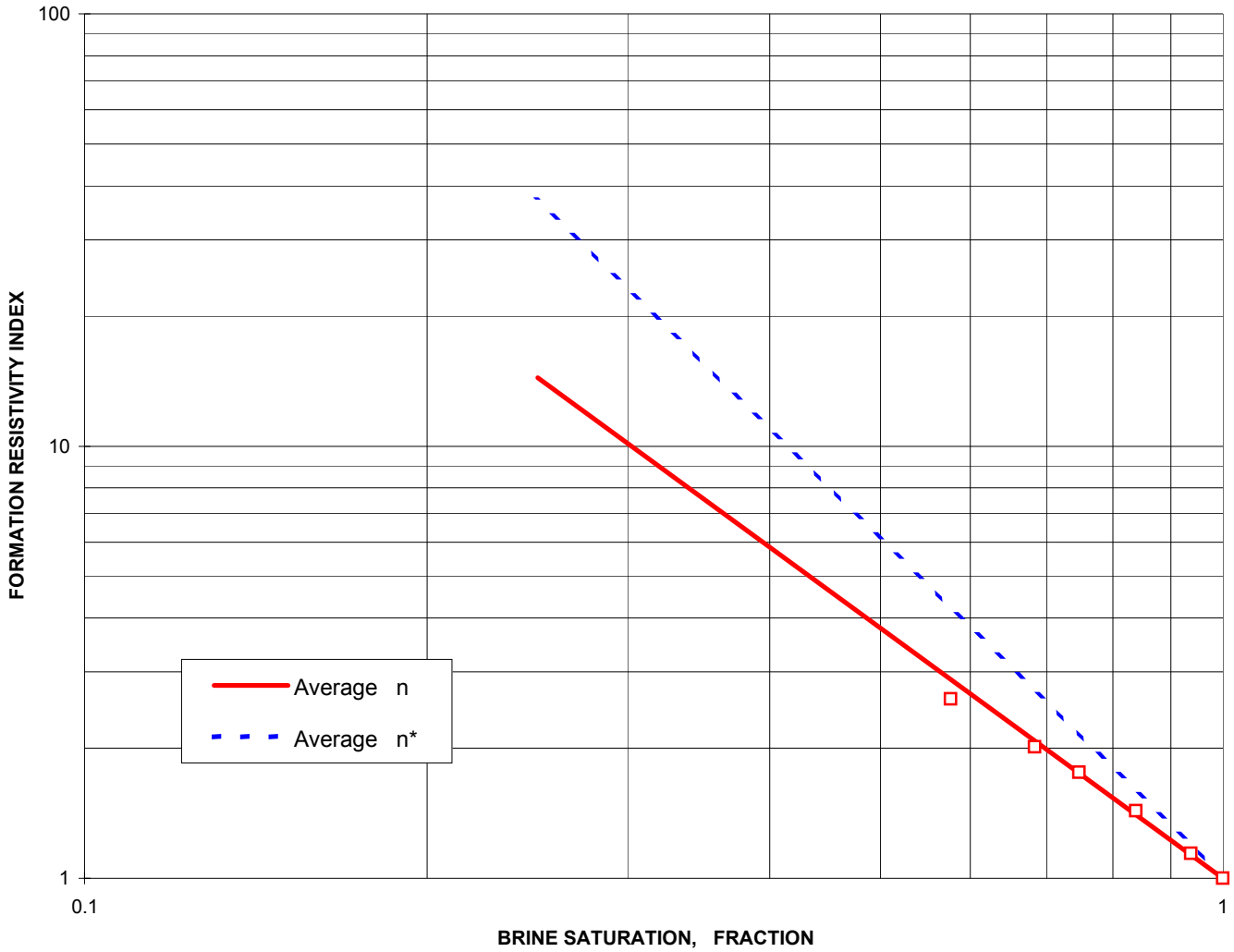

Formation resistivity index at 1910 psi NOBP.

(with simulated formation brine)

Sample no.	Depth (metres)	Grain density (gm/cc)	Determined at 1910 psi NOBP					
			Perm. to air (md)	Porosity (%)	Brine saturation (%pv)	Resistivity index	Sat. Exp. n	Corrected Sat. Exp. n *
24	2173.83	2.657	1150	18.0	100.0	1.00	-	-
					82.8	1.57	2.38	2.56
					61.8	2.68	2.05	2.25
					52.8	3.58	2.00	2.21
					37.0	6.70	1.91	2.16
					29.1	10.31	1.89	2.16
					19.5	23.63	1.94	2.25
					Average Exponent		2.03	2.27

FRF at NOBP	25.43
CEC (meq / 100gm)	3.13
FRF * at NOBP	30.45
Rw at 25°C, ohm-m	0.4150

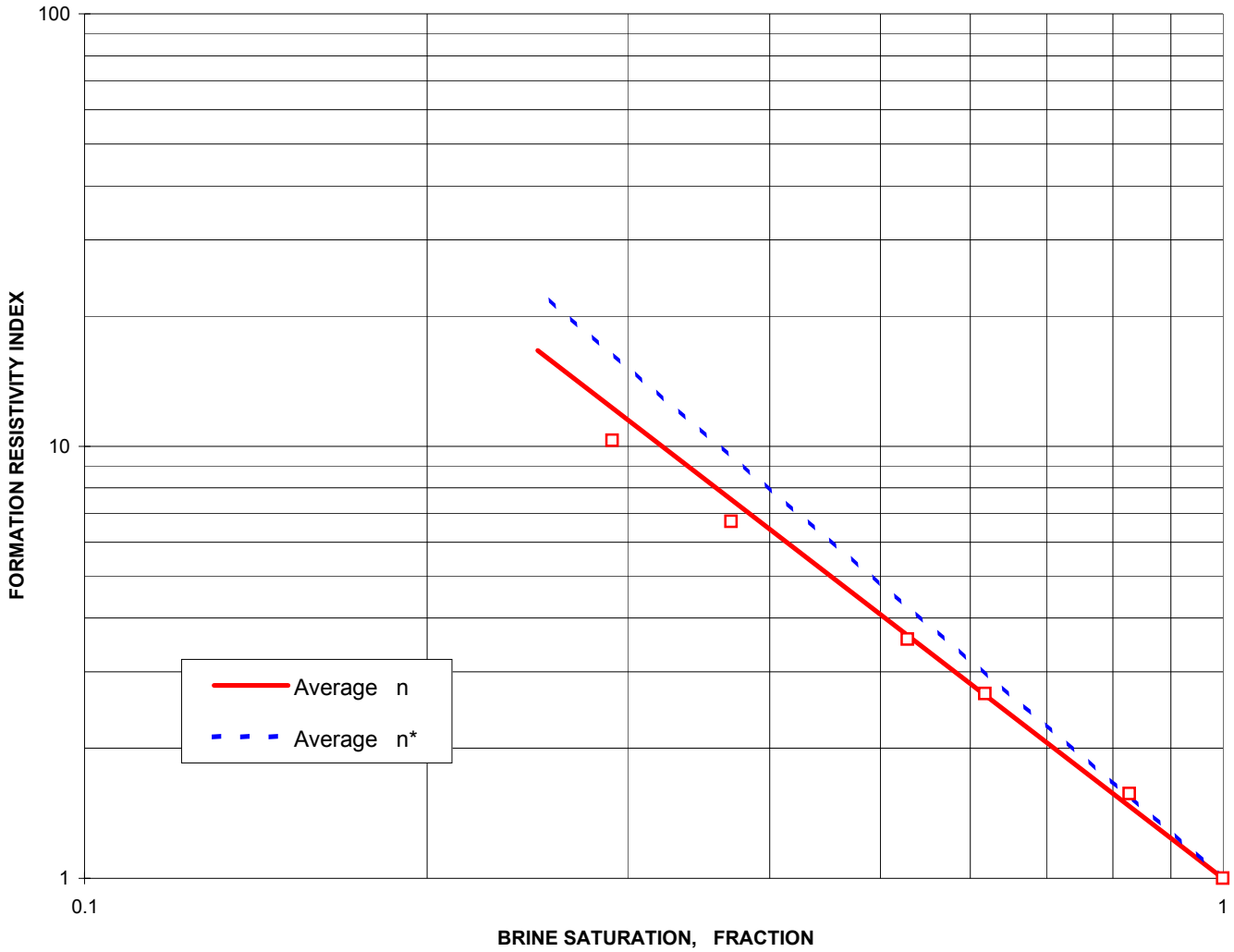

Formation resistivity index at 1910 psi NOBP.

(with simulated formation brine)

Sample no.	Depth (metres)	Grain density (gm/cc)	Determined at 1910 psi NOBP					
			Perm. to air (md)	Porosity (%)	Brine saturation (%pv)	Resistivity index	Sat. Exp. n	Corrected Sat. Exp. n *
25	2174.10	2.675	2.67	12.8	100.0	1.00	-	-
					89.4	1.24	1.91	2.26
					76.7	1.74	2.09	2.46
					69.6	2.16	2.13	2.52
					59.0	2.57	1.79	2.20
					54.1	3.60	2.08	2.50
					Average Exponent		2.00	2.39

FRF at NOBP	42.58
CEC (meq / 100gm)	2.57
FRF * at NOBP	64.73
Rw at 25°C, ohm-m	0.4150

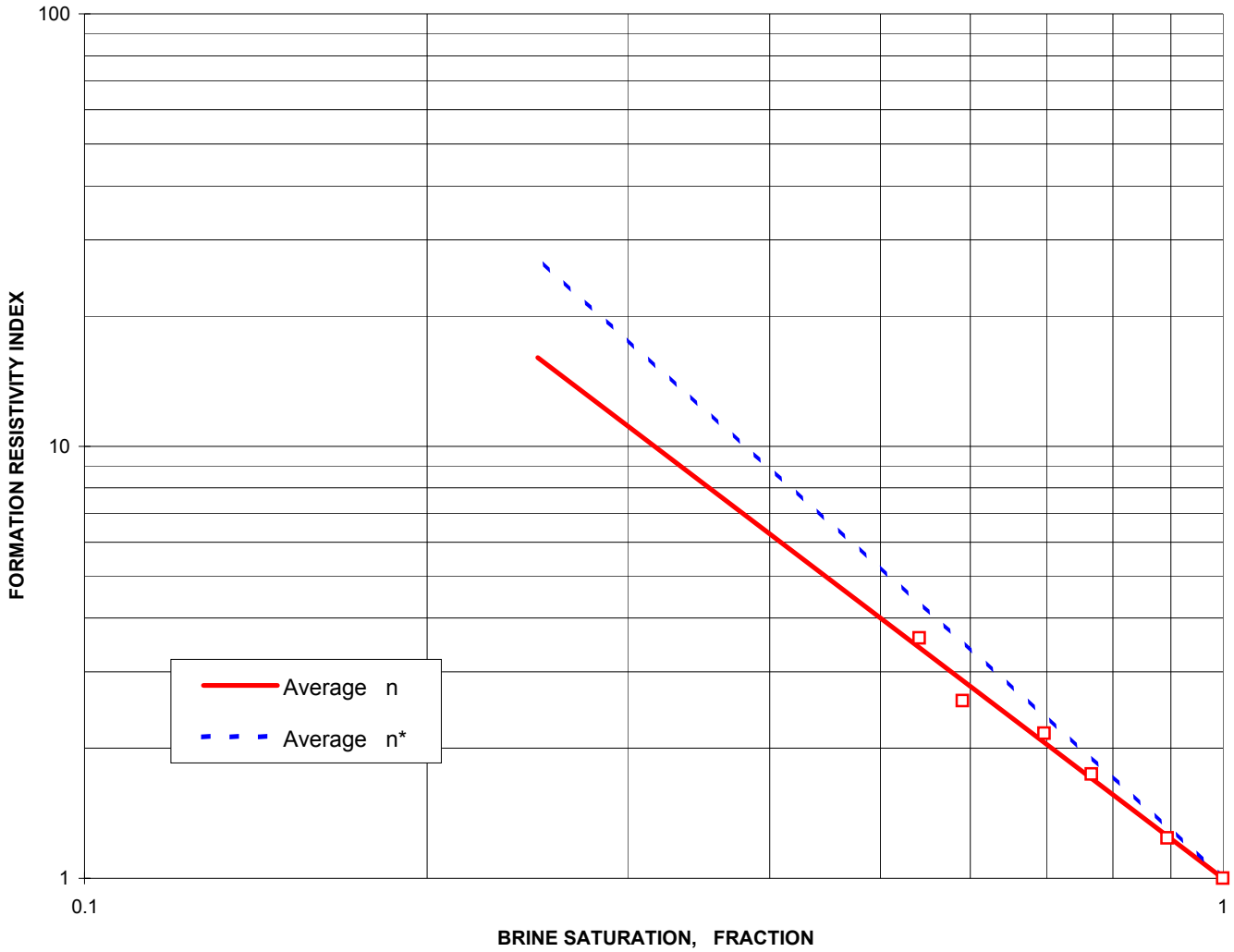

Formation resistivity index at 1910 psi NOBP.

(with simulated formation brine)

Sample no.	Depth (metres)	Grain density (gm/cc)	Determined at 1910 psi NOBP					
			Perm. to air (md)	Porosity (%)	Brine saturation (%pv)	Resistivity index	Sat. Exp. n	Corrected Sat. Exp. n *
28	2174.80	2.653	3170	20.2	100.0	1.00	-	-
					74.1	1.90	2.14	2.25
					63.5	2.55	2.06	2.19
					46.8	5.19	2.17	2.31
					40.9	6.46	2.09	2.24
					19.3	30.07	2.07	2.29
					Average Exponent		2.11	2.26

FRF at NOBP	20.92
CEC (meq / 100gm)	0.97
FRF * at NOBP	23.28
Rw at 25°C, ohm-m	0.4150

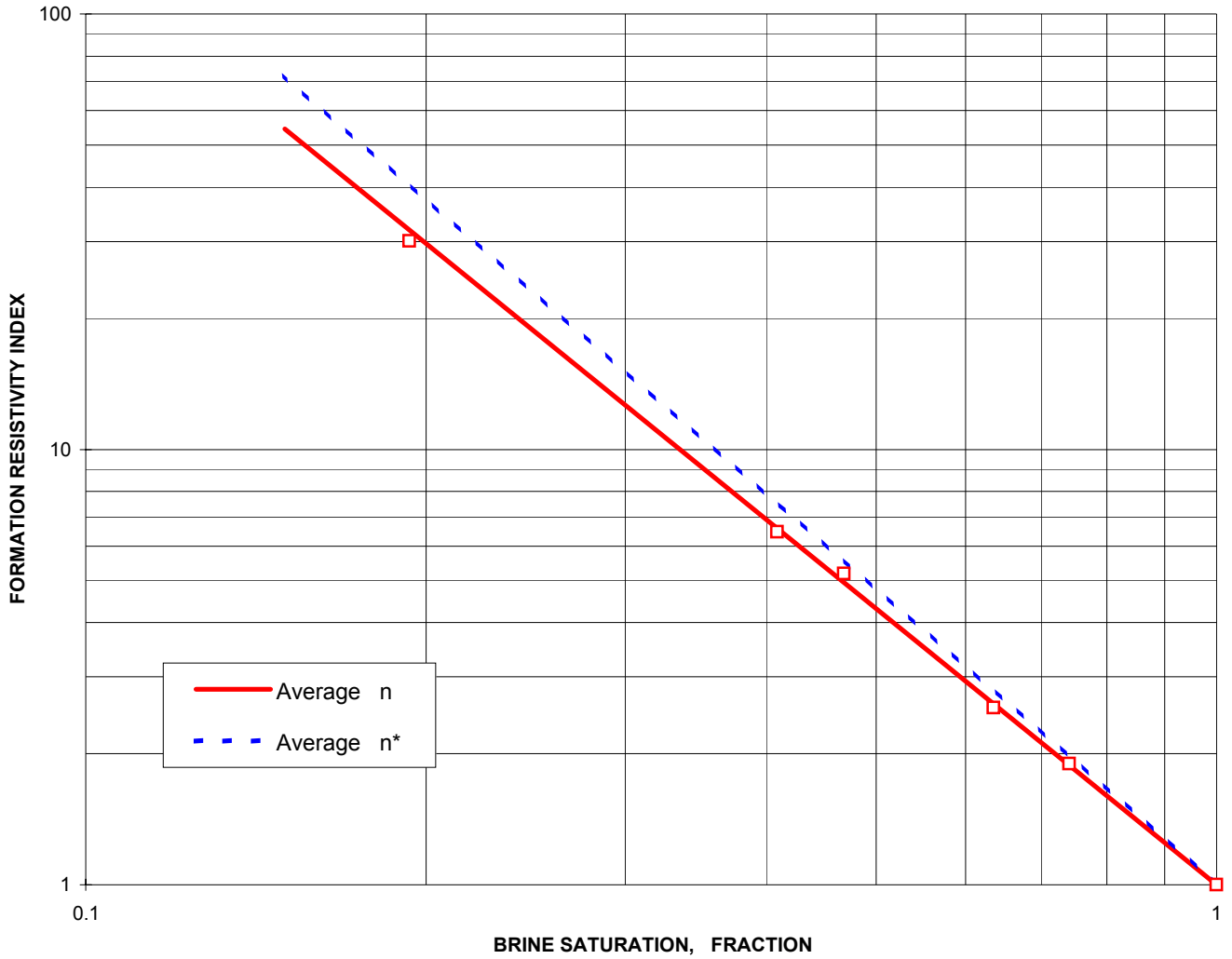

Formation resistivity index at 1910 psi NOBP.

(with simulated formation brine)

Sample no.	Depth (metres)	Grain density (gm/cc)	Determined at 1910 psi NOBP					
			Perm. to air (md)	Porosity (%)	Brine saturation (%pv)	Resistivity index	Sat. Exp. n	Corrected Sat. Exp. n *
46	2180.10	2.648	3980	22.5	100.0	1.00	-	-
					67.3	2.55	2.37	2.52
					51.0	3.51	1.86	2.04
					31.4	11.46	2.10	2.32
					18.3	28.55	1.97	2.24
					13.8	47.74	1.96	2.26
					Average Exponent		2.05	2.28

FRF at NOBP	15.51
CEC (meq / 100gm)	1.48
FRF * at NOBP	17.82
Rw at 25°C, ohm-m	0.4150

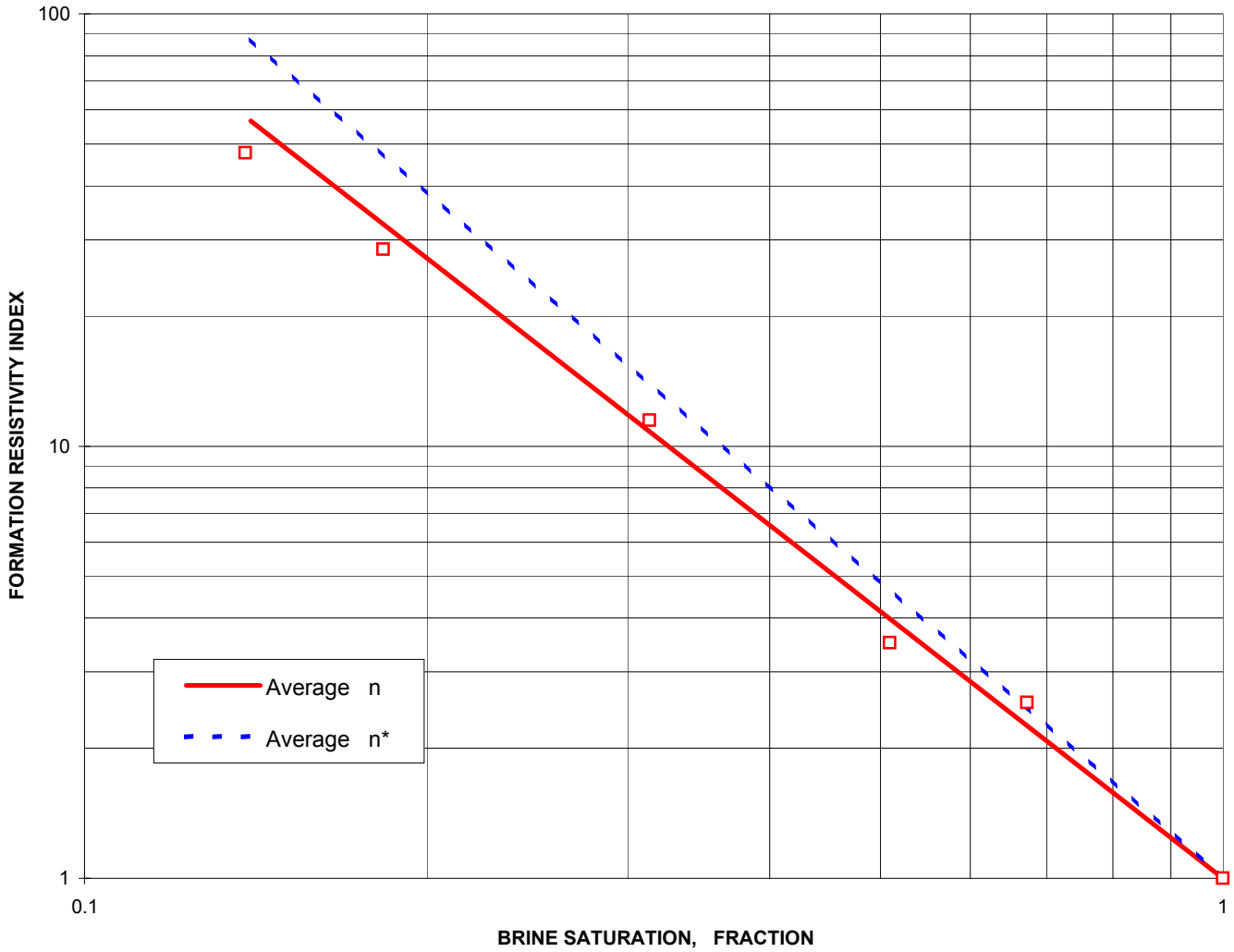

Formation resistivity index at 1910 psi NOBP.

(with simulated formation brine)

Sample no.	Depth (metres)	Grain density (gm/cc)	Determined at 1910 psi NOBP					
			Perm. to air (md)	Porosity (%)	Brine saturation (%pv)	Resistivity index	Sat. Exp. n	Corrected Sat. Exp. n *
55	2182.92	2.659	97.2	17.1	100.0	1.00	-	-
					73.1	1.92	2.09	2.47
					64.4	2.56	2.14	2.53
					53.4	3.35	1.93	2.35
					43.6	4.84	1.90	2.34
					32.1	7.64	1.79	2.27
					Average Exponent		1.97	2.39

FRF at NOBP	28.61
CEC (meq / 100gm)	3.72
FRF * at NOBP	43.83
Rw at 25°C, ohm-m	0.4150

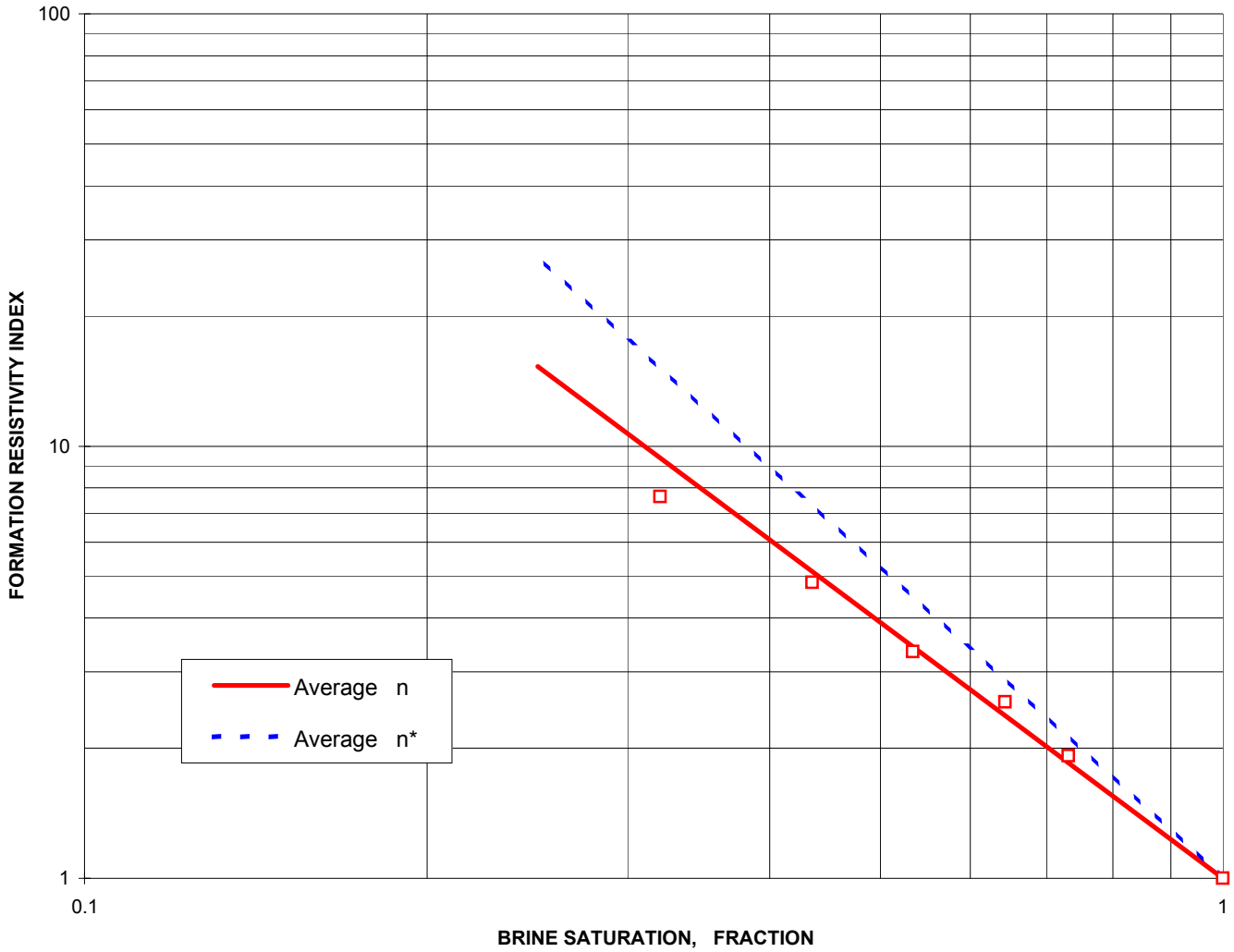

Formation resistivity index at 1910 psi NOBP.

(with simulated formation brine)

Sample no.	Depth (metres)	Grain density (gm/cc)	Determined at 1910 psi NOBP					
			Perm. to air (md)	Porosity (%)	Brine saturation (%pv)	Resistivity index	Sat. Exp. n	Corrected Sat. Exp. n *
62	2184.89	2.648	111	14.6	100.0	1.00	-	-
					73.9	2.00	2.30	2.68
					55.4	3.49	2.12	2.54
					49.0	4.04	1.95	2.39
					41.6	6.54	2.14	2.60
					24.0	16.27	1.96	2.48
					Average Exponent		2.09	2.54

FRF at NOBP	31.02
CEC (meq / 100gm)	3.14
FRF * at NOBP	47.73
Rw at 25°C, ohm-m	0.4150

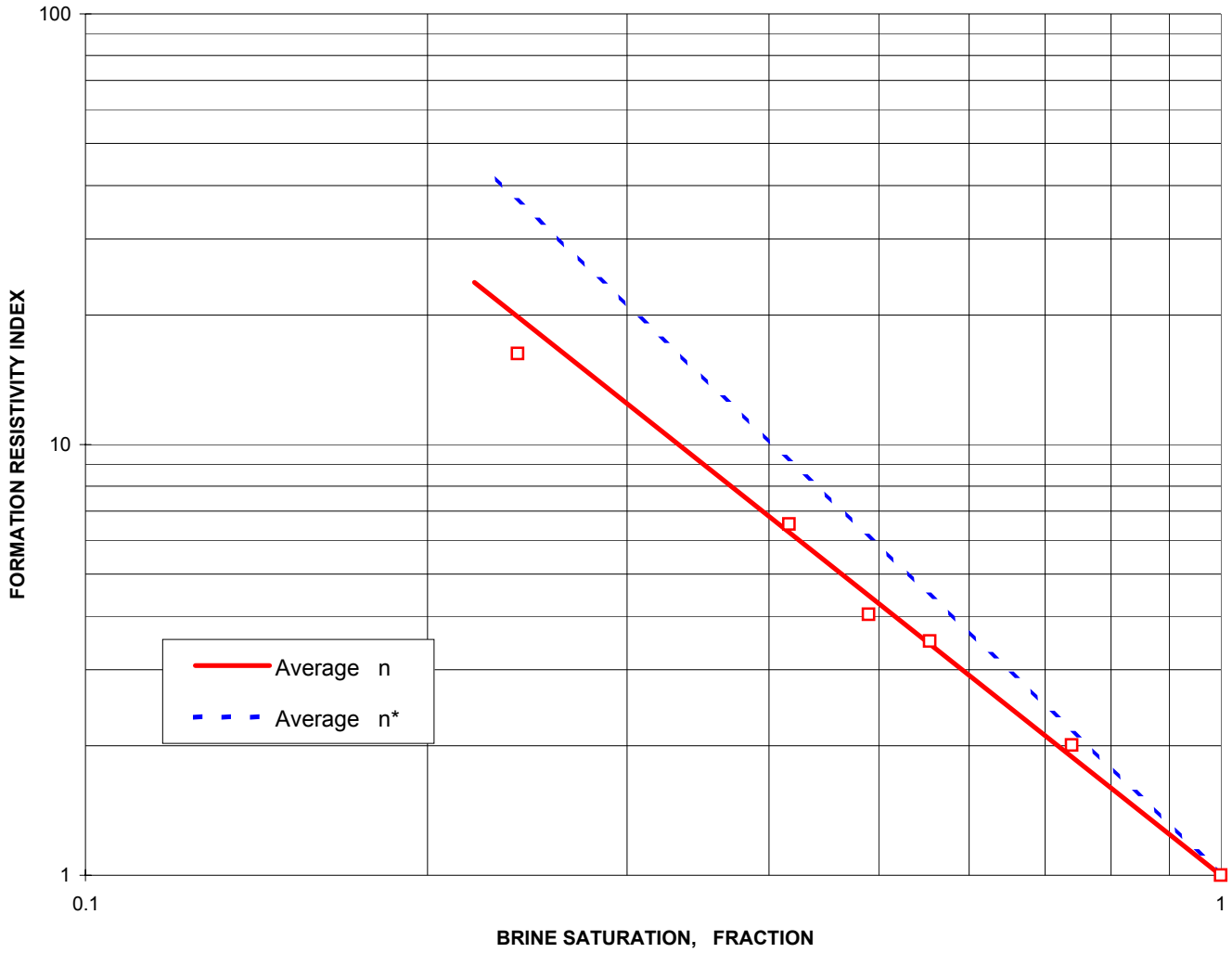

Formation resistivity index at 1910 psi NOBP.

(with simulated formation brine)

Sample no.	Depth (metres)	Grain density (gm/cc)	Determined at 1910 psi NOBP					
			Perm. to air (md)	Porosity (%)	Brine saturation (%pv)	Resistivity index	Sat. Exp. n	Corrected Sat. Exp. n *
67	2186.60	2.745	1.62	16.4	100.0	1.00	-	-
					80.9	1.42	1.66	2.07
					73.9	1.75	1.84	2.26
					67.4	1.91	1.64	2.07
					61.0	2.29	1.67	2.12
					53.3	2.78	1.62	2.09
					Average Exponent		1.69	2.12

FRF at NOBP	25.55
CEC (meq / 100gm)	4.01
FRF * at NOBP	41.45
Rw at 25°C, ohm-m	0.4150

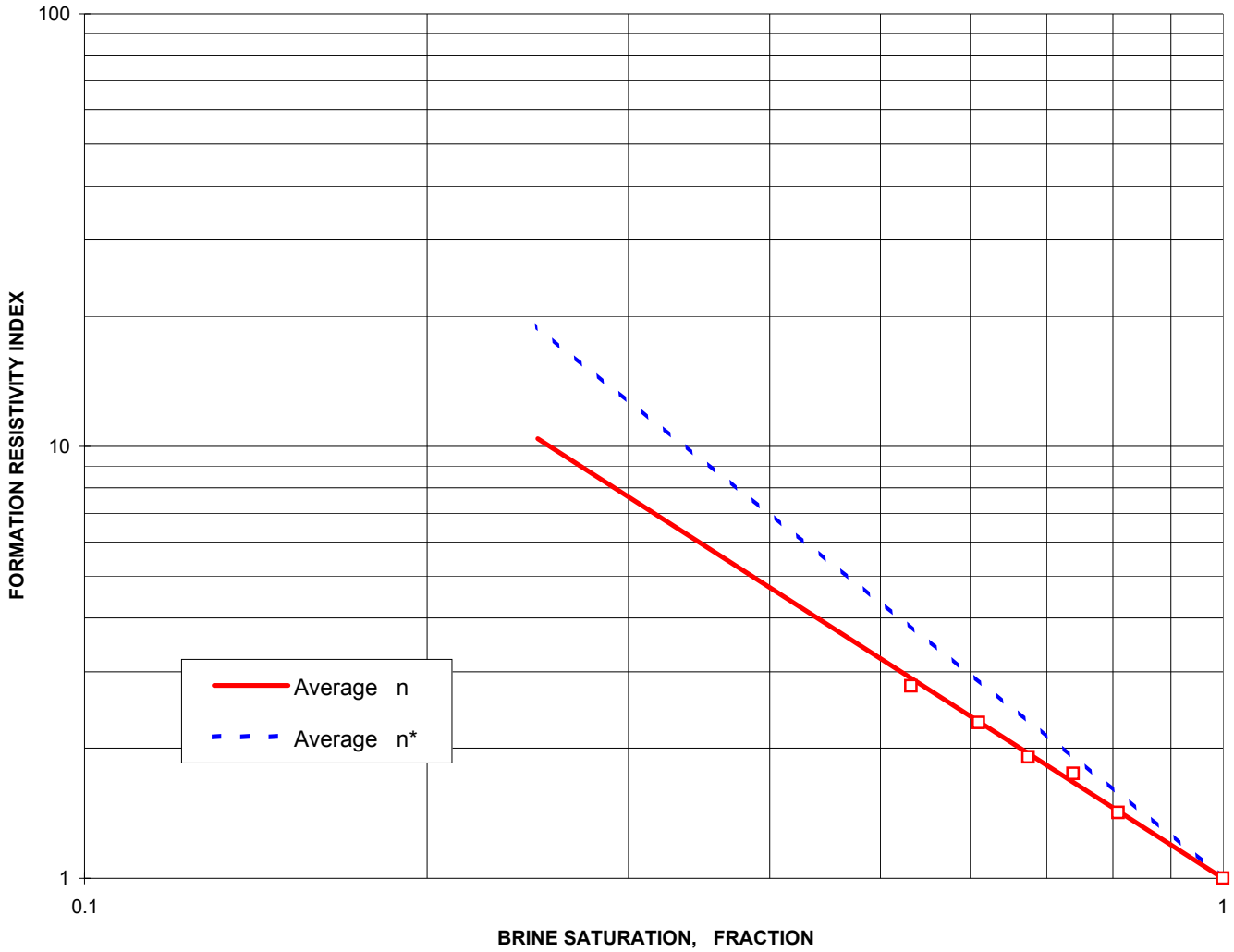

Formation resistivity index at 1910 psi NOBP.

(with simulated formation brine)

Sample no.	Depth (metres)	Grain density (gm/cc)	Determined at 1910 psi NOBP					
			Perm. to air (md)	Porosity (%)	Brine saturation (%pv)	Resistivity index	Sat. Exp. n	Corrected Sat. Exp. n *
69	2187.10	2.676	20.0	19.6	100.0	1.00	-	-
					77.5	1.63	1.93	2.19
					59.3	2.88	2.02	2.32
					47.0	4.13	1.88	2.20
					43.3	4.69	1.85	2.17
					36.5	5.87	1.76	2.10
					Average Exponent		1.89	2.20

FRF at NOBP	24.33
CEC (meq / 100gm)	2.60
FRF * at NOBP	31.99
Rw at 25°C, ohm-m	0.4150

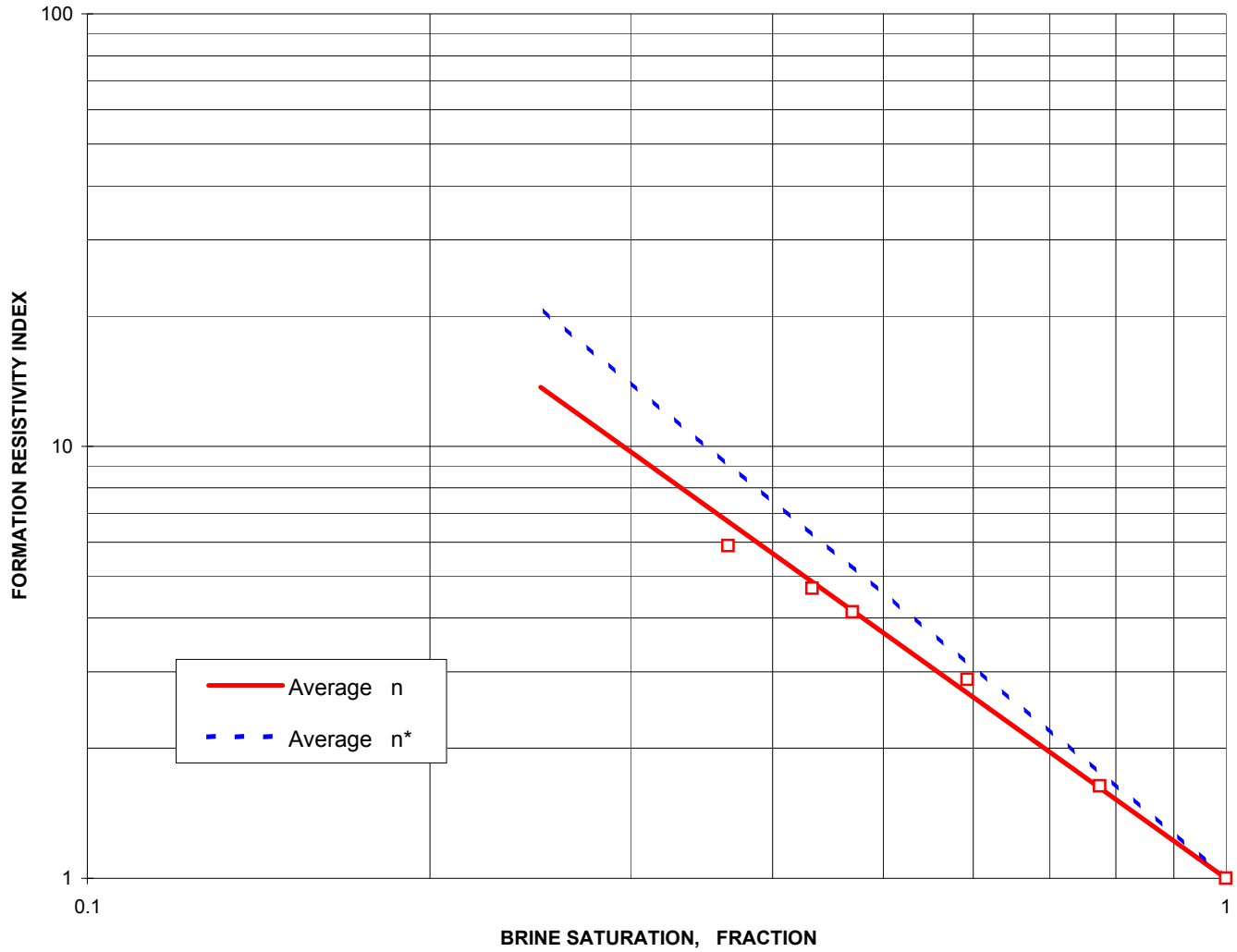

Formation resistivity index at 1910 psi NOBP.

(with simulated formation brine)

Sample no.	Depth (metres)	Grain density (gm/cc)	Determined at 1910 psi NOBP					
			Perm. to air (md)	Porosity (%)	Brine saturation (%pv)	Resistivity index	Sat. Exp. n	Corrected Sat. Exp. n *
80	2192.71	2.658	500	20.7	100.0	1.00	-	-
					74.8	1.90	2.21	2.38
					61.3	2.77	2.09	2.27
					50.2	4.49	2.18	2.38
					35.6	8.92	2.12	2.35
					27.8	14.49	2.09	2.34
					22.0	21.97	2.04	2.32
					Average Exponent		2.12	2.34

FRF at NOBP	23.57
CEC (meq / 100gm)	1.55
FRF * at NOBP	27.72
Rw at 25°C, ohm-m	0.4150

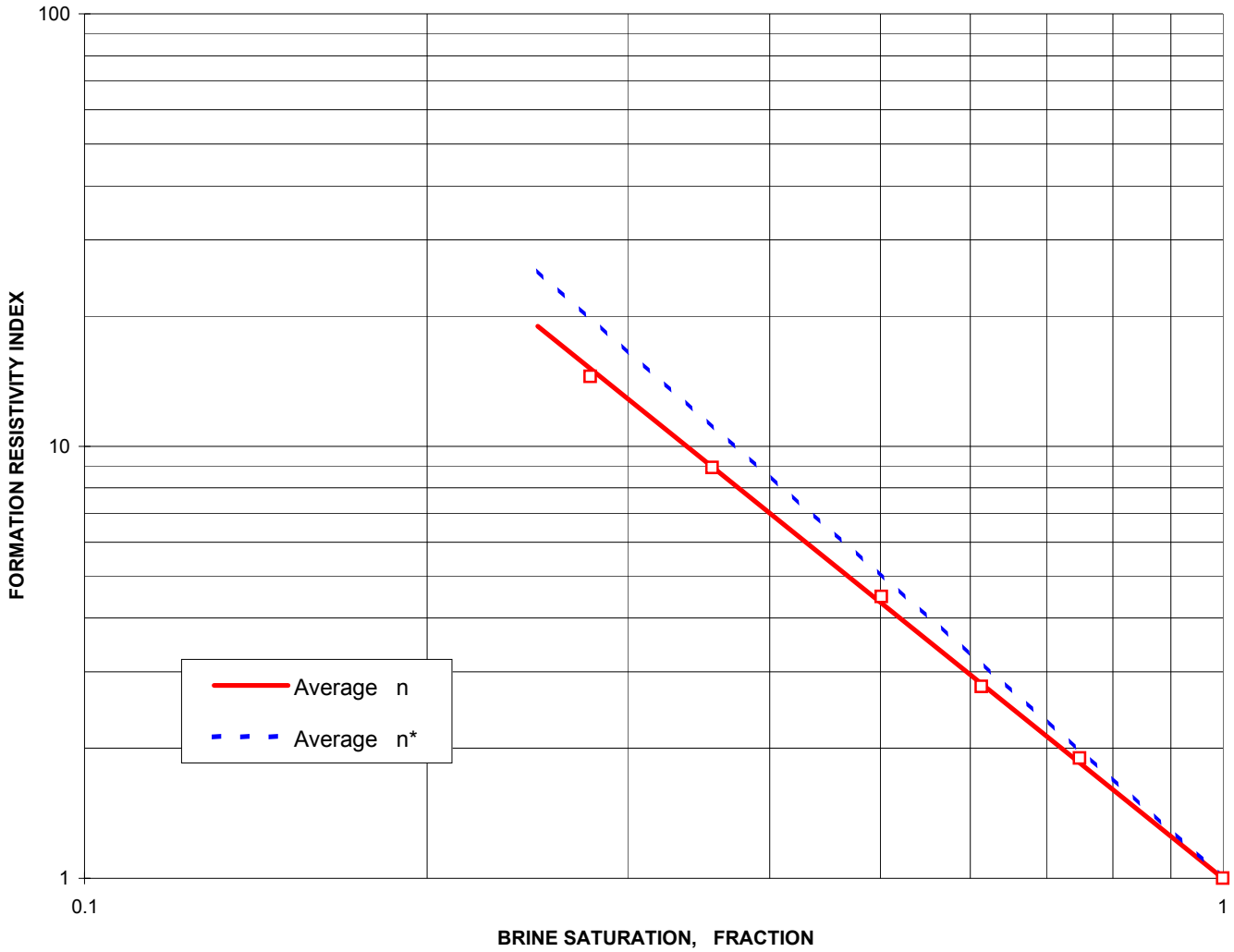

Formation resistivity index at 1910 psi NOBP.

(with simulated formation brine)

Sample no.	Depth (metres)	Grain density (gm/cc)	Determined at 1910 psi NOBP					
			Perm. to air (md)	Porosity (%)	Brine saturation (%pv)	Resistivity index	Sat. Exp. n	Corrected Sat. Exp. n *
83	2193.59	2.656	237	18.0	100.0	1.00	-	-
					79.8	1.62	2.13	2.39
					70.9	2.13	2.20	2.47
					43.8	5.69	2.11	2.43
					33.5	11.03	2.20	2.55
					27.6	14.37	2.07	2.45
					Average Exponent		2.14	2.46

FRF at NOBP	25.61
CEC (meq / 100gm)	2.34
FRF * at NOBP	33.64
Rw at 25°C, ohm-m	0.4150

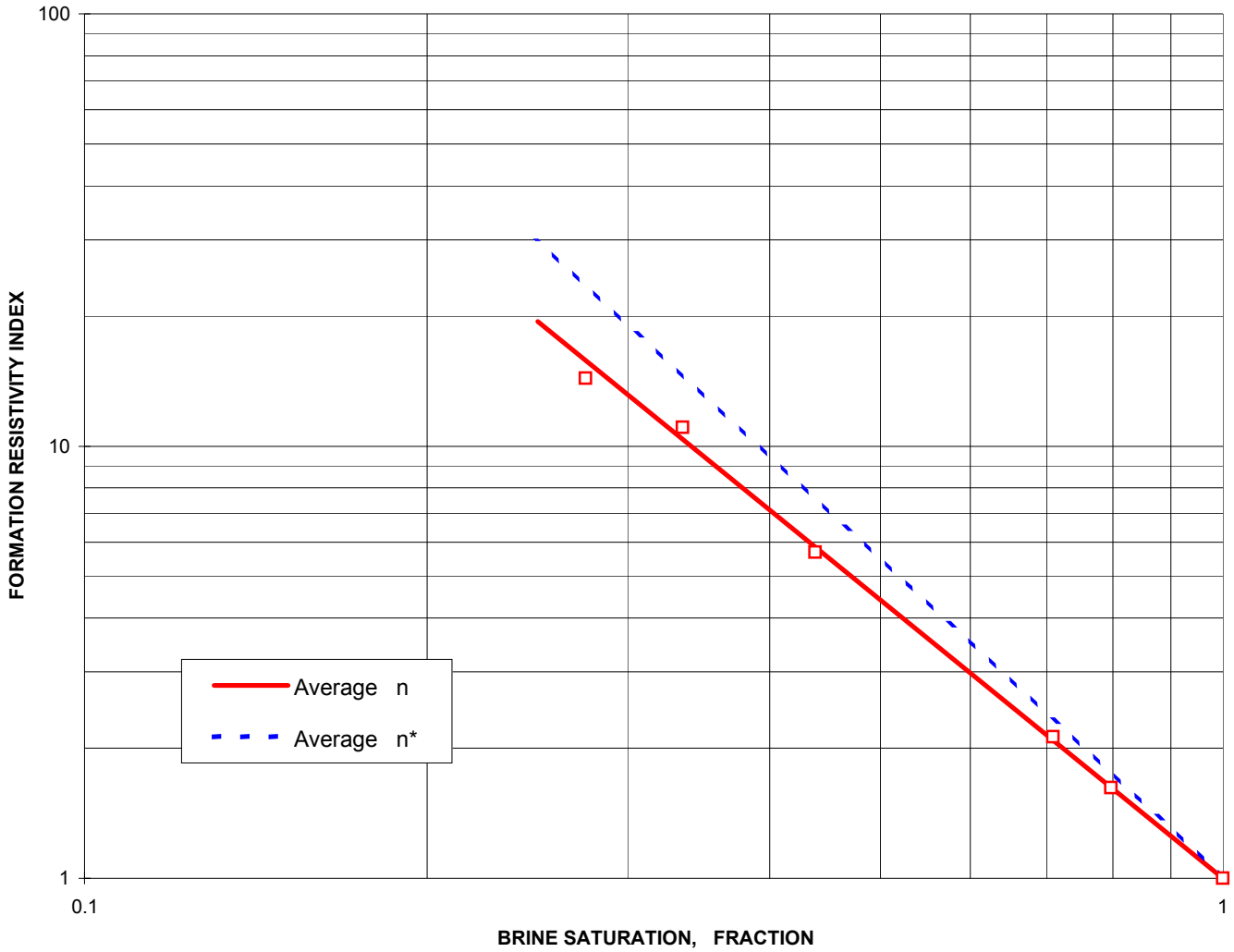

SECTION 3
CAPILLARY PRESSURE

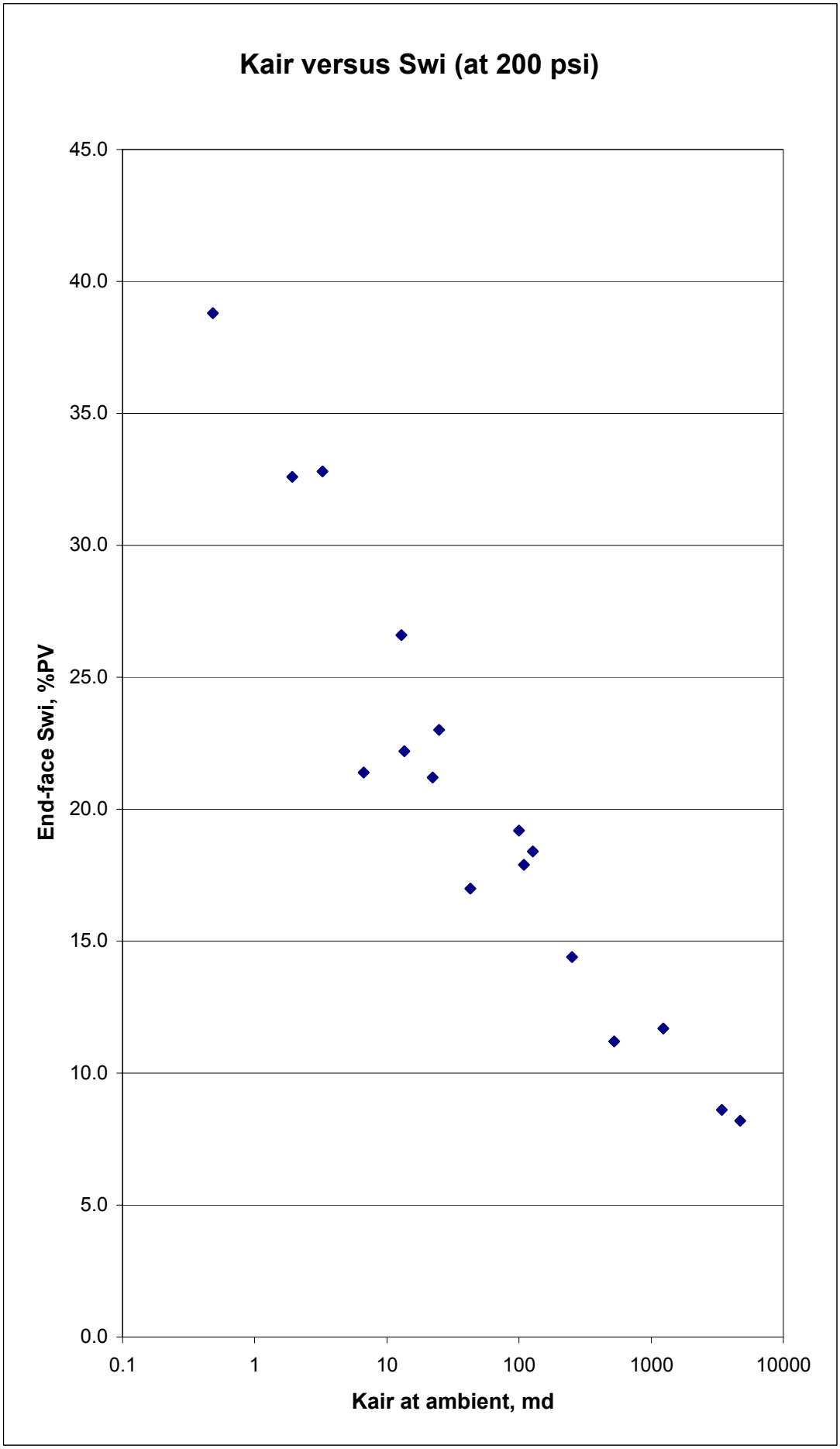
Kair versus Swi (at 200 psi)
End-face Swi, %PV
45.0
40.0
35.0
30.0
25.0
20.0
15.0
10.0
5.0
0.0
0.1
1
10
100
1000
10000
Kair at ambient, md

Summary of air-brine centrifuge capillary pressure data at ambient conditions

Sample no.	Depth (m)	Kair (md)	Porosity (%)	AIR - BRINE CAPILLARY PRESSURE (PSI)									
				0 psi	1 psi	2 psi	5 psi	10 psi	25 psi	50 psi	100 psi	200 psi	500 psi
				END FACE SATURATION Sw (%PV)									
MSCT-3	2055.00	13.5	19.9	100	100.0	100.0	79.7	63.4	46.9	32.6	25.6	22.2	20.0
MSCT-6	2092.20	42.8	23.2	100	100.0	91.0	62.0	48.8	37.5	23.7	18.8	17.0	15.3
MSCT-7	2094.00	12.9	21.1	100	100.0	100.0	76.1	62.8	48.2	36.3	29.6	26.6	23.0
MSCT-10	2143.60	24.9	20.8	100	100.0	100.0	65.6	53.7	41.2	33.7	27.6	23.0	20.9
5	2166.81	6.66	17.8	100	100.0	100.0	73.8	58.3	42.6	33.4	26.7	21.4	**
14	2171.19	99.5	21.8	100	88.3	72.0	54.9	44.8	34.2	28.0	23.2	19.2	**
22	2173.40	0.483	11.7	100	100	100	100	82.3	65.0	54.4	45.5	38.8	**
24*	2173.83	1240	18.5	100	53.7	47.6	34.7	24.3	17.5	15.9	13.8	11.7	**
25	2174.10	3.27	13.2	100	100	100	100	60.0	48.5	38.6	35.2	32.8	**
28*	2174.80	3430	20.9	100	41.8	32.0	22.5	17.4	13.8	11.6	9.7	8.6	**
46*	2180.10	4710	23.2	100	35.0	25.0	16.0	13.2	11.5	10.2	9.1	8.2	**
55	2182.92	109	17.7	100	79.4	65.4	50.5	41.6	32.1	26.5	21.8	17.9	**
62	2184.89	127	15.2	100	82.0	68.1	53.3	44.2	34.6	25.5	21.7	18.4	**
67	2186.60	1.93	17.0	100	100	100	100	85.9	65.9	52.8	41.7	32.6	**
69	2187.10	22.1	20.1	100	100	85.2	64.6	52.4	39.7	32.2	26.1	21.2	**
80	2192.71	524	21.1	100	57.9	44.4	31.2	23.9	16.8	14.4	12.2	11.2	**
83	2193.59	251	18.4	100	60.3	46.4	32.9	27.1	22.3	19.3	16.7	14.4	**

* Extrapolated at 200 psi.

** For the core plug samples, the maximum air-brine capillary pressure was limited to 200 psi.

MSCT-6 failed after capillary pressure measurements and was substituted with MSCT-2 for the subsequent electrical measurements.

Air-brine capillary pressure by centrifuge at ambient conditions.

Sample no.	Depth (m)	Determined at Ambient Conditions				
		Kinf (md)	Kair (md)	Porosity (%)	Capillary pressure (psi)	Brine saturation (%PV)
MSCT3	2055.00	11.6	13.5	19.9	0	100.0
					1	100.0
					2	100.0
					5	79.7
					10	63.4
					25	46.9
					50	32.6
					100	25.6
					200	22.2
					500	20.0

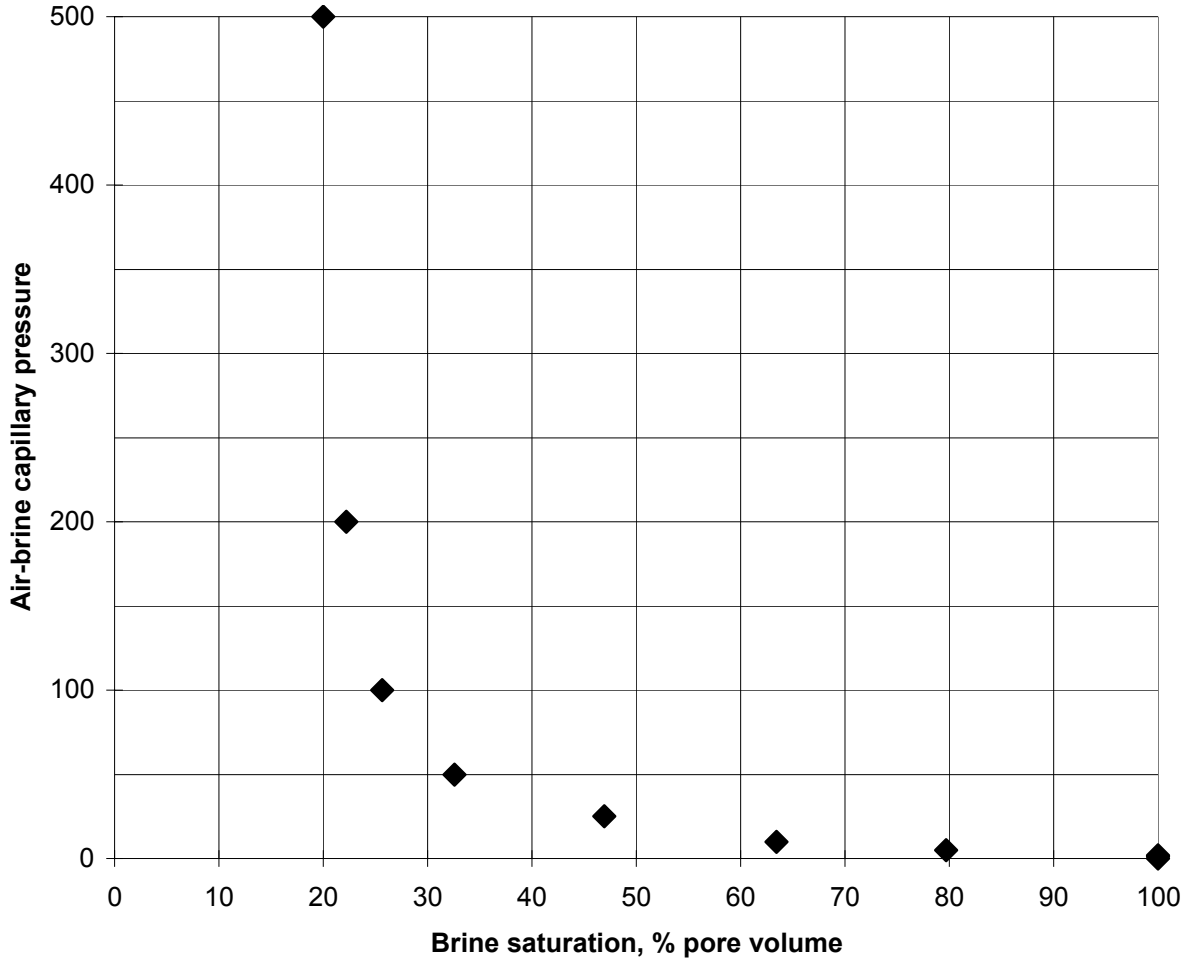

Air-brine capillary pressure by centrifuge at ambient conditions.

Sample no.	Depth (m)	Determined at Ambient Conditions				
		Kinf (md)	Kair (md)	Porosity (%)	Capillary pressure (psi)	Brine saturation (%PV)
MSCT6	2092.20	36.5	42.8	23.2	0	100.0
					1	100.0
					2	91.0
					5	62.0
					10	48.8
					25	37.5
					50	23.7
					100	18.8
					200	17.0
					500	15.3

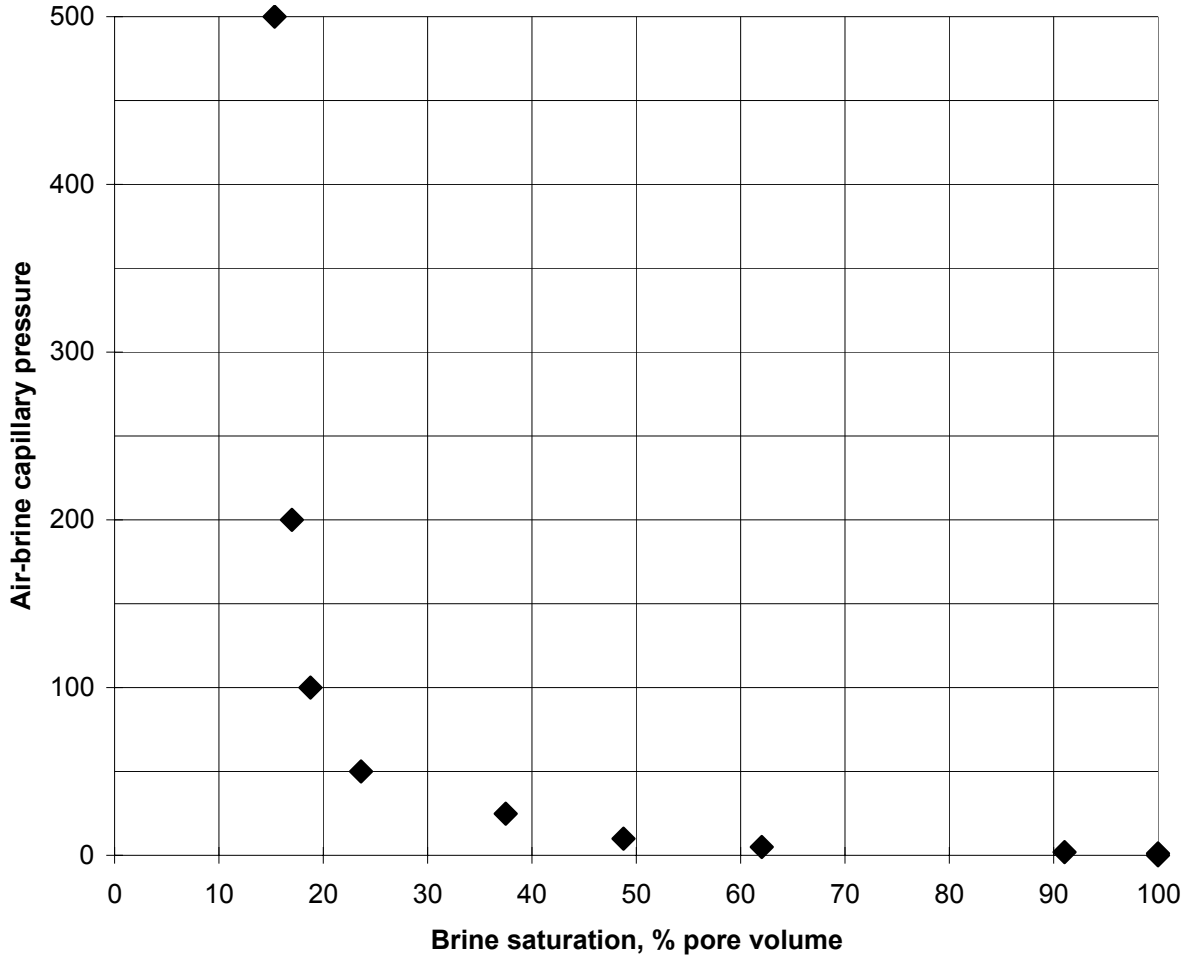

Air-brine capillary pressure by centrifuge at ambient conditions.

Sample no.	Depth (m)	Determined at Ambient Conditions				
		Kinf (md)	Kair (md)	Porosity (%)	Capillary pressure (psi)	Brine saturation (%PV)
MSCT7	2094.00	11.1	12.9	21.1	0	100.0
					1	100.0
					2	100.0
					5	76.1
					10	62.8
					25	48.2
					50	36.3
					100	29.6
					200	26.6
					500	23.0

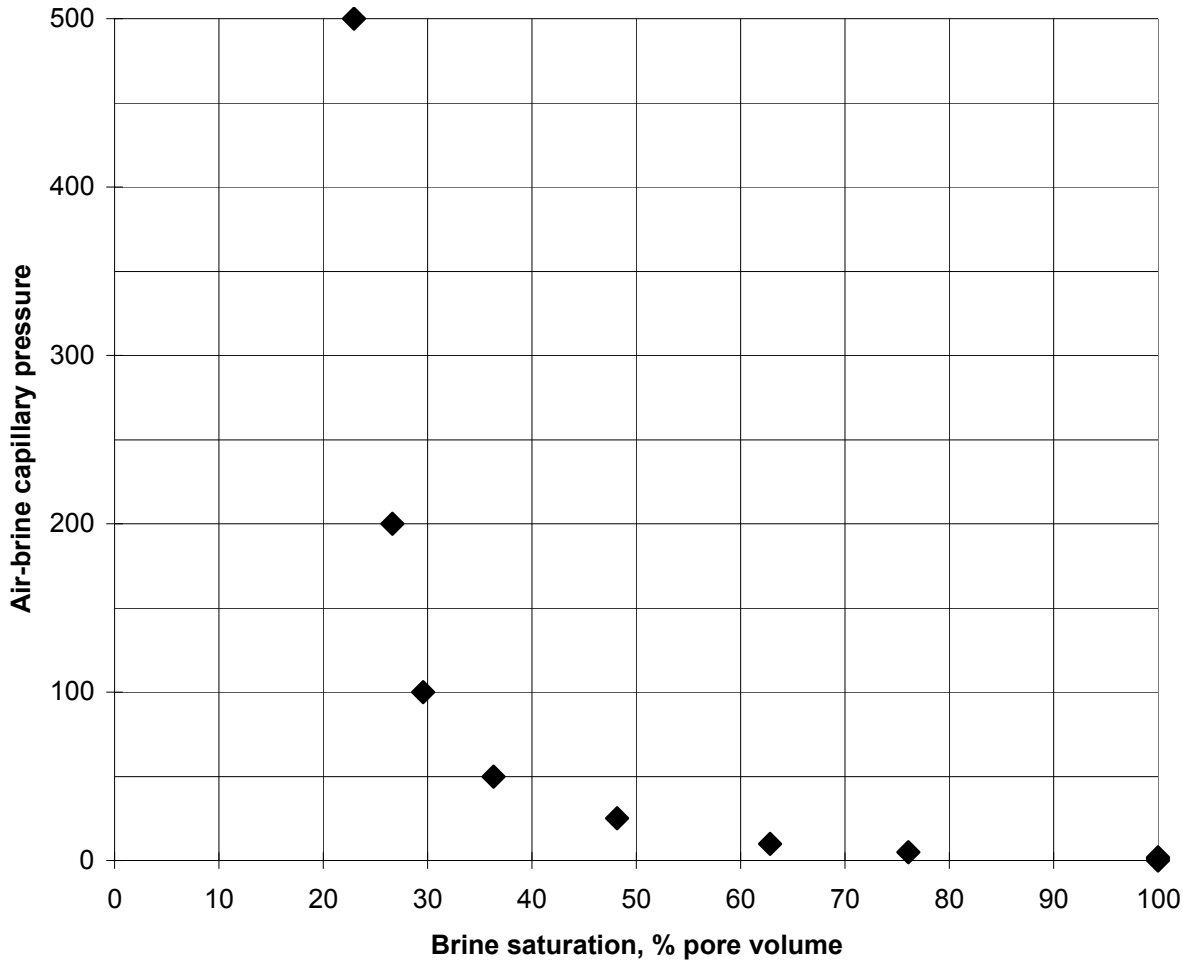

Air-brine capillary pressure by centrifuge at ambient conditions.

Sample no.	Depth (m)	Determined at Ambient Conditions				
		Kinf (md)	Kair (md)	Porosity (%)	Capillary pressure (psi)	Brine saturation (%PV)
MSCT10	2143.60	22.0	24.9	20.8	0	100.0
					1	100.0
					2	100.0
					5	65.6
					10	53.7
					25	41.2
					50	33.7
					100	27.6
					200	23.0
					500	20.9

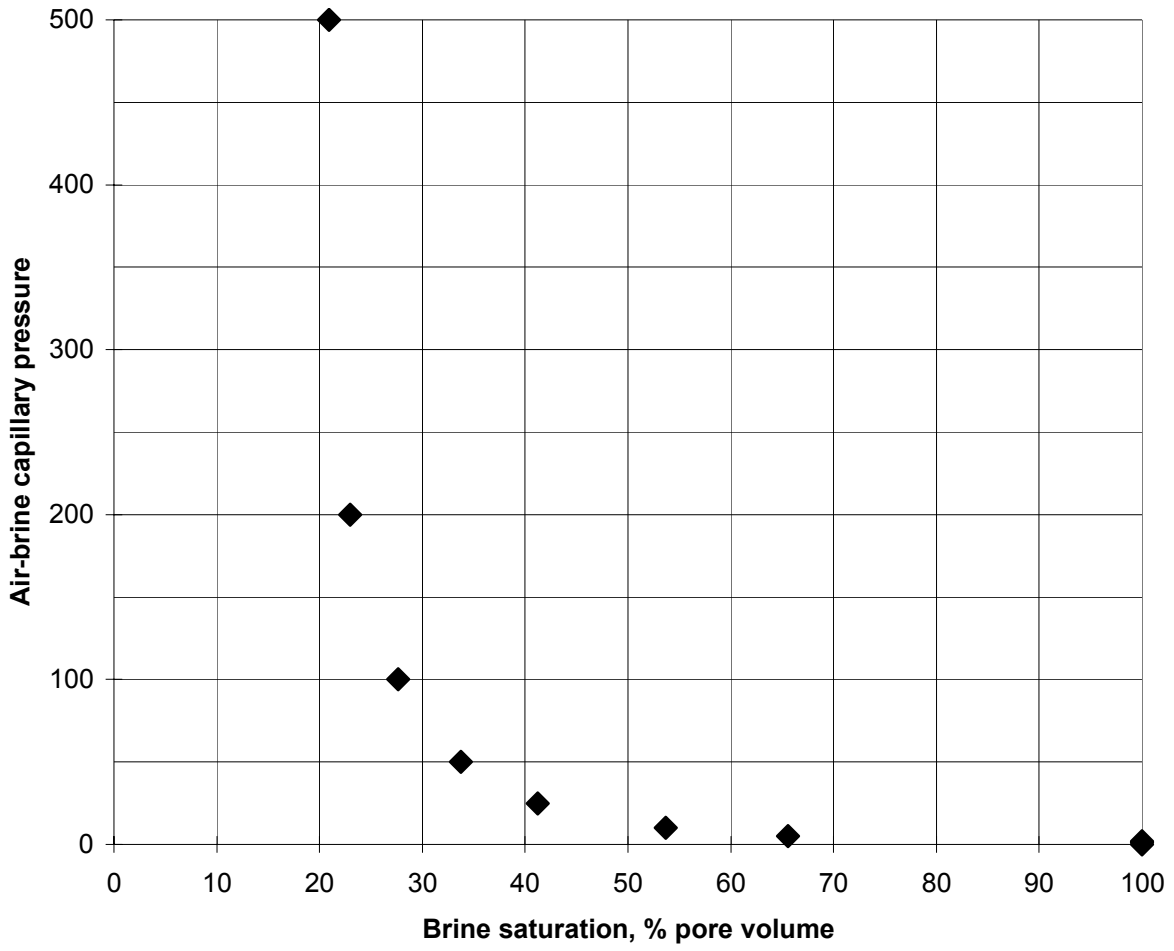

Air-brine capillary pressure by centrifuge at ambient conditions.

Sample no.	Depth (m)	Determined at Ambient Conditions				
		Kinf (md)	Kair (md)	Porosity (%)	Capillary pressure (psi)	Brine saturation (%PV)
5	2166.81	5.41	6.66	17.8	0	100.0
					1	100.0
					2	100.0
					5	73.8
					10	58.3
					25	42.6
					50	33.4
					100	26.7
					200	21.4

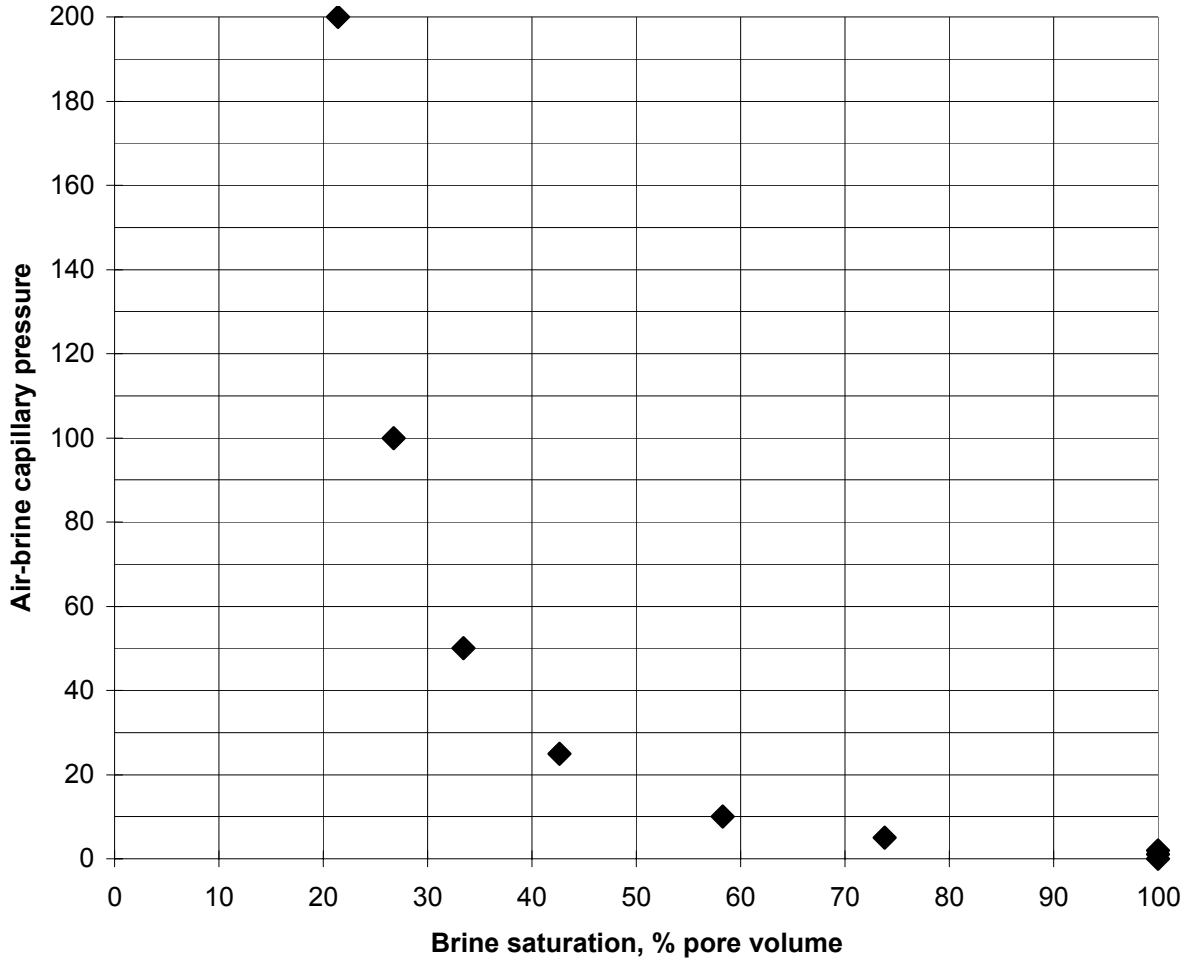

Air-brine capillary pressure by centrifuge at ambient conditions.

Sample no.	Depth (m)	Determined at Ambient Conditions				
		Kinf (md)	Kair (md)	Porosity (%)	Capillary pressure (psi)	Brine saturation (%PV)
14	2171.19	93.3	99.5	21.8	0	100.0
					1	88.3
					2	72.0
					5	54.9
					10	44.8
					25	34.2
					50	28.0
					100	23.2
					200	19.2

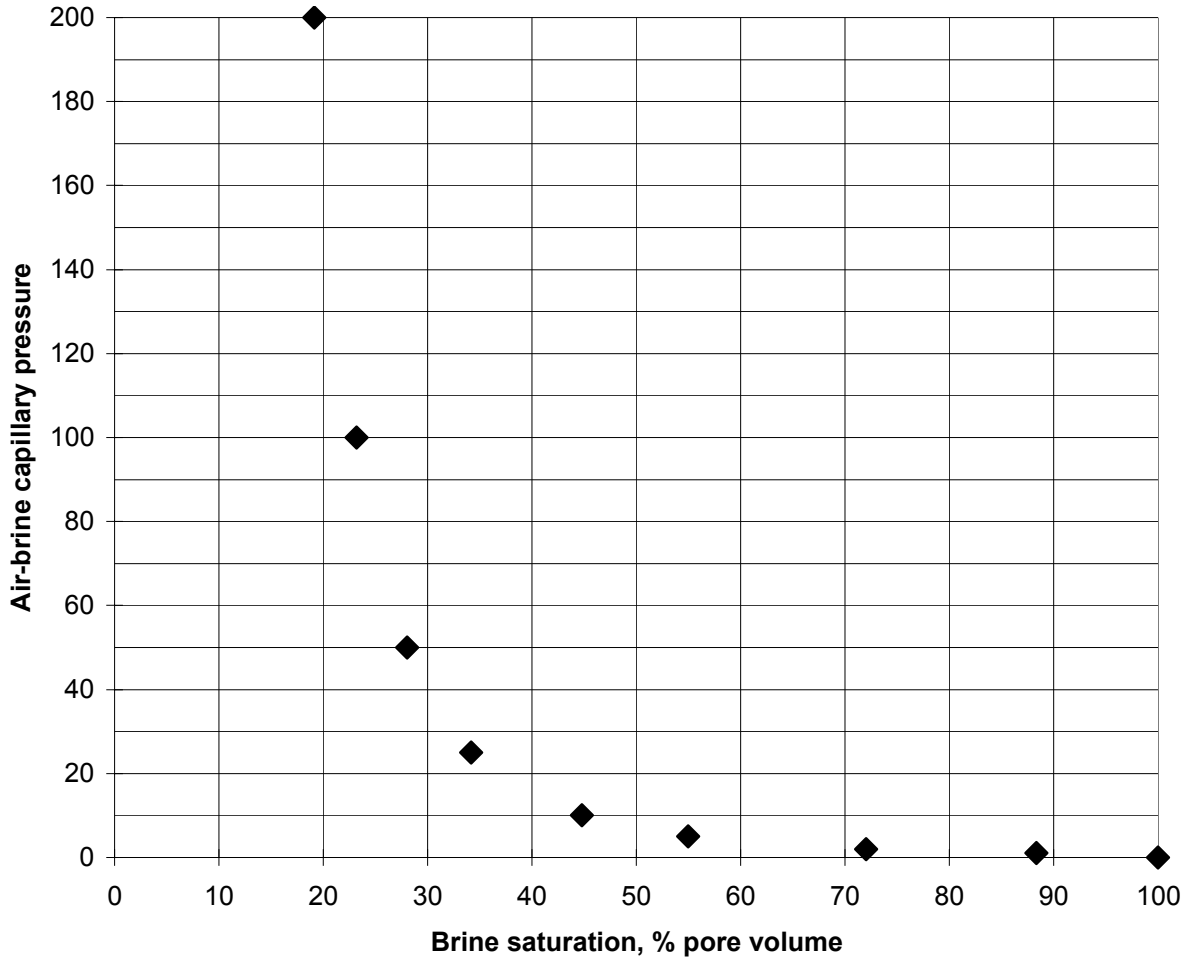

Air-brine capillary pressure by centrifuge at ambient conditions.

Sample no.	Depth (m)	Determined at Ambient Conditions				
		Kinf (md)	Kair (md)	Porosity (%)	Capillary pressure (psi)	Brine saturation (%PV)
22	2173.40	0.351	0.483	11.7	0	100.0
					1	100.0
					2	100.0
					5	100.0
					10	82.3
					25	65.0
					50	54.4
					100	45.5
					200	38.8

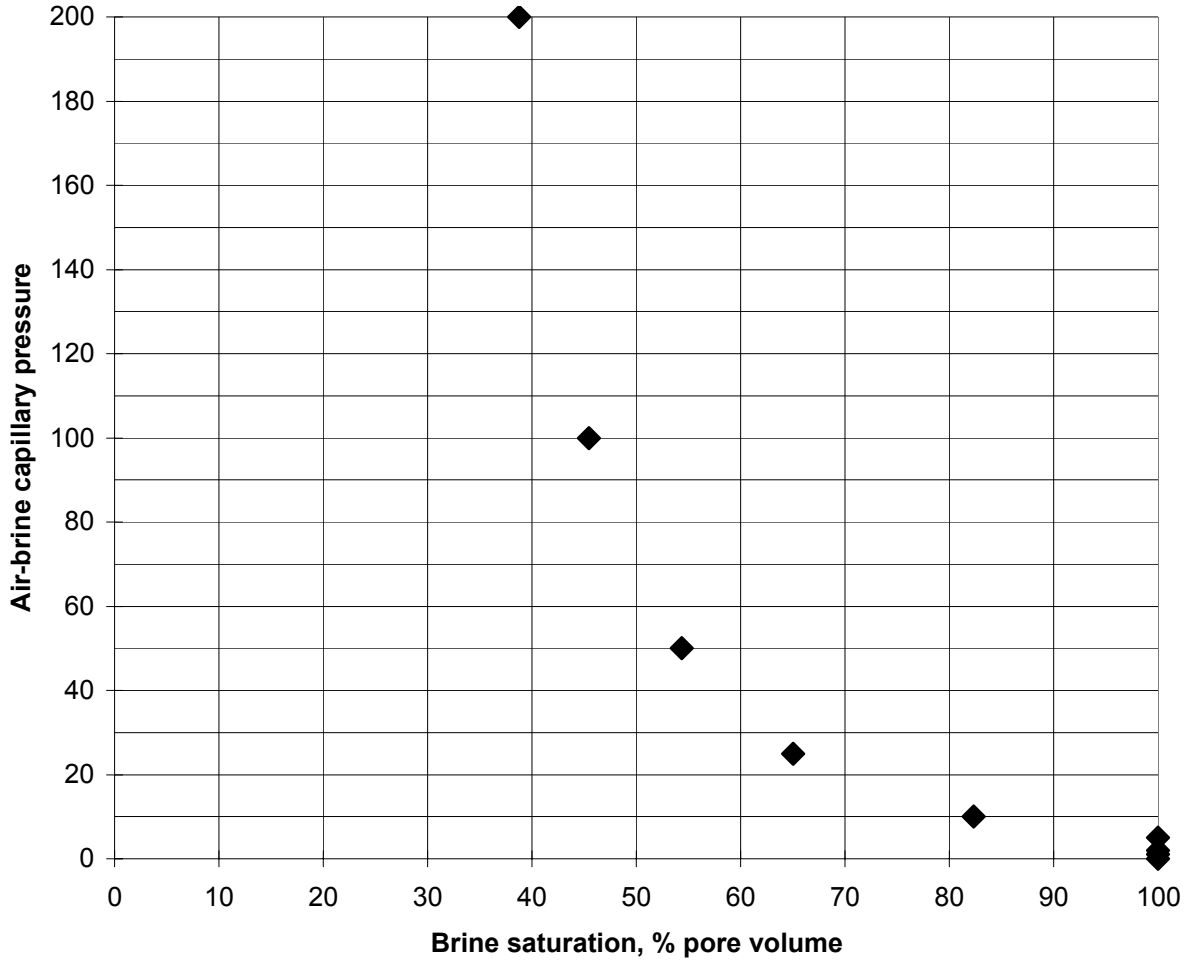

Air-brine capillary pressure by centrifuge at ambient conditions.

Sample no.	Depth (m)	Determined at Ambient Conditions				
		Kinf (md)	Kair (md)	Porosity (%)	Capillary pressure (psi)	Brine saturation (%PV)
24	2173.83	1060	1240	18.5	0	100.0
					1	53.7
					2	47.6
					5	34.7
					10	24.3
					25	17.5
					50	15.9
					100	13.8
					200	11.7

Brine saturation (Sw) at 200 psi is extrapolated.

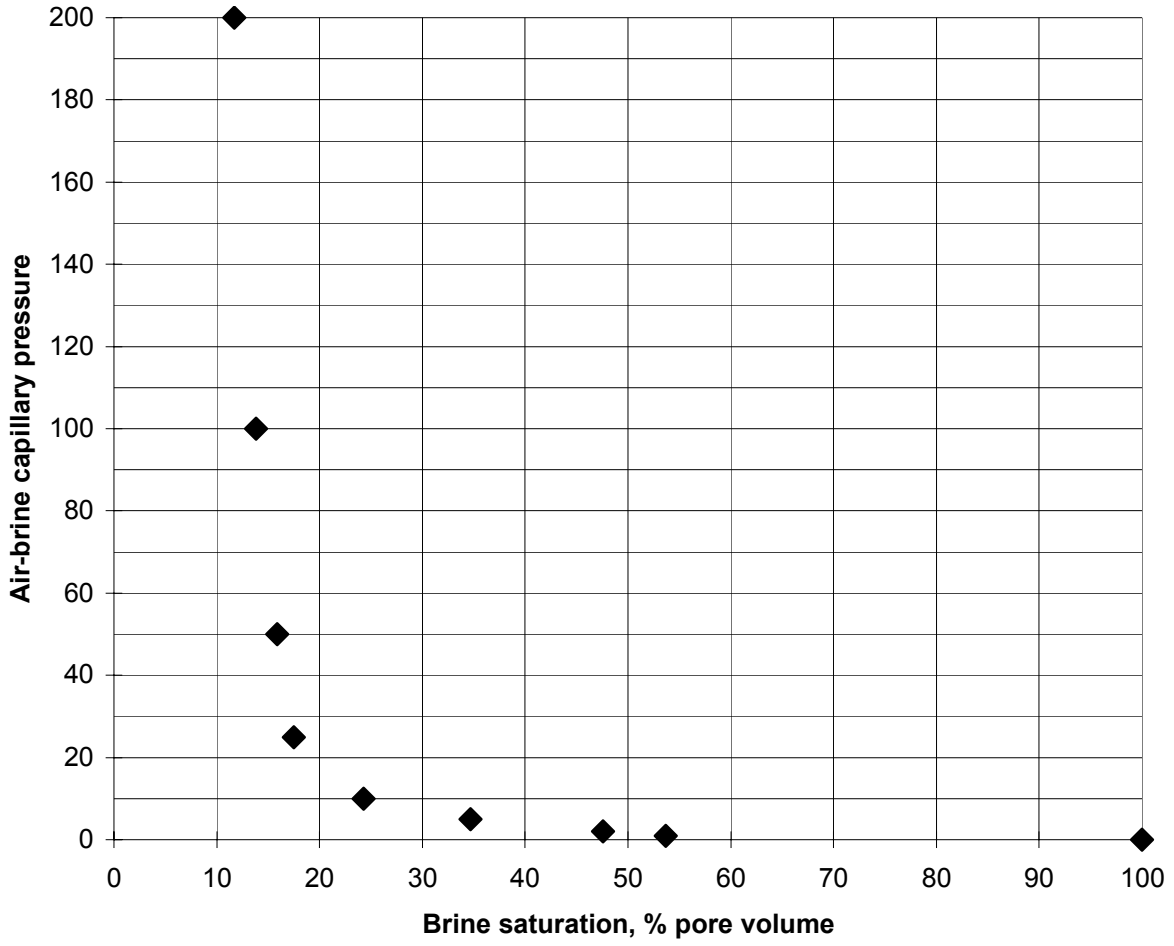

Air-brine capillary pressure by centrifuge at ambient conditions.

Sample no.	Depth (m)	Determined at Ambient Conditions				
		Kinf (md)	Kair (md)	Porosity (%)	Capillary pressure (psi)	Brine saturation (%PV)
25	2174.10	2.65	3.27	13.2	0	100.0
					1	100.0
					2	100.0
					5	100.0
					10	60.0
					25	48.5
					50	38.6
					100	35.2
					200	32.8

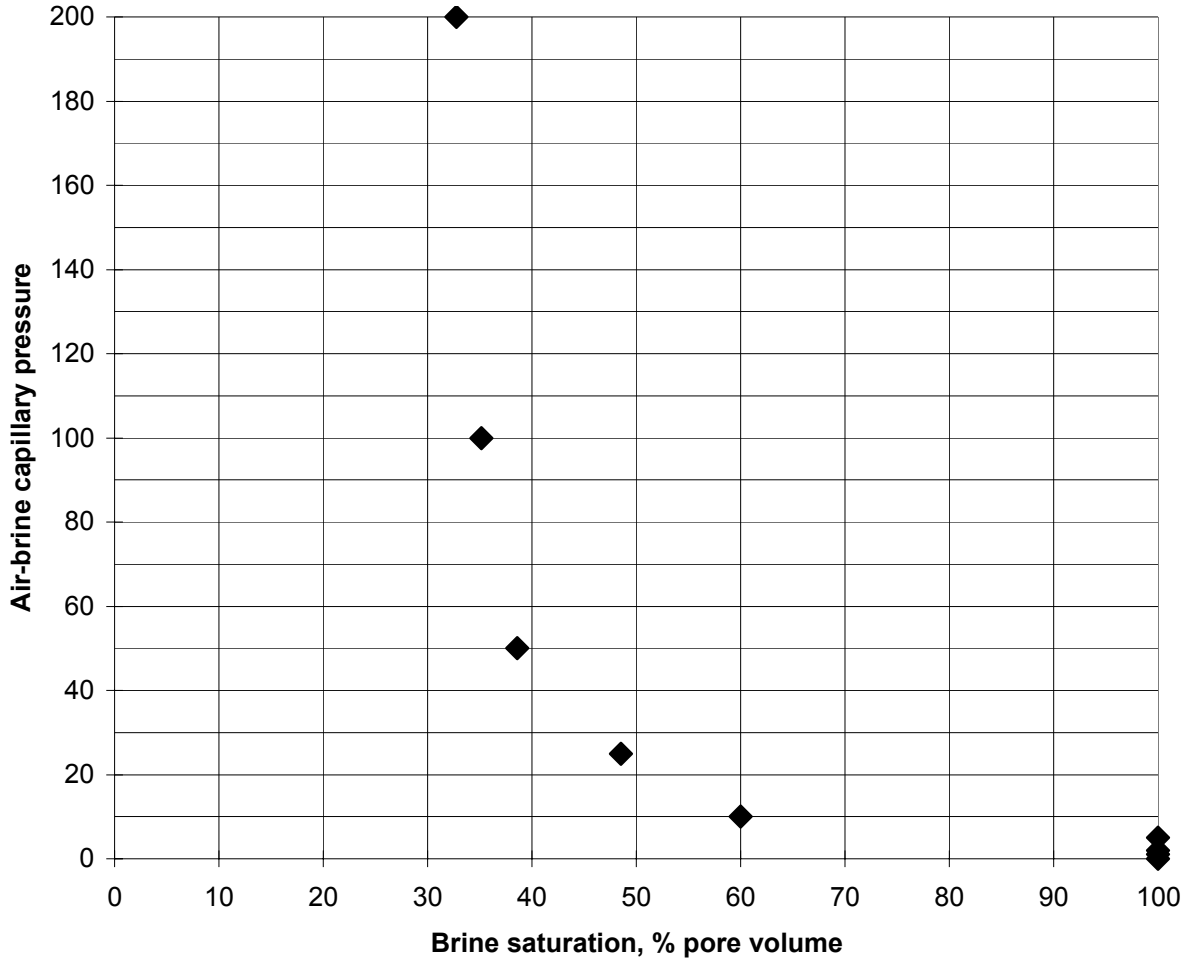

Air-brine capillary pressure by centrifuge at ambient conditions.

Sample no.	Depth (m)	Determined at Ambient Conditions				
		Kinf (md)	Kair (md)	Porosity (%)	Capillary pressure (psi)	Brine saturation (%PV)
28	2174.80	2910	3430	20.9	0	100.0
					1	41.8
					2	32.0
					5	22.5
					10	17.4
					25	13.8
					50	11.6
					100	9.7
					200	8.6

Brine saturation (Sw) at 200 psi is extrapolated.

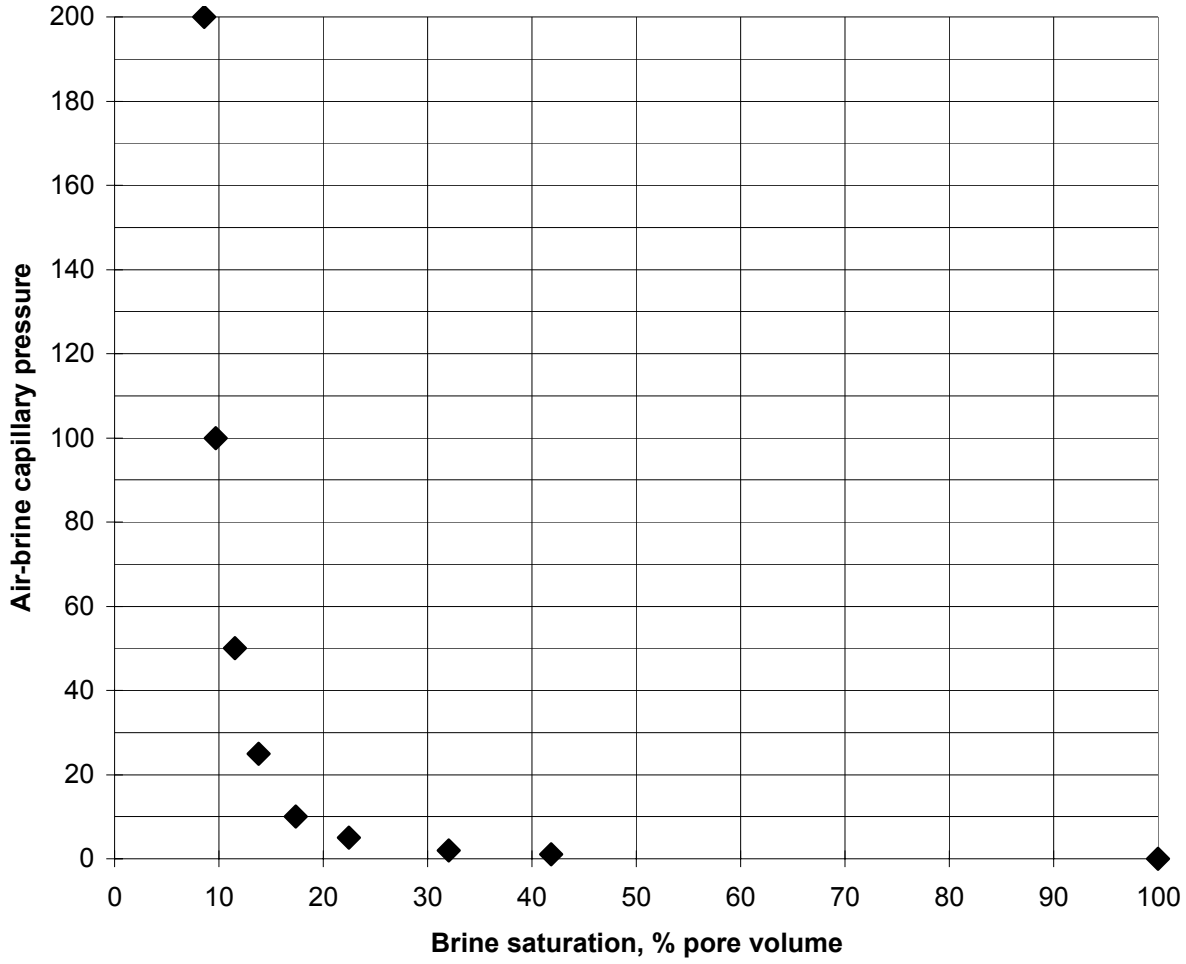

Air-brine capillary pressure by centrifuge at ambient conditions.

Sample no.	Depth (m)	Determined at Ambient Conditions				
		Kinf (md)	Kair (md)	Porosity (%)	Capillary pressure (psi)	Brine saturation (%PV)
46	2180.10	4670	4710	23.2	0	100.0
					1	35.0
					2	25.0
					5	16.0
					10	13.2
					25	11.5
					50	10.2
					100	9.1
					200	8.2

Brine saturation (Sw) at 200 psi is extrapolated.

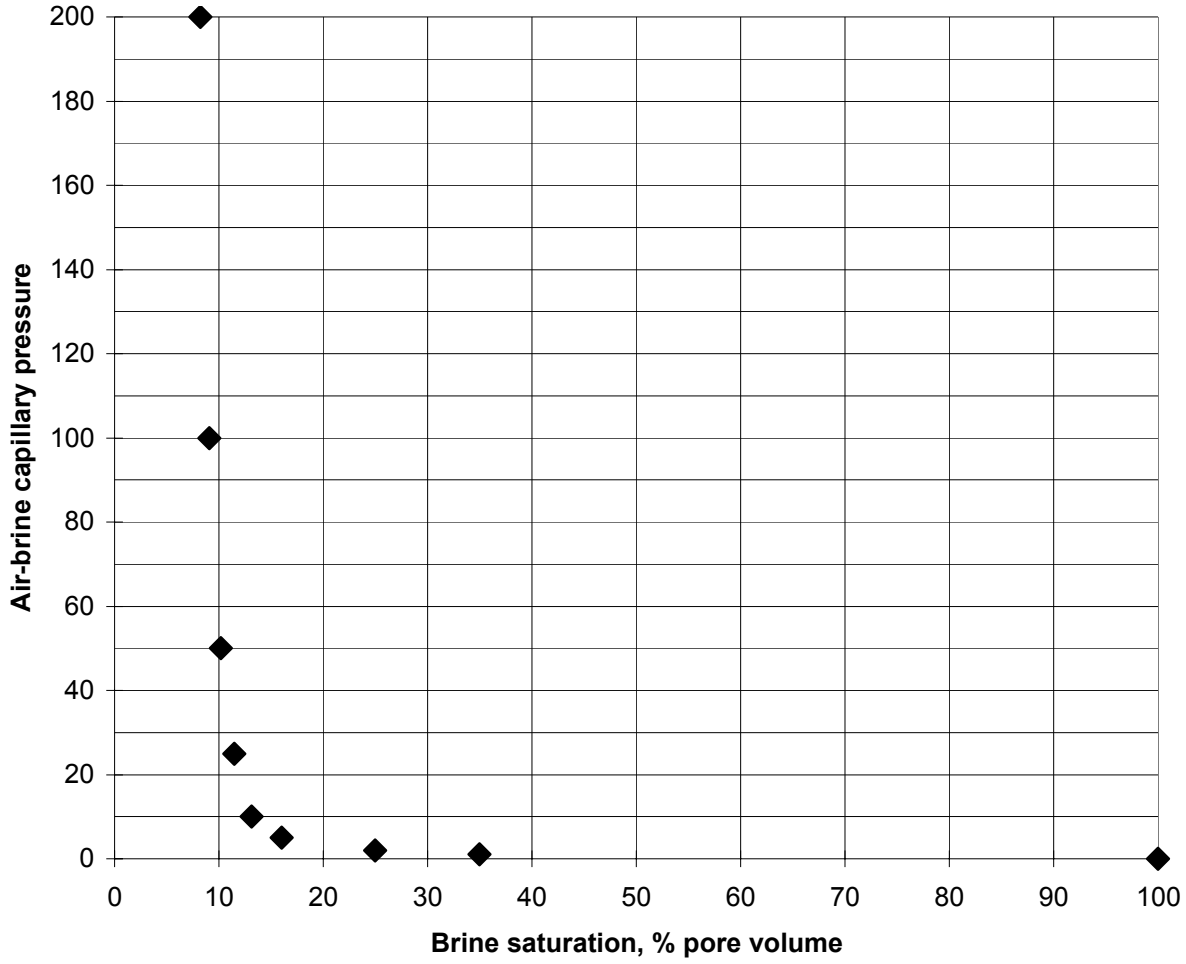

Air-brine capillary pressure by centrifuge at ambient conditions.

Sample no.	Depth (m)	Determined at Ambient Conditions				
		Kinf (md)	Kair (md)	Porosity (%)	Capillary pressure (psi)	Brine saturation (%PV)
55	2182.92	82.3	109	17.7	0	100.0
					1	79.4
					2	65.4
					5	50.5
					10	41.6
					25	32.1
					50	26.5
					100	21.8
					200	17.9

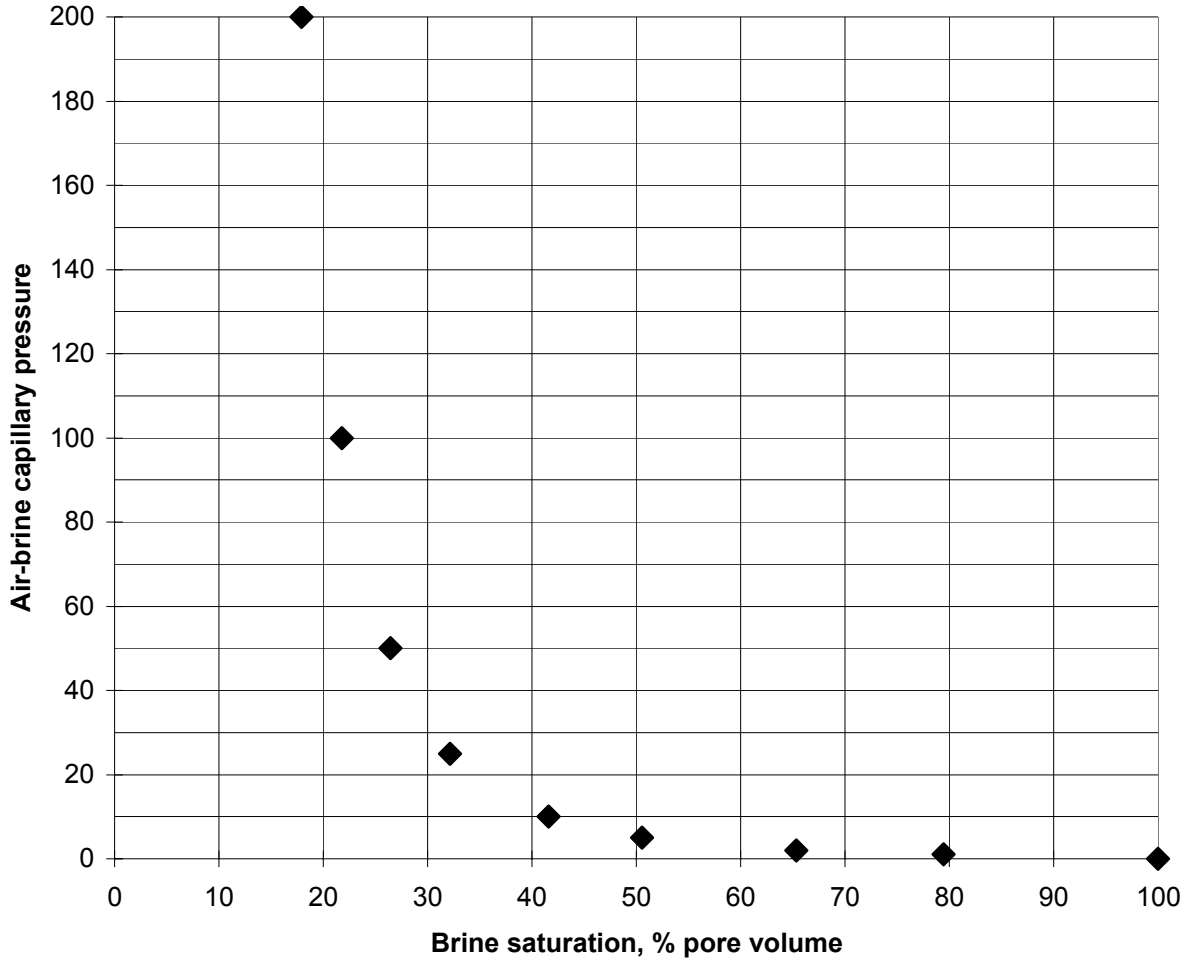

Air-brine capillary pressure by centrifuge at ambient conditions.

Sample no.	Depth (m)	Determined at Ambient Conditions				
		Kinf (md)	Kair (md)	Porosity (%)	Capillary pressure (psi)	Brine saturation (%PV)
62	2184.89	105	127	15.2	0	100.0
					1	82.0
					2	68.1
					5	53.3
					10	44.2
					25	34.6
					50	25.5
					100	21.7
					200	18.4

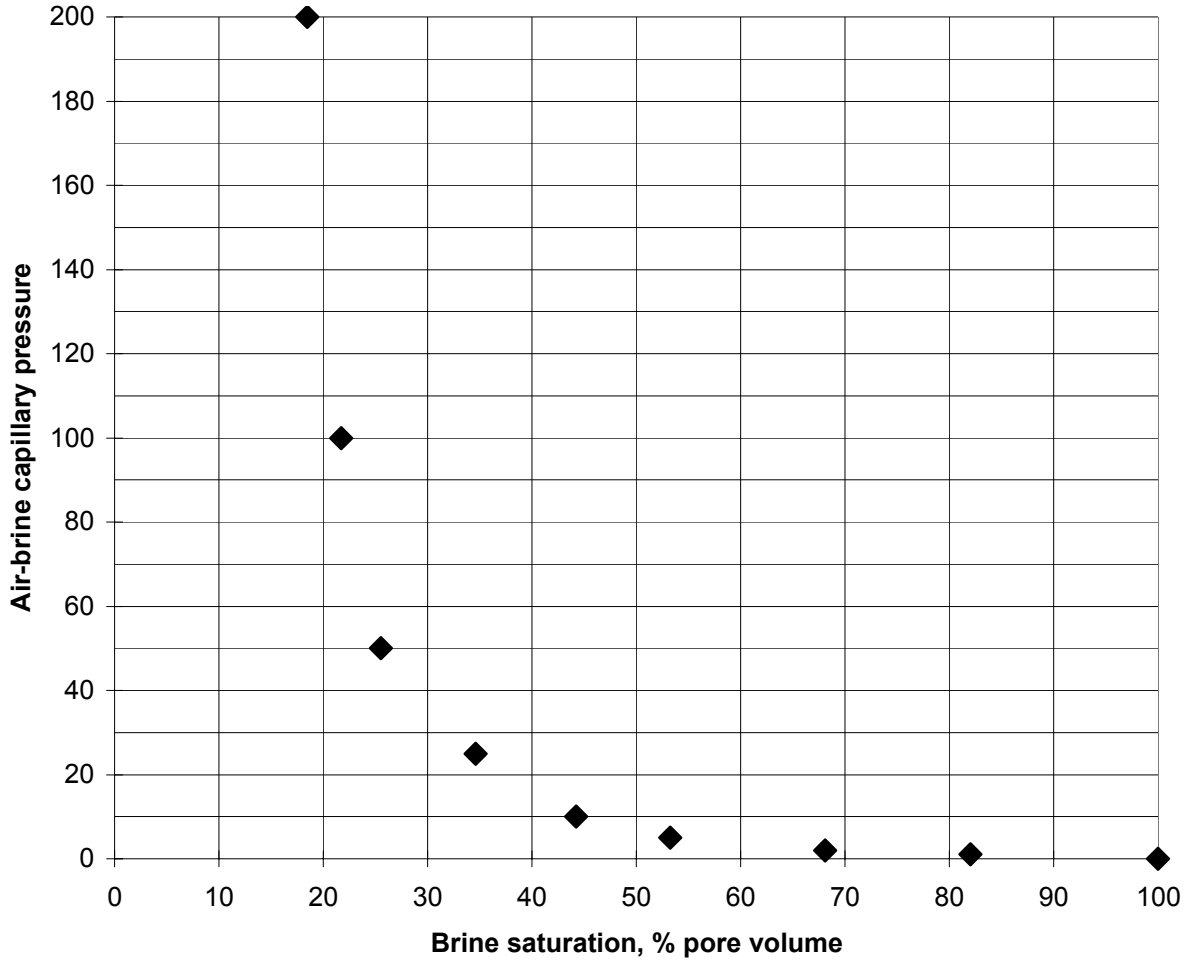

Air-brine capillary pressure by centrifuge at ambient conditions.

Sample no.	Depth (m)	Determined at Ambient Conditions				
		Kinf (md)	Kair (md)	Porosity (%)	Capillary pressure (psi)	Brine saturation (%PV)
67	2186.60	1.50	1.93	17.0	0	100.0
					1	100.0
					2	100.0
					5	100.0
					10	85.9
					25	65.9
					50	52.8
					100	41.7
					200	32.6

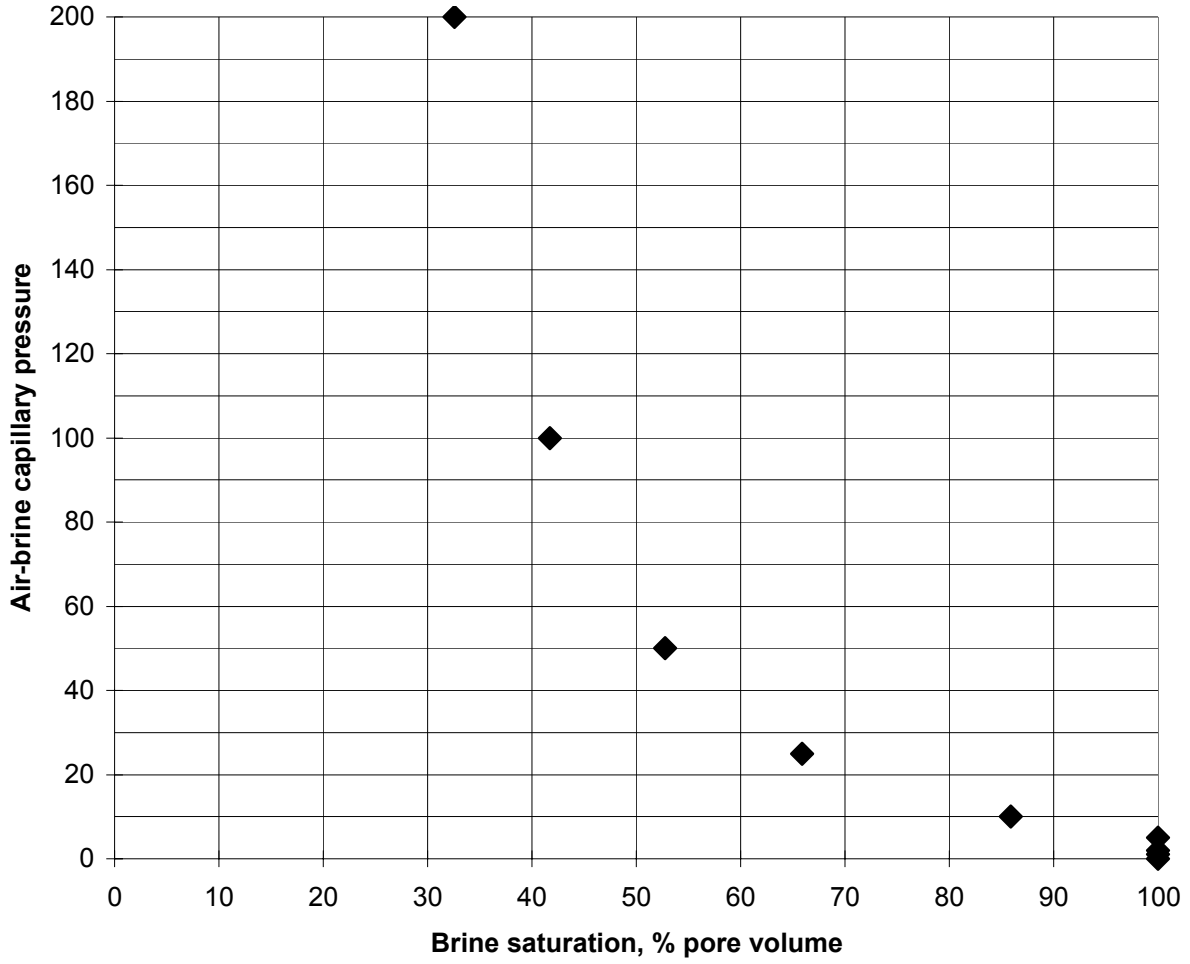

Air-brine capillary pressure by centrifuge at ambient conditions.

Sample no.	Depth (m)	Determined at Ambient Conditions				
		Kinf (md)	Kair (md)	Porosity (%)	Capillary pressure (psi)	Brine saturation (%PV)
69	2187.10	19.6	22.1	20.1	0	100.0
					1	100.0
					2	85.2
					5	64.6
					10	52.4
					25	39.7
					50	32.2
					100	26.1
					200	21.2

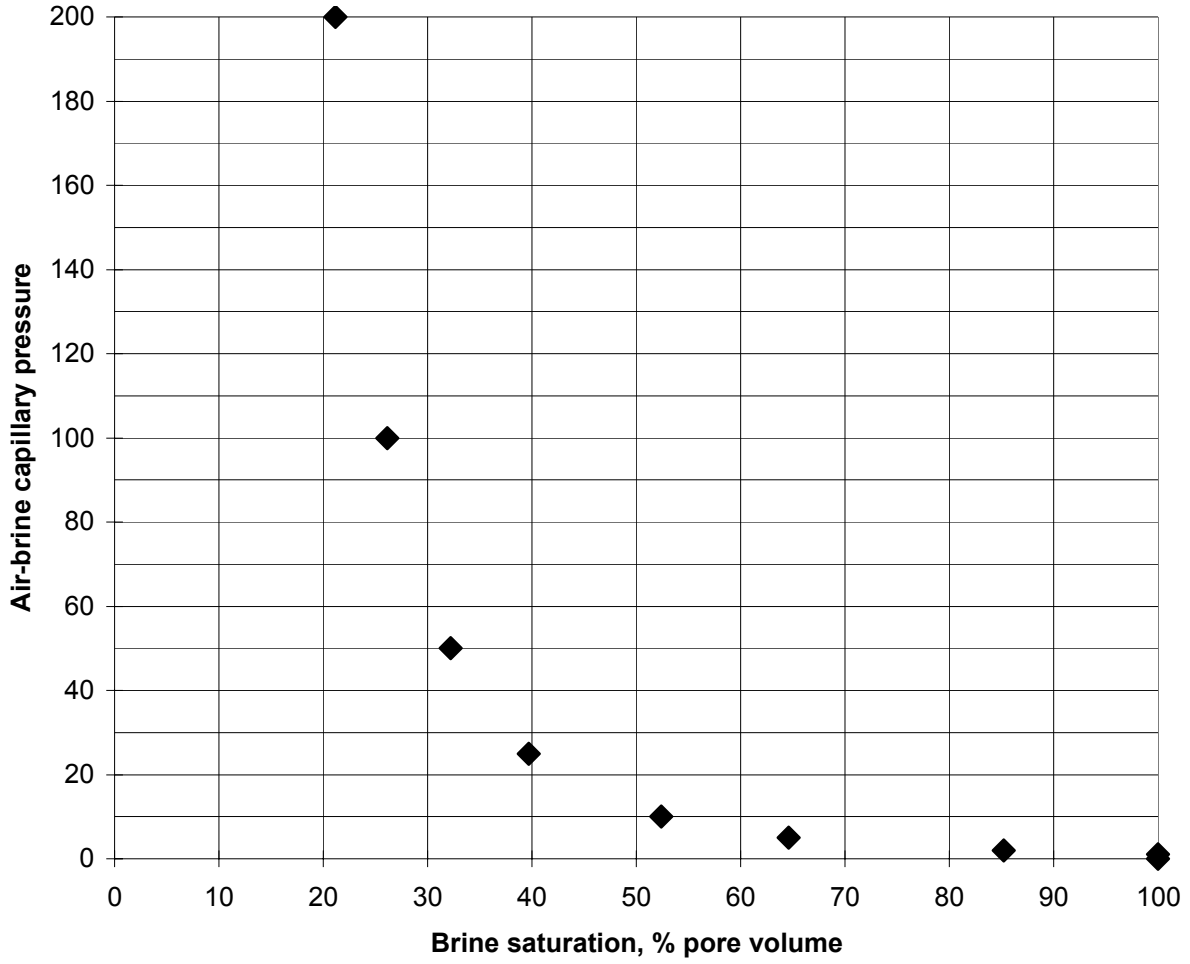

Air-brine capillary pressure by centrifuge at ambient conditions.

Sample no.	Depth (m)	Determined at Ambient Conditions				
		Kinf (md)	Kair (md)	Porosity (%)	Capillary pressure (psi)	Brine saturation (%PV)
80	2192.71	515	524	21.1	0	100.0
					1	57.9
					2	44.4
					5	31.2
					10	23.9
					25	16.8
					50	14.4
					100	12.2
					200	11.2

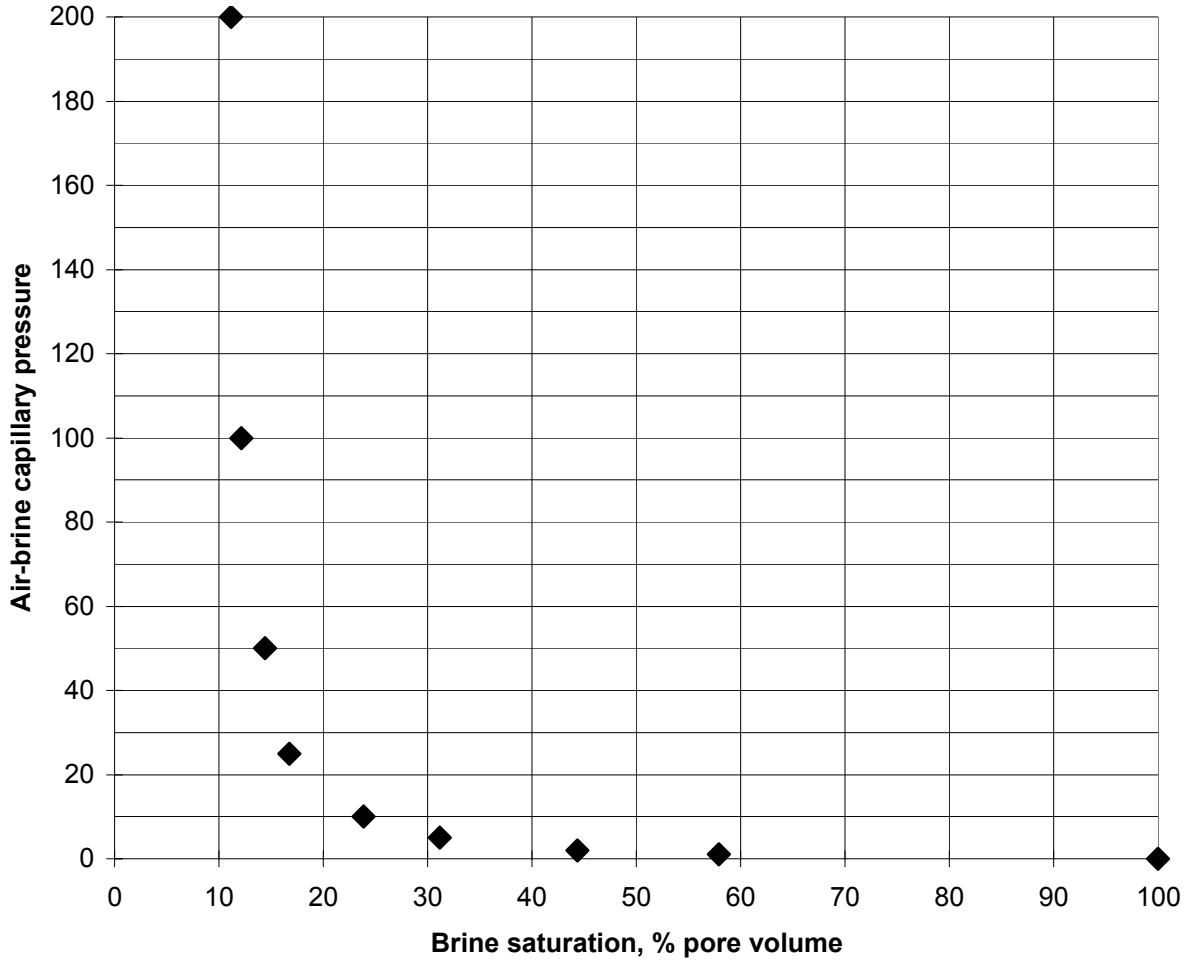

Air-brine capillary pressure by centrifuge at ambient conditions.

Sample no.	Depth (m)	Determined at Ambient Conditions				
		Kinf (md)	Kair (md)	Porosity (%)	Capillary pressure (psi)	Brine saturation (%PV)
83	2193.59	240	251	18.4	0	100.0
					1	60.3
					2	46.4
					5	32.9
					10	27.1
					25	22.3
					50	19.3
					100	16.7
					200	14.4

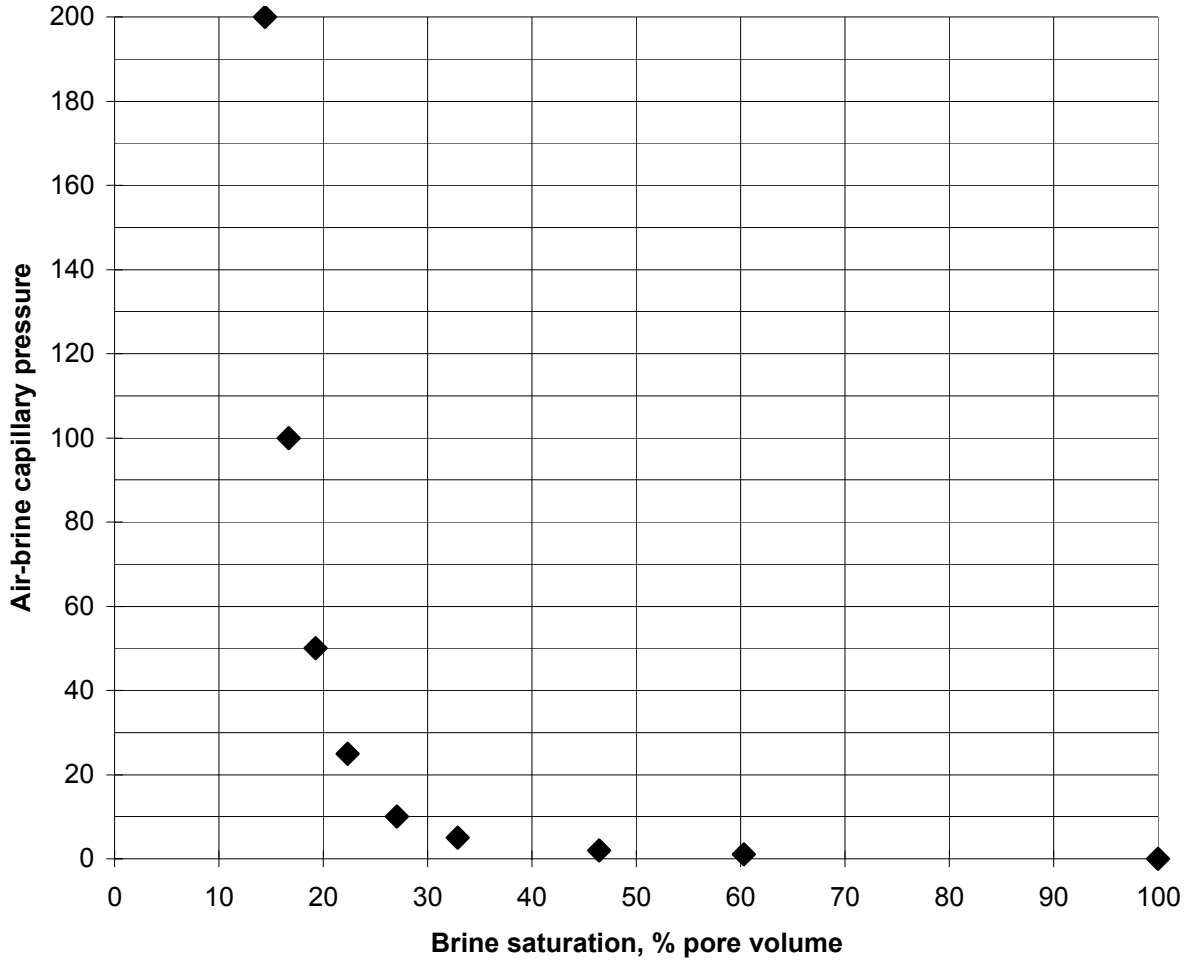

Comparison of air-brine centrifuge capillary pressure data at ambient versus NOBP

Sample no.	Depth (m)	Kair (md)	Porosity (%)	AIR - BRINE CAPILLARY PRESSURE (PSI)							
				0 psi	1 psi	2 psi	5 psi	10 psi	25 psi	50 psi	100 psi
				END FACE SATURATION Sw (%PV)							
14 (amb)	2171.19	99.5	21.8	100	88.3	72.0	54.9	44.8	34.2	28.0	23.2
14 (OB)	2171.19	94.7	21.4	100	81.2	66.5	51.1	41.8	32.1	26.3	21.5
22 (amb)	2173.40	0.483	11.7	100	100	100	100	82.3	65.0	54.4	45.5
22 (OB)	2173.40	0.298	11.3	100	100	100	100	86.0	65.4	53.1	43.2
25 (amb)	2174.10	3.27	13.2	100	100	100	100	60.0	48.5	38.6	35.2
25 (OB)	2174.10	2.67	12.8	100	100	100	100	60.4	48.6	41.3	35.1
46 (amb)	2180.10	4710	23.2	100	35.0	25.0	16.0	13.2	11.5	10.2	9.1
46 (OB)	2180.10	3980	22.5	100	38.0	29.3	20.8	15.7	11.5	10.4	9.6
62 (amb)	2184.89	127	15.2	100	82.0	68.1	53.3	44.2	34.6	25.5	21.7
62 (OB)	2184.89	111	14.6	100	73.4	59.6	45.2	36.7	29.8	25.7	22.1
80 (amb)	2192.71	524	21.1	100	57.9	44.4	31.2	23.9	16.8	14.4	12.2
80 (OB)	2192.71	500	20.7	100	53.8	41.3	29.1	22.3	14.6	13.3	12.4

(amb) : ambient conditions
(OB) : overburden pressure conditions, 1910 psi NOBP

Air-brine capillary pressure by centrifuge at 1910 psi NOBP.

Sample no.	Depth (m)	Determined at 1910 psi NOBP				
		Kinf (md)	Kair (md)	Porosity (%)	Capillary pressure (psi)	Brine saturation (%PV)
14	2171.19	88.8	94.7	21.4	0	100.0
					1	81.2
					2	66.5
					5	51.1
					10	41.8
					25	32.1
					50	26.3
					100	21.5

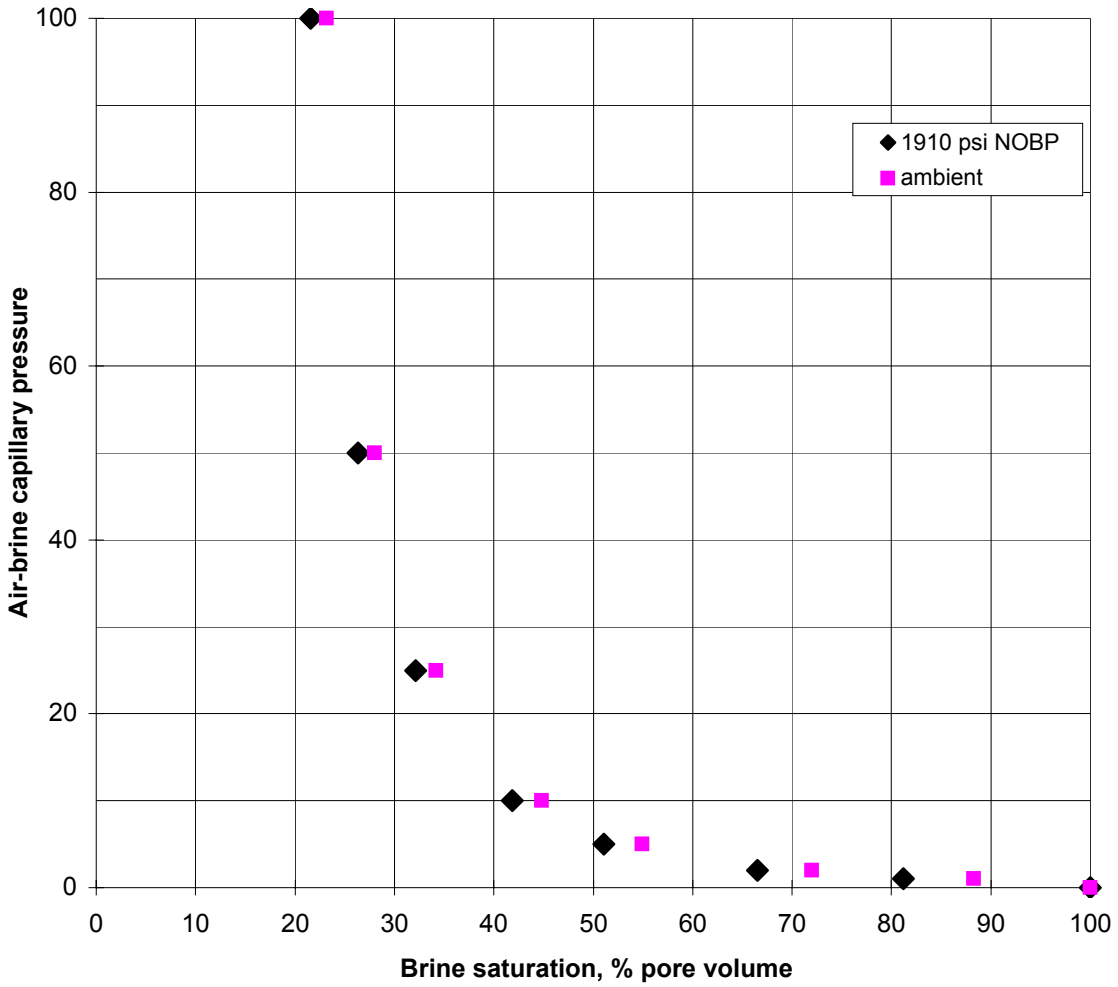

Air-brine capillary pressure by centrifuge at 1910 psi NOBP.

Sample no.	Depth (m)	Determined at 1910 psi NOBP				
		Kinf (md)	Kair (md)	Porosity (%)	Capillary pressure (psi)	Brine saturation (%PV)
22	2173.40	0.188	0.298	11.3	0	100.0
					1	100.0
					2	100.0
					5	100.0
					10	86.0
					25	65.4
					50	53.1
					100	43.2

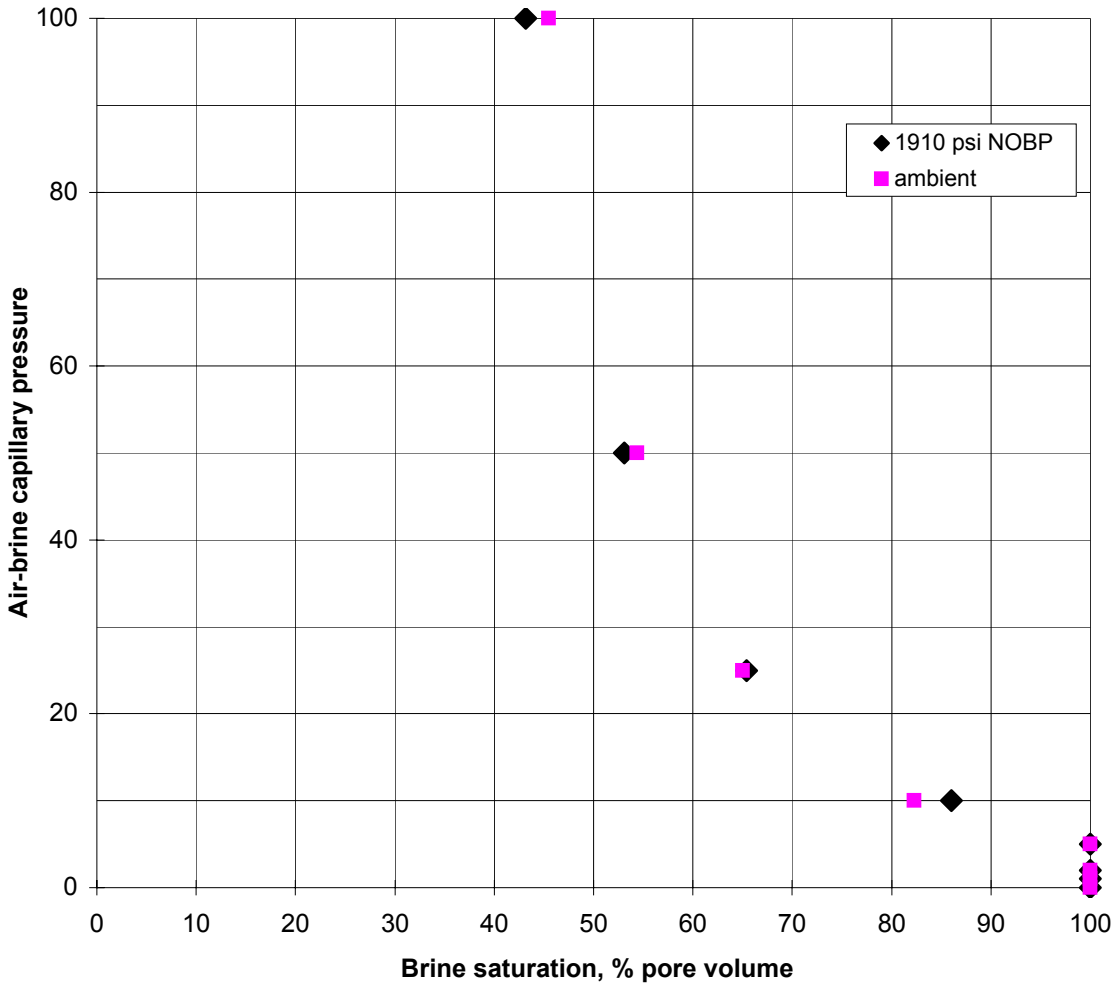

Air-brine capillary pressure by centrifuge at 1910 psi NOBP.

Sample no.	Depth (m)	Determined at 1910 psi NOBP				
		Kinf (md)	Kair (md)	Porosity (%)	Capillary pressure (psi)	Brine saturation (%PV)
25	2174.10	2.14	2.67	12.8	0	100.0
					1	100.0
					2	100.0
					5	100.0
					10	60.4
					25	48.6
					50	41.3
					100	35.1

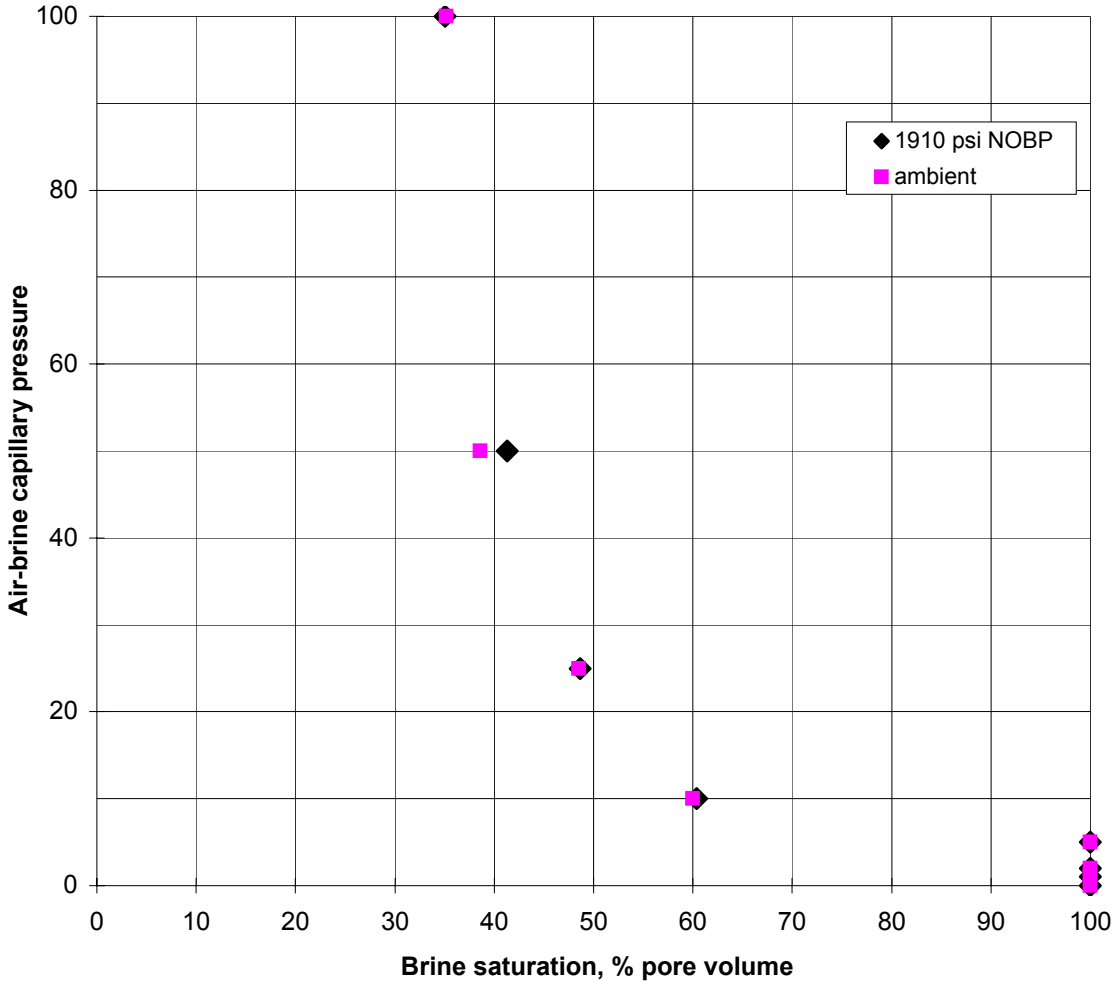

Air-brine capillary pressure by centrifuge at 1910 psi NOBP.

Sample no.	Depth (m)	Determined at 1910 psi NOBP				
		Kinf (md)	Kair (md)	Porosity (%)	Capillary pressure (psi)	Brine saturation (%PV)
46	2180.10	3370	3980	22.5	0	100.0
					1	38.0
					2	29.3
					5	20.8
					10	15.7
					25	11.5
					50	10.4
					100	9.6

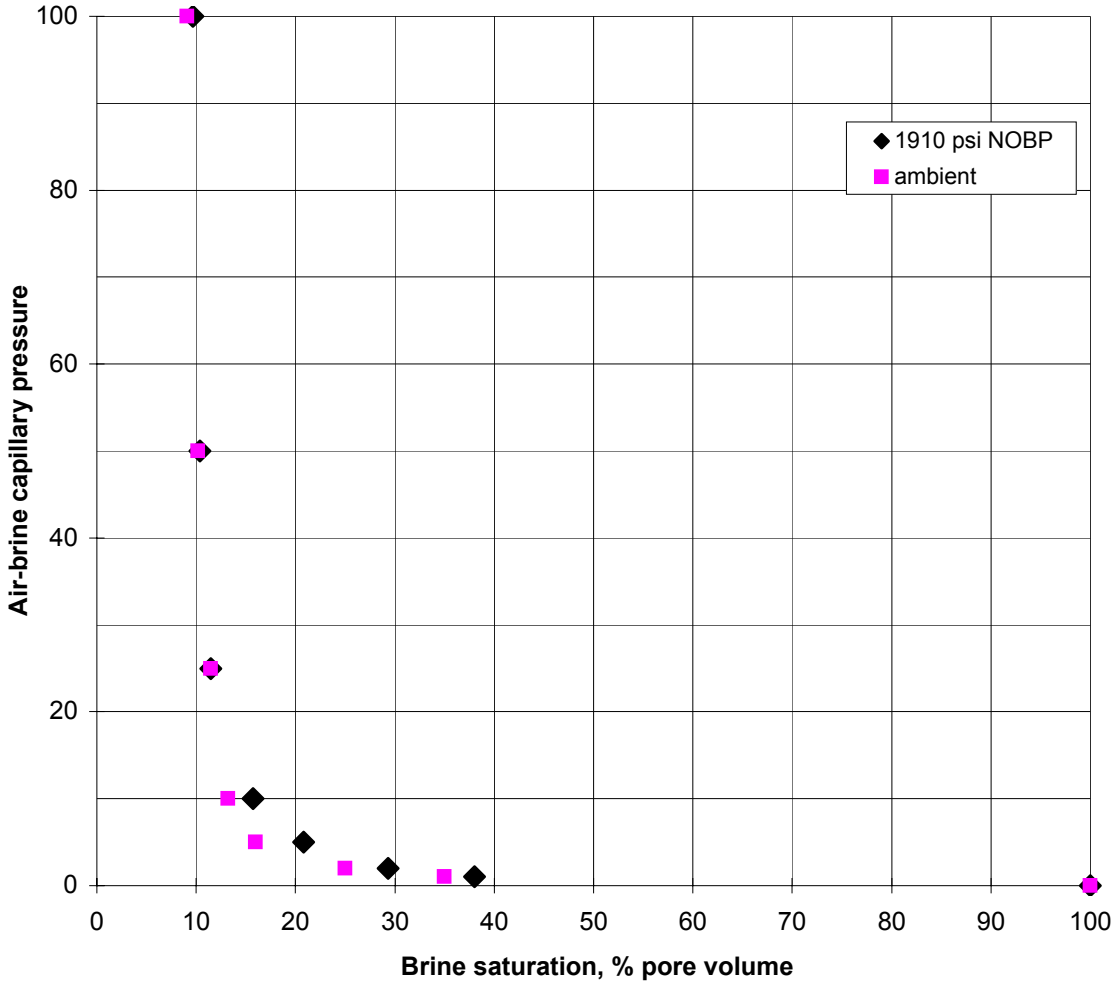

Air-brine capillary pressure by centrifuge at 1910 psi NOBP.

Sample no.	Depth (m)	Determined at 1910 psi NOBP				
		Kinf (md)	Kair (md)	Porosity (%)	Capillary pressure (psi)	Brine saturation (%PV)
62	2184.89	92.8	111	14.6	0	100.0
					1	73.4
					2	59.6
					5	45.2
					10	36.7
					25	29.8
					50	25.7
					100	22.1

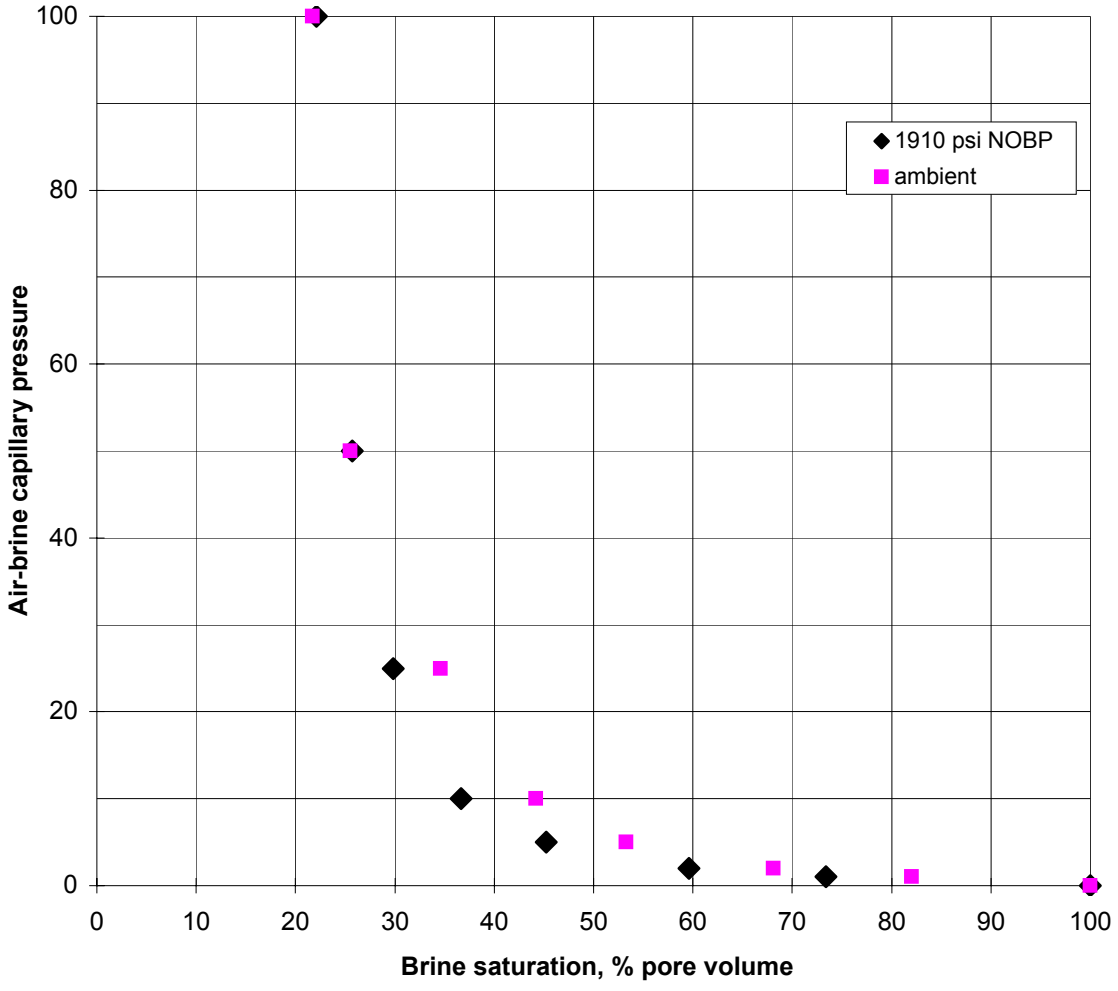

Air-brine capillary pressure by centrifuge at 1910 psi NOBP.

Sample no.	Depth (m)	Determined at 1910 psi NOBP				
		Kinf (md)	Kair (md)	Porosity (%)	Capillary pressure (psi)	Brine saturation (%PV)
80	2192.71	491	500	20.7	0	100.0
					1	53.8
					2	41.3
					5	29.1
					10	22.3
					25	14.6
					50	13.3
					100	12.4

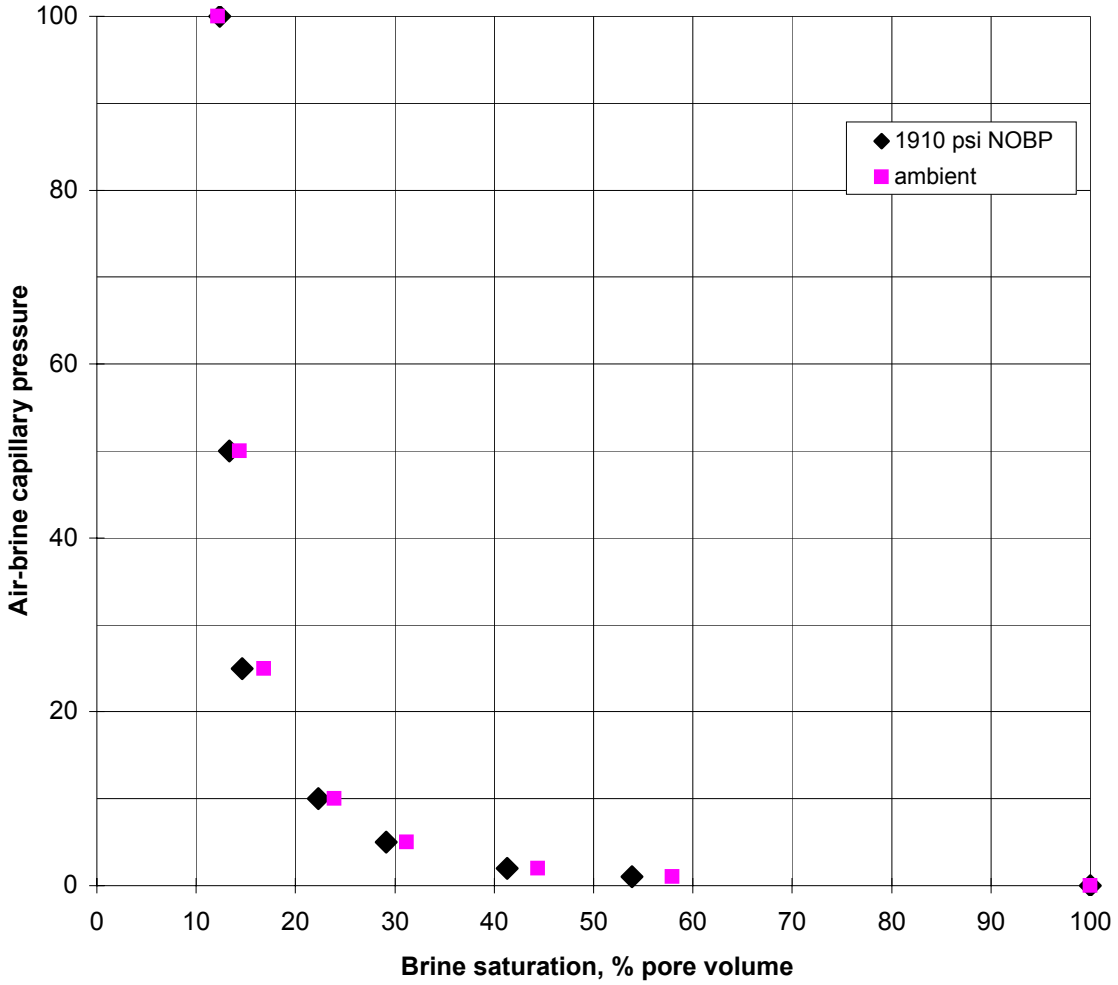

SECTION 4
RELATIVE PERMEABILITY

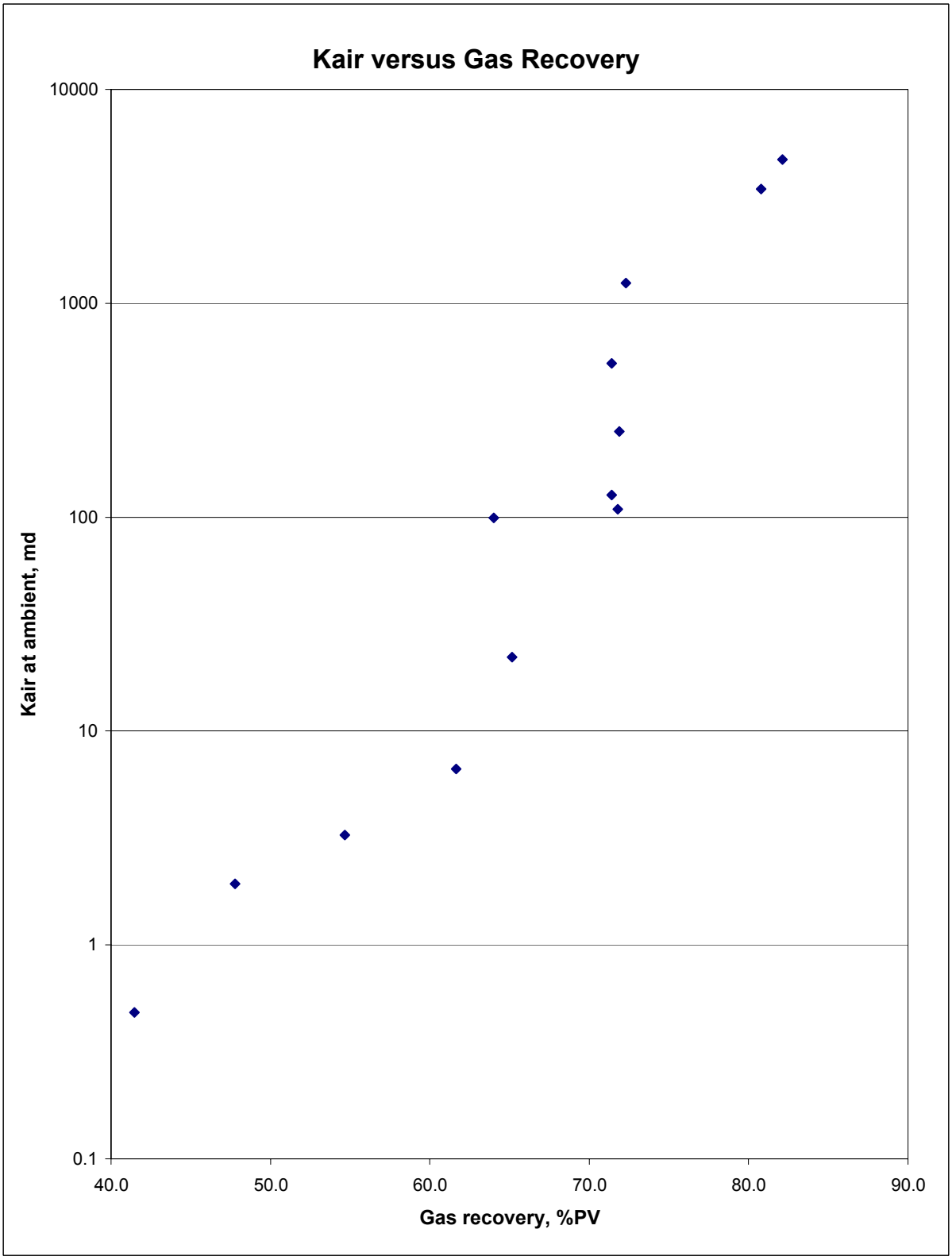
Kair versus Gas Recovery
10000
1000
100
10
1
0.1
Kair at ambient, md
40.0
50.0
60.0
70.0
80.0
90.0
Gas recovery, %PV

Summary of the WATER-GAS relative permeability by centrifuge (end-point) analysis results determined at ambient conditions.

Sample No.	Depth (m)	Kair at ambient (md)	Porosity at ambient (%)	INITIAL CONDITIONS			TERMINAL CONDITIONS			
				Average Swi (% pv)	Initial gas in place (% pv)	Kgas at Swi (md)	Sgr (% pv)	Gas Recovery (% pv)	Gas Recovery (% IIGP)	Kw at Sgr (md)
5	2166.81	6.66	17.8	30.3	69.7	4.70	8.1	61.7	88.5	1.38
14	2171.19	99.5	21.8	26.7	73.3	85.3	9.3	64.0	87.3	22.3
22	2173.40	0.483	11.7	53.0	47.0	0.165	5.5	41.5	88.2	0.057
24	2173.83	1240	18.5	15.9	84.1	1120	11.8	72.3	86.0	365
25	2174.10	3.27	13.2	40.4	59.6	2.90	4.9	54.7	91.7	0.567
28	2174.80	3430	20.9	11.1	88.9	3151	8.1	80.8	90.9	1442
46	2180.10	4710	23.2	9.9	90.1	3344	8.0	82.1	91.1	1615
55	2182.92	109	17.7	21.0	79.0	106	7.2	71.8	90.9	43.0
62	2184.89	127	15.2	21.0	79.0	120	7.6	71.4	90.4	39.0
67	2186.60	1.93	17.0	48.7	51.3	1.40	3.5	47.8	93.1	0.490
69	2187.10	22.1	20.1	30.2	69.8	15.1	4.7	65.2	93.3	5.15
80	2192.71	524	21.1	13.7	86.3	481	14.9	71.4	82.7	138
83	2193.59	251	18.4	16.8	83.2	246	11.3	71.9	86.4	45.5

SECTION 5
ROCK (PORE VOLUME) COMPRESSIBILITY

Rock (Pore Volume) Compressibility

Sample number	14A
Depth, metres	2171.24
Permeability to air , md	46.5
Porosity, %	19.9
Grain Density, gm/cc	2.67

Confining Stress (psi)	Porosity (%)	Compressibility (pv/pv/psi)	
		Hydrostatic	Uniaxial *
400	19.9	-	-
500	19.9	28.31E-6	17.27E-6
600	19.8	26.38E-6	16.09E-6
700	19.8	24.60E-6	15.01E-6
800	19.7	22.96E-6	14.01E-6
900	19.7	21.44E-6	13.08E-6
1000	19.7	20.04E-6	12.22E-6
1200	19.6	17.54E-6	10.70E-6
1400	19.5	15.41E-6	9.40E-6
1600	19.5	13.59E-6	8.29E-6
1800	19.5	12.03E-6	7.34E-6
2000	19.4	10.71E-6	6.53E-6
2500	19.3	8.17E-6	4.98E-6
3000	19.3	6.46E-6	3.94E-6
3500	19.2	5.31E-6	3.24E-6
4000	19.2	4.53E-6	2.76E-6
4500	19.2	4.00E-6	2.44E-6
5000	19.2	3.64E-6	2.22E-6
6000	19.1	3.23E-6	1.97E-6
7000	19.1	3.08E-6	1.88E-6

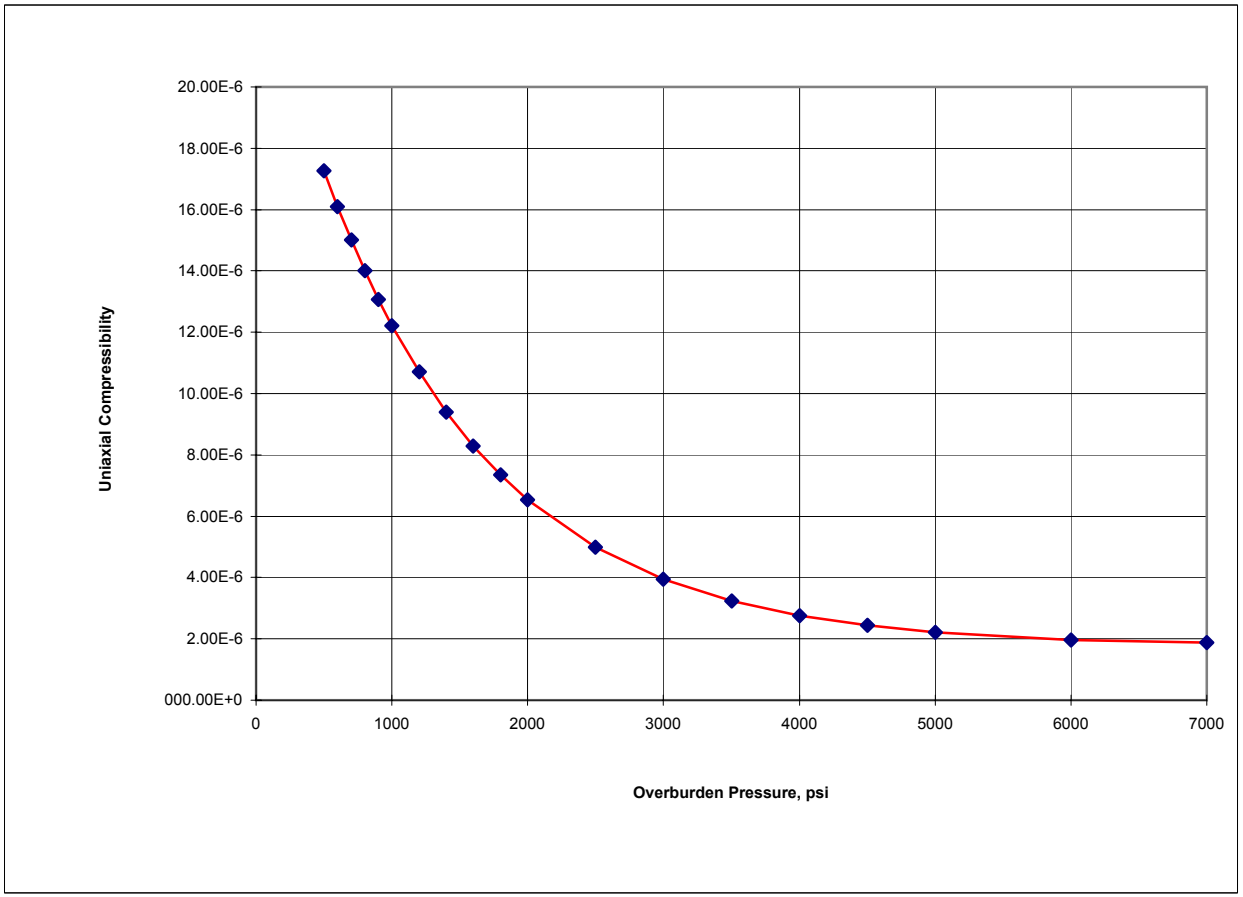

Compressibility under uniaxial loading conditions, transformed from hydrostatic data as per Teeuw, Dirk : "Prediction Of Formation Compaction From Laboratory Compressibility D
Trans: AIME (1971) 251, 263-271

Rock (Pore Volume) Compressibility

Sample number	22A
Depth, metres	2173.34
Permeability to air , md	0.198
Porosity, %	10.4
Grain Density, gm/cc	2.69

Confining Stress (psi)	Porosity (%)	Compressibility (pv/pv/psi)	
		Hydrostatic	Uniaxial *
400	10.4	-	-
500	10.4	33.00E-6	20.13E-6
600	10.4	31.32E-6	19.10E-6
700	10.4	29.73E-6	18.14E-6
800	10.4	28.23E-6	17.22E-6
900	10.3	26.82E-6	16.36E-6
1000	10.3	25.48E-6	15.54E-6
1200	10.2	23.03E-6	14.05E-6
1400	10.2	20.85E-6	12.72E-6
1600	10.1	18.90E-6	11.53E-6
1800	10.1	17.16E-6	10.47E-6
2000	10.1	15.62E-6	9.53E-6
2500	10.0	12.44E-6	7.59E-6
3000	10.0	10.06E-6	6.14E-6
3500	9.9	8.27E-6	5.05E-6
4000	9.9	6.93E-6	4.23E-6
4500	9.9	5.92E-6	3.61E-6
5000	9.9	5.17E-6	3.15E-6
6000	9.9	4.17E-6	2.54E-6
7000	9.9	3.60E-6	2.19E-6

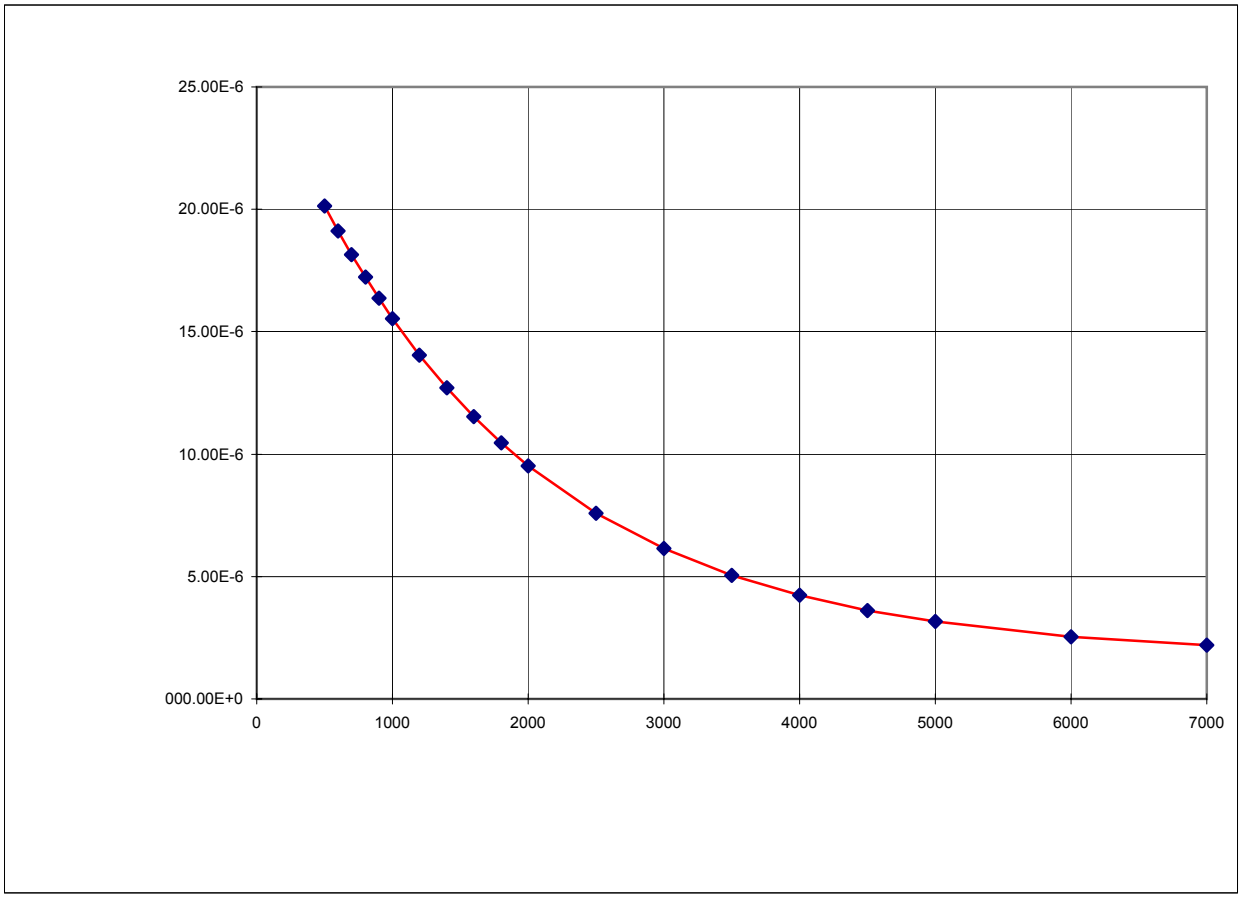

Compressibility under uniaxial loading conditions, transformed from hydrostatic data as per Teeuw, Dirk : "Prediction Of Formation Compaction From Laboratory Compressibility D
Trans: AIME (1971) 251, 263-271

Rock (Pore Volume) Compressibility

Sample number	46A
Depth, metres	2180.14
Permeability to air , md	2650
Porosity, %	22.7
Grain Density, gm/cc	2.65

Confining Stress (psi)	Porosity (%)	Compressibility (pv/pv/psi)	
		Hydrostatic	Uniaxial *
400	22.7	-	-
500	22.5	69.07E-6	42.14E-6
600	22.4	60.34E-6	36.81E-6
700	22.3	52.76E-6	32.18E-6
800	22.3	46.18E-6	28.17E-6
900	22.2	40.47E-6	24.69E-6
1000	22.1	35.52E-6	21.67E-6
1200	22.1	27.48E-6	16.77E-6
1400	22.0	21.43E-6	13.07E-6
1600	21.9	16.88E-6	10.29E-6
1800	21.9	13.44E-6	8.20E-6
2000	21.8	10.85E-6	6.62E-6
2500	21.7	6.84E-6	4.17E-6
3000	21.7	4.86E-6	2.97E-6
3500	21.6	3.89E-6	2.37E-6
4000	21.6	3.40E-6	2.07E-6
5000	21.5	3.03E-6	1.85E-6
6000	21.5	2.93E-6	1.79E-6
7000	21.4	2.89E-6	1.77E-6

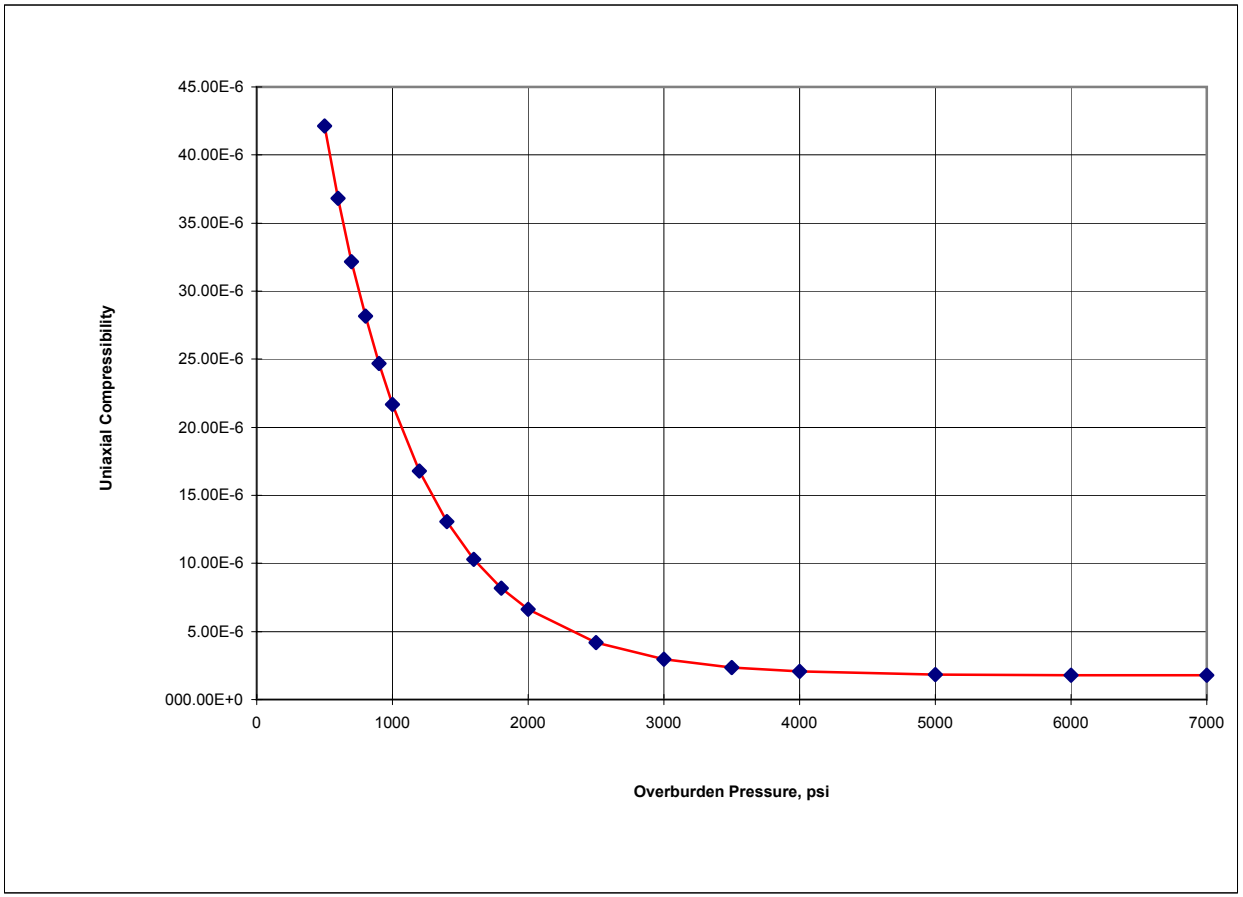

Compressibility under uniaxial loading conditions, transformed from hydrostatic data as per Teeuw, Dirk : "Prediction Of Formation Compaction From Laboratory Compressibility D
Trans: AIME (1971) 251, 263-271

Rock (Pore Volume) Compressibility

Sample number	62A
Depth, metres	2184.76
Permeability to air , md	192
Porosity, %	12.4
Grain Density, gm/cc	2.66

Confining Stress (psi)	Porosity (%)	Compressibility (pv/pv/psi)	
		Hydrostatic	Uniaxial *
400	12.4	-	-
500	12.3	82.33E-6	50.22E-6
600	12.2	72.90E-6	44.47E-6
700	12.1	64.58E-6	39.40E-6
800	12.0	57.26E-6	34.93E-6
900	12.0	50.81E-6	30.99E-6
1000	11.9	45.12E-6	27.52E-6
1200	11.9	35.70E-6	21.77E-6
1400	11.8	28.38E-6	17.31E-6
1600	11.8	22.70E-6	13.84E-6
1800	11.7	18.28E-6	11.15E-6
2000	11.7	14.86E-6	9.06E-6
2500	11.6	9.28E-6	5.66E-6
3000	11.6	6.31E-6	3.85E-6
3500	11.5	4.73E-6	2.88E-6
4000	11.5	3.88E-6	2.37E-6
4500	11.5	3.43E-6	2.09E-6
5000	11.4	3.19E-6	1.94E-6
6000	11.4	2.98E-6	1.82E-6
7000	11.4	2.91E-6	1.77E-6

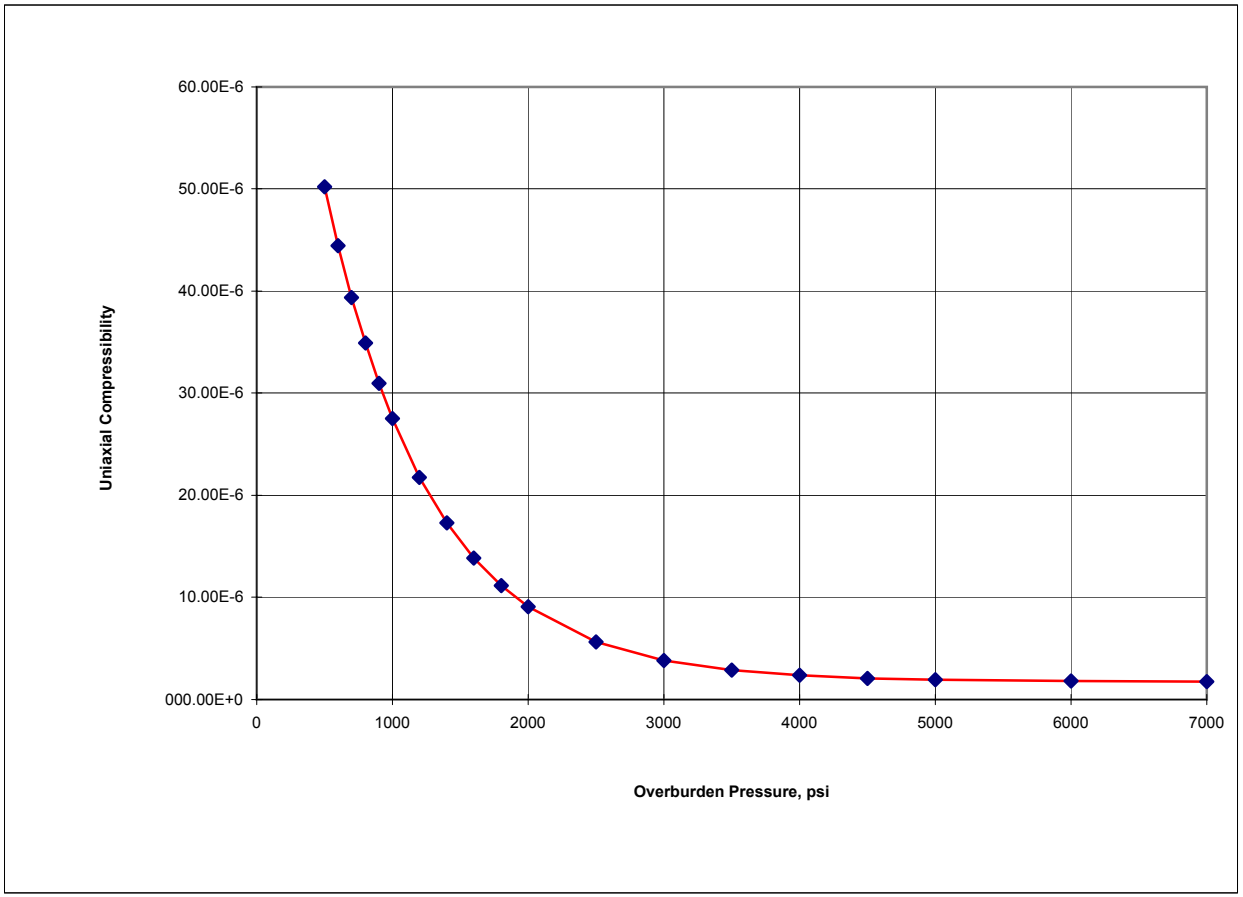

Compressibility under uniaxial loading conditions, transformed from hydrostatic data as per Teeuw, Dirk : "Prediction Of Formation Compaction From Laboratory Compressibility D
Trans: AIME (1971) 251, 263-271

APPENDIX-1

SUMMARY OF LABORATORY PROCEDURES

SUMMARY OF LABORATORY PROCEDURES

Sample selections were made by Mr Jon Kelly of Woodside on two separate occasions, in an attachment to an e-mail dated 28th August 2001 and in an e-mail dated 7th May 2002. The initial request covered the core plug samples whilst the latter covered the MSCT samples. These samples had originally undergone routine core analysis and so had been cleaned, dried and stored at ambient conditions following analysis.

All samples were screened visually initially, to determine if they were of suitable shape and size. Visual screening was followed by computerised tomography (CT) to detect any fractures or other heterogeneities which would render the samples unsuitable for analysis. Samples which failed the screening stage were replaced. Selected replacements were agreed by Woodside and they also underwent visual and CT screening.

For rock (pore volume) compressibility tests, additional duplicate samples (suffix "A") were drilled adjacent to the selected routine core analysis plugs. Following visual and CT screening, these duplicate samples were cleaned in methanol to remove residual salts. These samples were dried at 90°C in a non-humidified oven prior to measurement of porosity and air permeability at ambient conditions (no applied overburden pressure).

All routine core analysis samples which had been selected for analysis were also re-dried at 90°C and porosity, permeability, grain density values re-checked and compared to originally measured values.

A complete list of samples eventually selected for analysis and samples which failed screening is contained in SECTION 1 of this report.

Saturation

All samples undergoing analysis were evacuated and pressure saturated with a simulated formation brine of 13,500 ppm concentration (comprising 80% NaCl and 20% KCl). All samples were weighed after saturation to check measured pore volumes.

Formation Resistivity

Each fully saturated sample was loaded into a coreholder at the reservoir equivalent NOBP and the electrical resistivities measured on consecutive days until they were stable, indicating ionic eqilibrium in the pore spaces. Formation factor (FRF) and cementation exponent ("m") values were then calculated.

Each sample was then de-saturated at incrementally increasing pressures using humidified air as the displacement medium. Electrical resistivities of each sample were measured at the incrementally decreasing partial saturations. When each sample had attained electrical equilibrium at each incremental desaturation stage, values of resistivity index (RI) and saturation exponent ("n") were calculated.

The trimmed-ends of the plugs and the MSCT samples which underwent FRF and RI measurements were cleaned in methanol, dried at 60°C in a non-humidified oven and then subjected to determinations of cation exchange capacity (CEC) using the ammonium acetate wet chemistry technique on crushed sample. These CEC values were in turn used to calculate idealised "m*" and "n*" values using Waxman-Smits-Thomas equations. For comparative purposes, CEC values using similar wet chemistry technique were earlier determined on uncrushed sample splits from trim-ends of three samples which later underwent the standard "crushed" analysis.

All electrical resistivity data are presented in SECTION 2.

Following the resistivity index analysis, the samples were resaturated with the simulated formation brine for the capillary pressure analysis.

Air-brine capillary pressure by centrifuge.

Samples were each loaded into individual centrifuge coreholders. Samples were spun at incremental rotational speeds effecting capillary pressure. Each speed (RPM) was maintained for a minimum of 24 hours until production was stable. The speed was then raised to the next higher speed. Volumes of brine produced were monitored using a stroboscope.

Capillary pressure and end-face saturation data were then calculated from the raw data using data reduction techniques developed by Hassler-Brunner. These results are presented within SECTION 3 of this report.

Six of the thirteen samples which originally underwent air-brine capillary pressure (i.e #14, #22, #25, #46, #62, and #80) at ambient conditions were re-saturated (100% Sw) with the simulated formation brine. All samples were weighed after saturation to check measured pore volumes. Samples were each loaded into individual overburden centrifuge core holders and the requisite net overburden pressure (1910 psi) applied. Samples were then loaded into the centrifuge and spun at incremental rotational speeds to 3000 rpm (the maximum attainable speed in the overburden centrifuge).

Capillary pressure and end-face saturation data were then calculated from the raw data using data reduction techniques developed by Hassler-Brunner. These results are also presented in SECTION 3.

Water-gas relative permeability (end-point) analysis by centrifuge.

Following the air-brine capillary pressure analyses by centrifuge, the core plug samples were removed from the centrifuge core holders and each loaded into a hydrostatic core holder with the minimal 400 psi confining pressure (to seat sample against the sample boot) applied. Humidified nitrogen was flowed through each sample and the effective permeability to gas (Kgas) at Swi was determined.

Each sample was next loaded into individual brine-filled centrifuge cups. The samples were then spun at a maximum imbibition (equivalent to 200 psi), brine displacing air, capillary pressure to determine the end-point residual gas saturation (Sgr). The samples were removed from the centrifuge cups and the residual gas saturations were determined gravimetrically.

Each sample was then loaded into a hydrostatic core holder at 400 psi confining stress. Brine was flowed through the samples and effective permeability to brine at Sgr was then determined.
Results from the water-gas relative permeability (end-point) by centrifuge are presented in SECTION 4 of this report.

Water-gas relative permeability analysis was not performed on the MSCT samples.

Rock (pore volume) compressibility.

Four samples were selected to undergo rock (pore volume) compressibility analysis.

Each sample was evacuated and pressure saturated with the simulated formation brine. Samples were then loaded into a hydrostatic core holder and allowed to equilibrate at a low net overburden pressure. The net overburden pressure was then raised incrementally and the corresponding pore volume reductions monitored. The overburden pressure was raised to the next higher pressure only when pore volume reduction stabilised.

Hydrostatic compressibility data were then calculated from pore volume reduction data versus increasing overburden pressure. These data were converted to equivalent uniaxial loading following procedures outlined by Dirk Teeuw of Shell Research.

Results are presented in SECTION 5.

APPENDIX-2

RAWDATA FROM ELECTRICAL PROPERTIES, CAPILLARY PRESSURE AND ROCK COMPRESSIBILITY TESTS

RESISTIVITY MEASUREMENTS - RAWDATA

Sample	MSCT2
PV (NOBP),cc	1.779
Porosity (NOBP).%	19.3
Length,cm	2.18
Diameter,cm	2.35
Brine density,g/cc	1.007
Brine Rw.ohm-m	0.415

Saturation %PV	Rt ohm-m
60.1	27.96
47.9	34.23
35.6	50.77
32.5	52.47
28.8	61.09
18.4	116.19

Sample	MSCT3
PV (NOBP),cc	1.723
Porosity (NOBP).%	19.3
Length,cm	2.13
Diameter,cm	2.33
Brine density,g/cc	1.007
Brine Rw.ohm-m	0.415

Saturation %PV	Rt ohm-m
56.6	33.79
41.1	54.73
28.6	91.24
25.5	114.59
19.3	183.12

Sample	MSCT7
PV (NOBP),cc	1.912
Porosity (NOBP).%	20.5
Length,cm	2.23
Diameter,cm	2.35
Brine density,g/cc	1.007
Brine Rw.ohm-m	0.415

Saturation %PV	Rt ohm-m
54.6	40.53
48.4	50.72
42.7	57.53
37.6	64.79
21.7	110.54

Sample	MSCT10
PV (NOBP),cc	1.965
Porosity (NOBP).%	20.3
Length,cm	2.32
Diameter,cm	2.35
Brine density,g/cc	1.007
Brine Rw.ohm-m	0.415

Saturation %PV	Rt ohm-m
66.6	22.78
55.5	32.28
47.1	39.02
24.8	63.11
20.9	72.49

Sample	5
PV (NOBP),cc	9.201
Porosity (NOBP).%	17.3
Length,cm	4.95
Diameter,cm	3.73
Brine density,g/cc	1.007
Brine Rw.ohm-m	0.415

Saturation %PV	Rt ohm-m
74.5	20.88
69.5	23.59
66.7	24.73
57.8	30.79
51.1	39.35
39.4	58.99

Sample	14
PV (NOBP),cc	11.490
Porosity (NOBP).%	21.4
Length,cm	4.84
Diameter,cm	3.80
Brine density,g/cc	1.007
Brine Rw.ohm-m	0.415

Saturation %PV	Rt ohm-m
70.0	13.35
57.6	18.70
50.6	25.44
40.4	39.78
30.3	65.39

RESISTIVITY MEASUREMENTS - RAWDATA

Sample	22
PV (NOBP),cc	6.086
Porosity (NOBP).%	11.3
Length,cm	4.82
Diameter,cm	3.80
Brine density,g/cc	1.007
Brine Rw.ohm-m	0.415

Saturation %PV	Rt ohm-m
93.8	21.90
83.9	27.43
74.8	31.91
68.3	38.55
57.6	50.44

Sample	24
PV (NOBP),cc	9.244
Porosity (NOBP).%	18.0
Length,cm	4.72
Diameter,cm	3.79
Brine density,g/cc	1.007
Brine Rw.ohm-m	0.415

Saturation %PV	Rt ohm-m
82.8	14.87
61.8	25.38
52.8	33.92
37.0	63.51
29.1	97.87
19.5	224.09

Sample	25
PV (NOBP),cc	7.173
Porosity (NOBP).%	12.8
Length,cm	5.04
Diameter,cm	3.80
Brine density,g/cc	1.007
Brine Rw.ohm-m	0.415

Saturation %PV	Rt ohm-m
89.4	18.60
76.7	26.16
69.6	32.50
59.0	38.69
54.1	54.11

Sample	28
PV (NOBP),cc	9.929
Porosity (NOBP).%	20.2
Length,cm	4.56
Diameter,cm	3.78
Brine density,g/cc	1.007
Brine Rw.ohm-m	0.415

Saturation %PV	Rt ohm-m
74.1	13.95
63.5	18.74
46.8	38.16
40.9	47.51
19.3	221.12

Sample	46
PV (NOBP),cc	10.918
Porosity (NOBP).%	22.5
Length,cm	4.53
Diameter,cm	3.76
Brine density,g/cc	1.007
Brine Rw.ohm-m	0.415

Saturation %PV	Rt ohm-m
67.3	15.54
51.0	21.36
31.4	69.82
18.3	173.93
13.8	290.86

Sample	55
PV (NOBP),cc	9.343
Porosity (NOBP).%	17.1
Length,cm	5.06
Diameter,cm	3.78
Brine density,g/cc	1.007
Brine Rw.ohm-m	0.415

Saturation %PV	Rt ohm-m
73.1	19.82
64.4	26.42
53.4	34.53
43.6	49.91
32.1	78.79

RESISTIVITY MEASUREMENTS - RAWDATA

Sample	62
PV (NOBP),cc	7.177
Porosity (NOBP).%	14.6
Length,cm	4.50
Diameter,cm	3.79
Brine density,g/cc	1.007
Brine Rw.ohm-m	0.415

Saturation %PV	Rt ohm-m
73.9	23.22
55.4	40.47
49.0	46.78
41.6	75.82
24.0	188.59

Sample	67
PV (NOBP),cc	7.799
Porosity (NOBP).%	16.4
Length,cm	4.28
Diameter,cm	3.80
Brine density,g/cc	1.007
Brine Rw.ohm-m	0.415

Saturation %PV	Rt ohm-m
80.9	12.38
73.9	15.21
67.4	16.65
61.0	19.94
53.3	24.25

Sample	69
PV (NOBP),cc	8.436
Porosity (NOBP).%	19.6
Length,cm	3.95
Diameter,cm	3.79
Brine density,g/cc	1.007
Brine Rw.ohm-m	0.415

Saturation %PV	Rt ohm-m
77.5	14.56
59.3	25.68
47.0	36.84
43.3	41.76
36.5	52.32

Sample	80
PV (NOBP),cc	10.913
Porosity (NOBP).%	20.7
Length,cm	4.76
Diameter,cm	3.79
Brine density,g/cc	1.007
Brine Rw.ohm-m	0.415

Saturation %PV	Rt ohm-m
74.8	17.22
61.3	25.14
50.2	40.68
35.6	80.87
27.8	131.27
22.0	199.07

Sample	83
PV (NOBP),cc	9.557
Porosity (NOBP).%	18.0
Length,cm	4.79
Diameter,cm	3.79
Brine density,g/cc	1.007
Brine Rw.ohm-m	0.415

Saturation %PV	Rt ohm-m
79.8	15.19
70.9	19.96
43.8	53.37
33.5	103.50
27.6	134.83

Centrifuge Air-Brine Capillary Pressure - RAWDATA

Sample	5
Pore Vol	9.53
Length	4.95

RPM	Fluid Out (cc)
440	0.0
630	0.0
990	0.60
1540	2.26
2230	3.60
3160	4.93
4470	5.76
5500	6.26
6200	6.56

Sample	14
Pore Vol	11.9
Length	4.84

RPM	Fluid Out (cc)
440	0.0
630	0.33
990	2.66
1540	4.83
2230	6.23
3160	7.23
4470	8.23
5500	8.52
6200	8.72

Sample	22
Pore Vol	6.337
Length	4.82

RPM	Fluid Out (cc)
440	0.0
630	0.0
990	0.10
1540	0.60
2230	1.10
3160	1.60
4470	2.60
5500	2.93
6200	3.03

Sample	24
Pore Vol	9.579
Length	4.72

RPM	Fluid Out (cc)
440	1.67
630	3.33
990	5.33
1540	6.06
2230	6.99
3160	7.49
4470	7.83

Sample	25
Pore Vol	7.436
Length	5.04

RPM	Fluid Out (cc)
440	0.0
630	0.0
990	0.0
1540	1.07
2230	2.00
3160	3.33
4470	4.16
5500	4.36
6200	4.46

Sample	28
Pore Vol	10.327
Length	4.56

RPM	Fluid Out (cc)
440	3.00
630	5.00
990	6.49
1540	8.03
2230	8.49
3160	8.69
4470	8.99

Centrifuge Air-Brine Capillary Pressure - RAWDATA

Sample	46
Pore Vol	11.348
Length	4.53

RPM	Fluid Out (cc)
440	3.33
630	5.59
990	7.36
1540	7.99
2230	8.49
3160	8.99
4470	9.66

Sample	55
Pore Vol	9.743
Length	5.06

RPM	Fluid Out (cc)
440	0.33
630	1.00
990	2.40
2230	5.33
3160	6.29
4470	6.83
6200	7.33

Sample	62
Pore Vol	7.32
Length	4.28

RPM	Fluid Out (cc)
440	0.17
630	0.83
990	1.83
1540	2.5
2230	3.83
3160	5.00
4470	5.43
6200	5.76

Sample	67
Pore Vol	8.116
Length	4.28

RPM	Fluid Out (cc)
440	0.00
630	0.00
990	0.00
1540	0.67
2230	1.33
3160	2.33
4470	3.33

Sample	69
Pore Vol	8.7
Length	3.95

RPM	Fluid Out (cc)
440	0.03
630	0.67
990	1.27
1540	2.66
2230	3.66
3160	4.66
4470	5.39
6200	5.99

Sample	80
Pore Vol	10.724
Length	4.76

RPM	Fluid Out (cc)
440	0.50
630	3.63
990	5.16
2230	7.83
3160	8.66
4470	9.02
6200	9.26

Centrifuge Air-Brine Capillary Pressure - RAWDATA

Sample	83
Pore Vol	9.81
Length	4.79

RPM	Fluid Out (cc)
440	0.37
630	1.67
990	4.83
2230	6.99
3160	7.33
4470	7.73
6200	7.99

Sample	MSCT3
Pore Vol	1.79
Length	2.13

RPM	Fluid Out (cc)
1000	0.00
1380	0.00
2130	0.20
3080	0.55
4360	0.78
6170	1.00
8720	1.20
11540	1.29
14000	1.33

Sample	MSCT6
Pore Vol	2.04
Length	2.13

RPM	Fluid Out (cc)
1000	0.00
1380	0.35
2130	0.65
3080	0.98
4360	1.15
6170	1.44
8720	1.59
11540	1.64
14000	1.65

Sample	MSCT7
Pore Vol	1.917
Length	2.23

RPM	Fluid Out (cc)
1000	0.00
1380	0.10
2130	0.20
3080	0.59
4360	0.80
6170	0.99
8720	1.2
11540	1.31
14000	1.35

Sample	MSCT10
Pore Vol	2.03
Length	2.32

RPM	Fluid Out (cc)
1000	0.00
1380	0.20
2130	0.55
3080	0.85
4360	1.10
6170	1.25
8720	1.40
11540	1.50
14000	1.53

Centrifuge Air-Brine Capillary Pressure (1910psi NOBP) - RAWDATA

Sample	14
Pore Vol	11.045
Length	4.84

RPM	Fluid Out (cc)
310	1.0
440	1.1
700	2.93
990	4.44
1570	6.06
2220	7.07
2980	7.88

Sample	22
Pore Vol	5.938
Length	4.82

RPM	Fluid Out (cc)
310	0.0
440	0.0
700	0.0
990	0.0
1570	0.3
2220	1.41
2980	2.12

Sample	25
Pore Vol	6.98
Length	5.04

RPM	Fluid Out (cc)
310	0.0
440	0.0
700	0.0
990	1.11
1570	2.12
2220	2.83
2980	3.23

Sample	46
Pore Vol	9.90
Length	4.53

RPM	Fluid Out (cc)
310	3.54
440	5.05
700	6.46
990	7.27
1570	8.18
2220	8.48
2980	8.69

Sample	62
Pore Vol	6.667
Length	4.28

RPM	Fluid Out (cc)
310	0.1
440	0.8
700	2.0
990	3.03
1570	4.14
2220	4.34
2980	4.65

Sample	80
Pore Vol	10.284
Length	4.76

RPM	Fluid Out (cc)
310	2.32
440	3.23
700	5.25
990	6.57
1570	8.08
2220	8.48
2980	8.69

Rock Compressibility - RAWDATA

Company : **WOODSIDE ENERGY LIMITED**
Well : **THYLACINE-1**

Sample	14A		
Pore Vol.	10.775		
Porosity	19.9		
Bulk Vol.	54.096	Grain Vol.	43.321
Length	4.850		
Diameter	3.810		
Area	11.402		

OB (psi)	Pore Volume	Bulk Volume	Porosity (%)
400	10.765	54.086	19.9
500	10.735	54.056	19.9
600	10.706	54.027	19.8
700	10.679	54.000	19.8
800	10.654	53.975	19.7
900	10.630	53.951	19.7
1000	10.608	53.929	19.7
1200	10.566	53.887	19.6
1400	10.530	53.851	19.6
1600	10.497	53.818	19.5
1800	10.468	53.789	19.5
2000	10.442	53.763	19.4
2500	10.390	53.711	19.3
3000	10.351	53.672	19.3
3500	10.322	53.643	19.2
4000	10.300	53.621	19.2
4500	10.284	53.605	19.2
5000	10.272	53.593	19.2
6000	10.256	53.577	19.1
7000	10.247	53.568	19.1

Sample	46A		
Pore Vol.	12.118		
Porosity	22.7		
Bulk Vol.	53.469	Grain Vol.	41.351
Length	4.940		
Diameter	3.790		
Area	11.283		

OB (psi)	Pore Volume	Bulk Volume	Porosity (%)
400	12.135	53.486	22.7
500	12.031	53.382	22.5
600	11.952	53.303	22.4
700	11.889	53.240	22.3
800	11.837	53.188	22.3
900	11.793	53.144	22.2
1000	11.755	53.106	22.1
1200	11.693	53.044	22.0
1400	11.643	52.994	22.0
1600	11.601	52.952	21.9
1800	11.567	52.918	21.9
2000	11.537	52.888	21.8
2500	11.477	52.828	21.7
3000	11.431	52.782	21.7
3500	11.394	52.745	21.6
4000	11.364	52.715	21.6
4500	11.338	52.689	21.5
5000	11.316	52.667	21.5
6000	11.280	52.631	21.4
7000	11.251	52.602	21.4

Rock Compressibility - RAWDATA

Sample	22A		
Pore Vol.	5.799		
Porosity	10.4		
Bulk Vol.	55.628	Grain Vol.	49.8288
Length	4.947		
Diameter	3.805		
Area	11.372		

OB (psi)	Pore Volume	Bulk Volume	Porosity (%)
400	5.8	55.629	10.4
500	5.800	55.629	10.4
600	5.800	55.629	10.4
700	5.779	55.608	10.4
800	5.757	55.586	10.4
900	5.737	55.565	10.3
1000	5.718	55.546	10.3
1200	5.683	55.512	10.2
1400	5.653	55.482	10.2
1600	5.626	55.455	10.1
1800	5.603	55.432	10.1
2000	5.583	55.412	10.1
2500	5.544	55.373	10.0
3000	5.516	55.344	10.0
3500	5.496	55.324	9.9
4000	5.481	55.310	9.9
4500	5.471	55.300	9.9
5000	5.464	55.293	9.9
6000	5.455	55.284	9.9
7000	5.451	55.279	9.9

Sample	62A		
Pore Vol.	6.736		
Porosity	12.4		
Bulk Vol.	54.408	Grain Vol.	47.672
Length	4.890		
Diameter	3.820		
Area	11.462		

OB (psi)	Pore Volume	Bulk Volume	Porosity (%)
400	6.737	54.409	12.4
500	6.659	54.331	12.3
600	6.600	54.272	12.2
700	6.554	54.226	12.1
800	6.516	54.188	12.0
900	6.484	54.156	12.0
1000	6.457	54.129	11.9
1200	6.412	54.084	11.9
1400	6.377	54.049	11.8
1600	6.348	54.020	11.8
1800	6.324	53.996	11.7
2000	6.304	53.976	11.7
2500	6.263	53.935	11.6
3000	6.232	53.904	11.6
3500	6.207	53.879	11.5
4000	6.187	53.859	11.5
4500	6.171	53.843	11.5
5000	6.156	53.828	11.4
6000	6.133	53.805	11.4
7000	6.114	53.786	11.4

APPENDIX-3

SAMPLES DRILLED FOR MECHANICAL STRENGTH TESTS

Samples drilled for mechanical strength tests and forwarded to CSIRO

Sample ID	Depth (m)
G1	2187.65
G2	2187.75
G3	2187.79
G4	2187.85
G5	2169.34
G6	2169.54
G7	2169.59
G8	2169.65

THYLACINE 1
COMPOSITE WELL LOG

Origin Energy

Well Location Map

Thylacine 1 Story in plain view

Well Data Card

Well Name	Thylacine 1 Exploration Well
Operator	Origin Energy Resources Limited (Operator)
Rig Name	Ocean Patriot
Rig Type	Semi-Sub
Spud Date	1-Jan-00
Completion Date	1-Jan-00
Location	Lat: -38° 15' 0.00" S Easting: 484,000.00 m E
	Long: 146° 45' 0.00" E Northing: 5,760,000.00 m N
Datum	WGS 84, UTM Zone 55 S, CM = 147°E, Water Depth = 0 m
Water Depth	0 m
Total Depth	4,000.00 m MD, 3,987.00 m TVD
Penetration	4,000.00 m
Final Status	Gas Discovery
Rig Contractor	Ocean Patriot Pty Ltd
Rig Type	Semi-Sub
Rig Name	Ocean Patriot
Drilling Fluid Type	Seawater/Gel Sweeps
Elevation	22.00 m AMSL
Water Depth	0 m
Spud Date	1-Jan-00
Completion Date	1-Jan-00
Total Depth	4,000.00 m MD, 3,987.00 m TVD
Bottom Hole Temperature	120 °C
Max Deviation	0.00 °
Mud Type	Seawater/Gel Sweeps
Mud Weight	1.03 sg
Drilling Contractor	Ocean Patriot Pty Ltd
Rig Name	Ocean Patriot
Rig Type	Semi-Sub
Spud Date	1-Jan-00
Completion Date	1-Jan-00
Total Depth	4,000.00 m MD, 3,987.00 m TVD
Bottom Hole Temperature	120 °C
Max Deviation	0.00 °
Mud Type	Seawater/Gel Sweeps
Mud Weight	1.03 sg

Casing and Completion Schematic

Casing Record	Size	Weight	Grade	Set Depth (m MD)
Conductor Casing	30"	310 ppf	X-52	1,200
Surface Casing	20"	133 ppf	K-55	2,500
Intermediate Casing	13-3/8"	72 ppf	L-80	3,200
Production Casing	9-5/8"	53.5 ppf	P-110	3,800
Liner	7"	29 ppf	P-110	4,000
Tubing	5-1/2"	23 ppf	P-110	3,750

Completion Record	Top (m MD)	Bottom (m MD)
Perforations	3,850	3,900
Perforations	3,920	3,960
Packer	3,750	
Tubing Tail	3,750	

Marine Logging Survey Conditions

Survey	Date	Vessel	Water Depth (m)	Sea State	Wind (kn)	Current (kn)	Notes
Survey 1	1-Jan-00	MV Ocean Surveyor	0	Calm	5	0.5	Pre-spud survey
Survey 2	15-Jan-00	MV Ocean Surveyor	0	Moderate	15	1.2	Post-drilling survey

Lithology

Lithology	Description
Sandstone	Clastic sedimentary rock composed of sand-sized grains
Siltstone	Clastic sedimentary rock composed of silt-sized grains
Claystone	Fine-grained sedimentary rock composed of clay minerals
Limestone	Sedimentary rock composed of calcium carbonate
Coal	Organic-rich sedimentary rock
Volcanic	Igneous rock of volcanic origin
Basement	Crystalline basement rock

Legend

Gas	Oil
Water	Coal
Sandstone	Siltstone
Claystone	Limestone
Volcanic	Basement

Lithology Column